



## **4<sup>th</sup> International Conference on Environmental Radioactivity: Radionuclides as Tracers of Environmental Processes**

**29 May – 2 June 2017 Vilnius, Lithuania**

Thank you to our sponsors for their support to the International Conference on Environmental Radioactivity ENVIRA 2017!

### Organizers



### Sponsors





## Welcome to the ENVIRA2017 Conference

**Dear Colleagues,**

We welcome you to the ENVIRA2017, the International Conference on Environmental Radioactivity organized by the Centre for Physical Sciences and Technology (Institute of Physics) in Vilnius, Lithuania from Monday, May 29 to Friday, June 2, 2017. The venue and the Conference topics of the ENVIRA2017 which will be focusing on “Radionuclides as Tracers of Environmental Processes” were agreed on by the International Advisory Committee and confirmed at the closing session of the ENVIRA2015 conference held in Thessaloniki (Greece) in September 2015.

Following traditions of previous ENVIRA conferences, the ENVIRA2017 will consist of invited talks on relevant environmental radioactivity and radioanalytical topics, given by prominent representatives of the field, as well as by oral and poster contributions on various environmental radioactivity aspects. The conference will highlight the new scientific knowledge on the application of natural and anthropogenic radionuclides and isotopes in tracer studies in the terrestrial (atmosphere, hydrosphere, biosphere, pedosphere, etc.) and marine (seawater, marine biota, sediments, etc.) environments. The latest technological innovations in low-level radioactivity detection techniques including radiometric and low-energy and high-energy mass spectrometry methods, in situ measuring techniques, continuous monitoring systems, and other recent analytical developments will be included in the conference program as well. Radioecological topics, protection of the total environment against radiation including Chernobyl and Fukushima impacts on the environment, waste management and remediation actions on contaminated territories will be also covered.

Additionally, conference attendees and accompanying guests are invited to participate in our events: welcome reception, gala dinner, trip to Trakai.

If you have questions during the event, ENVIRA2017 committee staff will be available to assist you or you can contact [envira2017@ftmc.lt](mailto:envira2017@ftmc.lt) and visit <http://envira2017.ftmc.lt/> at any time.

Thank you for attending ENVIRA2017 and please enjoy the conference!

## Committees

### The Local Organizing Committee:

- G. Lujanienė (Chair), Center for Physical Sciences and Technology, Vilnius
- A. Mastauskas, Radiation Protection centre, Vilnius
- D. Šerėnaitė, Lithuanian Radiation protection society, Vilnius
- B. Šilobritienė, Environmental Protection Agency, Vilnius
- J. Mažeika, Nature Research Centre, Vilnius
- I. Kulakauskaitė, Center for Physical Sciences and Technology, Vilnius

### International Organizing Committee:

- P.P. Povinec (Chair), Comenius University, Bratislava
- G. Lujanienė, (Co-Chair), Center for Physical Sciences and Technology, Vilnius
- F. Bréchnignac, International Union of Radioecology, Paris
- A. Ioannidou, Aristotle University, Thessaloniki
- W. Plastino, Roma Tre University
- S.C. Sheppard, Chief Editor, Journal of Environmental Radioactivity
- I. Svetlik, Nuclear Physics Institute, Prague

### International Advisory Board:

- P.P. Povinec (Chair), Comenius University, Bratislava
- G. Lujanienė (Co-Chair), Center Phys. Sciences and Technology, Vilnius
- M. Aoyama, University of Fukushima
- M. Betti, EC, JRC Directorate for Nucl. Safety and Security, Karlsruhe
- F. P. Carvalho, University of Lisbon
- A. Chatt, Dalhousie University, Halifax
- M. Garcia-León - University of Seville
- R. Garcia-Tenorio, University of Seville
- K. Hirose, Sophia University, Tokyo
- X. Hou, Technical University of Denmark, Riso
- M. Hult, EC, Joint Research Centre, Inst. Ref. Mat. Measurements, Geel
- S. Jerome, National Physical Laboratory, Teddington
- A.J.T. Jull, University of Arizona, Tucson
- L. Kaihola, Littoinen, Finland
- S. Kalmykov, Moscow State University, Moscow
- C. Katzlberger, Austrian Agency for Health and Food Safety, Vienna
- W.E. Kieser, University of Ottawa
- T. Kovács, University of Pannonia, Veszprém
- O. Masson, Inst. Rad.Sûreté Nucléaire, Saint-Paul-lez-Durance
- J. W. Mietelski, Institute of Nuclear Physics, Polish Academy of Sciences, Krakow
- J. Mažeika, Nature Research Centre, Vilnius
- M. Molnár, Institute for Nuclear Research, Debrecen
- M. Oinonen, University of Helsinki
- S. Pan, University of Nanjing
- V. Remeikis, Center Phys. Sciences and Technology, Vilnius
- P. Vojtyla, CERN, Geneva



		Sun 5/28	Mon 5/29	Tues 5/30	Wed 5/31	Thurs 6/1	Fri 6/2														
<b>08:00</b>	0		Registration				Plenary session 5														
	10																				
	20																				
	30																				
	40																				
<b>09:00</b>	0		Opening ceremony				Plenary session 2	Plenary session 3	Plenary session 4	Plenary session 6											
	10																				
	20																				
	30																				
	40																				
<b>10:00</b>	0		Plenary session 1				Coffee break	Coffee break	Coffee break	Plenary session 7											
	10																				
	20																				
	30																				
	40																				
<b>11:00</b>	0		Coffee break				Fukushima impact/ NORMS	Atmosphere/ Natural Radionuclides	Monte carlo detection modeling/ impact of nuclear installations	Closing ceremony											
	10																				
	20																				
	30																				
	40																				
<b>12:00</b>	0		AMS applications/ Marine Environment				Lunch	Lunch	Lunch	Lunch											
	10																				
	20																				
	30																				
	40																				
<b>13:00</b>	0	Lunch	Poster session 1 & Coffee	Poster session 2 & Coffee	Presentations of companies	Poster session 3 & Coffee															
	10																				
	20																				
	30																				
	40																				
<b>14:00</b>	0	Registration	Enviromental proceses/ Reference materials and metods	Fukushima and chernobyl impacts/ Radon	Trip with a simple dinner	Sediments and soils/ Radionuclides in biota															
	10																				
	20																				
	30																				
	40																				
<b>15:00</b>	0		Registration	Poster session 1 & Coffee	Poster session 2 & Coffee	Poster session 3 & Coffee	Poster session 3 & Coffee														
	10																				
	20																				
	30																				
	40																				
<b>16:00</b>	0		Registration	Poster session 1 & Coffee	Poster session 2 & Coffee	Poster session 3 & Coffee	Poster session 3 & Coffee														
	10																				
	20																				
	30																				
	40																				
<b>17:00</b>	0		Registration	Poster session 1 & Coffee	Poster session 2 & Coffee	Poster session 3 & Coffee	Poster session 3 & Coffee														
	10																				
	20																				
	30																				
	40																				
<b>18:00</b>	0		Welcome party																		
	30																				
<b>19:00</b>	0	Welcome party																			
	30																				
<b>20:00</b>	0											Welcome party				Gala dinner					
	30																				
<b>21:00</b>	0																Welcome party				Gala dinner
	30																				

## Social events

On 31 June 2017, conference participants and guests are invited to experience the culture of the Trakai - the former capital of the Grand Duchy of Lithuania - is a small town located about 28 km from Vilnius. Situated in a picturesque lakeside area it is one of the most popular tourist attractions of the country. The historical part of the town– the famous insular Castle on the lake, the original gothic style architectural monument from the end of the XIV century. Trakai is also known for the Karaimes (a people speaking the Turkic language), who have lived there since the 14th century and have preserved their traditions. The 4-hour excursion departs from reception of Best Western Hotel. The trip includes a 30-minute drive by bus to Trakai, visit Takai island Castle and dinner featuring national dishes (the most popular is kybyn – a small pastry stuffed with minced meat).



## Local area information

The ENVIRA2017 conference venue will be the Best Western Hotel. The hotel is situated on the right bank of the Neris River of Vilnius, close to the historical town, just a 5 minutes walk to the Cathedral, Palace of the Grand Dukes of Lithuania, Gediminas Castle, as well as Pilies and Vokiečių streets so popular among the city guests and local inhabitants. Well-equipped and stylish rooms in the **BEST WESTERN Vilnius Hotel** will satisfy even the most demanding guests. The hotel offers 114 large and cosy rooms including 4 luxury rooms and one apartment with a private sauna.



## CONFERENCE PROGRAMME

Sunday 28, May 2017

15:00-18:00	<b>Registration</b>
18:00-20:00	<b>WELCOME PARTY</b>

Monday 29, May 2017

08:00-09:00	<b>Registration</b>
09:00-09:30	<b>OPENING OF THE CONFERENCE</b> Room: Glass A Chair: G. Lujanienė
	<b>Prof. Gintaras Valušis</b> , Director of SRI Center for Physical Science and Technology <b>Vitalijus Auglys</b> , Director of Pollution Prevention Department, Ministry of Environment <b>Julis Žiliukas</b> , Director of Expertise and Exposure Monitoring Department, Radiation Protection Centre <b>Darius Udrys</b> , Director of Go Vilnius, Vilnius City Municipality
09:30-11:30 PL1	<b>PLENARY SESSION I</b> Room: Glass A Chair: G. Lujanienė, P.P.Povinec
09:30-10:00 Id-1	Peter Steier, Austria <b>"New" environmental radionuclides made accessible by Ion-Laser Interaction (ILIA)</b> <i>P. Steier, J. Lachner, A. Kalb, Ch. Marek, M. Martschini, A. Priller, and R. Golser</i>
10:00-10:30 Id-2	William Kieser, Canada <b>Progress in AMS Radioisotope Analysis Using Fluoride Target Matrices</b> <i>W.E. Kieser, X-L. Zhou, C. McDonald and R.J. Cornett</i>
10:30-11:00 Id-3	Timothy Jull, USA <b>What can rapid carbon-14 excursions in the tree-ring record tell us about past "space weather" and the carbon cycle?</b> <i>A.J.T. Jull, F. Miyake, I. Panyushkina, K. Masuda, T. Nakamura, K. Kimura, M. Hakozaiki, L. Wacker, T.E. Lange, R.J. Cruz, Ch. Baisan. M.W. Salzer, R. Janovics, K. Hubay, M. Molnár</i>
11:00-11:30 Id-4	Filippo Terrasi, Italy <b>AMS studies of NPP environmental impact</b> <i>F. Terrasi</i>
11:30-12:00	Coffee break

### PARALLEL SESSIONS 1 12:00-13:00

SESSION 1A: AMS APPLICATIONS Room: Glass A Chair: W. Kieser, P. Steier		SESSION 1B: MARINE ENVIROMENT Room: Amber Chair: M. Eriksson, S.-H. Lee	
12:00 Id-5	Karin Hain, Austria <sup>233</sup> U/ <sup>236</sup> U – A new tracer for environmental processes? <i>K. Hain, P. Steier, R. Eigl, M. B. Froehlich, R. Golser, X. Hou, J. Lachner, J. Qiao, F. Quinto, A. Sakaguchi</i>	12:00 Id-9	Martina Rozmaric, Monaco <b>Marine environmental radioactivity off Namibia's coast</b> <i>M. Rozmaric, D.C. Louw, I. Osvath, O. Blinova, I. Levy, M.K. Pham, P. McGinnity, M. Fujak, J. Bartocci, S.B. Mudumbi, T.K.S. Kahunda, K. Grobler, E. Chamizo, M. Lopez, J.M. Lopez-</i>

			<i>Gutierrez , R. Garcia Tenorio and Lj. Benedik</i>
<b>12:15</b> Id-6	Francesca Quinto, Germany <b>Investigating the long-term behaviour of actinides in repository relevant conditions with the multi-actinides analysis and AMS</b> <i>F. Quinto, F. Geyer, M. Lagos , M. Plaschke, T. Schäfer, P. Steier and H. Geckeis</i>	<b>12:15</b> Id-10	Daniela Pittauer, Germany <b>Plutonium in Bismarck Sea sediments: South vs. North Pacific Signals</b> <i>D. Pittauer, P. Roos, J. Qiao , W. Geibert and H.W. Fischer</i>
<b>12:30</b> Id-7	Miroslav Jeřkovský, Slovakia <b>Preliminary study of AIN targets for accelerator mass spectrometry</b> <i>M. Jeřkovský, J. Pánik, J. Kaizer, P. Steier and P. P. Povinec</i>	<b>12:30</b> Id-11	Jerzy Mietelski, Poland <b><sup>241</sup>Pu/<sup>239+240</sup>Pu ratio in Antarctic marine and terrestrial samples</b> <i>K. M. Szufa, T. Mróz, J. W. Mietelski, K. Sobiech-Matura, P. Gaca , M.A.Olech</i>
<b>12:45</b> Id-8	Tiberiu Bogdan Sava, Romania <b>Dating in Romanian archaeology: comparison between radiocarbon and dendrochronology methods spanning over the last 1000 years</b> <i>T. Sava, I. Popa, G. Sava, A. Ion, M. Ilie, I. Stanciu , C. Simion, B. Ștefan, O. Gâza and D. Păceșilă</i>	<b>12:45</b> Id-12	Filothei Pappa, Greece <b>Chronological records of metal contamination at two mining areas using sediment profiles</b> <i>F.K. Pappa, C. Tsabaris , D.L. Patiris, E.G. Androulakaki, A. Ioannidou, M. Kokkoris , R. Vlastou.</i>

<b>13:00-14:00</b>	Lunch
<b>14:00-15:00</b>	Poster session 1& Coffee

**PARALLEL SESSION 2 15:00-17:00**

<b>SESSION 2A: ENVIROMENTAL PROCESSES</b> Room: Glass A Chair: H.-C. Li, E. Steinnes		<b>SESSION 2B: REFERENCE MATERIALS AND METODS</b> Room: Amber Chair: V. Remeikis, P. Vojtyla	
<b>15:00</b> Id-13	Wolfgango Plastino, Italy <b>Uranium time series analysis: a new methodological approach for event screening categorization</b> <i>S. Bianchi and W. Plastino</i>	<b>15:00</b> Id-20	Juan-Pedro Bolivar, Spain <b>Optimization and validation of the BCR sequential extraction procedure for natural radionuclides (U, Th, Po); application to phosphogypsum by-product</b> <i>S. Pérez-Moreno, M.J. Gázquez, and J. P. Bolívar</i>
<b>15:15</b> Id-14	Yihong Xu, China <b>Behaviours of plutonium isotopes in natural soil particles with different size</b> <i>Y.H. Xu, S.M. Pan and M.M. Wu</i>	<b>15:15</b> Id-21	Yanqin Ji, China <b>Preparation of strontium-90 pine needle reference material and the labs intercomparison radiochemical analysis</b> <i>Y. Ji, F. Chen, X. Shao, L. Yin, X. Kong</i>
<b>15:30</b> Id-15	Min Znao, China <b>Sources and transformation of carbon in an epikarst spring-fed pond system in central Guizhou: <math>\Delta^{14}\text{C}</math> and <math>\delta^{13}\text{C}</math> indicators</b> <i>M. Zhao, B. Chen, H.C. Li, Z. Liu, R. Yang</i>	<b>15:30</b> Id-22	Jose A. Corcho Alvarado, Switzerland <b>A procedure for the sequential determination of radionuclides: a case study in river sediments</b> <i>H. Sahli, S. Röllin, B. Balsiger, M. Burger, V. Putyrskaya, E. Klemt and J.A. Corcho Alvarado</i>
<b>15:45</b> Id-16	Marina Frontasyeva, Russia <b>Atmospheric deposition of radionuclides – assessment based on passive moss biomonitoring</b> <i>M. Frontasyeva, E. Steinnes</i>	<b>15:45</b> Id-23	András Bednár, Hungary <b>Determination of Sr-90 activity concentration and Strontium/Calcium ration in different matrices</b> <i>A. Bednár, G. Bátor, E. Tóth-Bodrogi, T. Kovács</i>
<b>16:00</b> Id-17	Almira Aidarkhanova, Kazakhstan <b>Radionuclide transport in the "sediments – water – plants" system of the water objects of the Semipalatinsk test site</b> <i>A.K. Aidarkhanova, S.N. Lukashenko, N.V. Larionova, V.V. Polevik</i>	<b>16:00</b> Id-24	Marina Sáez-Muñoz, Spain <b>Analysis of the evolution of gross alpha and beta activities in airborne samples in Valencia</b> <i>M. Sáez-Muñoz, M.C. Bas, J. Ortiz and S. Martorell</i>
<b>16:15</b> Id-18	Vivien Miller, USA <b>Monte Carlo Markov Chain Simulation of the Cesium Dynamics in the Small Mesotrophic Reservoir Pond 4</b> <i>V.J. Miller, T.E. Johnson and J.E. Pinder II</i>	<b>16:15</b> Id-25	Merja Lusa, Finland <b>Se uptake and reduction in two boreal Pseudomonas sp. Strains</b> <i>M. Lusa, J. Knuutinen, J. Lehto and M. Bomberg</i>



<b>16:45</b> Id-19	Alexandra Ioannidou, Greece <b>Time lag between the tropopause height and the levels of <sup>7</sup>Be concentrations in surface air in mid and high latitudes</b> <i>E. Ioannidou, A. – P. Leppänen, A. Vasileiadis, D. Melas and A. Ioannidou</i>		
<b>17:00-18:00</b>	Poster session 1 & coffee		

**Tuesday 30, May 2017**

<b>08:30-11:00</b> PL2	<b>PLENARY SESSION II</b> Room: Glass A Chair: A. J. T. Jull, O. Masson		
<b>08:30-09:00</b> Id-26	Michio Aoyama, Japan <b>Radiocaesium in the North Pacific Ocean derived from atmospheric weapons tests and Fukushima accident: past and present</b> <i>M. Aoyama</i>		
<b>09:00-09:30</b> Id-27	Katsumi Hirose, Japan <b>Atmosphere and marine impacts of the Fukushima Daiichi NPP accident: five years trends of Fukushima-derived radionuclides</b> <i>K. Hirose</i>		
<b>09:30-10:00</b> Id-28	Gi Hoon Hong, Korea <b>Radiocesium contamination in the North Pacific Ocean after 2011 Fukushima Nuclear accident</b> <i>G.H. Hong, S.H. Kim and H. Lee</i>		
<b>10:00-10:30</b> Id-29	Sang-Han Lee, Korea <b>Characteristics of artificial radionuclides in the food stuffs in Korea</b> <i>S.H. Lee, J.S. Oh, J.M. Lee, k. B. Lee, J.Y. Yun</i>		
<b>10:30-11:00</b> Id-30	Georg Steinhauser, Germany <b>Food Safety after the Fukushima Nuclear Accident</b> <i>Georg Steinhauser</i>		
<b>11:00-11:30</b>	Coffee Break		
<b>PARALLEL SESSION 3 11:30-13:00</b>			
<b>SESSION 3A: FUKUSHIMA IMPACT</b> Room: Glass A Chair: M. Aoyama, G. Hong		<b>SESSION 3B: NORMS</b> Room: Amber Chair: D. Degering, I. Krajcar-Bronić	
<b>11:30</b> Id-31	Daisuke Tsumune, Japan <b>Estimations of direct release rate of <sup>137</sup>Cs, <sup>90</sup>Sr and <sup>3</sup>H from the Fukushima Dai-ichi Nuclear Power Plant for four-and-a-half years</b> <i>D. Tsumune, M. Aoyama K. Hirose, T. Tsubono, K. Misumi and Y. Tateda</i>	<b>11:30</b> Id-37	Christian Katzlberger, Austria <b>Management of NORM legacy sites in Austria</b> <i>C. Katzlberger, M. Dauke, F. Rechberger, E. Lindner</i>
<b>11:45</b> Id-32	Jakub Kaizer, Slovakia <b>Tritium and radiocarbon in western North Pacific waters: post-Fukushima situation</b> <i>J. Kaizer, P.P. Povinec, M. Aoyama, Y. Kumamoto, M. Molnár and L. Palcsu</i>	<b>11:45</b> Id-38	Fernando P. Carvalho, Portugal <b>Environmental transfer of radionuclides from uranium mining and milling waste to biota and humans</b> <i>F. P. Carvalho, J.M. Oliveira, M. Malta</i>

<b>12:00</b> Id-33	Yutaka Tateda, Japan <b>Reconstruction of temporal change of radiocesium level in bottom sediment off Fukushima for evaluating contribution to benthic food chain transfer</b> <i>Y. Tateda, K. Misumi, D. Tsumune, M. Aoyama, Y. Hamajima, J. Kanda, T. Ishimaru, and T. Aono</i>	<b>12:00</b> Id-39	Rafael Garcia-Tenorio, Spain <b>Uranium concentrations in NORM efflorescences formed in a phosphogypsum legacy site determined by PIXE</b> <i>M.C. Jimenez-Ramos, I. Ortega-Feliu, J.P. Bolivarand R. García-Tenorio</i>
<b>12:15</b> Id-34	Mochamad Adhiraga Pratama, Japan <b>Time-dependent behaviour analysis and identification of factors affecting radiocaesium transfer to separate sewers in Fukushima Prefecture</b> <i>M.A. Pratama, S. Takahara, M. Munakataand, M. Yoneda</i>	<b>12:15</b> Id-40	Geert Biermans, Belgium <b>A survey of natural radioactivity in Belgian groundwater and its use in risk identification for water treatment and drinking water screening</b> <i>G. Biermans, J. Claes, B. Dehandschutter, S. Pépin, L. Sombé and M. Sonck</i>
<b>12:30</b> Id-35	Sarata Kumar Sahoo, Japan <b>Measurement of <sup>90</sup>Sr activity in Fukushima soil samples affected by Nuclear Accident</b> <i>S.K. Sahoo, N. Kavasi and T. Aono</i>	<b>12:30</b> Id-41	Jelena Ajtić, Serbia <b>REMdb as a framework for collaborations in environmental radioactivity research</b> <i>M. A. Hernández-Ceballos, E. Brattich, J. Ajtić, G. Cinelli, V. Djurdjevic, D. Sarvan, T. Tollefsen</i>
<b>12:45</b> Id-36	Yasushi Kino, Japan <b>Time course change of radiocesium concentration in wild mushrooms collected in Miyagi prefecture, Japan from 2011 to 2014</b> <i>A. Irisawa and Y. Kino</i>	<b>12:45</b> Id-42	Pawel Jodlowski, Poland <b>Radioactivity in the gas pipeline network in Poland</b> <i>J. Nowak, P. Jodłowski, J. Macuda, C. Nguyen Dinh and K. Liszka</i>

<b>13:00-14:00</b>	Lunch
<b>14:00-15:00</b>	Poster session 2& Coffee

**PARALLEL SESSION 4 15:00-16:30**

<b>SESSION 4A:</b> <b>FUKUSHIMA AND CHERNOBYL IMPACTS</b> Room: Glass A Chair: M. Frontasyeva, M.J. Oinonen		<b>SESSION 4B:</b> <b>RADON</b> Room: Amber Chair: R. Garcia-Tenorio, J. Mažeika	
<b>15:00</b> Id-43	Takuro Shinano, Japan <b>Secondary contamination of radioactive cesium to the plant in coastal area of Fukushima in 2013 and aftermath</b> <i>T. Shinano, H. Matunami, M. Sato, T. Saito, S. Fujimura, T. Ota, T. Eguchi, S. Horii and T. Murakami</i>	<b>15:00</b> Id-49	Véronique De Heyn, Belgium <b>Indoor Radon in Ardenne: A multivariate analysis</b> <i>V. De Heyn, C. Licour, F. Tondeur, I. Gerardy, B. Dehandschutter, G. Ciotoli, G. Cinelli</i>
<b>15:15</b> Id-44	Kazuma Koarai, Japan <b>Assessment of <sup>90</sup>Sr pollution from the Fukushima-Daiichi Nuclear Power Plant accident by measurement of cattle teeth</b> <i>K. Koarai, Y. Kino, A. Takahashi, T. Suzuki, Y. Shimizu, M. Chiba, K. Osaka, K. Sasaki, Y. Urushihara, T. Fukuda, E. Isogai, H. Yamashiro, T. Oka, T. Sekine, M. Fukumoto, H. Shinoda</i>	<b>15:15</b> Id-50	Qiuju Guo, China <b>Study on continuous radon measurement on based of Si-PIN detector</b> <i>L. Zhang, Q. Guo and Y. Wang</i>
<b>15:30</b> Id-45	Azusa Ishizaki, Japan <b>Estimation of dose reduction factor before and after decontamination</b> <i>A. Ishizaki, A. Mori, K. Kawase, M. Kato, M. Watanabe, I. Aoki and M. Munakata</i>	<b>15:30</b> Id-51	Jesús García-Rubiano, Spain <b>Radiological characterization of volcanic rocks from eastern Canary Islands</b> <i>J.G. Rubiano, H. Alonso, J.G. Guerra, M.A. Arnedo, A. Tejera, P. Martel</i>
<b>15:45</b> Id-46	Alexandra Ioannidou, Greece <b><sup>137</sup>Cs in surface soil samples in Northern Greece, 30 years after the Chernobyl accident</b> <i>A. Ioannidou, S. Stoulos, C. Betsou, E. Ioannidou, J. Hansman, M. Krmar, N. Kazakis, E. Tsakiri</i>	<b>15:45</b> Id-52	Vitaliy Romanenko, Kazakhstan <b>Characterisation of Radon Concentrations in the area of Kalachi village (North Kazakhstan)</b> <i>V.V. Romanenko, S.N. Lukashenko and Y.V. Garbuz</i>
<b>16:00</b> Id-47	Daniel Heine, Germany <b>Migration of Radionuclides in soil samples from Pripyat</b> <i>C. Walther, S. Bister, P. Brozynski, D. Heine</i>	<b>16:00</b> Id-53	Giancarlo Ciotoli, Italy <b>Geogenic radon as geophysical/Geochemical tracer of active faults</b> <i>G. Ciotoli, A.J.S.C. Pereira, P. Bossew, L. Ruggiero</i>



<b>16:15</b> Id-48	Natalia Kuzmenkova, Russia <b>Root uptake and translocation of <sup>137</sup>Cs by cultural and wild cereals, model pot experiment</b> <i>M.M. Godyaeva, N.V. Kuzmenkova and T.A. Paramonova</i>		
<b>16:30-18:00</b>	Poster session 2 & coffee		

## Wednesday 31, May 2017

<b>08:30-11:00</b> PL3	<b>PLENARY SESSION III</b> Room: Glass A Chair: K. Hirose, F. Terrasi		
<b>08:30-09:00</b> Id-54	Peter Bossew, Germany <b>Radon research as a discipline of radioecology – an overview</b> <i>P. Bossew</i>		
<b>09:00-09:30</b> Id-55	Ines Krajcar Bronić, Croatia <b>Environmental <sup>14</sup>C and <sup>3</sup>H levels in Croatia</b> <i>I. Krajcar Bronić</i>		
<b>09:30-10:00</b> Id-56	Mihály Molnár, Hungary <b>Enhanced atmospheric C-14 monitoring around the Paks NPP of Hungary</b> <i>M. Molnár, I. Major, T. Varga, G. Orsovski, M. Veres, T. Bujtás, L. Manga</i>		
<b>10:00-10:30</b> Id-57	Eiliv Steinnes, Norway <b>Influence of precipitation chemistry on the mobility of radionuclides in boreal forest ecosystems</b> <i>Eiliv Steinnes</i>		
<b>10:30-11:00</b> Id-58	Mats Eriksson, Sweden <b>On the radionuclide distribution in selected sediment cores from the Baltic Sea</b> <i>M. Eriksson, G. Olszewski, P. Lindahl, P. Andersson, E. Chamizo, R. García-Tenorio</i>		
<b>11:00-11:30</b>	Coffee Break		

### PARALLEL SESSION 5 11:30-13:00

<b>SESSION 5A: ATMOSPHERE</b> Room: Glass A Chair: T. Kovács, J.W. Mietelski		<b>SESSION 5B: NATURAL RADIONUCLIDES</b> Room: Amber Chair: L. Benedik, F.P. Carvalho	
<b>11:30</b> Id-59	Olivier Masson, France <b>Deposition of radionuclides by fog droplets on plants</b> <i>O. Masson, J. Tav, F. Burnet, P. Paulat, A. De Vismes</i>	<b>11:30</b> Id-64	Detlev Degering, Germany <b>Radium isotopes in saline deepwaters as tracers of the source aquifer</b> <i>D. Degering, N. Dietrich, F. Krüger.</i>
<b>11:45</b> Id-60	Wolfgang Plastino, Italy <b>Beryllium and Xenon time series analysis: a new methodological approach for Atmospheric Transport Modelling at small, synoptic and global scales</b> <i>S. Bianchi, A. Longo and W. Plastino</i>	<b>11:45</b> Id-65	Danyl Perez-Sanchez, Spain <b>Modelling the seasonal dynamics and influence in the transport of 238U-series radionuclides in soil to plant system</b> <i>D. Pérez-Sánchez, M.C. Thorne and R. Klos</i>
<b>12:00</b> Id-61	Antonio Baeza, Spain <b>Time evolution of atmospheric tritium concentration in two locations affected by different source terms: cosmogenic and cosmogenic plus anthropogenic</b> <i>A. Baeza, A. Rodríguez-Perulero, J. Guillén and E. García-Delgado</i>	<b>12:00</b> Id-66	Rafael García-Tenorio, Spain <b>Radiological evaluation associated to the mining and concentration of monazite in Central Spain</b> <i>R. García-Tenorio, G. Manjón, I. Diaz, I. Vioque, J. Galván and J. Mantero</i>

<b>12:15</b> Id-62	Angel, VIIBautista, Japan / Philippines <b>High resolution Iodine-129 and tritium bomb peak records in an ice core from SE-dome site, Greenland</b> <i>A.T. Bautista VII, Y. Miyake, H. Matsuzaki, Y. Iizuka, K. Horiuchi</i>	<b>12:15</b> Id-67	Jesús García-Rubiano, Spain <b>Gross alpha and radon: hidrogeochemical and radiological risk tracer in groundwater in Gran Canaria Island</b> <i>A. Tejera, H. Alonso, T. Cruz-Fuente, J. González-Guerra, A. Rodríguez-González, M.A. Arnedo, JG. Rubiano, M.C. Cabrera, F.J. Pérez-Torradoy, P. Martel</i>
<b>12:30</b> Id-63	Jelena Ajtic, Serbia <b>Analysis of beryllium-7 variability in northern Europe</b> <i>J. Ajtić, V. Djurdjevic, D. Sarvan, E. Brattich, M. A. Hernández-Ceballos</i>	<b>12:30</b> Id-68	Alexander Dario Esquivel López, República de Panamá <b>Annual cycle of <sup>7</sup>Be in soil in a micro-watershed of Mato Frio River, (Brazil)</b> <i>A.D. Esquivel L., R.M. Moreira, J. Juri Ayub and D.L. Valladares</i>
<b>13:00-14:00</b>	Lunch		
<b>14:00-15:15</b>	<b>PRESENTATIONS OF COMPANIES</b> Room: Glass A Chair: L. Kaihola		
<b>14:00</b>	Andrej Kováčik, Microstep-MIS, spol. s r.o., Slovakia <b>Integrated Environmental Monitoring System</b>		
<b>14:15</b>	Francesco Vicinanza, MEATECS, Singapur <b>State of the Art Design and Implementation of Environmental Radiation Monitoring Networks</b>		
<b>14:30</b>	Aude Bombard, Triskem International, France <b>New Developments in Triskem</b>		
<b>14:45</b>	Alan De Raedemaekere, InBio/PerkinElmer <b>New developments in the field of Liquid Scintillation Spectrometry for low level radio-analytical detection and environmental radioactivity screening</b>		
<b>15:00</b>	Mangirdas Zavackas, Baltic Scientific Instruments <b>Baltic Scientific Instruments product range Introduction</b>		
<b>15:30-20:00</b>	Trip with a Simple Dinner		

## Thursday 01, June 2017

<b>08:30-11:00</b> PL4	<b>PLENARY SESSION IV</b> Room: Glass A Chair: C. Katzlberger, W. Plastino		
<b>08:30-09:00</b> Id-69	Massimiliano Clemenza, Italy <b>Low background neutron activation analysis: an high sensitivity methods for long-lived radionuclides</b> <i>M. Clemenza</i>		
<b>09:00-09:30</b> Id-70	Amares Chatt, Canada <b>Separation of thorium and uranium using TEVA and TRU resins in tandem and quantification of uncertainty of their measurements using neutron activation</b> <i>S. Hevia and A. Chatt</i>		
<b>09:30-10:00</b> Id-71	Ljudmila Benedik, Slovenia <b>Neutron activation analysis and alpha-particle spectrometry in environmental research</b> <i>L. Benedik</i>		
<b>10:00-10:30</b> Id-72	Mikael Hult, Belgium		

	<b>Radioactivity measurements in the underground laboratory HADES</b> <i>M. Hult</i>		
<b>10:30-11:00</b> <i>Id-73</i>	Yasunori Hamajima, Japan <b>Low-Level Gamma-ray Counting in Ogoya Underground Laboratory</b> <i>Y. Hamajima</i>		
<b>11:00-11:30</b>	Coffee Break		
<b>PARALLEL SESSION 6 11:30-13:00</b>			
<b>SESSION 6A: MONTE CARLO DETECTION MODELING</b> Room: Glass A Chair: C. Katzlberger, Y. Hamajima		<b>SESSION 6B: IMPACTS OF NUCLEAR INSTALLATIONS</b> Room: Amber Chair: M. Molnár, I. Svetlík	
<b>11:30</b> <i>Id-75</i>	Miloslava Bagínová, Switzerland <b>Investigation of neutron-induced background in HPGe detectors – first phase</b> <i>M. Bagínová, P. Vojtyla and P. Povinec</i>	<b>11:30</b> <i>Id-80</i>	Róbert Janovics, Hungary <b>Inorganic and total <sup>14</sup>C in the vicinity of a Hungarian LILW</b> <i>R. Janovics, A. Molnár, T. Varga, M. Braun, I. Tóth, M. Molnár</i>
<b>11:45</b> <i>Id-76</i>	Robert Breier, Slovakia <b>Background of a HPGe detector in the Modane underground laboratory: Monte Carlo simulations</b> <i>R. Breier, P. Loaiza, F. Piquemal, P.P. Povinec</i>	<b>11:45</b> <i>Id-81</i>	Ivan Kontuľ, Slovakia <b>Radiocarbon record in modern tree rings from Slovakia</b> <i>I. Kontuľ, M. Ješkovský, J. Kaizer, P. P. Povinec, M. Richtáriková, I. Svetlík, A. Šivo</i>
<b>12:00</b> <i>Id-77</i>	Jonay González Guerra, Spain <b>Comparison of experimental vs Monte Carlo efficiency calibrations of an HPGe spectrometer</b> <i>J.G. Guerra, J.G. Rubiano, G. Winter, A.G. Guerra, H. Alonso, M.A. Arnedo, A. Tejera, P. Martel, J.P. Bolivar</i>	<b>12:00</b> <i>Id-82</i>	Gordana Pantelic, Serbia <b>Intercomparison of radionuclide measurements in Danube sediment</b> <i>G. Pantelić, P. Vančura, Z. Ulrich, E. Weiszenburger, D. Todorović, J. Krneta Nikolić, M. Janković, M. Rajačić, N. Sarap</i>
<b>12:15</b> <i>Id-78</i>	José Ordóñez Ródenas, Spain <b>Efficiency calibration of an HPGe detector for environmental radioactivity measurements. Influence of the geometric characterization using Monte Carlo methods.</b> <i>J. Ordóñez, S. Gallardo, J. Ortiz, S. Martorell</i>	<b>12:15</b> <i>Id-83</i>	Natalia Kuzmenkova, Russia <b>Radionuclides migration pathways in the artificial reservoirs</b> <i>N.V. Kuzmenkova, I.E. Vlasova, A.K. Rozhkova, E.A. Pryakhin, S.N. Kalmykov</i>
<b>12:30</b> <i>Id-79</i>	Elena Di Stefano, Italy <b>Liquid Scintillation Counting and Gamma Ray Spectroscopy for Ice Core Dating</b> <i>E. Di Stefano, M. Clemenza, V. Maggi, B. Delmonte, G. Baccolo</i>	<b>12:30</b> <i>Id-84</i>	Denis Turchenko, Kazakhstan <b>Tritium content insnowcover of nuclear explosion venues</b> <i>D. V. Turchenko, S.N. Lukashenko, O.N. Lyakhova</i>
<b>12:45</b> <i>Id-79</i>		<b>12:15</b> <i>Id-85</i>	Jixin Qiao, Denmark <b>Environmental radioactivity and tracer studies over the past sixty years in Denmark</b> Jixin Qiao
<b>13:00-14:00</b>	Lunch		
<b>14:00-15:00</b>	Poster session 3& Coffee		
<b>PARALLEL SESSION 7 15:00-17:00</b>			
<b>SESSION 7A: SEDIMENTS AND SOILS</b> Room: Glass A Chair: S. Jerome, S. Pan		<b>SESSION 7B: RADIONUCLIDES IN BIOTA</b> Room: Amber Chair: P. Bossew, Y. Tateda	
<b>15:00</b> <i>Id-86</i>	Olga Jefanova, Lithuania <b>Cs-137 and K-40 distribution in the Neris River basin, Lithuania</b>	<b>15:00</b> <i>Id-92</i>	Ján Mihalík, Portugal <b>The role of humic acids in <sup>137</sup>Cs mobility</b> <i>J. Mihalík, J.A. Corisco and M.J. Madruga</i>



	<i>O. Jefanova, E.D. Marčiulionienė, B. Vilimaitė Šilobritienė, J. Mažeika</i>		
<b>15:15</b> Id-87	Hong-Chun Li, Taiwan <b>Variations of <math>\Delta</math> 14CTOC and Acid-leachable elemental content in a 50-cm sediment core reflecting environmental changes over 200 years in Santa Barbara Basin, CA</b> <i>H.-C. Li, Y.-W. Zhang and W.M. Berelson</i>	<b>15:15</b> Id-93	Astrid Barkleit, Germany <b>Speciation of trivalent actinides and lanthanides in digestive media</b> <i>A. Barkleit and C. Wilke</i>
<b>15:30</b> Id-88	Andra-Rada Iurian, United Kingdom <b>Application of 210Pb and 137Cs for the study of marsh accretion and sediment accumulation. Examples of salt marshes from SW England</b> <i>A.R. Iurian, G. Millward, A. Taylor, W. Marshall, W. Blake</i>	<b>15:30</b> Id-94	Tatiana Ries, Germany <b>Accumulation of <sup>137</sup>Cs by fish and aquatic plants in a small eutrophic lake</b> <i>T. Ries, V. Putyrskaya, E. Klemt</i>
<b>15:45</b> Id-89	Alua Kabdyrakova, Kazakhstan <b>Distribution of radionuclides in granulometric fractions of soil in venues of underground nuclear tests in tunnels</b> <i>A.M. Kabdyrakova, A.T. Mendubaev and S.N. Lukashenko</i>	<b>15:45</b> Id-95	Chrysoula Betsou, Greece <b>Natural and artificial radionuclides in moss samples from the region of Northern Greece</b> <i>Ch. Betsou, E. Tsakiri, J. Hansman, M. Krmar, A. Ioannidou B.</i>
<b>16:00</b> Id-90	Robert-Csaba Begy, Romania <b>Investigation of sedimentation rates and sediment dynamics in Danube Delta lake system (Romania) by <sup>210</sup>Pb dating method</b> <i>R-Cs. Begy, Sz. Kelemen, L. Preoteasa, H. Simon</i>	<b>16:00</b> Id-96	Önder Kılıç, Turkey <b><sup>210</sup>Po and <sup>210</sup>Pb in various fish species from Gökçeada island, Northern Aegean Sea and contribution of 210Po to radiation dose</b> <i>Ö. Kılıç, M. Belivermiş, O. Gönülal, and N. Sezer</i>
<b>16:15</b> Id-91	Erol Sari, Turkey <b>Sedimentation rate and heavy metal pollution in core sediments from south western Black Sea derived from <sup>210</sup>Pb and <sup>137</sup>Cs chronology</b> <i>E. Sari, M. Belivermiş, Ö. Kılıç, T. N. Arslan, N. Sezer, N. Çağatay, D. Acar, A. Tutay and M. A. Kurt</i>	<b>16:15</b> Id-97	Murat Belivermiş, Turkey <b>Impacts of ocean acidification on <sup>57</sup>Co and <sup>134</sup>Cs bioconcentration in manila clam <i>Ruditapes philippinarum</i></b> <i>O. Kocaoğlan, N. Sezer, Ö. Kılıç and M. Belivermiş</i>
<b>17:00-18:00</b>	Poster session 3 & coffee		
<b>19:00</b>	<b>GALA DINNER</b>		

Friday 02, June 2017

<b>08:30-9:30</b> PL5	<b>PLENARY SESSION V</b> Room: Glass A Chair: A. Chatt, M. Hult		
<b>08:30-09:00</b> Id-98	Stepan N. Kalmykov, Russia <b>Plutonium environmental chemistry - from molecular to landscape level</b> <i>Stepan N. Kalmykov, Anna Yu. Romanchuk</i>		
<b>09:00-09:30</b> Id-99	Irka Hajdas, Switzerland <b>Bomb peak' radiocarbon a tracer and dating tool—an overview</b> <i>I. Hajdas</i>		
<b>09:30-10:00</b> Id-100	Simon Jerome, United Kingdom <b>Findings from NPL low-level proficiency testing</b> <i>S. Jerome</i>		
<b>10:00-11:15</b> PL6	<b>PLENARY SESSION VI</b> <b>Radioecology</b> Room: Glass A Chair: I. Hajdas, G. Steinhauser		
<b>10:00-10:15</b> Id-101	Peter Bossew, Germany <b>Long-term variation of cosmic dose rate</b> <i>G. Ginelli, P. Bossew, M.A. Hernández-Ceballos, T. Tollefsen and M. De Cort</i>		

<b>10:15-10:30</b> Id-103	Robert Froeschl, Switzerland <b>Environmental impact of the CHARM facility at the CERN East Experimental Area due to stray radiation and releases of airborne radioactivity</b> <i>R. Froeschl, P. Vojtyla and F. Malacrida</i>
<b>10:30-10:45</b> Id-104	Daniela Ene, Sweden <b>Environmental impact assessment of the European Spallation Source facility</b> <i>D. Ene, R. Avila, T. Hjerpe, B. Jaeschke and K. Stenberg</i>
<b>10:45-11:00</b> Id-105	Nele Horemans, Belgium <b>Do changes in whole genome methylation play a role in adaptations of plants to chronic radiation exposure in nuclear accidental affected areas?</b> <i>N. Horemans, J. Van de Walle, E. Saenen, M. Van Hees, R. Nauts</i>
<b>11:00-11:30</b> PL7 Id-106	<b>PLENARY SESSION VII</b> <b>Closing lecture</b> Room: Glass A Chair: G. Lujanienė, P.P.Povinec  François Brechignac, <b>Radioecology supports out future by preserving ecosystem health</b> <i>F. Brechignac</i>
<b>11:30-12:00</b>	Closing Ceremony (Student award for best oral and poster presentations)

## POSTER SESSION I

<b>PS1-1</b>	Natalia Alegria, Spain <b>Benchmarking of Monte Carlo simulations for a Cerium Bromide (CeBr3) detector</b> <i>F. Legarda, and N. Alegria</i>
<b>PS1-2</b>	Asta Orentienė, Lithuania <b>Vertical distribution of Cs-137 in soil profiles in Lithuania</b> <i>A. Orentienė, L. Pilkytė, R. Kievinas, A. Bogdanovič</i>
<b>PS1-3</b>	Tatsuo Aono, Japan <b>The activities of radiocaesium in marine fishes around off Fukushima in Japan</b> <i>T. Aono, M. Fukuda, S. Yamazaki, M. Akashi, T. Sohtome, T. Mizuno, M. Yamada, A. Yamanobe</i>
<b>PS1-4</b>	Angel, VII Bautista, Philipines <b>Comparison of coral 129I and 14C as proxy for human nuclear activities, age marker, and oceanographic tracer</b> <i>A.T. Bautista VII, H. Matsuzaki, Y.S. Tshuciya, and F.P. Siringan</i>
<b>PS1-5</b>	Fernando P.Carvalho, Portugal <b>Distribution of radionuclides in coastal mussels of the coast of Portugal, Northeast Atlantic</b> <i>F. P. Carvalho, J.M. Oliveira, M. Malta</i>
<b>PS1-6</b>	Chu-Ting Yang, China <b>Separation and Analysis of Uranium in the SRM IAEA-384 and 385</b> <i>Jun Han1, Sheng Hu1 and Chu-Ting Yang</i>
<b>PS1-7</b>	Detlev Degering, Germany <b>Simulation of the time evolution of radioactive disequilibria in IAEA reference materials IAEA-410 and -412</b> <i>Detlev Degering, Diana Walther</i>
<b>PS1-8</b>	Jeong-Hee Han, Republic of Korea <b>Absorption measurements to design small radiation irradiator</b> <i>Jeong Hee Han</i>
<b>PS1-9</b>	Olga Jefanova, Lithuania <b>Tritium in surface waters of Baltic, North and Norwegian Seas in 2016</b> <i>O. Jefanova, J. Mažeika, R. Petrošius, R. Paškauskas</i>

PS1-10	Miroslav Jeskovsky, Slovakia <b>Sample preparation and AMS analysis of hydrogen isotopes at CENTA laboratory</b> <i>J. Páňík, M. Ješkovič, J. Kaizer, I. Kontuľ, P.P. Povinec</i>
PS1-11	Miroslav Jeskovsky, Slovakia <b>Anthropogenic <sup>137</sup>Cs on atmospheric aerosols in Bratislava and around Jaslovské Bohunice NPP, Slovakia</b> <i>M. Ješkovič, M. Lištjak, I. Sýkora, O. Slávik and P. P. Povinec</i>
PS1-12	Jakub Kaizer, Slovakia <b>Sequential scavenging of radiocesium and plutonium from seawater and their determination by <math>\gamma</math>-spectrometry and AMS</b> <i>J. Kaizer, M. Aoyama, J. Páňík, P.P. Povinec, I. Sýkora, Y. Tateda, F. Terrasi</i>
PS1-13	Jakub Kaizer, Slovakia <b>Development of mass spectrometry methods for determination of uranium and thorium in the <sup>82</sup>Se source of the SuperNEMO experiment</b> <i>J. Kaizer, S. Dulanská, M. Bujdoš, P.P. Povinec and O. Kochetov</i>
PS1-14	Yohan Kim, Republic of Korea <b>Adsorptive removal of strontium-90 onto ordered granular mesoporous carbon</b> <i>Yohan Kim, Jung-Hyup Lee, Sangmyeon Ahn, Heechul Choi and Jinyong Park</i>
PS1-15	Jenna Knuutinen, Finland <b>Uptake of neptunium and technetium by bacteria isolated from a nutrient-poor boreal bog</b> <i>J. Knuutinen, M. Bomberg, J. Lehto and M. Lusa</i>
PS1-16	Ivan Kontuľ, Slovakia <b>Radiocarbon in wines: a useful tracer for studying environmental processes and wine dating</b> <i>P. P. Povinec, I. Kontuľ, J. Kaizer, A. Šivo, M. Richtáriková</i>
PS1-17	Ieva Kulakauskaitė, Lithuania <b>Dependences of heavy metals sorption on nano-magnetic sorbents</b> <i>I. Kulakauskaitė, G. Lujanienė, D. Valiulis</i>
PS1-18	Hyunmi Lee, Republic of Korea <b>Accumulation of <sup>239+240</sup>Pu and <sup>210</sup>Po in the marine biota living in the seas around Korean Peninsula</b> <i>S.H. Kim, H. Lee, B.E. Cho and G.H. Hong</i>
PS1-19	Agnė Leščinskytė, Lithuania <b>Application of Prussian blue based nano-composites for radiocesium pre-concentration from seawater</b> <i>A. Leščinskytė, G. Lujanienė, S. Šemčiuk, K. Mažeika, R. Juškėnas,</i>
PS1-20	Patric Lindahl, Sweden <b>Activity profiles of <sup>226</sup>Ra and <sup>228</sup>Ra in the euphotic zone of southwestern East/Japan Sea</b> <i>P. Lindahl, M. Eriksson, Suk Hyun Kim and Gi Hoon Hong</i>
PS1-21	Galina Lujanienė, Lithuania <b>Assessment of a potential risk to biota due to long-lived radionuclides in the Baltic Sea</b> <i>G. Lujanienė, B. Šilobritienė, D. Tracevičienė, S. Šemčiuk, N. Remeikaitė-Nikienė, G. Garnaga, V. Malejevas, P.P. Povinec, A. Stankevičius</i>
PS1-22	Shaoming Pan, China <b>Distribution and source identification of the radionuclide <sup>137</sup>Cs and <sup>239+240</sup>Pu in the sediments of the Liao River estuary</b> <i>S.M. Pan, K.X. Zhang, Z.Y. Liu, Y.H. Xu</i>
PS1-23	Pavel P. Povinec, Slovakia <b>Atmospheric <sup>13</sup>CO<sub>2</sub> and <sup>14</sup>CO<sub>2</sub> concentrations in different localities of Slovakia</b> <i>A. Šivo, K. Holý, P. P. Povinec, M. Richtáriková, J. Šimon, M. Müllerová</i>
PS1-24	Carlo Sabbarese, Italy <b>Actinides measurements on environmental and structural samples of the Garigliano Nuclear Power Plant (Italy) during the decommissioning phase</b> <i>A. Petraglia, C. Sirignano, R. Buompane, F. Terrasi, A. D'Onofrio, C. Sabbarese, A. M. Esposito</i>
PS1-25	Djibo Seydou, Republic of Niger <b>Radiological Monitoring of the Environment around Niger Uranium Mine Sites of Arlit</b> <i>D. Seydou, M. M. B. Babale, Fe. P. Carvalho, J. M. Oliveira, M. Malta</i>
PS1-26	Dagmara Strumińska-Parulska, Poland

	<p><b>Is ecological food radioecological as well – 210Po and 210Pb studies</b>  <i>D.I. Strumińska-Parulska</i></p>
PS1-27	<p>Ivo Svetlik, Czech Republic  <b>Determination of 14C forms in liquid releases from nuclear power plants: the first results</b>  <i>I. Svetlik, M. Fejgl, P.P. Povinec, T. Kořínková, L. Tomášková</i></p>
PS1-28	<p>Katarzyna Szufa, Poland  <b>Lichens and mosses as primary reference organisms of Antarctic terrestrial environment – dosimetric considerations.</b>  <i>K.M. Szufa, J.W. Mietelski and A.M. Olech, Kamil Brudecki</i></p>
PS1-29	<p>Jelena Ajtic, Slovenia  <b>Beryllium-7 correlations in total deposition (dry and wet) measured in Serbia and Slovenia</b>  <i>M. Rajačić, D. Sarvan, D. Todorović, J. Ajtić, N. Krneta Nikolić, B. Zorko, B. Vodenik, D. Glavič Cindro, J. Kožar Logar</i></p>
PS1-30	<p>Bu Wenting, China  <b>Determination of 135Cs and 137Cs in environmental samples by mass spectrometry: Current states and future perspectives</b>  <i>W.T. Bu, J. Zheng and S. Hu</i></p>
PS1-31	<p>Masatoshi Yamada, Japan  <b>Particle scavenging of 239+240Pu and 230Th in the western equatorial Pacific Ocean</b>  <i>M. Yamada and J. Zheng</i></p>
PS1-32	<p>Yoon Yeol Yoon, Korea  <b>Natural Isotopes as Tracers for the Monitoring of Artificial Groundwater Recharge System</b>  <i>Yoon Yeol Yoon, Yong Cheol Kim, Kil Yong Lee, Soo Young Cho</i></p>
PS1-33	<p>Jakub Zeman, Slovakia  <b>Development of nuclear microscopy techniques for mapping concentrations of radioactive and stable elements in environmental samples</b>  <i>J. Zeman, M. Jeřkovský, J. Kaizer, P.P. Povinec, D. Ozdín</i></p>
PS1-34	<p>Zita Žukauskaitė, Lithuania  <b>Possible influence of climate warming on lake water radioactive pollution</b>  <i>Z. Žukauskaitė, B. Lukšienė, N. Tarasiuk, D. Jasinevičienė, A. Puzas</i></p>
PS1-35	<p>Francesco Cardellini, Italy  <b>Radon in Water: Italian Standard Generator and comparison of different measurement methods.</b>  <i>M. Capogni, F. Cardellini, P. De Felice, E. Chiaberto, F. Berlier, M. Faure Ragani</i></p>
PS1-36	<p>Alicja Boryło, Poland  <b>Honey as bioindicators of pollution of the environment in Poland</b>  <i>A. Boryło, G. Romańczyk, B. Skwarzec</i></p>
PS1-37	<p>Alicja Boryło, Poland  <b>Lichens as bioindicators of environmental pollution in Poland</b>  <i>A. Boryło, G. Romańczyk, B. Skwarzec</i></p>
PS1-38	<p>Alyona Yankauskas, Kazakhstan  <b>Tritium effect on the anatomical structure of the common reed (Phragmites australis)</b>  <i>A.B. Yankauskas, N.V. Larionova, A.N. Shatrov</i></p>
PS1-39	<p>Pavel P. Povinec, Slovakia  <b>Anthropogenic radionuclide variations in the European atmosphere</b>  <i>P.P. Povinec, J. Bartok, I. Bartoková, M. Jeřkovský, A. Kováčik, G. Lujanienė, J.W. Mietelski, M.K. Pham, W. Plastino, I. Sýkora</i></p>
PS1-40	<p>Paweł Krajewski, Poland  <b>Challenges in assessments of radiological impacts</b>  <i>P. M. Krajewski and G. T. Krajewska</i></p>

## POSTER SESSION II

PS2-1	<p>Eleftheria Ioannidou, Greece  <b>Heavy metals and 210Pb in Finland for the years 2000 – 2005</b></p>
-------	---



	<i>E. Ioannidou , M. Manousakas K. Eleftheriadis , J. Paatero , A. Ioannidou</i>
PS2-2	Pavol Blahušiak, Slovakia <b>Development of a 222Rn in air secondary standard</b> <i>M. Krivošík, P. Blahušiak, J. Ometáková, M. Chytil, A. Javorník, M. Zálešáková</i>
PS2-3	José Luis Guerrero, Spain <b>Behavior of natural radionuclides during a hydrological year in an estuary affected by acid mine drainage and industrial effluents in Southwest of Spain</b> <i>J.L. Guerrero, A. Hierro , M. Ollas , J.P. Bolívar</i>
PS2-4	Juan Pedro Bolívar, Spain <b>Outdoor 222Rn concentrations in a city located nearby a large phosphogypsum repository</b> <i>I. Gutiérrez-Álvarez , J.E. Martín , C. Grossi, A. Vargas, J.P. Bolívar</i>
PS2-5	Robert Breier, Slovakia <b>Monte Carlo simulation gamma spectrometry of radon in air</b> <i>R. Breier, P.P. Povinec, M. Krivošík, P. Blahušiak, J. Ometáková , A. Javorník</i>
PS2-6	Steigvilė Byčenkienė, Lithuania <b>Temporal changes of 7Be, 137Cs, 241Am and Pu isotopes activity concentrations in surface air at Lithuania</b> <i>S. Byčenkienė, G. Lujanienė, B. Šilobritienė, P.P. Povinec</i>
PS2-7	Fernando P. Carvalho, Portugal <b>Radioactive elements and stable metals in uranium mine drainage</b> <i>F. P. Carvalho, J.M. Oliveira, M. Malta, M. Santos</i>
PS2-8	Tugulan Cornel-Liviu, Romania <b>Radon Concentration estimation for the working area within the Radioactive Waste Treatment Station from Bucharest, Romania</b> <i>L.C. Tugulan, A. Chiroasca, D. Vlaicu, C. Ciobanu, F. Dragolici and G. Chiroasca</i>
PS2-9	Tugulan Cornel-Liviu, Romania <b>The contribution of the natural radionuclides to the radiological hazard at the National Radioactive Waste Repository Baita Bihor, Romania</b> <i>L. C. Tugulan, C. Ricman, F. N. Dragolici, O. G. Dului</i>
PS2-10	Tugulan Cornel-Liviu, Romania <b>Environmental dose assessment for the radionuclides embedded in building materials used in residential buildings</b> <i>L.C. Tugulan, A. Chiroasca, A. F. Miclaus, F. Dragolici, D. Vlaicu and G. Chiroasca</i>
PS2-11	Georgios Eleftheriou, Greece <b>Use of gamma spectrometry for detection of 222Rn pre-earthquake anomalies</b> <i>G. Eleftheriou, V.K. Karastathis, K. Tsinganos, M. Kafatos, T. Aspiotis, D. Ouzounov and G. Tselentis</i>
PS2-12	Rafael Garcia-Tenorio, Spain <b>210Po determination in sandy soils by alpha-particle spectrometry</b> <i>C. Bañobre, I. Diaz-Francés, A. Noguera, H. Bentos Pereira, L. Fornaro, G. Manjón and R. García-Tenorio</i>
PS2-13	Dmitri Gudkov, Ukraine <b>Dynamics of radionuclide concentration in components of the Chernobyl NPP cooling pond ecosystem during drawdown of water level</b> <i>D.I. Gudkov, S.I. Kireev, A.Ye. Kaglyan, S.M. Obrizan, A.B. Nazarov and V.V. Belyaev</i>
PS2-14	Qiuju Guo Guo, China <b>Study on the correlation of the variation of ydose rate and radon progeny in the atmosphere</b> <i>Lei Zhang , Qiuju Guo and Yunxiang Wang</i>
PS2-15	Shin-Nosuke Hashida, Japan <b>The fate of contaminated radiocesium in forest litter during fungal lignin degradation as the late stage of decomposition process</b> <i>S.N. Hashida and T. Yoshihara</i>
PS2-16	Miguel Angel Hernandez-Ceballos, Italy <b>Elaboration and use of heat maps to assess of nuclear risk</b> <i>M.A. Hernández-Ceballos , L. De Felice</i>
PS2-17	Sy Minh Tuan Hoang, Korea <b>Experimental Measurement and Indirect Assessment Methods to Determine the Natural</b>

	<b>Background Gamma Radiation Dose Rate in Urban Region</b> <i>S.M.T Hoang, D.K. Tran, Y. Truong, and N.S. Le</i>
PS2-18	Karol Holý, Slovakia <b>On the relation between outdoor 222Rn and atmospheric stability determined using a modified Turner method</b> <i>M. Bulko, K. Holý, M. Müllerová</i>
PS2-19	Alexandra Ioannidou, Greece <b>Hot particles in air filters collected in Finland immediately after the Chernobyl accident</b> <i>J. Paatero, F. Groppi, A. Ioannidou</i>
PS2-20	Peter Ivanov, United Kingdom <b>Development of a rapid radioanalytical method for quantification of low levels of Ra-226 in aqueous samples by radiochemistry separation followed by <math>\alpha</math>-spectrometry</b> <i>E. M. van Es, B. Russell, D. Read, P. Ivanov</i>
PS2-21	Dainius Jasaitis, Lithuania <b>Assessment of natural radiation exposure caused by the 222Rn progeny gamma radiation in underground parking places in Vilnius</b> <i>D. Jasaitis, M. Pečiulienė, A. Girgždys and R. Girgždienė</i>
PS2-22	Mohammad Reza Kardan, Iran <b>Assessment of External Exposure to the Public from Natural Radionuclides in Soil in Iran</b> <i>M. R. Kardan, N. Fathabadi, A. Attarilar, N. Rastkhah</i>
PS2-23	Kil Yong Lee, Korea <b>Transitions of radon from groundwater to indoor air; Shower stall model</b> <i>K.Y. Lee, K.S. Ko, S.Y. Cho, D.H. Kim, Y.Y. Yoon, D.H. Koh, K. Ha</i>
PS2-24	Leanid Maskalchuk, Belarus <b>Radioactive contamination of soils of Japan and problems of their rehabilitation</b> <i>L.N. Maskalchuk</i>
PS2-25	Hitoshi Mimura, Japan <b>Multi-Nuclide Adsorption Properties of Granulated Composite Zeolites for Fukushima Advanced Decontamination</b> <i>H. Mimura, M. Matsukura, F. Kurosaki, T. Kitagawa</i>
PS2-26	Mohamed Nadri, Algeria <b>Activity Concentration of 210 Pb, 40K, 237Cs in surface soil samples from Southern Algeria</b> <i>M. Nadri, C. Khiari, A. Iouannidou</i>
PS2-27	Naoto Nihei, Japan <b>Secondary contamination of agricultural products by resuspension of radiocesium</b> <i>N. Nihei, Y. Ohmae, K.Tanoi, H. Mukai, T. Kogure and T.M. Nakanishi</i>
PS2-28	Deivis Plaušinitis, Lithuania <b>Monitoring the concentration of actinides and lanthanides in the Chernobyl exclusion zone</b> <i>D. Plausinitis, A. Budreika, A. Karaliunas, Y. Balashevskaya, L. Bogdan</i>
PS2-29	Pavel P. Povinec, Slovakia <b>Radionuclides in tree rings from the Fukushima region</b> <i>P.P. Povinec, M. Jeřkovský, J. Kaizer, I. Kontuř, I. Šýkora, A. Šivo, X. Hou, M. Laubenstein, L. Steinnes, I. Svetlik, S. Xu</i>
PS2-30	Andrius Puzas, Lithuania <b>Radioactive Contamination Source Determination by 137Cs, 129I and Pu Isotopic Ratios and its Emission Fallout Inhomogeneity Assessment</b> <i>A. Puzas, M. Konstantinova, A. Gudelis, Ž. Ežerinskis, X. Hou, R. Gvozdaitė, J. Šapolaitė, R. Druteikienė, E. Lagzdina, D. Lingis, V. Juzikienė, V. Remeikis</i>
PS2-31	Barbara Rubel, Poland <b>Assessment of radioactive contamination of surface water and sediments in Poland in 2016</b> <i>M. Kardaś, A. Fulara, B. Rubel, M. Suplińska, E. Starościk, K.Pachocki</i>
PS2-32	Paulo Sergio Cardoso Silva, Brazil <b>Cs-137 levels in Peruíbe Black Mud: a Medicinal Clay</b> Paulo Sergio Cardoso da Silva, Renato Semmler, Guilherme Soares Zahn, Paulo Flávio de Macedo Gouveia
PS2-33	Ewa Starościk, Poland

	<b>Determination of activity concentration of <sup>234</sup>U, <sup>238</sup>U, <sup>210</sup>Po, <sup>210</sup>Pb, <sup>90</sup>Sr, <sup>134</sup>Cs and <sup>137</sup>Cs in the water from wells Oligocene in Warsaw</b> <i>E. Starościak, M. Kardaś</i>
PS2-34	Dagmara Strumińska-Parulska, Poland <b>Polonium <sup>210</sup>Po, radiolead <sup>210</sup>Pb and uranium <sup>234</sup>U, <sup>238</sup>U in mushrooms from Northern Poland</b> <i>D.I. Strumińska-Parulska, K. Szymańska, B. Skwarzec and J. Falandysz</i>
PS2-35	Dagmara Strumińska-Parulska, Poland <b>Calcium and magnesium supplements as a source of polonium <sup>210</sup>Po and radiolead <sup>210</sup>Pb</b> <i>D.I. Strumińska-Parulska and B. Skwarzec</i>
PS2-36	DE HEYN Véronique, Belgium <b>Indoor Radon in Ardenne: A multivariate analysis</b> <i>V. De Heyn, C. Licour, F. Tondeur, I. Gerardy, B. Dehandschutter, G. Ciotoli, G. Cinelli</i>
PS2-37	Jun Wen, China <b>Solvent effects in the colorimetric detection of UO<sub>2</sub><sup>2+</sup> by substituted tetraphenylethene</b> <i>J. Wen, S. Hu, X. Wang</i>
PS2-38	Uk Yun, Korea <b>Radon levels in community groundwater systems in Korea</b> <i>U. Yun, M.S. Kim, H.K. Kim, D.S. Kim, S.Y. Cho, C.O. Choo, B.W. Cho</i>
PS2-39	Pavol Vojtyla, Switzerland <b>Background of HPGe gamma spectrometers: What can particle physics tell us?</b> <i>P. Vojtyla</i>

## POSTER SESSION III

PS3-1	Medet Aktayev, Kazakhstan <b>Features tritium distribution in the waters at the semipalatinsk test site</b> <i>M.R. Aktaev, S.N. Lukashenko, A.O. Aidarkhanov</i>
PS3-2	Vladimir Abdulajev, Lithuania <b>Peculiarities of burning the graphite samples</b> <i>V. Abdulajev, A. Garbaras, E. Lagzdina, D. Lingis, J. Garankin, A. Plukis, R. Plukienė, V. Remeikis, A. Gudelis</i>
PS3-3	Natalia Alegria, Spain <b>Prediction of the spectrum for a Cerium Bromide (CeBr<sub>3</sub>) detector combining RASCAL code and Monte Carlo simulations</b> <i>F. Legarda and N. Alegria</i>
PS3-4	Zhanat Baigazinov, Kazakhstan <b>Assessment of the possibility of farm animal breeding on the Semipalatinsk nuclear test site conditions</b> <i>Zh.A. Baigazinov, S.N. Lukashenko</i>
PS3-5	Byong Wook Cho, Korea <b>Dissolved uranium and radon in groundwater of the Goesan area, Korea</b> <i>B.W. Cho, M.S. Kim, H.K. Kim, B.K. Ju, J.H. Hwang, U. Yun, C.O. Choo</i>
PS3-6	Seokwon Choi, Korea <b>Concentration factors of fish, crustacean, cephalopod molluscs macroalgae and echinoderm.</b> <i>S.W. Choia, D.J. Kim, J.S. Chae</i>
PS3-7	NGUELEM MEKONGTSO Eric Jilbert, Cameroon <b>Radiological assessment of natural radioactivity level in some sediment samples along the coastal see of Limbe-Cameroon</b> <i>E.J.M. Nguelem, M.M. Ndontchueng, A. Simo, C.J.S. Guembou</i>
PS3-8	Alexander Dario Esquivel López, Panama <b>Annual cycle of <sup>7</sup>Be in soil in a micro-watershed of Mato Frio River, (Brazil)</b> <i>A.D. Esquivel L., R.M. Moreira, J. Juri Ayub and D.L. Valladares</i>
PS3-9	Lina Gaigalaitė, Lithuania <b>Tracing the migration of radionuclides using <i>Betula pendula</i> and <i>Pinus sylvestris</i> (Lithuania)</b> <i>A. Gudelis, L. Gaigalaitė, V. Abdulajev, D. Valiulis</i>

PS3-10	Inga Gorina, Lithuania <b>Temporal variations of 210Pb in groundwater near radioactive waste repository</b> <i>I. Gorina, A. Gudelis</i>
PS3-11	Andra-Rada Iurian, Romania <b>210Pb geochronology for the assessment of historical pollutants in the touristic area of Snagov Lake, Romania</b> <i>A.R. Iurian, R.C. Begy, K. Szabolcs, H. Simon, I.M. Martonos, D. Ciobotaru, I. Dumitrascu, R.M. Margineanu</i>
PS3-12	Olga Jefanova, Lithuania <b>The distribution of tritium in the aquatic environments, Lithuania</b> <i>O. Jefanova, J. Mažeika, R. Petrošius and Ž. Skuratovič</i>
PS3-13	Irina Kamenova, Kazakhstan <b>Distribution of 241Am and 137Cs in forest soil at «plumes» of radioactive fallout</b> <i>I.N. Kamenova, N.V. Larionova, A.O. Aidarkhanov, S.N. Lukashenko</i>
PS3-14	Beibit Kenessarın, Kazakhstan <b>Transfer parameters of 137Cs and 241Am into the tissues of sheep with soils in dependence to radioactive contamination form</b> <i>B.A. Kenessarın, Zh.A. Baigazinov, S.N. Lukashenko</i>
PS3-15	Pavel Krivitskiy, Kazakhstan <b>Technique to identify ground zeros of nuclear events of the Semipalatinsk test site</b> <i>P.Ye. Krivitskiy, S.N. Lukashenko, M.A Umarov</i>
PS3-16	Yuriy Kutlakhmedov, Ukraine <b>Radionuclides as tracers for assessing the radiocapacity and reliability of ecosystems</b> <i>Yu.A. Kutlakhmedov</i>
PS3-17	Natalya Larionova, Kazakhstan <b>Artificial radionuclides in the vegetation cover at areas adjacent to Semipalatinsk test site</b> <i>N.V. Larionova, V.V. Polevik, Yu.S. Shevchenko, I.N. Kamenova, A.O. Aidarkhanov, S.N. Lukashenko</i>
PS3-18	Junghyup LEE, Korea <b>Optimized Strontium-90 Analytical Methods for Groundwater Based on Properties</b> <i>Jung-Hyup Lee, Yo-Han Kim, Yong-Jae Kim, Ju-Yong Yoon, Sung-A Yim, Kyu-Jung Chae</i>
PS3-19	Tatjana Leontieva, Belarus <b>Sorption of 137Cs on aluminosilicate sorbents based on clay-salt slimes of JSC “Belaruskali”</b> <i>T.G. Leontieva, L.N. Maskalchuk</i>
PS3-20	Oxana Lyakhova, Kazakhstan <b>Tritium research in air at the territories affected by nuclear explosions</b> <i>O.N. Lyakhova, S.N. Lukashenko, L.V. Timonova and D.V. Turchenko</i>
PS3-21	Zhongtang Wang, China <b>Method for accurate determination of ultratrace level 241Am in soil and sediment samples by SF-ICP-MS</b> <i>Z.T. Wang, J. Zheng, K. Tagami and S. Uchida</i>
PS3-22	Carmel Mothersill, Canada <b>Environmental effects of low doses of ionising radiation: How do we deal with nontargeted effects?</b> <i>C. Mothersill and C. Seymour</i>
PS3-23	Laima Nedzveckienė, Lithuania <b>Soil as a barrier determining the radionuclide transport and availability</b> <i>L. Nedzveckienė, B Lukšienė, N. Tarasiuk, R. Gvozdaitė</i>
PS3-24	Leonid Nkuba, Tanzania <b>Radioactivity levels in maize from high background radiation areas and dose estimates for the public in Tanzania</b> <i>L. Nkuba, Y. Sungita</i>
PS3-25	Andrey Panitskiy, Kazakhstan <b>Radionuclides in Bodies of Wild Animals of Semipalatinsk Test Site</b> <i>A.V. Panitskiy, S.N. Lukashenko and N.Zh. Kadyrova</i>
PS3-26	Helen Papaefthymiou, Greece <b>Spatial distribution of natural radionuclides in soils surrounding a lignite-fired power plant in</b>

	<p><b>Greece</b>  <i>H. Papaefthymiou, M. Manousakas and M. Soupioni</i></p>
PS3-27	<p>Helen Papaefthymiou, Greece  <b>Honey as an environmental indicator in Achaia (Greece)</b>  <i>M. Soupioni, A. Kaponi and H. Papaefthymiou</i></p>
PS3-28	<p>Manuel Perez-Mayo, Germany  <b>Burullus lake, Egypt: Using natural and artificial radioisotopes for a chronology</b>  <i>M. Perez-May, N. Imam, D. Pittauer, H.W. Fischer</i></p>
PS3-29	<p>Yelena Polivkina, Kazakhstan  <b>Experimental studies of specifics of 3H transport in plant by root uptake</b>  <i>Y.N. Polivkina, N.V. Larionova, O.N. Lyakhova, S.N. Lukashenko</i></p>
PS3-30	<p>Sergey Pronin, Kazakhstan  <b>Reserch tritium migration with groundwater at the balapan in the territory of the memipalatinsk test site.</b>  <i>S.S. Pronin, S. N. Lukashenko, O.N. Lyakhova, M.R. Aktayev</i></p>
PS3-31	<p>Pavol Rajec, Slovakia  <b>Determination of important radionuclides in soil samples from the Island of Mljet, Croatia</b>  <i>S. Dulanská, M.Nodilo, P.Rajec, Ľ. Mátel, Ž. Grahek, I. Tucaković</i></p>
PS3-32	<p>Alexandra Rozhkova, Russia  <b>Radionuclides distribution in the artificial reservoir biota</b>  <i>A.K. Rozhkova, N.V. Kuzmenkova, I.E.Vlasova, E.A. Pryakhin, S.N. Kalmykov</i></p>
PS3-33	<p>Barbara Rubel, Poland  <b>Analysis of the 137Cs and 90Sr content in freshwater fish from northern Poland</b>  <i>B. Rubel, M. Suplińska, K.Pachocki, M.Kardaś</i></p>
PS3-34	<p>Enrique G San Miguel, Spain  <b>Constraints in the application of 210Pb dating method in a sediment core from a reservoir affected by Acid Drainage Mine</b>  <i>E.G. San Miguel, C.R. Cánovas, J.P. Bolívar</i></p>
PS3-35	<p>Sergej Šemčuk, Lithuania  <b>Radionuclides and heavy metal removal using chitosan-graphene oxide composite</b>  <i>S. Šemčuk, G. Lujanienė, D. Valiulis, A. Leščinskytė, S. Tautkus, D. Laurinavičius</i></p>
PS3-36	<p>Zarina Serzhanova, Kazakhstan  <b>Tritium speciations in soil as a factor, characterizing migration processes</b>  <i>Z.B. Serzhanova, A.K. Aydarkhanova and S.N. Lukashenko</i></p>
PS3-37	<p>Lyubov Timonova, Kazakhstan  <b>Tritium in soils of the «Experimental Field » of Semipalatinsk Test Site</b>  <i>L.V. Timonova, O.N. Lyakhova, S.N. Lukashenko</i></p>
PS3-38	<p>Andrey Toropov, Kazakhstan  <b>Speciation of artificial radionuclides in water objects of Semipalatinsk Test Site</b>  <i>A.S. Toropov, A.K. Aidarkhanova, S.N. Lukashenko</i></p>
PS3-39	<p>Diana Tracevičienė, Lithuania  <b>239,240Pu activity concentrations in biota of the Baltic Sea</b>  <i>D. Tracevičienė, G. Lujanienė and B. Šilobritienė</i></p>
PS3-40	<p>Pavol Vojtyla, Switzerland  <b>Calculation of net doses and their characteristic limits from readings of environmental strayradiation monitors at CERN</b>  <i>P. Vojtyla and F. Malacrida</i></p>



## Sponsor Advertisements



contact@triskem.fr  
www.triskem.com

### EXTRACTION CHROMATOGRAPHIC RESINS

TrisKem International resins are manufactured under ISO 9001 and used by international accredited laboratories. We provide R&D and technical support for your separation projects.

Unique Expertise in:

Environment

Decommissioning

Radiopharmacy

Bioassay

Geochemistry

Pb-210

Sr-89/90

Fe-55

Lanthanides

Tc-99

Ra-226/8

I-129

U. Th. Pu. Am

Ni-59/63

Cl-36

H-3

C-14

 Discover our new resins at our booth:

- Direct determination of Sr and Pb in water with TK100/1 Resins
- Separation of Pa and Nb with the new TK400 Resin
- Separation of Zr with our new hydroxamate based ZR Resin

 More developpements at:

our web site [www.triskem.com](http://www.triskem.com)



## ORAL PRESENTATIONS

## "New" environmental radionuclides made accessible by Ion-Laser Interaction (ILIA)

P. Steier, J. Lachner, A. Kalb, Ch. Marek, M. Martschini, A. Priller, and R. Golser

Faculty of Physics, University of Vienna, Austria  
 Keywords: AMS, Ion-Laser Interaction, radionuclides  
 Presenting author email: peter.steier@univie.ac.at

Short lived radio-nuclides can be efficiently measured with the various methods of decay counting, however, they become increasingly inefficient for half-lives above  $10^3$  years. Mass spectrometry can circumvent this limitation by counting the nuclides directly instead of waiting for their infrequent decay. Among the mass spectrometric methods, only AMS reaches the selectivity (*abundance sensitivity*) to single out the small number of trace nuclides at typical environmental levels. The list of suitable trace nuclides with half-lives between  $10^3$  and  $\sim 10^8$  years, inaccessible by other methods, is long:  $^{10}\text{Be}$ ,  $^{14}\text{C}$ ,  $^{26}\text{Al}$ ,  $^{36}\text{Cl}$ ,  $^{41}\text{Ca}$ ,  $^{53}\text{Mn}$ ,  $^{59}\text{Ni}$ ,  $^{60}\text{Fe}$ ,  $^{79}\text{Se}$ ,  $^{93}\text{Zr}$ ,  $^{92}\text{Nb}$ ,  $^{91}\text{Nb}$ ,  $^{93}\text{Mo}$ ,  $^{94}\text{Nb}$ ,  $^{97}\text{Tc}$ ,  $^{98}\text{Tc}$ ,  $^{99}\text{Tc}$ ,  $^{107}\text{Pd}$ ,  $^{126}\text{Sn}$ ,  $^{129}\text{I}$ ,  $^{135}\text{Cs}$ ,  $^{137}\text{La}$ ,  $^{146}\text{Sm}$ ,  $^{150}\text{Gd}$ ,  $^{154}\text{Dy}$ ,  $^{166\text{m}}\text{Ho}$ ,  $^{182}\text{Hf}$ ,  $^{186\text{m}}\text{Re}$ ,  $^{202}\text{Pb}$ ,  $^{205}\text{Pb}$ ,  $^{208}\text{Bi}$ ,  $^{210}\text{Bi}$ ,  $^{226}\text{Ra}$ ,  $^{236}\text{U}$ . Like other mass spectrometric methods, traditional AMS often suffers from limited *isobar suppression* i.e. the means to suppress atoms with the same mass, but from other elements. Therefore, only ten ( $^{10}\text{Be}$ ,  $^{14}\text{C}$ ,  $^{26}\text{Al}$ ,  $^{36}\text{Cl}$ ,  $^{41}\text{Ca}$ ,  $^{53}\text{Mn}$ ,  $^{59}\text{Ni}$ ,  $^{60}\text{Fe}$ ,  $^{129}\text{I}$ ,  $^{236}\text{U}$ ) out of the 34 isotopes enumerated above are presently detectable. Waggishly spoken, AMS is presently a method suitable for a small, selected number of isotopes, which are only the fortunate cases from a much larger set.

To extend the set, an Ion-Laser InterAction (ILIA) setup was developed (Martschini et al., 2016) and connected to the AMS facility VERA (Vienna Environmental Research Accelerator). ILIA allows to slow down negatively charged ions to thermal velocities in a linear radiofrequency quadrupole (RFQ) filled with helium gas. By means of element-selective laser photodetachment of the negative ions generally used for AMS, interfering isobaric species are suppressed. The method was verified by first measurements on  $^{36}\text{Cl}^-$  and  $^{26}\text{AlO}^-$ , where for the stable isobars  $^{36}\text{S}^-$  and  $^{26}\text{MgO}^-$  suppression factors of  $10^3$  and  $10^7$ , respectively, are realized. The VERA mass spectrometer then allows further identifying trace amounts of nuclides and molecules in the cleaned beam transmitted through the ion cooler.

Previous suppression of isobaric elements by chemistry is a prerequisite for successful separation in the spectrometer. However, chemical purification is efficient only for the first orders of magnitude. Once the interfering isobar is reduced to the ppm ( $10^{-6}$ ) level, further chemical processing often reintroduces as much contamination as it removes. Nevertheless, state-of-the-art chemical purification of the sample material cannot be neglected to reach the ambitious goals set by real applications. Also the necessary extraction from the isotope of interest from the sample matrix can be challenging. Though it is difficult to predict the potential of the individual isotopes, we want to discuss possible applications at this early stage, to attract radiochemists joining the development of the new applications.

Environmental tracer studies, based on natural or anthropogenic radionuclides, will profit if they are no longer restricted to the small group of present AMS isotopes. So far,  $^{129}\text{I}$  is the only naturally occurring AMS isotope between mass 60 and 210; its successful detection relies on the coincidental inability of the atomic isobars to produce negative ions.  $^{129}\text{I}$  is produced by fission of uranium and thorium and by spallation by cosmic radiation on atmospheric xenon. Its complex

environmental behavior has however complicated environmental studies, and its volatility fostered a worldwide anthropogenic contamination with material from nuclear power production, which obscures all natural signals. If the complete list of suitable radio-nuclides is made accessible, the fission products  $^{79}\text{Se}$ ,  $^{99}\text{Tc}$ ,  $^{107}\text{Pd}$ , and  $^{135}\text{Cs}$  would be available. Some of the nuclides are produced by thermal neutron capture ( $^{79}\text{Se}$ ,  $^{93}\text{Zr}$ ,  $^{94}\text{Nb}$ ,  $^{107}\text{Pd}$ ,  $^{186\text{m}}\text{Re}$ ,  $^{205}\text{Pb}$ ,  $^{210}\text{Bi}$ ,  $^{236}\text{U}$ ), others only by fast neutrons. Both groups are expected to be abundant both from natural and anthropogenic sources in the environment, however, their abundance (and thus suitability for widespread application) is expected to vary strongly. Mainly of natural origin may be  $^{93}\text{Zr}$ ,  $^{92,94}\text{Nb}$ ,  $^{97,98}\text{Tc}$ , which can serve as a tracer for atmospheric spallation. Rare projectiles like muons, which originate mainly from cosmic rays on earth, may produce  $^{137}\text{La}$ ,  $^{146}\text{Sm}$ ,  $^{150}\text{Gd}$ ,  $^{154}\text{Dy}$ ,  $^{182}\text{Hf}$ ,  $^{202}\text{Pb}$ ,  $^{205}\text{Pb}$ , or  $^{208}\text{Bi}$ . Especially for the very long half-lives, naturally produced nuclides can accumulate over geologic time spans, and reach significant quantities.

The long-term storage of radioactive waste is considered as a main drawback of nuclear power production. Even if nuclear energy production was cancelled immediately, a significant stockpile of waste waits for safe deposition. The question of the mobility of long-lived fission products, depending on the geological setting, is a main scientific challenge. Natural stable geological sites can be considered as a model for artificial waste dumps, with already millions of years of age. Their inventory of long-lived fission products is too small to be traced with any method other than AMS. There is probably no more convincing recommendation for a storage place than that it has already been working without leakage during the last few million years.

Metamorphosis of rocks fractionates elements based on their chemical properties. If radioactive elements are involved, this starts a natural clock. Many appropriate radio-nuclides are already widely used in geology. Natural long-lived fission products made accessible by ILIA will be quickly adopted for this purpose. They will likely extend the range of datable minerals, allow for more robust results since more isotopes can be measured on the same rock, and will extend the range of available half-lives.

We are optimistic that ILIA will vastly extend the domain of application of AMS, and will allow a decade of fruitful scientific developmental work, for physicists, radiochemists, and scientists from the applied fields.

Martschini, M., Pitters, J., Moreau, T., Andersson, P., Forstner, O., Hanstorp, D., Lachner, J., Liu, Y., Priller, A., Steier, P., Golser, R., 2016. Selective laser photodetachment of intense atomic and molecular negative ion beams with the ILIAS RFQ ion beam cooler. *Int. J. Mass Spectrom.* doi: 10.1016/j.ijms.2016.12.015.

## Progress in AMS Radioisotope Analysis Using Fluoride Target Matrices

W.E. Kieser<sup>1</sup>, X-L. Zhou<sup>1</sup>, C. McDonald<sup>1</sup> and R.J. Cornett<sup>2</sup>

<sup>1</sup>A. E. Lalonde AMS Lab, and Dept of Physics, University of Ottawa, Ottawa, Ontario, K1N 6N5, Canada

<sup>2</sup>A. E. Lalonde AMS Lab and Department of Earth and Environmental Science, University of Ottawa, Ottawa, Ontario, K1N 6N5, Canada

Keywords: Fluoride matrix, metallic molecular ions, actinides, fission fragments

Presenting author email: Liam.Kieser@uOttawa.ca

We have developed new AMS techniques to measure isotopes of Tc, Pb, Ra, Th, U, Pu, Am and Cm at sub-femtogram (fg) concentrations, using fluoride anions. These techniques are also applicable to Sr and Cs isotopes when additional isobar suppression is used. These concentrations are typical of those found in the marine, freshwater, and terrestrial environments.

The requirement in Accelerator Mass Spectrometry (AMS) to use negative ions of the analyte element has been problematic for many elements, typically metals, due to their low electron binding energy and thus low formation efficiency. From early in the history of AMS, this has led to the use of molecules containing the element of interest, frequently a hydride or an oxide. For example, for the analysis of <sup>41</sup>Ca, Fink et al (1984) explored the relative advantages of using target matrices of CaH<sub>2</sub>, CaO and CaF<sub>2</sub>.

The use of these hydride, oxide and fluoride molecules for target materials has continued to the present. The hydrides produce good ion currents, but the material is quite deliquescent and so difficult to handle. The oxides are quite stable but require a high power ion source to generate useful currents. In most cases, the fluorides produce the highest currents and F has the advantage of being mono-isotopic, especially useful for the heavier elements. Many F compounds are somewhat deliquescent, but can be handled with normal ion source loading procedures.

An additional advantage was discovered by Zhao et al (2010) during their investigation of the global properties of fluoride anions. For the frequent cases in which the atomic isobar of the isotope of interest resides in a different group of the periodic table, significant levels of isobar suppression can be achieved as the isobar preferentially forms a molecular anion containing a different number of F atoms. As the most probable negative molecular anion requires one more F atom than the neutral F-containing molecule, Zhao et al found that ion currents are enhanced by the addition of an additional fluoride compound to the target matrix. In their original work, the compound PbF<sub>2</sub> was found to be very effective, especially in view of its increased electrical and possibly ionic conductivity at elevated temperatures (>250°C).

However, the measurements in the 2010 work were carried out using the General Ionex model 834 sputter ion source at the IsoTrace Laboratory. In this source the high temperature (1200°C) ionizer, used to generate the Cs<sup>+</sup> primary sputtering beam is located in a separate vacuum chamber isolated from the sample.

Attempts to use fluoride target matrices in the typical high current ion source currently used in most AMS applications were initially problematic as the targets exhibited short life times characterized by a high initial burst of current followed by its rapid diminishment. It became clear that the proximity of the 1200°C ionizer, directly in front of the target in such sources (~2-3 cm) was a factor.

Further work, summarized in Zhou et al (2016), showed that thermal effects were only one factor and that the recycling of sputtered neutral material from the target as additional sputtering ions generated by the ionizer were also involved. To mitigate both these effects, a program of target material development and exploration of ion source operating parameters was begun. Initial results of this program can be seen in the increase in CsF<sub>2</sub><sup>-</sup> current from a CsF + PbF<sub>2</sub> target matrix in Zhao et al (2016), Figures 3 and 4.

Recently, further improvements in target lifetime and current stability have been obtained by the addition of other metallic powders to the target matrix. This increases the stability of the molecular anion beams for the analysis of isotopes of lead, thorium and plutonium

This presentation will review details of the fluoride molecular anion techniques which have allowed us to measure the sub-fg concentrations of a wide range of radionuclides in environmental matrices, ranging from Arctic Ocean water samples to uranium mine tailings.

This work was supported by NSERC Canada, research contracts with Canadian Nuclear Laboratories and Health Canada. The operation of the Lalonde AMS Lab is assisted by the Canada Foundation for Innovation.

- Fink, D., Middleton, R., Klein, J. and Sharma, P., 1984, <sup>41</sup>Ca Measurement by Accelerator Mass Spectrometry and Applications, Nucl. Instr. & Methods B 5, 79-96
- Zhao, X-L, Litherland, A.E., Eliades, J., Kieser, W.E. and Liu, Q., 2010, Studies of anions from sputtering I: Survey of MF<sub>n</sub><sup>-</sup>, Nucl. Instr. & Methods B 268, 807-811
- Zhao, X-L., Charles, C.R.J., Cornett, R.J., Kieser, W.E., MacDonald, C., Kazi, Z. and St-Jean, N., 2016, An exploratory study of recycled sputtering and CsF<sub>2</sub> current enhancement for AMS, Nucl. Instr. & Methods B 366, 96-107.

## What can rapid carbon-14 excursions in the tree-ring record tell us about past “space weather” and the carbon cycle?

A J Timothy Jull<sup>1,2,3</sup>, Fusa Miyake<sup>3,4</sup>, Irina Panyushkina<sup>5</sup>, Kimiaki Masuda<sup>4</sup>, Toshio Nakamura<sup>4</sup>, Katsuhiko Kimura<sup>6</sup>, Masataka Hakozaiki<sup>7</sup>, Lukas Wacker<sup>8</sup>, Todd E. Lange<sup>2</sup>, Richard J. Cruz<sup>2</sup>, Chris Baisan<sup>5</sup>, Matthew W. Salzer<sup>5</sup>, Robert Janovics<sup>3</sup>, Katalin Hubay<sup>3</sup> and Mihály Molnár<sup>3</sup>

<sup>1</sup>Department of Geosciences, University of Arizona, Tucson, Arizona USA, <sup>2</sup>Institute for Nuclear Research, Debrecen, Hungary. <sup>3</sup>AMS Laboratory, University of Arizona, Tucson, Arizona USA. <sup>4</sup>Institute for Space-Earth Environmental Research, Nagoya University, Nagoya, Japan. <sup>5</sup>Laboratory for Tree-Ring Research, University of Arizona, Tucson, Arizona USA. <sup>6</sup>Fukushima University, Fukushima, Japan. <sup>7</sup>National Museum of Japanese History, Sakura, Japan. <sup>8</sup>Laboratory for Ion Beam Physics, ETH-Zürich, Switzerland.

Keywords: carbon-14, tree rings, carbon cycle  
Presenting author email: jull@email.arizona.edu

A large amount of interest has been generated as a result of two <sup>14</sup>C excursions found in the Late Holocene (AD 774-775 and AD 993-994). This has been confirmed by multiple different measurements in many laboratories (Güttler et al. 2015). The most plausible cause of these events appears to be extreme Solar Proton Events (SPE), although other explanations such as gamma-ray bursts (GRB), supernovae and other more exotic explanations have been proposed. In essence, accepted explanations all require a rapid change in <sup>14</sup>C production rate from an external source. A larger event has also been reported at 5480 BC (Miyake et al. 2017a), which we attributed to a special mode of a grand solar minimum. Clearly, other events must exist. In order to detect more such events, we measured the <sup>14</sup>C contents in bristlecone pine tree rings during the periods when the <sup>14</sup>C increase rate is rapid and large in the international radiocarbon calibration curve (IntCal). Miyake et al. (2017b) looked for possible mid Holocene events (BC2479-BC2455, BC4055-BC4031, BC4465-BC4441, and BC4689-BC4681), but no significant events were discovered there. Dee et al. (2017) have also studied a number of events potentially associated with supernovae, but found no measurable effect.

We have now extended our survey to other time periods where we expect such events may be identified. We also assess whether there are different kinds of events which may be observed that are consistent with different types of solar phenomena, or other explanations. It is so far unexplored is whether other fluctuations in the atmospheric carbon exchange with other reservoirs could also generate rapid changes in the <sup>14</sup>C/<sup>12</sup>C ratio on these time scales.

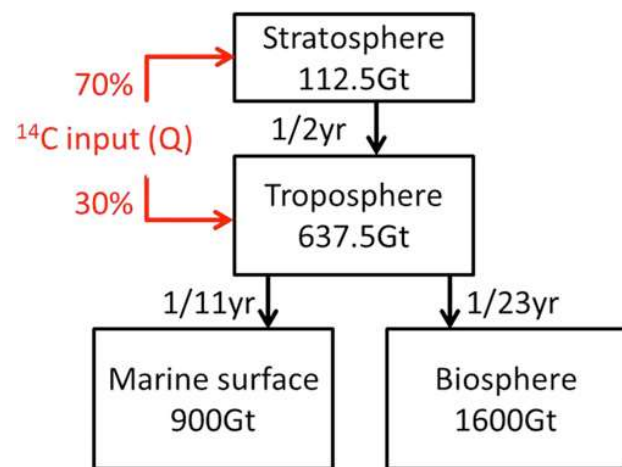


Figure 1: A greatly simplified model of the atmosphere carbon cycle. The mean exchange times between the boxes are ~ 2, 11 and 23 years respectively (Miyake et al. 2017a).

### References:

- Dee, M. et al. (2017) Radiocarbon 58 (2): in press. doi.org:10.1017/RDC.2016.50  
 Güttler D. et al. (2015) Earth Planet. Sci. Lett. 411: 290-297.  
 Miyake, F. et al. (2017a) Proc. Nat Acad. Sci. USA 114: 881-884. doi:10.1073/pnas.1613144114  
 Miyake et al. (2017b) Radiocarbon 58 (2): in press. doi: 10.1017/RDC.2016.54



## AMS studies of NPP environmental impact

F. Terrasi<sup>1</sup>

<sup>1</sup>CIRCE, Department of Mathematics and Physics, Campania University “L. Vanvitelli”, and INNOVA, 81100 Caserta (Italy)

Keywords: AMS, NPP, radiocarbon, actinides.

Presenting author email: filippo.terrasi@unicampania.it

Several Nuclear Power Plants (NPP) around the world are nowadays at - or close to - the end of their life cycle and are being, or will soon be, in the decommissioning phase. It is then important not only to assess the radiological status of the surrounding environment and of the plant structural material as a consequence of the past exercise, but also to monitor the radionuclide releases due to the decommissioning activities themselves.

In this respect, Accelerator Mass Spectrometry (AMS) plays a crucial role from several points of view. First, trees surrounding the NPP are a powerful natural archive of past <sup>14</sup>C releases in the environment. Radiocarbon measurements on tree rings around several NPP sites have been used to reconstruct the burn-up history of several reactors. A few examples of such investigations performed both at Center for Isotopic Research on the Cultural and Environmental heritage (CIRCE) and in other AMS laboratories (see e.g. Jeskovsky 2015) will be reported in the talk.

Another important contribution of AMS to the study of the environmental impact of an NPP is given by the ultrasensitive detection of Actinides. The measurement of the isotopic composition of U and Pu in environmental and structural samples is a very powerful tool to gain information about their origin in different matrices (natural, weapon grade, reactor burnup, fall out). Accelerator Mass Spectrometry (AMS) has proven to be characterized by an unparalleled sensitivity for rare isotopes detection via single ion counting, while current measurements in Faraday cups are used for normalization to abundant isotopes.

At CIRCE U and Pu AMS measurements are routinely performed. The relative abundances of the different isotopes may vary by several orders of magnitude – depending on the origin of the material analyzed –, as well as the absolute yields both for rare and abundant isotopes – depending on the absolute elemental concentration. In particular, <sup>235</sup>U yield is often too low for accurate current measurements, but at the same time too intense for particle detection.

We have performed an attempt to exploit the low isotopic abundance of <sup>17</sup>O in order to reduce the yield of <sup>235</sup>U measurements down to values compatible to the maximum count rate of the final detector. Actually, as U oxides (<sup>xxx</sup>U<sup>16</sup>O<sup>-</sup>) are normally used for injection into the accelerator, <sup>235</sup>U<sup>17</sup>O<sup>-</sup> injection will result in a <sup>235</sup>U beam intensity 2.6·10<sup>3</sup> times lower with respect to normal <sup>16</sup>O molecules injection. This will provide a means to measure <sup>235</sup>U abundance by atom counting, provided a negligible UOH<sup>-</sup> molecules production takes place at the

sputtering ion source. Similar considerations hold for <sup>234</sup>U detection using <sup>234</sup>U<sup>18</sup>O injection, with a reduction factor with respect to <sup>234</sup>U<sup>16</sup>O injection of 500.

In the present paper preliminary results about the application of the above described novel methodology will be presented. In particular, <sup>234,235,236</sup>U/<sup>238</sup>U isotopic ratios and absolute concentrations, using a <sup>233</sup>U spike for normalization, were measured using several samples of different isotopic composition and relative U concentrations, showing that UOH contamination is low enough and does not affect in any case the isotopic ratio results. New results of a monitoring campaign on environmental and structural materials from the site of the Garigliano NPP (De Cesare 2013), presently being dismantled by SoGIN will be presented as well.

M. Jeřkovsky, P. P. Povinec, P. Steier, A. Šivo, M. Richtarikova, R. Golser, 2015. *Retrospective study of <sup>14</sup>C concentration in vicinity of NPP Jaslovske Bohunice using tree rings and the AMS technique*, Nuclear Instruments and Methods in Physics Research Section B, 361, 129-132.

De Cesare, M., Fifield, L.K., Sabbarese, C., Tims, S.G., De Cesare, N., D'Onofrio, A., D'Arco, A., Esposito, A.M., Petraglia, A., Roca, V., Terrasi, F. *Actinides AMS at CIRCE and <sup>236</sup>U and Pu measurements of structural and environmental samples from in and around a mothballed nuclear power plant. (2013)* Nuclear Instruments and Methods in Physics Research, Section B, 294, 152-159

## $^{233}\text{U}/^{236}\text{U}$ – A new tracer for environmental processes?

K. Hain<sup>1</sup>, P. Steier<sup>1</sup>, R. Eigl<sup>2</sup>, M. B. Froehlich<sup>3</sup>, R. Golser<sup>1</sup>, X. Hou<sup>4</sup>, J. Lachner<sup>1</sup>, J. Qiao<sup>4</sup>, F. Quinto<sup>5</sup>, A. Sakaguchi<sup>2</sup>

<sup>1</sup>Faculty of Physics, University of Vienna, Währinger Str. 17, 1090 Vienna, Austria

<sup>2</sup>Graduate School of Science, Hiroshima University, Higashi-Hiroshima, Japan

<sup>3</sup>Department of Nuclear Physics, Australian National University, Building 57, Garran Road, ACT 2601, Australia

<sup>4</sup>Center for Nuclear Technologies, Technical University of Denmark, DTU Risø Campus, 4000 Roskilde, Denmark

<sup>5</sup>Institute for Nuclear Waste Disposal, Karlsruhe Institute for Technology, Hermann-von-Helmholtz Platz 1, 76344 Eggenstein-Leopoldshafen, Germany

Keywords:  $^{233}\text{U}/^{236}\text{U}$ , AMS, Sellafield, thermonuclear weapon

Presenting author email: karin.hain@univie.ac.at

Apart from the production of  $^{236}\text{U}$  by fast neutrons in thermonuclear weapons via the reaction  $^{238}\text{U}(n,3n)^{236}\text{U}$ ,  $^{236}\text{U}$  can be also produced in nuclear power plants and fission bombs via  $^{235}\text{U}(n,\gamma)^{236}\text{U}$  using thermal neutrons. In contrast, the principle production path for  $^{233}\text{U}$  is via the reaction  $^{235}\text{U}(n,3n)^{233}\text{U}$ , which requires fast neutrons with energies above 13 MeV (Gorbachev et al, 1980). Therefore, an increased production can be expected in thermonuclear weapons using Orallo (uranium enriched in  $^{235}\text{U}$ ) as blanket or tamper. Consequently, in average, fallout from nuclear weapons testings should show a higher  $^{233}\text{U}/^{236}\text{U}$  ratio than emissions from thermal nuclear power plants or reprocessing plants which allows source identification for contaminations present in the environment.

However, the cross section of the reaction  $^{235}\text{U}(n,3n)^{233}\text{U}$  for 14 MeV neutrons is only about 0.1 barn, as shown in Figure 1. As there is only little experimental data available for the cross-section of this reaction and the utilization of Orallo is not readily accessible for all nuclear devices which exploded during the period of atmospheric testing, the  $^{233}\text{U}$  fallout from thermonuclear weapons can be only roughly estimated to be around one to two orders of magnitude smaller than  $^{236}\text{U}$  fallout. Consequently, neglecting n capture on  $^{232}\text{Th}$  in rocks and local contaminations from the  $^{232}\text{Th}$  fuel cycle, the environmental concentrations of  $^{233}\text{U}$  can be expected to be extremely low, so that its detection is challenging also for the highly sensitive Accelerator Mass Spectrometry (AMS).

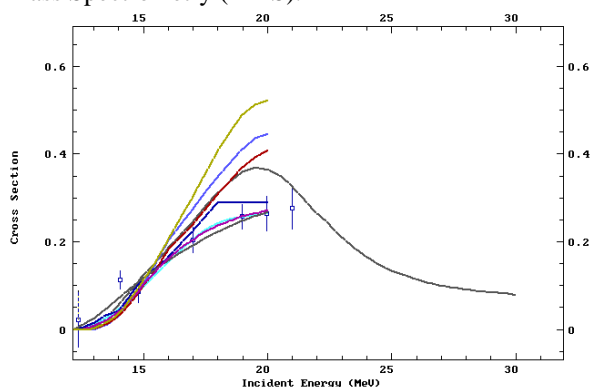


Figure 1. Cross section in barn for the reaction  $^{235}\text{U}(n,3n)^{233}\text{U}$  from model calculations (solid lines) and experimental data (blue squares) (EXFOR/ENDF, 2016)

$^{236}\text{U}$  in environmental samples is already routinely analysed at the Vienna Environmental Research Laboratory (VERA) (e.g. Froehlich et al, 2016). VERA has recently increased its detection efficiency such that it

is now capable to detect also  $^{233}\text{U}$ , which was demonstrated by analysing the concentration of this isotope in different types of environmental sampling material, including Irish Sea sediment, corals from the Pacific Ocean and peat bog samples from Germany. These samples were known to be affected by different contamination sources, i.e. nuclear weapons fallout and the reprocessing plant Sellafield, respectively. In average, the detected  $^{233}\text{U}/^{236}\text{U}$  ratio in the environment is at a level of around 1%. However, the  $^{233}\text{U}/^{236}\text{U}$  ratio in the Irish Sea sediments was around one order of magnitude lower than in the Pacific Ocean corals or the peat bog samples. These findings indicate that the  $^{233}\text{U}/^{236}\text{U}$  can be indeed used for the discrimination between these two contamination sources.

In contrast to Pu, whose isotopic ratios have been successfully used for source identification in the past (Lindahl et al, 2010), uranium shows a considerably higher solubility, and thus, a conservative behaviour in water so that it can be transported over large distances (Sakaguchi et al. 2012). Being isotopes of the same element, the  $^{233}\text{U}/^{236}\text{U}$  ratio is independent from the chemical behaviour in the environment as well as during sample preparation which significantly facilitates the interpretation of the measured data. For these reasons, the  $^{233}\text{U}/^{236}\text{U}$  ratio could serve as a powerful tracer for environmental processes when the principle contamination sources will have been characterized.

After an introduction to possible production paths of  $^{233}\text{U}$  and  $^{236}\text{U}$ , respectively, first results of the  $^{233}\text{U}/^{236}\text{U}$  ratio detected in samples from the different environmental reservoirs named before will be presented in this talk and the interpretation of the data will be discussed.

Gorbachev, V. M., et al. 1980. Nuclear Reactions in Heavy Elements, Pergamon Press, 1<sup>st</sup> edition  
EXFOR/ENDF database, 2016

[www-nds.iaea.org/exfor/servlet/X4sMakeX4](http://www-nds.iaea.org/exfor/servlet/X4sMakeX4)

M.B. Froehlich, et al. 2016. European roe deer antlers as an environmental archive for fallout U-236 and Pu-239. J. Environ. Radioact. 151, 587-592

Sakaguchi, A., et al. 2012. Uranium-236 as a new oceanic tracer: A first depth profile in the Japan Sea and comparison with caesium-137, Earth Planet. Sci. Lett., 333-334, 165–170

Lindahl, P., et al. 2010. Plutonium isotopes as tracers for ocean processes: A review. Mar. Environ. Res., 69, 73-84.

## Investigating the long-term behaviour of actinides in repository relevant conditions with the multi-actinides analysis and AMS

F. Quinto<sup>1</sup>, F. Geyer<sup>1</sup>, M. Lagos<sup>1</sup>, M. Plaschke<sup>1</sup>, T. Schäfer<sup>1</sup>, P. Steier<sup>2</sup> and H. Geckeis<sup>1</sup>

<sup>1</sup>Institut für Nukleare Entsorgung, Karlsruher Institut für Technologie, Hermann-von-Helmholtz-Platz 1, 76344 Eggenstein-Leopoldshafen, Germany

<sup>2</sup>VERA Laboratory, Faculty of Physics, University of Vienna, Währinger Straße 17, 1090 Vienna, Austria

Keywords: Accelerator Mass Spectrometry, actinides, *in situ* tracer test, geological disposal of nuclear waste.

Presenting author email: francesca.quinto@kit.edu

Laboratory and field experiments focusing on the geochemical behavior of the actinides provide relevant data for the evaluation of the safety of deep geological disposal of nuclear waste.

At the Grimsel Test Site (GTS) in Switzerland, several *in situ* radionuclide tracer tests were carried out (<http://www.grimsel.com/gts-phase-vi/cfm-section>). In these field experiments, actinide nuclides and bentonite colloids in a matrix of Grimsel groundwater were injected into a dipole of a water conducting granodiorite fracture.

Groundwater samples were collected continuously at the extraction point of the dipole and in the most recent *in situ* tests, run 12-02 and run 13-05, analyzed with sector field inductively plasma mass spectrometry (SF-ICPMS) and accelerator mass spectrometry (AMS) in order to determine the concentration of the eluted actinides. SF-ICPMS and AMS were employed as complementary analytical techniques: the first one providing an accurate description of the breakthrough curve above the detection limits (DL) of ca. 0.01 pg/g and the second one allowing for the determination of actinides far below the abovementioned DL and down to 10<sup>-7</sup> pg/g, as depicted in Figure 1.

In the actual contribution, we will present an overview of the *in situ* radionuclide tracer experiments performed at the GTS as well as the recent results obtained with AMS. We will describe the analytical method that was for this purpose developed (Quinto et al., 2015) and allowed for the investigation of the migration and retention of U(VI), Pu(IV), Am(III) and Np(V) in the granodiorite shear zone of the GTS in presence of bentonite colloids. In particular, in the frame of the radionuclide tracer test run 13-05 that took place in 2013, the behavior of the injected actinide nuclides, <sup>233</sup>U, <sup>237</sup>Np, <sup>242</sup>Pu and <sup>243</sup>Am, could have been investigated until 660 days from the start of the experiment. Furthermore, the determination in the groundwater samples of run 13-05 of <sup>241</sup>Am and <sup>244</sup>Pu, nuclides exclusively employed as tracers in a previous *in situ* experiment that took place in 2002 (Geckeis et al., 2004), paves the way to the capability of studying the actinides behavior for a time span of several years.

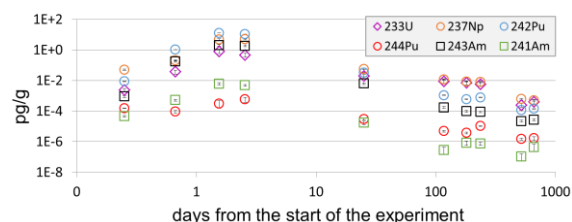


Figure 1. Concentrations expressed in pg/g of <sup>233</sup>U (violet rhombuses), <sup>237</sup>Np (orange circles), <sup>242</sup>Pu (blue circles), <sup>244</sup>Pu (red circles), <sup>243</sup>Am (black squares) and <sup>241</sup>Am (green squares) determined with AMS in chosen samples of the *in situ* tracer test run 13-05.

This work is funded by the Federal Ministry of Economics and Technology (BMWi) under the joint KIT INE, GRS research project “KOLLORADO-e2”, grants No. FKZ 02 E 11456 A. Furthermore, the authors would like to acknowledge the support of the CFM Project partners and the support of the local Grimsel Test Site/NAGRA staff.

<http://www.grimsel.com/gts-phase-vi/cfm-section>.

Quinto, F., Golser, R., Lagos, M., Plaschke, M., Schäfer, T., Steier, P., Geckeis, H. 2015. Accelerator Mass Spectrometry of Actinides in Ground- and Seawater: An Innovative Method Allowing for the Simultaneous Analysis of U, Np, Pu, Am and Cm Isotopes below ppq Levels. *Anal. Chem.* 2, 87 (11), 5766-73.

Geckeis, H., Schäfer, T., Hauser, W., Rabung, Th., Missana, T., Degueldre, C., Möri, A., Eikenberg, J., Fierz, Th., Alexander, W. R. 2004. Results of the colloid and radionuclide retention experiment (CRR) at the Grimsel Test Site (GTS), Switzerland – impact of reaction kinetics and speciation on radionuclide migration. *Radiochim. Acta.* 92, 765-774.

## Preliminary study of AlN targets for accelerator mass spectrometry

M. Ješkovský<sup>1</sup>, J. Pánik<sup>1</sup>, J. Kaizer<sup>1</sup>, P. Steier<sup>2</sup> and P. P. Povinec<sup>1</sup>

Center for Nuclear and Accelerator Technologies (CENTA), Faculty of Mathematics, Physics and Informatics, Comenius University, Bratislava, 84248, Slovakia

<sup>2</sup>VERA Laboratory, Faculty of Physics, University of Vienna, 1090 Vienna, Austria

Keywords: accelerator mass spectrometry, AlN, <sup>26</sup>Al

Presenting author email: jeskovsky@fmph.uniba.sk

<sup>26</sup>Al is a cosmogenic radionuclide which is produced by cosmic rays in terrestrial and extra-terrestrial matter. Therefore it can be used e.g. for environmental, geophysical, astrophysical and biomedical applications. It is a radioactive isotope of aluminium, decaying to <sup>26</sup>Mg with half-life of  $7.17 \times 10^5$  years. In higher concentrations it can be analysed by gamma-spectrometry by searching for the 1.809 MeV  $\gamma$ -line, however in many applications much lower concentrations or much smaller samples have to be analysed. Therefore accelerator mass spectrometry (AMS) technique is frequently used for analysis down to  $10^{-17}$  g of <sup>26</sup>Al. As far as main isobar <sup>26</sup>Mg does not form negative ions, many AMS laboratories use <sup>26</sup>Al<sup>-</sup> as injection ion for acceleration. It is well known, that aluminum does not yield high intensity negative ion beam, like other AMS elements. In most cases Al<sub>2</sub>O<sub>3</sub> is used in the ion source for production of aluminium negative ions because of high temperature stability, non-toxicity, in-air stability and a relative easy production from geological and biological samples. Another alternative is using AlN as target material, that can yield higher Al<sup>-</sup> currents but it is more difficult to synthesize and it decompose with water in air to form Al(OH)<sub>3</sub> and ammonia. However, several authors tested production of Al<sup>-</sup> and AlN<sup>-</sup> from AlN (Flarend et al., 2004, Janzen et al., 2015) and the ionization yields seems promising.

In this work, we tested possibility to use AlN<sup>-</sup> as an injection for <sup>26</sup>Al AMS measurements. Commercial available compounds of Al<sub>2</sub>O<sub>3</sub> and AlN were used for the mixtures with copper, silver and iron high purity powders and sputtered in MC-SNICS ion source for studying ionization yields. Mass spectrum of one AlN sample mixed with Ag powder in the 2:1 ratio is shown in Figure 1. Since production of magnesium and nitrogen negative ions is negligible, the production of MgN<sup>-</sup> molecule is questionable. Therefore preliminary tests of the formation of MgN<sup>-</sup> molecule were done at the CENTA laboratory (Povinec et al., 2015). The results of the MgN and AlN compounds AMS analyses in VERA laboratory will be discussed.

This work was supported by the EU Research and Development Operational Program funded by the ERDF (project No. 26240220004), and by the International Atomic Energy Agency (TC project SLR9013).

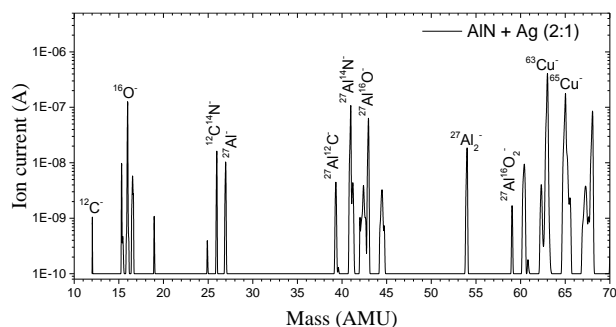


Figure 1. Low energy mass spectrum of AlN+Ag mixture from MC-SNICS ion source.

- Flarend, R., Hasan, M.E., Reed, C.S., 2004. Aluminum nitride as a novel aluminum-26 ion source material for accelerator mass spectrometry. Nucl. Instr. Meth. Phys. Res. B 223–224, 263–266.
- Janzen, M.S., Galindo-Uribarri, A., Liu, Y., Mills, G.D., Romero-Romero, E., Stracener, D.W., 2015. The use of aluminum nitride to improve Aluminum-26 Accelerator Mass Spectrometry measurements and production of Radioactive Ion Beams. Nucl. Instr. Meth. Phys. Res. B 361, 281–287.
- Povinec, P.P., Masarik, J., Kúš, P., Holý, K., Ješkovský, M., Breier, R., Staniček, J., Šivo, A., Richtáriková, M., Kováčik, A., Szarka, J., Steier, P., Priller, A., 2015. A new IBA-AMS laboratory at the Comenius University in Bratislava (Slovakia). Nucl. Instr. Meth. Phys. Res. B 342, 321–326.

## Dating in Romanian archaeology: comparison between radiocarbon and dendrochronology methods spanning over the last 1000 years

T. Sava<sup>1</sup>, I. Popa<sup>2</sup>, G. Sava<sup>1</sup>, A. Ion<sup>3</sup>, M. Ilie<sup>1</sup>, I. Stanciu<sup>1</sup>, C. Simion<sup>1</sup>, B. Ștefan<sup>1</sup>, O. Gâza<sup>1</sup> and D. Păceșilă<sup>1</sup>

<sup>1</sup>RoAMS Laboratory, Horia Hulubei National Institute for Physics and Nuclear Engineering, Măgurele, Ilfov, 077125, Romania

<sup>2</sup>Marina Dracea National Institute for Research and Development in Forestry, Câmpulung Moldovenesc, Suceava, 725100, Romania

<sup>3</sup>Faculty of Applied Chemistry and Material Science, University Politehnica of Bucharest, Bucharest, 060042, Romania

Keywords: tree rings radiocarbon dating, dendrochronology, wiggle match, calibration curve.

Presenting author email: tiberiu.sava@nipne.ro

At the RoAMS laboratory in Bucharest we have looked for a head-to-head meeting between AMS radiocarbon dating and dendrochronology methods, aiming to point out and explain any differences or similarities that might appear between their output results. As subject for this investigation we have fixed our attention on a sequence of tree rings spanning on last almost 1000 years. The sample were collected from the northern Romanian territory within Moldavia region and were provided by the “Marin Dracea - National Institute for Research and Development in Forestry”. The 25 samples were radiocarbon dated using alpha-cellulose extraction, followed by graphitization in an AGE3® [1] installation and subsequently AMS measurement within a 1 MV Tandetron® [2].

The results are showing good agreement at a large scale, even though, some differences were present in the analysis. The reasons for this behavior are explained in our paper.

### References

- [1] Nemeș M. et al., 2010, Optimization of the graphitization process at AGE-1, Radiocarbon 52(3):1380-1393.
- [2] Stan-Sion C. et al., 2014. A new AMS facility based on Cockcroft-Walton type 1MV Tandetron at IFIN-HH Magurele, Romania. 2014. NIM B 319, 117-122.



## Marine environmental radioactivity off Namibia's coast

M.Rozmaric<sup>1</sup>, D.C. Louw<sup>2</sup>, I. Osvath<sup>1</sup>, O. Blinova<sup>1</sup>, I. Levy<sup>1</sup>, M.K. Pham<sup>1</sup>, P. McGinnity<sup>1</sup>, M. Fujak<sup>1</sup>, J. Bartocci<sup>1</sup>, S.B. Mudumbi<sup>3</sup>, T.K.S. Kahunda<sup>2</sup>, K. Grobler<sup>2</sup>, E. Chamizo<sup>4</sup>, M. Lopez<sup>4</sup>, J.M. Lopez-Gutierrez<sup>4</sup>, R. Garcia Tenorio<sup>4</sup> and Lj. Benedik<sup>5</sup>

<sup>1</sup>International Atomic Energy Agency, Environment Laboratories (IAEA, NAEL), Monaco, MC 98000 Monaco

<sup>2</sup>Ministry of Fisheries and Marine Resources (MFMR), National Marine Information and Research Centre (NatMIRC), Swakopmund/Lüderitz, Namibia

<sup>3</sup>National Commission on Research Science and Technology (NCRST), Windhoek, Namibia

<sup>4</sup>Centro Nacional de Aceleradores (CNA), Universidad de Sevilla, Seville, 41092, Spain

<sup>5</sup>Jozef Stefan Institute, Ljubljana, 1000, Slovenia

Keywords: marine radioactivity, baseline study, natural and anthropogenic radionuclides, Namibia.

Presenting author email: M.Rozmaric@iaea.org

The International Atomic Energy Agency's Environment Laboratories in Monaco (IAEA, NAEL) are supporting Member States (MSs) in understanding the marine environment by applying isotopic and nuclear techniques. In this context NAEL may take part in scientific cruises with the aim to assist MSs in marine radioactivity monitoring and assessment.

The Ministry of Fisheries and Marine Resources in Namibia requested the IAEA NAEL to participate in a scientific sampling expedition on the R/V Mirabilis in May 2014 during a regular monthly oceanography monitoring survey along the Namibian coast. The main aim of the collaboration was to establish a baseline of marine radioactivity levels and to provide assistance to Namibia to set up a future marine radioactivity monitoring programme.

The Namibian coastline is approximately 1500 km long and is in a large proportion a marine protected area, considered as fairly unpolluted. The Namibian marine environment is part of the northern Benguela large marine ecosystem (BCLME), which is one of the most productive coastal ecosystems in the world and supports valuable fisheries and mariculture industries. Diamond mining, close to the southern border, is currently the only seabed mining activity. However, during the last decade, mining explorations for phosphate, petroleum and gas have increased and two existing harbours, Walvis Bay and Lüderitz, expanded. Namibia is one of the five leading countries in uranium mining and one of the countries with the largest proportion of uranium mines close to the coast, which might be an additional concern for the local population. The coastal population has increased and continuous growth of population in coastal cities is further expected. Therefore, Namibia needs regulations and a baseline study of marine radioactivity levels may assist to establish these regulations for any new coastal development, mining activity or sources of pollution.

During the two weeks' scientific survey, 20 seawater and approximately 450 sediment samples were collected at in-shore and off-shore stations along the Namibian coast (Figure 1). In addition, 22 biota (fish and mussels) and 22 seaweed (kelp and ulva) samples were collected close

to the three main coastal towns: Swakopmund, Walvis Bay and Lüderitz.

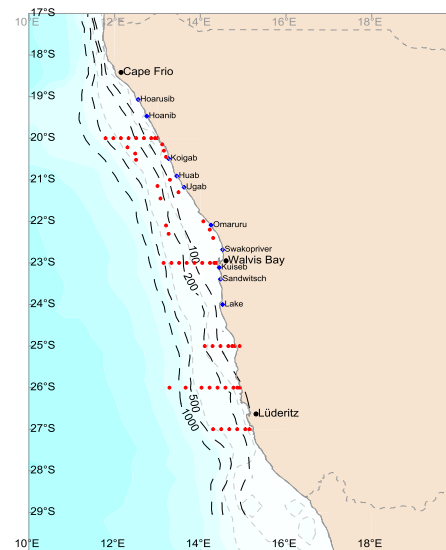


Figure 1: Sampling map showing the two coastal harbour towns (Walvis Bay and Lüderitz) and main dry rivers.

Natural (Po-210, Pb-210, radium and uranium isotopes) and anthropogenic (H-3, Sr-90, I-129, Cs-137, U-236 and Pu isotopes) radionuclides were determined by using different analytical techniques (alpha and gamma spectrometry, LSC, gas proportional counting and accelerator mass spectrometry) at the IAEA's Environment Laboratories in Monaco, the IAEA's Collaborating Centre the "Centro Nacional de Aceleradores" in Seville, Spain and Jozef Stefan Institute in Ljubljana, Slovenia.

The first results on the distribution of natural and anthropogenic radionuclides in marine environment of Namibia obtained within the project on baseline study of radioactivity levels will be presented in this paper.

This work was supported by the IAEA, NAEL Monaco and the Ministry of Fisheries and Marine Resources (MFMR), Namibia

## Plutonium in Bismarck Sea sediments: South vs. North Pacific Signals

D. Pittauer<sup>1,2</sup>, P. Roos<sup>3</sup>, J. Qiao<sup>3</sup>, W. Geibert<sup>4</sup> and H.W. Fischer<sup>2</sup>

<sup>1</sup>MARUM – Center for Marine Environmental Sciences, University of Bremen, Germany

<sup>2</sup>Institute of Environmental Physics, University of Bremen, Germany

<sup>3</sup>Center for Nuclear Technologies, Technical University of Denmark, Roskilde, Denmark

<sup>4</sup>Alfred Wegener Institute for Polar and Marine Research, Bremerhaven, Germany

Keywords: French Polynesia, Pacific Proving Grounds, ocean transport, radionuclides in sediments.

Presenting author email: dpittauer@marum.de

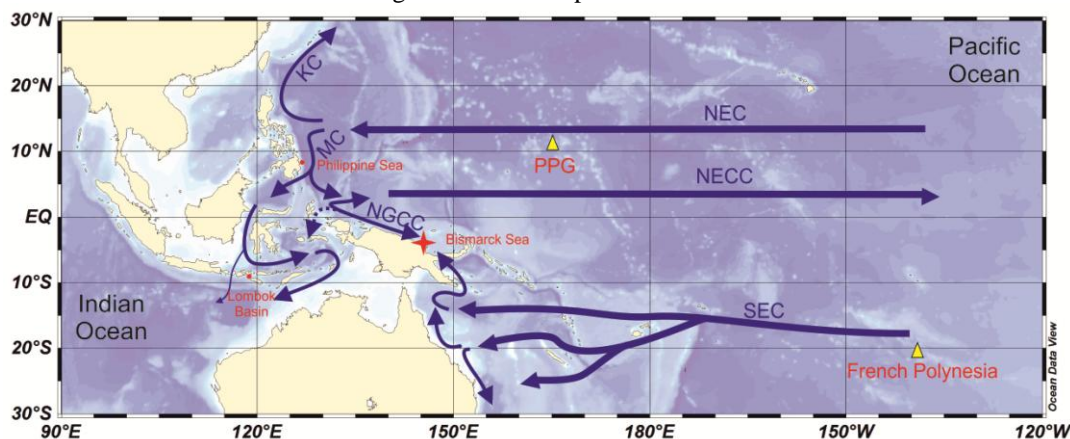


Figure 1. Study site located in the Bismarck Sea (star). Acronyms: North Equatorial Current (NEC), Kuroshio Current (KC), Mindanao Current (MC), North Equatorial Countercurrent (NECC), New Guinea Coastal Current (NGCC), South Equatorial Current (SEC), Pacific Proving Grounds (PPG).

Several major sources of anthropogenic radionuclides have contributed to radioactivity of the West equatorial Pacific Ocean. The global fallout, the omnipresent reminder of the Cold War atmospheric nuclear weapons testing, is one of the important constituents. Other major regional sources are nuclear weapon tests at the U.S. test sites at atolls Bikini and Enewetak (Pacific Proving Grounds, PPG) and at the French nuclear test sites Mururoa and Fangataufa (French Polynesia). An additional contribution arises from the 1964 satellite SNAP-9A burn up in the atmosphere, releasing <sup>238</sup>Pu from a thermoelectric generator.

Recently, it was shown that PPG plutonium is transported not only northwards via the Kuroshio Current (e.g. Lee et al., 2004, Zheng and Yamada, 2004, Wu et al. 2014), but also towards the south with the Mindanao Current, as recorded in a Philippine Sea sediment core (Pittauer et al., in prep.). It is further transported through the Indonesian archipelago towards the Indian Ocean, as demonstrated in a sediment core from Lombok Basin (Pittauer et al., submitted). The aim of our research is to evaluate the sources of plutonium in another area, where anthropogenic radionuclides have not been studied before: Bismarck Sea, off Papua New Guinea. This site potentially receives water masses from both North and South Pacific Ocean. The presented results are based on a deep sea sediment core taken in 2013.

We have analysed natural and artificial radionuclides (<sup>137</sup>Cs, <sup>241</sup>Am and plutonium isotopes) in the sediment core by means of HPGe gamma spectrometry, alpha spectrometry, as well as ICP-MS.

The age model based on <sup>210</sup>Pb shows, that the study site provides a high resolution archive of anthropocene marine deposition. The <sup>238</sup>Pu/<sup>239+240</sup>Pu activity ratios and <sup>240</sup>Pu/<sup>239</sup>Pu atom ratios provide a basis for quantifying contributions of individual sources of anthropogenic radionuclides and evaluating their depositional histories.

This study was funded through DFG-Research Center/Cluster of Excellence “The Ocean in the Earth System.” The authors appreciate the sediment sampling performed by the crew and the scientific party of SONNE 228 cruise.

### References

- Lee, S. Y., Huh, C. A., Su, C. C., You, C. F., 2004. Sedimentation in the Southern Okinawa Trough: enhanced particle scavenging and teleconnection between the Equatorial Pacific and western Pacific margins Deep-Sea Res. Pt I. 51, 1769–1780.
- Pittauer, D., Tims, S., Froehlich, M., Fifield, K., Wallner, A., McNeil, S., Fischer, H. W. Continuous transport of Pacific-derived anthropogenic radionuclides towards the Indian Ocean. Sci. Rep., Submitted.
- Wu, J., Zheng, J., Dai, M., Huh, C., Chen, W., Tagami, K., Uchida, S., 2014. Isotopic composition and distribution of plutonium in northern South China Sea sediments revealed continuous release and transport of Pu from the Marshall Islands. Environ. Sci. Technol. 48, 3136–3144.
- Zheng, J., Yamada, M., 2004. Sediment core record of global fallout and Bikini close-in fallout Pu in Sagami Bay, Western Northwest Pacific margin. Environ. Sci. Technol. 38, 3498–3504.

## $^{241}\text{Pu}/^{239+240}\text{Pu}$ ratio in Antarctic marine and terrestrial samples

K. M. Szufa<sup>1</sup>, T. Mróz<sup>2</sup>, J. W. Mietelski<sup>1</sup>, K. Sobiech-Matura<sup>3,\*</sup>, P. Gaca<sup>4</sup>, M.A. Olech<sup>3,5</sup>

<sup>1</sup>Institute of Nuclear Physics, Polish Academy of Sciences, Krakow Poland

<sup>2</sup>Pedagogical University, Krakow, Poland

<sup>3</sup>Institute of Botany, Jagiellonian University, Krakow, Poland

<sup>4</sup>Oceanic Center, Southampton University, Southampton, UK

<sup>5</sup> Institute of Biochemistry and Biophysics, Polish Academy of Sciences, Department of Antarctic Biology, Warsaw, Poland.

**Keywords:** radioactivity in Antarctic, plutonium,  $^{241}\text{Pu}$ , alpha spectrometry

**Presenting author email:** jerzy.mietelski@ifj.edu.pl

$^{241}\text{Pu}$  is beta emitter with half life time of 14.35 years. It decays to long lived  $^{241}\text{Am}$  (half live time 432 years), which is alpha and gamma emitter. The beta radiation emitted by  $^{241}\text{Pu}$  is of low energy (21.5 keV at maximum). It can be measured directly by LSC counting using  $^3\text{H}$  protocol. However, it can be measured also non directly, via ingrown of  $^{241}\text{Am}$  in old Pu alpha spectrometric sources. Both techniques were applied many years ago for samples from Poland (Mietelski et al, 1999). During last twenty years various environmental samples (both marine and terrestrial) collected in Antarctic environment (mostly Southern Shetlands and Antarctic Peninsula) were analysed for plutonium alpha emitters in our laboratory (IFJ PAN, Krakow Poland). Fifty eight preserved alpha sources (including blanks) prepared in years 2003-2008 (Mietelski et al. 2008, Sobiech-Matura, 2011) were re-measured in 2015 to find any ingrown of  $^{241}\text{Am}$ . In all those samples original Pu analyses were performed using  $^{242}\text{Pu}$  tracer. Therefore the other then  $^{241}\text{Am}$  decay products were not a problem. Blanks were used to control any  $^{241}\text{Am}$  ingrown from possible  $^{241}\text{Pu}$  impurities in  $^{242}\text{Pu}$  tracer. Additional eight sources from studies conducted in years 1997-1998 (Mietelski et al., 2000), when  $^{236}\text{Pu}$  was used could not be analysed this way due to presence of many other decay products. This tracer decays to  $^{232}\text{U}$  and subsequently to his progenies:  $^{228}\text{Th}$  plus all short lived isotopes from his decay. Those  $\text{NdF}_3$  alpha sources were dismounted. Removed filters were dissolved. To each sample tracer  $^{243}\text{Am}$  was added and Am fraction was separated using conventional method on Dowex 1 in methanol-acid solutions to measure it using alpha spectrometer.

In about 10% of samples the ingrown of  $^{241}\text{Am}$  was sufficient to calculate original  $^{241}\text{Pu}$  level. Project is not finished yet, the final results will be presented during Conference.

Mietelski, J.W., Dorda J., Wąs B., Pu-241 in samples of forest soli from Poland, *Applied Radiation and Isotopes*, 51 (4), 1999, 435-447

Mietelski J.W., Gaca P., Olech M. A., Radioactive contamination of lichens and mosses collected in South Shetlands and Antarctic Peninsula, *Journal of*

\* current affiliation: European Commission Joint Research Centre, Geel, Belgium

*Radioanalytical and Nuclear Chemistry*, 245 (3), 2000, 527-535.

Mietelski J.W., Olech M.A., Sobiech K., Gaca P., Zwolak M., Błażej S., Tomankiewicz E.  $^{137}\text{Cs}$ ,  $^{40}\text{K}$ ,  $^{238}\text{Pu}$ ,  $^{239+240}\text{Pu}$  and  $^{90}\text{Sr}$  in biological samples from King George Island (Southern Shetlands) in Antarctica. *Polar Biology*, 31 (9), 2008, 1081-1091.

Sobiech-Matura K., Badania poziomów skażeń radioaktywnych w lądowych i morskich ekosystemach Antarktyki, Jagiellonian University, 2011 (PhD thesis)

## Chronological records of metal contamination at two mining areas using sediment profiles

F.K. Pappa<sup>1,2</sup>, C. Tsabaris<sup>1</sup>, D.L. Patiris<sup>1</sup>, E.G. Androutakaki<sup>1,2</sup>, A. Ioannidou<sup>3</sup>, M. Kokkoris<sup>2</sup>, R. Vlastou<sup>2</sup>

<sup>1</sup>Institute of Oceanography, Hellenic Centre of Marine Research, Anavyssos, Attiki, 19013, Greece

<sup>2</sup>Department of Physics, National Technical University of Athens, Zografou, Athens, 15780, Greece

<sup>3</sup>Department of Physics, Aristotle University of Thessaloniki, Thessaloniki, 54124, Greece

Keywords: metal mines, sediment core, dating methods, radionuclides

Presenting author email: fkpappa@hcmr.gr

Radionuclide and heavy metal pollutants in the marine environment are important for protection issues and are used as tracers in environmental applications and studies. Additionally, sediments due to their adsorption capabilities contribute in accumulation and transportation processes and reflect the impact of human activities. Sediment profiles have been used in literature to assess the accumulation and pollution of metals, to describe the environmental conditions of the past and to investigate the contamination history of different areas (Vallette-Silver, 1993). Although heavy metal and radionuclide concentrations in sediment cores have been studied in many regions, there are very few well-documented studies in the marine environment near mining areas.

In general, mines are situated in the proximity of ecologically vulnerable areas. The ecological impact due to the mining wastes, either from accidents (Riba, 2002) or from waste disposals (Panagopoulos et al., 2009; Wang et al., 2015; Pappa et al., 2016), is under investigation by environmental agencies and local communities. In this study, two mining areas, an operative mine in Stratoni and an abandoned one in Lavrio, were studied. One sediment core was selected from each region. More specifically, in the coastal area of Ierissos Gulf – near the load out pier of Stratoni port and in the Oxygono Bay – near a mining waste disposal area.

The natural radionuclide concentrations (e.g. <sup>226</sup>Ra) were measured using gamma-ray spectrometry, while the major (e.g. Al, Ca) and minor elemental (e.g. As, Zn, Pb) concentrations were measured via X-ray fluorescence spectrometry, respectively. The measured element concentrations are depicted in Figs 1 and 2 in a time scale, taking into account the average sedimentation rates of the areas as they were derived from the concentrations of <sup>210</sup>Pb and <sup>137</sup>Cs (Tsabaris et al., 2012).

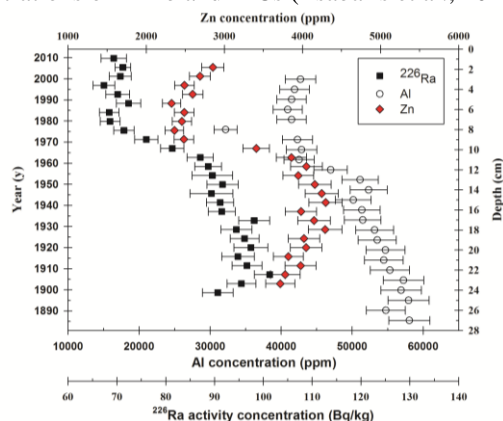


Figure 1. Characteristic core profiles of <sup>226</sup>Ra, Al and Zn concentrations in Ierissos Gulf (Stratoni).

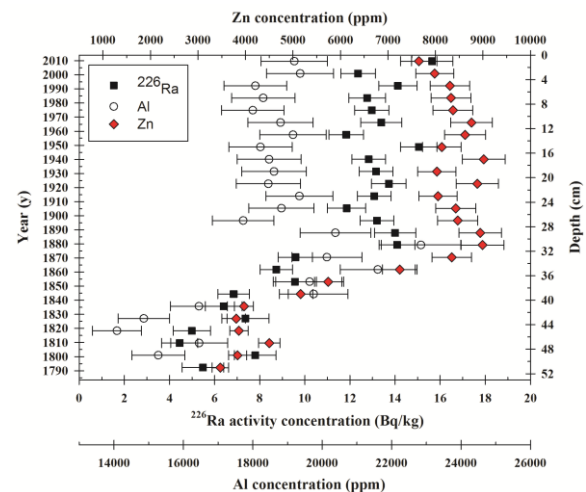


Figure 2. Characteristic core profiles of <sup>226</sup>Ra, Al and Zn concentrations in Oxygono Bay (Lavrio).

This work was supported by the A.G. Leventis Foundation by financially assisting Mrs F. K. Pappa.

Panagopoulos, I., Karayannidis, A., Adam, K., Aravossis, K., 2009. Application of risk management techniques for the remediation of an old mining site in Greece, *Waste Manag.* 29, 1739-1746.

Pappa, F.K., Tsabaris, C., Ioannidou, A., Patiris, D.L., Kaberi, H., Pashalidis, I., Eleftheriou, G., Androutakaki, A.G., Vlastou, R., 2016. Radioactivity and metal concentrations in marine sediments associated with mining activity in Ierissos Gulf, North Aegean Sea, Greece. *Appl. Radiat. Isot.* 116, 22-33.

Riba, I., DelValls, T.A., Forja, J.M., Gomez-Parra, A. 2002. Influence of the Aznacollar mining spill on the vertical distribution of heavy metals in sediments from the Guadalquivir estuary (SW Spain). *Mar. Pollut. Bull.* 44, 39-47.

Tsabaris, C., Kapsimalis, V., Eleftheriou, G., Laubenstein, M., Kaberi, H., Plastino, W., 2012. Determination of <sup>137</sup>Cs activities in surface sediments and derived sediment accumulation rates in Thessaloniki Gulf, Greece, *Environ Earth Sci* 67, 833-843.

Valette-Silver N.J., 1993. The use of sediment cores to reconstruct historical trends in contamination of estuarine and coastal sediments. *Estuaries* 16, 577-588.

Wang, S., Wang, Y., Zhang, R., Wang, W., Xu, D., Guo, J., Li, P., Yu, K., 2015. Historical levels of heavy metals reconstructed from sedimentary record in the Hejiang River, located in a typical mining region of Southern China, *Sci Total Environ.* 532, 645-654.



## Uranium time series analysis: a new methodological approach for event screening categorization

S. Bianchi<sup>1</sup> and W. Plastino<sup>1</sup>

<sup>1</sup>Department of Mathematics and Physics, Roma Tre University, Rome, I-00146, Italy

Keywords: Uranium, Groundwater, Time Series Analysis, Geodynamics.

Presenting author email: wolfango.plastino@uniroma3.it

Uranium was tested as a potential strain indicator of geodynamic processes occurring before an earthquake, rather than the consolidated scheme for radon release due to stress-strain processes in rocks (Plastino et al., 2010; Plastino et al., 2011).

The analysis supported the hypothesis that the uranium anomalies represented a key geochemical signal of the progressive increase of deep fluids fluxes at middle-lower crustal levels associated with the geodynamics of the earthquake (Plastino et al., 2013).

Now a new methodological approach for event screening categorization for uranium groundwater anomalies was tested. It was based on time series analysis and the flow chart of this method is showed in Figure 1. The first step of the analysis was inside (A), characterized by the trend removal. After the time series was detrended, the Lomb-Scargle (LS) spectrum can be computed for frequency domain analysis. Then, all frequencies were characterized in (B) by a notch filter for  $P(\omega)$  higher than a threshold, and reducing the time series to noise residuals. Starting from the top left in (C), the autocorrelation of the residuals was first computed, in order to test if they can be considered random or not. The Detrended Fluctuations Analysis (DFA) (Peng et al., 1995) was applied to noise residuals, and then for characterizing the statistical distributions two goodness of fit (GOF) tests were considered: Kolmogorov-Smirnov (KS) and Anderson-Darling (AD). The mean and variance of noise residuals were computed for the normalisation and outliers detection. Finally, in (D) was performed a noise analysis for ensuring that such outliers were not likely due to the particular noise configuration (white, pink, red).

This new methodological approach was tested on uranium groundwater time series collected before L'Aquila Earthquake (6<sup>th</sup> April, 2009) (Plastino et al., 2013). Finally, was possible to characterize an uranium groundwater anomaly (outlier) as well as the noise pattern in different sampling sites. The former was most likely associated with geodynamic processes occurring before the earthquake, and can be used as a possible strain meter in domains where continental lithosphere is subducted.

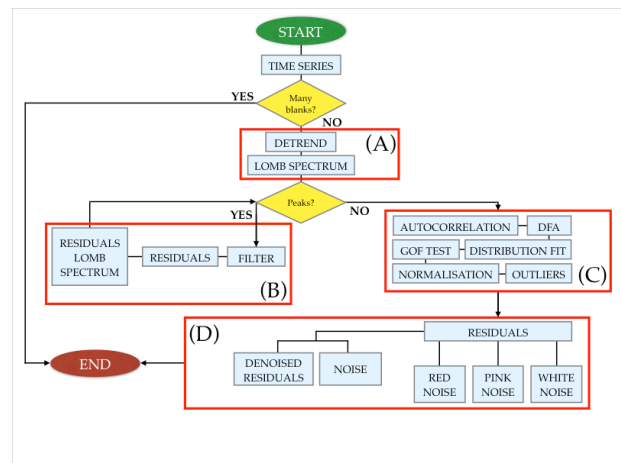


Figure 1. Time Series Analysis

The authors greatly acknowledge Mr Alessandro Longo for his kind contribution with scientific comments.

- Peng, C.K., Havlin, S., Stanley, H.E., Goldberger, A.L., 1995. Quantification of scaling exponents and crossover phenomena in nonstationary heartbeat time series. *Chaos* 5, 82-87.
- Plastino, W., Povinec, P.P., De Luca, G., Doglioni, C., Nisi, S., Ioannucci, L., Balata, M., Laubenstein, M., Bella, F., Coccia, E., 2010. Uranium groundwater anomalies and L'Aquila earthquake, 6th April 2009 (Italy), *J. Environ. Radioact.* 101, 45-50.
- Plastino, W., Panza, G.F., Doglioni, C., Frezzotti, M.L., Peccerillo, A., De Felice, P., Bella, F., Povinec, P.P., Nisi, S., Ioannucci, L., Aprili, P., Balata, M., Cozzella, M.L., Laubenstein, M., 2011. Uranium groundwater anomalies and active normal faulting, *J. of Radioanal. and Nucl. Chem.* 288, 101-107.
- Plastino, W., Laubenstein, M., Nisi, S., Peresan, A., Povinec, P.P., Balata, M., Bella, F., Cardarelli, A., Ciarletti, M., Copia, L., De Deo, M., Gallese, B., Ioannucci, L., 2013. Uranium, radium and tritium groundwater monitoring at INFN-Gran Sasso National Laboratory, Italy. *J. Radioanal. and Nucl. Chem.* 295, 585-592.

## Behaviours of plutonium isotopes in natural soil particles with different size

Y.H. Xu, S.M. Pan and M.M. Wu

The Key Laboratory of Coastal and Island Development of Ministry of Education, School of Geographic and Oceanographic Sciences, Nanjing University, Nanjing 210023, China

Keywords: Pu isotopes, Soil particles, size distribution, behavior

Presenting author email: yhxu@nju.edu.cn

Plutonium isotopes ( $^{239}\text{Pu}$  and  $^{240}\text{Pu}$ , with half-lives of 24110 and 6561 years, respectively) were recently used by some researchers as substitutes for  $^{137}\text{Cs}$  for investigation of soil erosion, due to their long half-lives, dominating source of global fallout worldwide, as well as their high retention and low mobility in soil. However, when using Pu isotopes for soil erosion tracing, researchers generally assumed that Pu isotopes closely associate with fine particles in soils similar to  $^{137}\text{Cs}$ , which was then used as the premise in explaining the physical migration process of Pu isotopes during soil erosion, without considering any different behaviors of Pu isotopes in soils compared to that of  $^{137}\text{Cs}$ . This approach might easily result in over-or undervalued soil erosion or deposition rates. Hence, in order to apply the Pu isotopes tracing method in soil erosion studies more scientifically, a systematical study of the behavior of Pu isotopes in natural soil particles is needed.

In this work, ten bulk soils collected from two different areas were separated into different particle size fractions by a combination of wet sieving and centrifugation techniques and the sub-samples were analyzed for  $^{137}\text{Cs}$ ,  $^{239}\text{Pu}$  and  $^{240}\text{Pu}$ . Results showed that the concentrations of both  $^{239+240}\text{Pu}$  and  $^{137}\text{Cs}$  increase with decreased particle sizes (Figure 1) and are closely related to the specific surface areas of soil particles (Figure 2), which demonstrated a similar preferential association of Pu with finer soil particles as  $^{137}\text{Cs}$ .

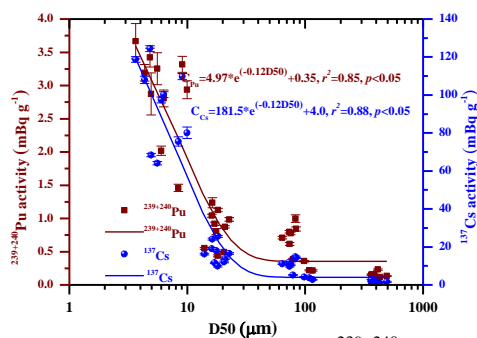


Figure 1. Relationships between  $^{239+240}\text{Pu}$  and  $^{137}\text{Cs}$  concentrations and the median diameter ( $D_{50}$ ) individual soil size fractions for all bulk samples. The smooth curves are the fitted results. Vertical error bars correspond to  $\pm 1$  standard deviation.

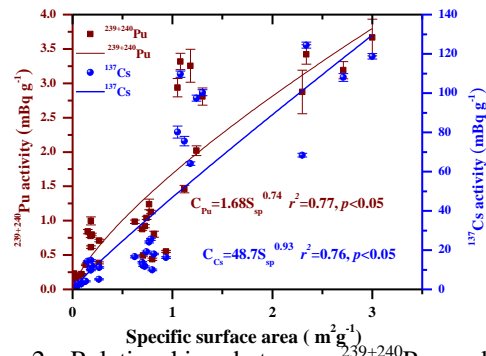


Figure 2. Relationships between  $^{239+240}\text{Pu}$  and  $^{137}\text{Cs}$  concentrations and the specific surface area of individual soil size fractions for all bulk samples.

The activity ratios of  $^{239+240}\text{Pu}/^{137}\text{Cs}$  in soil fractions increasing with increased particle size further indicated a less preferential transport of Pu with fine particles compared to  $^{137}\text{Cs}$ . These results not only highlight the suitability of Pu isotopes as soil erosion tracers, but also provide useful information for assessing the migration behavior of Pu in contaminated environments.

Speciation analysis of plutonium isotopes in soil samples using sequential extraction technique was also performed (Figure 3) to investigate their partitioning behavior and, thus, the potential mobility and bioavailability in the natural soil environment. The results provide a theoretical basis for the scientific use of plutonium isotopes in soil erosion tracing study in the future.

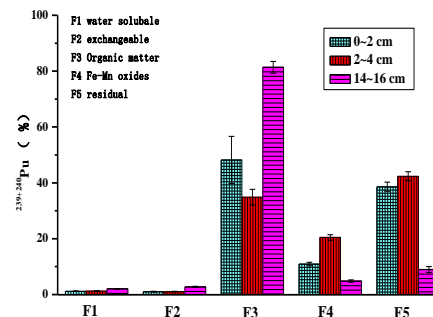


Figure 3 Fraction distribution of  $^{239+240}\text{Pu}$  activities in different layers of a soil core.



## Sources and transformation of carbon in an epikarst spring-fed pond system in central Guizhou: $\Delta^{14}\text{C}$ and $\delta^{13}\text{C}$ indicators

Min Zhao <sup>1,2,3</sup>, Bo Chen <sup>1,2</sup>, Hong-Chun Li<sup>3\*</sup>, Zaihua Liu <sup>1,2\*</sup>, Rui Yang <sup>1,2</sup>

<sup>1</sup> State Key Laboratory of Environmental Geochemistry, Institute of Geochemistry, CAS, Guiyang 550081, China  
<sup>2</sup> Puding Comprehensive Karst Research and Experimental Station, Institute of Geochemistry, CAS and Science and Technology Department of Guizhou Province, Puding 562100, China  
<sup>3</sup> Department of Geosciences, National Taiwan University, Taipei 10617, Taiwan

Presenting author email: zhaomin@mail.gyig.ac.cn

$\delta^{13}\text{C}$  and  $\Delta^{14}\text{C}$  of dissolved inorganic carbon (DIC), particulate organic carbon (POC) and aquatic plants from a karst spring and two spring-fed ponds in Laqiao (Fig.1), Maolan County, Guizhou Province in January, July and October of 2013 were measured to understand the roles of aquatic photosynthesis through DIC uptake in karst surface waters. The mean  $\Delta^{14}\text{C}$  and  $\delta^{13}\text{C}$  values of DIC for the spring pool, midstream and downstream ponds are  $-60.6 \pm 26.3\text{‰}$  and  $-13.53 \pm 1.97\text{‰}$ ,  $-62.8 \pm 62.9\text{‰}$  and  $-11.72 \pm 2.72\text{‰}$ , and  $-54.2 \pm 56.5\text{‰}$  and  $-9.40 \pm 2.03\text{‰}$ , respectively. Both  $\Delta^{14}\text{C}$  and  $\delta^{13}\text{C}$  show seasonal variations, with lower  $\Delta^{14}\text{C}$  values but heavier  $\delta^{13}\text{C}$  values in dry season and vice versa in summer rainy season (Fig.2). This observation indicates that (1) the main  $\text{CO}_2$  source of the spring DIC is from soil  $\text{CO}_2$  with higher contribution in summer due to higher productivity; (2) DIC in the stream ponds comes mainly from DIC of the spring, and contribution of DIC from the limestone bedrock dissolution is relatively small; (3) dilution of surface runoff (rainfall) to DIC in term of  $\Delta^{14}\text{C}$  and  $\delta^{13}\text{C}$  is not significant; and (4)  $^{13}\text{C}$  and  $^{14}\text{C}$  have different behaviors during DIC uptake by aquatic plants and during  $\text{CO}_2$  exchange between DIC and the atmospheric  $\text{CO}_2$ . Biological uptake of  $\text{CO}_2$  will not affect the  $\Delta^{14}\text{C}$  of DIC, but lead to  $\delta^{13}\text{C}_{\text{DIC}}$  enrichment.  $\text{CO}_2$  exchange between DIC and the atmospheric  $\text{CO}_2$  should elevate both the  $\Delta^{14}\text{C}$  and  $\delta^{13}\text{C}$  of DIC. In Laqiao system, it seems that the effect of biological uptake on the  $\Delta^{14}\text{C}$  and  $\delta^{13}\text{C}$  of DIC is much stronger than that of  $\text{CO}_2$  exchange with the atmosphere. The mean  $\Delta^{14}\text{C}$  values of POC from the spring pool, midstream and downstream ponds are  $-308.1 \pm 64.3\text{‰}$ ,  $-164.4 \pm 84.4\text{‰}$  and  $-195.1 \pm 108.5\text{‰}$ , respectively, indicating mixture of aquatic algae and detrital particle (clay and dust). More aquatic algae were formed in the stream ponds especially in the summer. SEM results of the POC samples support this conclusion. Furthermore, the  $\Delta^{14}\text{C}$  values of the submerged aquatic plants range from  $-200.0\text{‰}$  to  $-51.3\text{‰}$  and were similar to those of the DIC, indicating that the aquatic plants used DIC for photosynthesis. The  $\Delta^{14}\text{C}$  value of an emergent plant is  $-8.0 \pm 0.3\text{‰}$ , showing higher contribution of the atmospheric  $\text{CO}_2$  during photosynthesis.

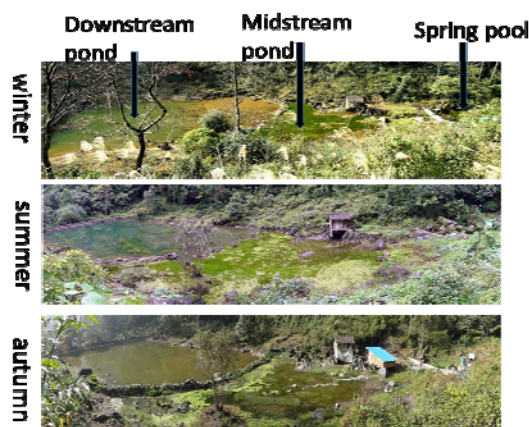


Fig.1 Full views of Maolan Spring and the spring-fed two ponds in winter, summer and autumn months.

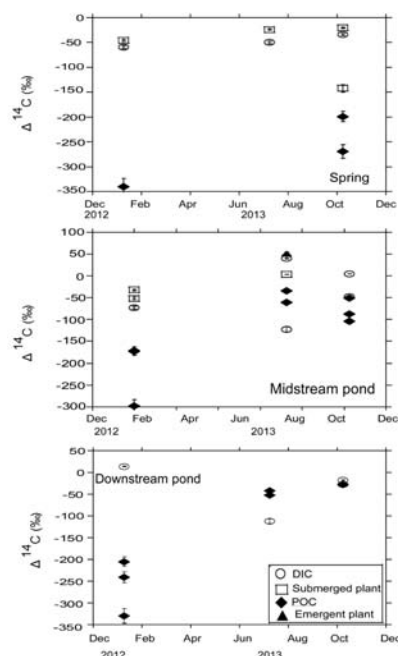


Fig.2 Seasonal variations in  $\Delta^{14}\text{C}$  values of DIC, POC and plant in Maolan spring and the two spring-fed ponds

Keywords: karst surface water, stable carbon isotope, radiocarbon, aquatic photosynthesis

This work was supported by the funds from NSFC (41673136, 41430753), 973 program (2013CB956703), the State Key Laboratory of Environmental Geochemistry (SKLEG2015404) of China

## ATMOSPHERIC DEPOSITION OF RADIONUCLIDES – ASSESSMENT BASED ON PASSIVE MOSS BIOMONITORING

Marina Frontasyeva & Eiliv Steinnes\*

*Sector of Neutron Activation Analysis and Applied Research, Division of Nuclear Physics,  
Frank Laboratory of Neutron Physics, Joint Institute for Nuclear Research, 141980 Dubna,  
Moscow Region, Russian Federation*

*\*Department of Chemistry, Norwegian University of Science and Technology, NTNU, NO-7491  
Trondheim, Norway*

Terrestrial moss has been used for the monitoring of atmospheric deposition of radionuclides since the late 50s of the last century, mostly for tracing deposition patterns of radionuclides due to technological accidents [1–3]. However, until recent time this aspect of investigations was absent in the UNECE ICP Vegetation (<http://icpvegetation.ceh.ac.uk/>) in spite of the great importance of knowledge on global mixing of long-lived radionuclides in the atmosphere and their deposition after the Chernobyl and Fukushima disasters. In the moss survey 2015/2016, an optional assessment of long-lived radionuclides such as  $^{137}\text{Cs}$  and  $^{210}\text{Pb}$  was suggested [4]. Low background gamma ray spectrometry is provided by several interested laboratories in Russia, Slovakia, Kazakhstan and Serbia, the JINR member-states. The feasibility of moss sampling to assess the atmospheric deposition of radionuclides is discussed and examples from the literature are reviewed.

**Keywords:** Moss, biomonitor, atmospheric deposition, radionuclides, nuclear accidents.

### References:

- [1] Svensson, G. K., & Liden, K. (1965). The quantitative accumulation of  $^{95}\text{Zr}$  +  $^{95}\text{Nb}$  and  $^{140}\text{Ba}$  +  $^{140}\text{La}$  in carpets of forest moss. *Health Physics* 11, 1033-1042.
- [2] Steinnes, E., & Njåstad, O. (1993). Use of mosses and lichens for regional mapping of  $^{137}\text{Cs}$  fallout from the Chernobyl Accident. *Journal of Environmental Radioactivity* 21, 65-73.
- [3] Aleksiyenak, Yu.V., Frontasyeva, M.V., Florek, M., Sykora, I., Holy, K., Masarik, J., Brestakova, L., Jeskovsky, M., Steinnes, E., Faanhof, A. & Ramatlhape, K.I. (2013). Distributions of  $^{137}\text{Cs}$  in moss collected from Belarus and Slovakia. *Journal of Environmental Radioactivity* 117, 19-24.
- [4] <http://icpvegetation.ceh.ac.uk/publications/documents/MossmonitoringMANUAL-2015-17.07.14.pdf>

## Radionuclide transport in the "sediments – water – plants" system of the water objects of the Semipalatinsk test site

A.K. Aidarkhanova<sup>1</sup>, S.N. Lukashenko<sup>1</sup>, N.V. Larionova<sup>1</sup>, V.V. Polevik<sup>2</sup>

<sup>1</sup>Institute of Radiation Safety and Ecology of the NNC RK, Kurchatov, East Kazakhstan region, 071100, Kazakhstan

<sup>2</sup>Shakarim State University, Semey, East Kazakhstan region, 071412, Kazakhstan

Keywords: radionuclides, water, sediments, water plants, transfer factors.

Presenting author email: Almira@nnc.kz

One of the main problems of radioecology is the migration of radionuclides in ecosystems, including water ecosystems. Water ecosystems can contribute to migration on a very long distance from the sources of formation of artificial radionuclides. Accumulating contamination during a long period, sediments remain accumulators of radionuclides and they are the source of secondary radioactive contamination of water objects. Water plants are also actively involved in the distribution of radioactive contamination of the water object. The aim of this work is assessment of levels of radioactive contamination and transfer in the "sediments – water – plants" system of the former Semipalatinsk Test Site (the STS) objects.

As objects of research surface water objects of STS are presented as the following types of sites: water objects of technogenic origin; water objects of naturally occurring; stream flows. In the frame of this work presents the water objects of technogenic origin. Water objects of technogenic origin in the territory of testing areas ("Experimental Field", "Balapan", "Telkem", "Sary-Uzen") are generally craters filled with water and formed due to surface or excavation explosions conducted. Total 11 of water objects on the "Experimental field" site, 3 – on the "Sary-Uzen" site, 2 – on the "Telkem" site and "Atomic" lake on the "Balapan" site was investigated.

At selected objects conjugated samples of water, sediments and plants were taken. 3 – 5 sampling points were on the each water object, and it depends on the size of the object. Samples were taken at the distance of 0.3 – 0.5 m from the costal line, the depth in sampling points was about 30 – 50 cm. Sampling of sediments was made to the depth of 0 – 10 cm, water – from a bottom layer, about 5 cm from the bottom. The water plants was sampling in the water, and the coastal plant – south cane (*Phragmites australis*), which most often meet in all water objects. Aboveground part of the south cane has been selected as a sample. Collected samples were used to determine concentration of artificial radionuclides <sup>90</sup>Sr, <sup>239+240</sup>Pu, <sup>241</sup>Am, <sup>137</sup>Cs, <sup>152</sup>Eu.

As a result of carried out researches the content of artificial radionuclides was determined in water, sediments and plants. Based on obtained data transfer factors (TF) for water and sediments, determining character of radionuclide contamination in water objects were calculated. Based on obtained data the TF decreases in <sup>239+240</sup>Pu > <sup>137</sup>Cs > <sup>90</sup>Sr line, i.e.  $n \times 10^5 > n \times 10^4 > n \times 10^3$  respectively. Radionuclide migration ability from sediment to water increases in this line. Nevertheless obtained TF values are  $\gg 1$ . This indicates that, most of researched radionuclides in "water-bottom sediments" system is concentrated in sediments.

In the case of plants, for example, the aboveground part of the south cane is able to accumulate up to 0.62% <sup>137</sup>Cs on the content in the sediments.

Distribution of radionuclides between the components of "sediments – water – plants" is one of the most important indicators of the radioecological situation in the water object.

Simpson SL, Batley GE, Chariton AA, Stauber JL, King CK, Chapman JC, Hyne RV, Gale SA, Roach AC, Maher WA (2005). Handbook for Sediment Quality Assessment (CSIRO: Bangor, NSW).

Handbook of Parameter Values for the Prediction of Radionuclide Transfer in Terrestrial and Freshwater Environments : Technical Reports Series. - No. 472. - Vienna: IAEA, 2010.

## Monte Carlo Markov Chain Simulation of the Cesium Dynamics in the Small Mesotrophic Reservoir Pond 4

V.J. Miller<sup>1</sup>, T.E. Johnson<sup>1</sup> and J.E. Pinder III<sup>1</sup>

<sup>1</sup>Dept. of Radiological and Environmental Health Sciences, Colorado State University, Fort Collins, Colorado, 80523 USA

Keywords: stochastic, aquatic model, Markov chain, cesium  
Presenting author email: millervi@colostate.edu

The mathematical modeling of the passage of radionuclides through ecosystems after initial release into the atmosphere or water column typically has employed continuous mathematics such as ordinary differential equations whereas in reality, the process involves discrete movements of the individual atoms of the released radionuclide. These movements are random and generally occur with low probabilities. The latter observation is supported by results regarding compartment retention from the Pond 4 kinetic model as described in “Model-Based Analysis of the Cesium Dynamics in the Small Mesotrophic Reservoir Pond 4 II. Development of a Rate-Based Kinetic Model” by Jeong, et. al (*in review*). However, there has been little investigation of the extent to which the random and improbable behavior of discrete units (such as atoms) modifies, describes, or controls the variation within the components of the system.

In this analysis we assess the discrete atom behaviors in influencing the midterm and long term distribution of Cs among the components using the robust and well documented experimental addition of <sup>133</sup>Cs into the 11.4 ha reservoir Pond 4 (a cooling pond of a decommissioned nuclear plant at the Savannah River Site, South Carolina). The following is a diagram of the primary biotic pathways sampled and utilized in our model.

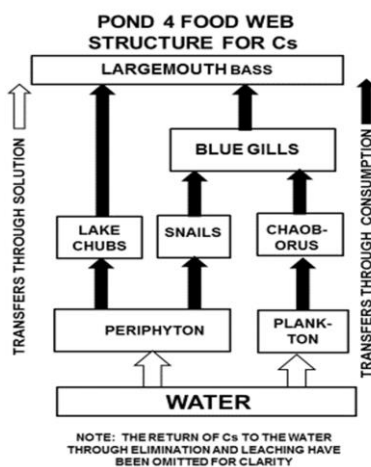


Figure 1. Pond 4 Modeled <sup>133</sup>Cs Biotic Pathways

The discrete atom behavior is modeled through the use of a Monte Carlo Markov Chain simulation for 1 million atoms. The result is stochastic in that no two simulations of individual atoms result in the same distributions of atoms among the components or the same fluxes of atoms along pathways through the system. Results indicate that overall the variability is low for this system, and the largest relative variability occurs 1) during time periods when components have smaller inventories of Cs and 2) for those components with smaller retention probabilities of retaining the Cs atoms per unit time. The effect of variability in one component on the subsequent component in the food chains was most noticeable for the snail to bluegill pathway.

Acknowledgments: Dr. Thomas Hinton, currently at Fukushima University Institute of Environmental Radioactivity, whom designed and conducted the original experiment along with the assistance of: A.E. De Biase, D. Coughlin, J. Gariboldi, K. Guy, A. Hays, B. Jackson, M. Johannsen, M. Jones, J. Joyner, R. Lide, L. Marsh, J. Novak, B. E. Taylor, F. W. Whicker, Y. Yi. Pond 4 original research was funded by DOE Contract No. DE-FC09-96SR18546.

JE Pinder III et. al, Cesium accumulation by aquatic organisms at different trophic levels following an experimental release into a small reservoir, *Journal of Environmental Radioactivity* 102 (2011) 283-293

JE Pinder III et. al, Cesium accumulation by fish following acute input to lakes: a comparison of experimental and Chernobyl-impacted systems (2009) 256-467

## Time lag between the tropopause height and the levels of $^7\text{Be}$ concentrations in surface air in mid and high latitudes

E. Ioannidou<sup>1</sup>, A. – P. Leppänen<sup>2</sup>, A. Vasileiadis<sup>1</sup>, D. Melas<sup>3</sup> and A. Ioannidou<sup>1</sup>

<sup>1</sup>Physics Department, Nuclear Physics Lab., Aristotle University of Thessaloniki, Thessaloniki 54124, Greece

<sup>2</sup>Environmental Surveillance and Measurement, Radiation and Nuclear Safety Authority – STUK, 96400 Rovaniemi, Finland

<sup>3</sup>Physics Department, Atmospheric Physics Lab., Aristotle University of Thessaloniki, Thessaloniki 54124, Greece

Keywords:  $^7\text{Be}$ , tropopause, correlation coefficient.

Presenting author email: [eleioann@physics.auth.gr](mailto:eleioann@physics.auth.gr) (Eleftheria Ioannidou)

The current study presents an analysis of  $^7\text{Be}$  concentrations data at mid and high geomagnetic latitudes, during the year 2009.

The  $^7\text{Be}$  is formed in the upper troposphere and lower stratosphere by spallation reactions of light atmospheric nuclei. The  $^7\text{Be}$  concentrations are affected by various meteorological conditions, one of which is the change in the level of the tropopause. The aim of the study is to define the time delay (time lag) between the changes of the tropopause height and the  $^7\text{Be}$  concentrations in surface air at Northern latitudes over 60°N and at mid latitudes, 40° N.

In mid latitudes, and more specifically in the region of Thessaloniki, Greece at 40°62'N, 22°95'E, the elevation of the tropopause during the warm summer months and the vertical exchange of air masses within the troposphere cause greater mixture of the air masses resulting in higher concentration levels for  $^7\text{Be}$  in surface air. The positive correlation between the monthly activity concentration of  $^7\text{Be}$  and the tropopause height, and also between  $^7\text{Be}$  and the temperature, confirm that the increased rate of vertical transport within the troposphere, especially during warmer summer months, has a result the descent to surface of air masses enriched in  $^7\text{Be}$ . However, the  $^7\text{Be}$  concentration levels in near surface air do not respond to the change of elevation of the tropopause immediately. It was found that there is a time delay of ~ 3 days (Fig. 1) between the change in the daily surface concentrations of  $^7\text{Be}$  and the change in the elevation of the tropopause (Ioannidou et al., 2014).

In case of high latitudes, the concentration of  $^7\text{Be}$  near surface air has been determined at three different locations in Finland, in Ivalo (68°64'N, 27°57'E), in Rovaniemi (66°51'N, 25°68'E) and in Kotka (60°48'N, 26°92'E). The large fluctuations in the values of the correlation factors represent a weak correlation between the  $^7\text{Be}$  and tropopause height (Fig. 2). In Ivalo and Rovaniemi, changes in the daily surface concentrations of  $^7\text{Be}$  lag the changes in the elevation of the tropopause by four days, however without clear maximum. In Kotka station, the influence of tropopause height on the surface concentrations of  $^7\text{Be}$  is the weakest and it seems that the influence of air masses from the East has greater influence on  $^7\text{Be}$  concentrations instead of the influence of the tropopause height.

$^7\text{Be}$  concentrations were found to have a distinct annual cycle with a clear maximum during warm summer months in both mid and high latitudes.

In high studied latitudes it seems that the ambient air  $^7\text{Be}$  activity is affected by climatic phenomena and that the impact of different climatic phenomena on  $^7\text{Be}$  activity is sensitive to location (Leppänen and Paatero, 2013). The changes in air mass transport patterns associated with NAO (North Atlantic Oscillation) and AMO (Atlantic Multidecadal Oscillation) were determined to be the main contributor to the interannual variability of surface air  $^7\text{Be}$  activities in Finland (Leppänen et al., 2012).

In general, at latitudes over 60°N the correlation between the tropopause height and  $^7\text{Be}$  concentrations is weak without any clear time delay, while in case of 40°N there is a clear time delay (time lag) of ~ 3 days.

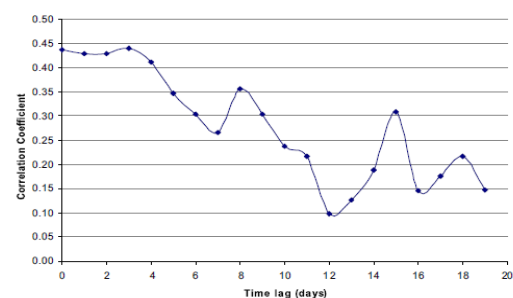


Figure 1. Day lag plot for the region of Thessaloniki.

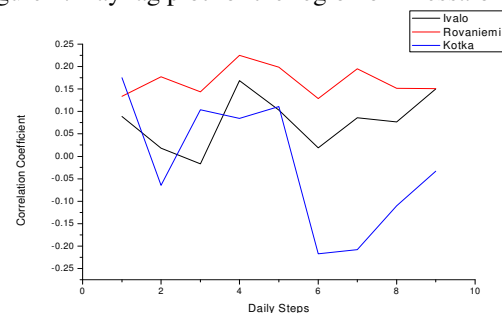


Figure 2. Day lag plot for the three locations in Finland.

### References

- Ioannidou A., Vasileiadis A. and D. Melas, 2014. J. Environm. Radioactivity 129, 80-85
- Leppänen A.-P., Usoskin I.G., Kovaltsov G.A., Paatero J., 2012. Journal of atmospheric and Solar-Terrestrial Physics 74, 164-180.
- Leppänen Ari-Pekka , Jussi Paatero, 2013. Journal of Atmospheric and Solar – Terrestrial Physics, 97, 1-10



## Optimization and validation of the BCR sequential extraction procedure for natural radionuclides (U, Th, Po); application to phosphogypsum by-product

S. Pérez-Moreno<sup>1</sup>, M.J. Gázquez<sup>2</sup>, R. Pérez-López<sup>3</sup> and J. P. Bolívar<sup>1</sup>

<sup>1</sup>Department of Applied Physics, University of Huelva, Huelva, 21071, Spain

<sup>2</sup>Department of Applied Physics, University of Cadiz, Cadiz, Spain.

<sup>3</sup>Department of Geology, University of Huelva, Huelva, Spain.

Keywords: BCR sequential extraction, validation, mobility radionuclides, phosphogypsum.

Presenting author email: sylvipm@gmail.com

The determination of total content of a contaminant in a waste is not a good measure to determine their potential radiological risk since only a proportion of the total content of the contained pollutants are mobile and/or bioavailable.

The optimized sequential extraction BCR procedure, acronym of Community Bureau of Reference (Rauret et al., 1999), allows obtaining information the mode of presentation of the trace metals in the sediments, as well as their physicochemical availability and mobilization.

The main purpose of this work is to validate for natural radionuclides BCR procedure, since this speciation method was only validated for heavy metals in the standard material called BCR-701. The second objective is to determine the mobility of uranium and thorium in phosphogypsum (PG) in order to evaluate the radiological and environmental risk during its future management.

The PG is a waste generated in the production of phosphoric acid by the sulphuric acid route, which contains high natural radionuclides concentrations. In the southwest of Spain, PG has been stored in piles on wetlands located at the Huelva estuary for 45 years, reaching 5 m of height, covering an area of about 1000 ha where about 100 millions of tons of PG are stored (Bolívar et al., 2009; Pérez-López et al., 2010).

Certified Reference Material BCR-701 and a PG core (6 samples, 2.5 m in depth) was subjected to BCR procedure. At each liquid fraction the heavy metals by ICP-MS were measured, while U-isotopes, Th-isotopes, and Po by alpha-particle spectrometry were determined.

The table 1 shows the certified heavy metals concentrations (Cr, Ni, Cu, Zn, Cd and Pb), which are in very good agreement with the measured ones. These results validate the BCR procedure applied in our laboratory.

Table 1. Concentration (mg/kg) of Cu and Zn in each fraction

	Cu		Zn	
	Measured Value (mg/kg)	Certified Value (mg/kg)	Measured Value (mg/kg)	Certified Value (mg/kg)
Step 1	52.9±14.8	49.3±1.7	185±55	205±6
Step 2	121±16	124±3	101.6±26.1	114.0±5.0
Step 3	56±10	55±4	48±3	46±4
Step 4	34.9±2.8	38.5±11.2	85.5±4.7	94.6±12.2

Figure 1 shows the distribution measured in the different operational phases; about 61±1% of U is bound to mobile fractions (step 1 + step 2 + step 3, being the

residual fraction the step 4. The thorium is only detected almost in the non-mobile fraction.

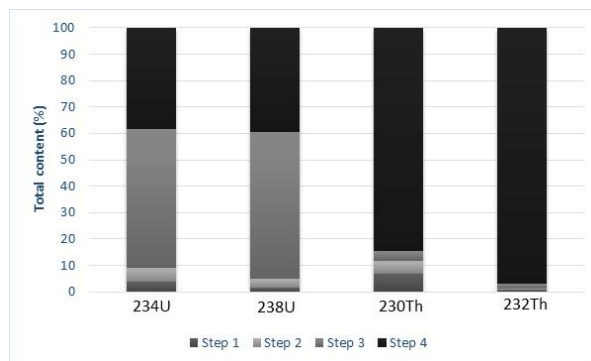


Figure 1. Distribution of U and Th radionuclides in each fraction from the BCR-701.

In the PG about 72±4% of U is bound to the mobile fraction (Fig. 2), whereas Th is fully found in the non-mobile fraction (98±1%).

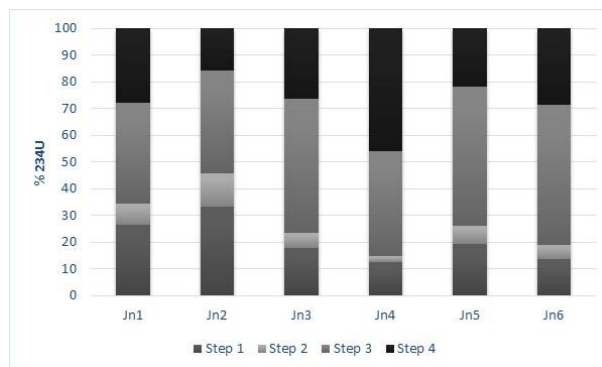


Figure 2. Distribution of <sup>234</sup>U in each fraction from PG core.

This study has concluded that BCR-701 standard can be used as Certified Reference Material for radionuclides measurement. In addition, the mobility of Th in phosphogypsum is very much low, whereas the mobility of uranium is high and can represent potential environmental risk.

J.P. Bolívar, J.E. Martín, R. García-Tenorio, J.P. Pérez-Moreno, J.L. Mas. (2009) *Applied Radiation and Isotopes* 67, 345–356.  
 R. Pérez-López, J. M. Nieto, I. López-Coto, J.L. Aguado, J.P. Bolívar, M. Santisteban. (2010) *Applied Geochemistry* 25, 705–715.  
 G. Rauret, J. F. Lopez-Sanchez, A. Sahuquillo, R. Rubio, C. Davidson, A. Ure and Ph. Quevauviller. (1999) *Journal Environmental Monitoring* 1, 57–6.



## Preparation of strontium-90 pine needle reference material and the labs intercomparison radiochemical analysis

Yanqin Ji\*, Fei Chen, Xianzhang Shao, Liangliang Yin, Xiangying Kong

China CDC Key Laboratory of Radiological Protection and Nuclear Emergency, National Institute for Radiological Protection, China CDC. 100088 Beijing, China

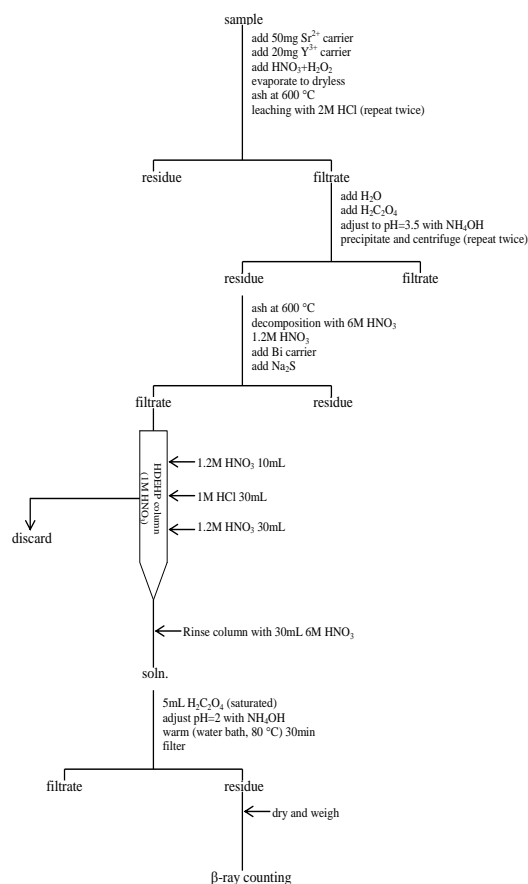
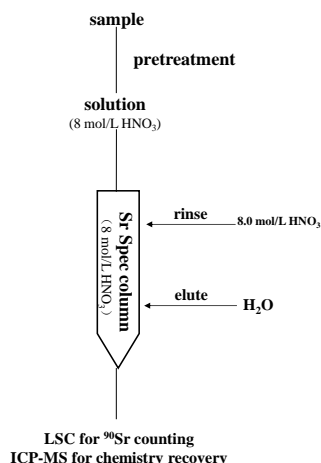
Keywords: strontium-90, reference material, pine needle, lab intercomparison

Presenting author email: jiyinqin@nirp.cn

Strontium-90 is one of the most important long-lived radionuclide with high-energy  $\beta$ -rays as the fission products of  $^{235}\text{U}$  and  $^{239}\text{Pu}$ . Its chemical characteristics are very similar with calcium and deposits mainly in the bones, teeth and damaging blood-producing cells of animals by uptake from the soil, food recycle results. Therefore, it is essential to precise detect low-level  $^{90}\text{Sr}$  in environmental and biological samples for environmental protection and health safety. The measurement of low-level  $^{90}\text{Sr}$  normally follows with a long radiochemical separation procedure. The purpose of this work is to prepare strontium-90 pine needle samples, as the higher strontium accumulation plant, reference materials primarily for use in evaluating the reliability of  $^{90}\text{Sr}$  analytical methods and the quality control organized nationwide radioactivity monitoring in foodstuffs samples in China.

The sample of pine needles were selected in Changping protected natural forest at the same age located in the north of Beijing, China. After water cleaned, dried at  $70^\circ\text{C}$ , jet milled and blended at about  $63\ \mu\text{m}$ . Spiked with  $^{90}\text{Sr}$  diluted solution and blended uniformly, liquid nitrogen fixed, then freeze-dried directly for one week. Finally it was completely blended again, filled bottles and Gamma ray irradiation sterilized with a total dose of  $25\text{kGy}$  using a  $^{60}\text{Co}$  source.

A unit of the sample consists of approximately 30 gram of pine needles powder. The batch experiments for the stability and uniformity performed by the Di-(2-ethylhexyl) phosphate (HDEHP) extraction chromatography separation, yttrium-90 precipitated and counting. The minimum sample amount for the measurement is about 8 gram under the satisfaction uncertainty.



This material was also used as a test material for the interlaboratory comparison exercise national-wide in China, for the determination of  $^{90}\text{Sr}$ . The main two methods for  $^{90}\text{Sr}$  measurement of HDEHP column separation with  $^{90}\text{Y}$  counting, the Sr-spec crown ether separation with liquid scintillation counter. The relative uncertainty of the recommended value is 3.1% of  $32.3\ \text{Bq/kg}$   $^{90}\text{Sr}$  in pine needle powder, the certificate RM number is GBW 04329. A description of the material collection and preparation, uncertainty analysis and the results of the interlaboratory comparison will be presented and discussed.

The authors acknowledge financial support by the Chinese Ministry of Science and Technology (Grant No. 2014FY211000 and 2013BAK03B00).

IAEA, 2009. Worldwide open proficiency test on the determination of radionuclides in spinach, soil and water. IAEA/AQ/8, IAEA-CU-2007-03. Vienna,

## A procedure for the sequential determination of radionuclides: a case study in river sediments

H. Sahli<sup>1</sup>, S. Röllin<sup>1</sup>, B. Balsiger<sup>1</sup>, M. Burger<sup>1</sup>, V. Putyrskaya<sup>2</sup>, E. Klemt<sup>2</sup> and J.A. Corcho Alvarado<sup>1</sup>

<sup>1</sup> Federal Office for Civil Protection, SPIEZ LABORATORY, Physics Division, 3700 Spiez, Switzerland

<sup>2</sup> Hochschule Ravensburg-Weingarten, University of Applied Sciences, Weingarten, Germany

Keywords: Rhine Sedimentes, radionuclides, Extraktion chromatography, ICP-MS,.

Presenting author email: [jose.corcho@babs.admin.ch](mailto:jose.corcho@babs.admin.ch)

We present a radiochemical procedure for the sequential determination of <sup>90</sup>Sr, <sup>241</sup>Am, Pu, Th and U isotopes in soil and sediment samples (Fig. 1). After drying, the samples are ashed at 520 °C. <sup>242</sup>Pu and <sup>115</sup>In tracers are added to the ashed sample and then digested by fusion. The silicates are precipitated with PEG in 4.5 M HNO<sub>3</sub>. Before filtration, an aliquot is taken for U and Th determinations by ICP-MS. Pu is separated using a TEVA resin and measured by ICP-MS (Röllin et al., 2009). <sup>243</sup>Am and stable Sr tracers are added to the breakthrough of the TEVA resin and the Ca-oxalates are precipitated. After dissolution, Am and Sr are separated in a TRU resin. The Am fraction is purified in a TEVA resin and, after electroplating, measured by alpha spectrometry. Sr was purified in a Sr-Spec resin and counted by gas proportional counting (LLC) in the form of SrCO<sub>3</sub>. The radiochemical method was tested and validated using several IAEA reference materials.

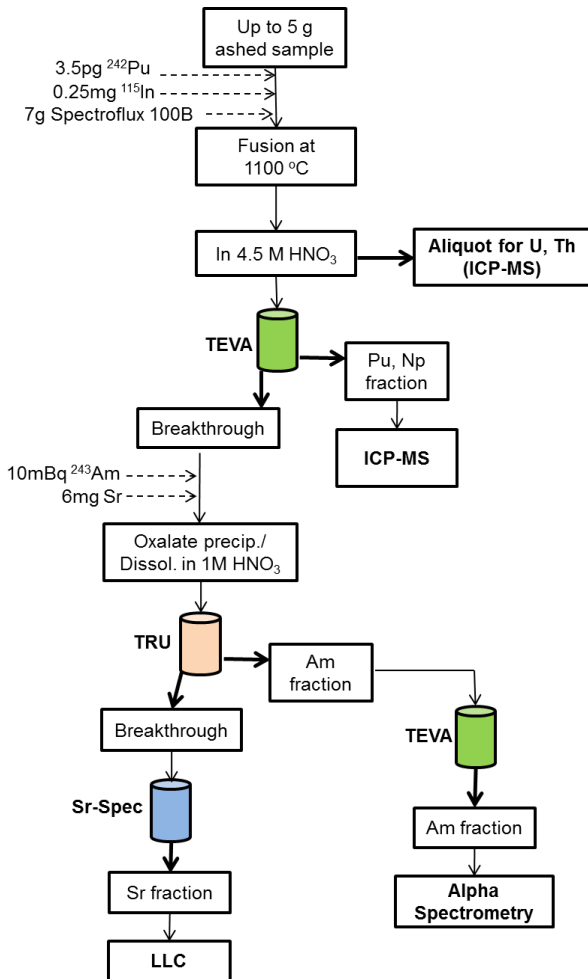


Figure 1. Flow chart of the radiochemical method.

This method was used to determine the radionuclide profiles in one sediment core collected in 2015 in the Rhine river, near Augst, downstream of Swiss nuclear power plants. The depth profiles of the anthropogenic radionuclides showed a well define maximum at 32-35 cm depth (Fig. 2). This depth horizon was related to the 1963 fallout maximum originated from the atmospheric nuclear weapon tests (NWT). The <sup>240</sup>Pu/<sup>239</sup>Pu and <sup>241</sup>Pu/<sup>239+240</sup>Pu isotope ratios corresponded to the typical ratios observed in global fallout from the NWTs and is therefore a strong indication that Pu originated mainly from this source(Fig. 2). This was further confirmed by the <sup>241</sup>Am/<sup>241</sup>Pu contamination dates which ranged between 1955 and 1970.

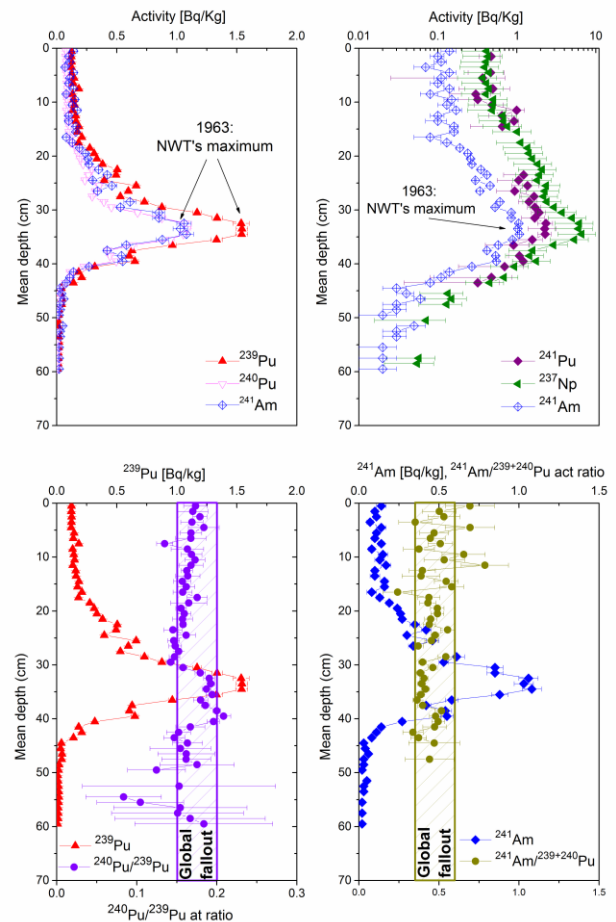


Figure 2. Vertical profiles of some of the investigated radionuclides and isotope ratios.

Röllin et al., 2009, Pu and Np analysis of soil and sediment samples with ICP-MS. App. Rad. Iso. 67 (5), 821-827

## Determination of Sr-90 activity concentration and Strontium/Calcium ration in different matrices

András Bednár<sup>1,2</sup>, Gergő Bátor<sup>1,2</sup>, Edit Tóth-Bodrogi<sup>2</sup>, Tibor Kovács<sup>1,2</sup>

<sup>1</sup>Social Organization for Radioecological Cleanliness, Egyetem u.10, 8200 Veszprém, Hungary

<sup>2</sup>Institute of Radiochemistry and Radioecology, University of Pannonia, PO Box 158, 8201 Veszprém, Hungary

Keywords: Radiostrontium, calcium, food-chain, liquid-scintillation, Cherenkov-counting

Presenting author email: bednar.andras@rttsz.hu

Several biologically active radioactive isotopes are produced in a uranium-235 nuclear bomb explosions and some nuclear power plant accidents; Sr-90 is a major problem when considering long-term consequences, because of its slow fallout from the atmosphere, its long half-life of 28.8 years and its biological similarity to calcium.

It is a well-known process that toxic elements going further along the food chain are concentrated during the steps. Milk has received attention as a source of Sr-90, since the radiostrontium found on the ground from fallout events can be readily dissolved in ground water, from where it can enter plant tissues. Cattle grazing these contaminated plants that way can produce milk containing an elevated amount of the material, which can be ingested by human beings afterwards (Crout et al. 1998). Because of the aforementioned facts during the experiments we made measurements from all the links in the chain.

There are a couple of methods for the determination of radiostrontium activity concentration in various containment matrices, during our experiments we used ashing followed by an acidic digestion step, and a microwave digestion of the samples in a strongly acidic media. During the measurements the Ca content and the strontium activity concentration were determined. The activity of the prepared samples were determined using a liquid scintillation counter (Wallac Quantulus 1220), the Ca content using an atomic emission spectrometer.

The experiments carried out lead to a conclusion that out of the two digestion methods the microwave method is better suited for the task as it has a higher chemical recovery factor and the resulting solution remaining after the process is much easier to handle. As an example figure 1 shows the comparison result of the two different methods in the case of soil digestion

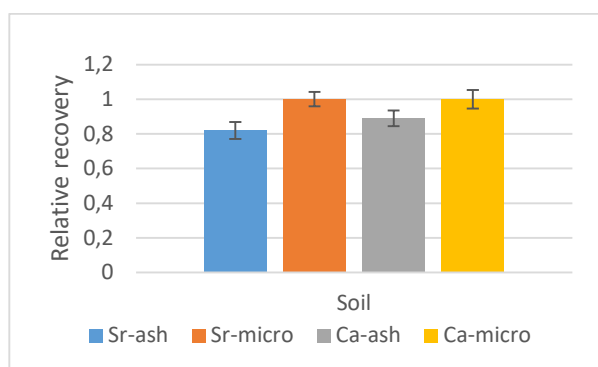


Figure 1: The comparison of relative recoveries in the case of soil digestion

The activity of the samples were measured by two different approaches: The classical liquid scintillation counting, and the measurement of the Cherenkov radiation of the prepared specimen (Stamoulis et al. 2007). Results indicate that both methods are suitable for these kinds of measurements, but the Cherenkov-counting has a slightly lower background which decreases detection limits.

After the optimization of the measurement conditions the measured activities and the strontium/calcium ratio were determined as shown on table 1.

Table 1: Sr-90 activity-concentration [Bq/kg], and Strontium/Calcium ratio in different matrices

	Sr-90 AC [Bq/kg] ± unc. [Bq/kg]	Sr/Ca ratio * 100
Soil	3.26E-01 ± 3.73E-02	0.123
Vegetation	4.82E-01 ± 7.63E-02	0.104
Animal Bones	6.35E-01 ± 5.16E-02	0.079
Milk (cow)	6.89E-01 ± 5.39E-02	0.075

As the presented results show, the activity of the radiostrontium following the food chain increases, but the Sr/Ca ratio decreases. This might be due to the fact that during the procession of the nutrients the various organisms acquire a slightly higher amount of Ca, and that despite the chemical similarities the processes still have a higher affinity towards calcium as opposed to strontium.

### Reference

- Crout, N.M.J. et al. 1998. "A Model of Radiostrontium Transfer in Dairy Goats Based on Calcium Metabolism." *Journal of Dairy Science* 81(1): 92–99.
- Stamoulis, K.C., K.G. Ioannides, D.T. Karamanis, and D.C. Patiris. 2007. "Rapid Screening of <sup>90</sup>Sr Activity in Water and Milk Samples Using Cherenkov Radiation." *Journal of Environmental Radioactivity* 93(3): 144–56.

## Analysis of the evolution of gross alpha and beta activities in airborne samples in Valencia

M. Sáez-Muñoz, M.C. Bas, J. Ortiz and S. Martorell

Laboratorio de Radiactividad Ambiental, MEDASEGI Research Group,  
 Universitat Politècnica de València, Valencia, Camino de Vera s/n, 46022, Spain

Keywords: gross alpha, gross beta, air, atmospheric factors

Presenting author email: masaemuo@etsii.upv.es

Gross  $\alpha$  and gross  $\beta$  determination is one of the most useful analysis for airborne radioactivity detection, together with gamma measurement. In normal situation, gross  $\alpha$  and gross  $\beta$  origin is mainly explained due to the presence of long-lived daughters of gaseous  $^{222}\text{Rn}$ . However, artificial radionuclides can be also detected, so it is one of the simplest technique as a method of “screening” in case of emergency or atmospheric radioactive release (Maiello and Hoover, 2011; EPA, 2009). Moreover, gross  $\alpha$  and  $\beta$  long-term monitoring also provides information about trends in radionuclide behavior. In this work, the “Laboratorio de Radiactividad Ambiental” of the Universitat Politècnica de València (LRA-UPV) presents the evolution of gross  $\alpha$  and gross  $\beta$  index in airborne of the city of Valencia over the period 2008-2016.

The ANOVA test (applied to Log  $\alpha$  and Log  $\beta$  to assume normality) shows that the differences in gross  $\alpha$  and  $\beta$  index considering the seasonal factor are statistically significant at a 95% confidence level. Therefore, it exists an intra-annual variability with maximum values in summer, minimum values in winter and similar values in spring and autumn (Figure 1). The variability observed could be mainly explained by the atmospheric factors.

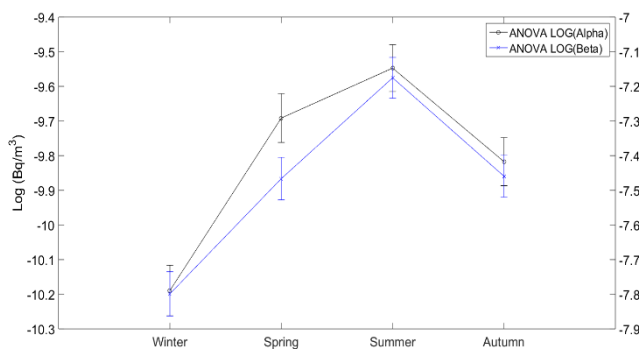


Figure 1. LSD intervals of the ANOVA analysis

The relation of atmospheric factors on total gross  $\alpha$  and  $\beta$  index are analyzed using the Spearman correlation. Results show a positive and strong relation of both index with relative humidity (RH), temperature (T) and dust content (D), and a negative influence of precipitations (PP) and wind speed (WS). A global Multiple Linear Regression (MLR) analysis was applied and results show that 52.68% and 57.99% of the variability of gross  $\alpha$  and  $\beta$  activity, respectively, is explained by the atmospheric factors.

However, considering the intra-annual variability observed in the ANOVA analysis, the atmospheric variables could have different influence on gross  $\alpha$  and  $\beta$  variability depending on the seasonal factor. Therefore, we proposed to apply a MLR analysis in summer months

(S), spring-autumn months (SA) and winter months (W) in order to identify the significant meteorological factors that affect the variability of gross  $\alpha$  and  $\beta$  index in different seasons.

Table 1. MLR of gross  $\alpha$  and  $\beta$  index by seasons

Models fitting for Gross $\alpha$ and $\beta$	$R^2$ (%)
$\text{Log}(A_\alpha)_S = -11.29 + 10.11\text{D} + 0.02\text{RH}$	14.09
$\text{Log}(A_\beta)_S = -9.11 + 0.026\text{RH}$	15.05
$\text{Log}(A_\alpha)_{SA} = -10.93 + 7.33\text{D} + 0.014\text{RH}$ $+ 0.003\text{T} - 0.1\text{WS}$	41.58
$\text{Log}(A_\beta)_{SA} = -7.89 + 2.79\text{D} + 0.007\text{RH} + 0.003\text{T}$ $- 0.0006\text{PP} - 0.14\text{WS}$	51.55
$\text{Log}(A_\alpha)_W = -10.81 + 21.40\text{D} + 0.01\text{RH} - 0.1\text{WS}$	70.66
$\text{Log}(A_\beta)_W = -7.35 + 11.45\text{D} - 0.13\text{WS}$	69.50

MLR analysis (Table 1) show that the influence of the atmospheric factors on  $\alpha$  and  $\beta$  variability is more significant in winter months (70.66% and 69.50% resp.) than in spring-autumn months (41.58% and 51.55% resp.). The variables that mainly and strongly influence on  $\alpha$  and  $\beta$  variability in winter months are D, RH and WS. In spring-autumn months there are more atmospheric variables (D, T, RH, PP, WS) that influence on  $\alpha$  and  $\beta$  variability and this result could be explained by the irregularity of these variables in these months.

However, the influence of the atmospheric factors on  $\alpha$  and  $\beta$  variability is much lower in summer (14.09% and 15.05% resp.). The atmospheric variables that slightly influence on  $\alpha$  and  $\beta$  variability are D and RH. These results suggest that the evolution of gross  $\alpha$  and gross  $\beta$  activity is more constant in summer and the atmospheric variables are more stable in these months and practically do not affect  $\alpha$  and  $\beta$  variability.

In conclusion, MLR provides information on significant meteorological factors that affect gross  $\alpha$  and gross  $\beta$  variability, which could be useful in identifying meteorological or atmospheric changes that could cause deviations in gross  $\alpha$  and gross  $\beta$  activity depending on the seasons considered.

This work was supported by the REM program of the Nuclear Safety Council SRA/2071/2015/227.06 of Spain.

EPA, 2009. Radiological Laboratory Sample Analysis Guide for Incidents of National Significance – Radionuclides in Air, Revision 0, EPA 402-R-09-007. Office of Air and Radiation, Washington, DC.  
 Maiello, M.L., Hoover, M.D., 2011. Radioactive Air Sampling Methods, CRC Press, Taylor & Francis Group, New York.



## Se uptake and reduction in two boreal *Pseudomonas* sp. strains

M. Lusa<sup>1</sup>, J. Knuutinen<sup>1</sup>, J. Lehto<sup>1</sup> and M. Bomberg<sup>2</sup>

<sup>1</sup>Department of Chemistry, Radiochemistry, University of Helsinki, Helsinki, FI-00014, Finland

<sup>2</sup>VTT Technical Research Centre of Finland, Espoo, FI-02044, Finland

Keywords: bacteria, selenium, reduction, uptake

Presenting author email: merja.lusa@helsinki.fi

<sup>79</sup>Se is one of the high priority radionuclides in the long-term biosphere safety assessment of spent nuclear fuel. In this study, the uptake and reduction of Se oxyanions by two previously isolated boreal bog *Pseudomonas* sp. strains, PS-0-L and T5-6-I (Lusa et al. 2016), was examined using batch experiments, transmission electron microscopy (TEM) and energy dispersive X-ray spectroscopy (EDX). In addition, SDS-PAGE was used to study the protein profiles in the presence of SeO<sub>3</sub><sup>2-</sup>/SeO<sub>4</sub><sup>2-</sup> and anionic macronutrients.

While Se reduction has been shown to be an environmentally important process, only a few SeO<sub>3</sub><sup>2-</sup>-respiring bacteria have been isolated and specific SeO<sub>3</sub><sup>2-</sup> uptake mechanisms and transporters have not yet been identified. Previously, we found the two *Pseudomonas* strains to remove <sup>75</sup>SeO<sub>3</sub><sup>2-</sup> from solutions under different nutrient conditions (Lusa et al. 2015). To study the transport systems present in these bacteria, we tested the effect of 0.1 % glucose (in 0.5% peptone+0.25% yeast extract) and cysteine (100 μM–5000 μM in 1 % Tryptone) on SeO<sub>3</sub><sup>2-</sup> uptake. We discovered a 2- to 7-fold increase in the SeO<sub>3</sub><sup>2-</sup> uptake in both bacteria when glucose was added. This stimulatory effect indicates active transport, which in turn should be affected by various inhibitors. In fact, S-containing amino acid L-cysteine inhibited SeO<sub>3</sub><sup>2-</sup> uptake in both studied bacteria, which indicates that SeO<sub>3</sub><sup>2-</sup> uptake may be regulated by cellular products formed in the sulphur metabolism.

Both intra- and extracellular reduced Se<sup>0</sup> granules have been found in distinct bacteria, but the generation process of these granules is still mainly unknown. In our study, formation of brick-red reduced Se<sup>0</sup> was observed after incubation in SeO<sub>3</sub><sup>2-</sup> containing cultures and intracellular Se<sup>0</sup> granules were verified using TEM and EDX in both *Pseudomonas* strains (Fig. 1). When SeO<sub>4</sub><sup>2-</sup> was used, these formations were absent.

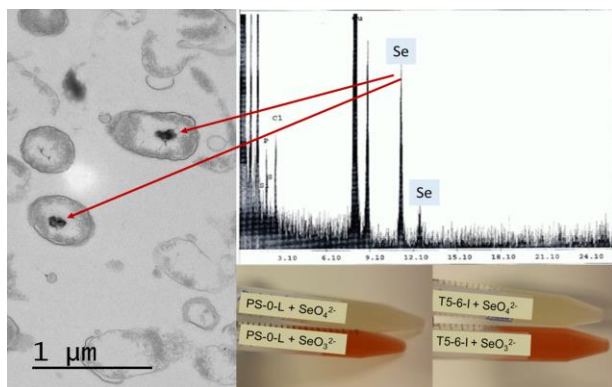


Figure 1. Reduced Se<sup>0</sup> found in two *Pseudomonas* strains after incubation in SeO<sub>3</sub><sup>2-</sup> solution.

Like other trace anions, SeO<sub>3</sub><sup>2-</sup> may share transporters with major anions. Therefore, we tested the roles of NO<sub>3</sub><sup>-</sup>, NO<sub>2</sub><sup>-</sup>, SO<sub>4</sub><sup>2-</sup> and SO<sub>3</sub><sup>2-</sup> in SeO<sub>3</sub><sup>2-</sup> uptake and assumed that with up-regulation of NO<sub>3</sub><sup>-</sup>/NO<sub>2</sub><sup>-</sup>/SO<sub>4</sub><sup>2-</sup>/SO<sub>3</sub><sup>2-</sup> the rate of SeO<sub>3</sub><sup>2-</sup> uptake would increase in the presence of these anions. We found NO<sub>3</sub><sup>-</sup>/NO<sub>2</sub><sup>-</sup>/SO<sub>4</sub><sup>2-</sup> addition to enhance SeO<sub>3</sub><sup>2-</sup> uptake in both bacteria, compared to the situation when only SeO<sub>3</sub><sup>2-</sup> or SeO<sub>3</sub><sup>2-</sup>+SO<sub>3</sub><sup>2-</sup> were present. This indicates two distinct SeO<sub>3</sub><sup>2-</sup> transport mechanisms; a low affinity transport system regulated by NO<sub>3</sub><sup>-</sup>/NO<sub>2</sub><sup>-</sup>/SO<sub>4</sub><sup>2-</sup> and a distinct SeO<sub>3</sub><sup>2-</sup> regulated transport system.

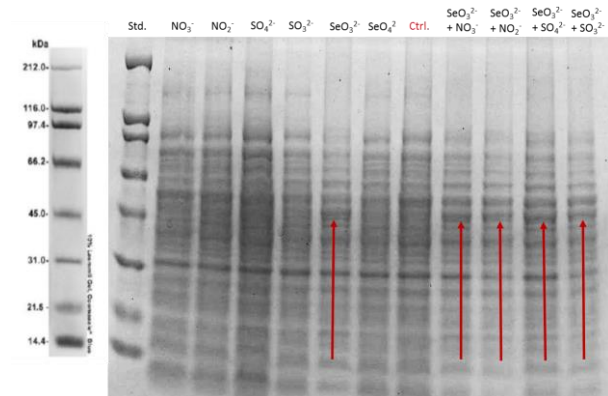


Figure 2. Proteins in *Pseudomonas* T5-6-I in NO<sub>3</sub><sup>-</sup>/NO<sub>2</sub><sup>-</sup>/SO<sub>4</sub><sup>2-</sup>/SO<sub>3</sub><sup>2-</sup>/SeO<sub>3</sub><sup>2-</sup>/SeO<sub>4</sub><sup>2-</sup> solutions.

Membrane transport proteins and/or reducing enzymes were examined by incubating the bacteria with NO<sub>3</sub><sup>-</sup>/NO<sub>2</sub><sup>-</sup>/SO<sub>4</sub><sup>2-</sup>/SO<sub>3</sub><sup>2-</sup> and SeO<sub>3</sub><sup>2-</sup>/SeO<sub>4</sub><sup>2-</sup>, which after soluble and inclusion body fractions were isolated and separated using SDS-PAGE. An additional soluble ~45 kDa protein was expressed as T5-6-I was incubated with only SeO<sub>3</sub><sup>2-</sup> or with SeO<sub>3</sub><sup>2-</sup>+NO<sub>3</sub><sup>-</sup>/NO<sub>2</sub><sup>-</sup>/SO<sub>4</sub><sup>2-</sup>/SO<sub>3</sub><sup>2-</sup> (Fig.2). In the absence of SeO<sub>3</sub><sup>2-</sup> this protein was not expressed. Based on the observed differences in reduction ability, relative toxicities of SeO<sub>3</sub><sup>2-</sup>/SeO<sub>4</sub><sup>2-</sup> and solubility of the 45 kDa protein, it is possible that this *Pseudomonas* strain uses SeO<sub>3</sub><sup>2-</sup> uptake and reduction as a detoxification mechanisms. However, further characterization of the protein is still needed and is ongoing at the moment.

Lusa, M, Bomberg, M, Aromaa, H, Knuutinen, J, Lehto, J, 2015. The microbial impact on the sorption behaviour of selenite in an acidic, nutrient-poor boreal bog. *J. Environ. Radioact.* 147, 85-96.

Lusa, M, Lehto, J, Aromaa, H, Knuutinen, J, Bomberg, M, 2016. The uptake of radioiodide by *Paenibacillus* sp., *Pseudomonas* sp., *Burkholderia* sp. and *Rhodococcus* sp. isolated from a boreal nutrient-poor bog. *J. Environ. Sci.* 44, 26-37.

## Radiocaesium in the North Pacific Ocean derived from atmospheric weapons tests and Fukushima accident: past and present

Michio Aoyama

Keywords: radiocaesium, Fukushima accident, atmospheric weapons tests, North Pacific Ocean,  
Presenting author email: r706@ipc.fukushima-u.ac.jp

### 1, Two major sources terms of radiocaesium to the Ocean from the Fukushima accident and fallout from atmospheric weapons tests before the accident

The  $^{137}\text{Cs}$  derived from atmospheric weapons test conducted late 1950s and early 1960s and the inventory in the North Pacific Ocean in 1970 was  $290 \pm 30$  PBq (Aoyama et al., 2006). Some portion of the  $^{137}\text{Cs}$  in the North Pacific Ocean were transported to South Pacific Ocean and Indian Ocean and also radioactive decay occurred with a half-life of 30.7 years, the  $^{137}\text{Cs}$  inventory in the North Pacific Ocean before the FNPP1 accident decreased to  $69 \pm 7$  PBq as of 2011 (Aoyama et al., 2016).

There are two major sources of radionuclides to the environment derived by the TEPCO Fukushima Dai-ichi Nuclear Power Plant (FNPP1) accident in 2011. The largest and earliest source of artificial radionuclide was atmospheric release from FNPP1, which led to atmospheric deposition on both land and in the ocean. Atmospheric release peaked mid of March 2011 and total amount of atmospheric release of  $^{137}\text{Cs}$  was estimated to be 15.2-20.4 PBq and same amount of  $^{134}\text{Cs}$  was also released because activity ratio of  $^{134}\text{Cs}$  vs.  $^{137}\text{Cs}$  was almost 1 (Aoyama et al., 2016). About 20 % of released radiocaesium fell on land and 80% of released radiocaesium fell on the ocean. Therefore 11.7-14.8 PBq of  $^{137}\text{Cs}$  was injected in the North Pacific Ocean as atmospheric deposition.

Second largest source was the direct discharge of contaminated waters to the ocean since 26 March 2011 and peaked on 6 April 2011 based on analysis of  $^{131}\text{I}$  vs.  $^{137}\text{Cs}$  activity ratio (Tsumune et al., 2012). Total amount of released  $^{137}\text{Cs}$  was estimated to be  $3.5 \pm 0.7$  PBq. A combined input to the North Pacific Ocean of  $^{137}\text{Cs}$  from both atmospheric deposition and direct discharge was therefore estimated to be 15.2 – 18.3 PBq. Thus, the  $^{137}\text{Cs}$  derived from the Fukushima accident increased the  $^{137}\text{Cs}$  inventory by up to 22–27 %.

### 2, Three major pathways of FNPP1 derived radiocaesium in the North Pacific Ocean

The fastest pathway of FNPP1 derived radiocaesium might be surface pathway. FNPP1-derived radiocaesium injected at north of Kuroshio front by atmospheric deposition and direct discharge spread eastward in surface water up to 200 meters by the North Pacific Current across the mid-latitude North Pacific (Aoyama et al., 2016). In 2013 main body of FNPP1 radiocaesium in surface layer was already in the eastern Pacific. A model simulation (Tsubono et al., 2016) also shows good agreement with the observed radiocaesium activities in the Pacific Ocean reported by several studies.

The second pathway is subduction of central mode water (CMW). A maximum of radiocaesium activity in June/July 2012 was observed at potential densities of 26.1–26.3 at 34 deg. N–39 deg. N, 165 deg. E, which

correspond to 400 meters depth. The density is in a range of density of CMW and radiocaesium activity was higher than those in the surrounding waters, including STMW. In June-July 2015 and June 2016 at 36°N–44°N along 165°E, there are only very weak signal of subduction of FNPP1 radiocaesium. This means that subducted radiocaesium might move eastward from this region. Before the Fukushima accident,  $^{137}\text{Cs}$  maximum corresponding CMW region was observed, however, it located at 20°N, 165°E because it was 40 years after subduction (Aoyama et al., 2008).

The third pathway is subduction of subtropical mode water (STMW). FNPP1-derived radiocaesium injected at south of Kuroshio front by atmospheric deposition transported to southward rapidly due to subduction of STMW at potential densities of 25.1–25.3. In 2015 along 165 deg. E, FNPP1 radiocaesium corresponding STMW spread entire subtropical gyre and a part of them reached 2 deg. N and recirculated in the subtropical gyre and reached Japanese coast.

This study was supported by Houshanou-chousa-kenkyuhi, FY2011–2014 and KAKENHI No. #24110005 of Ministry of Education, Culture, Sports, Science and Technology (MEXT), Japan.

Aoyama, M., Hirose, K. and Igarashi, Y. (2006) 'Reconstruction and updating our understanding on the global weapons tests  $^{137}\text{Cs}$  fallout', *J Environ Monit*, 8(4), pp. 431-8.

Aoyama, M., Hirose, K., Nemoto, K., Takatsuki, Y. and Tsumune, D. (2008) 'Water masses labeled with global fallout  $^{137}\text{Cs}$  formed by subduction in the North Pacific', *Geophysical Research Letters*, 35(1), pp. L01604.

Aoyama, M., Kajino, M., Tanaka, T. Y., Sekiyama, T. T., Tsumune, D., Tsubono, T., Hamajima, Y., Inomata, Y. and Gamo, T. (2016) ' $^{134}\text{Cs}$  and  $^{137}\text{Cs}$  in the North Pacific Ocean derived from the March 2011 TEPCO Fukushima Dai-ichi Nuclear Power Plant accident, Japan. Part two: estimation of  $^{134}\text{Cs}$  and  $^{137}\text{Cs}$  inventories in the North Pacific Ocean', *Journal of Oceanography*, 72(1), pp. 67-76.

Tsubono, T., Misumi, K., Tsumune, D., Bryan, F. O., Hirose, K. and Aoyama, M. (2016) 'Evaluation of radioactive cesium impact from atmospheric deposition and direct release fluxes into the North Pacific from the Fukushima Daiichi nuclear power plant', *Deep Sea Research Part I: Oceanographic Research Papers*, 115, pp. 10-21.

Tsumune, D., Tsubono, T., Aoyama, M. and Hirose, K. (2012) 'Distribution of oceanic  $^{137}\text{Cs}$  from the Fukushima Dai-ichi Nuclear Power Plant simulated numerically by a regional ocean model', *J Environ Radioact*, 111, pp. 100-108.



## Atmosphere and marine impacts of the Fukushima Daiichi NPP accident: five years trends of Fukushima-derived radionuclides.

K. Hirose

Department of Materials and Life Sciences, Faculty of Science and Technology, Sophia University, 7-1 Kioicho, Chiyodaku, Tokyo 102-8554, Japan

Keywords: Fukushima NPP,  $^{137}\text{Cs}$ , atmosphere, marine.

Presenting author email: hirose45037@mail2.accsnet.ne.jp

On 11 March 2011, the Richter scale 9.0 magnitude earthquake, so called “the 2011 Great East Japan Earthquake”, and Tsunami struck the northeast coast of Japan, resulting in widespread injury and loss of life. These natural disasters caused severe accident in the Fukushima Dai-ichi nuclear power plant (FDNPP). As a result, large amounts of radionuclides have been released in the environment (Hirose, 2016; Povinec et al., 2013). The released radionuclides, typically  $^{131}\text{I}$  and radiocesium, had been globally measured in environmental samples. After the initial emission in March 2011, the atmospheric emission rates of the FDNPP-derived radionuclides decreased rapidly. As a result, the global atmospheric effects of the FDNPP-derived radionuclides disappeared until the end of April 2011. However, local and regional effects of the FDNPP-derived radionuclides have continued in the atmosphere and marine environments; monthly deposition of  $^{137}\text{Cs}$  at monitoring sites within about 300 km from the FDNPP exceeded a pre-FDNPP accident level until early 2013, and  $^{137}\text{Cs}$  concentrations in coastal waters near FDNPP increased sporadically increased more than  $1 \text{ kBq m}^{-3}$  until early 2015.

In this paper, I review 5-years monitoring results conducted by Japanese government, local governments and Tokyo Electric Power Company.

### Effects to Atmospheric Environment

Although more than five years have passed since the FDNPP accident happened, Japanese government, research institutes and university have continuously monitored the FDNPP-derived radionuclides in the atmospheric and marine samples. Major target radionuclides are  $^{134}\text{Cs}$ ,  $^{137}\text{Cs}$  and  $^{90}\text{Sr}$  due to their long radioactive half-lives and potential possibility of post-accident releases.

The monitoring results revealed that  $^{137}\text{Cs}$  has been detected in monthly deposition samples collected at monitoring sites located in Kanto Plain and central Tohoku region in 2016. The high monthly  $^{137}\text{Cs}$  deposition at a site (Futaba) near the FDNPP ( $2000 \text{ Bq m}^{-2}$ ) was observed in January 2016. The monthly  $^{137}\text{Cs}$  deposition rapidly decreased with an apparent half-life of about 12 days during the period of March to June 2011. However, the decrease rate of the monthly  $^{137}\text{Cs}$  deposition slowed down. Since 2012, the monthly  $^{137}\text{Cs}$  deposition decreased with an apparent half-life of about 1 year at the monitoring sites within about 300 km from the FDNPP. Long-term atmospheric effects of the

FDNPP-derived  $^{137}\text{Cs}$  may be supported by post-accident emission of radionuclides from the FDNPP and natural and anthropogenic processes such as resuspension, production of  $^{137}\text{Cs}$ -bearing bio aerosols (Kajino et al., 2016) and others.

### Effects to Marine Environment

Concentrations of  $^{134}\text{Cs}$  and  $^{137}\text{Cs}$  in coastal waters near the FDNPP abruptly increased due to direct discharge of radioactive contaminated water and atmospheric deposition just after the FDNPP accident. The  $^{137}\text{Cs}$  concentrations in coastal waters rapidly decreased after cease of the direct discharge in early April 2011. The decrease rate of the  $^{137}\text{Cs}$  concentrations in coastal waters, which were related to release from the FDNPP, slowed down since May 2011. The  $^{137}\text{Cs}$  concentrations in coastal waters near the FDNPP were less than  $1 \text{ kBq m}^{-3}$  after October 2015. The  $^{137}\text{Cs}$  concentrations in coastal waters within 20 km from the FDNPP except two sites near the FDNPP were in the range of  $2$  to  $200 \text{ Bq m}^{-3}$  during the period of January 2015 to July 2016, which are still higher than background value. However, the enhanced  $^{137}\text{Cs}$  concentration in coastal waters near the FDNPP ( $>1 \text{ kBq m}^{-3}$ ) occurred in August 2016 after heavy rainfall accompanied with passages of typhoons.

The monitoring results reveal that there is possibility of the sporadic increase of the FDNPP-derived radionuclides in atmosphere and marine environments due to anthropogenic and natural events, although the effects of the FDNPP-derived radionuclides in atmosphere and marine environments decline gradually.

Hirose, K., 2016. Fukushima Daiichi Nuclear Power Plant Accident: Atmospheric and oceanic impacts over the five years. *J. Environ. Radioact.* 157, 1-18.

Kajino, M., Ishizuka, M., Igarashi, Y., Kita, K., Yoshikawa, C., Inatsu, M., 2016. Long-term assessment of airborne radiocesium after the Fukushima nuclear accident: re-suspension from bare soil and forest ecosystems. *Atmos. Chem. Phys.*, 16, 13149-13172.

Povinec, P.P., Hirose, K., Aoyama, M., 2013. Fukushima Accident: Radioactivity impact on the environment, Elsevier.

## Radiocesium contamination in the North Pacific Ocean after 2011 Fukushima Nuclear accident

G.H. Hong, S.H. Kim and H. Lee

Marine Radionuclide Research Center, Korea Institute of Ocean Science & Technology, Ansan, 15627, R. Korea

Keywords: Fukushima, radiocesium, Korea, Pacific Ocean.

Presenting author email: ghhong@kiost.ac.kr

Concentrations of radiocesium had been determined in the surface seawater and the fishery product of the several regions in the Pacific Ocean from 2012 to 2014 after 2011 Fukushima Nuclear accident following the 11 March 2011 Great East Japan Earthquake.  $^{134}\text{Cs}$  originated from Fukushima via wind was detected up to 1.10 mBq/kg in the surface seawater around Korean peninsula from March to June 2011. This is supported by the analysis of air mass back trajectory and atmospheric pressure systems which the Fukushima-derived radiocaesium had predominantly reached South Korea from the west by surface westerlies from 11 March to 5 April; however, after 6 April, air masses arrived from Japan directly due to a high pressure system that developed in the east of Japan (Hong et al., 2012). But  $^{134}\text{Cs}$  was not found in the fishery products caught in the sea areas around Korean peninsula from 2011 to 2013. Surface seawater were collected using six times of ships of opportunity of R/V Araon and R/V Onnuri in the Pacific Ocean from 2012 to 2014: three cruises in the Subarctic Pacific Ocean from Korea to Alaska, USA from 2012 to 2014; the northwest Pacific region of Kuroshio Current in June 2012, and line of Hawaii to Korea in September and October 2013, and in the crossing line between the North Pacific Ocean and the South Pacific Ocean from Korea to Christchurch, New Zealand in October and November 2013. Concentration of radiocesium was observed up to  $8.95 \pm 0.64$  mBq/kg of  $^{137}\text{Cs}$  and  $6.24 \pm 0.89$  mBq/kg of  $^{134}\text{Cs}$  in the surface waters of the subarctic North Pacific Ocean in July 2012.  $^{134}\text{Cs}$  activity concentrations were in the range of 0.23 - 0.29 mBq/kg in the surface waters of the East China Sea in June 2012.  $^{137}\text{Cs}$  activity concentrations were in the range of 2.40 - 2.76 mBq/kg and maximum level of  $^{134}\text{Cs}$  was found to be  $0.97 \pm 0.29$  mBq/kg in  $140^\circ\text{E}$  -  $150^\circ\text{E}$  of  $31^\circ\text{N}$  in the Pacific Ocean in October 2013. The presence of  $^{134}\text{Cs}$  ( $\sim < 1$  mBq/kg) was evident in the subarctic Pacific Ocean until 2014. However,  $^{134}\text{Cs}$  was not detected (detection limit  $\cong 0.2$  mBq/kg) in the surface water of the southbound cruise line from Korea to Christchurch, New Zealand in October and November 2013. Radiocesium was determined in the fishes caught in the marginal seas of the Pacific Ocean and the Pacific Ocean in 2012.  $^{137}\text{Cs}$  of  $2.69 \pm 0.26$  and  $^{134}\text{Cs}$  of  $1.81 \pm 0.44$  Bq/kg-fresh weight were found in the muscle tissue of mackerel caught in the Pacific Ocean near from Fukushima. And  $^{134}\text{Cs}$  was not detected (detection limit  $\cong 0.04$  Bq/kg-fresh weight) in the fishes caught in any other regions of the Pacific Ocean in 2012.

This work was funded by grants from the Korea Institute of Ocean Science & Technology (PE99403) and the Ministry of Food and Drug Safety (PG48320).

Hong, G.H., Hernández-Ceballos, M.A., Rozano, R.L., Kim, Y.I., Lee, H.M., Kim, S.H., Yeh, S-W., Bolívar, J.P. Baskaran, M.A. 2012. Radioactive impact in South Korea from the damaged nuclear reactors in Fukushima: evidence of long and short range transport. *J. Radiol. Prot.* 32, 397-411.

## Characteristics of artificial radionuclides in the food stuffs in Korea

S.H. Lee<sup>1</sup>, J.S. Oh<sup>1</sup>, J.M. Lee<sup>1</sup>, k. B. Lee<sup>1</sup>, J.Y. Yun<sup>2</sup>

<sup>1</sup>Center for ionizing radiation, Korea Research Institute of Standards and Science, Daejeon, 34113, Republic of KOREA

<sup>2</sup>Center for Environment Radiation and Radioactivity Assessment, Korea Institute of Nuclear Safety, Daejeon, 34142, Republic of KOREA

Keywords: Fukushima, food, monitoring, radionuclide.

Presenting author email: s.lee@kriss.re.kr

A large amount of artificial radionuclides were released into the environment as a result of the Fukushima Daiichi NPP accident occurred in March 11<sup>th</sup>, 2012. The public concerns have been growing on the food safety in terms of radionuclide contamination because of its radiological toxicity. Numerous number of radioactivity monitoring programme are being performed, not only on the agricultural products but also the seafood stuffs.

This study introduces the recent results of artificial radionuclides such as <sup>137</sup>Cs, <sup>239,240</sup>Pu and <sup>90</sup>Sr in the foods.

The activity concentration of <sup>137</sup>Cs in the foods produced from the terrestrial environment ranged from MDA (minimum detectable activity) to 41 Bq/kg (fresh weight) (Table 1). Most products grown in the rice paddy, the farm and the field showed the levels of <sup>137</sup>Cs below MDA, however, the elevated activity concentrations of <sup>137</sup>Cs were found in the mushrooms and brackens grown in the forest. Nevertheless, the highest level of <sup>137</sup>Cs observed from the study is lower than current national food safety control level (100 Bq/kg).

Table 1. Massic activities of <sup>137</sup>Cs in the mushroom and bracken samples collected from Korea

Species	<sup>137</sup> Cs (Bq/kg, fresh weight)
<i>Lentinula edodes</i>	0.14-3.18
<i>Sarcodon aspratus</i>	1.4-41
<i>Tricholoma Matsutake</i>	1.3-1.4
<i>Boletopsis leucomelas</i>	4.80
<i>Tricholomopsis rutilans</i>	1.30
<i>Collybia confluens</i>	7.60
<i>Sparassis crispa</i>	0.65
<i>Selaginella involvens</i> SPRING	0.54
<i>Pteridium aquilinum</i> var. <i>latius</i>	0.3-2.6

In all fish samples, massic activities of <sup>137</sup>Cs showed the radioactive concentration less than 1 Bq/kg (fresh weight). It is noted that the highest activity of <sup>137</sup>Cs was observed in the tuna fish that is well known as a top-level predator. The <sup>90</sup>Sr and <sup>239,240</sup>Pu were determined using the radioanalytical technique and the results were presented in Table 3. Although we employed a large quantity of samples (a few kgs) for the detection of <sup>90</sup>Sr and <sup>239,240</sup>Pu, most of seafood samples gave the MDA for <sup>90</sup>Sr.

The <sup>239,240</sup>Pu concentration in the fish is much lower than

ones observed in the seaweed samples and shellfish samples. Various parameters such as the plutonium's high particle affinity, vegetation and particle ingestion by shellfish could cause the different distribution of Pu among seafood samples.

Table 2. Massic activities of <sup>90</sup>Sr and <sup>239,240</sup>Pu in the fish, seaweed and shellfish samples collected from seas around Korea

Species	<sup>90</sup> Sr in fish (mBq/kg, fresh weight)	<sup>239,240</sup> Pu in fish (mBq/kg, fresh weight)
<i>Pleurogrammus azonus</i>	MDA	MDA
<i>Mugil cephalus</i>	20	0.079
<i>Paralichthys olivaceus</i>	MDA	0.045
<i>Pleuronichthys cornutus</i>	MDA	MDA
Species	<sup>90</sup> Sr in seaweed (mBq/kg, fresh weight)	<sup>239,240</sup> Pu in seaweed (mBq/kg, fresh weight)
<i>Undaria pinnatifida</i>	<11.9	2.6
<i>Sargassum fusiforme</i>	<14.1	2.0
Species	<sup>90</sup> Sr in shellfish (mBq/kg, fresh weight)	<sup>239,240</sup> Pu in shell fish (mBq/kg, fresh weight)
<i>Buccinidae</i>	<5.60	2.6
<i>Mytilus coruscus</i>	<7.7	1.2
<i>Atrina(Servatrina) pectinata</i>	<5.3	0.8

The atom ratio of Pu isotopes was determined using ICP-MS to identify their source. The fish samples, seaweed samples and shellfish samples presented 0.227 to 0.238 (mean value of 0.231), 0.233-0.238 (mean value of 0.236) and 0.206 to 0.240 (mean value of 0.227), respectively. The mean atom ratios found in the seafood in this study are corresponding to those measured in the seawater collected seas around the Korean Peninsula before the Fukushima NPP accident (Kim et al., 2004). Therefore, the artificial radionuclide found in the foods is thought to be originated from the global fallout rather than the FDNPP accident.

This work was supported by the Ministry of Food and Drug Safety under grant 15162 radioactivity 681.

Kim, C. K., Kim, C. S., Chang, B.U., Choi, S.W., Chung, C.S., Hong, G.H., Hirose, K., Igarashi, Y. 2004. Plutonium isotopes in seas around the Korean Peninsula. *Sci Total Environ.* 318(1-3),197-209.

## Food Safety after the Fukushima Nuclear Accident

G. Steinhauser<sup>1</sup>

<sup>1</sup>Institute of Radioecology and Radiation Protection, Leibniz Universität Hannover, 30419 Hannover, Germany

Keywords: Fukushima, food, radiocesium, radiostrontium

Presenting author email: steinhauser@irs.uni-hannover.de

The Fukushima nuclear accident (March 11, 2011) was the severest nuclear accident since Chernobyl. Ingestion of contaminated food is the most significant route of exposure to the general public and was taken very seriously by the Japanese authorities, as they initiated an unprecedented food monitoring campaign (Merz et al., 2015). In my presentation, I will give an overview on the characteristics of the monitoring, achievements and shortcomings.

Some food items were monitored with incredible density. Rice was monitored with a coverage of 100% (Nihei et al., 2015). In 2012, 72 rice bags of more than 10,000,000 exceeded the regulatory limit of 100 Bq/kg (Nihei et al., 2015).

Other foods, including beef, exhibited some problems in the monitoring. Here, food inspections began with delay and caused some above-limit items to reach the market (Steinhauser, 2017).

Overall, the monitoring for food was very effective and kept the Japanese population safe from the adverse health effects of radiation. In my presentation, I will also comment on quite recent reports of a drastically increased thyroid cancer cases and how these reports shall be viewed in the light of the obvious successes in food monitoring.

Merz S., Shozugawa K., Steinhauser G., 2015. Analysis of Japanese radionuclide monitoring data of food before and after the Fukushima nuclear accident.

*Environ. Sci. Technol.* 49, 2875-2885.

Nihei N., Tanoi K., Nakanishi T.M., 2015. Inspections of radiocesium concentration levels in rice from Fukushima Prefecture after the Fukushima Dai-ichi Nuclear Power Plant accident. *Sci. Rep.* 5, 8653.

Steinhauser G., 2017. Monitoring and radioecological characteristics of radiocesium in Japanese beef after the Fukushima nuclear accident. *J. Radioanal. Nucl. Chem.* 311, 1367-1373.

## Estimations of direct release rate of $^{137}\text{Cs}$ , $^{90}\text{Sr}$ and $^3\text{H}$ from the Fukushima Dai-ichi Nuclear Power Plant for four-and-a-half years

D. Tsumune<sup>1</sup>, M. Aoyama<sup>2</sup>, K. Hirose<sup>3</sup>, T. Tsubono<sup>1</sup>, K. Misumi<sup>1</sup> and Y. Tateda<sup>1</sup>

<sup>1</sup>Central Research Institute of Electric Power Industry, Abiko, Chiba, 270-1194, Japan

<sup>2</sup>Institute of Environmental Radioactivity, Fukushima University, Fukushima, Fukushima 960-1296, Japan

<sup>3</sup>Faculty of Science and Technology, Sophia University, Chiyodaku, Tokyo, 102-8554, Japan

Keywords: Fukushima Dai-ichi Nuclear Power Plant accident,  $^{137}\text{Cs}$ ,  $^{90}\text{Sr}$ ,  $^3\text{H}$ , Regional ocean model

Presenting author email: tsumune@criepi.denken.or.jp

A series of accidents at the Fukushima Dai-ichi Nuclear Power Plant (1F NPP) following the earthquake and tsunami of 11 March 2011 resulted in the release of radioactive materials to the ocean by two major pathways, direct release from the accident site and atmospheric deposition. Additional release pathways by river input and runoff from 1F NPP site with precipitation and were also effective for coastal zone in the specific periods before starting direct release on March 26 2011. The activities attributable to the direct release were observed adjacent to the 1F NPP site. The sea side impermeable wall was closed at 26 October 2015. We estimated the direct release rate of  $^{137}\text{Cs}$ ,  $^{90}\text{Sr}$  and  $^3\text{H}$  for more than four-and-a-half years after the accident by the Regional Ocean Model System (ROMS).

Direct release rate of  $^{137}\text{Cs}$  were estimated by comparing simulated results and measured activities adjacent to the 1F NPP site (at 5,6 discharge and south discharge, Tsumune et al., 2012; 2013)(Figure 1). Direct release rate of  $^{137}\text{Cs}$  was estimated to be  $2.2 \times 10^{14}$  Bq/day and decreased exponentially with time to be  $3.9 \times 10^9$  Bq/day by 26 October 2015. Estimated direct release rate have exponentially decreased with constant rate since 4 November 2011. Apparent half-life of direct release rate was estimated to be 346 days. The estimated total amounts of directly released  $^{137}\text{Cs}$  was  $3.6 \pm 0.7$  PBq from 26 March 2011 to 26 October 2015. Simulated  $^{137}\text{Cs}$  activities attributable to direct release were in good agreement with observed activities, a result that implies the estimated direct release rate was reasonable. Simulated  $^{137}\text{Cs}$  activity affected off coast in the Fukushima prefecture.

$^{90}\text{Sr}/^{137}\text{Cs}$  activity ratio of stagnant water was 0.05 in the basement of the 1F NPP reactor 2 turbine building on 27 March 2011(Nishihara et al., 2012). Direct release rate of  $^{90}\text{Sr}$  was estimated to be  $1.1 \times 10^{13}$  Bq/day from 26 March to 6 April 2011 using the activity ratio in stagnant water because the stagnant water released to the ocean in this period (Tsumune et al., 2012). And the temporal change of direct release rate was estimated by the measured  $^{90}\text{Sr}$  activity adjacent to 1F NPP (Figure 1). Directly release rate decreased exponentially to  $3.9 \times 10^{10}$  Bq/day by 30 April 2011. The direct release rate was constant and decreased exponentially from 27 June to 16 December 2013. And the direct release rate was  $2.9 \times 10^9$  Bq/day by 26 October 2015. The estimated total amounts of directly released  $^{90}\text{Sr}$  was  $208 \pm 42$  TBq.

$^3\text{H}/^{137}\text{Cs}$  activity ratio of stagnant water was  $8.7 \times 10^{-3}$  in the basement of the 1F NPP reactor 2 turbine building on 27 March 2011(Nishihara et al., 2012). Directly release rate of  $^3\text{H}$  was estimated to be  $1.9 \times 10^{12}$  Bq/day from 26 March to 6 April 2011 and decreased exponentially by 16 April 2011. The rate was decreased exponentially with constant rate by 26 October 2015. The direct release rate was estimated to be  $7.7 \times 10^9$  Bq/day at 26 October 2015. The estimated total amounts of directly released  $^3\text{H}$  was  $131 \pm 26$  TBq.

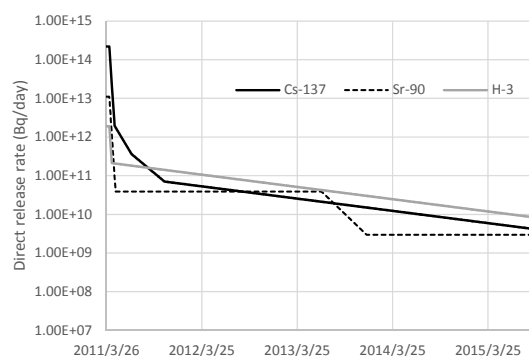


Figure 1. Estimated direct release rates of  $^{137}\text{Cs}$ ,  $^{90}\text{Sr}$  and  $^3\text{H}$  from 26 March 2011 to 26 October 2015.

This work was supported in part by a Grant-in-Aid for Scientific Research (A) (No. 23253001) from Ministry of Education, Culture, Sports, Science and Technology (MEXT), Japan.

Nishihara et al., 2012. Radionuclide Release to Stagnant Water in Fukushima 1 Nuclear Power Plant, Journal of Atomic Energy Society of Japan, doi:10.3327/taesj.J11.040 (In Japanese)

Tsumune, D., Tsubono, T., Aoyama, M., Hirose, K., 2012. Distribution of oceanic  $^{137}\text{Cs}$  from the Fukushima Daiichi Nuclear Power Plant simulated numerically by a regional ocean model, J. Environ. Radioact., 111, 100-108.

Tsumune, D., Tsubono, T., Aoyama, M., Uematsu, M., Misumi, K., Maeda, Y., Yoshida, Y., and Hayami, H., 2013. One-year, regional-scale simulation of  $^{137}\text{Cs}$  radioactivity in the ocean following the Fukushima Dai-ichi Nuclear Power Plant accident, Biogeosciences, 10, 5601-5617.



## Tritium and radiocarbon in western North Pacific waters: post-Fukushima situation

J. Kaizer<sup>1</sup>, P.P. Povinec<sup>1</sup>, M. Aoyama<sup>2</sup>, Y. Kumamoto<sup>3</sup>, M. Molnár<sup>4</sup> and L. Palcsu<sup>4</sup>

<sup>1</sup>Faculty of Mathematics, Physics and Informatics, Comenius University, 84248 Bratislava, Slovakia

<sup>2</sup>Institute of Environmental Radioactivity, Fukushima University, 1-1 Kanayagawa, Fukushima, Japan

<sup>3</sup>Research and Development Center for Global Change, Japan Agency for Marine-Earth Science and Technology, 2-15 Natushima-cho, Yokosuka, Kanagawa 237-0061, Japan

<sup>4</sup>Institute of Nuclear Research (ATOMKI), 4026 Debrecen, Hungary

Keywords: tritium, radiocarbon, Fukushima, North Pacific.

Presenting author email: kaizer@fmph.uniba.sk

The Fukushima Dai-ichi nuclear power plant (FDNPP) accident in 2011 resulted in significant releases of anthropogenic radionuclides into the environment. One of the most affected regions was undoubtedly the North Pacific Ocean whose radionuclide inventories were increased mainly through direct discharges of radioactive waters and by atmospheric deposition. Even though overall concentrations of long-lived radionuclides are very low in North Pacific waters, thus not posing radioecological problems for the marine environment, understanding of their distribution, which was disturbed after the Fukushima accident, can be important for oceanographic or climate change studies.

Tritium and radiocarbon belong into a group of radionuclides which have been studied post-Fukushima less frequently. In agreement with the expectance, releases of tritium and radiocarbon have been found much lower than e.g. releases of <sup>137</sup>C. Povinec et al. (2017) showed that tritium levels in waters offshore Fukushima were above the global fallout background by about factor of 6 only.

Regarding radiocarbon, recent data measured offshore Fukushima suggested that radiocarbon levels exceeded the background only by 9% (Povinec et al., 2017). Additionally, possible radiocarbon contribution of Fukushima were investigated by Xu et al. (2015) in tree rings of the Japanese cedar (originating from Iwaki, the Fukushima prefecture) who found a slightly higher <sup>14</sup>C concentration in the 2011 sample which may imply a release of radiocarbon during the FDNPP accident.

In this work, we shall present tritium and radiocarbon concentrations in surface water and water column samples collected from December 2011 to February 2012. The sampling sites were located approximately along the 149°E line, from the subarctic to the tropical region (42°N-4°S). Radiocesium levels in this specific transect were recently determined by Kumamoto et al. (2015), who concluded that the impact of the FDNPP accident in the western North Pacific in winter 2012 was almost the same as of global fallout which resulted from atmospheric nuclear weapons test.

Distribution of radiocarbon in surface waters of the investigated area shows a pattern typical for the western North Pacific Ocean. While the lowest value was determined on the site in the subarctic region, <sup>14</sup>C levels gradually increased downwards to the South Equatorial Current (Figure 1); the highest concentration was found in the subtropical area (149°20'E, 28°30'N). On top of that, we observed subsurface (depth range of

100-200 m) maxima of <sup>14</sup>C concentration in the vertical profiles of a few sampling locations. Similar results will be presented in the case of tritium measurements.

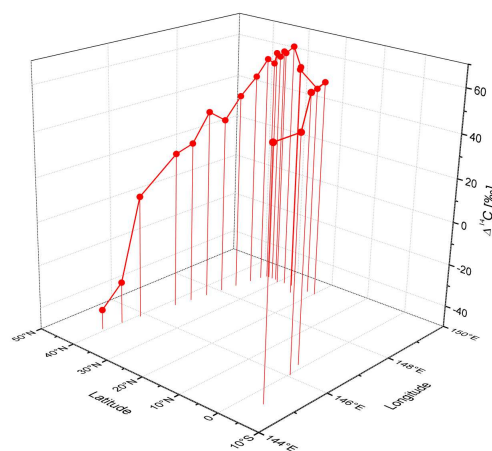


Figure 1 Radiocarbon concentration in surface waters of the North Pacific Ocean.

This work was supported by the EU Research and Development Operational Program funded by the ERDF (project No. 26240220004), and by the International Atomic Energy Agency (TC project SLR9013).

Kumamoto, Y., Aoyama, M., Hamajima, Y., Murata, A., Kawano, T., 2015. Impact of Fukushima-derived radiocesium in the western North Pacific Ocean about ten months after the Fukushima Dai-ichi nuclear power plant accident. *J. Environ. Radioact.* 140, 114-122.

Povinec, P.P., Liang Wee Kwong, L., Kaizer, J., Molnár, M., Nies, H., Palcsu, L., Pham, M.K., Jean-Baptiste, P., 2017. Impact of the Fukushima accident on tritium, radiocarbon and radiocesium levels in seawater of the western North Pacific Ocean: A comparison with pre-Fukushima situation. *J. Environ. Radioact.* 166, 56-66.

Xu, S., Cook, G.T., Creswell, A.J., Dunbar, E., Freeman, S.P.H.T., Hastie, H., Hou, X., Javobsson, P., Naymish, P., Sanderson, D.C.W., 2015. Radiocarbon concentrations in modern tree rings from Fukushima, Japan. *J. Environ Radioact.* 146, 67-72.



## Reconstruction of temporal change of radiocesium level in bottom sediment off Fukushima for evaluating contribution to benthic food chain transfer

Y. Tateda<sup>1</sup>, K. Misumi<sup>1</sup>, D. Tsumune<sup>1</sup>, M. Aoyama<sup>2</sup>, Y. Hamajima<sup>3</sup>, J. Kanda<sup>4</sup>, T. Ishimaru<sup>4</sup>, and T. Aono<sup>5</sup>

<sup>1</sup>Environmental Science Research Laboratory, Central Research CRIEPI, Abiko, Chiba, 270-1194, Japan

<sup>2</sup>Institute of Environmental Radioactivity, Fukushima University, Kanayagawa, Fukushima, 960-1296, Japan

<sup>3</sup>Institute of Nature and Environmental Technology, Kanazawa University, Nouni, Ishikawa, 923-1224, Japan

<sup>4</sup>Department of Ocean Science, Tokyo University of Marine Science and Technology, Minato, Tokyo, 108-8477, Japan

<sup>5</sup>Fukushima Project Headquarter, National Institute of Radiological Sciences, Inage-ku, Chiba, 263-8555, Japan

Keywords: radiocesium, Fukushima nuclear power plant accident, sediment, dynamic model

Presenting author email: tateda@criepi.denken.or.jp

The accident of Fukushima Dai-ichi Nuclear Power Plant (1FNPP) released radiocesium to the coastal waters along eastern Japan. Introduced radiocesium was transferred and distributed to continental shelf bottom (Ambe et al., 2014). Though radiocesium in marine sediment were mostly insoluble, labile fraction in fine sediment may be suggested to be transferred to benthos (Wang et al., 2016) and to demersal fish which feeds benthos (Tateda et al., 2016). To evaluate sediment contribution in radiocesium transfer through benthic food chain, temporal change data set of radiocesium level in sediment is necessary, because of kinetic transfer under transition state in case of short term introduction. We focus on fine particle which was commonly ingested by benthic biota, and apply dynamic model to reconstruct temporal radiocesium levels in sediment to understand its contribution as bioavailable component.

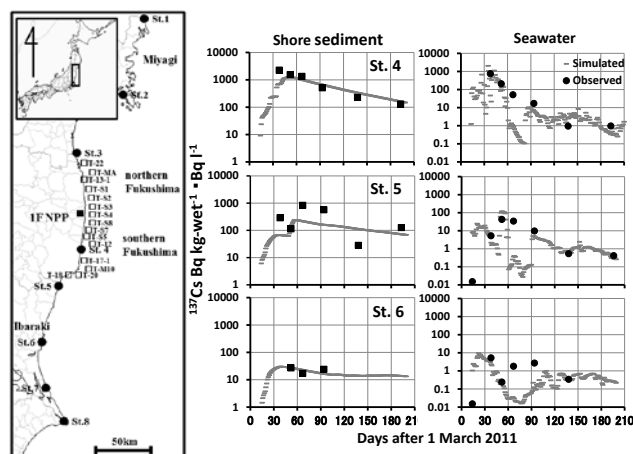


Figure 1. Study sites and simulated and observed <sup>137</sup>Cs levels in shore sediment of St. 4 to 6.

### Methods

Using the observed <sup>137</sup>Cs concentrations in bulk shore sediments and seawater at three coastal study sites (from St. 4 to 6, 30 to 80km south from 1FNPP, Fig. 1) those sampled during April to September 2011, the absorption/desorption kinetic parameters were derived. Temporal change of radiocesium concentrations in fine sediment (particle size < 75 μm) at seabed surface of 18 field study sites (from TS1 to St.8) off Fukushima were simulated from 2011 to 2014 by numerical model (Misumi et al., 2014) using derived transfer parameters. Calculated result was validated by measured <sup>137</sup>Cs concentrations in surface sediment collected by Research cruse UM-13-05 (Umitaka-maru, Tokyo University of Marine Science and Technology), SY-13-10 (Shinyo-maru) and Grant-in Aid field survey research program.

### Results

Filed absorption and desorption parameters were estimated as within ranges of 0.1 to 0.7 and 0.01 to 0.02 d<sup>-1</sup>, respectively, and the simulated levels were well agreed to observed concentrations at Fukushima southern coastal shore (Fig. 1). The radiocesium levels in bottom sediment of the Fukushima accident affected coastal bottom were reconstructed as levels normalized by particle size of <75 μm, those were commonly found in gut content of demersal fish which feeds benthos.

Part of this work was supported by the Grant-in-Aid for Scientific research on Innovative Areas Grant Number 2411005.

- Ambe, D., Kaeriyama, H., Shigenobu, Y., Fujimoto, K., Ono, T., Sawada, H., Saito, H., Miki, S., Setou, T., Morita, T., Watanabe, T., 2014. Five-minute resolved spatial distribution of radiocesium in sea sediment derived from the Fukushima Dai-ichi Nuclear Power Plant. *J. Environ. Radioact.* 138, 264-275.
- Wang, C., Baumann, Z., Madigan, D., Fisher, S., 2016. Contaminated marine sediments as source of cesium radioisotopes for benthic fauna near Fukushima. *Environ. Sci. Technol.* 50, 10448-10455.
- Tateda, Y., Tsumune, D., Tsubono, K., Misumi, K., Yamada, M., Kanda, J., Ishimaru, T. 2016. Status of <sup>137</sup>Cs contamination in marine biota along the Pacific coast of eastern Japan derived from a dynamic biological model two years simulation following the Fukushima accident. *J. Environ. Radioact.* 151, 495-501.
- Misumi, K., Tsumune, D., Tsubono, K., Tateda, Y., Aoyama, M., Kobayashi, T., Hirose, K. 2014. Factors controlling the spatiotemporal variation of <sup>137</sup>Cs in seabed sediment off Fukushima coast: implications from numerical simulations. *J. Environ. Radioact.* 136, 218-228.

## Time-dependent behaviour analysis and identification of factors affecting radiocaesium transfer to separate sewers in Fukushima Prefecture

M.A. Pratama<sup>1</sup>, S. Takahara<sup>1</sup>, M. Munakata<sup>1</sup> and M. Yoneda<sup>2</sup>

<sup>1</sup>Nuclear Safety Research Centre, Japan Atomic Energy Agency, Tokai-Mura, 319-1195

<sup>2</sup>Graduate School of Engineering, Kyoto University, Kyoto, 615-8245, Japan

Keywords: sewer sludge, radiocaesium, time-dependent

Presenting author email: pratama.mochamadadhiraga@jaea.go.jp

Separate sewers in Fukushima Prefecture have become contaminated by caesium released in March 2011. The time-dependent trend of caesium concentration in sewer sludge shows that they have an agreement with dietary intake of caesium. Considering the sewer sludge mostly consists of human excreta, it gave an opportunity to develop a new method for estimating radionuclide dietary intake based on the time-dependent concentration of caesium in the sludge. Towards the development of the new method, at first, the time-dependent behavior analysis, parameterization, and the identification of factors affecting parameter values were attempted. The analysis was based on the monitoring data of caesium concentration in sewer sludge from 10 wastewater treatment plants (WWTPs) in Fukushima Prefecture collected between 2011 to 2016 (MLIT, 2016).

The concentration of radionuclide in sewer sludge  $C(t)$  (Bq kg<sup>-1</sup>) resulting from the initial deposition  $D$  (Bq m<sup>-2</sup>) is given by

$$C_t(t) = D(A + Be^{-(\lambda+k_1)} + Ce^{-(\lambda+k_2)}) \quad (\text{Eq.1})$$

where  $k_1$  and  $k_2$  (day<sup>-1</sup>) are the fast and slow transfer coefficient, respectively, and  $A$ ,  $B$ , and  $C$  are the empirical coefficient representing the contribution of spontaneous, fast and slow transfer, respectively (Smith et al., 2000). However, not all the parameters are necessarily used since it depends on the best fit to the available data. Thus, several model configurations were set to find the best model that describes the time-dependent pattern of caesium concentration.

Table 1. The coefficient of determination ( $R^2$ ) of fits of various model configuration. FTC stands for failed to converge

WWTP	Determination coefficient $R^2$			
	$A, B, k_1$	$B, k_1$	$B, k_1, C, k_2$	$B, k_1, C$
Nihonmatsu	0.949	0.74	<b>0.957</b>	0.950
Aizuwakamatsu	0.860	0.73	<b>0.963</b>	0.948
Kunimi	0.856	0.6	<b>0.866</b>	0.858
Miharu	0.946	0.91	<b>0.947</b>	0.946
Minamisoma	0.827	0.74	FTC	FTC
Asakawa	0.964	0.95	<b>0.966</b>	0.964
Soma	0.799	0.44	FTC	FTC
Tamura	0.799	0.61	<b>0.979</b>	0.974
Shirakawa	0.930	0.68	<b>0.953</b>	0.933
Aizuwakamatsu 2	0.843	0.65	<b>0.846</b>	0.914

It is clearly seen in Table 1 that the time-dependent caesium concentration follows two exponentials model consisting of  $B$ ,  $k_1$ ,  $C$ , and  $k_2$  (bold font). Though, Minamisoma and Soma were FTC

because the starting point of the data collection was 2 years after the accident. It was likely that only slow transfer remained in the transfer process at those two WWTPs.

Table 2. The summary of the values for the double exponential equation based on 10 WWTPs in Fukushima Prefecture

coefficient	$B$	$k_1$	$C$	$k_2$
mean	0.0134	0.0126	0.0049	0.0015
standard deviation	0.0075	0.0044	0.0054	0.0003

The parameters values of two exponentials model were estimated by least square method and summarized in Table 2. Whereas values for the transfer coefficients are relatively the same between the WWTPs, the values of  $B$  and  $C$  significantly vary depending on the specific characteristic of each WWTP as shown in Table 3.

Table 3. Correlation coefficients ( $r$ ) between values of  $B$  and  $C$ , and various characteristics of the WWTP's service area.

Bold font shows a significant correlation ( $r > 0.5$ )

Parameter	$B$	$C$
percentage of built area ( $BA$ )	<b>0.50</b>	0.17
percentage of non-built area ( $NBA$ )	-0.02	<b>-0.50</b>
average slope of service area ( $s$ )	<b>-0.64</b>	-0.29
annual rainfall ( $R$ )	<b>0.53</b>	-0.20
percentage of decontaminated houses ( $R_{\text{house}}$ )	<b>-0.66</b>	-0.36
percentage of decontaminated public facilities ( $R_{\text{public}}$ )	<b>-0.73</b>	-0.49
percentage of decontaminated roads ( $R_{\text{road}}$ )	<b>-0.62</b>	<b>-0.54</b>

A multiple regression consisting of  $s$  and  $R_{\text{public}}$  gave a strong relationship with  $B$  ( $B=0.028-0.04s-0.01R_{\text{public}}$ ,  $R^2=0.8$ ) whereas the best multiple regression for  $C$  was obtained from  $NBA$  and  $R_{\text{road}}$  ( $C=0.013-0.007R_{\text{road}}-0.02NB$ ,  $R^2=0.7$ ).  $R_{\text{public}}$  has more influence to fast transfer while the slow transfer is more affected by  $R_{\text{road}}$ . This is because,  $R_{\text{public}}$  was set as the priority for the decontamination program. Slow transfer process is also affected by  $NBA$ , as soil on its surface has a strong sorption bond. Thus, the transfer process occurs slowly in a low rate for a long period.

Ministry of Land, Infrastructure, Transport and Tourism of Japan, Results of radioactivity concentration measurement in sewer sludge. *in Japanese*:

[http://www.mlit.go.jp/mizukokudo/sewerae/crd\\_sewerae\\_age\\_tk\\_000168.html](http://www.mlit.go.jp/mizukokudo/sewerae/crd_sewerae_age_tk_000168.html) (Accessed 30 July 2016)

Smith, J. T., Clarke, R. T., Saxén, R. 2000. Time-dependent behavior of radiocaesium: A new method to compare the mobility of weapons test and Chernobyl-derived fallout. *J. Environ. Radioact.* 49, 65–83.

## Measurement of $^{90}\text{Sr}$ activity in Fukushima soil samples affected by Nuclear Accident

S.K. Sahoo, N. Kavasi and T. Aono

Fukushima Research Headquarter, National Institutes for Quantum and Radiological Science and Technology, 4-9-1 Anagawa, Inage-ku, Chiba 263-8555, Japan

Keywords: Fukushima,  $^{90}\text{Sr}$ ,  $^{137}\text{Cs}$ , soil

Presenting author email: sahuo.sarata@qst.go.jp

Fukushima Daiichi Nuclear Power Plant (FDNPP) accident released  $\beta$ -particle emitter fission product,  $^{90}\text{Sr}$ , along with gamma-emitter nuclides, such as  $^{137}\text{Cs}$ ,  $^{134}\text{Cs}$ ,  $^{131}\text{I}$ ,  $^{132}\text{Te}$  into environment.  $^{137}\text{Cs}$ , and  $^{90}\text{Sr}$  have long-lasting radioecological impact due to their longer half-life ( $>30$  y). Furthermore, the  $^{90}\text{Sr}$  has long biological half-life ( $\sim 18$  y) in the human body. Due to its chemical similarity to calcium it accumulates in bones and irradiates the bone marrow, causing its high radiotoxicity.

Assessing  $^{90}\text{Sr}$  in the environment is therefore necessary in case of a nuclear disaster. For  $^{90}\text{Sr}$  measurement, a new separation laboratory was established at the National Institute for Quantum and Radiological Science and Technology, Japan (QST) in 2012.

Fukushima soil samples were collected in 2013. We have observed a weak correlation between  $^{90}\text{Sr}$  and  $^{137}\text{Cs}$  activity concentrations in samples (Figure 1), however, the  $^{90}\text{Sr}$  concentration was lower with three or four magnitudes than  $^{137}\text{Cs}$  (Sahoo et al., 2016, Kavasi et al., 2015)

This work was supported partially by a Grant-in-Aid for Scientific Research (15F14801) from the Japan Society for the Promotion of Science and Fukushima Prefecture related to Research and Development in Radiological Sciences.

Sahoo, S. K., Kavasi, N., Sorimachi, A., Arae, H., Tokonami, S., Mietelski, J.W., Lokas, E., Yoshida, S. 2016. Strontium-90 activity concentration in soil samples from the exclusion zone of the Fukushima daiichi nuclear power plant. *Sci. Rep.* 6, 23925.

Kavasi, N., Sahoo, S. K., Arae, H., Yoshida, S., Sorimachi, A., Tokonami, S. 2015. Measurement of  $^{90}\text{Sr}$  in contaminated Fukushima soils using liquid scintillation counter. *Radiat. Prot. Dosim.* 167 (1-3), 376-379.

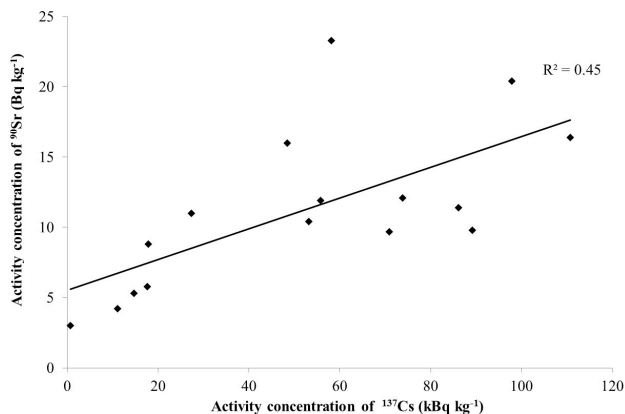


Figure 1. Correlation between  $^{90}\text{Sr}$  and  $^{137}\text{Cs}$  activity concentration in soil samples collected from the exclusion zone of the FDNPP (2013)

In this presentation, a soil sample collection survey in the Fukushima exclusion zone was accomplished in 2016 and some contaminated hot spots were revealed with air dose rate measurement ( $>20$   $\mu\text{Sv/h}$ ). In the collected soil samples,  $^{137}\text{Cs}$  activity concentrations were over 1000 Bq/g while the  $^{90}\text{Sr}$  were over 500 Bq kg $^{-1}$ .

## Time course change of radiocesium concentration in wild mushrooms collected in Miyagi prefecture, Japan from 2011 to 2014

Ayumi Irisawa and Yasushi Kino<sup>1</sup>

Department of Chemistry, Tohoku University, Sendai 980-8578, Japan

Keywords: radiocesium, Fukushima-Daiichi Nuclear Power Plant accident, mushroom, <sup>137</sup>Cs.

<sup>1</sup>Presenting author email: y.k@m.tohoku.ac.jp

### Introduction

It has been known that mushrooms accumulate larger amount of radiocesium than other agricultural products. In 1963, <sup>137</sup>Cs from fallout of atmospheric nuclear weapons testing was firstly found in mushrooms. (Grüter, 1964). Especially, after the Chernobyl Nuclear Power Plant accident, many papers about the accumulation of radiocesium by mushrooms have been published (see review papers and references therein: Gillett and Crout, 2000, Kalač, 2001, Duff and Ramsey, 2008). In some European countries, <sup>137</sup>Cs concentrations of wild mushrooms were found to be noticeably increased just after the accident. In Japan, however, the great part of <sup>137</sup>Cs found in wild mushrooms was originated from the global fall out of atmospheric nuclear weapons testing (Sugiyama, 1994, Yoshida, 1994). In this study, we have collected as many wild mushrooms as possible, and investigate tendency of the the radioactivity concentrations in wild mushrooms.

### Materials and Method

From 2011 when the Fukushima Daiichi Nuclear Power Plant accident to 2014, we have collected 739 samples of mushrooms (fruit bodies of basidiomycetes) belonging to 262 species of wild mushrooms in Miyagi prefecture that locates on the north of Fukushima prefecture. Mushrooms were cleaned carefully by removing attached soil and humus with wet tissues. They were cut into pieces and air-dried in the chamber at 50°C for a week. Dried samples were ground into powder and

were packed uniformly in plastic bottle (100 mL). Radioactivities of the samples were measured with highly pure Ge detectors. Radioactivities were decay-corrected to the day when the nuclear reactors were stopped, March 11, 2011.

### Results and discussion

Figure 1 shows time course change of the concentration of the radio cesium in wild mushrooms depending on the degree of pollution. The values sharply increased in the autumn of 2011. It tends to be higher in autumn than in summer. The concentrations varied more than three orders of magnitude, showing strong species dependence. The radioactivity ratios of <sup>134</sup>Cs to <sup>137</sup>Cs were around 1 except for mushrooms collected in lower pollution areas (< 0.1 μSv/h). Although the radioactivity of many agricultural products decreases below the detection limit, that of wild mushrooms is still high.

### References

- Grüter, H., 1964. *Naturwissenschaften*, 51, 161-162.
- Gillett, A.G., Crout, N.M.J., 2000. *J. Environ. Radioact.* 48, 95-121.
- Kalač, P., 2001. *Food Chem.* 75, 29-35.
- Duff, M.C., Ramsey, M.L., 2008. *J. Environ. Radioact.* 99, 912-932.
- Sugiyama, H., Shibata, H., Isomura, K., Iwashima, K., 1994. *J. Food Hyg. Soc. Japan* 35, 13-22.
- Yoshida S., Muramatsu Y., Ogawa M., 1994. *J. Environ. Radioact.* 22, 141-154.

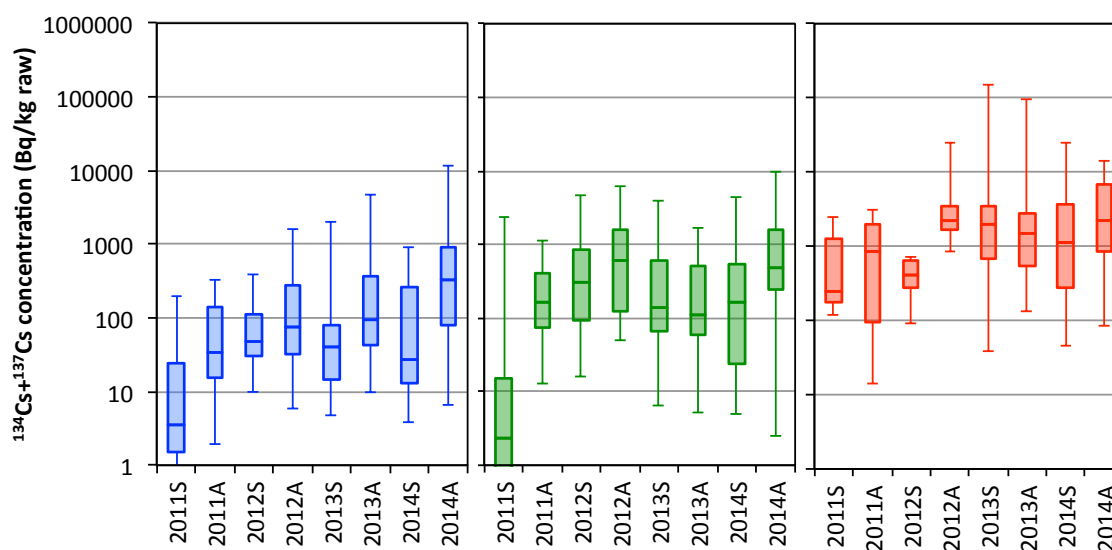


Figure 1. Time course change of the radiocesium concentration in wild mushrooms collected in Miyagi prefecture, Japan. The left, center, and right panels show low, middle, and high pollution areas. The letters S and A mean summer and autumn, respectively.

## Management of NORM legacy sites in Austria

C. Katzlberger<sup>1</sup>, M. Dauke<sup>1</sup>, F. Rechberger<sup>1</sup>, E. Lindner<sup>1</sup>

<sup>1</sup>Austrian Agency for Health and Food Safety, Radiation Protection Division, Vienna, Austria

Keywords: NORM, legacies, dose assessment, remediation,

Presenting author email: christian.katzlberger@ages.at

Following council directive 2003/122/EURATOM on the control of high-activity sealed radioactive sources and orphan sources and in preparation to implement the basic safety standards 2013/59/EURATOM several campaigns to identify potentially contaminated sites were performed in Austria in recent years. Results were summarized in a catalogue for suspected radiologically contaminated sites. Once potentially contaminated areas had been identified their priority was classified based on their potential radiological impact to the population. Priority sites – especially sites in cities and densely populated areas – were further investigated including on site measurements, sampling according to exposure scenarios and dose estimations. Verified sites were then classified as legacies and listed in a catalogue.

Starting at the end of the 19<sup>th</sup> century several factories and institutes especially in Vienna and its surroundings processed materials containing elevated levels of natural radioactivity (especially uranium ore, radium-226 salts and thorium compounds). Based on the legacy-catalogue several studies concerning former chemical factories were carried out by the Austrian Agency for Health and Food Safety. According to historical research one of these companies (founded around 1890) used to process pitch blende residues (uranium ore residue) for the production of radium-226 for research purposes as well as monazite sands for the production of thorium and subsequent manufacturing of incandescent gas lights. Another factory was processing uranium ores and radium-226 salts for the production of bathing additives.

The results of the radiological surveys for these two sites showed elevated concentrations of NORM in the surroundings of both former factory buildings. One legacy site has already been decontaminated and remediated; at the other site first protective measures were performed and further investigations are ongoing to find proper options for safeguarding and remediation.

Details concerning assessment procedures, exposure scenarios, dose estimations, safeguarding and remediation actions, the management and disposal of contaminated materials as well as environmental monitoring- and evidence collection programmes will be presented.

Based on the experiences gained during the investigation of different legacy sites, a systematic and standardized screening procedure for NORM legacies has been derived. This procedure includes combined sampling strategies and characterization models for radiological as

well as chemical parameters (mainly heavy metals) to assess their impact on the population and the environment.



## Environmental transfer of radionuclides from uranium mining and milling waste to biota and humans

F. P. Carvalho, J.M. Oliveira, M. Malta

Laboratório de Protecção e Segurança Radiológica, Instituto Superior Técnico/Universidade de Lisboa, Estrada Nacional 10, km 139, 2695-066 Bobadela LRS, Portugal

Keywords: uranium residues; soil to plant transfer; radionuclide accumulation in biota; radiation dose to humans.

Presenting author email: carvalho@itn.pt

Radioactive ores were exploited in Portugal for most of the 20th century and left 60 uranium legacy sites that under current environmental and radiation protection laws shall be remediated and currently are under remediation (Figure 1) (Carvalho, 2014). Many of these sites have been assessed for environmental contamination and radiological risks (Carvalho et al, 2007, 2014 b, c).

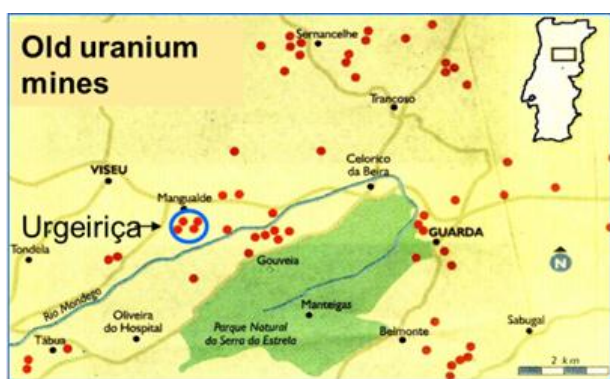


Figure 1. Old uranium and radium mine sites in Portugal.

Results from research and environmental monitoring near old uranium mine sites showed that some radionuclides, such as  $^{226}\text{Ra}$ , may be very mobile in the environment, transferred from waste piles and mine drainage to soils, and accumulated in horticulture products, while other radionuclides, such as  $^{238}\text{U}$ ,  $^{230}\text{Th}$  and  $^{210}\text{Po}$ , are much less mobile and little accumulated by plants. A detailed report on the environmental distribution of these radionuclides near the uranium mine of Cunha-Baixa is presented, including their accumulation in horticulture products (such as cabbage, lettuce, green beans, tomatoes) and farmed animals (rabbits and chicken). For example, irrigation water from a contaminated well contained dissolved  $^{238}\text{U}$ ,  $^{226}\text{Ra}$  and  $^{210}\text{Po}$  in activity concentrations of  $389\pm 15$ ,  $273\pm 11$  and  $19.8\pm 0.8$  mBq/L, respectively. Concentrations of the same radionuclides in cabbage from the farm were  $112\pm 6$ ,  $30220\pm 1540$ ,  $603\pm 22$  mBq/kg wet weight, respectively, and highlighting radium transfer. In chicken meat (muscle tissue) fed with cabbage and other vegetables in the same farm, radionuclide concentrations were  $208\pm 11$ ,  $3505\pm 310$ ,  $1689\pm 115$  mBq/kg wet weight, highlighting higher radium and polonium concentration in several internal organs (Figure 2).

Radiation dose assessment is made for animal farms and human consumers of locally produced foods and compared with other region with natural radiation background.

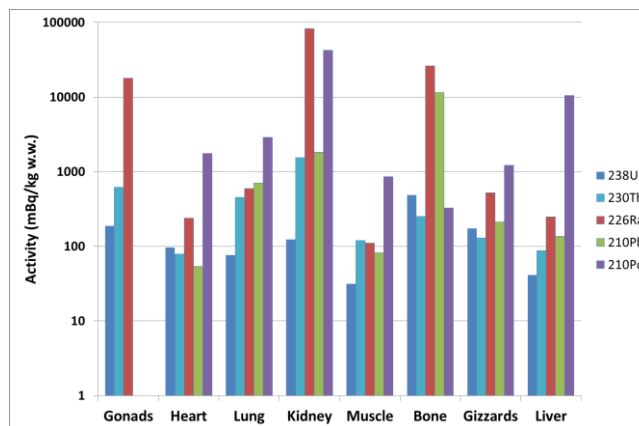


Figure 2. Activity concentration of uranium series radionuclides in internal organs of chicken.

### References

- Carvalho, F.P. 2014. The National Radioactivity Monitoring Program for the Regions of Uranium Mines and Uranium Legacy Sites in Portugal. *Procedia Earth Planet. Sci.* 8, 33–37.
- Carvalho FP, Oliveira, J.M., Malta, M. 2014a. Radioactivity in Iberian Rivers with Uranium Mining Activities in their Catchment Areas. *Procedia Earth Planet. Sci.* 8, 48–52.
- Carvalho FP, Oliveira, J.M., Malta, M. 2014b. Radioactivity in Soils and Vegetables from Uranium Mining Regions. *Procedia Earth Planet. Sci.* 8, 38–42.
- Carvalho FP, Oliveira, J.M., Malta, M. 2014c. Intake of Radionuclides with the Diet in Uranium Mining Areas. *Procedia Earth Planet. Sci.* 8, 43–47.
- Carvalho, F.P., Madruga, M.J., Reis, M.C., Alves, J.G., Oliveira, J.M., Gouveia J., Silva L. 2007. Radioactivity in the environment around past radium and uranium mining sites of Portugal. *Environ. Radioact.* 96, 39-46.

## Uranium concentrations in NORM efflorescences formed in a phosphogypsum legacy site determined by PIXE

M.C.Jimenez-Ramos<sup>1</sup>, I. Ortega-Feliu<sup>1</sup>, J.P.Bolivar<sup>2</sup> and R. García-Tenorio<sup>1,3\*</sup>

<sup>1</sup>Centro Nacional de Aceleradores, CNA, Sevilla, Spain

<sup>2</sup>Grupo Física de las Radiaciones y Medioambiente, University of Huelva (UHU), Spain

<sup>3</sup>Departamento Física Aplicada II, University of Sevilla, Spain

\*Presenting author email: gtenorio@us.es

In the vicinity of the town of Huelva (south-western coast of Spain) the restoration of a NORM legacy site covering some tens of hectares and accumulating around  $10^8$  tons of phosphogypsum (PG) is planned. This PG was generated during near 50 years as a by-product in the production of phosphoric acid in a big industrial complex located in the vicinity.

The legacy site is located on a salt-marsh area, on the margins of the Tinto river mouth and actually is, from a radioactive point of view, not a closed system because it presents direct and diffuse pollution points (leachates) to the surrounding compartments mainly generated by rainwater and tidal influences.



*Phosphogypsum disposal site*

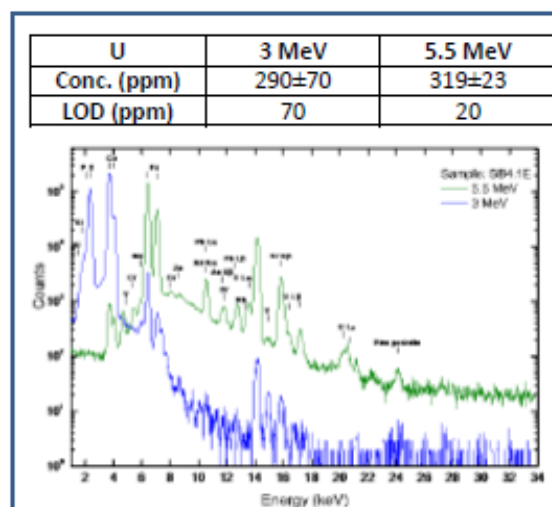
The landfill leachates are the source of efflorescences: precipitated crystallized salts in zones where the water drainage that has left the phosphogypsum piles has been evaporated. The efflorescent salts sequester acidity, metals and radionuclides temporarily and later release them during rain or melting events, thereby provoking the delayed dissemination of contaminants. Thus, the knowledge of efflorescent salt composition is needed for a proper evaluation of the environmental impact of the phosphogypsum stacks nowadays, and the design of the different countermeasures to be adopted associated to the restoration plans.

In this work we will present the uranium concentrations obtained by Proton Induced X-ray Emission (PIXE) in a wide range of efflorescences samples coming from the phosphogypsum disposal site. In particular, 28 samples of efflorescences have been analysed through this non-destructive and multielemental analytical technique. Typical analysis takes few minutes and does not need

chemical sample preparation (the samples only need to be powdered and homogenised before be pressed in pellets of 11mm diameter with a substratus of boric acid).

Analysis were performed with the 3 MV Tandem accelerator at CNA (Sevilla) in vacuum chamber with ion beam intensities of 2-2.5 nA and 3 mm spot diameter. The detector employed was a Si(Li) at 135° degrees with respect the beam direction. Quantification was done using SRM Montana 2710 (NIST).

The measurement of uranium concentrations in the interval of  $10$ - $10^2$  ppm is not trivial, for this reason the optimization of the technical issues was needed. Experiments with protons at different energies were carried out to decrease the limit of detection for uranium as much as possible.



*PIXE spectra obtained at different experimental conditions*

In this study, in addition to the majority elemental composition, other trace elements have been determined as for example: Se, Rb, Zr, Cd, Ba and Ra. To know the efflorescences composition is mandatory for a proper assessment of the environmental impact of the phosphogypsum stacks.

Finally, to validate the uranium measurements, an internal intercomparison between the uranium results obtained by PIXE and by alpha spectrometry has been performed. The Uranium content quantified by both techniques are in excellent agreement

## A survey of natural radioactivity in Belgian groundwater and its use in risk identification for water treatment and drinking water screening

G. Biermans<sup>1</sup>, J.Claes<sup>1</sup>, B.Dehandschutter<sup>1</sup>, S.Pépin<sup>1</sup>, L.Sombré<sup>1</sup> and M. Sonck<sup>1,2</sup>

<sup>1</sup>Federal Agency for Nuclear Control, Brussels, Belgium

<sup>2</sup>ETRO, Vrije Universiteit Brussel, Brussels, Belgium

Keywords: groundwater, NORM, drinking water

Presenting author email: geert.biermans@fanc.fgov.be

The presence of natural radionuclides in groundwater may under some conditions lead to potential exposure of workers, population or the environment. This is the case in groundwater treatment (workers and environment) and the use of groundwater as water for consumption (population). These risks are respectively covered by European Directive 2013/59/Euratom, which lists groundwater treatment as a NORM practice of concern, and European Directive 2013/51/Euratom, which deals with radiological quality of water intended for human consumption. In both cases, knowledge about the radiological composition of groundwater is essential for regulators to identify areas and operators likely to be of concern.

Despite its small area, Belgium has a complex geological history and a large number of aquifers of diverse geological composition. Previous surveys (e.g. ISP, 2007) have therefore, not surprisingly, hinted at a very heterogeneous radiological composition between aquifers, though no aquifer-dependent analysis of the data has been performed at that time.

Building upon these historical data, and in support of the transposition and application of both Directives, the Federal Agency for Nuclear Control (FANC) has initiated in 2014 a new survey of Belgian groundwater as part of its radiological surveillance program. By analysing groundwater data from existing monitoring programmes of operators, regional authorities or FANC and by performing additional sampling campaigns targeted on specific under-represented aquifers or regions, a substantial amount of representative data has been gathered to complement the data sets of previous surveys (150 samples in total).

For each sample, new or historical, at least three parameters were available: total alpha, total beta and <sup>40</sup>K, parameters which are also used in the screening for drinking water under 2013/51/Euratom. For some samples uranium content and radon concentrations were also available. For each aquifer, average values and standard deviation of each parameter were calculated. Aquifers with less than 5 samples were not taken into account.

The results show that none of the sampled aquifers, exceeds on average, the Directive's screening value of 1 Bq/l for total beta activity. In cases where

individual samples exceed this value, the beta activity can be completely explained by the presence of <sup>40</sup>K.

Total alpha activity varies greatly between aquifers (Fig.1), with average values exceeding the screening value of 0.1 Bq/l in several aquifers, notably the Cambrian Massif of Brabant and the aquifers in carboniferous limestone formations. Half of the samples in the survey exceeded the screening value.

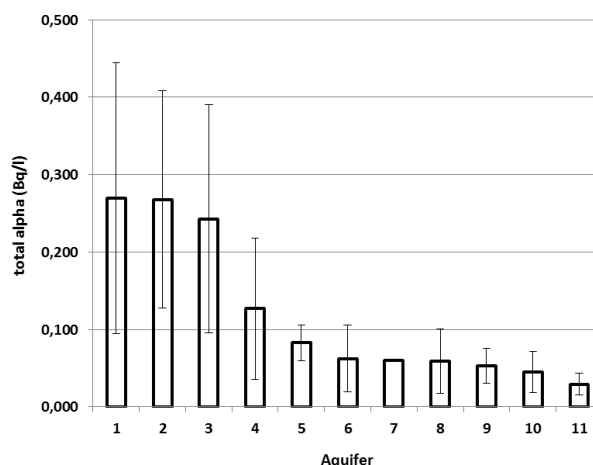


Figure 1: total alpha values (mean  $\pm$  SD) for the sampled Belgian aquifers.

These results were further interpreted to optimise risk identification in the application of the regulatory frameworks for NORM and radiological screening of drinking water. The survey also provides rudimentary reference values which for monitoring purposes.

Future work will focus on regional variability within aquifers and integrating feedback from regulatory practice into the measurement strategy to further optimise risk identification and monitoring.

ISP., 2007. Mesure de la radioactivité naturelle dans les eaux destinées à la consommation humaine : Méthodologie appliquée dans le cadre de la Directive 98/83/CE. Rapport D/2505/2007/40.

## REMdb as a framework for collaborations in environmental radioactivity research

M. A. Hernández-Ceballos<sup>1</sup>, E. Brattich<sup>2</sup>, J. Ajtić<sup>3,4</sup>, G. Cinelli<sup>1</sup>, V. Djurdjevic<sup>5</sup>, D. Sarvan<sup>3</sup>, T. Tollefsen<sup>1</sup>

<sup>1</sup>European Commission, Joint Research Centre, Directorate for Nuclear Safety & Security, Knowledge for Nuclear Safety, Security & Safeguards, Ispra, Italy

<sup>2</sup>Environmental Chemistry and Radioactivity Laboratory, Department of Chemistry “G. Ciamician”, Alma Mater Studiorum University of Bologna, 40126, Bologna (BO), Italy

<sup>3</sup>Faculty of Veterinary Medicine, University of Belgrade, Belgrade, 11000, Serbia

<sup>4</sup>Institute for Research and Advancement in Complex Systems, Belgrade, 11000, Serbia

<sup>5</sup>Institute of Meteorology, Faculty of Physics, University of Belgrade, Belgrade, 11000, Serbia

Keywords: REMdb, radioactivity, beryllium-7, Europe.

Presenting author email: miguelhceballos@gmail.com

### Radioactivity Environmental Monitoring database (REMdb)

Under the terms of Article 36 of the Euratom Treaty, European Union Member States (MSs) shall periodically communicate to the European Commission (EC) information on environmental radioactivity levels. These results have been introduced into the Radioactivity Environmental Monitoring database (REMdb) of the EC Joint Research Centre (JRC) sited in Ispra (Italy) (<https://rem.jrc.ec.europa.eu/RemWeb/>).

The initial purpose of the REMdb was to bring together environmental radioactivity data produced in the aftermath of the Chernobyl accident, and to store them in a harmonised manner. Thus the database has two main objectives: 1) to collect the environmental radioactivity data gathered through the national environmental monitoring programs of the MSs to prepare comprehensive annual monitoring reports; and 2) to keep a historical record of the radiological accidents for scientific studies.

Nowadays, containing nearly two million records of radioactivity levels in milk, water, air and mixed diet received from the MSs, the REMdb offers the scientific community dealing with environmental radioactivity endless research opportunities.

The records stored in REMdb prior to 2007 are fully public, while the access to the data from the 2007-2015 period can be granted only after explicit request. This fact makes the REMdb a useful and unique pillar on which to perform environmental radioactivity studies at the European level, and which can be considered as a liaison platform between national and international scientific groups conducting collaborative research.

### Example of collaboration: Analysis of <sup>7</sup>Be surface concentrations

As a valuable proof of this use, the present work provides an overview of the research activity undertaken by a friendly scientific collaboration network created by the University of Belgrade, the University of Bologna and the REM group of the JRC in the study of the <sup>7</sup>Be surface concentrations recorded across Europe. These sets of results represent one of the first attempts to better understand the <sup>7</sup>Be distribution in Europe, as well as the impact of tropopause height (TPH) and other meteorological parameters exert on it.

First, spatial and temporal distribution of the <sup>7</sup>Be specific activity in surface air was carried out using the long-term database (1984–2011) of 34 sampling sites, focusing on describing the impact of the latitude and solar cycle on yearly and monthly concentrations (Hernández-Ceballos et al., 2015). Further, a cluster analysis was instead applied to identify spatial patterns in <sup>7</sup>Be concentrations in Europe: results showed the presence of three distinguishable cluster groups (south, central and north of Europe) with clear differences between concentrations in both intensity and time trends, and with a latitudinal distribution of the sampling stations (Hernández-Ceballos et al., 2016a). These regions were also identified in an analysis of seasonal and spatial patterns of extremely high <sup>7</sup>Be surface concentration (values above 95<sup>th</sup> percentile in each site) recorded over the 2001–2010 period across Europe (Ajtić et al., 2016a). This study reported that most of the extremes occur over the March–August period, while at least 10 % of the total number of extremes take place during autumn and winter. In Ajtić et al., 2016b these “cold extremes” were analysed in more detail, showing three meteorological scenarios associated with their occurrence in northern Europe. In these works, the impact of TPH on <sup>7</sup>Be, and therefore, on the spatial distribution of <sup>7</sup>Be in Europe, was also suggested. The influence of TPH on <sup>7</sup>Be was further investigated in a separate study (Hernández-Ceballos et al., 2016b), which showed a larger TPH influence on <sup>7</sup>Be during summer and a large spatial variability of TPH on <sup>7</sup>Be levels with a clear gap between southern and northern Europe in the area of the polar front jet.

Ajtić et al., 2016a. Beryllium-7 surface concentrations extremes in Europe. Submitted to *Facta Universitatis*.

Ajtić et al., 2016b. Analysis of extreme beryllium-7 specific activities in surface air. *Rad. Applic. 1*, 216-221.  
Hernández-Ceballos et al., 2015. A climatology of <sup>7</sup>Be in surface air in European Union. *J. Environ. Radioact. 141*, 62-70.

Hernández-Ceballos et al., 2016a. Identification of airborne radioactive spatial patterns in Europe :Feasibility study using Beryllium-7. *J. Environ. Radioact. 155-156*, 55-62

Hernández-Ceballos et al., 2016b. Seasonality of <sup>7</sup>Be concentrations in Europe and influence of tropopause height. *Tellus B. 68*, 29534.



## Radioactivity in the gas pipeline network in Poland

J. Nowak<sup>1</sup>, P. Jodłowski<sup>1</sup>, J. Macuda<sup>2</sup>; C. Nguyen Dinh<sup>3</sup> and K. Liszka<sup>2</sup>

<sup>1</sup> Faculty of Physics and Applied Computer Science, AGH University of Science and Technology,  
Al. Mickiewicza 30, 30-059 Kraków, Poland

<sup>2</sup> Faculty of Drilling, Oil and Gas, AGH University of Science and Technology

<sup>3</sup> Faculty of Geology, Geophysics and Environmental Protection, AGH University of Science and Technology

Keywords: natural gas, radon, Pb-210, NORM.

Presenting author email: jodlowski@fis.agh.edu.pl

The radiological risk in natural gas pipeline transport is mostly connected with radon (Rn-222) and its progeny: Po-218, Pb-214, Bi-214, Po-214 and Pb-210.

The radon activity concentration in natural gas transported by gas pipelines varies in a wide range from dozens of Bq/m<sup>3</sup> to several thousand Bq/m<sup>3</sup> and mainly depends on the proximity of mines and geological structure of the deposit from which natural gas is extracted and transported.

The radon progeny are ion metals, which are easily adsorbed on aerosols and deposited on the inner surfaces of gas pipe and other gas processing equipment such as scrubbers, compressors, reflux pumps, control valves and product lines creating thin radioactive films. Additionally, radon progeny together with aerosols (in contrast to radon) are retained on filters. In the aftermath of successive radioactive decay of short-lived radon progeny, long-lived Pb-210 is accumulated on filters.

The paper presents the study of the Rn-222, Pb-210 and gamma radiation dose rates connected with the transport of natural gas by the gas pipeline network in Poland.

In the scope of the study the measurements of activity concentration of radon (Rn-222) in the gas samples (with alpha scintillation cells), radiolead Pb-210 in spent filter cartridges and dust samples collected from the gas pipeline network (with gamma-ray spectrometry) were performed. Additionally, gamma radiation dose rate at the selected points of the gas pipeline network were measured.

The results show that the Rn-222 activity concentration in natural gas varies from the detection limit of the applied method (30 Bq/m<sup>3</sup>) to around 1400 Bq/m<sup>3</sup>. Generally, the Rn-222 concentration in natural gas samples fluctuate around the mean radon concentration in the air of dwellings in Poland.

The elevated radon activity concentrations in natural gas of several hundreds of Bq/m<sup>3</sup> and more are observed at locations where the gas directly comes from local gas mines or where there is a blend of the national gas with imported one. Relatively low radon concentration in imported natural gas is connected with the fact that this gas was imported from abroad, e.g. from Belarus and Ukraine. Therefore, the time elapsed

from the gas extraction to the collection of samples was relatively long. In consequence, the concentration of Rn-222 in the gas significantly decreased due to radon decay (3.8 days).

Additionally, the temporal variability (daily and weekly) of the radon activity concentration in the natural gas were assessed. The results show radon concentrations does not statistically in daily or weekly time scale.

The Pb-210 activity concentration in dust ("black-powder") from gas filters and spent filter cartridges is high and varies from 500 to 17000 Bq/kg and from 200 to 2900 Bq/kg respectively.

The gamma radiation dose rates measured at the selected elements of the gas pipeline network are at the level of the natural background.

Al-Masri M.S., Shwiekani R., 2008. Radon gas distribution in natural gas processing facilities and workplace air environment, *J. Environ. Radioact.* 99, 574-580.

Godoy J.M. et al., 2005. 210Pb content in natural gas pipeline residues and its correlation with the chemical composition, *J. Environ. Radioact.* 83, 101-111.

IAEA, 2003. Radiation protection and the management of radioactive waste in the oil and gas industry, Safety Reports Series No. 34, International Atomic Energy Agency, Vienna.

Jodłowski P., 2016. A revision factor to the Cutshall self-attenuation correction in 210Pb gamma spectrometry measurements, *Appl. Radiat. Isot.*, 109, 566-569.

Jodłowski P., Kalita S., 2010. Gamma-Ray Spectrometry Laboratory for high-precision measurements of radionuclide concentrations in environmental samples, *Nukleonika*, 55, 143-148.

Kitto M., Torres M., Haines D., Semkow T., 2014. Radon measurement of natural gas using alpha scintillation cells, *J. Environ. Radioact.* 138, 205-207.

Kozak K. et al., 2011. Correction factors for determination of annual average radon concentration in dwellings of Poland resulting from seasonal variability of indoor radon, *Appl. Radiat. Isot.* 69, 1459-1465.



## Secondary contamination of radioactive cesium to the plant in coastal area of Fukushima in 2013 and aftermath

T. Shinano<sup>1</sup>, H. Matunami<sup>1</sup>, M. Sato<sup>2</sup>, T. Saito<sup>2</sup>, S. Fujimura<sup>1</sup>, T. Ota<sup>1</sup>, T. Eguchi<sup>1</sup>, S. Horii<sup>1</sup> and T. Murakami<sup>1</sup>

<sup>1</sup>Agricultural Radiation Research Center, TARC/NARO, Fukushima city, Fukushima, 9602156, Japan

<sup>2</sup>Hama Agricultural Regeneration Research Centre, Fukushima Agricultural Technology Centre, Minami-souma city, Fukushima, 975-0036, Japan

Keywords: radioactive cesium, agricultural products, contamination, imaging plate.

Presenting author email: shinano@affrc.go.jp

Two years after the Tokyo Electric Power Company's Fukushima Daiichi Nuclear Power Plant accident, countermeasures have been largely carried out and a large area of farmland have started their agricultural activity again. And in several areas have also started test cultivation to prepare the information whether the area is able to initiate agriculture again. In August 2013, pepper plant cultivated in Namie town was reported to have contaminated more than the standard value (100 Bq/kg). Plant samples pepper and soybean (which was cultivated adjacent to the pepper) were collected and subjected to the imaging plate analysis. It was clearly demonstrated that there was a lot of spot with high radioactivity in these samples. But at that time, as the cultivation activity in that area is very limited, detailed analysis had not been done. While in subsequent October, when the brown rice monitoring started in the Minami-souma city, some brown rice bag (30kg) exceeds the standard value.

There are several possibilities to increase the radioactivity of plant sample. 1) Uptake of radioactive cesium (Cs) from the soil, 2) Uptake of radioactive Cs from the water especially in the case of paddy field, 3) Direct attachment of radioactive Cs to the plant sample from air, or touching the soil. Twenty-eight bags among 11 million were reported to have higher activity, and all of them were concentrated in the southern area of the city where the rice cultivation was allowed from that year. Furthermore, more southern area, there was experimental fields for rice by our institute.

Comparing the transfer factor of radioactive Cs from soil to brown rice with other samples obtained in different areas, and obtaining the information of water usage of the paddy field, we have reached that the contamination was derived from direct attachment of radioactive Cs to the plant sample as observed in Namie town in August. From the border of the contamination reported paddy field *Miscanthus sinensis* and other plants were collected which are considered to be existed since summer. The imaging plate analysis shows a clear contamination by radioactive material to the plant (Fig. 1). Comparing the brown rice between those samples with similar contamination level shows a different cause of contamination (Fig.2). In 2012, some field where the brown rice exceeds more than 100 Bq/kg did not show any clear spotted contamination, which indicate that the radioactivity was transported from the soil to plant through uptake and unloading (Fig. 2 lower). But in the case of 2013, spotted contamination indicates the direct contamination to the upper part of plant occurred.

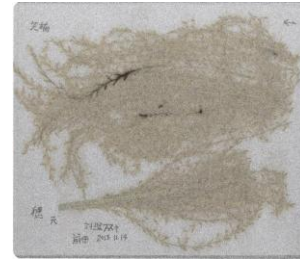


Fig. 1 Superimpose image of imaging plate and photograph of *Miscanthus sinensis* obtained from the border of paddy field. Black color indicate high radioactivity.

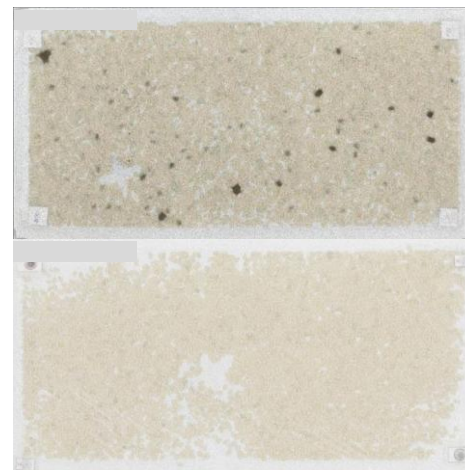


Fig. 2 Superimpose image of brown rice which exceed the standard value. Black color indicate high radioactivity. Upper: sample taken from Minamisoma with 180 Bq/kg in 2013. Lower: sample taken from Nakadori with 140 Bq/kg in 2012.

We have analysed the ratio of  $^{134}\text{Cs}/^{137}\text{Cs}$  in the spotted rice and others and found that the derived radioactive Cs is not from the soil underneath (Matsunami et al. 2016). After 2013, there was no report to exceed the standard value, but we need to keep paying attention to this type of contamination.

### Reference

Matsunami, H., Murakami, T., Fujiwara, H. and Shinano, T. 2016. Evaluation of the cause of unexplained radiocaesium contamination of brown rice in Fukushima in 2013 using autoradiography and gamma-ray spectrometry. Sci. Rep, 6, 20386

## Assessment of <sup>90</sup>Sr pollution from the Fukushima-Daiichi Nuclear Power Plant accident by measurement of cattle teeth

K. Koarai<sup>1</sup>, Y. Kino<sup>1</sup>, A. Takahashi<sup>1</sup>, T. Suzuki<sup>1</sup>, Y. Shimizu<sup>1</sup>, M. Chiba<sup>1</sup>, K. Osaka<sup>1</sup>, K. Sasaki<sup>1</sup>, Y. Urushihara<sup>2</sup>, T. Fukuda<sup>3</sup>, E. Isogai<sup>1</sup>, H. Yamashiro<sup>4</sup>, T. Oka<sup>1</sup>, T. Sekine<sup>1</sup>, M. Fukumoto<sup>1,5</sup>, H. Shinoda<sup>1</sup>

<sup>1</sup>Tohoku Univ., Japan. <sup>2</sup>QST, Japan, <sup>3</sup>Iwate Univ., Japan., <sup>4</sup>Niigata Univ. Japan., Japan. <sup>5</sup>Tokyo Med. Univ., Japan.

Keywords: <sup>90</sup>Sr, Fukushima-Daiichi Nuclear Power Plant accident, teeth, cattle.  
Presenting author email: koarai@dc.tohoku.ac.jp

**Introduction** <sup>90</sup>Sr has a bone-seeking property which may cause internal exposure together with its daughter nuclide, <sup>90</sup>Y. The nuclide was released into the environment by radioactive contamination, such as global fallout from past nuclear weapon testing and Chernobyl Nuclear Power Plant (ChNPP) accident. Attentions have been paid to the determination of <sup>90</sup>Sr in the environment.

Fukushima-Daiichi Nuclear Power Plant (FNPP) accident also have caused contamination of the environment, however, evaluation of the contamination is difficult. The amount of <sup>90</sup>Sr released from the FNPP was less than that released from global fallout and the ChNPP. Release of <sup>90</sup>Sr was smaller than volatile nuclides (include <sup>137</sup>Cs and <sup>131</sup>I) in case of the FNPP accident. Moreover, determination of <sup>90</sup>Sr required a great deal of effort. There is only limited information on the environmental <sup>90</sup>Sr pollution by the FNPP accident.

We examined <sup>90</sup>Sr activity concentrations in teeth of cattle caught within a 20-km radius around the FNPP (Koarai *et al.*, 2016). <sup>90</sup>Sr activity concentration in a given tooth reflects environmental <sup>90</sup>Sr contamination when the tooth was formed. We thus have little direct data on how much FNPP-related contamination affected animals. We had investigated activities of <sup>134</sup>Cs, <sup>137</sup>Cs, <sup>110m</sup>Ag and <sup>129m</sup>Te in organs of the cattle (Fukuda *et al.*, 2013), and the radioactive effect on cattle after the FNPP accident (Yamashiro *et al.*, 2013 and Urushihara *et al.*, 2016).

**Material and Method** We collected two young cattle in area A (10~30 μSv h<sup>-1</sup>, west 5 km from FNPP) and two young cattle in area B (0.8~1.2 μSv h<sup>-1</sup>, southwest 16 km from FNPP) from November 2011 to July 2012. Control samples of the cattle were two young cattle from the uncontaminated area C (north 250 km from FNPP). Nine molar teeth were dissected from the mandible. Radioactivity of <sup>90</sup>Sr in the teeth was determined by a low background 2π gas flow counter after chemical separations with fuming nitric acid. Concentrations of Ca were determined by ICP-AES.

**Results and Discussion** Figure 1 shows <sup>90</sup>Sr activity concentrations in teeth of cattle from area A, B and C. The activity concentrations of A and B were higher than those of control cattle (fig 1). <sup>90</sup>Sr in the control teeth from area C was originated from the global fallout. We observed the high activity concentrations in the teeth of cattle from the contaminated area.

Figure 1 shows <sup>90</sup>Sr activity concentrations in nine teeth (No. 1~9) of the cattle. The development stages of the teeth were different. The numbers of the teeth show chronological order of the development stage. Judging

from the ages of the cattle from area A and B, the No. 5~9 were developed after the FNPP accident, while the No. 1~4 were fully developed before the accident. Large changes of the activity concentrations were observed in the No.4~7. The changes represent that the cattle incorporated <sup>90</sup>Sr from the FNPP accident. We conclude that we detected the presence of <sup>90</sup>Sr from the FNPP accident in teeth of large animals for the first time.

Assessment of <sup>90</sup>Sr in teeth could allow for the measurement of time-course change of environmental <sup>90</sup>Sr pollution. We discuss the details of the changes and correlation between <sup>90</sup>Sr activity concentration in tooth with inventory of <sup>90</sup>Sr, chemical fraction of <sup>90</sup>Sr in soil.

- K. Koarai *et al.*, <sup>90</sup>Sr in teeth of cattle abandoned in evacuation zone: Record of pollution from the Fukushima-Daiichi Nuclear Power Plant accident., *Sci. Rep.*, **6**, 24077 (2016).
- T. Fukuda *et al.*, Distribution of Artificial Radionuclides in Abandoned Cattle in the Evacuation Zone of the Fukushima Daiichi Nuclear Power Plant., *Plos One*, **8**, e54312 (2013).
- H. Yamashiro *et al.*, Effects of radioactive caesium on bull testes after the Fukushima nuclear plant accident., *Sci. Rep.*, **3**, 2850 (2013).
- Y. Urushihara *et al.*, Analysis of plasma protein concentrations and enzyme activities in cattle within the ex-evacuation zone of the Fukushima Daiichi Nuclear Plant Accident., *Plos One*, **11**, e0155069 (2016).

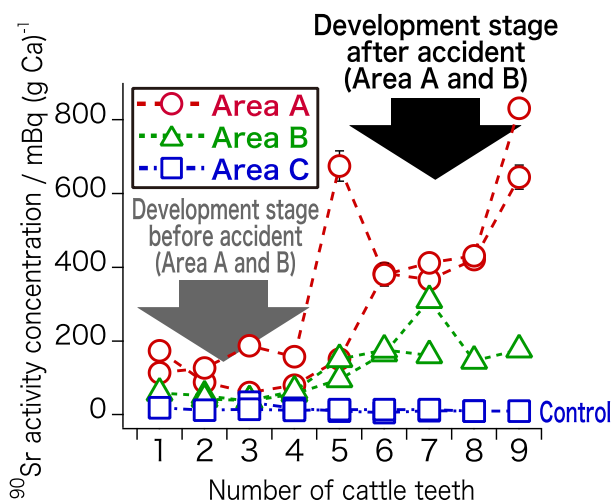


Figure 1. <sup>90</sup>Sr activity concentration in various teeth.

## Estimation of dose reduction factor before and after decontamination

A. Ishizaki<sup>1</sup>, A. Mori<sup>1</sup>, K. Kawase<sup>2</sup>, M. Kato<sup>2</sup>, M. Watanabe<sup>2</sup>, I. Aoki<sup>3</sup> and M. Munakata<sup>1</sup>

<sup>1</sup> Nuclear Safety Research Center, Japan Atomic Energy Agency, Shirakata 2-4, Tokai-mura, Naka-gun, Ibaraki, Japan

<sup>2</sup> Sector of Fukushima Research and Development, Japan Atomic Energy Agency, 10-2, Fukasaku, Miharu, Tamura-gun, Fukushima, Japan

<sup>3</sup> Nuclear Science Research Institute, Japan Atomic Energy Agency, Shirakata 2-4, Tokai-mura, Naka-gun, Ibaraki, Japan

Keywords: reduction factor, air dose rate, decontamination, Fukushima.

Presenting author email: ishizaki.azusa@jaea.go.jp

After the Fukushima Daiichi Nuclear Power Station (FDNPS) accident in 2011, a large amount of radionuclides was released to the environment. An exposed dose is one of indices for decision making of evacuations. To obtain the individual dose equivalent, the air dose rate and time to spend in an arbitrary place are necessary in each area where inhabitants stay. The place where inhabitants stay is categorized roughly according to indoor and outdoor in simple estimation of the exposed dose. It is known that the indoor air dose rate,  $D_i$ , can be obtained by multiplying the outdoor air dose rate,  $D_o$ , by dose reduction factor,  $RF$ . In case of wooden house,  $RF$  is reported as 0.4 which has the range from 0.2 to 0.5 (IAEA, 2000) and changes with floor area (Furuta and Takahashi, 2015) and indoor position, e.g. at the center of the house or by the window.

To evaluate the validity of  $RF$  represented as 0.4, in this study, we investigated  $D_i$  and  $D_o$  before and after decontamination for 17 Japanese wooden houses in four municipalities (A, B, C and D) of Fukushima prefecture. Air dose rates were measured using a survey meter with sodium iodide scintillator crystal. A measurement area of  $D_o$  was within a 250 m radius from a house, and  $RF$  was obtained as the ratio of an average of  $D_i$  to an average of  $D_o$ . Decontamination for areas A and B were limited within a few meters around a house. Decontamination for areas C and D were the whole community area.

Relation between area and  $RF$  before decontamination,  $RF_1$ , was shown in Fig. 1.  $RF$  was almost within the range from 0.2 to 0.5. Relation between area and  $RF$  after decontamination is shown in Fig. 2.  $RF$  after decontamination,  $RF_2$ , in area A and B increased in comparison with  $RF_1$ . In areas C and D, some  $RF_2$  increased and others decreased. From this results, it was clear that  $RF$  changes before and after decontamination despite of a same location. Change of  $RF$  before and after decontamination is caused by change of contaminant distributions. Depending on locations and materials where contaminants deposit, and decontamination method, decontamination efficiencies changed. Therefore, standard deviations of  $D_o$  after decontamination increased in comparison with those before decontamination. Location of measurement positions of  $D_o$  influences the evaluation of  $RF$ . Then,  $D_i$  obtained using  $RF$  is influenced by the location of  $D_o$  measurement. Additionally, an evaluation of individual dose and decision making of repatriation are also affected by the evaluation of  $RF$ . Therefore, it is

necessary to evaluate  $RF$  and  $D_i$  by simulating air dose rates on the basis of contaminant distributions around a house, especially after decontamination. In addition, we developed the preliminary estimation method of  $RF_2$  and compared with  $RF_2$  obtained with measured air dose rates.

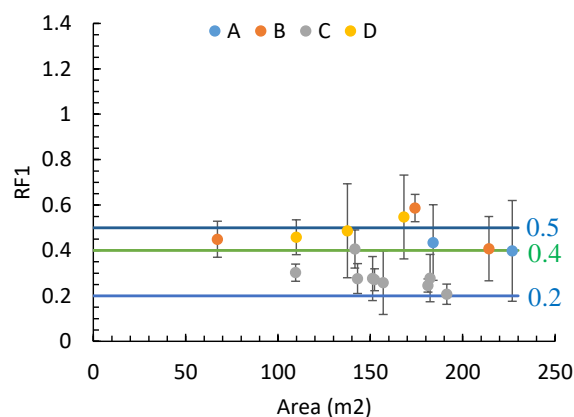


Figure 1 Reduction factor before decontamination in areas A, B, C and D.

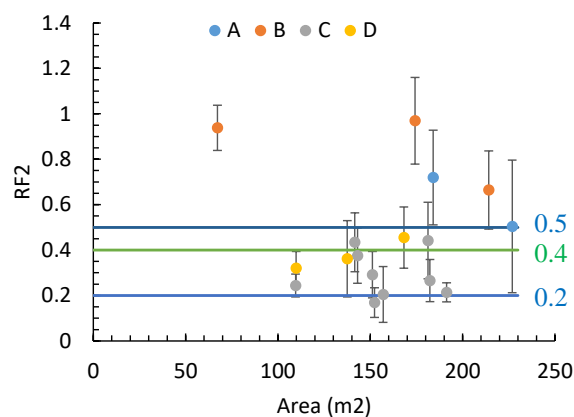


Figure 2 Reduction factor after decontamination in areas A, B, C and D.

### Reference

- Furuta, T., Takahashi, F., 2015. Study of radiation dose reduction of buildings of different sizes and materials. J. Nucl. Sci. Technol. 52, 897–904. doi:10.1080/00223131.2014.990939
- IAEA, 2000. Generic Procedures for Assessment and Response during a Radiological Emergency.

## $^{137}\text{Cs}$ in surface soil samples in Northern Greece, 30 years after the Chernobyl accident

A.Ioannidou<sup>1</sup>, S. Stoulos<sup>1</sup>, C. Betsou<sup>1</sup>, E. Ioannidou<sup>1</sup>, J. Hansman<sup>2</sup>, M. Krmar<sup>2</sup>, N. Kazakis<sup>3</sup>, E. Tsakiri<sup>4</sup>

<sup>1</sup>Physics Department, Nuclear Physics Lab., Aristotle University of Thessaloniki, Thessaloniki, 54124, Greece

<sup>2</sup>Physics Department, Faculty of Science, University of Novi Sad, Trg Dositeja Obradovica 4, Novi Sad, 21000, Serbia

<sup>3</sup>Geology Department, Engineering Geology and Hydrogeology, Aristotle University of Thessaloniki, Thessaloniki, 54124, Greece

<sup>4</sup>Biology Department, Division of Botany, Aristotle University of Thessaloniki, Thessaloniki, 54124, Greece

Keywords: nuclear accident, radioactive nuclides

Presenting author email: [anta@physics.auth.gr](mailto:anta@physics.auth.gr) (Alexandra Ioannidou)

The artificial radionuclide  $^{137}\text{Cs}$  contamination in Greece was mostly due to Chernobyl nuclear accident. After that, there were no other significant  $^{137}\text{Cs}$  emissions, and the atmospheric  $^{137}\text{Cs}$  was exposed to physical decay as well as to wet and dry deposition. In recent years the Fukushima accident contributed to the release of  $^{137}\text{Cs}$  in the atmosphere but with minor influence in regions far away from Japan.

Ninety three (93) samples of surface soil were collected from Northern Greece regions during July-September 2016, in order to determine the levels of  $^{137}\text{Cs}$  in surface soil after one half-life (30 years) of  $^{137}\text{Cs}$  released from Chernobyl accident.

The samples were dried at 60°C to constant weight, sieved below 600µm and put in a cylindrical plastic container of diameter 5.7 cm and height 2 cm. All samples were measured up to 200.000 sec in a low-background HPGe detector with relative efficiency 20%.

The highest observed  $^{137}\text{Cs}$  values (1536 Bq kg<sup>-1</sup> maximum) in surface soil samples are relatively higher than typically observed values over Europe nowadays. The coincidence of heavy rainfall during May 1986 with the passage of air masses from Chernobyl area to Northern Greece had as a result high  $^{137}\text{Cs}$  concentrations at the ground level in the site of investigation. The  $^{137}\text{Cs}$  ground deposition due to rainfall during May 1986 was approximately 23.9 kBq m<sup>-2</sup> in Thessaloniki areas (Papastefanou et al. 1988).

Immediately after the Chernobyl accident, during May-November 1986, soil samples collected and analyzed from all over Greece (Petropoulos et al. 2001) in order to define the levels of contamination (Fig. 1).

The present investigation showed that  $^{137}\text{Cs}$  activity concentrations in some regions are still high enough and that the highest  $^{137}\text{Cs}$  values observed in the same regions (Fig. 2) that were defined as high contaminated immediately after the Chernobyl accident. The levels of  $^{137}\text{Cs}$  in nowadays is one order of magnitude lower than it was immediately after the accident, due to radioisotope decay as well as the resuspension factor, movement in soils due to chemical or biological processes and other physical processes, such as erosion.

Moreover, elemental distribution and structure information of soil samples will be given by XRF analysis regarding to any possible correlation between  $^{137}\text{Cs}$  migration and geological background of the examined area.

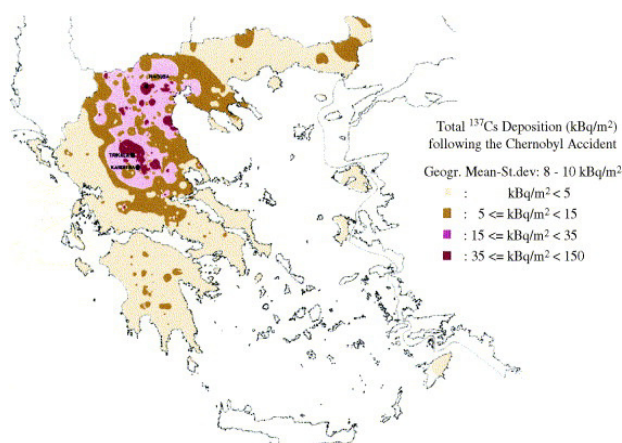


Figure 1.  $^{137}\text{Cs}$  activity concentrations in surface soil samples in Greece during May-November 1986 (Petropoulos et al., 2001)

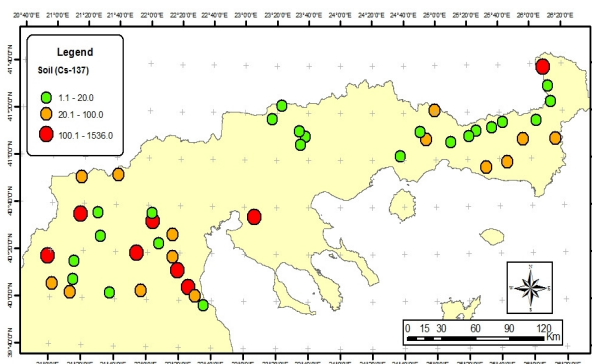


Figure 2.  $^{137}\text{Cs}$  activity concentrations in surface soil samples in Northern Greece during July-September 2016 (present work - 46 samples analysed up to now)

Papastefanou, C., Manolopoulou, M., Charalambous, S. 1988. Radiation Measurements and Radioecological Aspects of Fallout from the Chernobyl Reactor Accident, *J. Environ. Radioactivity* 7, 49-64.

Petropoulos N., Anagnostakis M., Hinis, E., Simopoulos, S. 2001. Geographical mapping and associated fractal analysis of the long-lived Chernobyl fallout radionuclides in Greece. *J. Environ. Radioactivity* 53(1), 59-66.



## Migration of Radionuclides in soil samples from Pripyat

Clemens Walther<sup>1</sup>, Stefan Bister<sup>1</sup>, Peter Brozynski<sup>1</sup>, Daniel Heine<sup>1</sup>

<sup>1</sup>Institut of Radioecology and Radiation Protection, Leibniz University of Hanover, 30167, Germany

Keywords: Pripyat, Chernobyl, contamination, migration in soil

Presenting author e-mail: heine@irs.uni-hannover.de

The accident of chernobyl led to significant contamination in large regions of Europe, particularly in Ukraine, Belarus and Russia. In the Chernobyl exclusion zone (CEZ), which includes a 2200 km<sup>2</sup> area around the Chernobyl nuclear plant, the highest amount of radioactivity was distributed. For predicting the temporal evolution of the contamination in this region the behaviour, and the transport of radioisotopes in the environment is just as important their physical half-lives.

In this study we investigated the vertical distribution of <sup>137</sup>Cs, <sup>90</sup>Sr, <sup>241</sup>Am and plutonium in upper soil layers from the exclusion zone to get information on the vertical migration of these nuclides. Therefore six drill cores of 30 cm length were collected in the city of Pripyat, which is about 4 km away from the power plant. It was cut into 10 layers of different thicknesses. Due to their half-lives <sup>137</sup>Cs (T<sub>1/2</sub>=30,17 a) and <sup>90</sup>Sr (T<sub>1/2</sub>=28,78 a) are still dominate the contamination in this region. Because of their relevance to long-term considerations the plutonium isotopes (<sup>238</sup>Pu, <sup>239</sup>Pu, <sup>240</sup>Pu) as well as <sup>241</sup>Am as a daughter of <sup>241</sup>Pu were also investigated.

### Methods and Measurements

In the first step, each sample were analyzed with  $\gamma$ -spectrometry to determine the amount of <sup>137</sup>Cs and <sup>241</sup>Am by their characteristic  $\gamma$ -lines (<sup>137</sup>Cs: E <sub>$\gamma$</sub> =661,7 keV; <sup>241</sup>Am: E <sub>$\gamma$</sub> =59,54 keV). In the next steps the soil samples have been ashed and plutonium and strontium where chemically seperated. For the detection of plutonium we used  $\alpha$ -spectrometry. The <sup>90</sup>Sr measurements were performed by liquid scintillation counting (LSC).

### First Results

Figure 1 shows the specific activities of <sup>241</sup>Am, <sup>137</sup>Cs and the three plutonium isotopes in different depths of one drill core. Comparing the activities in the same layers of different cores shows us, that there is a very inhomogeneous distribution of all these nuclides in the soil. While the absolute specific activities in layers of equal depth differ considerably, the decrease follows similar slopes in all cores and for every nuclide below the 12 cm horizon.

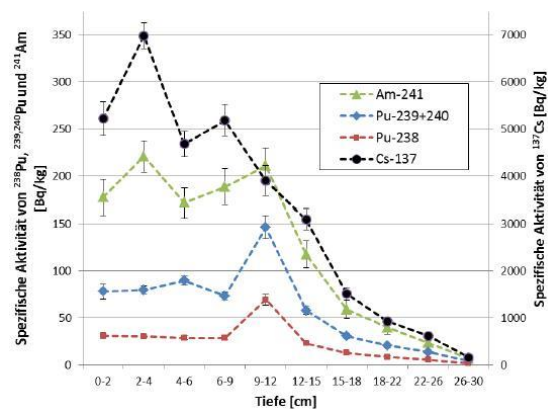


Figure 1: Specific activities in soil layers. [1]

### References

- [1] BROZYNSKI, P.; Migration of radionuclides in soil samples from northern Ukraine. Leibniz University of Hanover, Institute for Radioecology and Radiation Protection; 2016.
- [2] MANDEL, M.; POTTGIESSER, S.; Plutonium distribution in soil from northern Ukraine. Leibniz University of Hanover, Institute for Radioecology and Radiation Protection; 2016.



## Root uptake and translocation of <sup>137</sup>Cs by cultural and wild cereals, model pot experiment

M.M. Godyaeva<sup>1</sup>, N.V. Kuzmenkova<sup>2</sup> and T.A. Paramonova<sup>1</sup>

<sup>1</sup>Faculty of Soil Science, Lomonosov Moscow State University, Moscow, 199991, Russia

<sup>2</sup>Chemistry Faculty, Lomonosov Moscow State University, Moscow, 199991, Russia

Keywords: caesium-137 (<sup>137</sup>Cs), root uptake, translocation, cereals.

Presenting author email: kuzmenkova213@gmail.com

Cultural cereals represent the most valuable crops among the cultures of field rotation in post-Chernobyl areas in Russia. Moreover in terms of radioactive soil contamination cereals are proposed as reference crops for the prediction of <sup>137</sup>Cs root uptake by other plants groups (IAEA, 2006). Wild cereals in turn are frequently dominated in meadow plant community while grass vegetation (fodder crops) is considered as critical link in domestic animals food chain occurring on contaminated lands (IAEA, 2012).

The features of <sup>137</sup>Cs root uptake and translocation by selected cultural and wild cereals were estimated in model pot experiment with growing of oat (*Avena sativa*) and grass mixture of bluegrass (*Poa pratensis*) and fescue (*Festuca rubra*) on chernozems contaminated before seedling with 9.15 MBq/m<sup>2</sup> by <sup>137</sup>CsCl solution. Plants were grown at a temperature 20–22°C with additional lighting (regime 12/12 h) and were regularly watered with tap water by sprinkling according to needs of vegetation. After 16 weeks of growing the plants were removed from pots, separated into above- and belowground parts (belowground parts were simultaneously carefully washed out from soil particles), dried at 80°C, weighted and milled to powder for  $\gamma$ -spectrometry with the use of HPGe detector Canberra GR 3818. Two plants from every pot were dried under pressing for subsequent digital  $\gamma$ -autoradiography conducted with Cyclone. Soil cores were sliced down to thin layers and also were examined by  $\gamma$ -spectrometry and  $\gamma$ -autoradiography methods.

Distribution of <sup>137</sup>Cs within chernozem profiles after single accidental contamination appeared as sharply inhomogeneous with the radionuclide penetration in soil depth until 4–5 cm (Fig. 1). Root density of oat and grass mixture components was maximal at the same zone.

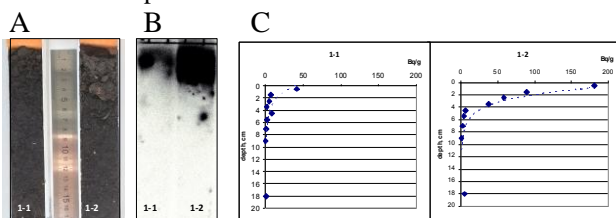


Figure 1. Distribution of <sup>137</sup>Cs in soil cores after growing oat: A – photography, B – digital autoradiography, C –  $\gamma$ -spectrometry

In this connection root uptake occurred from quite contrastingly contaminated local patterns of soil that gave rise to high variability in <sup>137</sup>Cs activities in experimental repetitions, especially for roots. Nevertheless the predominance of <sup>137</sup>Cs activities in

belowground biomass is evidently both for oat and for grass mixture (Table 1). In the field condition root biomass of meadow grasses normally exceeds aerial part biomass and in consequence it's could be presumed that not only peaks of <sup>137</sup>Cs activity, but the most part of the radionuclide inventory is also accumulated in roots of cereals.

Table 1. Ranges of <sup>137</sup>Cs root uptake indicators in experimental conditions

Crop	Part of biomass	<sup>137</sup> Cs activity, Bq/g	<sup>137</sup> Cs inventory, kBq/m <sup>2</sup>	TF <sub>agg</sub> *
oat	stems + leaves	7.5–10.8	0.57–0.73	0.25–0.44
	roots	39.8–121.8	0.09–0.46	1.72–3.60
	total	11.8–11.9	0.67–1.19	0.48–0.53
grasses	stems + leaves	2.3–4.1	0.44–0.77	0.46–0.65
	roots	15.7–32.9	0.23–0.44	2.44–7.66
	total	4.0–4.5	0.88–0.99	0.72–0.73

\* - TF<sub>agg</sub> – aggregated transfer factor = Bq/kg in plants / kBq/m<sup>2</sup> in soil

In general <sup>137</sup>Cs root uptake by both cultural and wild cereals was small intensive and demonstrated a discrimination of the radionuclide transport from contaminated soil into plant. At the same time the ability for <sup>137</sup>Cs accumulation in biomass of grass mixture was slightly more than in oat biomass, especially owing to increased deposition of <sup>137</sup>Cs in root biomass of wild cereals.

As a whole only small share of <sup>137</sup>Cs taken up by the roots was moved into aerial parts – stems and leaves. The values of translocation coefficient for oat and grass mixture varied in the range 0.06–0.27 without any clearly specificity by plant species of *Gramineae* family. Thus, the effect of rhizofiltration could be believed as general physiological strategy of cereals in connection with radioactive soil contamination. Appropriate land use with a high proportion of cereals in a field rotation of crops in the areas affected radioactive fallout is possible through this effect of rhizofiltration.

This work was supported by the Russian Foundation for Basic Research (project No. 14-05-00903).

IAEA, 2006. Classification of soil systems on the basis of transfer factors of radionuclides from soil to reference plants. Vienna. 1–19.

IAEA, 2012. Guidelines for remediation strategies to reduce the radiological consequences of environmental contamination. Vienna. 6–19.

## Indoor Radon in Ardenne: A multivariate analysis

V.De Heyn<sup>1</sup>, C.Licour<sup>1</sup>, F.Tondeur<sup>1</sup>, I.Gerardy<sup>1</sup>, B. Dehandschutter<sup>2</sup>, G. Ciotoli<sup>3</sup>, G. Cinelli<sup>4</sup>

<sup>1</sup>Laboratoire de Physique Nucléaire, ISIB, Haute Ecole Bruxelles-Brabant, Brussels, BE1000, Belgium

<sup>2</sup>Federal Agency for Nuclear Control, Brussels, BE1000, Belgium

<sup>3</sup>Istituto di Geologia Ambientale e Geoingegneria, Consiglio Nazionale delle Ricerche, Rome, I00016, Italy

<sup>4</sup>Independent Researcher, Italy

Keywords: natural radioactivity, soil uranium, soil radon, indoor radon

Presenting author email: [vdeheyn@he2b.be](mailto:vdeheyn@he2b.be)

Indoor radon being a product of the decay of <sup>238</sup>U present in the soil or sub-soil, it is often assumed that a correlation must exist between indoor <sup>222</sup>Rn the concentration of U in the soil or sub-soil, as well as with <sup>222</sup>Rn in the soil. These correlations should also be influenced by other physical and geochemical properties, like soil permeability, which in turn can be related to pedological, geological and lithological classes. Analyzing the relations between all these factors could allow developing a model that would predict areas affected by <sup>222</sup>Rn, even without any measurement in homes. This model would use the available data, which may differ according to the country or even the region.

Several data are available in Ardenne, a region of ~4000 km<sup>2</sup> in the south of Belgium: indoor Rn and soil gas Rn concentrations, soil permeability, soil U from an airborne campaign, which all show an important variability, although the area as a whole can be considered as radon-affected. Geological, pedological and lithological information is also available. As the datasets were not collected at the same sampling points, a first step of interpolation / smoothing was necessary for some of them before the multivariate analysis. The data were mapped on a kilometric grid. Soil Rn and soil permeability were combined into a “radon potential” applying the Czech definition. The numerical variables were transformed in a way to obtain roughly normal distributions (e.g. log-transform of indoor Rn data).

Figure 1 summarizes the absence of clear relationships between indoor Rn, soil Rn and permeability, and airborne soil U. As the radon potential is a function of soil Rn, the better correlation between them is obvious.

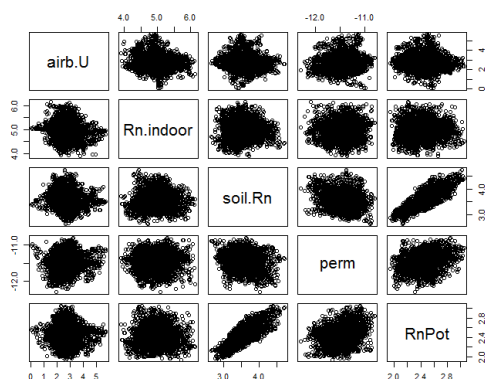


Figure 1. Scatterplot matrix of data collected in Ardenne

In Table 1, Pearson’s correlation coefficients of the global data lead to the same conclusion.

	Airb. U	indoor Rn	Soil Rn	perm	RnPot
Airb U	1.000				
indoor Rn	-0.110	1.000			
Soil Rn	-0.033	0.048	1.000		
Perm.	-0.085	0.030	0.817	1.000	
RnPot	0.086	0.033	0.368	-0.179	1.000

Table 1. Pearson Correlation coefficients of the smoothed and normalized data (N=3729)

We note a strong absence of correlation between indoor Rn and soil Rn or airborne soil U in this Rn-affected area. This result prevents further study by principal component analysis and leads to consider cartography by geological or lithological zone rather than on the kilometric grid. Table 2 gives the correlation coefficients between weighted mean values calculated for the 20 possible classes defined as lithology-geology pairs.

Data grouped by pairs lithology-geology					
Ave-rages	Airb. U	indoor Rn	Soil Rn	perm	RnPot
Airb U	1.000				
indoor Rn	-0.405	1.000			
Soil Rn	-0.044	0.375	1.000		
Perm.	-0.101	0.264	0.811	1.000	
RnPot	0.028	0.341	0.555	0.062	1.000

Table 2. Pearson Correlation coefficients of the smoothed and normalized grouped data by pairs lithology-geology (N=20)

## Study on continuous radon measurement on based of Si-PIN detector

Lei Zhang<sup>1</sup>, Qiuju Guo<sup>2</sup> and Yunxiang Wang<sup>2</sup>

<sup>1</sup>State Key Laboratory of NBC Protection for Civilian, Beijing, 102205, China

<sup>2</sup>State Key Laboratory of Nuclear Physics and Technology, School of Physics, Peking University, Beijing, 100871, China

Keywords: radon concentration, continuous measurement, Si-PIN detector, high-sensitivity.

Presenting author email: [qjguo@pku.edu.cn](mailto:qjguo@pku.edu.cn)

Long term continuous measurement on atmospheric radon concentration is important for the studies using radon as a tracer, and in some special cases, for example, on a small island or above sea surface, quite low level detection and high sensitive measurement are required.

To meet the need, a new continuous measurement equipment was developed with an effective drying system. The structure is shown by Figure 1.

Si-PIN detector (S3204-09, Hamamatsu, Japan) is adopted. 4500V high voltage is added on the surface of the detector, and the voltage drop on the opposite sides of the detector is designed to be 35V. For main continuous drying system, pure PD-50T-24MSS is adopted, and its structure is shown by Figure 2.

Radon gas is suctioned into the hemispheroid passing through a filter and the drying system. The fresh decay product, plus charged particle <sup>218</sup>Po, is adsorbed on detector surface in static electric field, and recorded by Si-PIN detector. Alpha spectrum can be given by mutual-spectrum analyser. Under the slow-work model, radon concentration can be gotten from the total counts of the alpha spectrum of <sup>218</sup>Po+<sup>214</sup>Po by the following equation:

$$C_{Rn} = CF_2 \times \frac{Counts(^{218}Po) + Counts(^{214}Po) - 0.56 \times Counts(^{212}Po)}{\Delta t}$$

Where, C<sub>Rn</sub> is radon concentration (Bqm<sup>-3</sup>), CF<sub>2</sub> is calibration factor for slow-work model, 0.04124Bqm<sup>-3</sup>/cph(got in our standard radon chamber); Δt is the cycle time of measurement; Counts(<sup>218</sup>Po), Count(<sup>214</sup>Po) and Count(<sup>212</sup>Po) are the counts of 6.0MeV, 7.69MeV and 8.78MeV alpha spectrum, respectively.

The new developed continuous radon measuring equipment was installed in an environmental monitor station in Beijing. Measurement result of outdoor radon concentration in November and December, 2016 is shown in Figure 3.

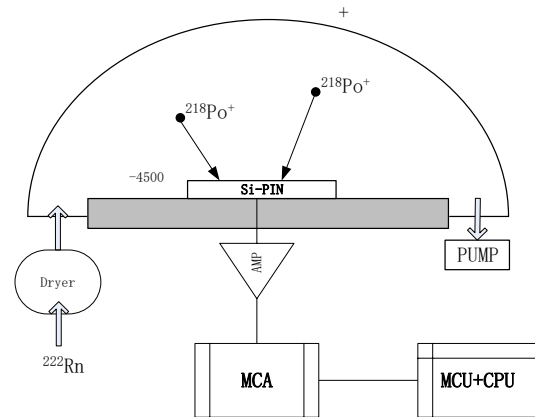


Figure 1. Structure of the radon measurement equipment

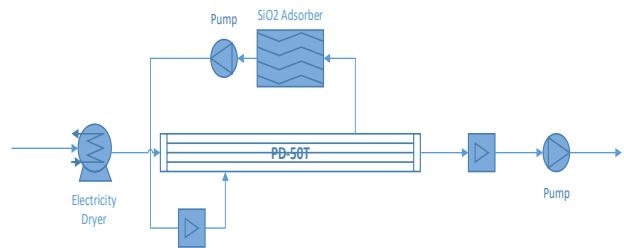


Figure 2. Structure of the continuous drying system

This work was supported by the National Found of Natural Science of China (No. 11355001).

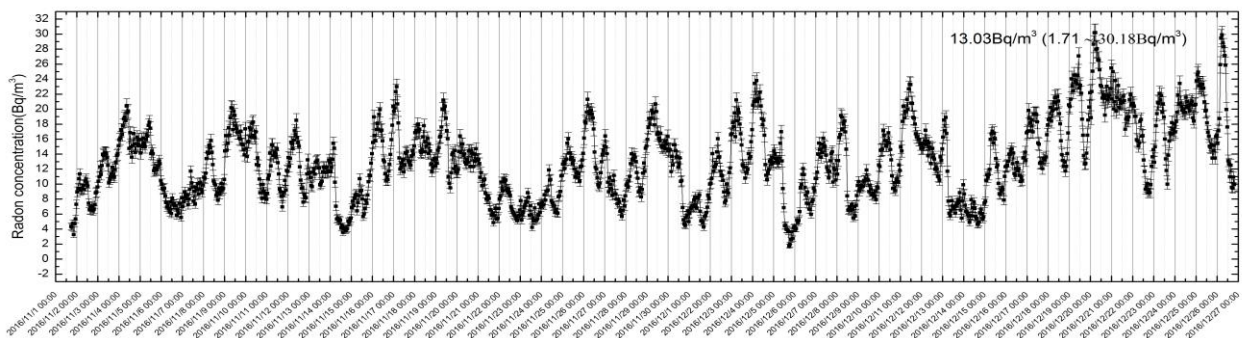


Figure 3. Measurement results of atmospheric radon concentration in Beijing in Nov. and Dec. 2016

## Radiological characterization of volcanic rocks from eastern Canary Islands.

J.G. Rubiano<sup>1</sup>, H. Alonso<sup>1</sup>, J.G. Guerra<sup>1</sup>, M.A. Arnedo<sup>1</sup>, A. Tejera<sup>1</sup>, P. Martel<sup>1</sup>

<sup>1</sup> Departamento de Física, Universidad de Las Palmas de Gran Canaria, 3501 Las Palmas de Gran Canaria, Spain,

Keywords: Gamma-ray spectrometry, natural radioisotopes, radon exhalation, Hazard indexes.

Presenting author email: [jesus.garciarubiano@ulpgc.es](mailto:jesus.garciarubiano@ulpgc.es)

The Canary Islands are located in the NE of the Central Atlantic Ocean (between 27° and 30°N and 19° to 13°W), off of the Western Sahara African coast. They are formed by a group of seven major islands (Tenerife, La Palma, La Gomera, El Hierro, Gran Canaria, Lanzarote and Fuerteventura) and six minor islets. One of the differential aspects of the Canary Islands with respect to the continental territory Spain is its characteristic lithology mainly dominated by volcanic materials.

The Canary Islands have a long volcanic history, with formations over 30 million years old, including submarine stages as well as subaerial volcanism. Three types of units can be found in the islands (1) Basal complex including turbiditic sediments belonging to oceanic crust, volcanic formations associated with the submarine growth of the islands, and intrusives (dike swarms and plutonic rocks of broad geochemical composition) related to submarine and subaerial volcanism, 2) Shield or juvenile volcanism (from basic to acidic rock), and 3) Post-shield or rejuvenated volcanism (rejuvenation stage with ultrabasic to acidic materials).

In this paper, we present a radiological characterization for the main lito-types of geological rock formations appearing in western Canary Islands (Gran Canaria, Lanzarote and Fuerteventura). Samples selected to cover the main categories of the TAS (Total Alkali-Silica) diagram for volcanic rocks have been Collected and analysed. For each sample of rock the content of natural radionuclides (<sup>226</sup>Ra, <sup>232</sup>Th, <sup>40</sup>K) as well as he rate of exhalation of <sup>222</sup>Rn has been determined.

The activity concentrations of natural radionuclides (<sup>226</sup>Ra, <sup>232</sup>Th, <sup>40</sup>K) were measured using a Canberra Extended Range (XTRa) HPGe spectrometer model GX3518. The detector has 38% relative efficiency and nominal FWHMs of 0.875 keV at 122 keV and 1.8 keV at 1.33 MeV, and it works coupled to a DSA-1000 Canberra multichannel analyzer. Radiochemical analysis of each sample has been also carried out.

The rate of exhalation of <sup>222</sup>Rn has been obtained by the technique of accumulation in sealed chamber. Three storage chambers made of methacrylate and equipped with the necessary instrumentation to analyse environmental conditions has been used- The chambers have been characterized to determine the leak rate and the importance of the back diffusion term. The growing curves are collected using the continuous solid-state radon monitors SARAD-SCOUT and AlphaGuard.

In figure 1 and 2 we show, as an example, the equipment setup for the accumulation experiences and the accumulation curves of concentration <sup>222</sup>Rn obtained for several of the litoypes studied.



Figure 1. Radon Accumulation chamber

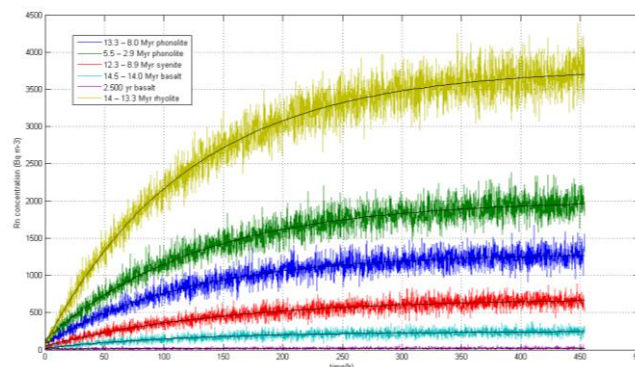


Figure 2. Accumulation curves of concentration <sup>222</sup>Rn for several litoypes.

The highest values activity concentration of natural radioisotopes has been found in intermediate and acidic rocks. These acidic magmatic rocks can accumulate variable amounts of trace elements (such as uranium, thorium, rubidium and strontium, rare earth elements), and major elements (such as potassium), which explains the presence of higher concentrations of natural radioisotopes. These rocks exhibit also the biggest level of <sup>222</sup>Rn exhalation, as expected.

In order to assess the radiological hazards from the litoypes studied, various parameters such as radium equivalent activity, absorbed dose rate, external and internal hazard index, gamma activity index and alpha index based upon the specific activities have been defined in the literature.

### Acknowledgements

This work was financed by the Nuclear Safety Council of Spain (CSN) through a grant from its R&D program 2009 and 2012, and by the European Development Fund (ERDF) through a research project granted by the Canary Agency for Research Innovation and Information Society (ACIISI) from its R&D program 2007.



## Characterisation of Radon Concentrations in the area of Kalachi village (North Kazakhstan)

V.V. Romanenko, S.N. Lukashenko and Y.V. Garbuz

National nuclear centre of the Republic of Kazakhstan, Kurchatov, 071100, Kazakhstan

Keywords: radon flux, doses, indoor radon, Kalachi village.

Presenting author email: Romanenko@nnc.kz

Kalachi settlement is located in the steppe zone on the bank of the Ishim river in the Northern Kazakhstan. On the eastern side of Kalachi settlement, at a distance of about 3 km the former Krasnogorskiy uranium mine is located. The mine is currently put to stand and reclaimed, in-place ore reserves were already depleted by 1983 y.

In 2012 Yesil regional hospital in the Northern Kazakhstan registered symptoms in Kalachi inhabitants which fell under unknown “sleeping” illness. Radon survey of the Kalachi area was conducted as part of the complex study the environmental situation to identify the causes of the mysterious “sleepy” sickness.

The study was carried out as follows:

1. Assessment of areal distribution of radon fluence from the ground surface at the territory of Kalachi village.
2. Survey of radon content indoors of residential accommodations.
3. Monitoring of radon and its daughter`s content in open air.
4. Assessment of radon activity in water.
5. Calculation of doses, received as the result of radon intake.

Studying radon hazard of the village we have revealed several zones with increased fluence of radon from the surface, covering skirts of western, northern and the northeastern part the village.

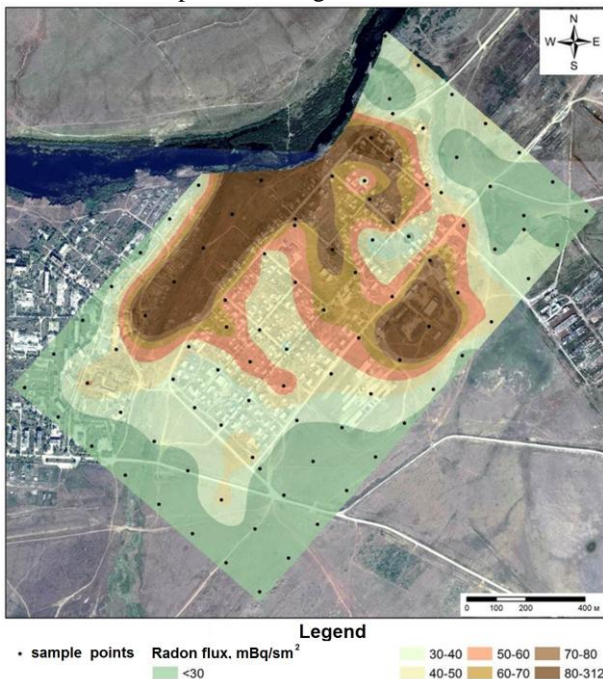


Figure 1. Radon flux

The range of obtained values of radon flux from the ground surface ranges within 4 to 312 mBq/m<sup>2</sup>·s. Increased radon hazard for local population is predetermined by the location of Kalachi village.

Average concentration of daughter products of radon decay in living premises is 130 Bq/m<sup>3</sup>. In 17 % of cases an exceedance of standardized value of 200 Bq/m<sup>3</sup> is observed. The maximal concentrations of radon can reach up to 1,500 Bq/m<sup>3</sup> in residential premises and 15,000 Bq/m<sup>3</sup> in cellars.

As the result of studying volumetric activity and equivalent equilibrium volumetric activity (EEVA) of radon daughters in the atmospheric air at the territory of the village increased and decreased activity cycles were discovered. The length of the period of increased values of radon VA in air is up to 40 days long.

Concentration of radon in groundwater between 2 and 40 Bq/l observed. Up to 2 days long periods of activity increase were registered.

Upon the results of measurements, mean value of internal exposure of village inhabitants by radon is approximately 5 mSv/year. This value exceeds the natural exposure effective dose (worldwide average value) almost 4 times. However, the radiation exposure over 6.4 mSv/year (formed at the average annual radon daughters` concentration indoors over 200 Bq/m<sup>3</sup>) is expected for only 17 % of the village population.

Thus, the increased radiation exposure from radon in the territory of Kalachi village were observed.

The part of this work was supported by the Government of Kazakhstan.



## Geogenic radon as geophysical/geochemical tracer of active faults

G. Ciotoli<sup>1,2</sup>, A.J.S.C. Pereira<sup>3</sup>, P. Bossew<sup>4</sup>, L. Ruggiero<sup>5</sup>

<sup>1</sup>Institute of Environmental Geology and GeoEngineering, Italian National Research Council, Rome, Lazio, 00015, Italy

<sup>2</sup>National Institute of Geophysics and Volcanology, Rome, Lazio, 00143, Italy

<sup>3</sup>CEMMPRE, Department of Earth Sciences, University of Coimbra, Portugal, 3030-790 Coimbra.

<sup>4</sup>German Federal Office for Radiation Protection, Berlin 10318, Germany

<sup>5</sup>Department of Earth Sciences, Rome University Sapienza, 00185 Italy

Keywords: geogenic radon, tracer, faults

Presenting author email: giancarlo.ciotoli@igag.cnr.it

Concentration of radon (Rn – isotopes <sup>222</sup>Rn and <sup>220</sup>Rn) in the ground, and its exhalation to the atmosphere depend on the strengths of their sources and of their capability to release Rn into the pore space, and to their ability to migrate in the ground. In general, radon background concentrations in the soil pore are typical for a specific lithology and depend on the local content of its parent nuclide <sup>226</sup>Ra in the subsurface rock. However, many investigations have reported radon anomalies at concentrations significantly higher than background levels along active faults, and many evidences suggest that these anomalies can provide reliable information about the locations of faults and the spatial distribution of fluid flow within fault zones. However, local increase in radon emanation along faults could be caused by a number of processes including the coprecipitation of parent nuclides in groundwater resulting in local changes of radium activity in the soil (Tanner, 1964), the increase of soil and rock permeability in the fracture zones surrounding active faults (also if buried under hundreds of meters of sedimentary cover; Mollo et al., 2011; Koike et al., 2015; Ciotoli et al., 2016), and the action of carrier gases (i.e., CO<sub>2</sub>, N<sub>2</sub>, and CH<sub>4</sub>) from deep sources that favour the advection and the velocity of gas migration along faulted zones (Ciotoli et al., 2016; Ciotoli et al., 2014; Pereira et al. 2010; Ciotoli et al., 2007).

Furthermore, it has been hypothesized that the stress-strain changes along seismogenic faults prior of earthquakes may be predicted by anomalous signals in geogenic Rn time series. In particular, it is evident that prediction of earthquakes is a potentially extraordinarily important topic (for a thorough discussion, Riggia and Santulin 2015). Therefore, it has been researched for many years, but results have not been sufficiently conclusive so that a certain frustration has taken place in this field of research. It seems however, that recently renewed interest can be noted, perhaps due to advances in Rn metrology and to better availability of statistical methodology for anomaly and signal analysis (e.g. Donner et al. 2015, Sabbarese et al. 2016, Stránský et al. 2016).

We think that characterization of faults with respect to their Rn signature and understanding of geophysical and geochemical processes in and around faults are prerequisites of evaluating them for seismic prediction.

Ciotoli G., Sciarra A., Ruggiero L., Annunziatellis A., Bigi S., 2016a. Soil gas geochemical behaviour across buried and exposed faults during the 24 August central

Italy earthquake. *Annals of Geophysics*, 59, Fast Track 5, 2016; DOI: 10.4401/ag-7242

Ciotoli G., Ascione A., Bigi S., Lombardi S., Mazzoli Soil gas distribution in the main coseismic surface rupture zone of the 1980, Ms=6.9, Irpinia earthquake (southern Italy). *Journal of Geophysical Research*, 119/3, 2440–2461, 2014 DOI:10.1002/2013JB010508

Ciotoli G., Lombardi S., Annunziatellis A., 2007. Geostatistical analysis of soil gas data in a high seismic intermontane basin: Fucino Plain, central Italy. *Journal of Geophysical Research - Solid Earth* Vol: 112 (B5) Article Number: B05407

Donner R.V., Potirakis S.M., Barbosa S.M., Matos J.A.O., Pereira A.J.S.C., Neves L.J.P.F. 2015. Intrinsic vs. spurious long-range memory in high-frequency records of environmental radioactivity. *Eur. Phys. J. Special Topics* 224, 741–762 DOI: 10.1140/epjst/e2015-02404-1

Koike, K., Yoshinaga, T., and Asaue, H. (2009). Radon concentrations in soil gas, considering radioactive equilibrium conditions with application to estimating fault zone geometry. *Environ. Geol.*, 56:1533–1549.

Mollo, S., Tuccimei, P., Heap, M.J., Vinciguerra, S., Soligo, M., Castelluccio, M., and Dingwell, D.B., 2011, Increase in radon emission due to rock failure: An experimental study: *Geo physical Research Letters*, v. 38, L14304, doi: 10.1029/2011GL047962.

Pereira A.J.S.C., Godinho M.M.N., Neves L.J.P.F. 2010. On the influence of faulting on small-scale soil-gas radon variability: a case study in the Iberian Uranium Province- *J. Environmental Radioactivity* 101, 875 – 882. doi: 10.1016/j.jenvrad.2010.05.014

Riggia A., Santulin M. 2015. Earthquake forecasting: a review of radon as seismic precursor. *Bollettino di Geofisica Teorica ed Applicata* 56 (2) 95-114 DOI 10.4430/bgta0148.

Sabbarese C., Ambrosino F., De Cicco F., Pugliese M., Quarto M., Roca V. 2016. Signal decomposition and analysis for the identification of periodic and anomalous phenomena in radon time series. 13th International Workshop GARRM (Geological Aspects of Radon Risk Mapping) 15-16 September 2016, Prague

Stránský V., erný L., Thinová L. 2016. Radon time series modelling based on the continual measurement of radon concentration and related atmospheric parameters. 13th International Workshop GARRM (Geological Aspects of Radon Risk Mapping) 15-16 September 2016, Prague.

## Radon research as a discipline of radioecology – an overview

P. Bossew

German Federal Office for Radiation Protection, Berlin, 10318, Germany

Keywords: radon, radioecology.

Presenting author email: pbossew@bfs.de

As exposure to indoor radon (Rn) is acknowledged as second cause of lung cancer, it has been given much attention for many years and in research practice it is mostly treated as a discipline on its own. Rn is perceived as air pollutant, and understandably, efforts are targeted towards exposure reduction. This implies, among other, modelling its geographical occurrence, its characteristics in various ecological compartments and its temporal behaviour.

Enter radioecology. Rn sources depend on concentrations of U and Th in the ground, in building materials and water. The availability of Rn to infiltrate houses depends on its capacity to migrate in the ground or to be carried by ground and well water. The dynamics of its indoor concentration is controlled by house physics and outdoor atmospheric dynamics. Risk caused by Rn depends on physiological properties of the persons who breathe the air containing it.

The pathway of Rn “from rock to risk” is very complex, as are dependencies and relations between physical and chemical quantities along this pathway. Some of them are control quantities or proxies which can be used for estimation purposes instead, or confounders in estimation procedures.

In this presentation, an overview of the “rock to risk” scheme is given, and certain sections addressed more closely. The pathway extends through several ecological compartments, thus involving a number of radio-ecological disciplines. This starts from the *geogenic compartment*, where the sources of Rn mainly reside, and from which it disperses into other compartments. Among processes in the geogenic compartment are geochemical fractionation, secondary mineralization, decay of radionuclides, decay chain disequilibrium, emanation, exhalation, and advective and diffusive transport.

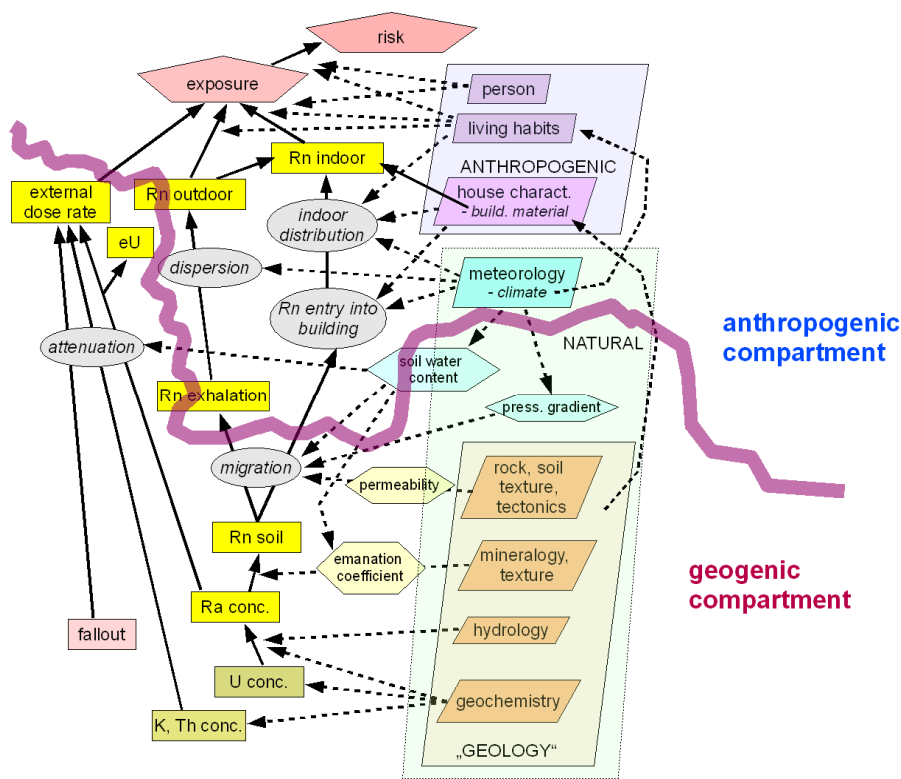
In the *hydrological compartment*, processes are sorption and dissolution, transport and exhalation. The *house ecosystem* has as sub-compartments the interface to the ground and indoor atmosphere. Processes are again advection and diffusion, attachment of progeny to aerosols and adhesion to surfaces, exhalation from building materials, tap water or even natural gas.

The behaviour of Rn and progeny in *living systems* which leads to exposure and finally risk, is again a different field, related to physiology, radiation biology and even sociology, as human behaviour is concerned.

It should be added that apart from its role as health hazard, Rn is increasingly studied as tracer of environmental processes in tectonic and climate studies.

Among challenges in Rn research are designing experimental schemes optimized to meet a given objective, quality assured sampling and measurement, identification of control factors across compartments, model building and calibration and validation.

Thus, the “supply chain” from rock to risk includes a number of radioecological disciplines which assist in achieving the main purpose of Rn research, namely risk reduction. Efforts of the IAEA and the EU to that objective through proposing regulatory frameworks, assisted by WHO, supported with radiological models by the ICRP and large epidemiological studies have led to an impressive volume of results and insights into Rn radioecology for the last years, still growing as countries strive for developing and implementing Rn action plans.



“From rock to risk” – simplified

## Environmental $^{14}\text{C}$ and $^3\text{H}$ levels in Croatia

I. Krajcar Bronić

Department of Experimental Physics, Ruđer Bošković Institute, Zagreb, HR-10000 Croatia

Keywords: atmosphere, biosphere,  $^{14}\text{C}$ ,  $^3\text{H}$

Presenting author email: [krajcar@irb.hr](mailto:krajcar@irb.hr)

A part of activities of Laboratory for low-level Radioactivities of the Ruđer Bošković Institute, Zagreb, Croatia, is devoted to monitoring  $^3\text{H}$  in precipitation and  $^{14}\text{C}$  in the atmosphere and biosphere. An overview of the results and comparison with the global trends will be presented in the talk. Results of monitoring  $^{14}\text{C}$  activity in the atmosphere and in biological samples in the vicinity of the Nuclear Power Plant Krško in Slovenia, about 30 km from Zagreb, will be also presented.

Activity concentration of  $^3\text{H}$  was measured by gas proportional counting technique until 2007 and since 2008 by liquid scintillation counting after electrolytic enrichment. A gas proportional counting technique for  $^{14}\text{C}$  was replaced by liquid scintillation counting following either benzene synthesis or direct absorption of  $\text{CO}_2$  (Horvatinčić et al., 2004, Krajcar Bronić et al., 2009).

Long-term data on  $^3\text{H}$  activity concentration in monthly precipitation in Zagreb and Ljubljana (Slovenia) exist for the period since 1976 and 1981, respectively (Krajcar Bronić et al., 1998, Vreča et al., 2014), while for shorter periods of time the data exist for several stations along the Adriatic coast (Krajcar Bronić et al., 2006, Vreča et al., 2006) and for the continental station Plitvice Lakes (Croatia). The long-term data records show seasonal variations superposed on the basic decreasing trend of mean annual values. The data recorded during last 2 decades, however, show almost constant mean annual  $^3\text{H}$  activity concentration of about 9 TU for the continental stations, while for coastal stations lower values were observed.

Data for  $^{14}\text{C}$  activity in the atmospheric  $\text{CO}_2$  in Zagreb are available for period 1985 – 2016 (Krajcar Bronić et al., 1998, 2010), while data for Plitvice Lakes are not continuous. A systematic decreasing trend of  $-0.46 \pm 0.04$  pMC per year is observed for Zagreb atmospheric  $\text{CO}_2$  in period 1993 – 2016 with seasonal variations superposed on the trend. The winter minima in atmospheric  $^{14}\text{CO}_2$  activity are systematically lower than 100 pMC, probably due to the contribution of fossil fuel combustion in the city area.

Systematic and continuous monitoring  $^{14}\text{C}$  activity in atmospheric  $\text{CO}_2$  and biological samples (mostly apples, vegetable, cereals, corn) in the vicinity of the Nuclear Power Plant Krško (NEK) in Slovenia has been performed since 2006. The  $^{14}\text{C}$  activity of atmospheric  $\text{CO}_2$  at two locations inside the NEK area is on the average slightly higher than that in Zagreb. It depends on the  $^{14}\text{C}$  activity released in air-born effluent. The influence of the  $^{14}\text{C}$  releases has been observed also

in plants. Higher  $^{14}\text{C}$  activity in plants is most pronounced shortly after spring refuelling, when plants use atmospheric  $\text{CO}_2$  that contains  $^{14}\text{C}$  released from NEK. The influence of the released air-born  $^{14}\text{C}$  activity is measurable in both atmospheric  $\text{CO}_2$  and in plants; the higher the activity of gaseous effluent, the higher the atmospheric and plant  $^{14}\text{C}$  activity (Krajcar Bronić et al., 2017). However, the influence is temporally and spatially limited. Average  $^{14}\text{C}$  activity in plants at the control location Dobova does not differ from the average atmospheric  $^{14}\text{C}$  activity in Zagreb.

- Horvatinčić, N., Barešić, J., Krajcar Bronić, I., Obelić, B. 2004. Measurement of low  $^{14}\text{C}$  activities in a liquid scintillation counter in the Zagreb Radiocarbon Laboratory. *Radiocarbon* 46, 105-116.
- Krajcar Bronić, I., Horvatinčić, N., Obelić, B. 1998. Two decades of environmental isotope records in Croatia: Reconstruction of the past and prediction of future levels. *Radiocarbon* 40, 399-416.
- Krajcar Bronić, I., Vreča, P., Horvatinčić, N., Barešić, J., Obelić B. 2006. Distribution of hydrogen, oxygen and carbon isotopes in the atmosphere of Croatia and Slovenia. *Arch. Ind. Hyg. Toxicol.* 57, 23-29.
- Krajcar Bronić, I., Horvatinčić, N., Barešić, J., Obelić, B. 2009. Measurement of  $^{14}\text{C}$  activity by liquid scintillation counting. *App. Radiat. Isotop.* 67, 800-804.
- Krajcar Bronić, I., Obelić, B., Horvatinčić, N., Barešić, J., Sironić, A., Minichreiter, K. 2010. Radiocarbon application in environmental science. *Nucl. instrum. Meth. Phys. Res. A* 619, 491-496.
- Krajcar Bronić, I., Breznik, B., Volčanšek, A., Barešić, J., Borković, D., Sironić, A., Horvatinčić, N., Obelić, B., Lovrenčić Mikelić, I. 2017.  $^{14}\text{C}$  activities in the atmosphere and biological samples in the vicinity of the Krško Nuclear Power Plant – 10 years of experience. In: Proc. 11<sup>th</sup> Symposium of the Croatian Radiation Protection Association, Osijek, Croatia. *in press*
- Vreča, P., Krajcar Bronić, I., Horvatinčić, N., Barešić, J. 2006. Isotopic characteristics of precipitation in Slovenia and Croatia: Comparison of continental and maritime stations. *J. Hydrol.* 330, 457-469.
- Vreča, P., Krajcar Bronić, I., Leis, A., Demšar, M. 2014. Isotopic composition of precipitation at the station Ljubljana (Reaktor), Slovenia – period 2007-2010. *Geologija* 57, 217-230.

## Enhanced atmospheric C-14 monitoring around the Paks NPP of Hungary

M. Molnár<sup>1</sup>, I. Major<sup>1</sup>, T. Varga<sup>1</sup>, G. Orsovszki<sup>2</sup>, M. Veres<sup>2</sup>, T. Bujtás<sup>3</sup>, L. Manga<sup>3</sup>

<sup>1</sup>Isotope Climatology and Environmental Research Centre, Institute for Nuclear Research, Hungarian Academy of Sciences, Debrecen Bem tér 18/c, Hungary

<sup>2</sup>Isotoptech Co., Debrecen Bem tér 18/c, Hungary

<sup>3</sup>Paks Nuclear Power Plant, Paks, Hungary

Keywords: atmospheric, radiocarbon, nuclear power plant

Presenting author email: molnar.mihaly@atomki.mta.hu

The estimated radiocarbon release of NPPs with VVER type light water pressurized reactors (PWRs), operating under standard conditions is cc. 1 TBqGWe<sup>-1</sup>y<sup>-1</sup> to the environment. In PWRs <sup>14</sup>C is produced by neutron activation of oxides in the fuel, moderators and coolant in <sup>17</sup>O(n,p)<sup>14</sup>C reaction and in the <sup>14</sup>N(n,p)<sup>14</sup>C reaction for nitrogen in the fuel, moderator and coolant. The <sup>14</sup>C produced in the coolant is released to the environment mainly via the stack; with <sup>14</sup>C activity discharged in the <sup>14</sup>C discharged with liquid and solid wastes is being less than 5% of the gaseous discharge.

The activity of <sup>14</sup>C in <sup>14</sup>CO<sub>2</sub> and <sup>14</sup>CnHm chemical forms is measured in the vicinity of the Paks Nuclear Power Plant (NPP), Hungary by sampling environmental ambient air. Differential <sup>14</sup>C samplers have been developed to obtain integrated samples for measuring of <sup>14</sup>C in chemical forms such as CO<sub>2</sub>, CH<sub>4</sub> and other hydrocarbons. Radiocarbon is trapped in the form of CO<sub>2</sub> for all chemical species since hydrocarbons are oxidised by a Pt-Pd catalyst heated at 450 C degree. The CO<sub>2</sub> is trapped in bubblers filled with 500 ml of 3M NaOH solution.

Nine differential sampling units at different sites collected samples less than 2 km away far from the 100-m-high stacks of the Paks NPP, and for reference a sampler is

operated at a station ca. 20 km away far from the Paks NPP. Previously atmospheric <sup>14</sup>C was monitored only at 5 stations using GPC counting technique around Paks NPP (Molnár et al, 2007).

We present the results of the continuous observations at the ten stations (A1-A9 and B24 as background reference, Figure 1.) covering the time span of 2 years (2015-2016). The samples have been analysed by AMS technique at the ICER Centre (Debrecen, Hungary). We evaluate the long-term impact of the NPP to on the <sup>14</sup>C content of the atmosphere in the surroundings of the Paks NPP. Comparing our <sup>14</sup>CO<sub>2</sub> measurements with data sets from Jungfraujoch and Schauinsland as well as from Hegyhátsál rural site (Hungary) we demonstrate that the NPP has a definite but minor influence to the <sup>14</sup>C content of the atmosphere.

This work was part of the National Nuclear Research Program (VKSZ\_14-1-2015-0021) supported by the National Research, Development and Innovation Office of Hungary.

Molnár M., Bujtás T., Svingor É., Futó I., Svetlik I.: Monitoring of atmospheric excess <sup>14</sup>C around Paks Nuclear Power Plant, Hungary. Radiocarbon 49 (2007)1031-

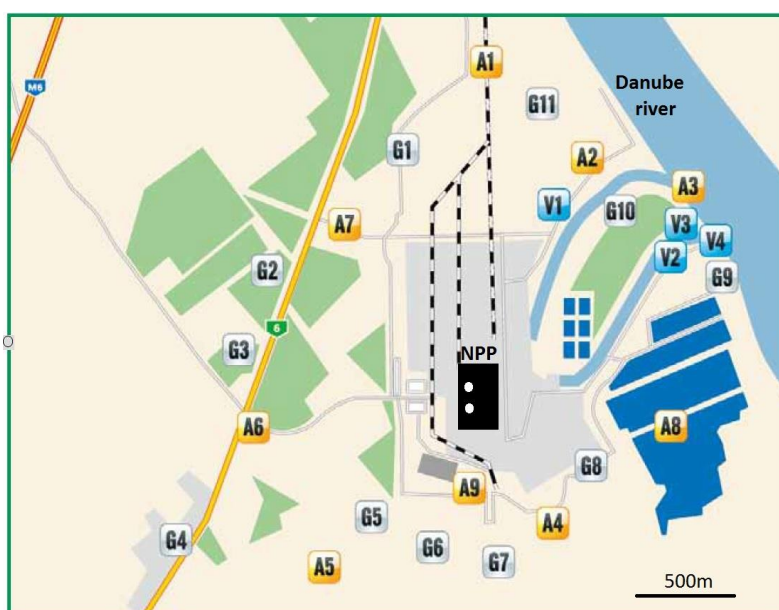


Figure 1. Location of the nine “A-type” atmospheric <sup>14</sup>C monitoring stations (A1 to A9) around the Paks Nuclear Power Plant (Paks, Hungary): One background station (B24) is located in 20 km distance from the NPP.



## Influence of precipitation chemistry on the mobility of radionuclides in boreal forest ecosystems

Eiliv Steinnes

*Department of Chemistry, Norwegian University of Science and Technology (NTNU),  
Trondheim, Norway. eiliv.steinnes@ntnu.no*

**Keywords: Radionuclides, precipitation chemistry, boreal forest, soil, vegetation**

Precipitation chemistry may vary substantially over short distances, particularly in countries with a complex topography. Not only is the amount of precipitation critically dependent on topography and meteorological factors, but also the chemical composition of the falling precipitation may vary substantially with distance to the ocean. In areas close to the coast the content of elements released from the ocean either as sea salt particles or by biogenic gaseous emission may be orders of magnitude higher in falling precipitation than what is the case in territories situated far from the ocean. Thus the atmospheric deposition of radionuclides at a given site does not only depend on the amount and frequency of precipitation, but perhaps even more on the chemical composition of the precipitation. After the radionuclide reaches the ground, other chemical substances supplied by precipitation may continue to influence its further mobility and biological uptake.

Norway is a country where the amount as well as the chemical composition of the precipitation varies substantially over its territory, depending on topography as well as distance from the ocean. This does not only strongly influence the atmospheric supply of chemical substances originating from the ocean, but also the mobility and hence the plant availability of other substances already present in the soil. This may influence the mobility and plant availability of several important radionuclides. Research in Norway has shown that the mobility of  $^{137}\text{Cs}$  from the Chernobyl accident in natural surface soil showed considerable variation over many years following the accident (Gjelsvik and Steinnes, 2013). Studies of marine influence of surface soil chemistry show that the atmospheric deposition of iodine in Norway and hence the availability of iodine in the soil varies by more than a factor of 10 over a 250-km transect from the ocean (Steinnes and Frontasyeva, 2002). Although not studied so far, this is likely to affect the fate of newly fallen  $^{131}\text{I}$  fallout and subsequent doses to humans and other biota, and should be considered in case of future nuclear accidents. Moreover, soil chemistry studies in Norway involving strontium indicate that the fate of  $^{89}\text{Sr}$ - $^{90}\text{Sr}$  fallout after a nuclear accident and the resulting radiation doses to humans and other biota may also depend on precipitation chemistry.

### REFERENCES

- Gjelsvik, R., Steinnes, E., 2013. Geographical trends in  $^{137}\text{Cs}$  fallout from the Chernobyl accident and leaching from natural soil in Norway. *Journal of Environmental Radioactivity* 126, 99-103.
- Steinnes, E., Frontasyeva, M., 2002. Marine gradients of halogens in soil studied by epithermal neutron activation analysis. *Journal of Radioanalytical and Nuclear Chemistry* 253, 173-177.



## On the radionuclide distribution in selected sediment cores from the Baltic Sea

M. Eriksson<sup>1</sup>, G. Olszewski<sup>1,2</sup>, P. Lindahl<sup>1</sup>, P. Andersson<sup>1</sup>, E. Chamizo<sup>3</sup>, R. García-Tenorio<sup>3,4</sup>

<sup>1</sup>Swedish Radiation Safety Authority, Stockholm, SE-171 16, Sweden

<sup>2</sup>University of Gdańsk, Faculty of Chemistry, Wita Stwosza 63, 80-308 Gdańsk, Poland

<sup>3</sup>Centro Nacional de Aceleradores, E-41092 Sevilla, Spain

<sup>4</sup>Applied Nuclear Physics Group, University of Seville, Avda. Reina Mercedes, 41012-Seville, Spain

Keywords: radionuclides, sediment, dating, Baltic Sea.

Presenting author email: mats.eriksson@ssm.se

The Swedish Radiation Safety Authority (SSM) collect jointly with the other Swedish authorities (e.g. Swedish Environmental Protection Agency and Geological Survey of Sweden (SGU)) samples for the marine environment surrounding Sweden. This activity is a part of the Swedish Marine Environmental Monitoring Program. Sampling station in this subproject have been revisit regularly and monitored since 1970s, but at its present form, including 16 stations, started 2003 and revisit every 5 year. The idea is to study trends in pollutions (including 68 elements and 66 organic compounds) at these stations that are carefully selected to be in deep bottom areas with undisturbed sediment, which forms excellent archives that can be dated.

SSMs role has been to study radioactivity in the sediments and to produce sediment dating results for the other collaborators monitoring metals and organic pollutants. The presentation will focus on the radionuclide (<sup>137</sup>Cs, Pu-isotopes and <sup>241</sup>Am) distribution in selected sediment profiles that have been dated using <sup>210</sup>Pb-models. The sediment cores were collected on the 2008 national sampling campaign. The distribution will be discussed with respect to sources of radionuclides in the Baltic Sea as well on redistribution of these radionuclides.

We could identify two main sources of radionuclide contamination in these cores, namely global fallout from nuclear weapons tests and from Chernobyl accident fallout. Plutonium mainly originate from the global fallout but Pu isotopic analysis showed a unique signal representing the Chernobyl fallout. For <sup>137</sup>Cs the contribution in the sediment cores was opposite, i.e. most of the activity originate from the Chernobyl fallout. For <sup>241</sup>Am we found similar activity concentrations in the sediment slices dated to Chernobyl accident and in those dated to the global fallout peak. Significant difference in the radionuclides distribution in the sediment cores from the two sites was observed. For Cs and Pu originating from the Chernobyl accident the fallout pattern do not agree. The Chernobyl fallout for <sup>137</sup>Cs seems to follow wet deposition and distance to the source of accident.

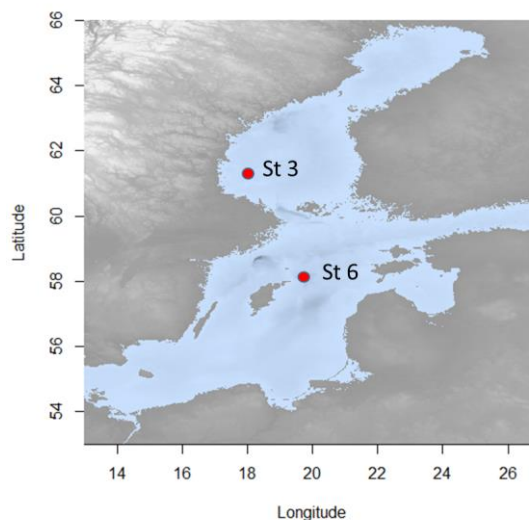


Figure 1. The two selected station in the Baltic Sea were radionuclide distribution have been studied in sediment cores.

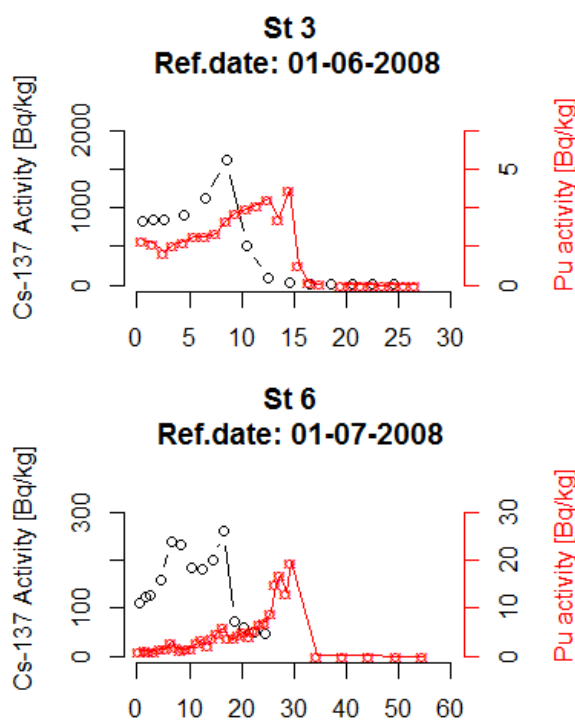


Fig 2. Radionuclide distribution in sediment cores (St 3 and St 6) from the Baltic Sea. Depth in cm.

## Deposition of radionuclides by fog droplets on plants

O. Masson<sup>1</sup>, J. Tav<sup>1</sup>, F. Burnet<sup>2</sup>, P. Paulat<sup>1</sup>, A. De Vismes<sup>3</sup>

<sup>1</sup> Institut de Radioprotection et de Sûreté Nucléaire (IRSN-LEREN), BP3, 13115, Saint Paul  
Lez Durance Cedex, France.

<sup>2</sup> CNRM/GAME, Météo-France/CNRS, 42 Av. De Coriolis, 31000 Toulouse, France

<sup>3</sup> Institut de Radioprotection et de Sûreté Nucléaire (IRSN-LMRE), Bois des rames 91400,  
Orsay, France.

Keywords: fog, deposition, radionuclides, plant

Presenting author e-mail: olivier.masson@irsn.fr

After a nuclear accident like Fukushima, airborne radionuclides released in the atmosphere can act as cloud condensation nuclei to form fog droplets, subject to a high ambient humidity and drop in temperature. Fog water deposition is rarely quantified and often considered as occult deposition. However the fog water chemistry exhibits higher concentrations than for rain water. A similar enrichment is expected for radionuclides compare with rain water. Fog contribution to radionuclide deposition on terrestrial ecosystem is thus legitimate, both on a regular basis i.e. during routine situations or after an accident release. This study focuses on radionuclide deposition by fog on different plants.

**Method.** An analysis of the fog water radioactivity levels and a quantification of the fog water deposition have been performed in the north east region of France. In order to quantify the deposition of cloud water, plants are exposed to fog and weighted with a precision balance every ten to twenty minutes. Three main plant species (small conifers with 3D shape; grasses and leaf-vegetable (cabbage) have been used for comparison of water deposition flux and velocity.

**Results.** Results show that the mass of water deposited ( $0.15$  to  $4 \text{ mL}\cdot\text{min}^{-1}\cdot\text{m}^{-2}$  of vegetation cover) is greater on small conifers than on other plants or bare soil. This is consistent with what was expected due to the larger impaction surface of the small conifers and turbulent induced droplet impaction. During the fog season (September to February) fogwater deposition can represent 1 to 2 % of total water deposition (mostly by rain and snow) but corresponds up to 12% of  $^{137}\text{Cs}$  or  $^{210}\text{Pb}$  deposited amount (in  $\text{Bq}/\text{m}^2$ ).

Apparent deposition velocities are at least those induced by sedimentation for 10 to 20  $\mu\text{m}$  aerosols and at most those assuming an additional contribution by turbulent impaction and deposition for smaller droplet sizes. The liquid water content (LWC) can be used to derive the sedimentation deposition velocity. The LWC is linked to the visibility which can be provided by usual sensor.

## **Beryllium and Xenon time series analysis: a new methodological approach for Atmospheric Transport Modelling at small, synoptic and global scales**

S. Bianchi<sup>1</sup>, A. Longo<sup>1</sup> and W. Plastino<sup>1</sup>

<sup>1</sup>Department of Mathematics and Physics, Roma Tre University, Rome, I-00146, Italy  
Keywords: Beryllium, Xenon, Time Series Analysis, Atmospheric Transport Modelling.  
Presenting author email: wolfango.plastino@uniroma3.it

Beryllium-7 is a cosmogenic radionuclide produced primarily in the lower stratosphere and the upper troposphere. It is useful to characterize the stratosphere–troposphere exchange of air masses and chemical species occurring at small, synoptic and global scales associated with the tropopause folding (Liu et al., 2016).

Xenon-133 is an anthropogenic radionuclide resulting from the nuclear fission process and released into the atmosphere from the Isotope Production Facilities (IPF), Nuclear Power Plants (NPP), and nuclear explosions. The knowledge of the activity concentration and isotopic composition of this radioactive noble gas in the atmosphere indicates the nuclear processes governing its formation (Plastino et al. 2010).

Now a new methodological approach based on time series analysis (Bianchi and Plastino, 2017) for event screening categorization of beryllium and xenon background and outliers was tested. Feedback induced by local meteorological patterns on the equipment and on the sampling procedures was included in the analysis to improve a possible event categorisation scheme. Furthermore, by use of atmospheric transport modelling (ATM) on aerosols and noble gas, knowledge of possible source characteristics, points of origination and potential contamination from other sources in the area of the sampling point can be established.

This new methodological approach was tested on radionuclides and meteorological data of the International Monitoring System (IMS) of the Comprehensive Nuclear-Test-Ban Treaty Organization (CTBTO), and for a period longer than 11-year solar cycle. The concentrations of beryllium and xenon in the atmosphere were being continuously monitored at 80 IMS stations around the world, and covering the Earth's hemispheres.

Furthermore, for beryllium time series analysis the data from the worldwide cosmic rays observatories were included.

Finally, was possible to characterize by ATM on noble gas (xenon) and aerosols (beryllium) the source-receptor relationship, and for beryllium to define the patterns at small, synoptic and global scales for testing the possible associated tropopause folding.

The authors greatly acknowledge the Comprehensive Nuclear-Test-Ban Treaty Organization for the kind contribution by the virtual Data Exploitation Centre.

- Bianchi, S., Plastino, W., 2017. Uranium time series analysis: a new methodological approach for event screening categorization. ENVIRA 2017 - Book of Abstracts.
- Liu, H., Considine, D.B., Horowitz, L.W., Crawford, J.H., Rodriguez, J.M., Strahan, S.E., Damon, M.R., Steenrod, S.D., Xu, X., Kouatchou, J., Carouge, C., Yantosca, R.M., 2016. Using beryllium-7 to assess cross-tropopause transport in global models. *Atmos. Chem. Phys.* 16, 4641–4659.
- Plastino, W., Plenteda, R., Azzari, G., Becker, A., Saey, P.R.J., Wotawa, G., 2010. Radioxenon Time Series and Meteorological Pattern Analysis for CTBT Event Categorisation, *Pure Appl. Geophys.* 167, 559–573.
- Schoeppner, M., Plastino, W., 2014. Determination of the Global Coverage of the IMS Xenon-133 Component for the Detection of Nuclear Explosions, *J. Sci. Global Secur.* 22, 209-234.

## Time evolution of atmospheric tritium concentration in two locations affected by different source terms: cosmogenic and cosmogenic plus anthropogenic

A. Baeza, A. Rodríguez-Perulero, J. Guillén and E. García-Delgado

LARUEX, Department of Applied Physics, University of Extremadura, Cáceres, 10003, Spain

Keywords: tritium, time evolution, NPP, cosmogenic

Presenting author email: abaeza@unex.es

Tritium concentration in near surface atmosphere has two main source terms: cosmogenic and anthropogenic. Due to this, time evolution of tritium concentration can differ significantly. The aim of this study is to analyse the dynamics of tritium in near surface atmosphere (water vapour and rainfall) in two different locations of Extremadura (West Spain): i) Cáceres and ii) surroundings of Almaraz Nuclear Power Plant (ANPP) (Serrejón and Almaraz). The first one is located more than 90 km away from ANPP and in the opposite direction from the prevailing winds. Therefore, it can be assumed that the source term for tritium in this area is mainly cosmogenic. While in the surroundings of the ANPP (Serrejón and Almaraz), there is also an antropogenic component due to this source term. In order to reduce the thermal impact in the Tagus River, several cooling towers were constructed on the ANPP reservoir. Its influence on tritium content in the surrounding was also analysed.

Tritium in water vapour was collected using an active tritium collector (MARC 7000) in each selected location. Rainfall was collected using trays with known surface. Tritium was determined by direct measurement, or previously concentrated by electrolyse if needed, in a Quantulus 1220. The quality control is assured by the ISO 17025 accreditation of LARUEX for the measurement of tritium in environmental samples. Table 1 shows the mean value, standard deviation (S.D.) and range of variation of tritium concentration in water vapour in air in the selected locations, being higher in the surrounding of ANPP than in Cáceres.

Table 1. Tritium concentration in  $\text{mBq m}^{-3}$  in near surface atmosphere in Cáceres (cosmogenic) and in Serrejón and Almaraz (cosmogenic+anthropogenic).

Location	Mean $\pm$ S.D	Range
Cáceres	$12 \pm 4$	6.3 – 16.8
Serrejón	$34 \pm 10$	24 – 49
Almaraz	$60 \pm 21$	26 – 86

Time evolution of tritium content in rainfall in Cáceres is shown in Figure 1, as a way of example. The mean value was  $0.64 \pm 0.44$  (S.D.) within the range (0.19 – 2.44) Bq/L. Seasonal variation were also observed in the other locations. In order to assess its dyanmics, tritium concentrations in rainfall and water vapour were modelled using meteorological variables (precipitation, solar radiation, relative humidity, etc.).

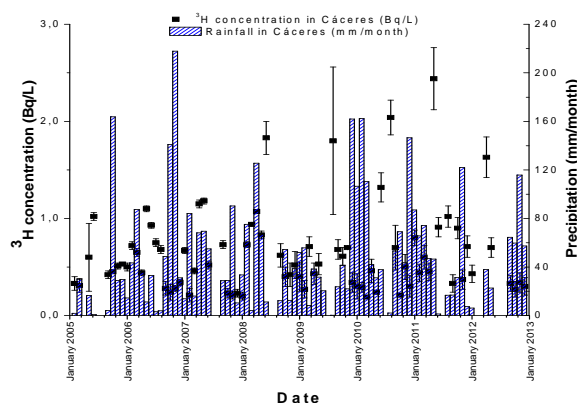


Figure 1. Tritium concentration in rainfall in Cáceres in Bq/L and precipitation in mm/month.

Figure 2 shows the influence of the cooling towers built on the ANPP reservoir on tritium concentration in water vapour. An enhancement regarding the initial situation was observed for the most of the year.

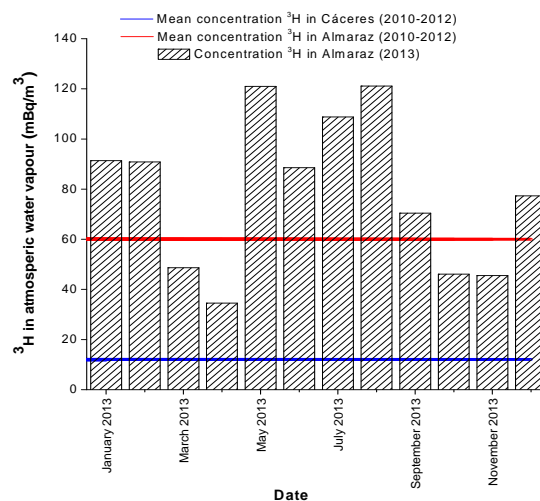


Figure 2. Tritium activity levels in near surface atmosphere in Almaraz just after the start-up of cooling towers in Almaraz Nuclear Power Plant water reservoir.

This work was financed by the Spanish Ministerio de Ciencia e Innovación in the project “Caracterización de la evolución temporal radiactiva de los aerosoles presentes en un emplazamiento exento de término fuente” (CTM2006-11105). We also want to thank the financial support granted to the LARUEX research group (FQM001).

## High resolution Iodine-129 and tritium bomb peak records in an ice core from SE-dome site, Greenland

A.T. Bautista VII<sup>1,2</sup>, Y.Miyake<sup>1</sup>, H. Matsuzaki<sup>1,3</sup>, Y. Iizuka<sup>4</sup>, K. Horiuchi<sup>5</sup>

<sup>1</sup>Department of Nuclear Engineering and Management, The University of Tokyo, Bunkyo-ku, Tokyo 113-8656, Japan

<sup>2</sup>Philippine Nuclear Research Institute – Department of Science and Technology, Quezon City 1101, Philippines

<sup>3</sup>MALT, The University Museum, The University of Tokyo, Bunkyo-ku, Tokyo 113-0032, Japan

<sup>4</sup>Institute of Low Temperature Science, Hokkaido University, Sapporo 060-0918, Japan

<sup>5</sup>Graduate School of Science and Technology, Hirosaki University, Hirosaki-shi, Aomori 036-8560, Japan

Keywords: ice core, iodine-129, tritium, bomb peak

Presenting author email: atbautistavii@pnri.dost.gov.ph

Iodine-129 and tritium are radionuclides that majorly come from human nuclear activities, such as nuclear bomb testing. These radionuclides are used in environmental studies as tracers and age markers. In particular, the tritium nuclear bomb peak is traditionally applied as an age marker for year 1963 in ice cores.

Ice cores that come from polar ice sheets, especially from domes, provide good historical records of paleoenvironmental events. Dome ice cores generally have low accumulation rates because these are often located in dry, inland areas. Ice cores with low accumulation rates can provide paleoenvironmental records of up to thousands of years. However, these ice cores have low temporal resolution and cannot reveal seasonal or annual events (Kameda et al., 2008).

In this paper, we report the results of <sup>129</sup>I and tritium measurements on an ice core from one of the highest accumulation dome sites (~ 0.9m per year) in Greenland – SE-dome (67.18°N, 36.37°W; Iizuka et al., 2016). This paper provides a record of <sup>129</sup>I deposition during years 1956-1976 with the highest temporal resolution (~ 6 months) to date. Given that these years mark the height of nuclear bomb testing, our aim in this study is to compare <sup>129</sup>I and tritium nuclear bomb signals found in the ice core and review their applications as age markers and environmental tracers.

The SE-dome ice core has a total length of 90.45m. Here we report measurements done on 66.9m to 90.35m of the ice core at 0.5m intervals. <sup>129</sup>I was measured using accelerator mass spectrometry in the MALT facility, University of Tokyo, Japan, while tritium was measured by Liquid Scintillation Counting in the National Institute for Polar Research, Japan (Iizuka et al., 2016b).

Results show that both <sup>129</sup>I and tritium record prominent peaks in years 1959 and 1963. These peaks are associated with nuclear bomb tests done by former Soviet Union in the Novaya Zemiya test site (70.72°N, 54.70°E) in year 1958 and 1962. In addition, <sup>129</sup>I records a peak in 1962, associated with Soviet tests done in 1961.

In terms of timing, <sup>129</sup>I bomb peaks are recorded in winter (1958.9, 1962.1, and 1963.0) while tritium bomb peaks show delay and are recorded in spring or summer of the same year (1959.3, and 1963.6). This discrepancy may have been caused by the difference in production or deposition mechanism between the two radionuclides.

Also notable is the large <sup>129</sup>I peak in year 1964, which cannot be attributed to nuclear bomb testing alone.

This enhanced signal is possibly due to additional contribution from nuclear fuel reprocessing from the Sellafield facility in the United Kingdom, which is believed to release large amounts of <sup>129</sup>I during these years (Reithmeier et al., 2006). We similarly attribute <sup>129</sup>I peaks in years 1972 and 1975 to emissions from Sellafield.

These results show that <sup>129</sup>I signals, like tritium, can also be used as age markers in ice cores. Although its analysis is less straightforward because of multiple <sup>129</sup>I sources (i.e., nuclear weapons testing and nuclear fuel reprocessing), additional signals available after 1963 provide more age markers that can be used well after the nuclear bomb testing period. Moreover, <sup>129</sup>I in this ice core may be used to reconstruct, with high temporal resolution, the impact of human nuclear activities on the area surrounding the SE-dome site. In the future, we plan to continue analysis of the rest of the ice core to reveal <sup>129</sup>I signals in years 1977-2015.

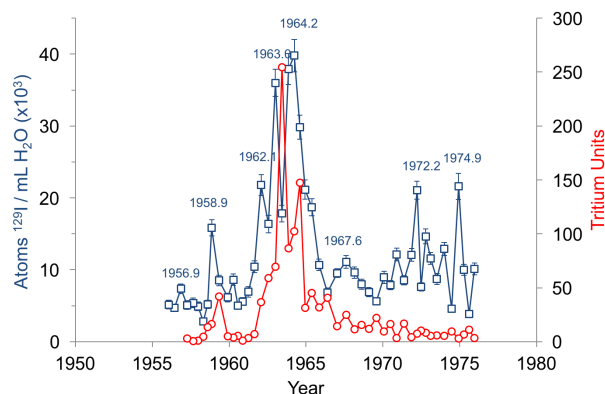


Figure 1. <sup>129</sup>I and tritium in the SE-dome ice core.

Iizuka, Y., Matoba, S., Yamasaki, T., Oyabu, I., Kadota, M., Aoki, T., 2016a. Bull. Glaciol. Res. 34, 1–10.  
 Iizuka, Y., Miyamoto, A., Hori, A., Matoba, A., Furukawa, R., Saito, T., Fujita, S., Hirabayashi, M., Yamaguchi, S., Fujita, K., Takeuchi, N., 2016b. Arctic, Antarctic, and Alpine Research, in press.  
 Kameda, T., Motoyama, H., Fujita, S., Takahashi, S., 2008. J. Glaciol. 54, 107–116.  
 Reithmeier, H., Lazarev, V., Rühm, W., Schwikowski, T.M., Gäggeler, H.W., Nolte, E., 2006. Environ. Sci. Technol. 40, 5891–5896.



## Analysis of beryllium-7 variability in northern Europe

J. Ajtić<sup>1,2</sup>, V. Djurdjevic<sup>3</sup>, D. Sarvan<sup>1</sup>, E. Brattich<sup>4</sup>, M. A. Hernández-Ceballos<sup>5</sup>

<sup>1</sup>Faculty of Veterinary Medicine, University of Belgrade, Belgrade, 11000, Serbia

<sup>2</sup>Institute for Research and Advancement in Complex Systems, Belgrade, 11000, Serbia

<sup>3</sup>Institute of Meteorology, Faculty of Physics, University of Belgrade, Belgrade, 11000, Serbia

<sup>4</sup>Environmental Chemistry and Radioactivity Laboratory, Department of Chemistry “G. Ciamician”, Alma Mater Studiorum University of Bologna, 40126, Bologna (BO), Italy

<sup>5</sup>European Commission, Joint Research Centre, Institute for Transuranium Elements, Nuclear 7 Security Unit, Ispra (VA), 21027, Italy

Keywords: Beryllium-7, meteorological parameters, SCAND index.

Presenting author email: erika.brattich@unibo.it

This work presents an overview of the results obtained in an analysis of the <sup>7</sup>Be activity concentrations recorded in surface air in Helsinki, Finland, over a 25-year period (1987-2011), and stored in the online Radioactivity Environmental Monitoring (REM) database.

First, lagged linear correlations of the <sup>7</sup>Be specific activity with several meteorological variables: tropopause height (TPH); mean, minimum and maximum temperature; precipitation (Prec); atmospheric pressure (Press); potential vorticity (PV) at 300 hPa and 200 hPa; solar zenith angle (SZA); and sunspot number are analysed (Tab. 1). The time lag in the correlation calculations is allowed to vary between 0 and 7 days for TPH, meteorological parameters and PV, and between 0 and 31 days for SZA and sunspot number. The correlations are calculated for the total set of measurements as well as for different seasons.

Table 1. Maximum correlation coefficients (m.c.c.) and number of days (n.d.) on which they are observed between <sup>7</sup>Be and meteorological variables. Empty cells indicate non-significant correlations.

Variable	Total set		Autumn		Winter		Spring		Summer	
	m.c.c.	n.d.	m.c.c.	n.d.	m.c.c.	n.d.	m.c.c.	n.d.	m.c.c.	n.d.
TPH	0.32	1	0.38	2	0.20	1	0.31	1	0.47	1
Mean T	0.41	0	0.33	0			0.40	0	0.48	1
Min T	0.37	0	0.34	0			0.33	0	0.39	0
Max T	0.44	0	0.31	0			0.42	0	0.50	1
Prec										
Press	0.29	2	0.29	2	0.31	3	0.34	2	0.43	2
PV (300 hPa)										
PV (200 hPa)										
SZA	0.48	0	0.3	0	0.20	0	0.34	31	0.08	15
Sunspot N										

Our results (Tab.1) indicate weak to moderate correlations for <sup>7</sup>Be with TPH, temperatures, and atmospheric pressure. The strongest relationship is observed in summer, when it is accompanied by a short time lag (within two days). The absence of significant correlations with PV is probably due to the fact that

stratospheric intrusions are not located directly above Helsinki.

In the second part of our analysis, we looked into the <sup>7</sup>Be extremes, defined as events with the <sup>7</sup>Be surface concentrations above the 95<sup>th</sup> percentile. Even though the <sup>7</sup>Be annual cycle is characterised by a maximum during the warm season and minimum during the cold period, 10% of the extreme events occur during cold months, between October and March. These “cold extremes” are analysed in more detail, and depending on their persistence, they are classified as “bursts” or “episodes”. Three representative episodes and one burst are analysed looking for common features. Our results imply that, in general, these events are characterised by anomalies in PV, sea level pressure, temperature and precipitation patterns over Europe and the North Atlantic. We further notice that the Scandinavia (SCAND) teleconnection index is above the 75<sup>th</sup> percentile during all the months in which the cold episodes are observed (Fig.1). This finding suggests a potential use of SCAND as a predictor of these events in the Scandinavian region.

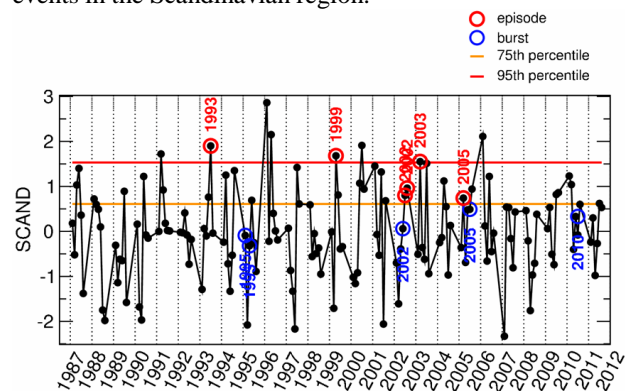


Figure 1. Monthly values of the SCAND index (black). In each year, six values, representing the cold months, are given. Red and blue circles annotate months when the cold episodes and bursts, respectively, are recorded. Orange and red lines are the 75<sup>th</sup> and 95<sup>th</sup> percentile thresholds for the SCAND distribution.

The work is a part of the research done within the project "Climate changes and their influence on the environment: impacts, adaptation and mitigation" (No. 43007) financed by the Ministry of Education, Science and Technological Development of the Republic of Serbia (2011–2017).

## Radium isotopes in saline deepwaters as tracers of the source aquifer

Detlev Degering<sup>1</sup>, Norman Dietrich<sup>1</sup>, Felix Krüger<sup>2</sup>

<sup>1</sup> VKTA - Strahlenschutz, Analytik & Entsorgung Rossendorf e. V., P.O. Box 510119, 01314 Dresden, Germany

<sup>2</sup> VacuTec Meßtechnik GmbH Dresden, Dornblüthstraße 14, 01277 Dresden, Germany

Keywords: Radium isotopes,  $\alpha$ -recoil, saline deepwaters.

Presenting author email: detlev.degering@vkta.de

A compilation of analyses on fluid samples from Germany used by geothermal energy, balneology etc. revealed a widespread variation of Radium activity concentration and  $^{228}\text{Ra}/^{226}\text{Ra}$  isotope ratios as well (Fig. 1). The highest Radium concentrations of several  $10 \text{ Bq}\cdot\text{l}^{-1}$  are correlated with enhanced salinities up to some  $100 \text{ g}\cdot\text{l}^{-1}$ . Such highly saline fluids can be found worldwide in waters from the crystalline basement at depths  $> 1500 \text{ m}$  (Bucher and Stober, 2010).

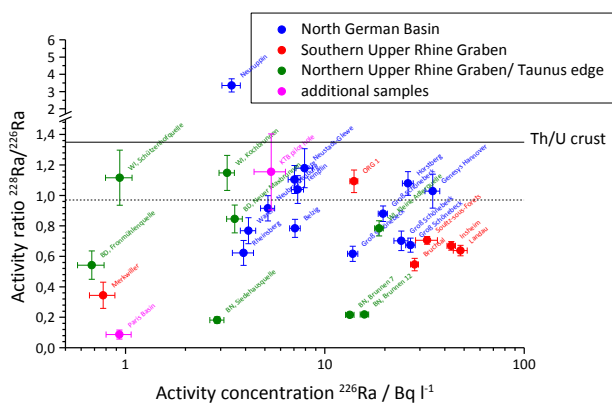


Figure 1. Summary of Radium isotope analyses performed on fluid samples mainly from Germany. The solid line gives the mean  $^{232}\text{Th}/^{238}\text{U}$  activity ratio of the earth's crust. The dashed line is explained in the text.

The aim of the presented investigation was the search for a link between the observed Radium isotope concentrations in the fluid and the characteristics of the storage aquifer rock.

$\alpha$ -recoil at the solid/fluid interface was identified as the prevailing mechanism for Radium release. In the fluid it is balanced by the contrary processes of sorption and radioactive decay, leading to equilibrium concentrations of the Radium isotopes in solution.

Short term laboratory experiments confirmed the role of  $\alpha$ -recoil effects as the main process at least in the release of  $^{224}\text{Ra}$  ( $T_{1/2} = 3.6 \text{ d}$ ) and showed a stabilisation of dissolved Radium species starting at salinities of some  $10 \text{ g}\cdot\text{l}^{-1}$  (Fig. 2).

Monte Carlo simulations were performed to focus on the modification of activity depth profiles at mineral surfaces caused by  $\alpha$ -recoil effects. The simulations included the different physicochemical behaviour of released recoil nuclei as well as the nuclear data of each  $\alpha$ -decay in the natural decay chain prior to the investigated Radium isotopes.

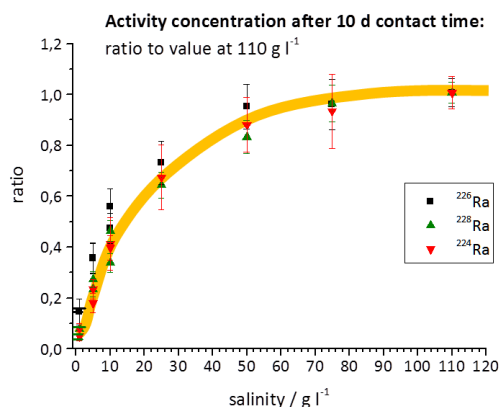


Figure 2. Radionuclide activity concentrations (normalised to the value at  $110 \text{ g}\cdot\text{l}^{-1}$ ) in solutions of variable salinity after 10 d contact time.

Main outcomes of the simulations were

- $\alpha$ -recoil release rates at the mineral surfaces depend only on the U- and Th- contents and on the specific surface area of the rock and are in the order of  $10^{-10} (\text{s}^{-1}\cdot\text{m}^{-2})\cdot(\text{Bq}\cdot\text{m}^{-3})^{-1}$ .

- A close relation exists between the  $^{228}\text{Ra}/^{226}\text{Ra}$  activity concentration ( $c_A$ ) ratio in the fluid and the  $^{232}\text{Th}/^{238}\text{U}$  activity (A) ratio of the aquifer rock:

$$\frac{c_A(^{228}\text{Ra})}{c_A(^{226}\text{Ra})}_{\text{fluid}} = 0.72 \cdot \frac{A(^{232}\text{Th})}{A(^{238}\text{U})}_{\text{rock}}$$

An illustration for this relation can be found in Fig.1: The mean  $^{232}\text{Th}/^{238}\text{U}$  activity ratio of the earth's crust (solid line, derived from Wedepohl, 1995) is obviously higher than the majority of the  $^{228}\text{Ra}/^{226}\text{Ra}$  ratios in fluids. Applying the factor of 0.72 it leads to the dashed line which is much closer to the "data cloud" shown in Fig.1. The Radium isotope signature of the fluid is thus a fingerprint of the aquifer rock responsible for the fluid storage.

The validity of the model was further verified by investigations on drilling cores from geothermal wells and by comparing a data set of  $> 100$  rock samples with fluid data of known origin.

Bucher, K., Stober, I., 2010. Fluids in the upper continental crust, *Geofluids* 10 (2010) 241-253.

Wedepohl, K. H., 1995. The composition of the continental crust, *Geochim. Cosmochim. Acta* 59 (1995) 1217-1232.

# Modelling the seasonal dynamics and influence in the transport of $^{238}\text{U}$ -series radionuclides in soil to plant system.

D. Pérez-Sánchez<sup>1</sup>, M.C. Thorne<sup>2</sup> and R. Klos<sup>3</sup>

<sup>1</sup>Department of Environment, CIEMAT, Madrid, 28040, Spain

<sup>2</sup>MTA Limited, Bishop Auckland, County Durham, DL13 3NJ, UK

<sup>3</sup>Aleksandria Sciences Limited, Sheffield, S7 2DD, UK

Keywords: modelling, seasonal dynamics, uranium series, soil to plant.

Presenting author email: d.perez@ciemat.es

## Introduction

Over the last few years, CIEMAT has made efforts to develop process-based models of radionuclide transport in soil-plant systems. This work has been very successful and has led to several peer-reviewed publications (Pérez-Sánchez et al., 2014a; Pérez-Sánchez and Thorne, 2014b; Klos et al., 2014). The development mathematical model, describes the radionuclide transport in soils with redox-sensitive behaviour in soils and their uptake by plants, taking into account seasonal variations in soil hydrology and considering long-term issues.

This paper reviews the processes that need to be represented in order to simulate the behavior of  $^{238}\text{U}$ -series radionuclides in long-term assessment models for radioactive waste disposal, and proposes a model structure and associated mathematical model that can be used to investigate the potential impacts of seasonally variable conditions on the calculated radionuclide concentrations in soils and plants. This work looks also at the potential for the inclusion of spatio-temporal variability in models for long-term dose assessments with alternative levels of detail.

## Results and Conclusions

Figure 1(a) provides a closer look at the results from the model. The top soil (0.1m) concentration as a function of time is shown for the first ten years from the commencement of irrigation. With its lower  $k_d$ , the inter-annual variation for U shows a series of peaks and troughs on an increasing trend with steady state established over a period of around ten years. For the more strongly sorbing Ra there is an increase during the irrigation period, as with the U, but the accumulated material is unaffected by varying water fluxes in the soil because of the high sorption. Concentration of Ra stays constant during this period and for the less strongly sorbed U there is a loss during this period.

Comparing the results with a simple one-compartment model, Figure 1(b), the Ra behaves in a similar way in both models in the long-term; the high  $k_d$  dominating over the variability caused by the fluctuating water table depth. The results show accumulation to similar concentrations in the upper soil. The single compartment results are somewhat higher, but this can be accounted for by the distribution of the activity over the remainder of the ten layer column in the multi-layer simulation. The long-term equilibrium concentrations of

U in the model are around one and a half orders of magnitude lower than are obtained using a simpler model that does not take changing hydrological and redox conditions into account.

Studies with the model for Spanish situation demonstrate that, it is a powerful tool for exploring the behaviour of redox-sensitive radionuclides in soil-plant systems under different hydrological regimes. These models are suitable for representing both the upward and downward migration of radionuclides in the soil column, uptake by plants. In particular, it permits studies of the degree to which secular equilibrium assumptions are appropriate when modelling the  $^{238}\text{U}$  decay chain.

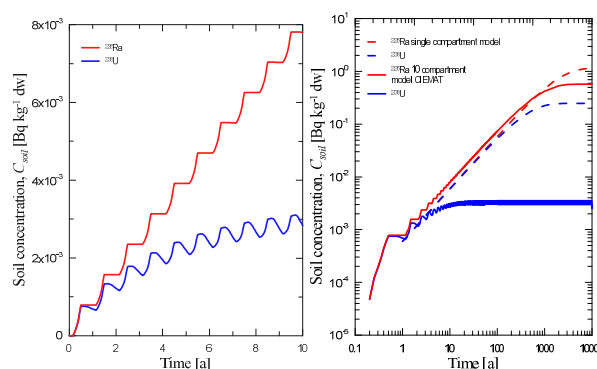


Figure 1. Comparison of the results from the model with variable water table height and those for a single compartment model. (a) Inter-annual variation in the concentration of the top soil as results of fluctuating water table. (b) Long term accumulation in the upper soil over a period of 10 ka

This work has been supported by the ENRESA/CIEMAT agreement.

Klos, R. Limer, L. Shaw, G. Pérez-Sánchez, D. and Xu, S., 2014. Advanced spatio-temporal modelling in long-term radiological assessment models- radionuclides in the soil column. *J. Rad. Prot.* 34, 31-50.

Pérez-Sánchez, D. and Thorne, M.C., 2014a. Modelling the behaviour of uranium-series radionuclides in soils and plants taking into account seasonal variations in soil hydrology. *J. Environ. Radioact.* 131, 19-30.

Pérez-Sánchez, D. and Thorne, M.C., 2014b. An Investigation into the Upward Transport of Uranium-series Radionuclides in Soils and Uptake by Plants. *J. Rad. Prot.* 34, 545-573.

## Radiological evaluation associated to the mining and concentration of monazite in Central Spain

R. García-Tenorio, G. Manjón, I. Díaz, I. Vioque, J. Galván and J. Mantero

Department of Applied Physics II, University of Sevilla, Spain

Keywords: NORM, rare earths, Th, U, monacite.

Presenting author email: gtenorio@us.es

A detailed radiological evaluation (occupational, public and environmental) has been performed associated with the mining and physical concentration of monazite, enriched in different rare earths, in a zone to be exploited commercially which is located 200 km at the south of Madrid (Spain). This evaluation is performed because the rare earth extraction mining and concentration steps are activities recognized in the positive list of NORM activities to be analysed for possible adoption of radiological controls.

The evaluation has been divided in two main parts: mining and physical concentration. And the evaluation of the mining activity has been based in the following studies:

- a) determination of the activity concentrations of several radionuclides from the uranium and thorium series in representative samples of the raw material mined,
- b) construction of an external gamma dose-rate map of the mining area,
- c) study of the distribution of the natural radioactivity in the material extracted in function of the grain size,
- d) radon determinations in the area, and
- e) laboratory leaching experiments.

All the results obtained allow concluding that the rare earth mining activity performed in Central Spain can be considered as exempted, being not needed the adoption of radiological measures associated to this activity. The monazite, although presents high activity concentrations of  $^{232}\text{Th}$  and  $^{238}\text{U}$  (6000 and 2000 Bq/kg, respectively) is found diluted in proportions less than 1% in the raw material mined. In addition the monazite is present as nodules with sizes in the range 0.5 – 1.5 mm (see Figure 1), playing for that reason the inhalation a minor role in the dosimetric evaluations.

The second part of the study was devoted to the radiological evaluation associated to the activities to be performed in a planned plant where the extraction and isolation of the monacite nodules from the raw mineral material mined will be performed. The isolation activities to be applied in the plant are all of them based in the application of physical processes that can alter the activity concentrations of Th and U along the process, but do not provoke the selective mobilization of some of

the daughters. The secular equilibrium in the Th and U series is not disrupted.

The plant evaluation performed, based in the application of simulations with well-established dosimetric models allowed us to conclude that this activity will be also exempted, being not necessary the adoption of any countermeasure from the radiological point of view.

The conclusions obtained in this work are different from the generalized statements found in reports devoted to the description of different NORM industries which indicates that the activities associated to the extraction of rare earths are paradigmatic examples of activities needing regulation from the radiological point of view.

Two are the key points that need to be considered to understand the conclusions obtained in our study

- a) The  $^{232}\text{Th}$  and  $^{238}\text{U}$  activity concentrations in the monazite extracted and isolated in central Spain are comparatively quite low in comparison with the values found in monacites extracted worldwide.
- b) The evaluation performed in this work, is restricted to the mining and physical concentration of the monazite. The posterior beneficiation, chemical treatment and concentration of the rare-earths from the monacite in beneficiation plants, activities that for the moment are not planned to be done in Spain, need an independent analysis. In the extraction and isolation of the different rare-earths from the monazite the secular equilibrium in the U and Th is disrupted, selective enrichments can be produced, and highly radioactive residues should be managed.

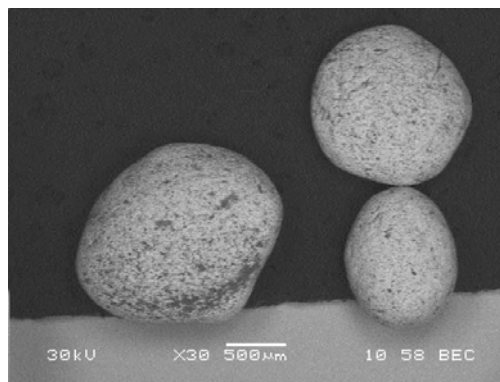


Figure 1.- Electron Microscope Image of monazite nodules enriched in Th and U



## Gross alpha and radon: hidrogeochemical and radiological risk tracer in groundwater in Gran Canaria Island

A. Tejera<sup>1</sup>, H. Alonso<sup>1</sup>, T. Cruz-Fuente<sup>1</sup>, J. González- Guerra<sup>1</sup>, A. Rodríguez-González<sup>1</sup>, M.A., Arnedo<sup>1</sup>, JG. Rubiano<sup>1</sup>, M.C. Cabrera<sup>1</sup>, F.J. Pérez-Torrado<sup>1</sup> y P. Martel<sup>1</sup>

<sup>1</sup>Department of Physics, University of Las Palmas de Gran Canaria, Gran Canaria, Canary Island, 35017, Spain

Keywords: radionuclide, gross alpha, groundwater, radon.

Presenting author email: alicia.tejera@ulpgc.es

The aim of the present work is to analyse the total alpha activity index of the groundwater wells located to the northwest of the island of Gran Canaria island (Spain). This study is focused in three points: First, to compare within the context of radiation protection with values of <sup>222</sup>Rn; second to study of the role of the index of total alpha activity and <sup>222</sup>Rn for the study of underground hydrogeology in the island; and finally to introduce of a new index, alpha<sub>less</sub> activity from the knowledge of the chemical composition of uranium was done.

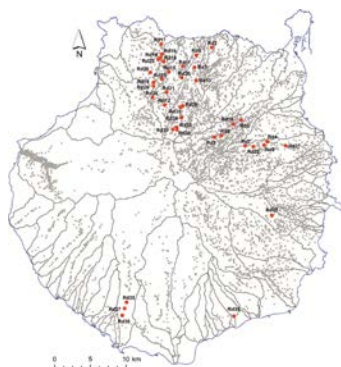


Figure 1.- Location of the points of water surveyed.

Thirty nine samples were analysed. The method used to measure gross alpha activity was coprecipitation (Suárez-Naranjo et al., 2002) and a ZnS (Ag) scintillation detector was used to count in. The radon activity concentration in a water sample is calculated by a closed loop system consisting of an AlphaGUARD monitor that measures the concentration of radon in the air by means of an ionization chamber, and AquaKIT set that is used to transfer dissolved radon in the water samples the air in the circuit.

The total alpha activity index and the radon activity concentrations of the well water samples were determined. Calculated statistical parameters are shown in Table 1. For gross alpha, values above 0.1 Bq/L were obtained in seven wells (four located in the north zone and three in the northeast), with two measurements above 1.0 Bq/L in the wells García Ruíz (1.46 Bq/L) and El Albercón (1.08 Bq/L) both located in the northeast area. However the values of radon concentration in the same points were below the limit of 100 Bq/L, 5.7 Bq/L and 19.2 Bq/L, respectively (Alonso et al, 2015).

Table 1.- Statistics of the gross alpha activities and radon concentration in Bq/L of the water samples.

	A	<sup>222</sup> Rn
Minimum	0.003±0.001	0.3±0.5
Maximum	1.46±0.02	91.6±7.3
Mean	0.149	14.05
Median	0.038	6.70
Standard deviation	0.313	18.75
Geometric mean	0.041	6.59

In accordance with the classification of Przylibski and Gorecka (2014), the waters of the wells analyzed 5 corresponded to the group of radon free water, 20 to that of water poor in Radon poor water and 14 to low radon water. In figure 2, the values of the total alpha index have been grouped according to the three types of water according to their radon concentration.

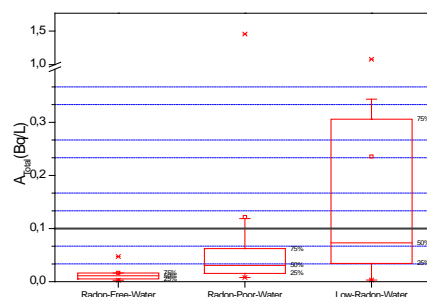


Figure 2.- Box-and whisker plot for gross alpha activity grouped depending on the concentration of <sup>222</sup>Rn.

A chemical analysis of the samples collected was performed. Only two wells showed thorium content in less than 0.5 µg / L. Their corresponding activities (Bq / L) were calculated from the uranium concentrations (µg / L) and the comparison with the total alpha index was 0.8052. A alpha<sub>less</sub> activity index was defined as the difference between the total alpha index and uranium activities, with values exceeding 0.1 Bq / L in 7 of the 39 wells.

Alonso, H., Cruz-Fuentes, T., Rubiano, JG, González-Guerra, J., Cabrera, MC., Arnedo, M.A., Tejera, A. Rodríguez-Gonzalez, A., Pérez-Torrado, F. and Martel, P. 2015. Radon in Groundwater of the Northeastern Gran Canaria Aquifer. *Water*, 7, 2575-2590.

Przylibski, T.A.; Gorecka, J. 2014. <sup>222</sup>Rn activity concentration differences in groundwaters of three Variscan granitoid massifs in the Sudetes (NE Bohemian Massif, SW Poland). *J. Environ. Radioact.* 134, 43–53.



## Annual cycle of <sup>7</sup>Be in soil in a micro-watershed of Mato Frio River, (Brazil)

A.D. Esquivel L.<sup>1</sup>, R.M. Moreira<sup>2</sup>, J. Juri Ayub<sup>3</sup> and D.L. Valladares<sup>3</sup>

<sup>1</sup>Universidad Tecnológica de Panamá, Ciudad de Panamá, Centro de Investigaciones Hidráulicas e Hidrotécnicas - (CIHH), Ciudad de Panamá, 0819-07289, El Dorado-Panamá, República de Panamá

<sup>2</sup>Setor de Meio Ambiente - (SEMAM), Centro de Desenvolvimento da Tecnologia Nuclear - (CDTN-CNEN), Belo Horizonte, Minas Gerais, 31270-901 Belo Horizonte, Brasil

<sup>3</sup>Grupo de Estudios Ambientales - (GEA), Instituto de Matemática Aplicada San Luis - (IMASL). Universidad Nacional de San Luis - CONICET, Ciudad de San Luis, Ejercito de los Andes 950, D5700HHW San Luis, Argentina

Keywords: Berillyum-7, atmospheric deposition, soil content, wet deposition.  
alexander.esquivel@utp.ac.pa

Beryllium-7 (<sup>7</sup>Be) is a natural radionuclide formed in the atmosphere by spallation nitrogen and oxygen atoms impacted by cosmic rays atoms (Lal et al., 1958). It can be used to estimate soil erosion and/or sedimentation caused by rainfall events. Kaste et al. (2011) pointed out that, in order to evaluate the potential of <sup>7</sup>Be as a tracer in this application, it is necessary to know its seasonal and spatial depositional variability as well as quantify the relationship between precipitation and surface inventories. The aim of the present work research is to investigate the content of <sup>7</sup>Be in soil, its seasonal variation along the year and its relationship with the rainfall regime in the Mato Frio creek micro-watershed (Brazil).

### Results

A highly linear relationship between <sup>7</sup>Be deposition and the amount of rainfall, has been observed in the studied region (Fig. 1). Similar results have been found in others environments (Kaste et al., 2011; Juri Ayub et al., 2012). Thus the expected value of the <sup>7</sup>Be

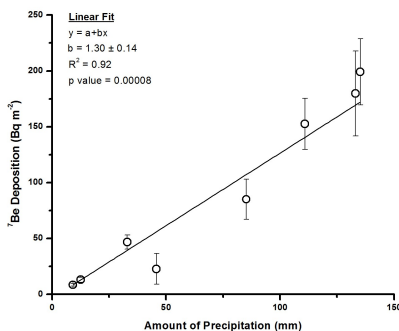


Figure 1. <sup>7</sup>Be deposition versus rainfall amount.

content in the soil due to wet deposition could be calculated from the slope ( $1.30 \pm 0.14 \text{ Bq L}^{-1}$ ) and the daily precipitation record of the 2015/2016 biennium. In the upper part of Figure 2 is shown the expected <sup>7</sup>Be soil content, whereas the bars in the lower part show the <sup>7</sup>Be atmospheric input. From October 2015 to October 2016, soil samples were sampled monthly down to a depth of 5 cm, and the <sup>7</sup>Be total content measured (Fig. 2, circles). This figure reveals that: 1) the <sup>7</sup>Be deposition exhibits oscillation cycles due to the asymmetric precipitation pattern, 2) the measured <sup>7</sup>Be content is close to the value expected from wet deposition; 3) seasonal changes in

soil <sup>7</sup>Be content could be predicted from the atmospheric deposition in rainfall episodes.

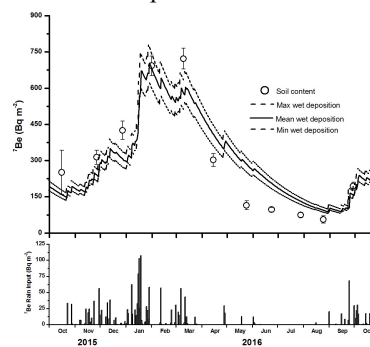


Figure 2. <sup>7</sup>Be wet deposition and <sup>7</sup>Be soil content (upper) and <sup>7</sup>Be input by rains (lower).

The <sup>7</sup>Be content in soil indicates a marked seasonal variation along the year. This could be explained by the local precipitation pattern; the region shows well marked rainy and dry seasons, with at least 80% of the precipitation occurring during the wet season. The good agreement between the measured <sup>7</sup>Be content in the soil and the expected value due to wet deposition confirms: 1) that the general assumption that wet deposition is the main mechanism by which <sup>7</sup>Be reaches the soil, 2) that the <sup>7</sup>Be content in the soil can be accurately estimated by the <sup>7</sup>Be content in the rain.

This work has been supported by the Brazilian Nuclear Energy Commission (CNEN).

Lal, D., Malhotra, P.K., Peters, B., 1958. On the production of radioisotopes in the atmosphere by cosmic radiation and their application to meteorology. *Journal of Atmospheric and Terrestrial Physic.* 12. 306 to 328.

Kaste, J.M., Elmore, A.J., Vest, K.R., Okin, G.S., 2011. Beryllium-7 in soils and vegetation along an arid precipitation gradient in Owens Valley, California. *Geophysical Research Letters.* 38.

Juri Ayub, J., Lohaiza, F., Velasco, H., Rizzotto, M., Di Gregorio, D., Huck, H., 2012. Assessment of <sup>7</sup>Be content in precipitation in precipitation in a South American semi-arid environment. *Science of the Total Environment.* 441. 111 to 116.

## Low background neutron activation analysis: an high sensitivity methods for long-lived radionuclides

M. Clemenza<sup>1,2</sup>

<sup>1</sup> INFN, Sezione di Milano-Bicocca, Milano, Lombardia, 20126, Italy

<sup>2</sup> Dipartimento di Fisica “G. Occhialini”, Università degli Studi Milano-Bicocca, Milano, Lombardia, 20126, Italy

Keywords: <sup>232</sup>Th, <sup>238</sup>U, Low background NAA,

Presenting author email: massimiliano.clemenza@mib.infn.it

The Low Background Neutron Activation Analysis (LBNAA) foresee to minimize all sources of noise that limit the sensitivity of the INAA, as the contamination in materials containers used during sample irradiation, the radioactive background due to the major and minor elements of the sample matrix, as well as the use of detector with very low intrinsic radioactive background. In particular in this work is show a case studies of application of LBNAA in the ultra-radio pure materials selection for a physics of rare events experiments.

Among the different techniques usually adopted for bulk analysis, for example ICP-MS inductively coupled plasma mass spectrometry, or gamma spectroscopy, LBNAA can be used with success to reach sensitivity of the order of  $10^{-13}$  g/g for the long-lived radionuclides such as <sup>232</sup>Th and <sup>238</sup>U.

Instrumental Neutron Activation Analysis (INAA) is a common method of trace element analysis whose sensitivity depends, as with almost all the analytical techniques used in the various fields of research, from the signal to noise ratio. In the case of INAA the sensitivity is limited by interference from other trace elements (and in some case from major elements) in the sample, or by interference from background radiation due to the radio-contaminations in the detection system. Usually the first choice is to maximize the signal by increasing all those parameters, which in principle can be improved as much as possible in sample irradiation process and in gamma spectroscopy measurements such as neutron flux intensity, irradiation-waiting-measuring times, detector efficiency, sample mass.

The new generation of Physics of rare events experiments needs increasing constraints in the radio-purity of materials. The natural radioactive background can cover the signal of extremely rare processes, such as neutrino oscillation, double beta decay and dark matter searches. Normally these experiments are situated in underground labs in order to reduce the natural background due to cosmic radiations, but not from the one due to the experimental apparatus itself. For example, the radiations emitted from radio-nuclides presents in the experimental set-up can often have the same energy signature of the rare processes studied.

In order to reduce the intrinsic background of these experiments is widespread the utilization of shieldings and structures made of ultra-pure materials (generally with high atomic number, Z and density). In these latest years it has become of great importance to found an

optimal analytical method in order to reach detection limits on the radio-purity of the materials of  $10^{-12}$  -  $10^{-14}$  g of contaminants / g of materials. In particular our goal is to determine <sup>232</sup>Th and <sup>238</sup>U contaminations in ultra-pure materials such as copper (NOSV and OFHC type) and lead (commercial ultra-pure lead and ancient “Roman” lead). In this way also the evaluation of <sup>232</sup>Th and <sup>238</sup>U contaminations in ultra-pure materials becomes very important, because this two radionuclides are the principal cause of radioactive background due to the detectors facilities.

These materials are chosen because almost all the radiation detectors in low background facilities and shielding of many experiments of Physics of Rare Events (GERDA, MAJORANA) are made by these two materials and in particular for the CUORE Experiment it was necessary to select the materials for inner and external shielding, but also for the detector holders.

LBNAA can be also used for environmental researches for example to elemental analysis of atmospheric mineral dust entrapped in ice core; this kind of samples requires the specific development of a “low level counting” analytical technique that can reach sub-ng detection limits for many elements.

## Separation of thorium and uranium using TEVA and TRU resins in tandem and quantification of uncertainty of their measurements using neutron activation

S. Hevia and A. Chatt

Trace Analysis Research Centre, Department of Chemistry, Dalhousie University,  
6274 Coburg Road, Room 212, PO BOX 15000, Halifax, Nova Scotia, B3H 4R2, Canada

Keywords:  $^{232}\text{Th}$ ,  $^{238}\text{U}$ , TEVA/TRU resins, expanded uncertainty.

Presenting author email: chatt@dal.ca

A pseudo-cyclic epithermal instrumental neutron activation analysis (PC-EINAA) method in conjunction with Compton suppression spectrometry (CSS) was initially developed for the determination of thorium and uranium in water and food items with detection limits of  $0.05 \mu\text{g g}^{-1}$  (Hevia, 2006). Our first approach to preconcentration of uranium and thorium involved coprecipitation with  $\text{Ca}_3(\text{PO}_4)_2$  (Dang and Chatt, 1986). A better separation method for thorium and uranium was then used to further improve the detection limits using a coprecipitation step followed by a separation step using TEVA.Resin and TRU.Spec resins in tandem. The detection limits for thorium and uranium were 2 and  $0.8 \text{ ng g}^{-1}$ , respectively. The method was applied to food items and drinking water. The relative expanded uncertainties for thorium varied between 2.5 and 5.0% and that for uranium between 1.4 and 4.7% at a coverage factor of 2 for the samples analyzed (Hevia, 2006). The methods are briefly described in this abstract.

Considering the very low levels of thorium and uranium in food and water, preconcentration methods for have been widely used for the quantitative separation of these elements. The common techniques employed for this purpose are coprecipitation, solvent extraction, ion exchange and extraction chromatography. Typical coprecipitating agents include  $\text{Pb}_3(\text{PO}_4)_2$ ,  $\text{CaC}_2\text{O}_4$ ,  $\text{Fe}(\text{OH})_3$ ,  $\text{Ca}_3(\text{PO}_4)_2$  and  $\text{MnO}_2$ . Solvent extraction with the following compounds are also applied extensively: CMPO/TBP, PIA-8, HDEHP, N-alkyl amides, N, N-alkyl amides, TBSA in n-dodecane, TBSA in toluene, TOPO in toluene, and Cyanex-923. Ion exchange chromatography using Dowex 1x4, Dowex 1x8, Dowex 50 Wx8, and TEVA.Resin have also been employed widely. Extraction chromatographic methods using resins like Kelf-TBP, Silica gel-TBP, Levextrel-TBP, U/TEVA and TRU.Spec have become quite popular.

Tandem column arrangements incorporating TEVA.Resin, U/TEVA.Resin and TRU.Spec resin were successfully used for the simultaneous separation of actinides from high-level nuclear waste solutions. (Horwitz *et al.*, 1995). Another tandem method using TEVA.Resin followed by TRU.Spec resin was developed for the separation of thorium, uranium, plutonium and americium in human soft tissues (Moody *et al.*, 1998). The tandem approach allows for simple, flexible, rapid, efficient and cost-effective separations. For these reasons, we have used TRU.Spec and TEVA.Resin in tandem to separate thorium and uranium in water and food samples (Hevia, 2006).

Thorium and uranium were first coprecipitated with  $\text{Ca}_3(\text{PO}_4)_2$  (Dang and Chatt, 1986). The precipitate

was dissolved in conc.  $\text{HNO}_3$  and treated with  $\text{C}_6\text{H}_8\text{O}_6$  (Eichrom, 2001). Preliminary experiments involved independent separation of thorium from a thorium-uranium mixture using TEVA.Resin and that of thorium and uranium from their mixture using TRU.Spec Resin. Finally, thorium and uranium were separated using TEVA.Resin and TRU.Spec resin in tandem arrangement.

About  $100 \mu\text{L}$  ( $100 \mu\text{g}$ ) of a thorium standard solution and  $250 \mu\text{L}$  ( $25 \mu\text{g}$ ) of a uranium standard solution were spiked onto  $10 \text{ mL}$   $1 \text{ M Al}(\text{NO}_3)_3$ - $3 \text{ M HNO}_3$  loading solution. It was then passed through the TEVA.Resin-TRU.Spec columns arranged in series. Following a rinsing step, the columns were separated for the elution of uranium and thorium. Thorium was eluted from TEVA.Resin using  $0.5 \text{ M C}_2\text{H}_2\text{O}_4$  and the column was rinsed with  $0.01 \text{ M HNO}_3$ . Uranium was eluted from the TRU.Spec column with  $0.1 \text{ M NH}_4\text{HC}_2\text{O}_4$  and was also rinsed with  $0.01 \text{ M HNO}_3$ . The eluent solutions of both columns from the loading step to the last rinsing step were collected in portions of  $1\text{-mL}$  in small polyethylene vials, air-dried in a fumehood, and head-sealed.

Thorium and uranium were determined through  $^{239}\text{U}$  ( $74.67 \text{ keV}$  gamma-ray) and  $^{233}\text{Th}$  ( $86.50 \text{ keV}$ ) radioisotopes by neutron activation analysis (NAA). The irradiations were carried out in the DUSR facility at a thermal neutron flux of  $2.5 \times 10^{11} \text{ cm}^{-2} \text{ s}^{-1}$ . The conditions for thorium and uranium working standard solutions and drinking water certified standards were 10, 5, 10 min for irradiation, decay and counting, respectively, and were counted using a Canberra Ge(Li) detector. The recoveries for thorium was  $91 \pm 5\%$  and that of uranium  $97 \pm 3\%$  using the above procedure.

This work was financially supported by the Natural Sciences and Engineering Research Council of Canada.

Hevia, S., 2006. Studies of naturally occurring radioactive materials by direct gamma-ray spectrometry and after chemical separation. PhD Thesis, Dalhousie University, Halifax, Nova Scotia, Canada.

Dang, H.S., Chatt, A., 1986. *Trans. Am. Nucl. Soc.* 52, 169-170.

Horwitz, E.P., Dietz, M.L., Chiarizia, R.; Diamont, H., Maxwell, S.L., Nelson, M.R., 1995. *Anal. Chim. Acta.* 310, 63-78.

Moody, C.A., Glover, S.E., Stuit, D.B., Filby, R.H., 1998. *J. Radioanal. Nucl. Chem.* 234, 183-187.

Eichrom Technologies, Inc., 2001. *Anal. Procedures.*

## Neutron activation analysis and alpha-particle spectrometry in environmental research

L. Benedik

<sup>1</sup>Department of Environmental Sciences, Jožef Stefan Institute, Jamova 39, SI-1000 Ljubljana, Slovenia

Keywords: Neutron activation analysis, alpha-particle spectrometry, environment, radionuclides

Presenting author email: [ljudmila.benedik@ijs.si](mailto:ljudmila.benedik@ijs.si)

Neutron activation analysis (NAA) is an isotopic-specific analytical technique for the qualitative and quantitative measurement of the elemental mass. It offers important advantages for analysis of trace and minor elements. Since NAA requires access to a nuclear reactor it is less widely applied than other analytical techniques for elemental analysis. Its adherent freedom from blanks, the use of isotopic tracers and carriers for minimisation of losses by adsorption and evaluation of the chemical yield, are only few the most important features of NAA. Instrumental NAA (INAA) is applied much more frequently than NAA using radiochemical separation (RNAA), in spite of the fact that the latter reaches a higher accuracy and sensitivity. The choice of NAA technique is dependent upon the radionuclide being measured and the sample material being analysed. NAA is based upon the conversion of stable atomic nuclei by irradiation into radioactive nuclei by irradiation with neutrons and measurement of the radiation emitted during the decay of induced radioactive nuclei. The radionuclide's half-life, the type of radiation it emits as it decays, and the energy of its radiations as well as the radioactivity induced in the other elements in the sample matrix, must be considered in selecting the method to be followed. One of the most important stages relating to quality control in RNAA procedures is the determination of the chemical yield. Radiotracer techniques are the most accurate and simple way to measure the chemical yield for each sample aliquot.

Determination of the activity concentrations of natural and man-made radioisotopes in environmental samples by alpha-particle spectrometry (AS) following their radiochemical separation is widely practiced in radiochemical laboratories. Such data are required in many studies related to radioecology; to exposure, uptake and elimination of these radionuclides and their dosimetry; and to a variety of environmental, geological, geochronological, and other processes. Often the isotopic ratios and the equilibrium or disequilibrium of the isotopes are of the prime interest or represent an important methodological tool.

Determination of radionuclides may be performed either by direct activity measurement, usually termed radiometric analysis or by mass measurement. However, the required sensitivity usually limits the choice of mass measurement to spectroscopic techniques, mass spectrometry and neutron activation analysis.

Radiometric methods become less favourable for long lived, low specific activity radionuclides, while mass-based ("atom-counting") techniques become more advantageous. NAA is thus also more favourable for low

specific activity, i.e. longer lived nuclides and becomes worth considering when the nuclear characteristics are highly favourable. It means, that the nuclide has a large capture cross section for formation of a product nuclide of relatively short half-life with good measurement properties, preferably for gamma-ray spectrometry. In the most favourable cases INAA is useful for determination of U-238 and Th-232 via Np-239 and Pa-233, respectively, in many materials at natural levels. In cases where radiochemical separation of the induced radionuclide has to be conducted after irradiation to improve the signal/noise ratio and the sensitivity, this radioactive measurement possesses some important advantages over normal radiometry of the original nuclide in that added carrier could be used to optimize and control chemical recovery, and crucially, the procedure is not subject to blank corrections. The blank is the factor limiting the sensitivity and accuracy of all other techniques, including mass spectrometry.

It is possible to quantify the advantages of NAA with respect to radiometry of the original radionuclide in terms of an advantage factor (AF). The advantage factors for some radionuclides are shown in Table 1.

Table 1. Values of AF for NAA of some long/lived radionuclides (Byrne and Benedik, 1999)

Nuclide pair	AF
U <sup>238</sup> /U <sup>239</sup>	7.0x10 <sup>6</sup>
U <sup>238</sup> /Np <sup>239</sup>	8.0x10 <sup>5</sup>
Th <sup>232</sup> /Pa <sup>233</sup>	4.0x10 <sup>5</sup>
Th <sup>230</sup> /Th <sup>231</sup>	27
Np <sup>237</sup> /Np <sup>238</sup>	640
Pa <sup>231</sup> /Pa <sup>232</sup>	106

As shown in Table 1, extremely high values of AF are found for NAA of U-238 and Th-232, and lower but still favourable values for Np-237, Pa-231 and Th-230.

The use of NAA and AS in environmental research with emphasis on their combination will be presented.

Byrne, AR., Benedik, L., 1999. Application of neutron activation analysis in determination of natural and man-made radionuclides, including Pa-231. Czech. J. Phys. 49/S1, 263-267.



## Radioactivity measurements in the underground laboratory HADES

M. Hult<sup>1</sup>

<sup>1</sup>European Commission, Joint Research Centre, Directorate for Nuclear Safety & Security, Geel, 2400, Belgium

Keywords: HPGe-detector, gamma-ray, underground, EU-policy

Presenting author email: Mikael.hult@ec.europa.eu

In 1992, the former IRMM (Institute for Reference Materials and Measurements) (since 1 July 2016 called JRC-Geel) installed its first HPGe-detector in the underground laboratory HADES, which is located 225 m underground at the premises of the Belgian nuclear centre SCK•CEN. Back then, it was an exploratory research project. Soon, it was realised that performing gamma-ray spectrometry in an underground location is a great asset due to the reduction of the muon flux. In HADES, the muon flux is reduced by a factor 5000 compared to measurements above ground at sea level. At present there are 11 HPGe-detectors in operation. The reason for the expansion was that the detectors proved useful in many projects in a wide range of fields. The presentation will focus on the technical developments that enabled underground gamma-ray spectrometry to be a new important method in diverse fields. Examples of applications will be given.

Initially, in Europe and world-wide, the major driving force for going underground was to perform experiments looking for rare events like double-beta decay, neutrino interactions and dark matter. It was soon realised that not only those large-scale experiments had to be underground but also detectors used for selecting radiopure materials (i.e. materials with extremely low levels of radioactivity) necessary for the construction of the big experiments. In HADES, materials used for the construction of the Borexino neutrino detector and the GERDA double-beta decay experiment have been selected. Also materials to be used in the construction of more standard type of detectors, like HPGe-detectors, benefitted from having their components tested in an underground laboratory. This has led to an iterative improvement of the radiopurity of detectors.

At JRC-Geel it was soon realized that the HPGe-detectors located underground were a perfect complement to "the fleet" of radiation detectors present in the above ground laboratory for radionuclide metrology. The RadioNuclide Metrology laboratory (RN) was set up as a consequence of Article 8 in the EURATOM Treaty to work on ensuring a uniform nuclear terminology and a standard system of measurements. Its key activities are therefore linked to the (i) realization of the unit Bq (ii) production of radioactive reference materials (iii) generation of reference decay data (iv) organization of proficiency tests for EU Member State laboratories (v) harmonization of radioactivity measurements and (vi) contribution and development of international standards.

### Characterisation of reference materials

Many reference materials intended for laboratories that monitor radioactivity in the environment have very low activity levels. This is important as monitoring labs are required to be able to measure a factor 10 below legal limits (Jerome et al., 2015). Certification measurements of reference materials produced by IRMM, NIST, IAEA, KRISS, NMIJ and others have been performed in HADES. Examples of such materials from organic matrices are bilberries, shell fish, rice and milk powder. Furthermore, also larger reference materials with higher activity levels (and non-organic matrices), for example for nuclear decommissioning, benefit from low-level measurements. In a recent publication, Hult et al. (2016) describe how the homogeneity of a 240 kg metal tube material was determined by sampling 0.3 g chips (or swarfs) from about 100 locations. So although the total activity of the 240 kg calibration standard was high, it was necessary to use low-level measurements for a proper characterization.

### Radiotracer studies

Many processes in nature and industries can be followed if mBq-levels of radioactivity can be measured. One current example important for climate change studies is the tracing of ocean currents following the Fukushima NPP accident. The level of <sup>134</sup>Cs in Pacific sea water far from Fukushima is, today (2017), less than 1 mBq/L. In recent years, measurements in HADES in collaboration with both Japanese and US scientists have helped to shed light on the complex processes taking place in the Northern Pacific.

Jerome, S.M., Inn, K.G.W., Wätjen, U., Lin, Z. 2015. Certified reference, intercomparison, performance evaluation and emergency preparedness exercise materials for radionuclides in food. *J. Radioanal. Nucl. Chem.* 303, 1771–1777.

Hult, M., Stroh, H., Marißsens, G., Tzika, F., Lutter, G., Šurán, J., Kovar, P., Skala, L., Sud, J. 2016. Distribution of radionuclides in an iron calibration standard for a free release measurement facility. *Appl. Radiat. Isot.* 109, 96-100.

Aoyama, M., Hamajima, Y., Hult, M., Uematsu, M., Oka, R., Tsumune, D., Kumamoto, Y. 2016. <sup>134</sup>Cs and <sup>137</sup>Cs in the North Pacific Ocean derived from the March 2011 TEPCO Fukushima Dai-ichi Nuclear Power Plant accident, Japan. Part one: surface pathway and vertical distributions, *J Oceanogr* 72:53–65.



## Low-Level Gamma-ray Counting in Ogoya Underground Laboratory

Y. Hamajima

Low Level Radioactivity Laboratory, Kanazawa University, Nomi, Ishikawa, 9231224, Japan

Keywords: low level counting, underground, gamma-ray, HPGe.

Presenting author email: hamajima@se.kanazawa-u.ac.jp

The Ogoya Underground Laboratory (OUL) is located in a tunnel of the former Ogoya Copper Mine with overburden of 270 m w.e., where 12 well, 5 planar, and 1 coaxial low background HPGe detectors for low-level radioactivity measurement have been in operation (Table 1). All detectors have large active volume, high resolution, and excellent counting efficiency. Ultra-low-background aluminium has been used for end-caps. Cryostats are of the J-type or U-type and preamplifiers are located outside of the lead shield. The lead shield is 15 to 20 cm thick, and its upper part is covered by about 10 cm of iron plate. The inner 3 to 5 cm of the lead shield is made of old lead refined 200 years ago or Oxygen-Free Copper. The nitrogen gas from the Dewar is blown to the top of the end cap. Due good shielding conditions, the background count rates of detectors are about 1/100 of the aboveground ones (Hamajima and Komura, 2004; Komura and Hamajima, 2004).

Several low-level gamma-ray measurements in OUL will be presented, i.e. the detection of low-level cosmogenic radionuclides in a few grams of a chondrite (Jenniskens et al., 2012), on natural radionuclides, fission products such as Ag110m, Cs137 and Cs134 in seawater and in marine organisms from the Pacific Ocean (e. g. Aoyama et al., 2012; Kumamoto et al., 2014) and on activated nuclides induced by environmental neutrons and by fission neutrons (e.g. NAA of Asteroid Itokawa (Ebihara et al., 2011)). The number of recent measured samples related to the Fukushima accident (precipitation of AMP/Cs and Cs<sub>2</sub>PtCl<sub>6</sub>, filtrated suspended solids, and biological samples), chondrite samples, and nuclear reaction products for each year is summarized in Table 2. Corrections for the cascade sum coincidences in the HPGe detector will also be discussed.

Aoyama M., D Tsumune, M Uematsu, F Kondo, Y Hamajima. 2012. Temporal variation of I34Cs and I37Cs activities in surface water at stations along the coastline near the Fukushima Dai-ichi Nuclear Power Plant accident site, Japan. *Geochemical Journal* 46, 321-325.

Ebihara, N. S Sekimoto, N Shirai, Y Hamajima, M Yamamoto, K Kumagai. 2011. Neutron activation analysis of a particle returned from asteroid Itokawa. *Science* 333 (6046), 1119-1121

Jenniskens, P. et al., 2012. Radar-Enabled Recovery of the Sutter's Mill Meteorite, a Carbonaceous Chondrite Regolith Breccia. *Science*, 338, 1583-1587.

Kumamoto, Y., M Aoyama, Y Hamajima, T Aono, S Kouketsu, and A Murata. 2014. Southward spreading of the Fukushima-derived radiocesium across the Kuroshio Extension in the North Pacific. *Scientific reports* 4, 4276

Komura, K., Y.Hamajima, 2004. Ogoya underground laboratory for the measurement of extremely low levels of environmental radioactivity: review of recent projects

carried out at OUL, *Appl. Radiation and Isotopes*, 61, 185-189.

Hamajima, Y., K.Komura, 2004. Background components of Ge detectors in Ogoya underground laboratory. *Appl. Radiation and Isotopes*, 61, 179-183.

Table 1. Specifications and performances of HPGe detectors in OUL and background count rate.

name	Type of detector (well size)	Relative Eff (Abs Eff at 662keV for well) (size, active volume)	BG* (min <sup>-1</sup> )
J	planar	34% (38.6cm <sup>2</sup> x 29.9cm, 113cm <sup>3</sup> )	0.57
K	planar	34% (38.6cm <sup>2</sup> x 29.9cm, 113cm <sup>3</sup> )	0.52
L	planar	18.2% (28cm <sup>2</sup> x 2cm, 56cm <sup>3</sup> )	0.57
M	planar	22% (28cm <sup>2</sup> x 2.8cm, 78.4cm <sup>3</sup> )	
N	planar	22% (28cm <sup>2</sup> x 3cm, 79cm <sup>3</sup> )	
A	well(21mmφx62.5mm)	19.2% (72.0φx75.0mm, 272cm <sup>3</sup> )	1.90
B	well(21mmφx62.5mm)	20.0% (72.0φx74.7mm, 272cm <sup>3</sup> )	1.40
D	well(21mmφx62mm)	18.1% (72.0φx74.8mm, 271cm <sup>3</sup> )	2.35
E	well(21mmφx66.0mm)	21.5% (74.0φx80mm, 310cm <sup>3</sup> )	1.63
F	well(21mmφx62mm)	18% (70.0φx75.0mm, 252cm <sup>3</sup> )	1.88
H	well(21mmφx66.5mm)	21.2% (74.0φx80mm, 309cm <sup>3</sup> )	2.19
P	well(16mmφx55mm)	16% (61φx62mm, 166cm <sup>3</sup> )	0.89
Q	well(21mmφx66.0mm)	21% (74.0φx80mm, 308cm <sup>3</sup> )	1.49
S	well(21mmφx66.5mm)	17% (71.7φx74.8mm, 260cm <sup>3</sup> )	5.45
W	well(21mmφx60mm)	21.1% (75.1φx80.6mm, 344cm <sup>3</sup> )	1.80
Y	well(21mmφx68mm)	22.1% (74.3φx80mm, 311cm <sup>3</sup> )	1.41
Z	well(16mmφx62.5mm)	20.5% (67.6φx70mm, 231cm <sup>3</sup> )	1.56
U	coaxial	93.5% (78.9φx80.9mm, 379cm <sup>3</sup> )	1.12

BG\*: integrated count rate (50 – 2000 keV), 2015-2016

Table 2. Samples measured in OUL.

yr	total	FINPP			Chond	Nucl
		AMP/Cs	Cs <sub>2</sub> PtCl <sub>6</sub>	Filt(SS)		
2011	478	478				
2012	625	510	106		7	2
2013	298	243	54			1
2014	525	300	1	90	134	
2015	788	706	10		67	5
2016	701	563	47		88	3

## Investigation of neutron-induced background in HPGe detectors – first phase

M. Baginova<sup>1</sup>, P. Vojtyla<sup>1</sup> and P. Povinec<sup>2</sup>

<sup>1</sup>CERN, Geneva 1211, Switzerland

<sup>2</sup>Faculty of Mathematics, Physics and Informatics, Comenius University, Mlynská dolina F1,  
842 48 Bratislava, Slovakia

Keywords: Monte Carlo simulations, detector background, GEANT4, neutron calculations.

Presenting author email: miloslava.baginova@cern.ch

Background induced by neutrons is a poorly understood background component for all low-level systems. In shielded laboratories, neutrons can still be produced by interactions of cosmic rays (hadronic cascades, negative muon capture) and by natural radioactivity, via spontaneous fission or ( $\alpha$ , n) reactions. Predicting all background components correctly is crucial for designing efficient shielding and applying appropriate event-rejection strategies.

The interactions of fast neutrons in a coaxial p-type high-purity germanium detector (HPGe) have been studied experimentally and by the detector simulation tool GEANT4.

Neutrons and  $\gamma$ -rays emitted from a <sup>241</sup>Am-Be source with an activity 370 MBq were used for a detailed investigation of their interactions in a coaxial p-type HPGe.

In HPGe detector, the main energy deposition mechanisms of neutrons with energies between 0.5 and 10 MeV, are elastic and inelastic scattering. Elastic and inelastic scattering of neutrons for HPGe energy thresholds below about 50 keV give the largest contribution to the interaction probability, and may be an important effect to take into account in future  $\gamma$ -ray spectrometers based on  $\gamma$ -ray tracking. (Ljungvall and Nyberg, 2005)

The experimental setup consisted of a <sup>241</sup>Am-Be source encapsulated in a case of stainless steel and in an aluminium shell placed coaxially 161.2 mm above a 50% coaxial p-type HPGe detector in a low-level shield. Two circular iron absorbers were placed above the detector to absorb the abundant gamma rays of <sup>241</sup>Am and so reduce the dead time and a plastic beaker was used to keep the distance of the source to the detector. This setup was implemented in the GEANT4 simulation as shown in Figure 1.

The experimental results were compared with GEANT4 simulations of the neutron and  $\gamma$ -ray interactions with the detector and shielding. Precise geometry of the setup was coded including individual material impurities. Detailed analysis of both, experimental and simulated spectra was carried out. Elastic and inelastic scattering of fast neutrons were observed, as well as their capture. Ge peaks at energies 68.6 keV, 564.0 keV, 597.0 keV, 688.1 keV, 836.1 keV, 1039.6 keV and 1215.7 keV have typical triangular shape, which is due to the inelastic scattering of fast neutrons on Ge. A Peak at the energy of 68.8 keV corresponds to the reaction <sup>73</sup>Ge(n, n' $\gamma$ )<sup>73</sup>Ge\*, peaks at energies 564.0 keV and 597.0 keV to the reaction <sup>76</sup>Ge(n, n' $\gamma$ )<sup>76</sup>Ge\*, peaks at

energies 688.1 keV and 836.1 keV to the reaction <sup>72</sup>Ge(n, n' $\gamma$ )<sup>72</sup>Ge\*, and the peak at the energy of 1215.7 keV to the reaction <sup>70</sup>Ge(n, n' $\gamma$ )<sup>70</sup>Ge\*.

The results of this work have shown that the GEANT4 simulation tool and the neutron cross section data implemented into GEANT4 are suitable for neutron simulations and give good results at least up to neutron energy 11 MeV, which is the maximum energy of neutrons from <sup>241</sup>Am-Be source. Concluding, GEANT4 was validated for further studies by comparing experimental results with simulations.

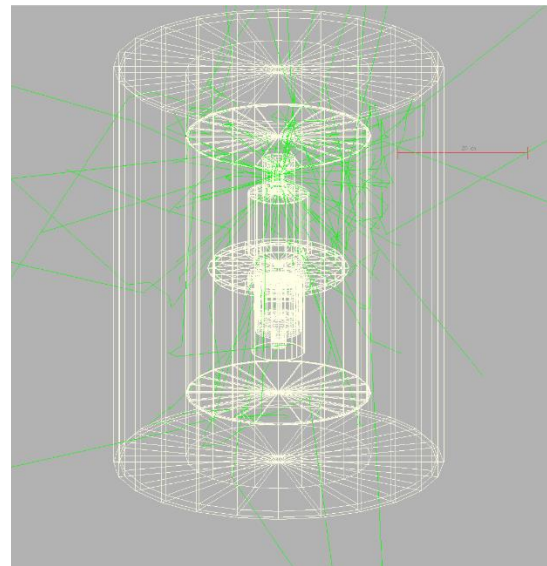


Figure 1. Simulation of neutron and  $\gamma$ -ray interactions with HPGe detector and shielding.

Ljungvall, J., Nyberg, J., 2005. Nucl. Instr. Meth. in Phys. Res. A 546, 553–573.

## Background of a HPGe detector in the Modane underground laboratory: Monte Carlo simulations

R. Breier<sup>1</sup>, P. Loaiza<sup>2</sup>, F. Piquemal<sup>2,3</sup>, P.P. Povinec<sup>1</sup>

<sup>1</sup>Department of Nuclear Physics and Biophysics, Faculty of Mathematics, Physics and Informatics, Comenius University, 84248 Bratislava, Slovakia

<sup>2</sup>Laboratoire Souterrain de Modane, 73500 Modane, France

<sup>3</sup>Centre Etudes Nucléaires de Bordeaux Gradignan, CNRS/ IN2P3, 33175 Gradignan, France

Keywords: Monte-Carlo, HPGe, Background, muon, cosmic rays,

Corresponding author email: breier@fmph.uniba.sk

Simulations of cosmic-ray background components of the low-level HPGe gamma-ray spectrometer operating in a deep underground laboratory was carried out using Monte Carlo codes GEANT 4 and MUSIC. The simulated background gamma-ray spectrum was compared with the gamma-ray spectrum measured at the Modane underground laboratory operating at the depth of 4800 m water equivalent (Arnold et al., 2005). The experimental results showed the total background of the HPGe detector is ( $81.068 \text{ imp day}^{-1} \text{ kg}^{-1}$ ), about three orders of magnitude higher than the Monte Carlo simulated cosmic-ray background ( $0.0228 \text{ imp day}^{-1} \text{ kg}^{-1}$ ).

The higher measured background should be due to radioactive contamination of the construction parts surrounding the HPGe crystal, as well as due to presence of radon and its decay products in the laboratory. This part of the HPGe background which has been due to contamination of construction materials (Povinec et al., 2008) has also been studied using the Monte Carlo method. The construction materials of the detector and the shield are mainly contaminated by  $^{40}\text{K}$  and decay products of  $^{238}\text{U}$  and  $^{232}\text{Th}$ . Geant4 module G4Decay has been used in the Monte Carlo simulations (Martineau et al., 2004; Breier and Povinec, 2010).

The HPGe semiconductor detector under investigation was a coaxial type with relative efficiency of 93% (relative to a 3 inch in diameter and 3 inch thick NaI(Tl) detector). The diameter of the Ge crystal was 7.9 cm, and its length was 8.1 cm. The sensitive volume of the detector was  $379 \text{ cm}^3$ . The detection system is placed in the deep underground laboratory, operating at the depth of 4800 m w.e.), where the muon flux is only about  $5 \text{ muons/m}^2/\text{day}$  (Schmidt et al., 2013). The passive shielding of the HPGe detector consisted of lead (thickness of 20–25 cm), and on the top of the shielding an additional layer of iron (10–15 cm) has been added. The inner layer of the shielding (3–5 cm) is composed of very old (Roman) lead.

The blue line in Fig. 1 shows the Monte Carlo simulated background spectrum induced by cosmic-ray muons, the black line is the Monte Carlo spectrum from contamination of the surrounding of the HPGe detector, and the red line is the experimental gamma-ray spectrum. Activities of  $^{40}\text{K}$ ,  $^{238}\text{U}$  and  $^{232}\text{Th}$  in contaminated materials have been assumed to be  $0.1 \text{ mBq/kg}$ .

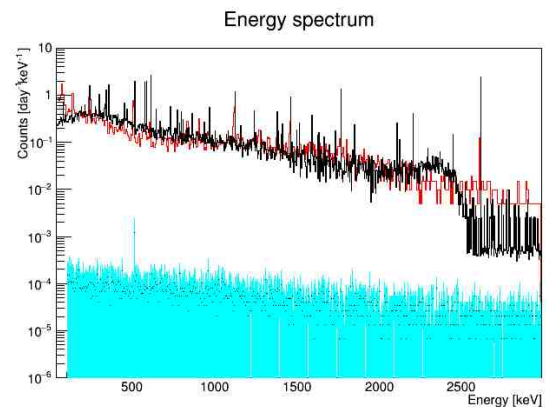


Figure 1 Experimental (top-red) and Monte Carlo simulated (top-black and bottom) background gamma-ray spectra of the HPGe detector.

The Monte Carlo simulated background from cosmic rays is by about three orders of magnitude lower than the experimental background, which is similar to the background from contamination of construction parts of the HPGe detector.

This work was supported by the Slovak Research and Development Agency under the contract No. APVV-15-0576,

Arnold, J., et al., 2005. Technical description and performance of the NEMO 3 detector. Nucl. Instr. Meth. Phys. Res. A 536, 79–122.

Breier, R., P. P. Povinec, 2010. Simulation of background characteristics of low-level gamma-ray spectrometers using Monte Carlo method. Applied Radiation and Isotopes 68 (2010) 1231–1235.

Martineau, O., et al., 2004. Calibration of the EDELWEISS cryogenic heat-ionization germanium detector for dark matter. Nucl. Inst. Meth. Phys. Res. A 530, 426–439.

Povinec, P. P., Betti, M., Jull, A.J.T., Vojtyla, P. 2008. New isotope technologies in environmental physics. Acta Phys. Slovaca 58, 1–154.

Schmidt et al., 2013. Muon-induced background in the EDELWEISS dark matter search. Astroparticle Physics Volume 44, April 2013, Pages 28–39

## Comparison of experimental vs Monte Carlo efficiency calibrations of an HPGe spectrometer

J.G. Guerra<sup>1</sup>, J.G. Rubiano<sup>1</sup>, G. Winter<sup>2</sup>, A.G. Guerra<sup>1</sup>, H. Alonso<sup>1</sup>, M.A. Arnedo<sup>1</sup>, A. Tejera<sup>1</sup>, P. Martel<sup>1</sup>, J.P. Bolivar<sup>3</sup>

<sup>1</sup> Departamento de Física, Universidad de Las Palmas de Gran Canaria, 3501 Las Palmas de Gran Canaria, Spain,

<sup>2</sup> Instituto Universitario de Sistemas Inteligentes y Aplicaciones Numéricas en la Ingeniería, Universidad de Las Palmas de Gran Canaria, 3501 Las Palmas de Gran Canaria, Spain

<sup>3</sup> Departamento de Física Aplicada, Universidad de Huelva, 21071 Huelva, Spain

Keywords: Gamma-ray spectrometry, Certified Reference Materials, Efficiency calibration, Monte Carlo simulation.  
Presenting author email: jglezg2002@gmail.com

When determining the activity concentration of radionuclides by gamma spectrometry, it is needed to know the full energy peak efficiency (FEPE) for the relevant energies, which significantly varies depending on the photon energy, material and geometry of the sample, and source-detector arrangement. Due to the difficulties related to the efficiency calibration by experimental procedures using certified reference materials (CRMs), an alternative method for FEPE determination may well be rather useful for any standard research laboratory. The most common alternative is the Monte Carlo Simulation, which allows performing computational efficiency calibrations for a large variety of geometries and materials of samples without the need to use CRMs once the detector has been characterized, which is to say, it has been achieved an appropriate knowledge of the characteristics of the detector.

In this work we perform a comparison between experimental FEPEs, and the corresponding ones calculated by the LabSOCS code for an HPGe XtRa detector characterized by Canberra. The experimental FEPEs has been determined using the IAEA CRMs, RGU-1, RGTh-1 and RGK-1, with various gamma emissions distributed throughout the range of interest for environmental samples (45-1800 keV), which has been prepared in a frustoconical beaker for five different volumes. FEPEs for these geometries and materials have also been generated by LabSOCS and the relative deviation between both (experimental and computational FEPEs) for each geometry and energy have been computed.

From the 27 emissions considered within the mentioned range, it has been observed a good agreement for 14 emissions (see Table 1), taking into account the experimental uncertainties (within the range of 1 - 8 %) and the LabSOCS ones which are over the 4% (Bronson, 2003). The poor agreement in the rest of emissions arises mainly due to two difficulties in the experimental measurements, large uncertainties in the peak area determination (either because of interferences among close peaks or too low Peak-to-Compton ratios), and the coincidence summing effect in the case of radionuclides with several probable emissions. This latter source of error has been studied for the emissions most strongly affected by it, obtaining the Coincidence Summing Correction Factors (Table 2), which would allow measuring environmental samples with enough accuracy using the emissions affected by such an effect.

Table 1. Relative deviations between LabSOCS and experimental FEPEs, using as reference the experimental ones

CRM	En (keV)	Sample volumes (ml)				
		40	60	80	100	145
RGU-1	46.5	-0.1	1.1	0.9	-0.3	-0.4
	63.3	-1.8	-3.1	0.4	-0.8	-3.0
	143.8	-3.4	0.2	-4.5	0.0	-3.2
	186.0	-4.6	-3.1	-3.7	-4.1	-4.3
	242.0	3.7	5.0	3.4	3.2	3.3
	295.2	4.3	6.0	4.4	4.6	4.4
	352.0	-1.0	0.9	-0.8	-0.8	-0.7
RGTh-1	1001.0	-3.7	-3.8	0.3	-4.2	-2.3
	1764.5	-0.5	1.4	0.4	0.6	0.6
	338.3	1.3	-0.3	-0.6	-3.1	-3.3
	727.3	6.1	5.4	5.8	4.4	3.7
RGK-1	860.0	5.6	3.6	4.3	4.3	2.7
	911.0	4.3	4.5	3.8	2.5	3.1
1460.8	0.4	-1.7	-2.9	1.9	-0.5	

Table 2. Correction Factors for the most affected emissions by Coincidence Summing

CRM	En (keV)	Sample volumes (ml)				
		40	60	80	100	145
RGU-1	609.3	0.84	0.84	0.86	0.86	0.87
	768.4	0.82	0.82	0.84	0.85	0.85
	934.1	0.79	0.81	0.83	0.83	0.85
	1120.3	0.82	0.83	0.85	0.85	0.87
	1238.1	0.83	0.84	0.86	0.88	0.88
RGTh-1	583.2	0.85	0.87	0.88	0.88	0.91

J.G. Guerra acknowledges a PhD fellowship through the "Programa de personal investigador pre-doctoral en formación" of the ULPGC.

Bronson, F. L., 2003. Validation of the accuracy of the LabSOCS software for mathematical efficiency calibration of Ge detectors for typical laboratory samples. J. Radioanal. Nucl. Chem. 255 (1), 137-141.



## Efficiency calibration of an HPGe detector for environmental radioactivity measurements. Influence of the geometric characterization using Monte Carlo methods.

J. Ordóñez<sup>1</sup>, S. Gallardo<sup>2</sup>, J. Ortiz<sup>3</sup>, S. Martorell<sup>1,3,4</sup>

<sup>1</sup>Grupo de Medioambiente y Seguridad Industrial.

<sup>2</sup>Instituto Universitario de Seguridad Industrial, Radiofísica y Medioambiental.

<sup>3</sup>Laboratorio de Radiactividad Ambiental.

<sup>4</sup>Departamento de Ingeniería Química y Nuclear.

Universitat Politècnica de València, Valencia, 46022, Spain.

Keywords: Detector calibration, HPGe, MCNP6, Dead layer.

Presenting author email: joorro1@etsii.upv.es

High Purity Germanium (HPGe) detectors are widely used in gamma spectrometry to determine the activity of environmental samples. In order to obtain accurate measurements, a detailed characterization of the efficiency response of the system is required. In this frame, Monte Carlo methods represent a powerful tool to complement these measurements, being able to carry out rapid and realistic simulations.

Previous studies conclude that the efficiency obtained by simulation considering the data provided by the manufacturer, differs from the experimental results. Parameters such as the thickness of the germanium dead layer or the active crystal are of particular relevance in the efficiency calculation (Ródenas et al., 2003; Chuong et al., 2016). Moreover, the germanium dead layer thickness increases over time, producing a decrease in the efficiency and being necessary to adjust the model during the lifetime of the detector (Huy et al., 2007).

In this work, different models of a GMX HPGe detector (ORTEC) are developed using the MCNP6 code. The aim of this work is to study the geometric features of these models to determine the level of detail required to obtain accurate efficiency values. In this frame, a sensitivity analysis of geometric parameters is carried out, revealing those parameters with greater incidence in the efficiency system. This analysis also allows identifying the components that require a more detailed modelling.

With MCNP6, the photon and electron fluence can be obtained in a superimposed mesh using the F4 MESH tally. On the other hand, F8 (pulse height distribution, PHD) tally enables to collect the deposited energy in the active crystal. Both tallies allow improving the model with a better characterization of the geometry. Furthermore, with these tools it is possible to analyze the gamma absorption in the crystal and thus, the penetration depending on the gamma energy.

Results obtained show the influence of geometric parameters on the efficiency depending on the gamma emitter energy. The dead layer has a great influence on low energies (<sup>241</sup>Am and <sup>109</sup>Cd) due to their low penetration and therefore, most interactions take place close to the surface of the crystal. On the other hand, for high-energy gamma emitters, interactions occur throughout the crystal, hence, they are affected mostly by the active germanium volume and not by the dead layer.

Table 1 shows the efficiencies corresponding to a multigamma standard source covering the energy range

between 56.54 keV and 1836.01 keV, using a detailed detector model and considering the data provided by the manufacturer. The obtained ratio show significant discrepancies between experimental and simulated efficiencies, highlighting the need to adjust the geometric model of the detector. <sup>60</sup>Co and <sup>88</sup>Y present true summing coincidence effect, decreasing the efficiency of the detection. Relative errors of experimental measurements are about 2%, whereas simulated relative errors are lower than 1%.

Table 1. Experimental and simulated efficiencies

Isotope	Energy (keV)	Exp. Eff.	MCNP6 Eff.	Ratio
<sup>241</sup> Am	59.54	0.0915	0.0989	1.081
<sup>109</sup> Cd	88.03	0.0972	0.0979	1.007
<sup>57</sup> Co	122.06	0.0899	0.0942	1.048
<sup>139</sup> Ce	165.85	0.0717	0.0840	1.171
<sup>51</sup> Cr	320.08	0.0473	0.0521	1.102
<sup>113</sup> Sn	391.69	0.0396	0.0442	1.117
<sup>85</sup> Sr	513.99	0.0306	0.0357	1.168
<sup>137</sup> Cs	661.66	0.0264	0.0293	1.109
<sup>54</sup> Mn	834.83	0.0219	0.0247	1.129
<sup>88</sup> Y	898.02	0.0185	0.0235	1.269
<sup>65</sup> Zn	1115.52	0.0174	0.0202	1.159
<sup>60</sup> Co	1173.24	0.0154	0.0194	1.258
<sup>60</sup> Co	1332.50	0.0137	0.0174	1.268
<sup>88</sup> Y	1836.01	0.0106	0.0138	1.306

- Rodenas, J., Pascual, A., Zarza, I., Serradell, V., Ortiz, J., Ballesteros, L., 2003. Analysis of the influence of germanium dead layer on detector calibration simulation for environmental radioactive samples using the Monte Carlo method. Nucl. Instrum. Methods A 496, 390–399.
- Huynh Dinh Chuong, Tran Thien Thanh, Le Thi Ngoc Trang, Vo Hoang Nguyen, Chau Van Tao., 2016. Estimating thickness of the inner dead-layer of n-type HPGe detector. Applied Radiation and Isotopes, 116, 174–177.
- Huy, N.Q., Binh, D.Q., An, V.X., 2007. Study on the increase of inactive germanium layer in a high-purity germanium detector after a long time operation applying MCNP code. Nucl. Instrum. Methods A 573, 384–388.



## Liquid Scintillation Counting and Gamma Ray Spectroscopy for Ice Core Dating

E. Di Stefano<sup>1,2</sup>, M. Clemenza<sup>2,3</sup>, V. Maggi<sup>1</sup>, B. Delmonte<sup>1,2</sup>, G. Baccolo<sup>1,2</sup>

<sup>1</sup>Dipartimento di Scienze dell'Ambiente e del Territorio, Università degli Studi Milano-Bicocca, Milano, Lombardia, 20126, Italy

<sup>2</sup>INFN, Sezione di Milano-Bicocca, Milano, Lombardia, 20126, Italy

<sup>3</sup>Dipartimento di Fisica "G. Occhialini", Università degli Studi Milano-Bicocca, Milano, Lombardia, 20126, Italy

Keywords: LSC, <sup>137</sup>Cs, ice core dating, Adamello glacier

Presenting author email: edistefano3@campus.unimib.it

The aim of this work is to use a combination of liquid scintillation counting and gamma ray spectroscopy to date an ice core. It is possible to link defined nuclear events to the presence of <sup>137</sup>Cs in ice core samples, thus providing an absolute method for ice core dating. The main events taken into account to explain release of <sup>137</sup>Cs in the atmosphere, and possible subsequent deposition, are the nuclear tests that took place before the Partial Test Ban Treaty (PTBT) entered into force in 1963 and the nuclear accident occurred in Chernobyl in 1986.

This work focuses on the study of the 45m ice core drilled at Pian di Neve site, Adamello glacier, in the Italian Alps, during summer 2016. Analysis were carried out on the chips of the ice core, which were divided in 71 runs covering the entire length of the ice core.

Total beta activity analysis was performed with spectrometer Quantulus 1220<sup>TM</sup> on aqueous samples extracted from chips of the ice core. HNO<sub>3</sub> was added to the samples prior to analysis in order to reach 1.7 pH and avoid deterioration. Quenching curves with HNO<sub>3</sub> will be performed in the near future to assess the influence of HNO<sub>3</sub> on the shifting of the spectrum due to quench. The analysis was carried out on 20mL Polyethylene vials containing 8mL of sample water from the ice core and 12mL of Ultima Gold scintillation cocktail. Each sample was analyzed for 1000 minutes with a PSA level of 81, determined with a PSA calibration done using <sup>90</sup>Sr and <sup>238</sup>Pu standards. The resulting spectra were compared to blank runs to assess the background spectrum. A clear excess was found in some samples.

Gamma ray spectroscopy was performed using a high-purity germanium detector. Water samples from the ice core were stored in 1000mL Polyethylene bottles. Samples from the chips that had shown a surplus in total beta activity were analyzed with HPGE detector with counting times of 160 hours on average. A peak at 661,6 keV, corresponding to gamma ray emission of <sup>137</sup>Cs, was recorded in some samples, showing a good agreement with beta activity levels. Absolute efficiencies for the HPGE detector containing the water samples were calculated with Monte Carlo simulation using the Geant4 code (Agostinelli et al, 2003). For samples that showed an <sup>137</sup>Cs excess, the specific activity was calculated, whilst for samples without any excess a detection limit was calculated.

Measurements clearly indicate a radioactive contamination of <sup>137</sup>Cs. The annual megaton release due to the nuclear test explosions which were carried out in the year 1963, prior to the PTBT, was compared to the <sup>137</sup>Cs concentrations measured in the ice core samples, and a correlation was found. No evidence of the Chernobyl nuclear accident was found so far.

In conclusion, regarding the work that has been done up to now, we can assess the value of LSC in ice core dating as it provides a quick way of analyzing the total depth of the ice core with a high efficiency. Moreover, we can link the presence of <sup>137</sup>Cs in the Adamello ice core to the nuclear tests performed in 1963, confirming the value of gamma ray-spectroscopy in this type of analysis.

S.Agostinelli et al., Nucl. Instrum. Methods A 506,250 (2003)

## Inorganic and total <sup>14</sup>C in the vicinity of a Hungarian LILW

R. Janovics<sup>1</sup>, A. Molnár<sup>2</sup>, T. Varga<sup>1</sup>, M. Braun<sup>1</sup>, I. Tóth<sup>2</sup>, M. Molnár<sup>1</sup>

<sup>1</sup>Institute for Nuclear Research, Hungarian Academy of Sciences, Debrecen Bem tér 18/c, Hungary

<sup>2</sup>Isotoptech Co., Debrecen Bem tér 18/c, Hungary

Keywords: disposal facility, radiocarbon, DI<sup>14</sup>C, T<sup>14</sup>C

Presenting author email: janovics@atomki.hu

The monitoring of the radiocarbon emission of nuclear facilities into the groundwater is generally performed on the basis of the measurement of the inorganically bound radiocarbon (DI<sup>14</sup>C). However, the exact monitoring of the emission would only be possible, if the total radiocarbon activity of the groundwater or other media (T<sup>14</sup>C) is known.

Our previous studies proved that there is some artificial radiocarbon in the groundwater of the Püspökszilágy Radioactive Waste Treatment and Disposal Facility, (RWTDF) Hungary, which cannot be detected by the current conventional methods (Molnár et al, 2013).

Within the framework of this study, the determination of the radiocarbon activity concentration of the inorganic and total carbon of groundwater was performed for the complete monitoring well network of the RWTDF together with the analysis of soil samples. The measurements were performed by a MICADAS type of AMS in Debrecen.

In the site of the RWTDF, the most significant radiocarbon source is one of the cells in the vicinity of the well T-24 (Figure 1.).

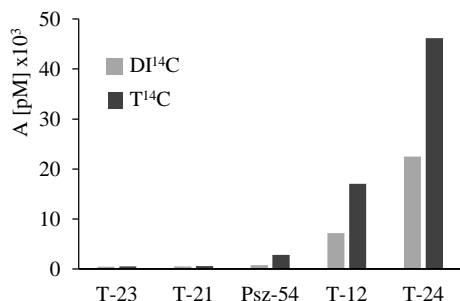


Figure 1. DI<sup>14</sup>C and T<sup>14</sup>C in the groundwater samples [uc.:±5%]

The spread of the contamination is towards the well Psz-54 in the main flow direction of groundwater. It is proved that by the current monitoring practice based on the determination of the inorganic fraction, only less than 50% of the total radiocarbon content of groundwater can be detected in certain wells of higher radiocarbon content in the RWTDF.

The soil sample were taken from the unsaturated zone from different depth in the main groundwater spreading direction for parallel measurement of the water soluble inorganic and the total radiocarbon activity (Figure 2.). The soluble inorganic carbon has respectively higher specific <sup>14</sup>C activity compared to the results of the total carbon. The most significant excess was observed in the top layer where the T<sup>14</sup>C was the half of the DI<sup>14</sup>C. The activity is decreasing with depth but it is still remains

above the natural background even under 3.5 m deep. These results suggest that the <sup>14</sup>C in the unsaturated soil zone is mainly falls out from the air.

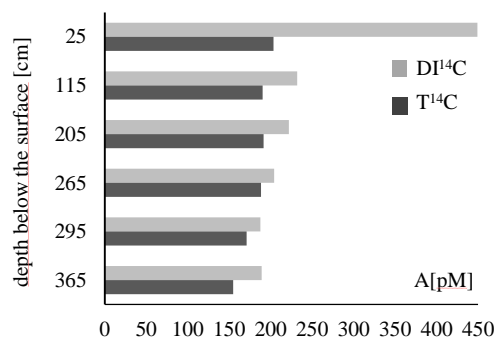


Figure 2. I<sup>14</sup>C and T<sup>14</sup>C in the soil [uc.:±5%]

On the basis of these observations it can be stated that to receive more precise emission control and dose estimation during the environmental monitoring of the RWTDF, the radiocarbon concentration of the total dissolved carbon content of groundwater should be measured, not only the inorganic fraction. The measurement of the total carbon fraction is even more justifiable as it is obvious that significant part of the radiocarbon activity restored in the RWTDF is in organic matrix (scintillation cocktails, wastes of biological researches etc.).

This work was carried out in part in the frame of Task „3.1.4. Development of radiochemical measurement technique of hardly measurable isotopes” of the National Nuclear Research Program VKSZ\_14-1-2015-0021 supported by the National Research, Development and Innovation Office of Hungary.

The research was supported by the European Union and the State of Hungary, co-financed by the European Regional Development Fund in the project of GINOP-2.3.2.-15-2016-00009 ‘ICER’.

The research was also supported by the Hungarian Atomic Energy Authority in the project of OAH-ABA-01/16-M.

Molnár, M., Hajdas, I., Janovics, R., Rinyu, L., Synal, H. A., Veres, M., Wacker, L., C-14 analysis of groundwater down to the milliliter level. 2013. Nuclear Instruments and Methods in Physics Research Section B: Beam Interactions with Materials and Atoms 294 573-576

## Radiocarbon record in modern tree rings from Slovakia

I. Kontul<sup>1</sup>, M. Ješkovec<sup>1</sup>, J. Kaizer<sup>1</sup>, P. P. Povinec<sup>1</sup>, M. Richtáriková<sup>1</sup>, I. Svetlík<sup>2</sup>, A. Šivo<sup>1</sup>

<sup>1</sup>Centre for Nuclear and Accelerator Technologies (CENTA), Faculty of Physics, Mathematics and Informatics, Comenius University, 842 48 Bratislava, Slovakia

<sup>2</sup>Department of Radiation Dosimetry, Nuclear Physics Institute of the CAS, 180 86 Prague, Czech Republic

Keywords: radiocarbon, tree rings, AMS, radiometric counting

Presenting author email: ivan.kontul@fmph.uniba.sk

Radiocarbon  $^{14}\text{C}$  is produced mainly by nuclear reactions between secondary neutrons from the cosmic radiation and nuclei in the atmosphere. After production, it quickly oxidizes into  $^{14}\text{CO}_2$  and takes part in the global carbon cycle. In the process of photosynthesis it is absorbed by trees and used during its growth to create the wood structure. Most of the trees growing in the temperate climate zones have well-defined annual growth rings and they can be used to study past variations of radiocarbon concentrations in the atmosphere and biosphere.

Three radiocarbon records from tree rings covering years 1974-2013 will be presented and discussed: Vysoká pri Morave, Žilkovce and Bratislava (Fig. 1). Samples from Vysoká pri Morave and Žilkovce were taken using an increment borer, and their radiocarbon content was analyzed by accelerator mass spectrometry. In the case of Bratislava tree rings, whole section of the tree was used to produce enough sample material for radiometric counting of  $^{14}\text{C}$ .

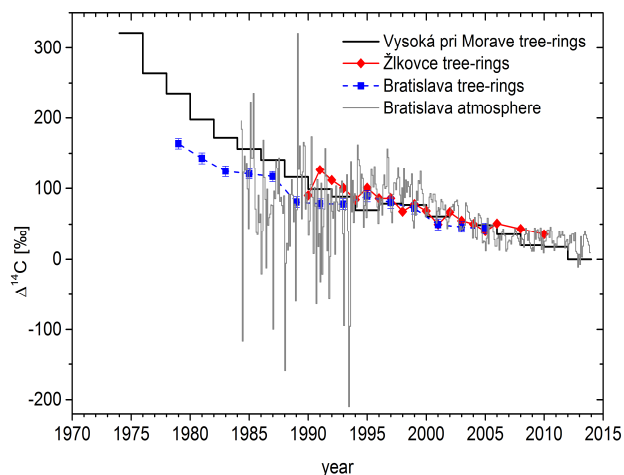


Figure 1. Radiocarbon concentration in annually growth rings from three sampling stations in Slovakia, and monthly atmospheric data from Bratislava. The Vysoká pri Morave data are shown as a histogram, because they represent two-year averages (Žilkovce and Bratislava results represent annual data).

The Žilkovce sampling site is in close proximity to the Jaslovské Bohunice nuclear power plant (NPP). The tree-ring samples from this site show an influence of anthropogenic radiocarbon released by the. A comparison of Bratislava tree-ring and atmospheric data with clean air radiocarbon levels from Schauinsland

sampling station (Levin, 2004; Levin et al., 2013) shows a dilution of radiocarbon concentration by  $^{14}\text{C}$ -free carbon dioxide from fossil fuel emissions by about 5 % (i. e. Suess effect), especially until 1993. Bratislava as the capital city of Slovakia is heavily urbanized and industrialized. Regional Suess effect is also responsible for lower radiocarbon levels in tree rings from Vysoká pri Morave (Kontul' et al., 2016).

Changes in industrial activities in Slovakia after 1993 caused a decrease in fossil fuel emissions in the region. These changes are clearly visible in the tree-ring radiocarbon data (Figure 1) as a slight increase of  $^{14}\text{C}$  concentration in annual growth rings in 1993-1997 superimposed on the prevalent decrease of radiocarbon levels from the bomb peak maximum in 1963. Absence of extremely deep minima in atmospheric  $^{14}\text{C}$  after this period supports this interpretation. Tree rings retain atmospheric carbon only from the growing season of the source trees (usually spring, summer and the beginning of autumn) and therefore their radiocarbon content is not heavily influenced by the winter deep minima in 1984-1993.

The expected exponential decrease of  $^{14}\text{C}$  concentration in the atmosphere and biosphere can also be observed in the presented data sets. The rate of this decrease is different for the examined sites because of the different local sources of fossil  $\text{CO}_2$  emissions and impact of the Jaslovské Bohunice NPP.

Tree-ring records from Slovakia provide an excellent tool for reconstructing past changes in the radiocarbon concentration in the regional environment and their comparison with available atmospheric data, which allows to explore the dynamics between the atmosphere and biosphere, important for climate change studies.

This work was supported by the EU Research and Development Operational Program funded by the ERDF (projects No. 26240120012, 26240120026, and 26240220004), and by the International Atomic Energy Agency (TC project SLR9013).

Levin, I., 2004. The tropospheric  $^{14}\text{CO}_2$  level in mid-latitudes of the northern hemisphere (1959-20036). Radiocarbon 46, 1261-1272.

Levin, I., Kromer, B., Hammer, S., 2013. Atmospheric  $\Delta^{14}\text{CO}_2$  trend in Western European background air from 2000 to 2012. Tellus B 65, 20092.

Kontul' et al., 2016. Radiocarbon concentration in tree-ring samples collected in the south-west Slovakia (1974-2013). Appl. Rad. Isot. doi.org/10.1016/j.apradiso.2016.12.001.

## Intercomparison of radionuclide measurements in Danube sediment

G. Pantelić<sup>1</sup>, P. Vančura<sup>2</sup>, Z. Ulrich<sup>3</sup>, E. Weiszenburger<sup>3</sup>, D. Todorović<sup>1</sup>, J. Krneta Nikolić<sup>1</sup>,  
M. Janković<sup>1</sup>, M. Rajačić<sup>1</sup>, N. Sarap<sup>1</sup>

<sup>1</sup>University of Belgrade, Vinča Institute for Nuclear Sciences, Belgrade, Serbia

<sup>2</sup>South Transdanubian Inspectorate for Environmental Protection, Nature Conservation and Water Management, Pécs, Hungary

<sup>3</sup>Government Office of Baranja County, Pécs, Hungary

Keywords: radionuclide, Danube, intercomparison.

Presenting author email: pantelic@vinca.rs

Potential pollutants of the river Danube are the Paks Nuclear Power Plant situated 85 km from Serbian-Hungarian border and long-lived fission products from the accident of Chernobyl nuclear power plant. For this reason, radioactivity monitoring of Danube by the countries of Serbia and Hungary was conducted more than 20 years.

Regarding the external quality control of the measurements, during 2015 Vinča Institute for Nuclear Sciences from Belgrade, Serbia and Government Office of Baranja County, Pécs, Hungary, have participated in intercomparison exercise, which has been organized and developed in the framework of Serbian-Hungarian Subcommittee for water quality. The scope of this intercomparison was to obtain the information on the degree of agreement between the results on gross beta activity and gamma spectrometry measurement in the sediment samples.

The monitoring did not emphasise only on fallout radionuclides like <sup>137</sup>Cs, but also took into account the presence of naturally occurring radionuclides from uranium and thorium series, as well as <sup>40</sup>K and <sup>7</sup>Be.

The samples were taken at the border profiles Bezdan (Serbia) and Mohacs (Hungary). The sediments samples from Danube river were collected in April (sediments 1-2), September (sediments 3-5) at Bezdan and in November (sediments 6-9) at Mohacs. Samples were prepared in Hungary, and after measurement were sent to Serbia.

Results obtained by the two laboratories participating in the intercomparison exercise, along with their respective combined standard uncertainties are presented in Tables 1 and 2.

Table 1. Gross beta activity in the sediments

Sample	SRB Activity (Bq/kg dry weight)	HU Activity (Bq/kg dry weight)
Sediment 1	610 ± 70	710 ± 90
Sediment 2	890 ± 80	650 ± 90
Sediment 3	520 ± 80	580 ± 90
Sediment 4	650 ± 80	590 ± 90
Sediment 5	690 ± 90	550 ± 90
Sediment 6	870 ± 90	700 ± 110
Sediment 7	900 ± 90	850 ± 110
Sediment 8	800 ± 90	750 ± 110
Sediment 9	880 ± 90	780 ± 110

Table 2. <sup>137</sup>Cs activity concentration in the sediments

Sample	SRB <sup>137</sup> Cs activity (Bq/kg dry weight)	HU <sup>137</sup> Cs activity (Bq/kg dry weight)
Sediment 1	10.0 ± 0.7	14.5 ± 1.5
Sediment 2	8.9 ± 0.6	14.8 ± 1.5
Sediment 3	7.2 ± 0.5	9.5 ± 1.0
Sediment 4	11.2 ± 0.8	9.1 ± 1.0
Sediment 5	5.3 ± 0.4	7.9 ± 0.9
Sediment 6	12.4 ± 0.9	14.0 ± 1.4
Sediment 7	22.0 ± 1.1	27.2 ± 1.9
Sediment 8	13.6 ± 0.9	17.5 ± 1.6
Sediment 9	11.6 ± 0.9	13.7 ± 1.2

There is good agreement between SRB and HU results for gross beta activity in all sediments within the limits of measurement uncertainty, except for sediment 2 (Table 1).

Comparing gamaspectrometry results for all natural radionuclides (<sup>232</sup>Th, <sup>226</sup>Ra and <sup>40</sup>K) in all sediments we concluded that the obtained activity concentrations are in agreement within the measurement uncertainty. Results for <sup>137</sup>Cs activity concentration in the sediments agreed within 2 σ (Table 2).

Results of intercomparison showed good agreement between the results obtained by two laboratories similar to the previous measurements (Pantelić et al. 2015).

The research was supported by the Ministry of Education and Science of Serbia under the Project III43009 - New Technologies for Monitoring and Protection of Environment from Harmful Chemical Substances and radiation impact.

Pantelić, G., Vancsura, P., Krneta Nikolić, J., Janković, M., Sarap, N., Todorović, D., Rajačić, M., 2016. Results from radionuclide interlaboratory intercomparison in sediment and fish. 2016. Rad.Applic. 1,1, 36-39

## Radionuclides migration pathways in the artificial reservoirs

N.V. Kuzmenkova<sup>1</sup>, I.E. Vlasova<sup>1</sup>, A.K. Rozhkova<sup>1</sup>, E.A. Pryakhin<sup>2</sup>, S.N. Kalmykov<sup>1</sup>

<sup>1</sup>Department of Chemistry, Lomonosov MSU, Moscow, 119991, Russia

<sup>2</sup>Urals Research Center for Radiation Medicine, Chelyabinsk, 454076, Russia

Keywords: PA "Mayak», ecosystem, radionuclides, concentration ratio.

Presenting author email: kuzmenkova213@gmail.com

Production Association "Mayak", Chelyabinsk region, Russia, - one of the largest nuclear facility in the Russian Federation. Reservoir R-17 was used as intermediate level liquid radioactive wastes (ILLW) storage and reservoir R-4 was used as low level liquid radioactive wastes (LLLW) storage. The aim of this study is to investigate radionuclides migration pathways in the reservoirs using the activity and concentration factor (CR (ratio of activity of radionuclides in the studied biota to their activity in water)).

The following samples were collected: reservoir water, bottom sediments, benthos (*Chironomidae lavrae*), reed (*Phragmites australis*), zooplankton and phytoplankton. Plant samples have been washed out of the soil residues and sediments, air dried and divided into roots, stems and leaves. Pore water separated from the bottom sediment by high-speed centrifugation (10,000 RPM for 20 minutes). All samples were analyzed using gamma-spectrometry (Canberra GR 3818), strontium-90 was determined by Cherenkov counting. Alpha spectrometry was used for alpha-emitting nuclides (CANBERRA Model 7401) after separation using extraction chromatography (DGA, UTEVA, TRU (TrisKem International)). To determine the way of hydrobionts accumulate radionuclides, the samples were analyzed by radiography (Cyclone Plus Storage Phosphor System, PerkinElmer). The activity of <sup>3</sup>H, <sup>90</sup>Sr, <sup>99</sup>Tc, <sup>137</sup>Cs, <sup>60</sup>Co, <sup>241</sup>Am, <sup>238,239,240</sup>Pu, <sup>234,238</sup>U, <sup>244</sup>Cm and <sup>237</sup>Np in biotic and abiotic components of two reservoirs in "Mayak" territory - R-17 ("old swamp") and R-4 were determined.

In the aquatic ecosystems most of the radionuclides are accumulated in bottom sediments that play the "geochemical barrier" role in the radionuclides migration processes. Biota is also involved in the radionuclides redistribution processes within the aquatic ecosystem (Figure 1).

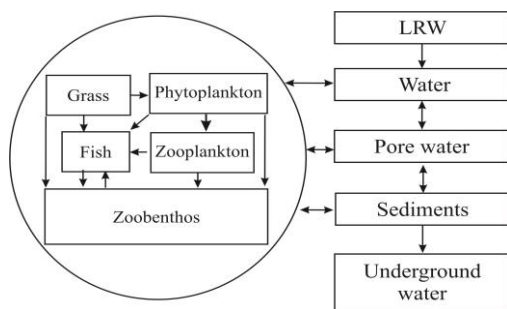


Fig.1 The model of radionuclides migration pathways in artificial reservoirs.

Maximum CR values for sediment (in respect to water) was found for Am-241 for all studied objects in both reservoirs. The plutonium CR in two reservoirs varied as much as two orders of magnitude that is probably due to the reservoir R-4 sediments properties, the total activity and speciation of this radionuclide.

Phyto- and zooplankton rapidly absorbs radionuclides from water. The maximum CR revealed for Am, Pu and Cs for the two reservoirs. Phytoplankton accumulates radionuclides better than zooplankton (except of Cs in the R-4). The minimum CR in the studied aquatic organisms was found for U. Chironomids CR in the R-17 show different ways of radionuclides intake in benthos. It was established that Am, Cs and Pu chironomids accumulates from water, while Sr from the bottom sediments. The vegetation CR revealed most of the radionuclides contained in the roots of plants, the leaves are less active, minimum activity was found in the stems (except of strontium). Maximum CR was found for plutonium and americium, minimum - for uranium.

Integrated approach for the samples and standards (digital radiography) along with Alpha Track radiography and  $\gamma$ -spectroscopy were used to estimate the contribution of the main nuclides in specific parts of samples. The data show uneven distribution of radionuclides in benthos bodies also showing the presents of radioactive particles that stick to the hydrobionts surface.

The main contribution to the total activity in the biotic components is due to <sup>90</sup>Sr (up to 55%) and <sup>137</sup>Cs (up to 47%), in abiotic (water, pore water, sediments): <sup>137</sup>Cs (up to 80%), <sup>90</sup>Sr (up to 17%) and <sup>241</sup>Am (2.5%). The contribution of other radionuclides is less than 1%. The values of the radioactivity in reservoir R-17 is 2-3 orders higher than in R-4. The maximum concentration factor was found for the Am-241 in all ecosystems components for both reservoirs. Phytoplankton revealed as more effective scavenger for radionuclides compares with zooplankton. Aquatic plants accumulate more in roots than in leaves and stems. The following series of accumulation of radionuclides for the bottom sediments R-17 was detected (CR sediments/water from highest to lowest): Am → Pu → Cs → Co → Sr → U.

This work was supported by the Russian Scientific Foundation (project 16-13-00049).



## TRITIUM CONTENT IN SNOW COVER OF NUCLEAR EXPLOSION VENUES

Turchenko D.V., Lukashenko S.N., Lyakhova O.N.

Branch «Institute of Radiation Safety and Ecology» of the NNC RK, Kurchatov, Kazakhstan

Keywords: UNE, ICE, CCE, ground water, tritium, snow cover, STS, migration of radionuclides,

Presenting author email: turchenko@nnc.kz

Previously carried out researches revealed high concentrations of tritium in environmental components of Semipalatinsk Test Site (water objects, animal products, plants, atmospheric and soil air, and soil cover). It's assumed that the main source of tritium is gopher cavities of underground nuclear explosions (UNE), tritium was out with ground waters subsequently appearing at the daily surface. The highest concentrations of tritium were found in surface and ground waters of the STS water objects (Shagan river and creeks of Degelen site) reaching the value of  $n \cdot 10^5$  Bq/kg.

Over 130 underground nuclear explosions (UNE) of various types and yields was made at Semipalatinsk Test Site, including 106 UNEs at «Balapan» site, 24 UNEs at «Sary-Uzen» site. UNEs were aimed at nuclear weapons invention and modification, and for peaceful purposes well. As expected, the main sources of tritium emanation to the environment are surface and ground waters of the STS, nevertheless epicentral zones of UNE boreholes at «Balapan» and «Sary-Uzen» sites, can be potential sources of tritium entry to the environment.

Work objective: Research of the character of tritium distribution in snow cover in venues of underground nuclear explosions.

### Methodology.

Since such research works haven't been carried out ever before, while researching peri-portal sites of warfare boreholes of «Balapan» site different methodological approaches were used. General assessment of tritium content in snow cover was carried out in boreholes. To assess background concentrations of tritium in snow cover, research lines were drawn at wellhead sites of warfare boreholes. At the boreholes 1355 and 1010 areal survey of tritium content in the snow cover was carried out. In 2011 and 2012 snow cover on the borehole 1355 was sampled by 1x1km grid.

To determine specific activity of tritium in snow samples TRI-CARB 2900 TR and Quantulus 1220 liquid scintillation spectrometers were used with standard technique

### Results.

Researches carried out have revealed sites with increased tritium concentrations in the snow cover. As a rule, maximum concentrations of tritium in snow are observed at the wellhead of boreholes 1355 and 1010, in some cases achieving 75 Bq/kg. It should be noted also, that maximum concentrations of tritium in snow were found not only at the wellhead, but also 200-300 away from the nuclear test epicenter southward (see. Figure 1).

Comparing data for the bottom and the top snow cover layer revealed that tritium concentration in the bottom layer is higher than in the top layer. This fact proofs an

assumption made before on tritium entry (emanation) from soil.

Nevertheless, an issue of the origin of tritium in snow cover remains open: tritium enters the top soil layer from either UNE gopher cavity or a closely-spaced water-bearing layer.

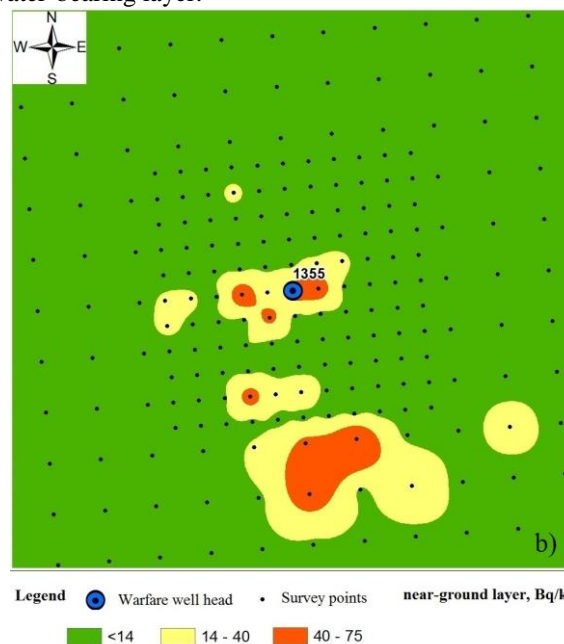


Figure 1. Tritium content in the snow cover of warfare boreholes 1355 bottom layer

For more detailed research of mechanisms of tritium entry into the snow cover, at peri-portal sites of warfare boreholes it is necessary to carry out additional works to study geological structure and chemical composition if the soil cover at various depths from the bottoming surface. Besides that additional researches of snowcover need to be carried out at «Balapan» site, allowing to assess global fallout background of tritium from atmosphere for this area.

This research shows that tritium at the STS is distributed in much larger scales, than we expected before. This method can be successfully used in identification of underground test venues. The method developed is cheap enough and easy to be implemented.

### Conclusion.

The paper provides concentrations of tritium in snow cover in venues of underground nuclear tests. Gopher cavities of underground explosions were found to be potential sources of tritium entry into environment. Levels and tritium distribution in snow cover vary significantly depending on type and yield of nuclear explosion. It was found, that in venues of nuclear tests the main mechanism of tritium entry into snow cover is emanation from soil.

## Environmental radioactivity and tracer studies over the past sixty years in Denmark

J. Qiao<sup>1</sup>

<sup>1</sup>Center for Nuclear Technologies, Technical University of Denmark, Risø Campus, 4000 Roskilde, Denmark

Keywords: Environmental radioactivity, tracer studies, North Atlantic, Arctic, North Sea, Baltic Sea, Greenland

Presenting author email: jiqi@dtu.dk

Studies of environmental radioactivity were initiated in 1956 at the Research Establishment Risø located at Roskilde, Denmark. This paper aims to give a brief overview of the investigations carried out in Denmark for environmental radioactivity and tracer studies over the past sixty years.

Our systematic record of environmental radioactivity data clearly indicate the anthropogenic radionuclides signal originated from global fallout of nuclear weapons testing during the 1960's, fallout of the Chernobyl accident in 1986 as well as the Fukushima accident in 2011 (see Fig.1). After the accident at Thule, Greenland in 1968, comprehensive studies have been carried out to investigate the local radioactive pollution (<sup>137</sup>Cs, <sup>90</sup>Sr, <sup>238,239,240</sup>Pu, <sup>237</sup>Np, <sup>99</sup>Tc, <sup>241</sup>Am) and its radiological impact to the Arctic marine and terrestrial environment. Radioactive tracers (e.g., <sup>99</sup>Tc, <sup>129</sup>I) released from the two major European reprocessing plants (La Hague and Sellafield) have been employed as point source tracers to studies the water movement in the North Atlantic-Arctic region. In recent years, <sup>236</sup>U oceanographic studies have also been carried out to investigate the source term of <sup>236</sup>U in North Sea-Baltic Sea region as well as along Greenland coast.

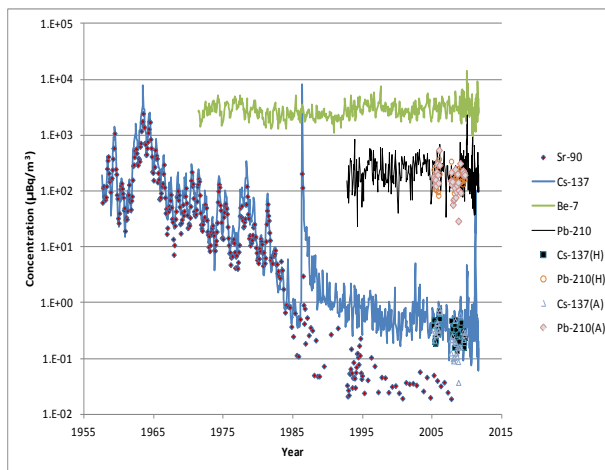


Fig1. Time series record of radioactivity in the air at Risø, Roskilde, Denmark

## Cs-137 and K-40 distribution in the Neris River basin, Lithuania

O. Jefanova<sup>1</sup>, E.D. Marčiulionienė<sup>1</sup>, B. Vilimaitė-Šilobritienė<sup>2</sup>, J. Mažeika<sup>1</sup>

<sup>1</sup>State Research Institute Nature Research Centre, Akademijos Str. 2, LT-08412 Vilnius, Lithuania

<sup>2</sup>Environmental Protection Agency, A. Juozapaviciaus Str. 9, LT-09311 Vilnius, Lithuania

Keywords: Neris River basin, macrophytes, bottom sediment, molluscs

Presenting author email: olga.jefanova@gamtostyrimai.lt

Nowadays is poorly information about the accumulation of Cs-137 in components of the Neris River Basin, however it is very actual in context of environmental protection. The aim of this work is to present established distribution of Cs-137 and K-40 in Neris Rivers basin Lithuanian territory.

It were three sampling point: the Neris River (Buivydziai and Vilnius) and Lake Karackiai. The collection and preparation for gamma-measurements described in detail in (Jefanova, 2016).

It was found that at Buivydziai, Cs-137 activity concentration in macrophytes ranged from 6 to 21 Bq kg<sup>-1</sup>; in shells of small molluscs (2-4 year old) *Anadonta sp.* – were <mda (Table 1). However, in soft tissues of molluscs, Cs-137 activity concentration was 7 Bq kg<sup>-1</sup> and in shells and soft tissues of large molluscs (5-7 year old) it was about 1 Bq kg<sup>-1</sup>. Data of Environmental Protection Agency (gamta.lt/..., assessed 2017-01-20) shows Cs-137 activity concentrations fluctuation in bottom sediment from Buivydziai in range from 2 to 20 Bq kg<sup>-1</sup> during 2007-2015 period (Figure 1).

Table 1. Cs-137 and K-40 activity concentrations (Bq kg<sup>-1</sup>) in molluscs and macrophytes

Sampling point	Species	Cs-137	K-40
Neris River, Buivydziai	<i>Elodea canadensis</i>	21.0±4.5	890±60
	<i>Potamogeton lucens</i>	6.0±3.2	820±50
	<i>Anadonta sp.</i> (small, 2-4 year)		
	shells	<mda	24±19
	soft tissues	6.8±0.8	86±9
	<i>Anadonta sp.</i> (large, 5-7 yaer)		
	shells	1.0±0.6	13±9
	soft tissues	1.0±0.9	79±16
Neris River, Vilnius	<i>Elodea canadensis</i>	8.0±2.5	880±50
	<i>Potamogeton lucens</i>	<mda	1200±80
Lake Karackiai	<i>Elodea canadensis</i>	12.0±4.3	1450±80
	<i>Potamogeton lucens</i>	16.0±5.0	2270±110
	<i>Chara sp.</i>	6.0±2.3	180±30

mda - minimum detectable activity

In the Neris River near the Žirmūnai residential district (Vilnius), Cs-137 activity concentration in macrophytes was lower than that at Buivydziai and ranged from <mda up to 8 Bq kg<sup>-1</sup> (Table 1). In the Neris River both at Buivydziai and near Žirmūnai, Cs-137 activity concentration in sediments was found to be slightly different, reaching 16 and 18 Bq kg<sup>-1</sup> respectively.

In macrophytes of Lake Karackiai, Cs-137 activity concentrations ranged from 6 to 16 Bq kg<sup>-1</sup> (Table 1). However, concentrations of this radionuclide

in lake bottom sediments were up to 130 Bq kg<sup>-1</sup>. Significantly larger amounts of Cs-137 in bottom sediments of the lake compared to those of the Neris River could be accounted for by differences in ecological conditions, grain size composition and organic matter content of lake and river sediments.

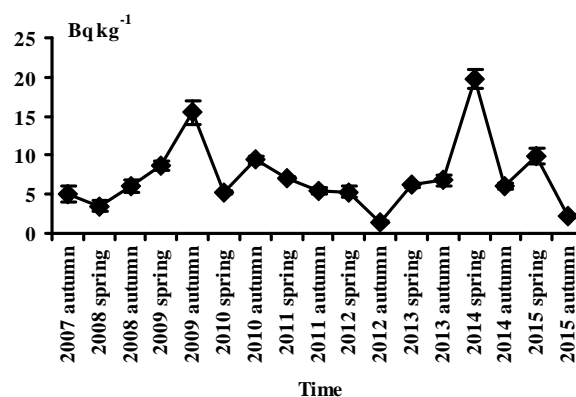


Figure 1. Cs-137 activity concentration in bottom sediments of the Neris River at Buivydziai during 2007-2015 period (gamta.lt/..., assessed 2017-01-20)

The largest K-40 activity concentration in the Neris River was determined in macrophytes (from 824 to 1202 Bq kg<sup>-1</sup>), while the lowest in shells of mollusks *Anadonta sp.* (13 and 24 Bq kg<sup>-1</sup>) (Table 1). K-40 activity concentration in soft tissues of mollusks was higher (79 and 86 Bq kg<sup>-1</sup>) than in shells. K-40 activity concentrations in the Neris River sediments ranged from 481 to 724 Bq kg<sup>-1</sup>.

Based on the Cs-137/K-40 ratio established in macrophytes, mollusks and sediments, it is possible to infer that Cs-137 accumulation properties of the mollusks *Anadonta sp.* are better than those of macrophytes or even those of bottom sediments. Although Karackiai Lake sediments have the highest concentration of Cs-137 activity, the Cs-137/K-40 ratio for sediments was lower than for mollusks *Anadonta sp.* Among the studied macrophytes, *Chara sp.* (Cs-137/K-40 ratio 0.033) showed the greatest ability to accumulate Cs-137.

Jefanova O., 2016. The distribution of artificial radionuclides in different components of aquatic and terrestrial ecosystem under various environmental conditions. Summary of doctoral dissertation, Biomedical sciences, Biology (01B). Gamtos tyrimų centras, Vilnius. p. 60.  
<http://gamta.lt/cms/index?rubricId=7a9a8309-05de-4580-836c-cfff1327d18b> (Assessed 2017-01-20) Reports of Environmental Protection Agency radiological monitoring

**Variations of  $\Delta^{14}\text{C}_{\text{TOC}}$  and Acid-leachable elemental content in a 50-cm sediment core reflecting environmental changes over 200 years in Santa Barbara Basin, CA**

H.-C. Li<sup>1\*</sup>, Y.-W. Zhang<sup>1</sup> and W.M. Berelson<sup>2</sup>

<sup>1</sup>Department of Geosciences, National Taiwan University, Taipei 10617, Taiwan, ROC

<sup>2</sup>Department of Earth Sciences, University of Southern California, Los Angeles, CA 90089, USA

Keywords: AMS <sup>14</sup>C dating, <sup>210</sup>Pb dating, elemental content, Santa Barbara Basin.

Presenting author email: hcli1960@ntu.edu.tw

A 51-cm gravity core (SBB-8-2012) collected from Santa Barbara Basin (SBB) of California in 2012 has been dated by <sup>210</sup>Pb dating method, spanning about 210 years of depositional history with a mean sedimentation rate of 0.29cm/y. The core was X-ray radiographed by an Itrax-XRF Core Scanner, showing laminations and biological stratigraphic features. Elemental analyses on the acid (0.5N HCl) leaching phase of the bulk sediments have been done by an ICP-OES. We have done AMS <sup>14</sup>C dating on TOC of the bulk sediments in 34 layers from the upper 40.1 cm of the core. Excluding the <sup>14</sup>C date (2983±99 yr BP) at 35-35.2 cm depth, the other 33 uncorrected <sup>14</sup>C dates range from 508±4 yr BP to 2214±19 yr BP and form two linear lines (Fig. 1):

$$\text{age} = 417 + 35.9 \text{ depth (cm)}, R^2 = 0.976$$

$$\text{age} = 665 + 37.4 \text{ depth (cm)}, R^2 = 0.949$$

The AMS <sup>14</sup>C dating results indicate that both total organic carbon and inorganic carbon in the sediments contain reservoir ages. For the TOC in the sediments, the minimal reservoir age may be about 417 years which may be caused by DIC uptaking through photosynthesis (autochthonous source) in the water column and by terrestrial input from river flow and dust fallout (allochthonous source). At 35.5-37 cm depth, the AMS <sup>14</sup>C date of a plant remain sample was 520±12 yr BP. If this age subtracts the reservoir age of 417 years, the corrected age is close to the results of <sup>210</sup>Pb dating and lamination counting. A shell sample at 38.5 cm depth provides a <sup>14</sup>C age of 915±47 yr BP, showing even older reservoir age for carbonate. The old carbon influence from the autochthonous source on the TOC <sup>14</sup>C ages varied through time depending on water mixing rate in the basin. When the mixing rate of the water column in the basin was slower, the reservoir age became older. Based on the chronology from the <sup>210</sup>Pb dating, we are able to determine the  $\Delta^{14}\text{C}$  fluctuations of the TOC in the bulk sediments of the core. The variation of the  $\Delta^{14}\text{C}$  may let us evaluate basin mixing during the past 200 years. In addition, XRF scan results and acid leachable elemental concentrations (ALEC) show high biological shells, clear and thicker laminations, high ALECs of all elements especially heavy metals, and brown color bands (high Fe and Mn) between 36-20 cm depths (AD 1887 ~1943)(Fig. 2). These evidences indicate that the basin had extremely strong changes during this period.

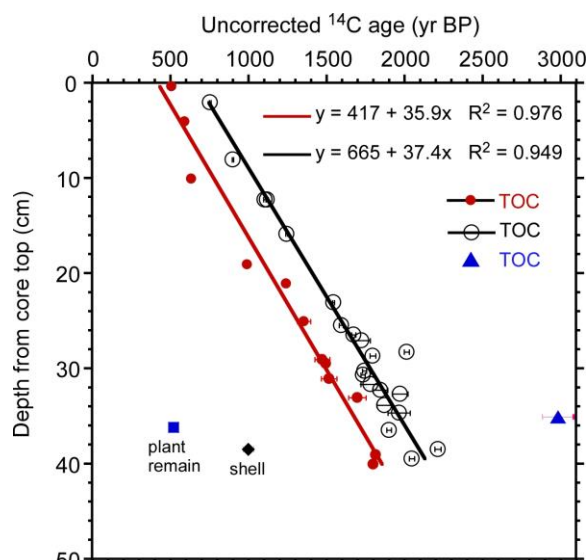


Figure 1. AMS <sup>14</sup>C dating profile of SBB-82012.

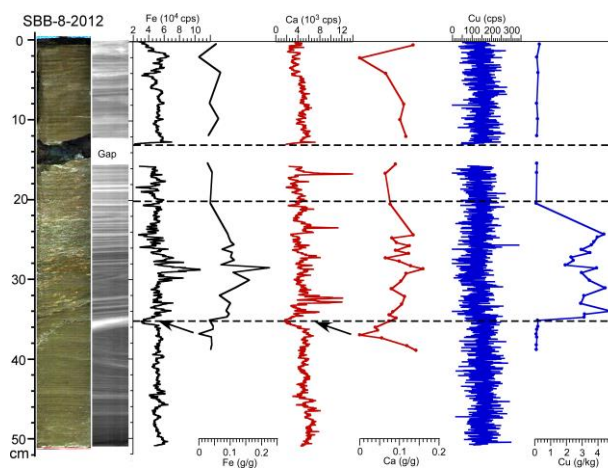


Figure 2. XRF scan and ICP-OES measured acid-leachable elemental concentrations.

This work was supported by the Ministry of Science and Technology of Taiwan under grant MOST 104-2116-M-002-017.



## Application of <sup>210</sup>Pb and <sup>137</sup>Cs for the study of marsh accretion and sediment accumulation. Examples of salt marshes from SW England

A.R. Iurian, G. Millward, A. Taylor, W. Marshall, W. Blake

School of Geography, Earth and Environmental Sciences, Plymouth University, Plymouth, Devon, PL4 8AA, United Kingdom

Keywords: <sup>210</sup>Pb geochronology, gamma-ray spectrometry, accretion rate, saltmarsh. Presenting author email: andra.iurian@plymouth.ac.uk

Coastal sediment systems (e.g. saltmarshes, wetlands, inter-tidal mudflats) are recognised as highly productive natural ecosystems with great ecological value, but are also among the most vulnerable areas to climate change, natural hazards and contamination from human riverine inputs. These environments can preserve sedimentary sequences with continuous accumulations over centuries, through integration of the atmospheric and aquatic deposition which enhance their accretion rates. Different processes affect accretion rates of tidal marshes, such as: (1) deposition of mineral suspended sediment (especially silt and clay), which is strongly influenced by land use practices (e.g. agriculture and deforestation, reservoir building) in the upland; (2) organic matter accumulation (from local humic-rich soils, on site vegetation) and on site degradation; (3) erosion, and (4) auto-compaction of the soil sediment with the increasing age of the saltmarsh. Saltmarsh sedimentary sequences have shown promise for the reconstruction of wetland ecosystem development and in providing information for forecasting future trends of coastal evolution, where accurate and precise chronologies are required.

This work uses short-lived radionuclides <sup>210</sup>Pb and <sup>137</sup>Cs, supported by sedimentary physical properties (bulk density, granulometry and organic carbon content): (1) to assess the historical spatial variation of vertical accretion among five salt-marshes environments in the River Tamar system, SW England, and (2) to determine the relative influences of mineral sediment versus organic matter accumulation on measured rates of accretion thereby developing insights on the biogeochemical and physical processes of marsh formation. The conclusions of this study can assist local authority's development of adaptation measures for sustaining salt marsh ecosystems under the present, and future, rate of sea-level rise.

The sediment water content, organic content, and dry bulk density varied widely among cores. The results indicate that marsh accretion is driven by a combination of mineral sediment and organic matter accumulation, the relative proportions of which vary among and within the marsh units. Organic matter and mineral sediment accumulation rates were calculated from the accretion rate and the mass inventory. In most cores, the water content decreased (and bulk density increased) with depth below the living root zone on account of changes in sediment structure and compaction. An example of the correlation between sedimentation rates determined by the CRS model (Appleby et al., 1979) and sediment

physical properties is given in Figure 1 for the Treluggan Marsh.

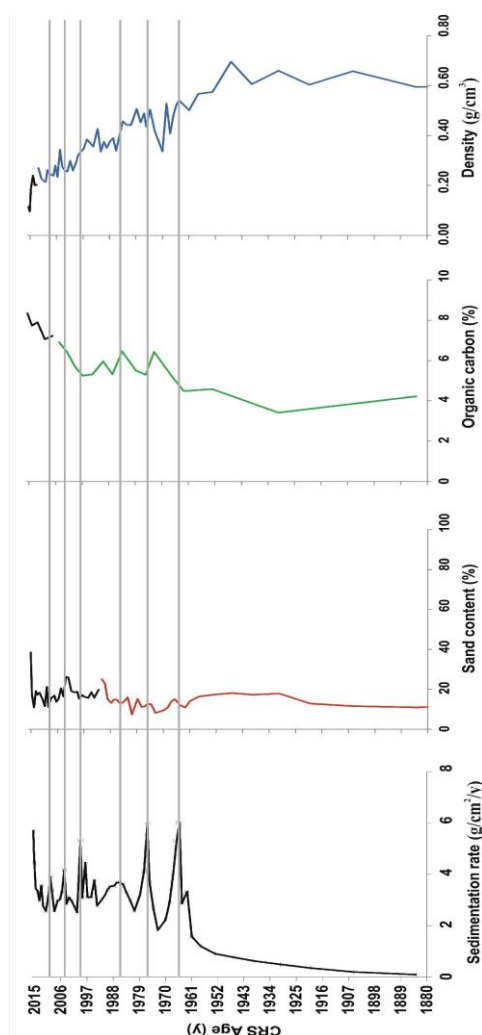


Figure 1. Sedimentation rates, sand content, organic carbon and bulk density for Treluggan Marsh. The different colours of the same plot mark the combined use of two cores for the same site

A.R. Iurian acknowledges the support of a Marie Curie Fellowship (H2020-MSCA-IF-2014, Grant Agreement no.: 658863) within the Horizon 2020.

Appleby, P.G., F. Oldfield, R. Thompson, P. Huttunen & K. Tolonen, 1979. <sup>210</sup>Pb dating of annually laminated lake sediments from Finland. *Nature*, 280:53-55.



## Distribution of radionuclides in granulometric fractions of soil in venues of underground nuclear tests in tunnels

A.M. Kabdyrakova, A.T. Mendubaev and S.N. Lukashenko

Branch “Institute of Radiation safety and Ecology” of the RSE “National Nuclear Center of the Republic of Kazakhstan”, Kurchatov city, East-Kazakhstan, 071100, Kazakhstan

Keywords: soil, granulometric fractions, nuclear tests, Semipalatinsk Test Site.

Presenting author email: kabdyrakova@nnc.kz

The paper presents results of researching distribution of  $^{137}\text{Cs}$ ,  $^{241}\text{Am}$ ,  $^{239+240}\text{Pu}$  and  $^{90}\text{Sr}$  radionuclides in granulometric soil fractions of the near-portal areas of the tunnels used for underground nuclear tests in the «Degelen» mountain massif of the Semipalatinsk Test Site.

Radioactive contamination of the soils studied was caused by carrying-out of radioactive substances by ground waters rising up on the day surface and running out through the tunnel cavities.

Water streams running out through the tunnels have resulted in formation of small brooks and spatially confined meadow ecosystems.

The research was aimed at revealing peculiarities of technogenic radionuclides distribution in granulometric soil fractions caused by their migration by water.

The research methodology included soil sampling, granulometric fractionation of soil samples and radionuclide analyses of fractions.

The topsoil samples were taken to the depth of 5 cm. Sampling points were located in flooded waterside zones of the brooks.

Granulometric fractioning was performed using «wet» sieving and sedimentation methods. Using sieving method the samples were separated into 5 fractions with the particle size ranging from 1000 to 40  $\mu\text{m}$ . Soil fractions with particle size ranging from 40 to 1  $\mu\text{m}$  were separated using sedimentation method.

Enrichment factor (Ef) was used for quantitative assessment of radionuclides distribution in granulometric soil fractions. Ef was calculated as the ratio of activity concentrations of the radionuclide in granulometric fraction ( $A^{fr}$ ) to soil ( $A^{soil}$ ):  $Ef = A^{fr} / A^{soil}$ . This parameter is the indication of the enrichment or depletion degree of granulometric fractions relative to average concentration of radionuclides in soil.

According to results, increasing of radionuclides concentration in granulometric fractions of soil with decreasing of size of particles is typical for water migration of radionuclides (fig. 1 and 2). This fact shows that distribution of radionuclides in granulometric soil fractions occurs due to sorption processes and the accumulation of radionuclides in soil particles (fractions) depends on the specific surface area of soil particles, their composition and properties. Besides that, sorption intensity probably depends on own nature and properties of the radionuclides. For example, Ef of  $^{239+240}\text{Pu}$  in soil fraction with the particle size of <1  $\mu\text{m}$  is 2-3 times lower than of  $^{137}\text{Cs}$ .

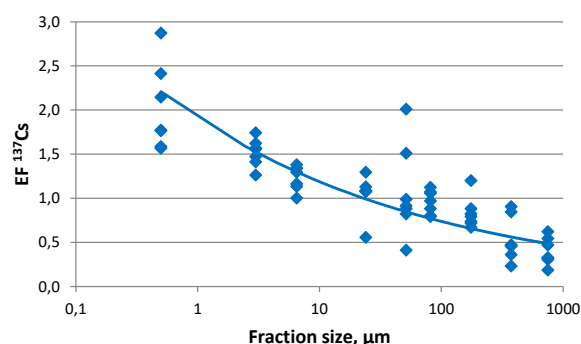


Figure 1. Distribution of  $^{137}\text{Cs}$  in granulometric soil fractions of the brook zone

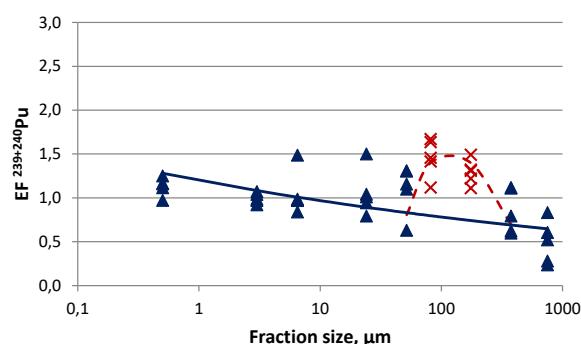


Figure 2. Distribution of  $^{239+240}\text{Pu}$  in granulometric soil fractions of the brook zone

However the results obtained also show that distribution of  $^{239+240}\text{Pu}$  is caused not only by sorption, but by other processes as well. So enrichment of the fraction with the particle size of 250 to 63  $\mu\text{m}$  (fig.2, red crosses) can be caused by presence of high-activity particles were formed during the nuclear explosion and taken out from the tunnel cavity with water streams. Also there is a possibility that «secondary» high-activity particles can be formed as the result of selective sorption of  $^{239+240}\text{Pu}$  with some definite soil particles.

## Investigation of sedimentation rates and sediment dynamics in Danube Delta lake system (Romania) by <sup>210</sup>Pb dating method

R-Cs. Begy<sup>1,2</sup>, Sz. Kelemen<sup>1</sup>, L. Preoteasa<sup>3</sup>, H. Simon<sup>1</sup>

<sup>1</sup>Babeş-Bolyai University, Faculty of Environmental Science and Engineering, 30 Fântânele Street, 400294, Cluj-Napoca, Romania

<sup>2</sup>Interdisciplinary Research Institute on Bio-Nano-Science, Babeş-Bolyai University, Treboniu Laurean 42, 400271 Cluj-Napoca, Romania

<sup>3</sup> University of Bucharest, Faculty of Geography, M. Kogalniceanu Blvd 36-46, Sector 5, 050107, Bucharest, Romania

Keywords: Danube Delta, <sup>210</sup>Pb dating method, sedimentation rates

Presenting author email: robert.begy@ubbcluj.ro

Being a dynamic environment associated with complex coastal, fluvial and marine processes, only a few studies regarding the evolution of the Danube Delta and human impacts on its ecosystem have been made carried out. Being a sensible to all processes occurring in its catchment area, information is stored in the deposited sediments, which can be used as tracers for natural and anthropic processes. The aim of this study is to determine a detailed reconstruction of the sedimentation rates in the last two centuries by applying the <sup>210</sup>Pb dating method validated by <sup>137</sup>Cs profiles for the first time in this area. <sup>210</sup>Pb<sub>sup</sub> and <sup>137</sup>Cs were determined using gamma spectrometry, while <sup>210</sup>Pb<sub>tot</sub> was measured via alpha spectrometry (<sup>210</sup>Po), using the CRS model for age determination. Additionally the impacts of the construction of river-regulating structures (mainly the Iron Gates Hydro-energetic Power Plants) are investigated, along with the assessment of the natural phenomena (floods, storms etc.). To achieve this, 27 sediment cores from seven lakes were collected: Cruhlig Lake lies north of the Sf. Gheorghe Branch; Uzlina, Isac, Cuibida and Iacob lakes are located between the Sf. Gheorghe and Sulina branches, while Matița and Merhei lakes are situated between the Chilia and Sulina branches. After the construction of the Iron Gates the sediment retention can not be observed in all lakes because of the many other factors which has accentuated effects on sedimentation. On average, an increase in the mass sedimentation rates can be observed, of 81.64% in Matița, 27.37% in Iacob and 26.53% in Cuibida lakes (Fig.1). The retention effects appear with 7.79% decreasing in Merhei, 58.74% in Cruhlig, 16.12% in Uzlina and 42.35% in Isac lakes (Fig.2) in the 1972-1980 period compared to the average from 1940-1972. Sedimentation rates show growths of 4.14 times after 1989, the most affected being the two northern lakes with an average increase of 7.6 times, while the central lakes sediment intake increased 2.88 times and the southern one 2.25 times. Physical parameters (water content, porosity and bulk density) and LOI (organic matter and inorganic carbon content) were determined for each core, to differentiate carbon and non-carbon sedimentation. However, a good similarity can be observed between the two sedimentation types, therefore no significant amount of organic matter contributes from the decaying vegetation contributes to the sedimentation of the analyzed lakes.

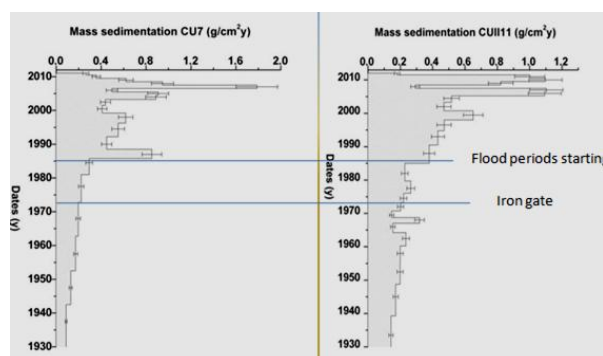


Figure 1. Cuibida lake mass sedimentation.

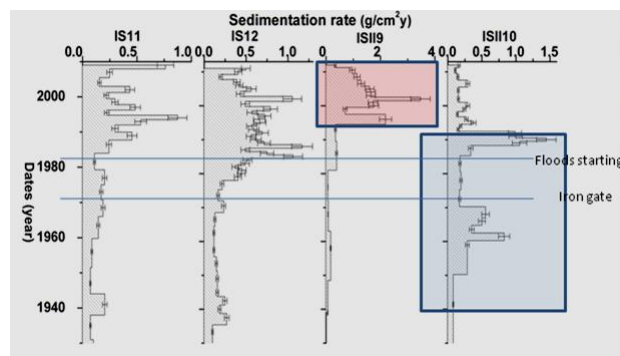


Figure 2. Isac lake mass sedimentation.

Table 1. Integrated mass sedimentation values for the investigated lakes, and percentual changes in sedimentation

	Matita	Merhei	Cruhlig	Iacob	Uzlina	Isac	Cuibida	Average
1940-1972	0.156	0.266	0.238	0.418	0.264	0.446	0.181	<b>0.281</b>
1972-1980	0.208	0.216	0.098	0.376	0.222	0.197	0.230	<b>0.221</b>
	<b>81.64%</b>	-7.79%	-58.74%	<b>27.37%</b>	-16.12%	-42.35%	<b>26.53%</b>	<b>-31.25%</b>
1972-1989	0.422	0.466	0.136	0.209	0.269	0.268	0.357	<b>0.303</b>
1989-2013	2.082	0.846	0.307	0.677	1.002	0.715	0.674	<b>0.901</b>
	13.01x	2.19x	2.25x	3.19x	3.74x	2.53x	2.05x	<b>4.14x</b>

This work was supported by the Ministry of National Education, Romania under the grant 61/30.04.2013, PN-II-RU-TE-2011-3-0351 project.

## Sedimentation rate and heavy metal pollution in core sediments from south western Black Sea derived from $^{210}\text{Pb}$ and $^{137}\text{Cs}$ chronology

E. Sarı<sup>1</sup>, M. Belivermiş<sup>2</sup>, Ö. Kılıç<sup>2</sup>, T. N. Arslan<sup>1</sup>, N. Sezer<sup>2</sup>, N. Çağatay<sup>3</sup>, D. Acar<sup>3</sup>, A. Tutay<sup>4</sup> and M. A. Kurt<sup>5</sup>

<sup>1</sup>Institute of Marine Science and Management, Istanbul University, Istanbul, 34134, Turkey

<sup>2</sup>Department of Biology, Istanbul University, Istanbul, 34134, Turkey

<sup>3</sup>Department of Geological Engineering, Istanbul Technical University, Istanbul, 34469, Turkey

<sup>4</sup>Faculty of Sciences, Department of Physics, Istanbul University, Istanbul, 34134, Turkey

<sup>5</sup>Department of Environmental Engineering, Mersin University, Mersin, 33343, Turkey

Keywords: Southwestern Black Sea sediment, heavy metal,  $^{210}\text{Pb}$  dating,  $^{137}\text{Cs}$ .

Presenting author email: erolsari@istanbul.edu.tr

$^{210}\text{Pb}$  and  $^{137}\text{Cs}$  have been widely applied as environmental tracers in the study of recent sediment deposition history, chemical scavenging and particulate transport in fluvial, lacustrine and marine environments (Appleby et al., 1979; Garcia-Tenorio, 1988; Lima et al., 2005; Alvarez-Iglesias et al., 2007). Geochemical studies of two cores from the south western continental slope of the Black Sea Basin at water depths of 350 m (KD12-04) and 302 m (KD 12-07) revealed heavy metal pollution history and sedimentation rate in the Black Sea over the last century. These changes were dated using the  $^{210}\text{Pb}$  and  $^{137}\text{Cs}$  analysis of this study. The studied cores were collected using a stainless gravity corer sampler on board of the R. V. ALEMDAR of Istanbul University in 2012 (Fig. 1).

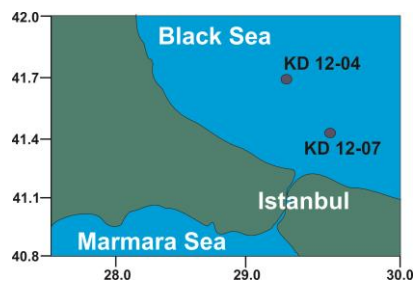


Figure 1. Sampling area and locations

The core sediments consist mainly of clay (49–80%) and silt (15–41%) with small amounts of sand and gravel (0.04–14%). The average concentrations of metals measured in  $\text{mg kg}^{-1}$  are: 55400 (Al), 37800 (Fe), 1125 (Mn), 464 (Ba), 2 (Cd), 11.2 (Co), 90 (Cr), 32.4 (Cu), 4 (Mo), 67.4 (Ni), 44.3 (Pb), 2063 (Ti), 212 (Sr), 128 (V) and 123 (Zn). Cu, Ni, Zn, Mo and Pb showed an increasing trend from 40 cm to the top of the core KD 12-04, while the concentration of Cd, Cr, Cu, Co, Ni, Mo, Ti, V and Zn are enriched between 0–48 cm for the core KD 12-07. The activity ranges of  $^{137}\text{Cs}$  and  $^{210}\text{Pb}$  in cores were found to be 0.4–76 and 12–527  $\text{Bq kg}^{-1}$ , respectively. Sedimentation rates based on  $^{210}\text{Pb}$  and  $^{137}\text{C}$  dating are  $0.716 \text{ cm.y}^{-1}$  for KD12-04 and  $0.857 \text{ cm.y}^{-1}$  for Core KD12-07, respectively (Fig. 2).  $^{137}\text{Cs}$  and  $^{210}\text{Pb}$  dating indicated that south western Black Sea continental slope sediments have been contaminated by strong industrial metal pollution for the last 50 years. The

ongoing pollution has also been supported by Enrichment Factor (EF), Contamination Factor (CF) and Pollution Load Index (PLI) values.

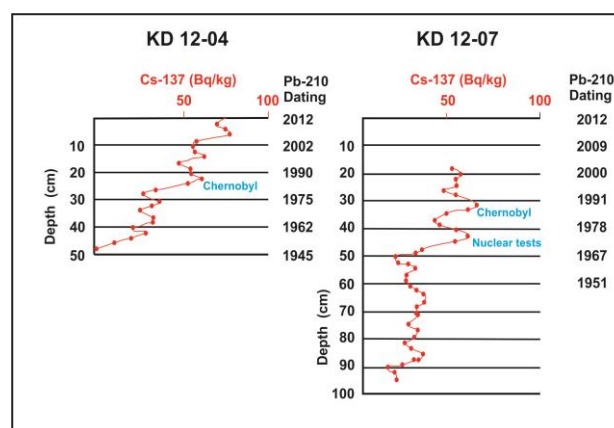


Figure 2. Distribution of  $^{137}\text{Cs}$  activity and  $^{210}\text{Pb}$  dating in cores.

### Acknowledgments

This work was supported by The Scientific and Technological Research Council of Turkey (TÜBİTAK, Project number: 114Y240).

### References

- Appleby, P.G., Oldfield, F., Thompson, R., Hottunen, P., 1979.  $^{210}\text{Pb}$  dating of annually laminated lake sediments from Finland. *Nature* 280, 53–55.
- Garcia-Tenorio, R., 1988. El metodo de fechado por  $^{210}\text{Pb}$  y su aplicacion a sedimentos. *Rev. Geofis.* 44, 225–234.
- Lima, A.L., Bradford Hubeny, J., Reddy, C.M., King, J.W., Huguen, K.A., Eglinton, T.I., 2005. High resolution historical records from Pettaquamscutt River Basin sediments: 1.  $^{210}\text{Pb}$  and varve chronologies validate record of  $^{137}\text{Cs}$  released by the Chernobyl accident. *Geochim. Cosmochim. Acta* 69, 1803–1812.
- Alvarez-Iglesias, P., Quintana, B., Rubio, B., Perez-Arlucea, M. 2007. Sedimentation rates and trace metal input history in intertidal sediments from San Simo'n Bay (Ría de Vigo, NW Spain) derived from  $^{210}\text{Pb}$  and  $^{137}\text{Cs}$  chronology. *J. Environ. Radioactivity* 98, 229–250.

## The role of humic acids in $^{137}\text{Cs}$ mobility

J. Mihalík<sup>1</sup>, J.A. Corisco<sup>1,2</sup> and M.J. Madruga<sup>1,2</sup>

<sup>1</sup>Centro de Ciências e Tecnologias Nucleares (C2TN), Instituto Superior Técnico (IST), Universidade de Lisboa,

<sup>2</sup>Laboratório de Proteção e Segurança Radiológica (LPSR), Instituto Superior Técnico (IST), Universidade de Lisboa, E.N. 10 (km 139.7), 2695-066 Bobadela LRS, Portugal

Keywords: radiocesium, humic acid, clay, sorption.

Presenting author email: jmihalik@ctn.tecnico.ulisboa.pt

The research was focused on the role of humic acids (HA) in mobility of  $^{137}\text{Cs}$ . With the help of HPLC (High pressure liquid chromatography) and gamma spectrometry we found that in the course of composting of contaminated biomass,  $^{137}\text{Cs}$  is associated with fresh humic acids in water eluates. Fresh humic acids in these eluates differ to well stabilized humic acids in soil: they have usually lower molecular weight and lower content of oxygen than HA in soil (Droussi et al., 2009). These differences could influence also their ability to adsorb  $^{137}\text{Cs}$  in soil.

We distinguished two cases: i) internally contaminated biomass (ICB), ii) externally contaminated biomass (ECB). While the rate of  $^{137}\text{Cs}$  release from ICB decreased during composting (fig. 1), in the case of ECB this rate increased (fig. 2).

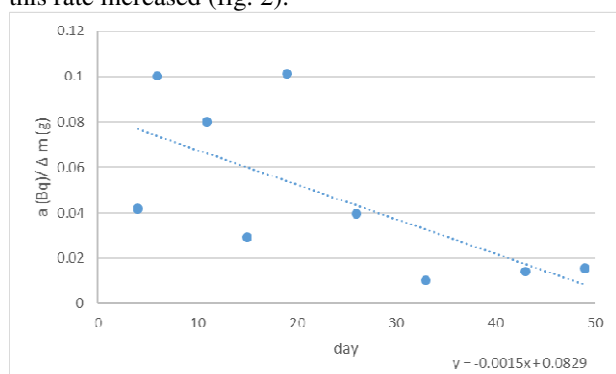


Figure 1. The rate of  $^{137}\text{Cs}$  release from ICB. “a” is the activity of  $^{137}\text{Cs}$  in eluates,  $\Delta m$  is the difference of the fresh weight of biomass in container, “day” is a period of composting.

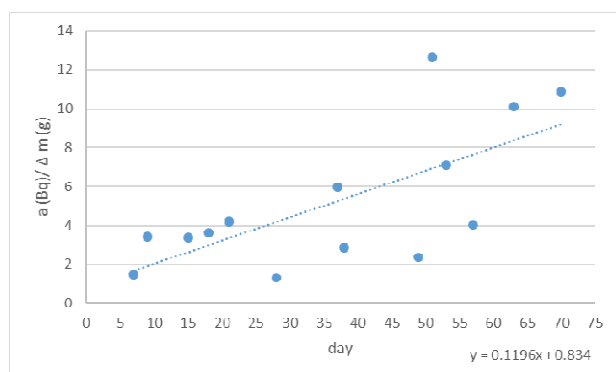


Figure 2. The rate of  $^{137}\text{Cs}$  release from ECB. “a” is the activity of  $^{137}\text{Cs}$  in eluates,  $\Delta m$  is the difference of the fresh weight of biomass in container, “day” is a day of composting.

The different behavior of  $^{137}\text{Cs}$  probably results from different characteristic of retention in biomass: in the ICB the  $^{137}\text{Cs}$  can stay in plant sap (Fuhrmann et al., 2003) which is easily released in the early phase of composting, in the ECB the  $^{137}\text{Cs}$  is probably absorbed in the structure of leaf surface.

Humic acids serve as a vector of  $^{137}\text{Cs}$  in soil. The more alkaline pH favors the adsorption on humic acids compared to clay (Warwick et al., 2005).

The batch experimental procedure contains four variants: A) clay immersed by a pure solution of  $^{137}\text{CsCl}$ ,

B) clay firstly incubated with humic acids and then the solution of  $^{137}\text{Cs}$  is added,

C) clay immersed with an eluate from compost rich on humic acids and  $^{137}\text{Cs}$ ,

D) clay immersed with a solution of  $^{137}\text{Cs}$  and humic acid (analytic).

The variant B is the concept which was repeatedly investigated (Warwick et al., 2005). In this case, HA eliminate adsorption of  $^{137}\text{Cs}$  on clay because HA itself is adsorbed on clay. Moreover, bonds between  $^{137}\text{Cs}$  and HA are weaker than between  $^{137}\text{Cs}$  and clay which made  $^{137}\text{Cs}$  more bioavailable.

The results of this study will be the kinetic of the transport of  $^{137}\text{Cs}$  with humic acids in clay.

### Abstract review

C2TN/IST authors gratefully acknowledge the Fundação para a Ciência e a Tecnologia (FCT) support through the UID/Multi/04349/2013 project.

Droussi, Z., D’Orazio, V., Hafidi, M., Ouattmane, A., 2009. Elemental and spectroscopic characterization of humic-acid-like compounds during composting of olive mill by-products, *J. Hazard. Mater.* 163, 1289–1297.

Fuhrmann, M., Lasat, M., Ebbs, S., Cornish, J., Kochian, L., 2003. Uptake and release of cesium-137 by five plant species as influenced by soil amendments in field experiments, *J. Environ. Qual.* 32, 2272–2279.

Warwick, P., Lewis, T., Evans, N., Bryan, N., Knight, L., 2005. Sorption of selected radionuclides to clay in the presence of humic acid. EC-FP FUNMIG IP 1<sup>st</sup> Annual Workshop Proceedings, Saclay, France, Nov, pp. 184-189.



## Speciation of trivalent actinides and lanthanides in digestive media

A. Barkleit and C. Wilke

Helmholtz-Zentrum Dresden-Rossendorf, Institute of Resource Ecology, Dresden, Germany

Keywords: curium, europium, fluorescence spectroscopy, body fluids

Presenting author email: a.barkleit@hzdr.de

In case of incorporation into the human body, radionuclides potentially represent serious health risks due to their chemo- and radiotoxicity. In order to assess their toxicological behavior, such as transport, metabolism, deposition, and elimination from the human organisms, the understanding of their *in vivo* chemical speciation on a molecular level is crucial. Nevertheless, little is known about the speciation of not only trivalent actinides (An(III)) but also trivalent lanthanides (Ln(III)), non-radioactive chemical analogs of An(III), in human body fluids. In order to improve our understanding of the behavior of An(III) and Ln(III) in the human body, the present study focuses on the chemical speciation of An(III) and Ln(III) in the gastrointestinal tract. The human gastrointestinal system was simulated by using an *in vitro* digestion model, part of an international unified bioaccessibility method (UBM), developed by the Bioaccessibility Research Group of Europe (BARGE) (Wragg et al., 2009). To verify the model, natural human saliva samples were also investigated (Barkleit et al., 2017).

The speciation of trivalent curium (Cm(III)) and europium (Eu(III)) in the gastrointestinal tract and in human natural saliva has been studied by means of time-resolved laser-induced fluorescence spectroscopy (TRLFS). The standard model body fluids and the natural saliva samples were spiked *in vitro* with Cm(III) or Eu(III) with a trace metal concentration. Figure 1 shows the selected luminescence spectra of Cm(III).

The dominant chemical species in the body fluids were determined by linear combination fitting (LCF) analysis based on the reference spectra for individual components in the body fluids. The results indicate the formation of inorganic- (60-90%) and organic species (10-40%) of Cm(III)/Eu(III) in the salivary media. Ternary M(III) complexes containing phosphate and carbonate anions with the additional counter-cation calcium is found to be the main inorganic species, while the complexes with the digestive enzyme  $\alpha$ -amylase and the protein mucin represent the major part of the organic species.

When the M(III) reached the stomach, the metal complexes are dissociated due to the high acidic conditions in the stomach. That is, Cm(III) and Eu(III) are mainly present as aquo complexes, while a small part (about 20%) is coordinated by the protein pepsin. When entering the intestine the M(III) strongly interact with the protective protein mucin (about 65%) and inorganic ligands (mainly carbonate and phosphate).

These speciation results in different body fluids of the gastrointestinal tract pointed out that An(III) and Ln(III) are coordinated by both inorganic and organic molecules in the human digestive system. Proteins (e.g.,  $\alpha$ -amylase,

pepsin, mucin) would be the important organic binding partners. Furthermore, ternary inorganic complexes containing phosphate and carbonate anions with the additional counter-cation calcium are expected to be formed as the main inorganic species in the whole body fluids.

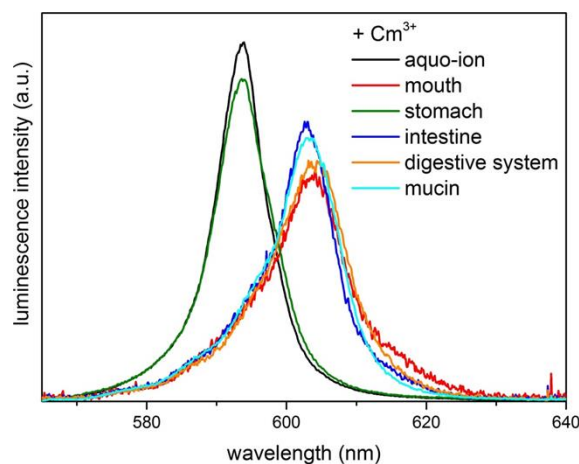


Figure 1. Luminescence spectra of Cm(III) in the simulated media of mouth, stomach and small intestine as well as the reference spectra of pure Cm(III) aquo complex (black data) and the species with mucin (light blue data).  $[Cm(III)]_{total} = 0.3 \mu M$ .

This work was supported by the Federal Ministry of Education and Research (Bundesministerium für Bildung und Forschung, BMBF) under contract number 02NUK030F.

- Wragg, J., Cave, M., Taylor, H., Basta, N., Brandon, E., Casteel, S., Gron, C., Oomen, A., van de Wiele, T., 2009. British Geological Survey Open Report OR/07/027, Keyworth, Nottingham, 90 pp.
- Barkleit, A., Wilke, C., Heller, A., Stumpf, T., Ikeda-Ohno, A., 2017. Trivalent f-elements in human saliva: a comprehensive speciation study by time-resolved laser-induced fluorescence spectroscopy and thermodynamic calculations. *Dalton Trans.* DOI: 10.1039/c6dt03726g



## Accumulation of $^{137}\text{Cs}$ by fish and aquatic plants in a small eutrophic lake

T. Ries, V. Putyrskaya, E. Klemt

University of Applied Sciences, Hochschule Ravensburg-Weingarten, Weingarten, D-88250, Germany

Keywords:  $^{137}\text{Cs}$ , accumulation, fish, aquatic plants.

Email: tatiana.ries@hs-weingarten.de

Lake Vorse, a glacially formed small and shallow eutrophic lake in Southern Germany, belongs to the areas in Germany with rather high Chernobyl fallout deposition of  $^{137}\text{Cs}$  (about 30 kBq/m<sup>2</sup>). Even decades after the  $^{137}\text{Cs}$  fallout considerable amounts of  $^{137}\text{Cs}$  are still transported from the catchment area into the lake, and the  $^{137}\text{Cs}$  activity concentration in the lake water and the transfer into aquatic plants and fish is relatively high compared with other lakes (Pröhl et al., 2006).

The following measurements have been performed to describe the accumulation and transport of  $^{137}\text{Cs}$  in different parts of the lake ecosystem:

- 1) 1987-2016:  $^{137}\text{Cs}$  activity concentration in lake water and suspended matter;
- 2) 2013-2016:  $\text{NH}_4^+$  and  $\text{K}^+$  ions competing with  $^{137}\text{Cs}$  in the lake water;
- 3) 1987-2016:  $^{137}\text{Cs}$  activity concentration in fish species (*Esox lucius*, *Perca fluviatilis*, *Silurus glanis*, *Abramis brama*, *Blicca bjoerkna*, *Cyprinus carpio*, *Rutilus rutilus*, *Scardinius erythrophthalmus*, *Alburnus alburnus*);
- 4) 2013-2016:  $^{137}\text{Cs}$  activity concentration in aquatic and terrestrial plants (*Myriophyllum spicatum*, *Nymphaea alba*, *Menyanthes trifoliata*, *Carex rostrata*, *Typha latifolia*, *Phragmites australis*, *Rubus fruticosus*, *Dryopteris carthusiana*).

Time dependence of  $^{137}\text{Cs}$  activity concentration in lake water can be well described by a sum of two exponential functions superimposed by some seasonal cycling. The seasonal cycling of the  $^{137}\text{Cs}$  activity concentration in water and its correlation with different influencing factors (competing ions concentration, weather conditions, biological activity of water plants, etc.) will be discussed.

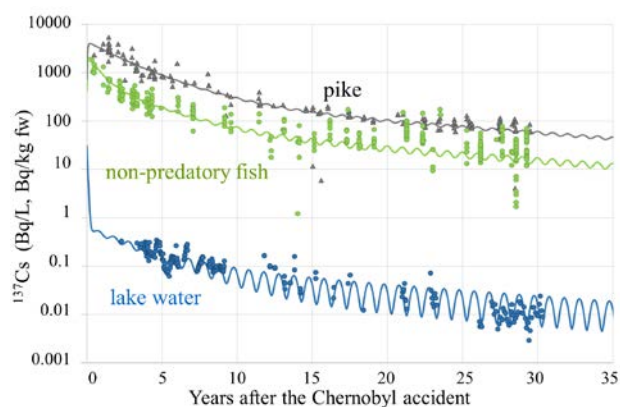


Figure 1. Time dependence of  $^{137}\text{Cs}$  activity concentration in water and fish from Vorse.

To describe the accumulation of  $^{137}\text{Cs}$  in different fish species and aquatic plants a simple uptake and loss model (Smith et al., 2002) was used.  $^{137}\text{Cs}$  accumulation in the trophic chain via water to non-predatory and predatory fish was observed. Estimations on the uptake and loss rate parameters for fish species from different trophic levels will be presented. Analysis of  $^{137}\text{Cs}$  accumulation in fish in the last 4 years showed the decrease of  $^{137}\text{Cs}$  concentration in some fish species with increasing mass.

Table 1.  $^{137}\text{Cs}$  distribution in aquatic and terrestrial plants from Vorse, summer 2016

Plant type	Name	$^{137}\text{Cs}$ activity concentration, Bq/kg (dw)		
		Leaves	Stems	Roots
Submerged	<i>Myrioph. spicatum</i>	45 ± 3	15 ± 1	89±5
Floating	<i>Nymphaea alba</i>	113 ± 2	183 ± 7	
Emerged	<i>Menyan. trifoliata</i>	31 ± 1	40 ± 2	141±6
	<i>Carex rostrata</i>	68 ± 5		
	<i>Typha latifolia</i>	198 ± 5		
Terrestrial	<i>Phragm. australis</i>	41 ± 1		
	<i>Rubus fruticosus</i>	47 ± 2	49 ± 3	
	<i>Dryopteris carth.</i>	1735 ± 97		

Distribution of  $^{137}\text{Cs}$  concentration in the different parts of aquatic plant varies strongly for different species. Correlations with different factors influencing  $^{137}\text{Cs}$  concentration in *Myriophyllum spicatum* (dominant plant in the lake) will be presented.

This work was supported by the Federal ministry of education and research under grant 02NUK030.

Pröhl, G., Ehlken, S., Fiedler, I., Kirchner, G., Klemt, E., Zibold, G. 2006. Ecological half-lives of  $^{90}\text{Sr}$  and  $^{137}\text{Cs}$  in terrestrial and aquatic ecosystems. *Journal of Environmental Radioactivity* 91, 41–72.

Smith, J.T., Kudelsky, A.V., Ryabov, I.N., Daire, S.E., Boyer, L., Blust, R.J., Fernandez, J.A., Haddingh, R.H., Voitsekhovitch, O.V. 2002. Uptake and elimination of radiocesium in fish and the “size effect.” *J. Environ. Radioact.* 62, 145-164.

## Natural and artificial radionuclides in moss samples from the region of Northern Greece

Betsou Ch.<sup>1</sup>, Tsakiri E.<sup>2</sup>, Hansman J.<sup>3</sup>, Krmar M.<sup>3</sup>, Ioannidou A.<sup>1</sup>

<sup>1</sup>Physics Department, Nuclear Physics Lab., Aristotle University of Thessaloniki, Thessaloniki, 54124, Greece

<sup>2</sup>Biology Department, Division of Botany, Aristotle University of Thessaloniki, Thessaloniki, 54124, Greece

<sup>3</sup>Physics Department, Faculty of Science, University of Novi Sad, Trg Dositeja Obradovica 4, Novi Sad, 21000, Serbia

Keywords: moss technique, airborne radionuclides, bio-monitoring, <sup>137</sup>Cs

Presenting author email: chbetsou@physics.auth.gr

Naturally occurring radionuclides <sup>7</sup>Be and <sup>210</sup>Pb together with the artificial <sup>137</sup>Cs are a useful tool in studying the environmental processes. The <sup>7</sup>Be is formed by spallation reaction between cosmic rays and nuclei of oxygen and nitrogen in the stratosphere and upper troposphere. After production, the <sup>7</sup>Be atoms are attached to aerosol particles and the fate of <sup>7</sup>Be will become the fate of the carrier aerosols. Since aerosol particles contain most of the air pollutants, the transport of the last ones can be investigated by tracking the <sup>7</sup>Be pathway. The radionuclide <sup>210</sup>Pb is widely found in the terrestrial environment and it present in the atmosphere due to the decay of <sup>222</sup>Rn diffusing from the ground. The artificial radionuclide <sup>137</sup>Cs was mostly released in the atmosphere during atmospheric nuclear weapon tests and the Chernobyl nuclear accident. After that, there were no other significant <sup>137</sup>Cs emissions, and the atmospheric <sup>137</sup>Cs was exposed to physical decay as well as wet and dry deposition. In recent years the Fukushima accident contributed to the release of <sup>137</sup>Cs in the atmosphere but with minor influence in regions far from Japan.

Terrestrial mosses can be used for investigation and monitoring of airborne radionuclide depositions. Many mosses, obtain most of their nutrients directly from precipitation and dry deposition. The absence or strong reduction of the cuticle and thin leaves allows easy uptake from the atmosphere. Lack of an elaborate rooting system also means that uptake from the substrate is normally insignificant. These properties make mosses an ideal sampling medium for metals and airborne radionuclides deposited from the atmosphere, as they are accumulated by the moss, producing concentrations much higher than those in the original wet or dry deposition (Krmar, 2009; Krmar 2013). The sample collection is so simple, that a high sampling density can be achieved, in contrast to the conventional precipitation analysis and the air sampling. High resolution gamma spectrometry measurements can be carried out with the moss technique, without any chemical treatment of the samples.

The aim of this study is to measure activities of the radionuclides <sup>137</sup>Cs, <sup>7</sup>Be, <sup>210</sup>Pb and <sup>40</sup>K in mosses and investigate their possible variabilities over different places in Northern Greece. The different meteorological conditions, the wind direction and precipitation can influence the deposition of airborne radionuclides, as well as their activities in mosses.

Ninety five (95) samples of Hypnum Cupressiforme were collected in Northern Greece. All samples were collected in a short time interval during the end of summer 2016. After sampling, mosses were dried

at 105°C for 2 hours and all the impurities were removed manually. After the preparation, mosses were put in two cylindrical plastic containers, diameter 67 mm and height 31 mm. They were measured in a low-background HPGe detector with relative efficiency 36%.

The range of activity concentrations of <sup>7</sup>Be, <sup>137</sup>Cs, <sup>210</sup>Pb and <sup>40</sup>K in moss samples are shown in Table 1. Differences have been observed in the activity concentrations between the mosses collected from ground surface, rocks, branches and roots. <sup>7</sup>Be and <sup>210</sup>Pb activity concentrations are higher in moss samples from the ground surface and rocks than those near roots. <sup>137</sup>Cs concentrations are higher in mosses collected near roots and rocks than those collected near the ground surface. <sup>40</sup>K concentrations are higher in mosses collected from branches and near roots than those collected from rocks.

Table 1. Radionuclides activity concentrations in Bq kg<sup>-1</sup> in moss samples

Radionuclide	Range (mean value) Bq kg <sup>-1</sup>
<sup>7</sup> Be	69-1280 (388)
<sup>137</sup> Cs	0-425 (35)
<sup>210</sup> Pb	147-1920 (817)
<sup>40</sup> K	120-750 (269)

Between the concentrations of <sup>7</sup>Be and <sup>210</sup>Pb there is a good correlation, indicating that the major quantity of <sup>210</sup>Pb in mosses has arrived from aerosol deposition. There is not any correlation between <sup>7</sup>Be and <sup>40</sup>K, pointing out that <sup>40</sup>K was transferred to mosses due to the re-suspension and the decayed plant matter covering them. A big number of sampling sites was covered and the information obtained using mosses as biomonitors, provide the spatial distribution of all the radionuclides over Northern Greece.

### References

- Krmar, M., Wattanavatee, K., Radnović, D., Slivka, J., Bhongsuwan, T., Frontasyeva, M.V., Pavlov, S.S., 2013. Airborne radionuclides in mosses collected at different latitudes. *Journal of Environmental Radioactivity* **117**, 45-48.
- Krmar, M., Radnović, D., Mihailović, D.T., Lalić, B., Slivka, J., Bikit, I., 2009. Temporal variations of <sup>7</sup>Be, <sup>210</sup>Pb and <sup>137</sup>Cs in moss samples over 14 month period. *Applied Radiation and Isotopes* **67**, 1139-1147.

## <sup>210</sup>Po and <sup>210</sup>Pb in various fish species from Gökçeada island, Northern Aegean Sea and contribution of <sup>210</sup>Po to radiation dose

Ö. Kılıç<sup>1</sup>, M. Belivermiş<sup>1</sup>, O. Gönülal<sup>2</sup> and N. Sezer<sup>1</sup>

<sup>1</sup>Department of Biology, Faculty of Science, Istanbul University, Istanbul, 34134, Turkey

<sup>2</sup>Gökçeada Marine Research Department, Istanbul University, Çanakkale, 17100, Turkey

Keywords: <sup>210</sup>Po, <sup>210</sup>Pb, fish, Gökçeada.

Presenting author email: kilic\_onder@yahoo.com

In the marine environment, the main contribution of radiation comes from naturally occurring radionuclides. Among these radionuclides <sup>210</sup>Po ( $t_{1/2} = 138$  day) and <sup>210</sup>Pb ( $t_{1/2} = 22.3$  year), which are the members of the <sup>238</sup>U decay series, are the most significant since they are known strongly accumulated by marine organisms and transferred to people through consumption of marine organisms. In addition to their particle-reactive property, <sup>210</sup>Po is an alpha emitter with a high energy (5.30 MeV) and which accumulates in organic matter and <sup>210</sup>Pb is a beta emitter which adsorbs to inorganic minerals.

The main objectives of the present study are to 1) determine activity concentrations of <sup>210</sup>Po and <sup>210</sup>Pb in various economical fish species collected from Gökçeada which is the largest island of Turkey, 2) to investigate distribution of <sup>210</sup>Po and <sup>210</sup>Pb in edible part, gill and liver, 3) to calculate committed effective dose level due to <sup>210</sup>Po to public health through consumption of fish.

Fish samples were collected from locations around Gökçeada island and they were immediately transported the laboratory (Figure 1).

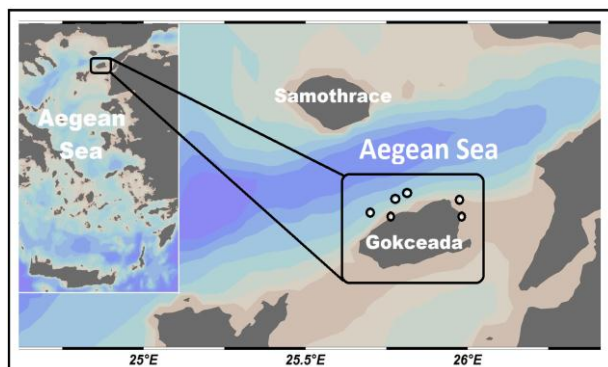


Figure 1. Sampling locations around Gökçeada island

All samples were digested using a microwave digestion system (Milestone). Po-210 was spontaneously deposited on a rotating silver disc-over with <sup>209</sup>Po as a standard tracer (100 mBq) during 12 h at room temperature (Olivera and Carvalho, 2006). The activity concentrations of <sup>210</sup>Po in the samples were measured using silicon surface-barrier detectors connected to the multi-channel analyser of an ORTEC alpha spectrometer. Afterwards the samples sealed for six months, which is adequate time to allow the ingrowth of <sup>210</sup>Po from <sup>210</sup>Pb. Following this, the samples were re-

plated onto a silver disc, and measured for determination of <sup>210</sup>Pb activity.

According to the data set, it was observed that the activity concentrations (Bq kg<sup>-1</sup>, dry weight) of <sup>210</sup>Po and <sup>210</sup>Pb are variable among the various fish species. Besides, activities of <sup>210</sup>Po were found higher comparing with <sup>210</sup>Pb in the samples. Also the trend of the accumulation of <sup>210</sup>Po was observed in order as liver > gill > edible part in all fish species (Figure 2).

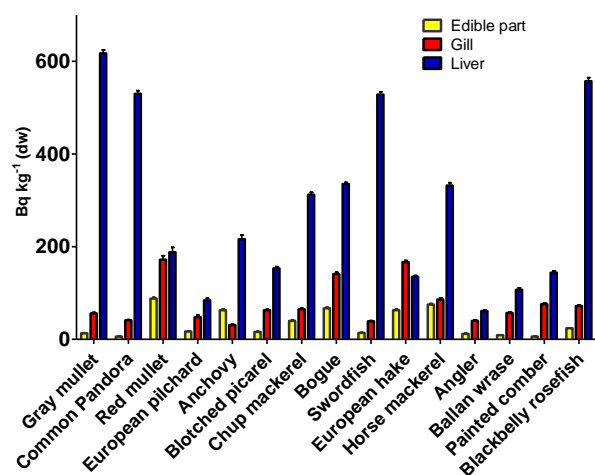


Figure 2. The activity concentrations (Bq kg<sup>-1</sup>, dry weight) of <sup>210</sup>Po in edible part, gill and liver of various fish species

Po-210 is a primary dose contributor among natural radionuclides due to seafood consumption. Therefore, collective committed effective dose level of <sup>210</sup>Po was calculated (IAEA, 2003). The mean and range dose levels were found to be 4.54 and 0.54-12.26  $\mu$ Sv y<sup>-1</sup>. The maximum dose level was found in red mullet. This study provides the first data related to activity concentrations of <sup>210</sup>Po and <sup>210</sup>Pb in various economical fish species from Gökçeada.

Olivera, J.M., Carvalho, F.P. 2006. Sequential extraction procedure for determination of uranium, thorium, radium, lead and polonium radionuclides by alpha spectrometry in environmental samples. Czech. J. Phys. 56,545-555.

IAEA (International Atomic Energy Agency), 1995. Sources of radioactivity in the marine environment and their relative contributions to overall dose assessment from marine radioactivity (MARDOS). IAEA Technical Report Series No. 838.

## Impacts of ocean acidification on $^{57}\text{Co}$ and $^{134}\text{Cs}$ bioconcentration in manila clam *Ruditapes philippinarum*

O. Kocaođlan, N.Sezer, Ö.Kılıç and M. Belivermiş

<sup>1</sup>Department of Biology, University of Istanbul, Istanbul, 34134, Turkey  
 Keywords: Ocean acidification,  $\text{CO}_2$ ,  $^{57}\text{Co}$ ,  $^{134}\text{Cs}$ , manila clam, radiotracer  
 Presenting author email: belmurat@istanbul.edu.tr

Anthropogenic activities like fossil fuel burning have increased atmospheric  $\text{CO}_2$  concentration. Since one third of atmospheric  $\text{CO}_2$  stored in ocean that increase declined pH of seawater at 0.1 pH level and altered its carbonate chemistry. That phenomenon is named as “ocean acidification”. Seawater pH decreased 26% since industrial revolution and it is expected to decrease 170% in year 2100 according to high  $\text{CO}_2$  emission scenarios (IGBP, 2013).

Bioconcentration of a metal or radionuclide in a marine shelled mollusk is dominated by its own ecophysiological characteristics and the physical and chemical properties of surrounding seawater. Economically important shelled mollusks are generally exposed to a high level of trace metals in coastal areas. Acidified seawater poses a risk of increased accumulation and toxicity of trace metals and radionuclides in the calcifying marine organisms, including bivalves. Hence the bioconcentration of  $^{134}\text{Cs}$  and  $^{57}\text{Co}$  was investigated in manila clam *Ruditapes philippinarum* under three pH level (ambient seawater: 8.1; estimated conditions by 2100: 7.8, estimated conditions by 2200: 7.5). The  $p\text{CO}_2$  levels were calculated to be, 460, 620 and 1100  $\mu\text{atm}$ , for the pH levels 8.1, 7.8 and 7.5 respectively. Clams were exposed to dissolved  $^{134}\text{Cs}$  and  $^{57}\text{Co}$  at those levels in controlled laboratory conditions (aerated 20 L seawater; salinity: 22 p.s.u; light/dark cycle: 14 h/10 h; temperature 20 °C). Uptake and depuration kinetics of the two metals in the clam were followed for 21 and 35 days, respectively.

The Co and Cs uptake kinetics in whole-body clams under the three conditions were best fitted by a 2-parameter asymptotic exponential model, whatever the pH. The steady state concentration factor ( $\text{CF}_{\text{ss}}$ ) of  $^{57}\text{Co}$  was found to be  $258 \pm 10$ ,  $194 \pm 6$  and  $130 \pm 5$  at pH levels 7.5, 7.8 and 8.1 (control), respectively (Figure 1), thus demonstrating more efficient accumulation in acidified seawater compared to the control ( $P < 0.001$ , one way ANOVA). Increased accumulation of cobalt in the lowered pH was elucidated mainly with the aragonitic shell of the clam, low salinity and alkalinity of seawater used in the experiment. However, the elimination of cobalt by the manila clam did not vary with regard to pH level. In the case of the clam’s shell, 1.39 and 1.23 times higher  $^{57}\text{Co}$  activity was observed in the two acidified seawater conditions (7.8 and 7.5, respectively) compared to normocapnia at the end of the depuration phase. Accumulation of  $^{134}\text{Cs}$  was not strongly influenced by reduced pH ( $P > 0.05$ , one way

ANOVA), represented by an analogous uptake constant rate and  $\text{CF}_{\text{ss}}$  in each treatment (Figure 1).

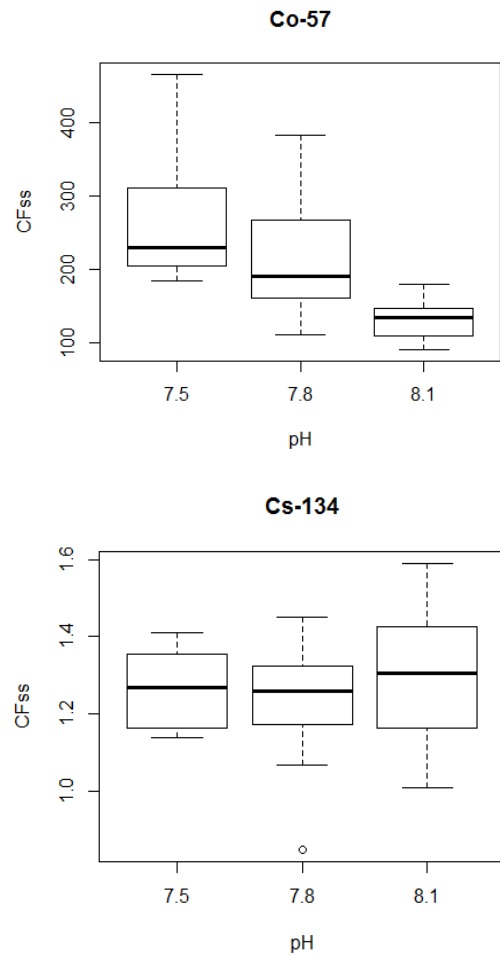


Figure 1.  $\text{CF}_{\text{ss}}$  (Steady state concentration factor) values for  $^{57}\text{Co}$  and  $^{134}\text{Cs}$  in three pH levels

This study was supported by the Scientific Research Projects Coordination Unit of Istanbul University, Project No. 2117 and 2146.

IGBP, IOC. SCOR (2013). Ocean Acidification Summary for Policymakers–Third Symposium on the Ocean in a High- $\text{CO}_2$  World. International Geosphere-Biosphere Programme. Stockholm, Sweden.

## Plutonium environmental chemistry - from molecular to landscape level

Stepan N. Kalmykov, Anna Yu. Romanchuk  
Department of Chemistry, Lomonosov Moscow State University

Plutonium is the element of the major concern in both nuclear waste management and environmental restoration at the legacy sites. Its chemistry is complicated by the multiple oxidation states in which it could be present under environmental conditions.

The partitioning and speciation of plutonium and other actinides is studied in various samples collected at the contaminated areas including nuclear test sites, nuclear reprocessing plants and territories affected by nuclear accidents. The advanced spectroscopic and microscopic techniques are used to trace both local distribution and chemical speciation of actinides in the samples. The attempt to link the release scenario with chemical speciation and bioavailability is done. A specific feature of the behavior of plutonium is that it can form extremely poorly soluble crystalline oxides (and mixed oxides with other actinides) at high temperatures. Plutonium oxides can form particles with different sizes including micrometer and submicrometer particles as a result of nuclear explosions, fires, explosions, and other high-temperature impacts. The environmental behavior of these "hot" particles is controlled by sources of their origin, i.e., their formation scenarios: temperature conditions, presence of oxygen, presence of other elements, etc. Thus, in "hot" particles, radionuclides occur in extremely kinetically stable physicochemical forms far from thermodynamic equilibrium with the environment. Extremely slow dissolution of these "hot" particles can proceed on contact with water.

The speciation of plutonium in samples from contaminated sites is compared with those studied under well-defined laboratory conditions. The interfacial behavior of Pu in mineral colloid suspensions is studied in batch sorption tests accompanied by XAFS and HR-TEM measurements. The formation of crystalline oxide nanoparticles with the sizes of 1.5 – 2.0 nm is established that result in formation of low soluble refractory species.

The conclusions concerning the effect of chemical speciation on the migration behavior, bioavailability and landscape distribution at contaminated sites is done.



## 'Bomb peak' radiocarbon a tracer and dating tool—an overview

I. Hajdas

Laboratory of Ion Beam Physics, ETH, Zurich, 8093, Switzerland

Keywords: radiocarbon, bomb peak, anthropogenic

Presenting author email: hajdas@phys.ethz.ch

Radiocarbon ( $^{14}\text{C}$ ), a naturally present radioactive isotope of carbon is produced in the atmosphere by thermal neutrons, which are products of cosmic rays interaction with the atmosphere. The nuclear tests in the 1950ties caused additional production of radiocarbon atoms (artificial). The effect has been almost double of the natural production and created an excess  $^{14}\text{C}$  activity in the atmosphere and in terrestrial carbon bearing materials. The bomb produced  $^{14}\text{C}$  has been identified soon after the tests started but the peak (ca. 100% above the normal levels) reached its maximum in 1963 in the northern Hemisphere where most of the tests took place. In the southern Hemisphere the bomb peak reached lower values (ca. 80 % of normal level) and was delayed by ca. 2 years. After the ban on nuclear tests the atmospheric  $^{14}\text{C}$  content began to decrease mainly due to the uptake by the ocean but also due to addition of old ( $^{14}\text{C}$  free)  $\text{CO}_2$  which is a product of fossil carbon combustion. Continuous monitoring of the atmospheric  $^{14}\text{C}$  ratio during the years that followed the nuclear tests, provides data (Fig. 1), which forms essential basis for environmental studies (Reimer et al., 2004).

present an overview of this wide spectrum of interdisciplinary studies as well as discuss effects that the present development of the atmospheric  $^{14}\text{C}$  content (Graven, 2015), might have on the applications of  $^{14}\text{C}$  in the future.

- Hua, Q., Barbetti, M. and Rakowski, A.Z., 2013. Atmospheric radiocarbon for the period 1950–2010. *Radiocarbon*, 55(4), pp.2059-2072.
- Graven, H.D., 2015. Impact of fossil fuel emissions on atmospheric radiocarbon and various applications of radiocarbon over this century. *Proceedings of the National Academy of Sciences* 112, 9542-9545.
- Levin, I., Kromer, B., Hammer, S., 2013. Atmospheric Delta ( $\text{CO}_2$ )- $\text{C}$ -14 trend in Western European background air from 2000 to 2012. *Tellus Series B-Chemical and Physical Meteorology* 65.
- Reimer, P.J., Brown, T.A. and Reimer, R.W., 2004. Discussion: reporting and calibration of post-bomb  $^{14}\text{C}$  data. *Radiocarbon*, 46(03), pp.1299-1304.

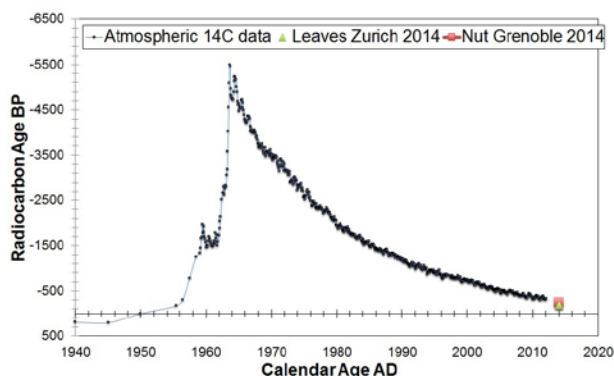


Figure 1. Bomb peak atmospheric from various monitoring stations compiled by Hua et al., (2013) and additional data from Levin et al, (2013) are used as reference in  $^{14}\text{C}$  analysis. The trend towards 'old' atmosphere is clearly visible for 2014 analysis of short lived vegetation.

During the last 60 year applications of the 'bomb peak'  $^{14}\text{C}$  analysis ranged from studies of ocean circulation,  $\text{CO}_2$  uptake, carbon storage in soils and peat, root turn-over time to the medical, forensic and detection of forgeries. This paper will

## Findings from NPL low-level proficiency testing

Simon Jerome

Nuclear Metrology Group, National Physical Laboratory, Teddington, MIDDLESEX TW11 0LW, United Kingdom

Keywords: first, second, third, fourth.

simon.jerome@npl.co.uk

The quality of monitoring data, provided to the UK Government and public in the aftermath of the Chernobyl accident in 1986 was variable and contradictory; in some cases, the validity of such data was questionable.

Accordingly, the National Physical Laboratory (NPL) was tasked by the UK Government with running a proficiency test exercise to gauge the quality of data provided by radioactivity monitoring laboratories in the UK. Thus, in 1989, samples containing  $^{90}\text{Sr}$ ,  $^{106}\text{Ru}$ ,  $^{134}\text{Cs}$  and  $^{137}\text{Cs}$  were prepared for this purpose; the nuclides selected were those observed in the fall-out across the UK after Chernobyl.

Seventy UK laboratories took part in the first exercise, and included laboratories funded by the UK Government in support of statutory monitoring of the nuclear industry, local authority laboratories charged with environmental monitoring, commercial monitoring laboratories, nuclear site operators and the academic sector. The results of this first exercise revealed some interesting outcomes:

- All of the participants were from the UK,
- Calibration techniques were extremely variable, and measurement traceability to national standards was not clear in many cases,
- Decay data used in calculating measurement results was drawn from a number of sources, some of which were rather obscure,
- There was little or no appreciation of the subtleties of  $\gamma$ -ray spectrometry, such as the effects of cascade summing,
- The derivation of uncertainty budgets was limited mainly to the consideration of uncertainties arising from the numbers of counts observed, and
- There were no participants holding accreditation to ISO 17025 (or the equivalents used at that time).

All of these observations made for an interesting discussion of the results after the exercise. At that time, the analysis of the exercise data was limited to the calculation of the deviation of the result:

$$dev(\%) = \frac{V_{(lab)} - V_{(ref)}}{V_{(ref)}} \times 100\%$$

And a u-test (Brookes, *et al*, 1979) :

$$u = \frac{[|V_{(lab)} - V_{(ref)}|]}{\sqrt{u_{V_{(lab)}}^2 + u_{V_{(ref)}}^2}}$$

In this initial exercise, compared to the reference values, approximately 40% of the results were compliant, where  $u < 1.64$ , 50% of the results were discrepant, where  $u > 3.29$ , and 10% of the results were in the 'grey zone',

where  $1.64 < u < 3.29$  (Jerome, 1990). Since then, these proficiency tests have expanded in scope to meet the changing needs of users, and have included a wider range of  $\beta$ - and  $\gamma$ -emitters (from 1990),  $\alpha$ -emitters (from 1992), solids (intermittently since 1997) and low energy  $\beta$ -emitters (from 2004). These changes have been made over the years to respond to changes in the nuclear and environmental monitoring industries and to respond to the needs of the user community.

Since then, the outlook has changed and we find that:

- Participation is international,
- Calibration techniques deliver traceability to national standards,
- Decay data sources are rationalised and draw mainly from the DDEP project and ENSDF,
- Cascade summing effects still influence results, but the principles are better understood,
- Uncertainty budgets mostly (but not always) include a more reasonable list of inputs and hence are more realistic, and
- Many participants now hold accreditation to ISO 17025, with NPL holding accreditation to ISO 17043 (previously ISO Guide 43) since 2010.

Furthermore, the analysis of data is more subtle; the deviation and the u-test (now called the  $\zeta$ -test) are still used, but the relative uncertainty ( $R_L$ ) and z-scores are also calculated. These lead to the following assessment of data:

Table 1. Proficiency test assessment

$\zeta$ test	$R_L$ test	z score	Outcome
Pass	Pass	Pass	Agreement
Pass	Fail	Pass	Questionable
Fail	Pass	Pass	Questionable
Pass	-	Fail	Questionable
Fail	-	Fail	Discrepant

The presentation will describe the history of the NPL proficiency test programme and how it has developed over the years with observations on the trends in results. The current data analysis will be discussed in more detail, and a forward look centring on future development of the proficiency test programme and how it will address the growing needs of the nuclear decommissioning industry in the UK and beyond.

Brookes C.J., Betteley I.G. and Loxton S.M., 1979. Fundamentals of Mathematics and Statistics. Wiley, New York.

Jerome, S.M., 1990. Environmental Radioactivity Measurement Intercomparison Exercise. NPL Report RSA(EXT)5

## Long-term variation of cosmic dose rate

G. Ginelli<sup>1</sup>, P. Bossew<sup>2</sup>, M.A. Hernández-Ceballos<sup>3</sup>, T. Tollefsen<sup>3</sup> and M. De Cort<sup>3</sup>

<sup>1</sup>Independent researcher, Italy

<sup>2</sup>German Federal Office for Radiation Protection, Berlin, 10318, Germany

<sup>3</sup>European Commission, JRC, Directorate G – Nuclear Safety & Security, Radioactivity Environmental Monitoring (REM) group, 21027 Ispra (VA), Italy

Keywords: cosmic radiation, dose rate, solar cycle.

Presenting author email: pbossew@bfs.de

The surface of the earth and its biosphere including humans are exposed to secondary cosmic radiation (SCR). It consists mainly of muons and neutrons and is generated by nuclear processes in the upper atmosphere, when the primary cosmic radiation interacts with atmospheric matter. Primary cosmic radiation consists of protons, alpha particles and heavier nuclei and originates mainly from outer space, with a smaller but temporally variable fraction from the sun. Apart from SCR, these nuclear reactions result in generation of so-called cosmogenic radionuclides, such as <sup>7</sup>Be and <sup>14</sup>C.

For Europe, the annual cosmic dose to humans amounts from a few hundred to a few thousand micro-Sievert. The geographical annual average has been estimated to be 0.39 mSv, with a demographical weighted mean of about 0.33 mSv (Cinelli et al. 2017). Very roughly, SCR contributes one-twentieth to one-tenth of overall exposure to natural radiation sources.

SCR intensity in open locations depends on attenuation by the atmosphere, apart from the intensity of the incoming primary flux. In practice, the mid-term average, which refers to periods longer than typical meteorological variability (days) or episodes of high incoming flux (short pulses to hours), can be estimated as a function of geographical altitude (e.g. Bouville and Lowder 1988) and latitude. The latter amounts to a few percent over Europe, but this will not be further discussed here. Over long term, however, SCR intensity is subject to variations of solar activity, which shows an approximate 11 year cycle. In this framework, we attempt to estimate the corresponding long-term variability of the annual mean SCR doses.

Ambient dose rate (ADR, which includes SCR) is continuously measured at more than 5000 stations all over Europe for the purpose of radiological emergency monitoring. In routine situations the generated data represent background radiation. The data are collected by the EURDEP (European Radiological Data Exchange Platform) system operated by the Joint Research Centre of the European Commission, <https://eurdep.jrc.ec.europa.eu/basic/pages/public/home/default.aspx>. In a previous publication (Bossew et al. 2017) it has been shown how the terrestrial component of the ambient dose rate can be estimated from the data.

In this contribution, we extend that method to estimate long-term variations of the normalized ADR background. “Normalized” means ADR in situations of identical environmental conditions. We attempt to relate the reconstructed long-term variation to the one of

reported <sup>7</sup>Be concentrations (also stored in EURDEP, REMdb (Radioactivity Environmental Monitoring database) and available in literature, e.g. Ajtić et al. 2013, Hernández-Ceballos et al. 2015), of reported neutron flux which is monitored by a world-wide network (e.g. Moscow monitor, <http://cr0.izmiran.rssi.ru/mosc/main.htm> and Oulo monitor, <https://cosmicrays oulu.fi/>), and to solar activity (among many others, Kanzelhöhe observatory, [https://www.kso.ac.at/spots/spot\\_graph.php](https://www.kso.ac.at/spots/spot_graph.php)). Although accurate estimation of the absolute value of SCR dose rate from ADR monitors is difficult, due to the fact that response to SCR of these monitors (GM probes, proportional counters) is not accurately known in most cases, its relative variability can still be calculated approximately.

- Ajtić J.V., Todorović D.J., Nikolić D.J., Nikolić J.D., Djurdjević V.S. 2013. A multi-year study of radioactivity in surface air and its relation to climate variables in Belgrade, Serbia. *Nuclear Technology & Radiation Protection* 28 (4), 381 – 388.
- Bossew P., Cinelli G., Hernández-Ceballos M., Cernohlawek N., Gruber V., Dehandschutter B., Menneson F., Bleher M., Stöhlker U., Hellmann I., Weiler F., Tollefsen T., Tognoli P.V., De Cort M. 2017. Estimating the terrestrial gamma dose rate by decomposition of the ambient dose equivalent rate. *J. Environmental Radioactivity* 166, 296 – 308
- Bouville, A. and Lowder W.M. 1988. Human population exposure to cosmic radiation. *Radiat. Dosim.* 24(1), 293-299
- Cinelli G., Gruber V., De Felice L., Bossew P., Angel Hernández-Ceballos M., Tollefsen T., Mundigl S., De Cort M. 2017. Development of the European annual cosmic-ray dose map and estimation of population exposure. Submitted.
- Hernández-Ceballos M.A., Cinelli G., Marín Ferrer M., Tollefsen T., De Felice L., Nweke E., Tognoli P.V., Vanzo S., De Cort M. 2015. A climatology of <sup>7</sup>Be in surface air in European Union. *J. Environmental Radioactivity* 141, 62 – 70.

## Environmental impact of the CHARM facility at the CERN East Experimental Area due to stray radiation and releases of airborne radioactivity

R. Froeschl, P. Vojtyla and F. Malacrida

CERN, Geneva 1211, Switzerland

Keywords: Environmental impact assessment, accelerator facilities, Monte Carlo simulations

Presenting author email: robert.froeschl@cern.ch

The CERN High energy Accelerator Mixed field (CHARM) facility has been constructed in 2014 in the CERN East Experimental Area to study radiation effects on electronic components (Froeschl et al., 2015). It receives a primary proton beam from the CERN Proton Synchrotron at a beam momentum of 24 GeV/c and a maximum average beam intensity of  $6.6 \times 10^{10}$  protons/second. The beam impinges on one out of a set of dedicated targets to produce the desired radiation fields at several experimental positions.

In total,  $2.91 \times 10^{17}$  protons have been delivered to the CHARM facility in 2015, 93% to a copper target.

Stray radiation and releases of gaseous airborne radioactivity are the two main contributors to the radiological impact of the CHARM facility beyond the borders of the CERN site.

The stray radiation consists of the neutron radiation emerging from the roof of the facility known as sky shine. The effective dose due to stray radiation is assessed using a FLUKA Monte Carlo simulation (Bohlen et al, 2014, Fassò et al., 2005) of the CHARM facility and its surroundings. The simulated process includes: (1) Interactions of the proton beam with the target; (2) Attenuation of the emerging neutron radiation through the facility shielding; and (3) The transport of the radiation to the location of the reference population group, predominantly via scattering. This simulation has to heavily employ biasing techniques to provide an estimate with the required uncertainty in a reasonable computing time. The roof shielding, which is 4.8 meter thick, was segmented in the FLUKA Monte Carlo simulation into several layers. Region Importance Biasing was then applied for these layers to accelerate the convergence of the effective dose estimate at the location of the reference population group.

Ambient dose equivalent data measured by an hydrogen-filled ionization chamber (20 bar) located directly above the CHARM target on the roof of the shielding of the CHARM facility have been used to normalize the Monte Carlo simulation results to reduce the uncertainty originating in the attenuation of the neutron radiation while traversing the roof shielding. Based on these calculations and measurements, the estimated effective dose to a member of the public due to neutron stray radiation from CHARM was smaller than  $0.58 \mu\text{Sv}$  in 2015.

The calculation of annual releases of airborne radioactivity is based on FLUKA Monte Carlo simulations to determine the activation of the air inside the CHARM facility while taking the beam-exploitation and ventilation parameters into account (Froeschl, 2014).

The resulting annual effective dose to members of the public is then obtained by a Monte Carlo integration of the dose kernel that is attributable to the photon radiation from radionuclides dispersed in the air under various meteorological conditions occurring during the year (Vojtyla, 2006).

The releases of gaseous airborne radioactivity – essentially short-lived radionuclides ( $^{11}\text{C}$ ,  $^{13}\text{N}$ ,  $^{14}\text{O}$ ,  $^{15}\text{O}$  and  $^{41}\text{Ar}$ ) – are continuously monitored by a semiconductor gross beta counter. The measured release term, obtained by using a calibration based on the estimated activity ratios of the radionuclides, in 2015 has been compared to the estimate yielding an agreement at the level of a factor 1.2, validating the assessment methodology. In 2015, the annual release was 2.54 TBq. The resulting effective dose to any member of the public was smaller than  $0.084 \mu\text{Sv}$ .

The total effective dose to any member of the public due to operation of the CHARM facility in 2015 was smaller than  $0.7 \mu\text{Sv}$ . It remained below the facility design goal of  $1 \mu\text{Sv}$  per year.

### References

- T.T. Bohlen, et al, (2014). The FLUKA Code: Developments and Challenges for High Energy and Medical Applications, Nuclear Data Sheets 120, pp. 212–214.
- A. Fassò, A. Ferrari, J. Ranft, P.R. Sala, 2005. FLUKA: a multi-particle transport code, CERN-2005-10, INFN/TC-05/11, SLAC-R-773.
- R. Froeschl, 2014. Radiation Protection Assessment of the Proton Irradiation facility and the CHARM facility in the East Area, CERN-RP-2014-008-REPORTS-TN, EDMS 1355933.
- R. Froeschl, M. Brugger, S. Roesler, 2015. The CERN High Energy Accelerator Mixed Field (CHARM) facility in the CERN PS East Experimental Area, Proceedings of SATIF12, NEA/NSC/R(2015)3, Batavia, Illinois, United States, pp. 14–25.
- P. Vojtyla, 2006. Calculation of the external effective dose from a radioactive plume by using Monte Carlo dose kernel integration, Applied Modeling and Computations in Nuclear Science. Semkow, T. M., Pommé, S., Jerome, S. M. and Strom, D. J. Eds. A.C.S. Symposium Series 945 (Washington, DC: American Chemical Society) pp. 104–114 (2006).



## Environmental impact assessment of the European Spallation Source facility

D. Ene<sup>1</sup>, R. Avila<sup>2</sup>, T. Hjerpe<sup>2</sup>, B. Jaeschke<sup>2</sup> and K. Stenberg<sup>2</sup>

<sup>1</sup>Environment, Health and Safety Department, European Spallation Source ESS-ERIC, Lund, Sweden

<sup>2</sup>Facilia AB, Gustavslundsvägen 151C, SE-167 51 Bromma, Sweden

Keywords: source term, modelling of environmental processes, human dosimetry, environment impact.

Presenting author email: daniela.ene@esss.se

Like other accelerator-based installations, the European Spallation Source ESS facility will not be a totally isolated system; it will interact with the environment. The Swedish legislation requires a demonstration that the sum of the doses resulting from the exposure of any member of the public to ionizing radiation does not exceed the specified dose constraint of 50  $\mu\text{Sv}/\text{year}$ . A radiological assessment, based upon the actual status of the ESS design, has been produced to provide that demonstration.

A graded approach was adopted in the assessment. The relative importance of the dose contributions was initially assessed by comparing doses calculated using the IAEA SRS19 screening approach against the predefined dose value of 0.1  $\mu\text{Sv}/\text{year}$ . In the second step, for all radionuclides identified as having significant dose contribution, realistic dose factors were derived using dispersion and radio-ecological realistic models. The total dose rate was finally obtained by summing all the dose rates from the realistically-treated radionuclides and from the radionuclides which were screened out in the first step.

### 1. Stray radiation

Stray radiation fields were studied under the assumption of 5 MW beam power at 2 GeV and it was found that the maximum annual dose to members of the public is lower than 10  $\mu\text{Sv}/\text{year}$ .

### 2. Radioactive releases to the surrounding environment

The evaluation of exposures to impacted environmental media considers three main pathways: i) airborne releases of radionuclides through ventilation, ii) liquid discharges of radionuclides to the sewage system and downstream surface water (rivers and sea), iii) migration of radionuclides with groundwater following activation of the surrounding soil. The impact assessment has two main phases: i) estimation of the source term (ST), by means of calculation of radioactivity (Monte Carlo radiation transport simulations coupled with activation calculations by means CINDER'90 code) that can be released annually and taking into account the design parameters of the abatement systems, e.g. ventilation system (HVAC), and ii) applying dispersion and radionuclide transport models to calculate concentrations in the environment and dose models to calculate doses to reference groups of the population around the site. The considered land-use classes are: 1) residential building and garden plot, 2) cropland, 3) pastureland, 4) forest, 5) lake, 6) freshwater body, and 7) sea basins. In addition, sewage plant is considered as a type of land use.

### *Releases to the atmosphere*

The calculation of effective doses to the reference population due to the airborne releases to the environment was performed for two scenarios: i) a chronic constant 50 year long-term release with average atmospheric dispersion conditions and radionuclide accumulation in the environment, and ii) short-term periodic atmospheric releases during which atmospheric dispersion conditions may significantly differ from the average conditions. Two main release points were accounted for: i) main stack, the exhaust of both continuous releases from the accelerator tunnel, target station and instrument systems as well as the periodic short-term releases from the hot cell, and ii) waste stack, the point of releases from the waste facility, during short-term campaigns. The total annual dose obtained is below 1  $\mu\text{Sv}/\text{year}$  and is dominated by N-13, C-11, Ar-41, O-15 and I-125. The reduction effect of the filtration system on the total doses from continuous releases is marginal, since the total doses are dominated by radionuclides that are released in gas form.

### *Discharge to the sewage system*

All radioactive wastewater produced during the operation will be sent to the waste facility for treatment and further discharged to the sewage plant. Radionuclides potentially contained in the wastewater originate from: i) activation of the water, and ii) contamination of water with corrosion products and dust. Realistic dose factors were used to derive discharge limits (Bq/year), for each radionuclide.

### *Migration of contaminants with the groundwater*

The results of modeling show that doses will be formed practically 100% by tritium. Tritium concentrations in well water are approximately one order of magnitude below the admissible level of 100 Bq/L. Transport of other radionuclides to the well is delayed by sorption, and their predicted concentrations are negligible.

### 3. Impact to non-human biota

Assessment of the dose for non-human biota required development of the ERICA computer code to address data and exposure pathways gaps relevant to the ESS site. The results indicate that no organisms are subjected to dose rates above the screening value of 10  $\mu\text{Gy}/\text{h}$ .

### 4. Conclusion

It was concluded from this assessment that during normal operation, the ESS facility will comply with the dose constraints imposed by the Swedish Authority. The current data are estimations subject to evolution and regular updates.



## Do changes in whole genome methylation play a role in adaptations of plants to chronic radiation exposure in nuclear accidental affected areas?

N. Horemans<sup>1,2</sup>, J. Van de Walle<sup>1,2</sup>, E. Saenen<sup>1</sup>, M. Van Hees<sup>1</sup>, R. Nauts<sup>1</sup>

<sup>1</sup>Belgian Nuclear Research Centre (SCK•CEN), Biosphere Impact Studies, Boeretang 200, B-2400 Mol, Belgium,

<sup>2</sup>Centre for environmental research, University of Hasselt, Universiteitslaan 1, 3590 Diepenbeek, Belgium

Keywords: nuclear accident, plant adaptation, transgenerational effects, DNA methylation.

Presenting author email: nhoremans@sckcen.be

The impact on plants of long-term (transgenerational) exposure to radiation coming from nuclear accidents like Fukushima and Chernobyl is investigated at a molecular level. Ionising radiation can induce genotoxic effects by interacting with DNA either directly or indirectly and as such can induce DNA damage, oxidative stress and lead to alterations in proteins and lipids. Methylation is one of the epigenetic mechanisms that is involved in the expression of genes and is said to be important in the induction of transgenerational memory in different organisms. Additionally a decrease in global methylation may lead to DNA instability and contribute to mutations and chromosomal recombinations.

In order to study the long-term impact (within and across generations) of gamma radiation in plants a field campaign was performed in both Chernobyl (CEZ) and Fukushima affected areas (FEZ) in the course of May 2016. Annual Brassicacea plants, *Arabidopsis thaliana* and *Capsella bursa pastoris* in CEZ and FEZ respectively, were sampled alongside a gradient of enhanced radiation ranging from 0.5 to 50  $\mu\text{Gy}\cdot\text{h}^{-1}$ . In total 15 (CEZ) or 10 (FEZ) sampling sites were visited that could be divided in low medium (3-10  $\mu\text{Gy}\cdot\text{h}^{-1}$ ), high radiation levels (15-80  $\mu\text{Gy}\cdot\text{h}^{-1}$ ) or control conditions. For CEZ control sites were visited both within and out of the exclusion zone. For analysis of methylation, leaves were harvested from flowering plants and frozen in liquid nitrogen as soon as possible in the field. The reproductive stage was chosen to increase identification of plants. For *A. thaliana* rosette leaves were taken whereas for *C. bursa pastoris* leaves present on the flowering stem were harvested as rosettes where senescent and wilting in flowering *C. bursa pastoris* plants. To have a first indication of radiation levels the average dose rates at the level of the plants was measured. For correct dosimetry both soil samples (at least three per sampling spot) and above ground plant material was sampled. Plants and soils were dried prior to measurement of most important radionuclides (Cs, Sr and Am). For FEZ additional samples for heavy metal contamination were taken. In addition *A. thaliana* plants coming from seeds harvested in the field were grown in the lab together with control plants of our *A. thaliana* col 0 stock. A radiation exposure experiment was performed on 7-day old lab *A. thaliana* col 0 seeds by exposing them to different gamma dose rates (delivered by a Cs-137 source) for ranging from 20 to 400  $\text{mGy}\cdot\text{h}^{-1}$  for 14 days and this for three subsequent

generations (F0-S1-S2). Leaves were snap-frozen in  $\text{N}_2$  and stored at  $-80^\circ\text{C}$  until further analysis.

To determine whole genome methylation genomic DNA was extracted from the frozen leaves using DNeasy 96 Plant Kit protocol of QIAGEN (QIAGEN GmbH, Hilden, Germany). The concentration and purity of extracted DNA was checked using NanoDrop 2000 (Thermo Fisher Scientific, USA). DNA was subsequently broken down to single nucleosides using a 2-hour DNA Degradase Plus protocol (Zymo Research Corporation). Percentage of methylated cytosines was determined after separation on UCLP-MS/MS as described by (Lisanti et al., 2013). To follow up the possible role of methylation gene expression of different methylation related genes was additionally measured in both lab and field exposed plants. RNA was extracted using RNeasy Plant Mini kit according to the manufacturers' instructions (Qiagen, Venlo, Netherlands). A first indication of the possible involvement of a changed methylation in adaptation of plants to radiation was found in lab-exposed plants. Global DNA methylation in lab exposed *A. thaliana* plants showed a significant increase which was both dose and generation dependent. With a stronger induction in plants exposed for the second (S2) or third generation (S3). Significant changes in transcription of methylation regulating genes was also measured in the different generations. The field plants did not show any abnormalities that could be correlated with the exposure gradient. At this moment the measurement of methylation levels on field collected samples is ongoing but results will be compared to lab acquired data.

This work was supported by European project COMET (7th PCRD EURATOM Contract Number: Fission-2012-3.4.1-604794) ([www.comet-radioecology.org](http://www.comet-radioecology.org))

Lisanti S, Omar WA, Tomaszewski B, et al., 2013. Comparison of methods for quantification of global DNA methylation in human cells and tissues. *PLoS ONE* 8, e79044.

## Radioecology supports out future by preserving ecosystem health

François Bréchnignac  
IRSN & IUR

**ABSTRACT:** Ecological impact of radiation, as resulting from nuclear accidents or potential malevolent actions, has become a global environmental issue within the list of current concern (climate change impact, biodiversity decline and stressor's impact on the biosphere). Indeed, despite 3 majors accidents (Three Miles Island, Chernobyl, Fukushima), nuclear activities continue to spread throughout the world together with associated waste issues, and often in countries with limited or no expertise on environmental risks. Furthermore, understanding the ecological impact of radiation is still debated within the scientific community, leading to potentially unjustified distrust from society with respect to the ability of authorities to take adequate measures for mastering nuclear risk. This is particular critical when realizing that unplanned dispersion of radioactivity over large areas no longer can be considered as unlikely. It is therefore crucial to maintain worldwide expertise such as to make sure that we have the operational capacity to face risk. An intensive body of work and brainstorming is under development internationally in order to identify how best improving our limited understanding of what is the actual ecological impact of radiation. Further to traditional lines of thinking in human radioprotection which involve radiobiological inferences in individual organism level, ecosystem approaches, featuring consideration of populations and interspecies interactions, appear necessary for adequate ecological risk assessment of radiation. An ecocentric vision is under construction which conceptualizes how human health is also bound to ecosystem health which therefore needs to be preserved from potential radiation alteration. Within this movement, radioecology contributes to the urgent and general commitment to preserving ecosystem health.

## **POSTER PRESENTATIONS**

## Benchmarking of Monte Carlo simulations for a Cerium Bromide (CeBr<sub>3</sub>) detector

F. Legarda<sup>1</sup>, and N. Alegría<sup>1</sup>

<sup>1</sup>Department of Nuclear Engineering and Fluid Mechanics, University of the Basque Country, Bilbao, 48013, Spain

Keywords: CeBr<sub>3</sub> detectors, gamma spectrometry, MCNP simulations

Presenting author email: natalia.alegria@ehu.eus

In order to improve Environmental Radiation Monitoring Networks, new systems with spectrometric capacity have been studied, including Caesium Bromide detectors (CeBr<sub>3</sub>).

Cerium Bromide (CeBr<sub>3</sub>) detectors are scintillators that offer significantly better resolution (<3 percent at 662 keV) than sodium iodide (NaI(Tl)) detectors and a lower level of radioactive contamination than Lanthanum Bromide (LaBr<sub>3</sub>) detectors.

The first part of the study dealt with the acquisition of spectra in our laboratory, figure 1, using a 1 x 1 inch CeBr<sub>3</sub> detector and several point sources (<sup>241</sup>Am, <sup>137</sup>Cs and <sup>60</sup>Co).

The distance between the detector window and the source was 35 cm, figure 1, and the experimental spectra of <sup>241</sup>Am, <sup>137</sup>Cs and <sup>60</sup>Co had at least 10000 counts at the central channel of the photopeaks.

In parallel, using the Monte Carlo code MCNP-5 the same situation was simulated: the detector geometry, the point source and the constructive details of the laboratory, figure 1, such as the floor, walls, detector and source holders. Gaussian energy broadening was used to model the resolution of the CeBr<sub>3</sub> detector.

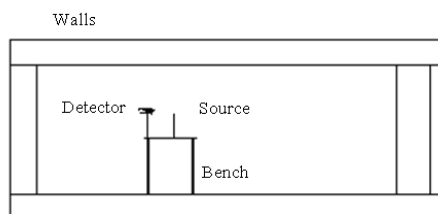


Figure 1, simulation of the experimental conditions

The first spectra (experimental and simulated) comparison showed an excellent coincidence. As an example of the results, <sup>137</sup>Cs spectra (experimental and simulated) are shown in figure 2.

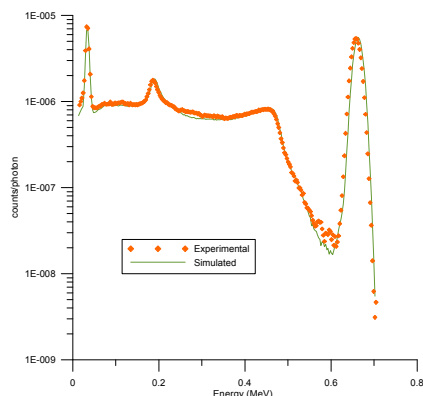


Figure 2, <sup>137</sup>Cs spectra

The second part of the study was the analyses of the angular response of the detector.

Spectra were collected at 45° and 90° beam incidence with respect to detector axis. They were simulated using the Monte Carlo code MCNP-5.

At 45° and 90° the experimental measurements and the simulated results in all situations are in excellent agreement.

Finally, the result of the comparison of the efficiencies versus energies for the 3 position (0°, 45° and 90°) is shown in figure 3

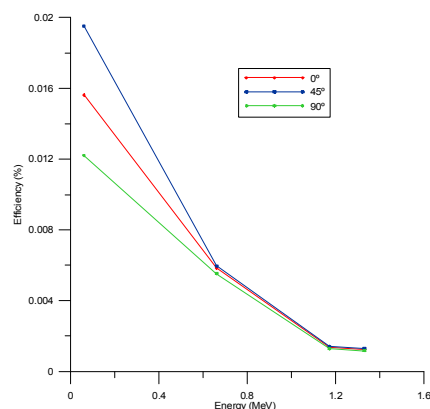


Figure 3, Comparison of the efficiencies

We can conclude that the detector response can be simulated using MCNP-5 with high accuracy and that the angular dependence is higher for low energies, being very small for energies above ~700 keV.

### References

- Los Alamos National Laboratory. MCNP-5. Monte-Carlo N-Particle Transport Code System, versión 5. New México. USA, 2005.
- Scintillation and detection characteristics of high-sensitivity CeBr<sub>3</sub> gamma-ray spectrometers. F. G. A. Quarati et al. Nuclear Instruments and Methods in Physics Research A 729 (2013) 596
- CeBr<sub>3</sub> Scintillators for Gamma-Ray Spectroscopy. Kanai S. Shah et al. IEEE Transactions on Nuclear Science, Vol 52 N° 6, December 2005
- Radiopurity of CeBr<sub>3</sub> crystal used as scintillation detector. G. Lutter et al. Nuclear Instruments and Methods in Physics Research A 703 (2013) 158-162
- New information on the characteristics of 1 in. X 1 in. Cerium bromide scintillation detectors. R. Billnert et al. Nuclear Instruments and Methods in Physics Research A 647 (2011) 94-98

## Vertical distribution of <sup>137</sup>Cs in soil profiles in Lithuania

Asta Orentienė, Laima Pilkytė, Remigijus Kievinas, Aneta Bogdanovič  
Radiation Protection Centre, Vilnius, LT-08221, Lithuania

Keywords: <sup>137</sup>Cs specific activity, vertical distribution, soil samples, gamma spectrometry.  
asta.orentiene@rsc.lt

The nuclear weapon tests (1946-1980) and the Chernobyl accident (1986) are the main contributors to the soil pollution with artificial radionuclides in Lithuania, and in most of the places elsewhere. After Chernobyl nuclear power plant (NPP) accident, the increase of the contamination in artificial radionuclides was observed, among which, the most notable being <sup>137</sup>Cs. For instance, the measured of <sup>137</sup>Cs specific activity varied between 2–600 Bq/kg in the most contaminated areas, that is, the southern, south-western, and western parts of Lithuania and furthermore, due to a very slow vertical migration process (0.1-0.2 cm/year), the upper layer of soil still remains contaminated. (Butkus et al., 1992) The accumulation of <sup>137</sup>Cs in the environment poses a serious threat to human health, especially taking into account various pathways this pollutant can enter into human body through food chain. Therefore, the monitoring of the distribution and dynamics of this particular radionuclide is of utmost importance.

In order to evaluate the residual contamination with <sup>137</sup>Cs caused by the Chernobyl NPP disaster and also to trace its vertical migration in the soil, detailed measurements were conducted in the different areas across Lithuania. The territory of Lithuania was covered by 10x10 km grid and the sampling of the soil were performed on every segment in different parts of Lithuania (Fig 1.).

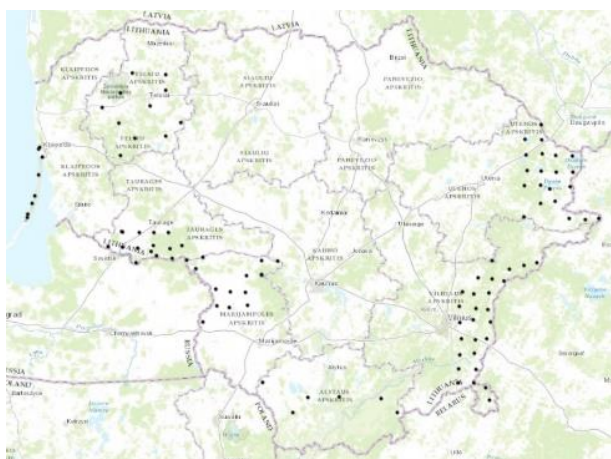


Figure 1. Soil sampling points in the territory of Lithuania.

The vertical distribution of <sup>137</sup>Cs was evaluated at every 5 cm of the soil profile, up to 30 cm depth. High purity germanium detectors and spectrum analysis software Genie2000 were used for all measurements.

In accord with general trends (WHO working group, 1989), the highest <sup>137</sup>Cs specific activity values were measured in the southwest part of Lithuania. As expected, the highest <sup>137</sup>Cs specific activity values were detected in the upper layers of soil, up to 20 cm, and reaches up to 18 Bq/kg. As shown in Fig. 2, the specific activity of <sup>137</sup>Cs varies depending on the type of soil and the intensity of the agricultural activity in the area.

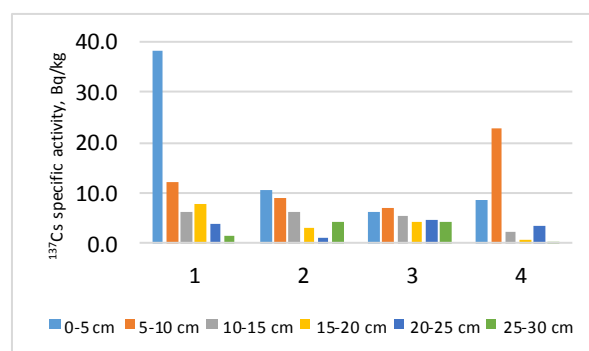


Figure 2. The <sup>137</sup>Cs specific activity in a different type of soil. (1-forest floor, 2-undisturbed area, 3-farmland, 4-Curronian Spit).

The variation in activity is also caused by the very complex nature of the <sup>137</sup>Cs migration process itself, the rate of which is affected by the kinetics of sorption-desorption equilibrium and the type of the soil as well as other factors such as humidity, flora and agriculture. The results indicate that the amount of <sup>137</sup>Cs is smaller in actively cultivated soil as a result of efficient mixing of the surface layers. In such areas <sup>137</sup>Cs specific activity do not depend on the sampling depth and equals to 2-5 Bq/kg. On the other hand, <sup>137</sup>Cs specific activity in the forest floor, where the migration process is very slow, is the highest in 0-5 cm layer, and exceed 40 Bq/kg. (Fig. 2, data set. 1). As a comparison, <sup>137</sup>Cs specific activity in the eastern part of the country, where the influence of Chernobyl accident was not significant, varies 4-8 Bq/kg only.

The results obtained indicates that, although the activity of <sup>137</sup>Cs is decreasing, but due to long half-life and slow migration process the residual activity of this radionuclide still remains in the upper layer of the soil and may contribute to human exposure.

Butkus D. et al. 1992, The evaluation of <sup>137</sup>Cs contamination in the territory of Lithuania, Vilnius, Academia, 21-31.

WHO working group, 1989. Health hazards from radiocaesium following the Chernobyl nuclear accident. Journal of Environmental radioactivity. 10, 257-295.



## The activities of radiocaesium in marine fishes around off Fukushima in Japan

T. Aono<sup>1</sup>, M. Fukuda<sup>1</sup>, S. Yamazaki<sup>1</sup>, M. Akashi<sup>1</sup>, T. Sohtome<sup>2</sup>, T. Mizuno<sup>2</sup>, M. Yamada<sup>2</sup>, A. Yamanobe<sup>2</sup>

<sup>1</sup>National Institute of Radiological Sciences(NIRS), National Institute for Quantum and Radiological Science and Technology(QST), Fukushima, 960-1295, Japan

<sup>2</sup>Fukushima Prefectural Fisheries Experiment Station, Fukushima, 970-0316, Japan

Keywords: radiocaesium, marine fishes, Fukushima

Presenting author email: aono.tatsuo@qst.go.jp

About six years have passed since an accident of the Fukushima Daiichi Nuclear Power Station (FDNPS). Dispersion of radionuclides in the FDNPS accident have been caused environmental changes around Fukushima immediately. It is important that monitoring of radionuclide activities in seawater, sediments and fishes in the marine environment off the coast of Fukushima in the Pacific Ocean for understanding the dispersion and behaviour of radionuclides after the FDNPS accident. This study aimed to examine the temporal and spatial variation of radionuclide activities in marine fishes and to discuss concentration ratio (CR) of marine organisms around Fukushima.

Marine samples such as seawater, sediment and fishes were collected with some research and fishing vessels after this accident. Radioactive Cs in seawater were determined with the AMP/Cs method (Aoyama and Hirose, 2008) and the  $\gamma$  spectrometry using Ge detectors. Regarding sediment, radionuclides were measured with the Ge detector used for the seawater samples. In case of marine fishes, after being classified into species and weighed, each sample was packed into a plastic container (U-8). The radionuclide activities were determined by gamma-ray spectrometry using a HP-Ge detector. These of marine samples in the sampling date were calculated with the correction of the decay and the coincidence-summing of <sup>134</sup>Cs. Detection limits of <sup>134</sup>Cs, <sup>137</sup>Cs, and <sup>110m</sup>Ag in marine fishes were estimated within 1 and 0.5 Bq/kg [wet weight (wet-wt)], respectively.

<sup>134</sup>Cs, <sup>137</sup>Cs, <sup>110m</sup>Ag and <sup>239+240</sup>Pu were detected in fish and shellfish collected off Onahama (the southern area from FDNPS) in June and December 2011, and then <sup>90</sup>Sr were not detected in the bony part of fish and the <sup>239+240</sup>Pu activities in visceral parts were almost same levels as before this accident. The radiocaesium activities in fishes were shown in Table 1. The <sup>40</sup>K activities were almost similar in fishes.

Table 1 The activities of radionuclides in fishes collected off Naraha in Nov. 13th, 2013 (Bq/Kg-wet).

Species	Edible parts		
	<sup>134</sup> Cs	<sup>137</sup> Cs	<sup>40</sup> K
Bastard halibut	18.80	46.74	159.79
Fat greenling	11.23	27.93	135.38
Common skete	29.84	79.13	86.35
Cloudy catshark	4.12	9.54	93.38

The large differences of observed radionuclide activities in edible parts of fishes was not recognized between individuals, as radiocaesium activities in seawater off Fukushima were gradually decreased until almost the same levels as before this accident(Table 2).

Table 2 The average of radionuclide activities in edible parts of fishes collected around off Fukushima.

(1) Fishes collected off Naraha in Nov. 24th, 2014 (Bq/Kg-wet)				
Species	n	Cs-134	Cs-137	K-40
		Av.	Av.	Av.
Japanese blue crab	3	0.04	0.09	18.14
Mackerel	7	< 0.05	0.08	34.53
Common skete	4	2.11	6.51	16.92

(2) Fishes collected off Naraha in Jan. 29th, 2015 (Bq/Kg-wet)				
Species	n	Cs-134	Cs-137	K-40
		Av.	Av.	Av.
Common skete	6	1.34	4.35	10.86
Fat greenling	6	0.78	2.51	27.63

No significant influence from the accident was observed in the fish as a foodstuff collected off Fukushima in 2014 and 2015. The variations of radiocaesium activities in bottom fishes such as *Common skete* were depended on feeding habits and the sediment in their habitat. It seemed that the particles such as suspend matter and sediment led to high CRs-Cs after this accident, as the estimated these values in the bottom fishes around Fukushima were higher than the reported values in TRS-422,

This work was partly supported by a Research on Food Safety in the Health and Labour Sciences Research Grant by MLHW.

### References

- Aoyama, M., Hirose, K., 2008. Radiometric determination of anthropogenic radionuclides in seawater, In P. P. Pavel (Ed.), Radioactivity in the Environment (pp. 137–162). Hungary: Elsevier.

## Comparison of coral $^{129}\text{I}$ and $^{14}\text{C}$ as proxy for human nuclear activities, age marker, and oceanographic tracer

A.T. Bautista VII<sup>1,2</sup>, H. Matsuzaki<sup>1,3</sup>, Y.S. Tsuchiya<sup>3</sup>, and F.P. Siringan<sup>4</sup>

<sup>1</sup>Department of Nuclear Engineering and Management, The University of Tokyo, Bunkyo-ku, Tokyo 113-8656, Japan

<sup>2</sup>Philippine Nuclear Research Institute – Department of Science and Technology, Quezon City 1101, Philippines

<sup>3</sup>MALT, The University Museum, The University of Tokyo, Bunkyo-ku, Tokyo 113-0032, Japan

<sup>4</sup>Marine Science Institute, University of The Philippines, Diliman, Quezon City 1101, Philippines

Keywords: coral, iodine-129, carbon-14, Philippines

Presenting author email: atbautistavii@pnri.dost.gov.ph

Iodine-129 ( $^{129}\text{I}$ ) and carbon-14 ( $^{14}\text{C}$ ) in coral core samples can be used as (1) proxy for human nuclear activities (HNA); (2) age marker – for establishing or confirming coral age models; and (3) oceanographic tracer – for understanding ocean mixing and variabilities. In the case of  $^{129}\text{I}$ , these applications are being studied only recently, with a handful of published works (Bautista et al., 2016; Biddulph et al., 2006; Chang et al., 2016). For  $^{14}\text{C}$ , these applications are more extensively known, with numerous published studies available (Andrews et al., 2016; review by Grottoli and Eakin, 2007). Nonetheless, a direct and comprehensive comparison of the applications of  $^{129}\text{I}$  and  $^{14}\text{C}$  in coral samples has never been done.

In this paper, we show  $^{129}\text{I}$  and  $^{14}\text{C}$  levels in two coral cores from the Philippines – Baler and Parola, located in the Pacific Ocean (east) and South China Sea (west) sides of the country, respectively. We provide a direct comparison of the applications of the newer  $^{129}\text{I}$  and the better known  $^{14}\text{C}$  in these corals as proxies for HNA, age markers, and oceanographic tracers. To aid in the comparison, a simple box mixing model to simulate  $^{129}\text{I}$  and  $^{14}\text{C}$  signals observed in Baler and Parola was also constructed.

Results show that as proxies for HNA,  $^{129}\text{I}$  in the Baler and Parola corals record nuclear weapon testing (e.g., 1962 peak), nuclear fuel reprocessing (e.g., 1977, 1980, and 1989 peaks), and nuclear accident (Chernobyl, 1986 peak) signals separately (Bautista et al., 2016), while  $^{14}\text{C}$  only registers a broad peak for both sites, attributed to nuclear weapons testing only. Hence,  $^{129}\text{I}$  is a better HNA proxy than  $^{14}\text{C}$ , and it provides a better measure of the impact of HNA on the vicinity of the corals.

As age markers, nearly identical  $^{129}\text{I}$  bomb peaks are recorded in the year 1962 in both Baler and Parola. In contrast,  $^{14}\text{C}$  bomb peaks in Baler and Parola and even those from published records varied in timing, shape, and magnitude depending on the location of the coral. We attribute this discrepancy to the large difference in atmospheric lifetimes between the two radionuclides i.e., centuries to millennia for  $^{14}\text{C}$  (Joos et al., 2001) and 2 weeks to 2 years for  $^{129}\text{I}$  (Moran et al., 1999; UNSCEAR, 2000). The quicker  $^{129}\text{I}$  atmospheric lifetime results to a sharper bomb peak that is not affected by ocean processes. Thus,  $^{129}\text{I}$  bomb peak should be consistently observed with the same timing regardless of the location of the coral. On the other hand, the slower  $^{14}\text{C}$  atmospheric results to a broad peak that is affected by ocean processes.

Thus,  $^{14}\text{C}$  bomb peak should vary in timing, magnitude, and shape depending on the location of the coral. This explanation was successfully demonstrated in our box model simulation, which was done in two cases – one with a radionuclide atmospheric lifetime of 1.125 years and another at 300 years. Hence,  $^{129}\text{I}$  bomb peak is the better age marker since it is observed with consistent timing regardless of the location of the coral.

As oceanographic tracers, results show that  $^{129}\text{I}$  signals can be used to estimate the speed, direction, and amount of ocean circulation and radionuclide transport. This capability is observed in the 9 to 11-year timing discrepancy in NFR and Chernobyl signals between Parola and Baler and a large difference in  $^{129}\text{I}$  levels of the two corals after the year 1996. On the other hand,  $^{14}\text{C}$  signals reflected large and long-term scale changes in circulation such intrusion of South Pacific waters to the North Equatorial Current, northward shift in the North Equatorial Current bifurcation latitude, and increased upwelling in the Central American region. The latter two are variabilities caused by the El Niño Southern Oscillation and the 1976 Pacific Decadal Oscillation shift. Hence, both  $^{129}\text{I}$  and  $^{14}\text{C}$  offer oceanographic tracer applications that are unique from each other.

Andrews, A.H., Asami, R., Iryu, Y., Kobayashi, D.R., Camacho, F., 2016. *J. Geophys. Res. Ocean.* 7772–7793.

Bautista, A.T., VII, Matsuzaki, H., Siringan, F.P., 2016. *J. Environ. Radioact.* 164, 174–181.

Biddulph, D.L., Beck, J.W., Burr, G.S., Donahue, D.J., 2006. *Radioact. Environ.* 8, 592–598.

Chang, C.-C., Burr, G.S., Jull, A.J.T., Russell, J.L., Biddulph, D., White, L., Prouty, N.G., Chen, Y.-G., Shen, C.-C., Zhou, W., Lam, D.D., 2016. *J. Environ. Radioact.* 165, 144–150.

Grottoli, A.G., Eakin, C.M., 2007. *Earth-Science Rev.* 81, 67–91.

Joos, F., Prentice, I.C., Sitch, S., Meyer, R., Hooss, G., Plattner, G.K., Gerber, S., Hasselmann, K., 2001. *Global Biogeochem. Cycles* 15, 891–907.

Moran, J.E., Oktay, S., Santschi, P.H., Schink, D.R., 1999. *Environ. Sci. Technol.* 33, 2536–2542.

UNSCEAR, 2000. Sources and effects of ionizing radiation. UNSCEAR 2000 Report to the General Assembly, Annex C: exposures from man-made sources of radiation. New York.

## Distribution of radionuclides in coastal mussels of the coast of Portugal, Northeast Atlantic

F. P. Carvalho, J.M. Oliveira, M. Malta

Laboratório de Protecção e Segurança Radiológica, Instituto Superior Técnico/Universidade de Lisboa, Estrada Nacional 10, km 139, 2695-066 Bobadela LRS, Portugal

Keywords: coastal monitoring, radioactivity, land-based discharges.

Presenting author email: carvalho@itn.pt

Naturally-occurring radionuclides mostly alpha emitters of uranium series, namely  $^{238}\text{U}$ ,  $^{235}\text{U}$ ,  $^{234}\text{U}$ ,  $^{230}\text{Th}$ ,  $^{226}\text{Ra}$ ,  $^{210}\text{Pb}$ ,  $^{210}\text{Po}$ , and artificial radionuclides such as  $^{137}\text{Cs}$ ,  $^{239+240}\text{Pu}$ , and  $^{238}\text{Pu}$  were determined in mussel samples (*Mytilus galloprovincialis*) collected annually at the coast of Portugal over several years.

A large data set on natural radionuclides showed that activity concentrations of radionuclides in mussels ranked from very low, such as in the case of  $^{230}\text{Th}$  with  $0.031 \pm 0.014 \text{ Bq kg}^{-1}$  (wet weight) and  $^{238}\text{U}$  with  $0.24 \pm 0.03 \text{ Bq kg}^{-1}$  (ww), to high values such as  $^{210}\text{Po}$   $93 \pm 7 \text{ Bq kg}^{-1}$  (ww), as measured at station 3 near Cascais. The pattern of distribution of activity concentrations of radionuclides in mussels' soft tissues was similar in all stations, with  $^{210}\text{Po}$  concentrations being the highest among radionuclides analysed. At the same station, fluctuations in activity concentrations among the years seem related to river discharges. Other parameters are known to have influence on the reported activity concentrations, but adequate sampling was performed to minimize these effects (Carvalho et al., 2011a, 2012b).

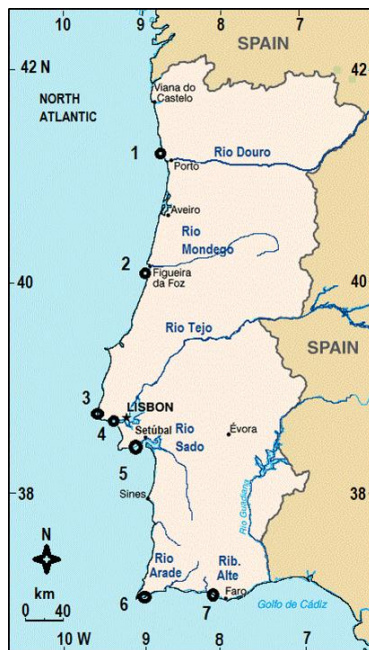


Figure 1. Map of Portugal and coastal sampling stations (circles).

Cesium-137 concentrations was always below  $0.15 \text{ Bq kg}^{-1}$  (ww) and its concentration in mussels did not increased significantly in samples collected after the Fukushima nuclear accident in 2011, although

radioactive atmospheric depositions have been recorded in this region (Carvalho et al, 2012).

Plutonium concentrations in mussels (station 3) were  $(1.98 \pm 0.32) \times 10^{-3} \text{ Bq kg}^{-1}$  (ww) for  $^{239+240}\text{Pu}$  and generally  $< 1.28 \times 10^{-4} \text{ Bq kg}^{-1}$  (ww) for  $^{238}\text{Pu}$ . Plutonium low isotopic ratios in the coastal environment suggest that it was originated in radioactive global fallout following nuclear weapon tests carried in the second half of last century.

No significant radioactive contamination was detected in this coastal sea area. Overall concentrations of naturally occurring radionuclides in this NE Atlantic region are similar to values reported in other coastal seas of Europe, despite intensive uranium mining and milling in the country during the 20<sup>th</sup> century.

Concentrations of artificial radionuclides, namely caesium and plutonium were consistently lower than in other coastal sea areas of Europe reflecting the absence of anthropogenic discharges in this region.

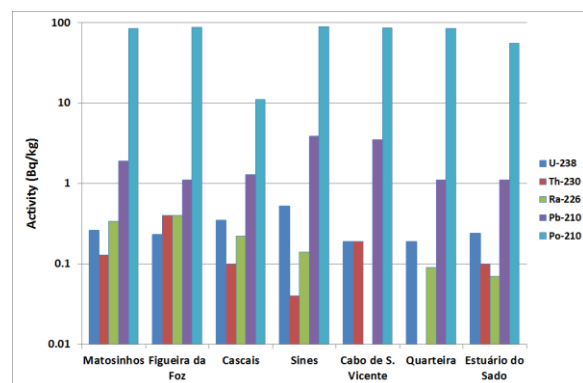


Figure 2. Concentrations of natural radionuclides in mussels (year 2015).

### References

- Carvalho, F.P., Oliveira, J.M., Alberto, G., Vives i Batlle, J., 2011a. Allometric relationships of  $^{210}\text{Po}$  and  $^{210}\text{Pb}$  in mussels and their application to environmental monitoring. *Mar. Pollut. Bull.* 60, 1734–1742.
- Carvalho, F.P., Oliveira, J.M., Alberto, G., 2011b. Factors affecting  $^{210}\text{Po}$  and  $^{210}\text{Pb}$  activity concentrations in mussels and implications for environmental bio-monitoring programmes. *J. Environ. Radioact.* 102, 128–137.
- Carvalho F.P., Reis M.C., Oliveira J.M., Malta M., Silva L. (2012). Radioactivity from Fukushima nuclear accident detected in Lisbon, Portugal. *Journal of Environmental Radioactivity* 114: 152-156

## Separation and Analysis of Uranium in the SRM IAEA-384 and 385

Jun Han<sup>1</sup>, Sheng Hu<sup>1</sup> and Chu-Ting Yang<sup>1</sup>

<sup>1</sup> Institute of Nuclear Physics and Chemistry, China Academy of Engineering Physics, Mianyang, 621900, China

Keywords: TIMS; reference materials; uranium; abundance

Presenting author email: yangchuting@caep.cn

The IAEA reference material can be used for assurance/quality control of the analysis of radionuclides in the environment, as well as for the development and validation of analytical methods (Moody et al., 2005; Mayer et al., 2005, 2013; Wallenius et al., 2006). Furthermore, the isotope ratio may provide a valuable contribution to environmental monitoring. Herein, the pretreatment, separation, and analysis of the IAEA -384 and 385 samples have been done. Quantitative analysis values of uranium measured by TIMS were  $1.37\text{E-}4(^{234}\text{U})$ ,  $0.0161(^{235}\text{U})$ ,  $2.26(^{238}\text{U})$  ug/g in IAEA-384, and  $1.24\text{E-}4(^{234}\text{U})$ ,  $0.0164(^{235}\text{U})$ ,  $2.30(^{238}\text{U})$  ug/g in IAEA-385. The massic activities of uranium isotopes were  $42.1408\pm 0.19(^{234}\text{U})$ ,  $1.7284(^{235}\text{U})$ ,  $37.5892\pm 0.19(^{238}\text{U})$  Bq/Kg in IAEA-384, and  $27.1015\pm 0.05(^{234}\text{U})$ ,  $1.3166(^{235}\text{U})$ ,  $29.2706\pm 0.06(^{238}\text{U})$  Bq/Kg in IAEA-385, respectively (See Table 1). The results were in line with the certified mass activity of CRM (dw 95% confidence interval). The isotope ratios of  $^{235}\text{U}$  and  $^{238}\text{U}$  in the environmental soil samples were in good agreement with natural Uranium.

Table 1. The massic activities of uranium isotope in IAEA-384 and IAEA-385 samples by TIMS

Sample No.	R( $^{234}\text{U}$ )	R( $^{235}\text{U}$ )	R( $^{238}\text{U}$ )
	Bq/kg	Bq/kg	Bq/kg
IAEA-384-1	$42.01 \pm$	$1.72 \pm$	$37.42 \pm$
	0.05	0.06	0.06
IAEA-384-2	$42.27 \pm$	$1.74 \pm$	$37.76 \pm$
	0.05	0.06	0.05
IAEA-384-3	$42.16 \pm$	$1.73 \pm$	$37.58 \pm$
	0.05	0.06	0.05
Av.	42.15	1.73	37.59
Reference value	$40 \pm 5$	$1.74 \pm$	$35.3 \pm$
		0.16	1.7
95% confidence interval		1.60-	33.4-
	35-43	1.96	36.8
IAEA-385-1	$28.05 \pm$	$1.31 \pm$	$28.48 \pm$

	0.06	0.05	0.06
IAEA-385-2	$26.15 \pm$	$1.32 \pm$	$28.74 \pm$
	0.05	0.06	0.06
IAEA-385-3	$27.38 \pm$	$1.31 \pm$	$28.61 \pm$
	0.06	0.05	0.06
Av.	27.19	1.31	28.61
Reference value	$27 \pm$	$1.35 \pm$	$29 \pm$
	1	0.09	1
95% confidence interval	26-28	1.25-1.44	28-30

This work was supported by the National Council Research under grant AB/001.

Moody K. J., Hutcheon I. D., Grant P. M., 2005. Nuclear Forensic Analysis. CRC Press: Boca Raton, FL. ISBN 978-0-8493-1513-8.

Mayer K., Wallenius M., Ray I., 2005. Nuclear forensics—a methodology providing clues on the origin of illicitly trafficked nuclear materials. Analyst 130, 433-441.

Mayer K., Wallenius M., Varga Z., 2013. Nuclear Forensic Science: Correlating measurable material parameters to the history of nuclear material. Chem. Rev. 113, 884-900.

Wallenius M., Mayer K., Ray I., 2006. Nuclear forensic investigations: two case studies. Forensic Sci. Int. 156 (1), 55–62.

## Simulation of the time evolution of radioactive disequilibria in IAEA reference materials IAEA-410 and -412

Detlev Degering, Diana Walther

VKTA - Strahlenschutz, Analytik & Entsorgung Rossendorf e. V., P.O. Box 510119, 01314 Dresden, Germany

Keywords: Reference materials, radioactive disequilibria.

Presenting author email: detlev.degering@vkta.de

The use of certified reference materials is an imperative for a good laboratory praxis in radionuclide analysis. Recently two sediment materials were certified as IAEA-410 (Bikini Atoll) and IAEA-412 (Pacific Ocean) by inter-laboratory exercises (Pham et al., 2016). One important feature of these materials is the occurrence of radioactive disequilibria. Although this fact is mentioned in the reference, the future activity evolution is not investigated in detail yet. Since simple exponential decays will fail for the description of the future of the certified activity values we investigated their time evolution on the base of the available radioanalytical data and of additional own analyses.

### IAEA-410

#### <sup>238</sup>U decay series

The sediment is characterised by a large excess of sorbed <sup>230</sup>Th (Ivanovich and Harmon, 1992) over uranium. <sup>226</sup>Ra as well as <sup>210</sup>Pb show a lower excess but have also enhanced concentrations.

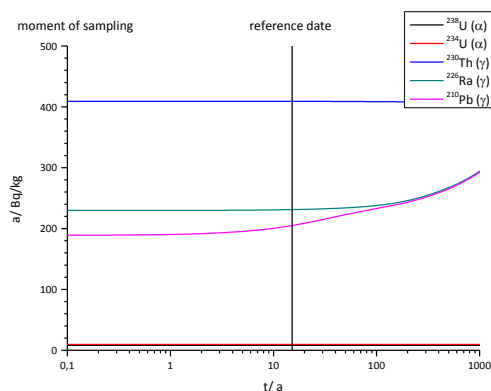


Figure 1. Evolution of the specific activities a with time t of members of the <sup>238</sup>U decay chain in sediment IAEA-410.

Time evolutions of long living <sup>238</sup>U chain members are shown in Figure 1. The long living <sup>238</sup>U, <sup>234</sup>U and <sup>230</sup>Th will not vary during the next decades. <sup>210</sup>Pb is increasing and tends to an equilibrium with <sup>226</sup>Ra whose activity increases by a few per cent during the next 100 years.

#### <sup>235</sup>U decay series

In contrast to the <sup>238</sup>U series, the simulation of the future <sup>235</sup>U chain is more uncertain. Reasons are the much lower activities and analytical problems especially in the case of <sup>231</sup>Pa. Similar to <sup>230</sup>Th, <sup>231</sup>Pa is attached to sediment particles by sorption. <sup>227</sup>Ac is produced mainly by the decay of <sup>231</sup>Pa. In the present material occurs an

equilibrium between <sup>231</sup>Pa and <sup>227</sup>Ac, so the <sup>227</sup>Ac fate is ruled by the half life of <sup>231</sup>Pa ( $3.267 \cdot 10^4$  a).

#### <sup>241</sup>Pu – <sup>241</sup>Am

<sup>241</sup>Am in the environment originates mainly from the nuclear weapons tests at the beginning of the 1960s. The global fallout did also contain its precursor <sup>241</sup>Pu (half life 14.33 a). Now the majority of <sup>241</sup>Pu nuclei decayed to <sup>241</sup>Am, this means that <sup>241</sup>Am reaches soon an activity maximum. Currently the <sup>241</sup>Pu in the sediment is below detection limit. The uncertainty of the initial <sup>241</sup>Pu activity in the sediment causes a maximum uncertainty of about 10 % in the future evolution of the <sup>241</sup>Am content.

### IAEA-412

#### <sup>238</sup>U decay series

In IAEA-412 the <sup>238</sup>U series is marked by an excess of <sup>234</sup>U over <sup>238</sup>U. Reasons may be a combination of  $\alpha$ -recoil effects in the water column and subsequent binding onto the organic phase. The mineral fraction of the sediment can be considered as close to radioactive equilibrium. <sup>226</sup>Ra is slightly depleted by leaching processes. <sup>210</sup>Pb is in excess due to an input from <sup>222</sup>Rn decay in air. The non-exponential decay of unsupported <sup>210</sup>Pb will be the main effect in the next decades.

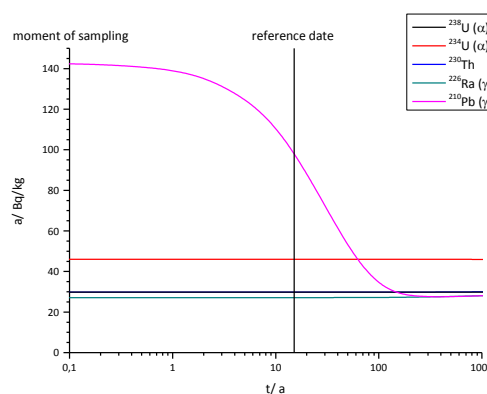


Figure 2. Evolution of the specific activities a with time t of members of the <sup>238</sup>U decay chain in sediment IAEA-412.

Ivanovich, M., Harmon, R.S. (eds.), 1992. Uranium-series Disequilibrium: Applications to Earth, Marine and Environmental Sciences, Clarendon Press, Oxford  
Pham, M.K. et al., 2016. Certified reference materials for radionuclides in Bikini Atoll sediment (IAEA-410) and Pacific Ocean sediment (IAEA-412), Appl. Rad. Isot. 109 (2016) 101-104.



## Absorption measurements to design small radiation irradiator

Jeong Hee Han

Division of Environmental and Material Sciences, Korea Basic Science Institute, Cheongju-si, Chungcheongbuk-do, 28119, Republic of Korea

Keywords : irradiator, portable, calibration, monitoring  
Email : hanjh@kbsi.re.kr

Radioactive contamination and those possibilities for food or surroundings of living, although those don't have critical activity for their health and life, have been being cause of sensitive reaction by Korean ordinary people. Thus, the government and public organizations have been demanded to establish planning to manage the entire cycle for potential future crisis, including nuclear disaster or terrorism by them.

Our colleagues are studying to establish the action plan to protect water sources for public water service from nuclear disaster or terrorism, and this study is a part of monitoring system development for gamma radiation measurements in water. This monitoring system is operated independently with real-time data measurements, and the data are transferred to a control center.

Generally, there are no supplementary equipment in monitoring system itself to check their performance and status. If the standard radiation source to check these is equipped, the reliability of the data obtained from in situ measuring systems must be highly improved. The data reliability is very important to use for rapid response action by government or official institutes in the event of an emergency.

Our plan is to develop the radiation irradiator of small size, which is optimized to be equipped to in situ gamma radiation measurement system with easy handling. It must be structurally simple, not heavy and small, but perfect to shield gamma radiation from standard nuclides.

To calculate optimized shield thickness for each gamma-ray energy of typical radionuclides, the ratio between I, measured activity penetrating lead plates, and I<sub>0</sub>, no absorbance, was directly measured by HPGe gamma-ray detector with lead plate and multi-nuclides radioactive source for gamma-ray detector calibration (Fig. 1). The thickness of lead to reduce 99% of radiation beam was calculated by the equations derived from the ratio of I and I<sub>0</sub> (Table 1).

Because low energy the gamma-ray below 165.9 keV (Ce-139) can't be penetrated only 5 mm lead plate, the absorbed activity, I, can't be measured. The gamma-ray from Cr-51 (320.08 keV) is shielded more than 99% of radiation flux with only 10 mm lead.

For gamma-ray over 500 keV, more than 20mm thickness for lead material is needed to reduce more than 99% of incident gamma radiation and it makes total weight of shield system too heavy, thus the nuclides emitting high energy gamma are not adequate for our purpose. As a result, the nuclides emitting gamma-ray less than 500 keV

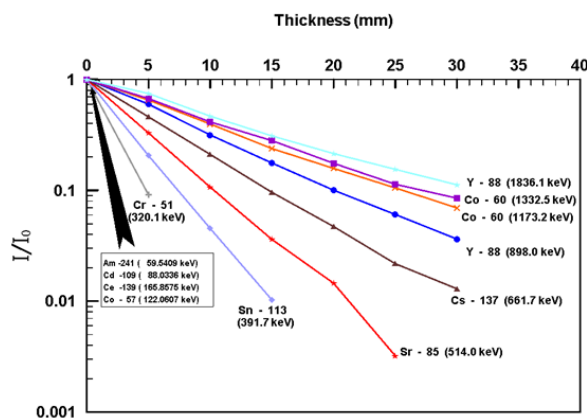


Figure 1. The relationships between the ratio I/I<sub>0</sub> and thickness of lead plate for gamma-ray energies.

Table 1. The slopes between the ratio, I/I<sub>0</sub> and thickness of lead plate at gamma-ray energies. The last column is thicknesses required to reduce 99% of incident radiation beam.

Nuclides	Half Life (day)	γ-ray energy (keV)	Slope of equation	Z <sub>99%</sub> (mm)
Am-241	158004	59.5409	-	< 5
Cd-109	461.9	88.0336	-	< 5
Co-57	271.8	122.0607	-	< 5
Ce-139	137.641	165.8575	-	< 5
Cr-51	27.704	320.08	-0.48	9.60
Sn-113	115.09	391.698	-0.30	15.11
Sr-85	64.85	514.005	-0.22	20.59
Cs-137	10976	661.657	-0.15	31.24
Y-88	106.63	898.036	-0.11	41.15
Co-60	1925.23	1173.228	-0.09	51.29
Co-60	1925.23	1332.492	-0.08	54.57
Y-88	106.63	1836.052	-0.07	61.48

are selected as appropriate radiation source for our irradiator.

The small radiation irradiator with optimized lead shield was designed with circular shield to minimize the weight of lead shield, and large prototype to test various functions was developed (Fig. 2).

Figure 2. Large prototype of irradiator to test mechanics of a moving lead shield and electronics.



This work was supported by grants from NST (CAP-15-07-KICT) and KBSI (C36701)

## Tritium in surface waters of Baltic, North and Norwegian Seas in 2016

O. Jefanova<sup>1</sup>, J. Mažeika<sup>1</sup>, R. Petrošius<sup>1</sup>, R. Paškauskas<sup>1,2</sup>

<sup>1</sup>State Research Institute Nature Research Centre, Akademijos Str. 2, LT-08412 Vilnius, Lithuania

<sup>2</sup>Klaipėda University, Herkaus Manto Str. 84, LT-92294, Klaipėda, Lithuania

Keywords: tritium, sea surface waters, liquid scintillation counting

Presenting author email: olga.jefanova@gamtostyrimai.lt

The radioactive isotope of hydrogen, tritium (<sup>3</sup>H or T, T<sub>1/2</sub>=12.32 years), included in the structure of water molecule, is almost an ideal water tracer and can be nowadays measured at very low concentration in water using electrolytic enrichment and low level liquid scintillation counting.

Natural <sup>3</sup>H concentrations in surface waters are of the order of 10<sup>-18</sup> tritium atoms per hydrogen atom. Therefore in hydrological studies <sup>3</sup>H concentrations are reported as TU (Tritium Units) which mean a tritium to hydrogen ratio [T]/[H] of 10<sup>-18</sup> what is equivalent to an activity of 0.118 Bq per litre H<sub>2</sub>O.

The average production rate of natural tritium is about 0.2 <sup>3</sup>H atoms/cm<sup>2</sup> sec leading to natural <sup>3</sup>H values in mean continental precipitation of about 5 TU (Craig and Lal, 1961). Shortly after the discovery of natural <sup>3</sup>H in the environment (von Faltings and Harteck, 1950), the <sup>3</sup>H as a tracer of water movement in natural water systems, including the ocean was considered (Grosse et al., 1951; Kaufman and Libby, 1954; Begemann and Libby, 1957).

Starting in the early 1950's <sup>3</sup>H from anthropogenic sources (mainly nuclear weapon tests) was added to the atmosphere what created the peak <sup>3</sup>H concentration of 5000 TU during spring 1963 in precipitation of northern hemisphere. This peak was slowly disappearing and nowadays yearly averaged <sup>3</sup>H concentration in precipitation is below 10 TU approaching to natural tritium level.

A surface water of ocean environment is low in <sup>3</sup>H content due to the long residence time of water in the ocean. In the ocean the maximum <sup>3</sup>H concentrations observed in the northern hemisphere surface waters are of the order of 1 TU.

This study presents the initial data on <sup>3</sup>H concentrations in surface marine waters along the profile from South eastern Baltic Sea towards North and Norwegian Seas and along the coastline of Iceland. (Figure 1). The samples were collected during marine research and educational voyage of Klaipėda University sailboat Brabander carried out in June-September 2016.

The variation of <sup>3</sup>H concentration along profile is shown in Figure 2. The averaged value of <sup>3</sup>H concentration in surface waters of Baltic Sea was 8.2 TU, similar in Kattegat (8.3 TU), and slightly higher in Skagerrak close to Norwegian coast (13.2 TU).

Regions with high runoff components or locations with nearly hosted big nuclear facilities could have elevated <sup>3</sup>H concentrations. Present day <sup>3</sup>H concentrations in distant from the coast surface waters of northern Atlantic (North and Norwegian Seas) are of the order of 0.6 TU (Figure 2).



Figure 1. Localization sampling stations within the voyage transect of sailboat Brabander of Klaipėda University (25-06 – 10-09, 2016)

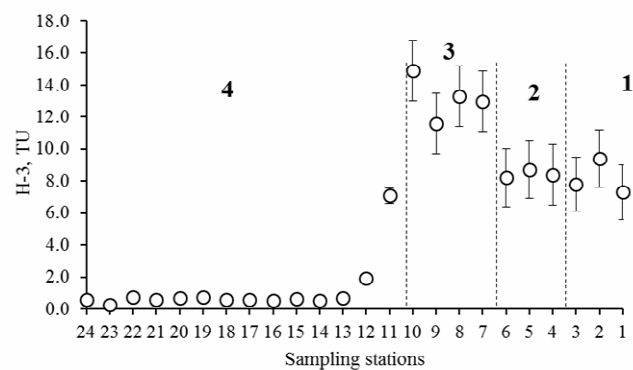


Figure 2. <sup>3</sup>H activity concentration in surface marine waters from west (Islandic coast) to east (South eastern Baltic) (1 – Baltic Sea, 2 – Kattegat, 3 – Skagerrak, 4 – North and Norwegian Seas)

- Begemann, F., Libby, W.F., 1957. Continental water balance, ground water inventory and storage times, surface ocean mixing rates and world-wide water circulation patterns from cosmic-ray and bomb tritium. *Geochim. Cosmochim. Acta*, 12, 277-296.
- Craig, H., Lal, L., 1961. The production rate of natural tritium. *Tellus*, XIII, 85-105.
- von Faltings, V., Harteck, P., 1950. Der Tritiumgehalt der Atmosphäre. *Zs. fuer Naturf.*, 5a, 438-439.
- Grosse, A.V., Johnston, W.M., Wolfgang, R.L., Libby, W.F., 1951. Tritium in Nature. *Science*, 113, 1-2.
- Kaufman, S., Libby, W.F., 1954. The natural distribution of tritium. *Phys. Rev.*, 93, 1337-1344.

## Sample preparation and AMS analysis of hydrogen isotopes at CENTA laboratory

J. Pánik, M. Ješkovský, J. Kaizer, I. Kontuľ, P.P. Povinec

Center for Nuclear and Accelerator Technologies (CENTA), Faculty of Mathematics, Physics and Informatics, Comenius University, Bratislava, 84248, Slovakia

Keywords: AMS, hydrogen isotopes, hydrogen isotopes ratio.

Presenting author email: jeskovsky@fmph.uniba.sk

Hydrogen consists of three naturally occurring isotopes. The most common stable isotope of hydrogen is protium ( $^1\text{H}$ ) with an abundance of 99.9885%; it can be found in the atmosphere in the form of  $\text{H}_2$ ,  $\text{H}_2\text{O}$  and  $\text{CH}_4$ . The second stable isotope of hydrogen is deuterium ( $^2\text{H}$  or D). In nature, one atom of deuterium is found in 6500 atoms of hydrogen ( $\text{D}/\text{H} = 1.5 \times 10^{-4}$ ) and its preferred form is HD, HDO or  $\text{CH}_3\text{D}$ . Due to various physico-chemical processes, the deuterium isotope content in various waters changes up to about 70%. The heaviest naturally occurring hydrogen isotope is unstable tritium ( $^3\text{H}$  or T) with the half-life of  $T_{1/2} = 12.32$  year; it beta-decays into  $^3\text{He}$  with maximum energy of 18.3 keV. Tritium itself has three main sources of origin: (i) natural production in the upper atmosphere in reactions of cosmic ray neutrons with nitrogen ( $^{14}\text{N} + n \rightarrow ^{12}\text{C} + \text{T}$ ); (ii) residual T activities still observed in the environment from nuclear weapons testing; (iii) and ongoing nuclear fuel cycle operations. Tritium in the atmosphere is in the form of HTO, HT and  $\text{CH}_3\text{T}$ , however, because of rapid oxidation of molecular hydrogen and very low production of tritiated methane, the significant atmospheric components are only tritiated molecules of water HTO, rarely  $\text{T}_2\text{O}$ . Tritium activities are commonly reported in terms of tritium units (TU), where 1 TU represents one  $^3\text{H}$  atom per  $10^{18}$  protium atoms, which is equivalent to the activity of 0.118 Bq/L.

Centre for Nuclear and Accelerator Technologies (CENTA) at the Comenius University in Bratislava operates a tandem laboratory, comprising of two ion sources (MC-SNICS and RF source), an ion injection system, a 3 MV Pelletron with nitrogen stripping column, and analyzers of accelerated ions. The laboratory was designed for Accelerator Mass Spectrometry (AMS) and Ion Beam Analysis (IBA) studies (Povinec et al., 2015).

AMS is one of the most sensitive techniques for detecting and quantifying different isotopes with a high precision in milligram-sized samples. AMS analyses of tritium have been applied in environmental studies, in biomedical research, as well as in clinical investigations (Roberts et al., 1994).

The presented work has focused on several aims. The first one has been studying preparation of hydride targets for AMS according to two step method. It is based on the reduction of water to hydrogen gas using zinc, followed by the reaction of the hydrogen gas with titanium at elevated temperature ( $\sim 500^\circ\text{C}$ ) to produce solid  $\text{TiH}_2$  (Chiarappa-Zucca et al., 2002). Robustness of

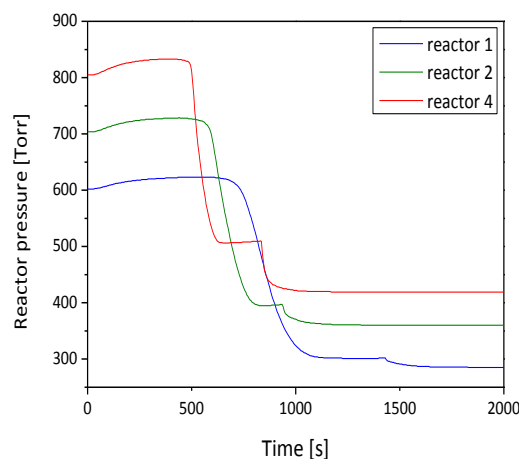


Figure 1. History of preparation of  $\text{TiH}_2$  from hydrogen gas and titanium powder.

the latter reaction has been successfully tested in our laboratory with the use of high purity hydrogen gas and Ti powder (Figure 1).

In order to optimize individual steps of the methodology, as well as its efficiency, the quality of prepared hydride targets has been evaluated. For this purpose, series of standard samples were prepared by dilution of water standards with known concentration of deuterium and tritium, and subsequently analysed in the tandem accelerator laboratory. Results of AMS measurements of the standards prepared in the form of  $\text{TiH}_2$  targets will be presented.

This work was supported by the EU Research and Development Operational Program funded by the ERDF (projects No. 26240120012 and 26240120026).

- Chiarappa-Zucca, M.L., Dingley, K.H., Roberts, M.L., Velsko, C.A., Love, A.H., 2002. Sample preparation for quantitation of tritium by accelerator mass spectrometry. *Anal. Chem.* 74, 6285-6290.
- Povinec, P.P., et al., 2015. A new IBA-AMS laboratory at the Comenius University in Bratislava (Slovakia). *Nucl. Instrum. Meth. B* 342, 321-326.
- Roberts, M.L., Velsko, C., Turteltaub, K.W., 1994. Tritium AMS for biomedical applications. *Nucl. Instrum. Meth. B* 92, 459-462.

## Anthropogenic $^{137}\text{Cs}$ on atmospheric aerosols in Bratislava and around Jaslovské Bohunice NPP, Slovakia

M. Ješkovský<sup>1</sup>, M. Lišťjak<sup>2,3</sup>, I. Sýkora<sup>1</sup>, O. Slávik<sup>2</sup> and P. P. Povinec<sup>1</sup>

<sup>1</sup>Department of Nuclear Physics and Biophysics, Comenius University, Bratislava, 84248, Slovakia

<sup>2</sup>VUJE, Inc., Trnava, 91864, Slovakia

<sup>3</sup>Faculty of Electrical Engineering and Information Technology, Slovak University of Technology, Bratislava 81219, Slovakia

Keywords: aerosols,  $^{137}\text{Cs}$ , nuclear power plant.

Presenting author email: jeskovsky@fmph.uniba.sk

Monitoring of radioactivity around nuclear power plants (NPP) has been very often discussed topic, especially after the Fukushima accident. In this study, variations of  $^{137}\text{Cs}$  concentrations in atmospheric aerosols have been investigated at few sampling sites in Slovakia. Most of the atmospheric  $^{137}\text{Cs}$  in this region comes, from the resuspension of the Chernobyl-derived  $^{137}\text{Cs}$ , as well as caesium produced during nuclear weapons testing, mainly during the 1960's (Kulan, 2006). The objective of this work has been to study local trends and variations of anthropogenic  $^{137}\text{Cs}$  in the atmosphere at few sampling sites in Slovakia. First one is around Jaslovské Bohunice NPP, where NPP A1 is under decommissioning after accident in 1977 and another NPP V1 is under decommissioning as part of the agreement for EU accession negotiations. The Jaslovské Bohunice NPP V2 is still in operation as Mochovce NPP, which was chosen for another sampling site. The results from those sites will be compared with the results obtained in Bratislava station.

Aerosol samples were collected on monthly basis in Katlovce (located about 5 km from the Jaslovské Bohunice NPP in north east direction) and in Regional Repository of Radioactive Waste in Mochovce. Katlovce samples are collected by Laboratory of NPP surroundings radiation control within NPP V2 monitoring plan and Mochovce samples are collected by repository personnel within its monitoring plan. Both samples were analysed by VUJE, Inc. Another sampling site is located in Bratislava, where atmospheric aerosols were collected by Department of Nuclear Physics and Biophysics of the Comenius University (Povinec et al., 2012a, b; Sýkora et al., 2017).

Aerosols collected at each station were analysed for trace concentrations of  $^{137}\text{Cs}$  by low-level gamma-ray spectrometry. Development of the  $^{137}\text{Cs}$  activity concentration in the air at Katlovce and Bratislava is presented in Figure 1. Seasonal variations in  $^{137}\text{Cs}$  concentrations can be clearly recognized in the Bratislava data (similarly as at other monitoring stations (e.g. Kulan, 2006; Bourcier et al., 2011), while in the Katlovce data such trend is hardly noticed. The  $^{137}\text{Cs}$  concentrations at both sites are in the same range (a few  $\mu\text{Bq}/\text{m}^3$ ) with slightly elevated values at Katlovce site, except the higher concentrations observed during March 2011, which are associated with transport of radioactive masses from the Fukushima accident (Povinec et al., 2012b). Local sources of  $^{137}\text{Cs}$  at each sampling site will

be discussed and contribution of the sources to overall activity will be estimated, however, the monitoring interval is too short to make some conclusions.

This work was supported by the EU Research and Development Operational Program funded by the ERDF (project No. 26240220004), and by the International Atomic Energy Agency (TC project RER7008).

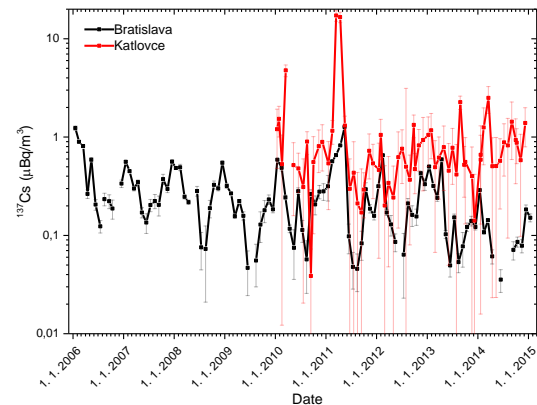


Figure 1. Concentrations of  $^{137}\text{Cs}$  in Bratislava and Katlovce.

- Bourcier, L., Masson, O., Laj, P., Pichon, J.M., Paulat, P., Freney, E., Sellegri, K., 2011. Comparative trends and seasonal variation of  $^7\text{Be}$ ,  $^{210}\text{Pb}$  and  $^{137}\text{Cs}$  at two altitude sites in the central part of France. *J. Environ. Radioact.* 102, 294-301.
- Kulan, A., 2006. Seasonal  $^7\text{Be}$  and  $^{137}\text{Cs}$  activities in surface air before and after the Chernobyl event. *J. Environ. Radioact.* 90, 140-150.
- Povinec, P.P., Holý, K., Chudý, M., Šivo, A., Sýkora, I., Ješkovský, M., Richtáriková, M., 2012a. Long-term variations of  $^{14}\text{C}$  and  $^{137}\text{Cs}$  in the Bratislava air - implications of different atmospheric transport processes. *J. Environ. Radioact.* 108, 33-40.
- Povinec, P.P., Sýkora, I., Holý, K., Gera, M., Kováčik, A., Brest'áková, L., 2012b. Aerosol radioactivity record in Bratislava/Slovakia following the Fukushima accident - A comparison with global fallout and the Chernobyl accident. *J. Environ. Radioact.* 114, 81-88.
- Sýkora, I., Holý, K., Ješkovský, M., Müllerová, M., Bulko, M., Povinec, P.P., 2017. Long-term variations of radionuclides in the Bratislava air. *J. Environ. Radioact.* 166, 27-35.



## Sequential scavenging of radiocesium and plutonium from seawater and their determination by $\gamma$ -spectrometry and AMS

J. Kaizer<sup>1</sup>, M. Aoyama<sup>2</sup>, J. Pánik<sup>1</sup>, P.P. Povinec<sup>1</sup>, I. Sýkora<sup>1</sup>, Y. Tateda<sup>3</sup>, F. Terrasi<sup>4</sup>

<sup>1</sup>Faculty of Mathematics, Physics and Informatics, Comenius University, 84248 Bratislava, Slovakia

<sup>2</sup>Institute of Environmental Radioactivity, Fukushima University, 1-1 Kanayagawa, Fukushima, Japan

<sup>3</sup>Environmental Science Research Laboratory, Central Research Institute of Electric Power Industry, 1646 Abiko, Abiko-shi, Chiba-ken, Japan

<sup>4</sup>CIRCE, 2nd University of Naples, 81100 Caserta, Italy

Keywords: radiocesium, plutonium, AMS,  $\gamma$ -spectrometry.

Presenting author email: kaizer@fmph.uniba.sk

Distribution of long-lived radionuclides, such as  $^{137}\text{Cs}$  and plutonium ( $^{239,240}\text{Pu}$ ) in the World Ocean has been studied since their potential for better understanding of various oceanographic processes had been discovered. The first data were reported in the early 1970s when the Geochemical Ocean Section Study (GEOSECS) was conducted. After that, more projects and expeditions followed (e.g., WOMARS, WOCE, SHOTS), resulting in acquiring of extensive data on the fate of radionuclides in the marine environment, though the need for an additional update of their distribution is still very actual, as a single unfortunate event, such as Fukushima Dai-ichi Nuclear Power Plant (FNPP1) accident, has been altering already obtained information.

$^{137}\text{Cs}$  with a half-life of 30.17 y is by far the most frequently studied anthropogenic radionuclide present in seawater. Because of its high abundance and high energy of the  $\gamma$ -rays (662 keV), it is usually measured by  $\gamma$ -spectrometry, although it emits beta-particles as well. Other advantageous property of  $^{137}\text{Cs}$  is possibility of direct measurements and a minimal risk of contamination during sample preparation. Recent developments in  $\gamma$ -spectrometry, mainly introduction of high-efficiency HPGe detectors and effective shielding (including underground operation), led to significant reduction of sample volume or even omitting the sample processing altogether; which has been common in analysis of  $^{137}\text{Cs}$  in raw surface waters with activity levels of  $\sim 10$  mBq/L.

Plutonium isotopes  $^{239}\text{Pu}$  ( $T_{1/2} = 24.1$  ky) and  $^{240}\text{Pu}$  ( $T_{1/2} = 6.56$  ky) noticeably became part of the environment as a consequence of nuclear weapon tests in the last century. Conventionally, their combined activity is measured by alpha-spectrometry, although only the development of advanced mass spectrometric techniques, such as inductively coupled plasma mass spectrometry (ICP-MS) and accelerator mass spectrometry (AMS), has enabled to determinate their separate concentrations and the atomic ratio. With a proper use of radioanalytical chemistry and AMS, one is able to reach detection levels of  $\sim 1$  fg levels (De Cesare et al., 2013), meaning that  $<10$  L of seawater should be sufficient for successful measurements.

If one is interested in determination of more than one radionuclide in a water sample, the water is usually divided into portions whose volumes depend on the respective radionuclide. In this work we used a different

approach for simultaneous processing of several samples, which originated from the coastal region of the FNPP1 (Fig. 1, green diamonds) from different time frames, based on the sequential scavenging of radiocesium and plutonium from the same volume, following the procedures described by Levy et al. (2011). In short, plutonium was co-precipitated on Fe hydroxide and separated by filtration, the remaining supernatant was then acidified and radiocesium was concentrated with the use of AMP. While the AMP was dissolved and radiocesium was measured by  $\gamma$ -spectrometry, the Fe precipitate was processed by anion exchange chromatography to prepare a target for AMS analysis of the  $^{240}\text{Pu}/^{239}\text{Pu}$  ratio. Moreover, the results from direct counting of  $^{137}\text{Cs}$  in seawater, sampled in the same area in 2015, shall be presented as well (Fig. 1, blue dots).

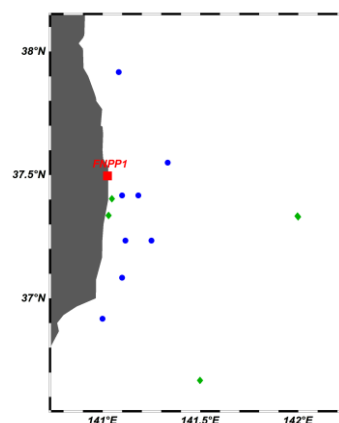


Figure 1. Locations of the sampling sites in the Fukushima coastal region.

This work was supported by the EU Research and Development Operational Program funded by the ERDF (projects No. 26240120012, 26240120026, and 26240220004), and by the International Atomic Energy Agency (TC project SLR9013).

De Cesare, M., et al., 2013. Actinides AMS at CIRCE and  $^{236}\text{U}$  and Pu measurements of structural and environmental samples from in and around a mothballed nuclear power plant. Nucl. Instrum. Meth. B 294, 152-159.

Levy, I., et al., 2011. Marine anthropogenic radiotracers in the Southern Hemisphere: New sampling and analytical strategies. Prog. Oceanogr 89, 120-133.

Povinec, P.P., Comanducci, J.-F., Levy-Palomo, I., 2008. IAEA-MEL's underground counting laboratory in Monaco. Appl. Radiat. Isotopes 61, 85-93.



## Development of mass spectrometry methods for determination of uranium and thorium in the $^{82}\text{Se}$ source of the SuperNEMO experiment

J. Kaizer<sup>1</sup>, S. Dulanská<sup>2</sup>, M. Bujdos<sup>2</sup>, P.P. Povinec<sup>1</sup> and O. Kochetov<sup>3</sup>

<sup>1</sup>Faculty of Mathematics, Physics and Informatics, Comenius University, 84248 Bratislava, Slovakia

<sup>2</sup>Faculty of Natural Sciences, Comenius University, 84215 Bratislava, Slovakia

<sup>3</sup>Dzhelepov Laboratory of Nuclear Problems, Joint Institute for Nuclear Research, Dubna, Russia

Keywords: SuperNEMO experiment, radiopurity, uranium, thorium.

Presenting author email: kaizer@fmph.uniba.sk

Unlike the two neutrino double beta-decay process, which has been already observed in the case of several isotopes (e.g.,  $^{48}\text{Ca}$ ,  $^{96}\text{Zr}$ ,  $^{100}\text{Mo}$ ), the neutrinoless double beta-decay with a reported upper half-life limit of the order of  $10^{24}$  y would violate the basic principles of the Standard Model (Arnold et al., 2015). The SuperNEMO experiment, which is based on the tracking and calorimetry techniques, shall be devoted exclusively to the search for this rare process. While following the fundamental concept of the NEMO-3 detector, several improvements have been applied for main components of the SuperNEMO detector.

In its full scale, the SuperNEMO experiment will comprise twenty planar modules, identical in height, length and width. The source foil, made of enriched and purified  $^{82}\text{Se}$  powder, will be situated in the middle of each module. Tracking chambers and calorimeters for energy and time of flight measurements will be placed at both sides of the module. The detector is planned to be surrounded by water and iron shielding to lower the background from neutrons and gamma rays, respectively. It is expected that the first module, Demonstrator, will start operation in 2017.

One of the biggest challenges in the current stage of the development of the SuperNEMO experiment is to reduce the background radiation to minimal values (Povinec, 2017). The constraints of the experiment are determined by external and internal sources of background. As already stated, suppression of the external background can be achieved by effective shielding, however, diminishing of the internal radiation is more complicated and requires to use construction materials of highest radiopurity. The most sensitive parts of the SuperNEMO detector include inner components of the tracker, the isotope source and foil supporting the source itself.

From the point of view of internal contamination, there are two beta emitters,  $^{214}\text{Bi}$  and  $^{208}\text{Tl}$ , which are especially dangerous as energy of beta-electrons of these short-lived radionuclides is above the double beta-decay energy of the  $^{82}\text{Se}$  source ( $\sim 3$  MeV). While  $^{214}\text{Bi}$  is part of the uranium decay chain,  $^{208}\text{Tl}$  is a progeny of  $^{232}\text{Th}$ .

First measurements of  $^{238}\text{U}$  and  $^{232}\text{Th}$  in construction materials (Cu) and the  $^{82}\text{Se}$  source of the SuperNEMO experiment with the use of radiochemical neutron activation analysis (RNAA) have been recently conducted by Kučera et al. (2017). Although RNAA showed promising results (and its sensitivity can still be enhanced), further radiopurity measurements will

probably need to exploit mass spectrometric techniques, such as inductively coupled plasma mass spectrometry (ICP-MS) or accelerator mass spectrometry (AMS; Table 1).

Table 1. Estimated detection limits (in nBq) for analysis of  $^{238}\text{U}$  and  $^{232}\text{Th}$  in construction materials using different analytical techniques.

Nuclide	RNAA <sup>a</sup>	ICP-MS <sup>b</sup>	AMS <sup>c</sup>
$^{232}\text{Th}$	80	3	0.2
$^{238}\text{U}$	200	10	0.1

<sup>(a)</sup> estimated from Kučera et al., 2017, <sup>(b)</sup> LaFerriere et al., 2015, <sup>(c)</sup> Famulok et al., 2015

Determination of long-lived radionuclides by ICP-MS or AMS is not straightforward and generally requires pre-concentration of the radionuclides of interest from the sample matrix. Here we shall present a simple method for separation of  $^{238}\text{U}$  and  $^{232}\text{Th}$  from the  $^{82}\text{Se}$  powder which will be used in the SuperNEMO experiment. The method has been developed on the basis of anion exchange / extraction chromatography and tested on several modelled samples prepared from high purity selenium and natural uranium and thorium. Preliminary results of measurements of  $^{238}\text{U}$  and  $^{232}\text{Th}$  in the  $^{82}\text{Se}$  source by mass spectrometric techniques shall be presented as well.

This work was supported by the Slovak Research and Development Agency under the contract No. APVV-15-0576, and by the EU Research and Development Operational Program funded by the ERDF (projects No. 26240120012 and 26240120026).

Arnold, A., et al., 2015. Results of the search for neutrinoless double- $\beta$  decay in  $^{100}\text{Mo}$  with the NEMO-3 experiment. *Phys. Rev. D* 92, 72011.

Famulok, N. et al., 2015. Ultrasensitive detection method for primordial nuclides in copper with Accelerator Mass Spectrometry. *Nucl. Instrum. Meth. Phys. B* 361, 193–196.

Kučera, J., Kamenik, J., Povinec, P.P., 2017. Radiochemical separation of mostly short-lived neutron activation products. *J. Radioanal. Nucl. Chem.* 311, 1299–1307.

LaFerriere, B.D. et al., 2015. A novel assay method for the trace determination of Th and U in copper and lead using inductively coupled plasma mass spectrometry. *Nucl. Instrum. Meth. Phys. A* 775, 93–98.

Povinec, P.P., 2017. Background constrains of the SuperNEMO experiment for neutrinoless double beta-decay searches. *Nucl. Instrum. Meth. A*, <http://dx.doi.org/10.1016/j.nima.2016.06.104>.

## Adsorptive removal of strontium-90 onto ordered granular mesoporous carbon

Yohan Kim<sup>1</sup>, Jung-Hyup Lee<sup>1</sup>, Sangmyeon Ahn<sup>1</sup>, Heechul Choi<sup>2</sup> and Jinyong Park<sup>1\*</sup>

<sup>1</sup> Department of Radiation Protection and Radioactive Waste Safety, Korea Institute of Nuclear Safety, 62 Gwahak-ro, Yuseong-gu, Daejeon, 34142, Republic of Korea

<sup>2</sup>School of Environmental Science and Engineering, Gwangju institute of Science and Technology, 123 Cheomdangwagi-ro, Buk-gu, Gwangju, 61005, Republic of Korea

Keywords: Adsorption, Waste management, Granular mesoporous carbon, radionuclide.

Presenting author email: john@kins.re.kr

Radioactive materials produced from nuclear reactions have been considered as widespread contaminants to threaten human health and environment due to their radioactivity in aqueous phase. Among them, strontium-90 is selected as a target material in this study due to a typical fission product and one of important radioactive isotopes of strontium with a half-life of 28 years (Kaçan and Kütahyalı, 2012). It is exposed from nuclear power plant and ubiquitously presented in water. To protect human health and environment, it is necessary to remove strontium-90 from water. Adsorptive removal is one of the most effective technology for separation and purification of radiostrontium from water due to its simplicity and convenience compared to other water treatment processes (Kim et al., 2014). Porous carbon material is one of versatile and excellent adsorbents due to its high surface area and pore characteristic. Among carbonaceous adsorbents, ordered granular mesoporous carbon (GMC) synthesized by facile method was used in this study for removal of strontium-90 in water environment (Kim et al., 2016). Kim et al. reported that GMC with three dimensional spherical mesoporous symmetry showed higher adsorption capacity and kinetics of organic contaminant than granular activated carbon due to ordered mesoporous structure and excellent textural properties.

In this study, GMC is successfully synthesized by using powdered mesoporous carbon and organic binders through a one-step and economical granulation approach. The physical properties of synthesized carbon adsorbents were calculated by the BET and BJH methods and presented in Table 1. The textural properties of prepared GMC revealed that GMC showed the similar pore structures and characteristics compared to powdered mesoporous carbon after granulation process. Characterization results were obtained by scanning electron microscope, X-ray diffraction, as well as surface and porosity analysis. This result indicated that GMC had more available adsorption sites and higher adsorption capacity of target compound than GAC.

Batch adsorption experiments for removal of strontium-90 were carried out onto GMC and GAC to evaluate the adsorption affinity by using sea water collected in South Korea. Adsorption characteristics of strontium-90 revealed that synthesized GMC showed better adsorption capacity and kinetics than GAC due to ordered mesoporous structure and excellent physical properties such as BET surface area and pore volume. Therefore,

this study indicates that GMC could be a promising adsorbent for removal of radioactive materials exposed from the radioactive waste in aqueous phase.

Table 1. Physical properties of synthesized mesoporous carbon adsorbents

Sample	BET (m <sup>2</sup> /g)	PV (cm <sup>3</sup> /g)	APS (nm)
GMC <sup>1</sup>	900.84	1.90	8.4
GAC <sup>2</sup>	1015.87	0.55	2.16
PMC <sup>3</sup>	960	1.42	6.1

BET, PV, and APS indicate BET surface area, total pore volume, and average pore size, respectively.

<sup>1</sup>GMC: granular mesoporous carbon, <sup>2</sup>GAC: commercial granular activated carbon, and <sup>3</sup>PMC: powdered mesoporous carbon.

This work has been supported by the R&D program funded by Korea Institute of Nuclear Safety.

Kaçan, E., Kütahyalı, C. 2012. Adsorption of strontium from aqueous solution using activated carbon produced from textile sewage sludges. *J. Anal. Appl. Pyrol.* 97, 149-157.

Kim, Y., Bae, J., Park, J., Suh, J., Lee, S., Park, H., Choi, H. 2014. Removal of 12 selected pharmaceuticals by granular mesoporous silica SBA-15 in aqueous phase. *Chem. Eng. J.* 256, 475-485.

Kim, Y., Bae, J., Park, H., Suh, J., Yoo, Y., Choi, H. 2016. Adsorption dynamics of methyl violet onto granulated mesoporous carbon: Facile synthesis and adsorption kinetics. *Water Res.* 101, 187-194.

## Uptake of neptunium and technetium by bacteria isolated from a nutrient-poor boreal bog

J. Knuutinen<sup>1</sup>, M. Bomberg<sup>2</sup>, J. Lehto<sup>1</sup> and M. Lusa<sup>1</sup>

<sup>1</sup>Department of Chemistry, Radiochemistry, University of Helsinki, 00014 Helsinki, Finland.

<sup>2</sup>VTT Technical Research Center of Finland, 02044 Espoo, Finland

Keywords: neptunium, technetium, uptake, bacteria.

Presenting author email: jenna.knuutinen@helsinki.fi

The potentially high mobility of neptunium (<sup>237</sup>Np) and technetium (<sup>99</sup>Tc) can present concerns for long-term safety of spent nuclear fuel disposal. Only limited data is available about the ability of microorganisms to remove Np and Tc from solutions. Previously, some Fe(III)-reducing bacteria have shown to be able to reduce soluble Np(V) (NpO<sub>2</sub><sup>+</sup>) into Np(IV), which in turn may be removed from the solution as phosphate complexes by for example *Citrobacter* sp. In aqueous solutions and under oxidizing conditions the most stable species of technetium is TcO<sub>4</sub><sup>-</sup>. TcO<sub>4</sub><sup>-</sup> is highly mobile and behaves similarly to other oxyanions (e.g. sulphate, selenite) and is therefore susceptible for various microbiological processes. In the boreal regions, nutrient-poor bogs provide unique growth environments for distinct microbial populations, but only limited knowledge about their metabolism is available. In this study, bacterial strains belonging to the genera *Peaenibacillus* (KV-0-YR, IV-0-L and VV-0-L), *Massilia* (K5-6-BS and P5-6-BD), *Burkholderia* (V4-5-SB and RP-0-BL) and *Methylobacterium* (P4-5-LR) were isolated from a boreal bog, identified using 16S rRNA gene sequencing and their ability to remove <sup>237</sup>Np and <sup>99</sup>Tc from solution was examined using batch experiments (in 1 % Yeast extract and 1 % Tryptone, at 20°C, incubation time 7 or 14 days). In addition, previously isolated bacterial strains, capable of selenite and iodide removal, *Pseudomonas* (PS-0-L and T5-6-I), *Peaenibacillus* (B6-7-W) and *Burkholderia* (K5-6-SY) (Lusa et al., 2016) were used.

All studied isolates, unaccompanied by other bacteria, removed Np(V) from the nutrient solutions, depending on used broth and incubation time (Figure 1). The highest Np uptake was shown by the two *Burkholderia* strains V4-5-SB and RP-0-BL. However, the maximum Np uptake of previously isolated *Burkholderia* K5-6-SY was significantly lower, which indicates notable variation in the Np uptake ability among different species of the same bacterial genus.

High Np uptake was in addition observed for the *Pseudomonas* strains PS-0-L and T5-6-I. For PS-0-L, the maximum uptake was found in 1% Yeast extract, but for T5-6-I in 1% Tryptone. In general, *Pseudomonas* sp. have broad metabolic versatility and genetic plasticity. Previously we found that the PS-0-L and T5-6-I strains differ significantly in the utilization patterns of different substrates tested by the RapID system (Lusa et al., 2016), which may also affect their ability to remove Np under variable nutritional conditions.

In addition to Np removal, all studied bacteria were able to remove Tc from solutions, although some more variation between strains and broths was observed

(Figure 1). In consistence with Np uptake, *Burkholderia* RP-0-BL showed high Tc retention, while the Tc uptake of *Burkholderia* V4-5-SB was ten times lower. Highest Tc uptake ability was however observed in *Peaenibacillus* VV-0-L in 1 % Yeast extract, with a maximum K<sub>d</sub> value of 28 000 L/kg DW. Compared to other *Peaenibacillus* strains KV-0-YR (max K<sub>d</sub> 300 L/kg DW) and IV-0-L (max K<sub>d</sub> 360 L/kg DW), which had corresponding substrate utilization patterns in the RapID test, Tc uptake was 80-fold higher in *Peaenibacillus* VV-0-L.

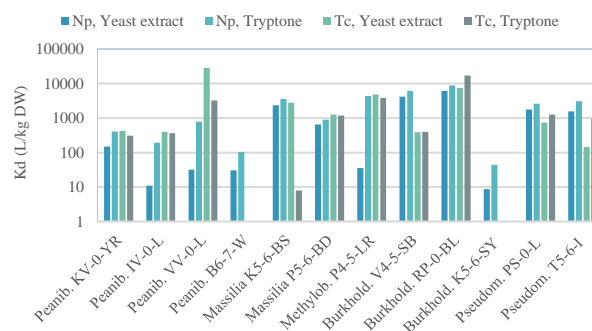


Figure 1. Uptake of Np and Tc by bacterial strains in Yeast extract and Tryptone (incubation time 7d)

These differences may reflect distinct uptake mechanisms (reduction, biosorption, detoxification) among these bacteria. Energy-independent uptake mechanisms (e.g. direct biosorption on cell wall functional groups) would be affected by the pH of the solution, as pH affects both the protonation of functional groups, as well as the speciation of Np and Tc. However, in this study, varying pH did not significantly influence the uptake for either nuclide (Figure 2). This may refer to other uptake mechanisms, involving membrane proteins or enzymes, on which further research is on-going in our laboratory at the moment.

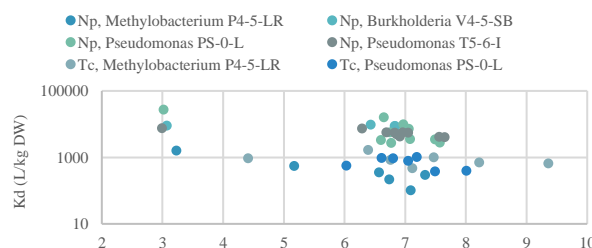


Figure 2. Np and Tc uptake as a function of pH

Lusa M., Lehto J., Aromaa H., Knuutinen J., Bomberg M. 2016. Uptake of radioiodide by *Peaenibacillus* sp., *Pseudomonas* sp., *Burkholderia* sp. and *Rhodococcus* sp. isolated from a boreal, nutrient-poor bog. *J. Environ. Sci.* 44, 26-37.

## Radiocarbon in wines: a useful tracer for studying environmental processes and wine dating

P. P. Povinec, I. Kontuľ, J. Kaizer, A. Šivo, M. Richtáriková

Center for Nuclear and Accelerator Technologies (CENTA), Faculty of Mathematics, Physics and Informatics, Comenius University, Bratislava, 84248, Slovakia

Keywords: Radiocarbon, wine, bomb effect, Suess effect, wine dating

Presenting author email: povinec@fmph.uniba.sk

Annually produced and well-preserved wines have good potential for studying radiocarbon variations in the environment, similarly e.g. to annual tree-ring samples, although the time span for wines is much shorter. Radiocarbon in wines has been used in the past for studying radiocarbon variations associated with:

- (i) 11-yr solar cycle during the 20<sup>th</sup> century. Cosmogenic radiocarbon has been produced in the atmosphere by neutrons originating in interactions of galactic cosmic-ray protons with nitrogen and oxygen. As the flux of galactic cosmic-ray particles has been fluctuating during the 11-yr solar activity due to its modulation by solar wind, it has been expected that radiocarbon should follow these variations. The radiocarbon 11-yr solar cycle was discovered in well-preserved Georgian wines from Tbilisi, although the amplitudes of the radiocarbon variations during various solar cycles was very small (in average about 0.4 %, Burchuladze et al., 1980).
- (ii) bomb effect – a large, about 100 % increase in atmospheric/biospheric <sup>14</sup>C concentrations observed in 1963/1964 due to atmospheric tests of nuclear bombs carried out mostly in 1961 and 1962. As contributions from nuclear bomb tests carried out later were negligible, the bomb peak and subsequent decline in the radiocarbon concentration has been used for studying radiocarbon exchange processes in stratosphere-troposphere, troposphere-biosphere, troposphere-ocean, as well as for dating of wines (Burchuladze et al., 1989).
- (iii) Suess effect – a relative decrease in radiocarbon concentration in the atmosphere and biosphere due to releases of fossil fuel CO<sub>2</sub> to the air by industrial activities (Povinec et al., 1986). Radiocarbon thus became a strong tool to study climate change effects on the local, regional and global scales (Levin et al., 2004; 2008).

The present work has been focused on radiocarbon studies of Slovak wines with the aim to develop a radiocarbon bomb curve for the central Europe corrected for the Suess effect, so exact dating of wines could be possible. Any artificial contributions to wine during its production or storage could be thus discovered, as a clean wine without any additives should carry out the radiocarbon concentration of the respective year of its production.

Well-preserved wines originating from eastern Slovakia and produced during the last century have been used in this study. It has been carefully checked that the

wines stored in bottles have been well closed so no exchange between the wine and the air could be possible. For calibration purposes recent wines produced in the south-western and southern Slovakia has also been used, as well as wines from Austria, Hungary, Bavaria, Slovenia and Italy.

Wine samples without sediments were carefully distilled and checked for ethylalcohol content. The alcohol samples were then slowly combusted in a stream of oxygen. The produced CO<sub>2</sub> was either converted to methane (Povinec, 1972) and counted in proportional counters (Povinec, 1978), or graphite samples were prepared for accelerator mass spectrometry (Povinec et al., 2016). A comparison of obtained radiocarbon concentrations in wines with atmospheric and tree-ring data will be presented and discussed.

This work was supported by the EU Research and Development Operational Program funded by the ERDF (projects No. 26240120012, 26240120026 and 26240220004).

- Burchuladze, A.A., Pagava, S.V., Povinec, P., Togonidze, G.I., Usacev, S., 1980. Radiocarbon variations with the 11-year solar cycle during the last century. *Nature* 287, 320-322.
- Burchuladze, A.A., Chudý, M., Eristavy, I.V., Pagava, S.V., Povinec, P., Sivo, A., Togonidze, G.I., 1989. Anthropogenic <sup>14</sup>C variations in atmospheric CO<sub>2</sub> and wines. *Radiocarbon* 31, 771-776.
- Levin, I., Kromer, B., 2004. The tropospheric <sup>14</sup>CO<sub>2</sub> level in mid-latitudes of the northern hemisphere (1959-2003). *Radiocarbon* 46, 1261-1272.
- Levin, I., Samuel Hammer, S., Kromer, B., Meinhardt, F., 2008. Radiocarbon observations in atmospheric CO<sub>2</sub>: Determining fossil fuel CO<sub>2</sub> over Europe using Jungfraujoch observations as background. *Sci. Total Environ.* 391, 211-216.
- Povinec P. 1972. Preparation of methane gas filing for proportional <sup>3</sup>H and <sup>14</sup>C counters. *Radiochem. Radioanal. Lett.* 9, 127-35.
- Povinec P. 1978. Multiwire proportional counters for low-level <sup>14</sup>C and <sup>3</sup>H measurements. *Nucl. Instrum. Meth.* 156, 441-445.
- Povinec, P., Chudý, M., Sivo, A., 1986. Anthropogenic radiocarbon: past, present and future. *Radiocarbon* 28, 668-672.
- Povinec, P.P., et al., 2016. Recent results from the AMS/IBA laboratory at the Comenius University in Bratislava: preparation of targets and optimization of ion sources. *J. Radioanal. Nucl. Chem.* 307, 2101-2108.



## Dependences of heavy metals sorption on nano-magnetic sorbents

I. Kulakauskaitė, G. Lujanienė, D. Valiulis

SRI Center for physical sciences and technology, Savanorių ave. 231, LT-02300 Vilnius, Lithuania

Keywords: heavy metals, sorption, nanomaterials

Presenting author email: ieva.kulakauskaite@gmail.com

Water pollution has recently turned into a main global problem due to the rapid development of the modern industrial activities. The use of metals and chemicals results in large quantities of wastes. Heavy metals are contaminants with the serious potential threat to living organisms and the whole ecological system, even at low concentrations in the environment.

Today many methods, including chemical precipitation, coagulation, ion exchange, filtration, and electrochemical technologies, have been proposed for the removal of heavy metals and harmful radionuclides (e.g.  $^{64}\text{Cu}$ ,  $^{67}\text{Cu}$ ,  $^{59}\text{Ni}$ ,  $^{63}\text{Ni}$ ,  $^{58}\text{Co}$  and  $^{210}\text{Pb}$ ) and/or pre-concentrations from various water solutions. However, their applications have been restricted by limitations; for example, precipitation or coagulation techniques require various chemicals and involve high sludge volumes while filtration or electrochemical technologies require relatively large capital investments and electricity supplies.

Adsorption is a simple, effective, and economical method for the heavy metal removal. Many adsorbents have been used for that purpose. Price, availability, adsorption capacity and strong affinity to pollutants are limiting factors for sorbent application. Nano-materials in the form of nano-metal oxides have been used for the heavy metal removal and extraction from aqueous solutions because of their high surface area, efficient adsorption capacity, incorporated selectivity, fast equilibration time and excellent recovery values. Magnetite ( $\text{Fe}_3\text{O}_4$ ) nano-composites have great potential for water treatment. These materials are non-toxic, hydrophilic, chemically stable and can be isolated from medium using the external magnetic field (Kumari et.al. 2015).

The aim of this study is to synthesize nano sorbents based on magnetite and Prussian blue and to use them to remove heavy metals from water solutions.

Magnetite nano-particles are synthesized by the co-precipitation method, using ferric and ferrous salts in basic medium. Magnetic graphene oxide was synthesized via a chemical deposition of  $\text{Fe}_3\text{O}_4$  nanoparticles onto graphene oxide (Yunjin et. al. 2012). Magnetic Prussian blue (PB) and magnetic Prussian blue-graphene oxide composites were prepared by anchoring  $\text{Fe}_3\text{O}_4$  magnetic nanoparticles onto a large surface area of GO and in situ coating  $\text{Fe}_3\text{O}_4$  magnetic nanoparticles with PB (Hongjun et.al. 2014).

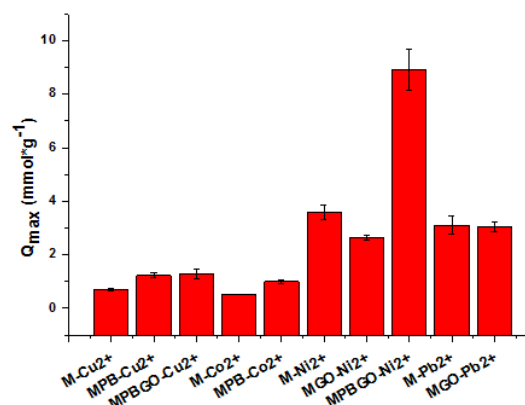


Figure 1.  $Q_{\max}$  values for nano-magnetic sorbents.

Sorption experiments were performed with the initial concentration of 50 - 700 mg L<sup>-1</sup> of Cu, Co, Ni, Pb and 1g ·L<sup>-1</sup> dosage (1:1000 g/ml ratio) of adsorbent. The pH of solution was adjusted with 0.1M NaOH and HCl. The reaction mixture of metal solution and adsorbent was shaken for the time intervals of 5 – 1440 min at room temperature and pH was controlled using a pH –meter WTW inoLab Multi Level 1 m. The sorbed metal ions on the surface of magnetic nano-sorbent were separated from solution by the action of an external magnet.

The potential applicability of designed nano-sorbents was further studied and evaluated using mix solution with all four heavy metals. The ratio of Cu (II), Co (II), Ni (II) and Pb (II) in solution was 1:1:1:1.

To develop sorbents for water treatment in natural aqueous systems, to check the interference of others ions on the removal efficiency adsorption experiments were carried out using seawater collected in the Baltic Sea at the state monitoring stations. A known weight of nano-sorbents was added to the samples and shaken at room temperature for 72h. Magnetic particles were removed using a magnet and solutions were analyzed for their residual metal concentration.

M. Kumari, C. Pittman, D. Mohan. *Journal of Colloid and Interface Science*. 442 2015 120-132  
 Y. Yunjin, M. Shiding, L. Shizhen, *Chemical Engineering Journal* 184 2012 326– 332  
 Y. Hongjun, L. Haiyan, Z. Jiali Zhai, *Chemical Engineering Journal* 246 2014 10–19



## Accumulation of $^{239+240}\text{Pu}$ and $^{210}\text{Po}$ in the marine biota living in the seas around Korean Peninsula

S.H. Kim, H. Lee, B.E. Cho and G.H. Hong

Marine Radionuclide Research Center, Korea Institute of Ocean Science & Technology, Ansan, 15627, R. Korea

Keywords:  $^{239+240}\text{Pu}$ ,  $^{210}\text{Po}$ , marine biota, Korea.

Presenting author email: hmlee@kiost.ac.kr

The activity concentrations of  $^{239+240}\text{Pu}$  and  $^{210}\text{Po}$  were determined in the marine biota of several tropic levels living in the seas around Korean Peninsula to understand the bioaccumulation of these alpha emitting radionuclides. Marine biota including plankton, macroalgae, crustaceans, mollusks, surface and bottom water dwelling fishes, and cephalopods were collected in 2014. The body concentrations were determined as a whole and in their skin, muscle and internal organs in some samples.

The activity concentrations of  $^{239+240}\text{Pu}$  in collected biota were the highest in plankton [20 - 300  $\mu\text{m}$ ] with  $58 \pm 10$  mBq/kg·ww and were exhibited in the descending order of plankton [20 - 300  $\mu\text{m}$ ] > plankton [ > 300  $\mu\text{m}$ ] ( $13 \pm 4.0$ ) > abalone ( $5.4 \pm 1.2$ ) > sea mustard ( $0.80 \pm 0.06$ ) > laver ( $0.64 \pm 0.08$ ) > prawn ( $0.50 \pm 0.20$ ) > mackerel ( $0.30 \pm 0.02$ ) > anchovy ( $0.27 \pm 0.10$ ) > squid ( $0.26 \pm 0.06$ ) > flat fish ( $0.24 \pm 0.13$ ) : (unit: mBq/kg·ww). This order indicates that  $^{239+240}\text{Pu}$  is highly accumulated in plankton but the accumulation factor does not increase in upper tropic levels. The activity concentrations of  $^{210}\text{Po}$  in plankton were  $140 \pm 50$  in the 20 - 300  $\mu\text{m}$  plankton fraction and  $110 \pm 2$  Bq/kg·ww in the > 300  $\mu\text{m}$  plankton fraction, respectively. The activity concentration of  $^{210}\text{Po}$  in the whole body of anchovy preying on plankton was in the order of  $390 \pm 2$  Bq/kg·ww and it was higher than that in plankton. The activity concentrations of  $^{210}\text{Po}$  in the muscle tissues of squid, abalone, prawn, mackerel and flat fish were  $8.6 \pm 2.0$ ,  $2.9 \pm 0.9$ ,  $2.8 \pm 0.2$ ,  $0.8 \pm 0.1$  and  $0.5 \pm 0.1$  Bq/kg·ww. However, the concentrations of  $^{210}\text{Po}$  in the internal organ tissues of these species were two or three orders of magnitude higher than reported in their muscle tissues. This suggests that  $^{210}\text{Po}$  transferred through food chain is not easily accumulated in muscle but is highly so in internal organ tissues.

The concentration factors of  $^{239+240}\text{Pu}$  for plankton and macroalgae for biota samples in this study were lower by one order of magnitude than the recommended value (IAEA, 2004). The concentration factors of  $^{210}\text{Po}$  for plankton and macroalgae in this study were comparable to the recommended value of IAEA (2004). But the concentration factor of  $^{210}\text{Po}$  for anchovy in this study was higher by two orders of magnitude than the recommended value for surface fish (IAEA, 2004).

This work was funded by grants from the Korea Institute of Ocean Science & Technology (PE99403) and the Ministry of Food and Drug Safety (PG48320).

IAEA, 2004. Sediment Distribution Coefficients and Concentration Factors for Biota in the Marine Environment. TECHNICAL REPORTS SERIES No. 422, Vienna.

## Application of Prussian blue based nano-composites for radiocesium pre-concentration from seawater

Agnė Leščinskytė, Galina Lujanienė, Sergej Šemčiuk, Kęstutis Mažeika, Remigijus Juškėnas

Center of physical sciences and technology, Savanorių ave. 231 LT-02300 Vilnius

Keywords: radiocesium, seawater, nano-composites, Prussian blue.

Presenting author email: lescinskyte.agne@gmail.com

Radiocesium is one of the toxic radionuclides which was released into the environment (e.g., after nuclear accidents at the Chernobyl nuclear power and the Fukushima nuclear power plant in March 2011) and is present in the radioactive waste. In order to protect the environment from radioactive Cs isotopes modern, efficient and cost-effective technologies are required. One of the possible ways of removing and pre-concentration of radioactive Cs from contaminated liquid media and environmental samples is based on the application of sorption techniques.

Various sorbents and technologies were applied for decontamination of water from Cs isotopes and the Cs pre-concentration in environmental samples. The most specific adsorbents suitable for seawater samples were reported to be based on ammonium molybdophosphate (AMP) and Prussian blue (PB). AMP was used for  $^{137}\text{Cs}$  extraction from unfiltered and filtered seawater and the reported chemical yield of  $^{137}\text{Cs}$  was approximately 80% (Park et al, 2008). The porous silica based nano-composites containing PB nano-particles ( $\text{Co}^{2+}/[\text{Fe}(\text{CN})_6]^{3-}$ , 10 nm) showed maximum adsorption capacities of  $Q_{\text{max}} = 0.4\text{-}1.3$  mmol/g for  $\text{Cs}^+$  ions from contaminated solutions simulating the effluents of the Fukushima reactors (Delchet et al., 2012).

The aim of this work was to synthesize and characterize adsorbents as well as investigate sorption of radiocesium to Magnetic Prussian blue (MPB), Prussian blue magnetic graphene oxide (PBMGO) and Prussian blue graphene oxide (PBGO) from various solutions including seawater samples collected in the Baltic sea.

Graphite oxide (GO) synthesis was performed from the graphite powder (<20 $\mu\text{m}$  synthetic, Sigma-Aldrich, Switzerland) using the modified Hummer's method. The PBMGO sorbent was synthesized by mixing together aqueous solutions of GO and magnetite, which were dispersed ultrasonically. The resulting brown precipitate was separated with a magnet and re-dispersed in water. Then aqueous solution of  $\text{FeCl}_3$  and aqueous solution of  $\text{K}_4[\text{Fe}(\text{CN})_6]$  were slowly introduced into the mixture. The obtained precipitate was washed with water and dried at 50° C. MPB, MPBGO and PBGO were characterized by Mössbauer spectroscopy, X-ray diffraction (XRD) and Transmission electron microscopy (TEM). The batch technique was used to study the adsorption of elements and three sets were conducted for each experiment. In experiments with Cs, in addition to CsCl solutions, 100 mg L $^{-1}$  of CsCl in seawater (35‰) and natural seawater from the

State monitoring stations located in the Baltic Sea were used.

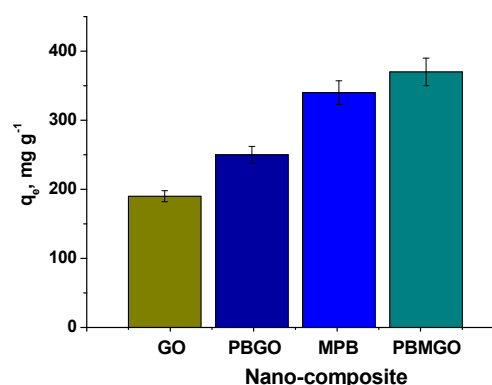


Figure 1. Maximum adsorption capacities of Cs on nano-composites.

The maximum adsorption capacities of Cs(I) on GO, MPB, PBGO and PBMGO varied from 190 to 370 g g $^{-1}$  (Figure 1). The lowest adsorption capacity was found for GO while the highest one was obtained for PBMGO. The obtained Langmuir and Freundlich constants indicated the dominating physisorption mechanism and favorable adsorption conditions. The competitive adsorption experiments have indicated that the MPBGO nano-composite can effectively adsorb Cs even at high concentration of  $\text{K}^+$ ,  $\text{Na}^+$  and other ions naturally occurring in seawater. The efficiency of MPBGO for Cs(I) sorption from natural seawater was close to 100%.

Delchet C., Tokarev A., Dumail X., Toquer G., Barré Y., Guari Y., Guerin Ch., Larionova J., Grandjean A. 2012. Extraction of radioactive cesium using innovative functionalized porous materials. *RSC Adv.* 2, 5707-5716.

Park J.H., Chang B.U., Kim Y.J., Seo J.S., Choi S.W., Yun J.Y. 2008. Determination of low ( $^{137}\text{Cs}$ ) concentration in seawater using ammonium 12-molybdophosphate adsorption and chemical separation method. *J Environ Radioact.* 99(12), 1815-8.

## Activity profiles of $^{226}\text{Ra}$ and $^{228}\text{Ra}$ in the euphotic zone of southwestern East/Japan Sea

P. Lindahl<sup>1</sup>, M. Eriksson<sup>1</sup>, Suk Hyun Kim<sup>2</sup> and Gi Hoon Hong<sup>2</sup>

<sup>1</sup>Swedish Radiation Safety Authority, Stockholm, SE-171 16, Sweden

<sup>2</sup>Korea Institute of Ocean Science and Technology, Ansan, Republic of Korea

patric.lindahl@ssm.se

Distributions of the naturally occurring radionuclides  $^{226}\text{Ra}$  and  $^{228}\text{Ra}$  in the water column were studied at the southwestern part of the East/Japan Sea. Activity concentration depth profiles in the thermocline (depth 200 m) of  $^{226}\text{Ra}$  and  $^{228}\text{Ra}$  were obtained at four stations along a transect from 35°N to 36°N at 130°50'E (Fig. 1).

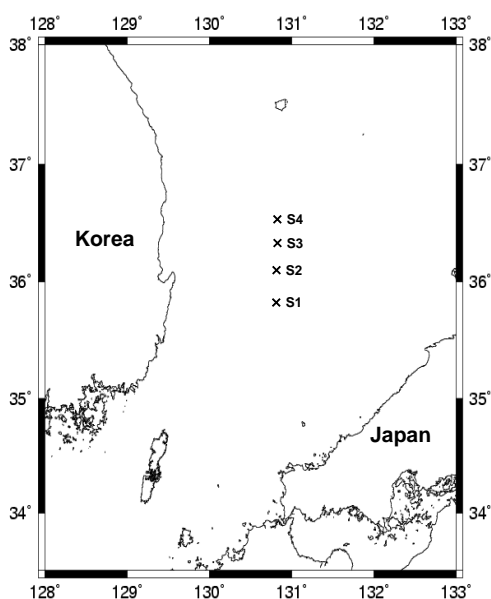


Figure 1. Locations of sampling stations in southwestern East/Japan Sea.

The upper 150 m of the southwestern East/Japan Sea consists of warm and saline water transported by the Tsushima Current through the Korea/Tsushima Strait with about 20 % originating from the continental shelf waters of the East China Sea and the Yellow Sea with the remaining 80 % from the Kuroshio Current waters (Nozaki et al., 1989).

Radium was extracted from seven depths by pumping seawater through  $\text{MnO}_2$ -impregnated filters in tandem with an overall extraction efficiency of  $90 \pm 6\%$ . The  $^{226}\text{Ra}$  and  $^{228}\text{Ra}$  activity concentrations were determined by gamma-ray spectrometry with well-defined geometry.

$^{226}\text{Ra}$  activity concentrations in the water column showed minor variations in the upper 200 m with an average of  $1.9 \pm 0.3 \text{ Bq m}^{-3}$ . The  $^{228}\text{Ra}$  activity concentrations decreased with depth from  $\sim 4 \text{ Bq m}^{-3}$  at the surface to  $\sim 1 \text{ Bq m}^{-3}$  at depth 100 m reflecting the contribution of the

Tsushima Current water in the southwestern East/Japan Sea.

From the  $^{228}\text{Ra}/^{226}\text{Ra}$  activity ratios in the upper 100 m water column (Fig. 2), mixing ratios in the seawater at the sampling site was estimated by using endmembers for the Tsushima Current and eastern coast of Korea (Inoue et al., 2013; Lee et al., 2005; Yang et al., 2002)

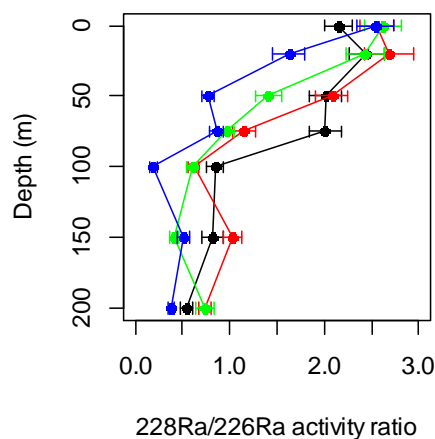


Figure 2. Depth profiles of  $^{228}\text{Ra}/^{226}\text{Ra}$  activity ratio in the euphotic zone of southwestern East/Japan Sea.

The authors are very grateful to the captain and crew of R/V Onnuri and KIOST (Korea Institute of Ocean Science and Technology) personnel for preparation and assistance during sampling.

Inoue et al., 2013.  $^{228}\text{Ra}/^{226}\text{Ra}$  ratio and  $^7\text{Be}$  concentration in the Sea of Japan as indicators for water transport: comparison with migration pattern of Fukushima Dai-ichi NPP-derived  $^{134}\text{Cs}$  and  $^{137}\text{Cs}$ . *J. Environ. Radioact.* 126, 176-187.

Lee, J.S., Kim, K.H., Moon, D.S., 2005. Radium isotopes in the Ulsan Bay. *J. Environ. Radioact.* 82, 129-141.

Nozaki, Y., Kasemsupaya, V., Tsubota, H., 1989. Mean residence time of the shelf water in the East China and the Yellow Seas determined by  $^{228}\text{Ra}/^{226}\text{Ra}$  measurements. *Geophys. Res. Lett.* 16, 1297-1300.

Yang, H.S., Hwang, D.W., Kim, G., 2002. Factors controlling excess radium in the Nakdong River estuary, Korea: submarine groundwater discharge versus desorption from riverine particles. *Mar. Chem.* 78, 1-8.

## Assessment of a potential risk to biota due to long-lived radionuclides in the Baltic Sea

G. Lujaniene<sup>1</sup>, B. Šilobritienė<sup>2</sup>, D. Tracevičienė<sup>1</sup>, S. Šemčuk<sup>1</sup>, N. Remeikaitė-Nikienė<sup>1,2</sup>, G. Garnaga<sup>2</sup>, V. Malejevas<sup>2</sup>, P.P. Povinec<sup>3</sup>, A. Stankevičius<sup>2</sup>

<sup>1</sup>SRI Center for Physical Sciences and Technology, Vilnius, Savanorių pr. 231, LT-02300, Lithuania

<sup>2</sup>Environmental Protection Agency, A. Juozapavičiaus g. 9, LT-09311 Vilnius, Lithuania

<sup>3</sup>Comenius University, 84248 Bratislava, Slovakia

Keywords: <sup>137</sup>Cs, <sup>241</sup>Am, <sup>239,240</sup>Pu

Presenting author email: lujaniene@ar.fi.lt

Long-lived radionuclides were introduced into the Baltic Sea due to the global fallout from atmospheric nuclear weapon tests, the Chernobyl and other nuclear accidents, as well as due to the transport of radionuclides with river water inflows from contaminated areas (HELCOM, 1995; Livingston & Povinec, 2002).

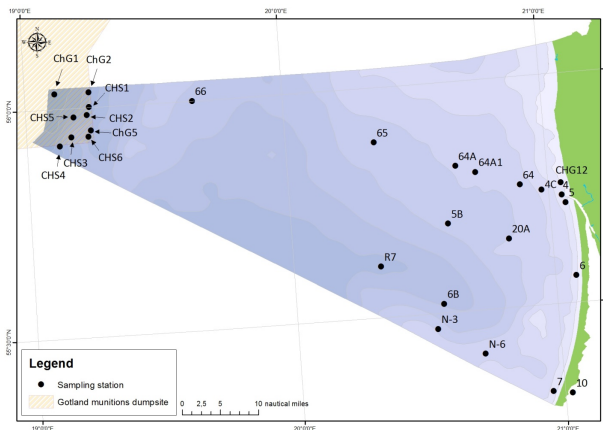


Figure 1. Sampling locations.

The aim of this study was to estimate long-lived radionuclide concentrations in surface water, sediments and biota as well as to assess the risk to biota.

The location of sampling stations is presented in Figure 1. Bottom sediment samples were collected using a Van Veen grab and Gemini Corer samplers during the sampling campaigns in the frame of the State Environmental Monitoring. Large-volume water samples (up to 1,000 L) were collected during several cruises in the Lithuanian economic zone of the Baltic Sea and the Curonian Lagoon. Suspended particles were collected in situ by filtering a large volume of water (from 400 to 1000 L).

<sup>137</sup>Cs activities were measured with HPGe detectors (GEM40P4-76, efficiency 40%, resolution 1.85 keV (FWHM) at 1.33 MeV and GX4018, resolution 1.8 keV/1.33 MeV and efficiency 42 %). Samples were ashed at 550 °C and then dissolved in strong acids (HNO<sub>3</sub>, HCl, HF and HClO<sub>4</sub>). The TOPO/cyclohexane extraction and radiochemical purification using UTEVA, TRU and TEVA resins (100 – 150 μm) were employed for separation of Am and Pu isotopes. <sup>242</sup>Pu and <sup>243</sup>Am (AEA Technology UK, Isotrak, QSA Amersham international, PRP10020 and ATP10020) were used as yield tracers in the separation procedure. The overall recovery of <sup>242</sup>Pu tracers was about 80% and 70%, respectively (Lujaniene, 2013). Pu isotopes were

measured using mass spectrometry (Lujaniene et. al., 2017)

Wide variations of <sup>137</sup>Cs and <sup>239,240</sup>Pu activity concentrations in bottom sediments of the Lithuanian waters of the Baltic Sea were observed in 2011-2015. Average <sup>137</sup>Cs activity concentrations varied from 7.6±0.5Bq/kg to 200±10Bq/kg, while in the Curonian Lagoon activities ranged from 1.24±0.07Bq/kg to 10.4±0.5Bq/kg.

Measured activity concentrations of <sup>239,240</sup>Pu in seaweed were between 0.44±0.04 and 12.6±0.9 mBq/kg, whereas in fish the activities ranged from 0.5±0.1 to 5.9±0.4 mBq/kg.

The assessment of biota exposure was performed for the Baltic Sea (Lithuanian economic zone). Average activity concentrations of <sup>137</sup>Cs, <sup>40</sup>K, <sup>90</sup>Sr, <sup>239</sup>Pu and <sup>240</sup>Pu in surface water, sediments and biota from EPA and SRI CPST database were used for modelling. The species considered for this part of the sea included seaweed (*Furcellaria lumbricalis*) and three types of fish (*Platichthys flesus*, *Gadus morhua*, *Clupea harengus*).

ERICA Assessment Tool to calculate dose rates was used for evaluation of dose rates for biota. The screening value 10 microGy/h proposed in ERICA tool was used for evaluation of the risk. The total (internal and external summed) estimated dose rates were compared directly to the selected screening dose rate to enable the assessment of the risk to biota.

HELCOM. Radioactivity in the Baltic Sea 1984-1991.

Baltic Sea Environment Proceedings. 1995; 61, Helsinki Commission, Helsinki, Finland.

Livingston, H.D., Povinec, P.P., 2002. A Millennium Perspective on the Contribution of Global Fallout Radionuclides to Ocean Science. Health Physics, 82, 656–668.

Lujaniene, G., 2013. Determination of Pu, Am and Cm in environmental samples. In: Isotopes in hydrology, marine ecosystems and climate change studies: proceedings of the international symposium held in Monaco, March 27 - April 1, 2011. Vol. 2. Vienna: International Atomic Energy Agency, 411-418.

Lujaniene G., Povinec P.P., Li H.-C., Barisevičiūtė R., Remeikaitė-Nikienė N., Malejevas V., Garnaga-Budrė G., Terrassi F., Pánik J., Kaizer J., Šemčuk S., Jokšas K., Tracevičienė D., Stankevičius

A. Carbon and Pu isotopes in Baltic Sea sediments. Appl. Radiat. isotopes. (2017) <http://dx.doi.org/10.1016/j.apradiso.2017.02.026>.

# Distribution and source identification of the radionuclide <sup>137</sup>Cs and <sup>239+240</sup>Pu in the sediments of the Liao River estuary

S.M. Pan<sup>1</sup>, K.X. Zhang<sup>1</sup>, Z.Y. Liu<sup>2</sup>, Y.H. Xu<sup>1</sup>

<sup>1</sup> School of Geographic and Oceanographic Sciences, Nanjing University, Nanjing210023, P.R. China

<sup>2</sup> School of Radiation Medicine & Protection, Medicine College, Soochow University, Suzhou 215123, P.R. China

Keywords: Pu, <sup>137</sup>Cs, sedimentation rate, Liao River estuary

Presenting author email: span@nju.edu.cn

The Liao River is the principal river in southern Northeast China, and one of the seven main river systems in mainland China. Along with the increasing activities of human beings, the sedimentary environments have been changing all the time, posing serious problems at present in the aspects of ecology and economy in the Liao River estuary. In this work, 17 sediment cores collected from the Liao River coastal zone were subjected to analyze <sup>137</sup>Cs, Pu isotopes activities and <sup>240</sup>Pu/<sup>239</sup>Pu atom ratios. The <sup>137</sup>Cs and the <sup>239+240</sup>Pu activities in the surface sediments (0 ~ 5 cm) were 1.03 ~ 15.68 Bq/kg with an average of 5.09 ± 0.34 mBq/g (n=17) (Figure 1) and 0.103 ± 0.008 to 0.978 ± 0.035 mBq/g with an average of 0.294 ± 0.053 mBq/g (n=7) (Figure 2), respectively. Increased from tidal flat to land and east to west in the Liao River estuary.

consistent with global fallout. Additionally, the linear correlativity between <sup>239+240</sup>Pu and <sup>137</sup>Cs in the surface sediment is statistically significant at the 1% significance level.

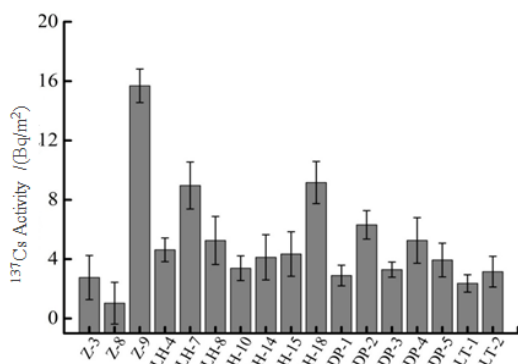


Figure 1. Distribution of the <sup>137</sup>Cs activities in surface sediment of the Liao River estuary.

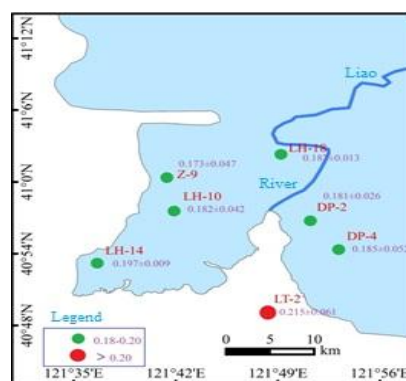


Figure 3. <sup>240</sup>Pu/<sup>239</sup>Pu atom ratios of surface sediments in the Liao River estuary.

Sedimentation rates calculated from <sup>137</sup>Cs maximum ranged from 0.48 to 1.63 cm/a, with a mean of 0.70 cm/a. The sedimentation rates increased from north to south and land to sea in the Liao River estuary. The <sup>137</sup>Cs inventories vary from 980 ± 46 to 6094 ± 92 Bq/m<sup>2</sup>, with an average of 2278 ± 42 Bq/m<sup>2</sup>.

Except for the sediment core LT-2, the <sup>240</sup>Pu/<sup>239</sup>Pu atom ratios in the sediment cores ranged from 0.180 to 0.199, which was close to the global fallout value of 0.18 ± 0.02. The mean of <sup>240</sup>Pu/<sup>239</sup>Pu atom ratios for the sediment core LT-2 was 0.217 ± 0.050. This indicated that the Pu on the tidal flat in the Liao River estuary is sourced from a combination of global fallout and close-in fallout from the Pacific Proving Grounds (PPG). The relative proportions of global fallout and PPG close-in fallout presented in the tidal flat sediment in the Liao River estuary were estimated, using a two end-member mixing model. The relative contribution of the PPG close-in fallout to core LT-2 is 26.57%. The remaining 73.43% can be attributed to global fallout and drainage input. The contribution of PPG close-in fallout was around 29.2 Bq/m<sup>2</sup> and the remaining 80.7 Bq/m<sup>2</sup> derived from global fallout and basin input. At 30~40°N region, contribution of the direct global fallout to Pu inventory is about 42 Bq/m<sup>2</sup>. Assuming all the direct global fallout was transferred to the sediment, we estimate the contribution from the land-origin global fallout transported by the Liao River.

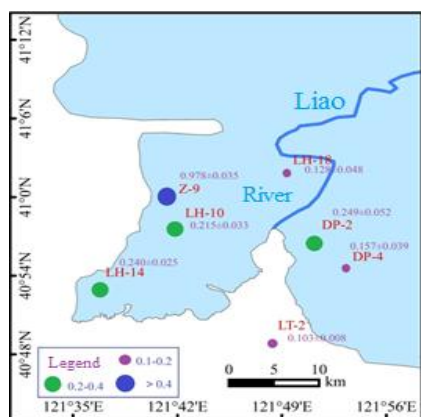


Figure 2. <sup>239+240</sup>Pu activities in surface sediment of the Liao River estuary.

The <sup>240</sup>Pu/<sup>239</sup>Pu atom ratios in surface sediments ranged from 0.173 ± 0.047 to 0.215 ± 0.061, with an average of 0.188 ± 0.039 (n=7) (Figure 3), which is



## Atmospheric $^{13}\text{C}$ and $^{14}\text{C}$ concentrations in different localities of Slovakia

A. Šivo<sup>1</sup>, K. Holý<sup>1</sup>, P. P. Povinec<sup>1</sup>, M. Richtáriková<sup>1</sup>, J. Šimon<sup>2</sup>, M. Müllerová<sup>1</sup>

<sup>1</sup>Faculty of Mathematics, Physics and Informatics, Comenius University, Mlynská dolina F-1, 842 48 Bratislava, Slovakia

<sup>2</sup>Faculty of Mechanical Engineering, University of Žilina, Univerzitná 1, 010 26 Žilina, Slovakia

Keywords: atmosphere, carbon dioxide,  $^{14}\text{C}$ ,  $^{13}\text{C}$ , variations.

Presenting author email: [Pavel.Povinec@fmph.uniba.sk](mailto:Pavel.Povinec@fmph.uniba.sk)

Anthropogenic  $^{14}\text{C}$  present in atmospheric carbon dioxide has been used during the last 60 years as a tracer in numerous environmental studies (e.g. Levin, 2004). In Slovakia (Bratislava station),  $^{14}\text{C}$  activity in atmospheric  $\text{CO}_2$  has been measured since 1967 (e.g. Povinec et al., 1968). In the present work, the results of  $^{14}\text{CO}_2$  and  $^{13}\text{CO}_2$  monitoring at six regional stations in Slovakia during the period 2007-2014 are presented. The measurements provide information about the variations of  $^{13}\text{C}$  and  $^{14}\text{C}$  in a clean high mountain area (Chopok station at 2000 m a.s.l.), suburban areas of Bratislava (Rovinka and Vysoká na Morave stations), rural and agriculturally active locality (Žilkovce station), as well as in the urban region contaminated by fossil fuels (stations BA-Mlynská dolina and BA-centre). Additionally, Žilkovce station is located in the very vicinity of Jaslovské Bohunice nuclear power plant and monitors its environmental impact as well.

For the carbon isotope measurements in the atmosphere, samples of  $\text{CO}_2$  have been continuously collected at a height of 3 m above the ground by dynamic absorption of  $\text{CO}_2$  in  $\text{NaOH}$  solution. Subsequently,  $\text{CH}_4$  was prepared from the samples as a filling of low-level proportional counter, which was used for counting  $^{14}\text{C}$  decays (Povinec et al., 2009). For the determination of  $\delta^{13}\text{C}$  in samples, a mass spectrometry was used.

maximum in summer and minimum in winter months (December-February). While in summer months the differences in  $\Delta^{14}\text{C}$  measured at individual stations are minimal, in winter months, e.g. in Bratislava centre,  $\Delta^{14}\text{C}$  are up to 40‰ lower than at Chopok station (Fig. 1). This has been caused by high fossil fuel  $\text{CO}_2$  emissions in Bratislava centre during winter months.

In contrast to this, the lowest yearly values of  $\delta^{13}\text{C}$  (with the average  $\sim 13.9\text{‰}$ ) were found at the locality of Žilkovce, possibly as a result of more intensive soil respiration in this agricultural area. The most pronounced seasonal variation of  $\delta^{13}\text{C}$  was observed at Vysoká na Morave station, with the minimum in winter ( $\sim 13.2\text{‰}$ ) and the maximum in summer ( $\sim 10.7\text{‰}$ ). The values of  $\delta^{13}\text{C}$  measured at the remaining stations during summer were similar, at the level of  $-10\text{‰}$ , and the differences in individual values of  $\delta^{13}\text{C}$  were observed mostly in winter months.

The obtained data can be utilized e.g. for quantification of fossil  $\text{CO}_2$  emissions into the atmosphere (e.g. Levin et al., 2008), for testing of new approaches of their calculations that will be independent on statistical data, and in climate change studies.

This work has been supported by the the Scientific Grant Agency of the Ministry of Education of the Slovak republic under the VEGA projects No. 1/3046/06, 1/0678/09 and 1/0143/14.

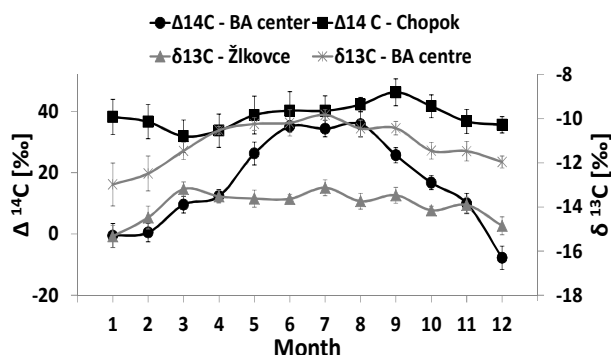


Figure 1. Average seasonal (monthly) variations of  $\Delta^{14}\text{C}$  and  $\delta^{13}\text{C}$  and their standard uncertainties in atmospheric carbon dioxide obtained during the years 2007-2014.

Significant seasonal variations of  $\Delta^{14}\text{C}$  were found at every station except Chopok station, with

Levin, I., 2004. The tropospheric  $^{14}\text{CO}_2$  level in mid latitudes of the Northern Hemisphere (1959-2003). *Radiocarbon* 46, 1261-1272.

Levin, I., Hammer, S., Kromer, B., Meinhardt, F., 2008. Radiocarbon observations in atmospheric  $\text{CO}_2$ : Determining fossil fuel  $\text{CO}_2$  over Europe using Jungfrauoch observations as background. *Sci. Total Environ.* 391, 211-216.

Povinec, P. P., Chudý, M., Šivo, A., Šimon, J., Holý, K., Richtáriková, M., 2009. Forty years of atmospheric radiocarbon monitoring around Bohunice nuclear power plant, Slovakia. *J. Environ. Radioact.* 100, 125-130.

Povinec, P., Šáro, Š., Chudý, M., Šeliga, M., 1968. The rapid method of carbon-14 counting in atmospheric carbon dioxide. *Int. J. Appl. Rad. Isotop.* 19, 877-881.

## Actinides measurements on environmental and structural samples of the Garigliano Nuclear Power Plant (Italy) during the decommissioning phase

A. Petraglia<sup>1</sup>, C. Sirignano<sup>1</sup>, R. Buompane<sup>1</sup>, F. Terrasi<sup>1</sup>, A. D'Onofrio<sup>1</sup>, C. Sabbarese<sup>1</sup>, A. M. Esposito<sup>2</sup>

<sup>1</sup>Departimento di Matematica e Fisica, Università degli studi della Campania "L. Vanvitelli" Caserta, Italy

<sup>1</sup>SoGIN, Garigliano NPP

Presenting author email: carlo.sabbarese@unicampania.it

The study of the radiological impact of a nuclear power plant (NPP) is important for the population and the environment of the area surrounding the plant, for the workers operating inside the plant and for characterisation and classification of the structural materials to be removed. The Gargliano Nuclear Power Plant is in the decommissioning phase from 90s. Previous surveys has been carried (Petraglia et al., 2005) to assess the contamination levels over the years in order not only to safeguard the health of people and the environment, but also to lower the level of risk perception among the population, for which an objective and verifiable scientific campaign can be very effective. An extraordinary survey was carried out in order to provide an adequate and updated assessment of the radiological impact that the decommissioning operations of the Garigliano NNP may have procured to the soils of the surrounding area. To characterize and classify structural material to be removed sampling were made on metallic and concrete materials. The isotopes of uranium ( $^{235}\text{U}$ ,  $^{236}\text{U}$ ,  $^{238}\text{U}$ ) and plutonium ( $^{239}\text{Pu}$ ,  $^{240}\text{Pu}$ ) and some their significant ratios were measured to identify the origin source actinides with the AMS technique that is able to also measure elements in traces and reach sensitivity that cannot be obtained with other methods. The results of the soils show that the anthropogenic component is essentially due to the atmospheric fallout and no or a negligible contamination can be charged to the NPP. They are represented in geo-referenced maps to highlight the distribution area and some particular aspects of each measured radionuclide. The results of the structural materials indicate the different source and quantify the specific contamination.

## Radiological Monitoring of the Environment around Niger Uranium Mine Sites of Arlit

Djibo Seydou\*<sup>1</sup>, Mahaman Moussa Bachirou Babale<sup>1</sup>, Fernando P. Carvalho<sup>2</sup>, João Maria Oliveira<sup>2</sup>, Margarida Malta<sup>2</sup>.

1 Ministry of Mines, Republic of Niger, B.P 11700 Niamey, Niger Tel: +227 20736529

Fax: +227 20731810.

2 Laboratório de Protecção e Segurança Radiológica/ Instituto superior Técnico, Estrada Nacional 10, km 139,7; 2695-

066 Bobadela LRS. Portugal

\*Corresponding author: seydou\_djibo@yahoo.com

### Abstract

Uranium mining activities started in Niger since 1968, but up to now, in terms of radiological monitoring of the environment, it is the mining operator who collect, prepare and analyze samples, interpret radiological data and evaluate the dose received by the receiving medium. The State does not have the material and human resources to verify the reliability of the data provided by the mining operator. A start is now taking place with the support of International Atomic Energy Agency (IAEA) Technical Cooperation projects with the endowment of the state with equipment's for radiation measurement and control; the training of technical staff on radiation safety for surveillance of workers health as well as radiological monitoring of the environmental and finally the financing of a field mission around the mining areas to collect environmental samples and their analysis at the Nuclear and Technological Institute of Lisbon, Portugal, to determine the concentration of radionuclides from the  $^{238}\text{U}$  and  $^{232}\text{Th}$  series in the environmental samples including soils, water and food chain. The results are presented in this work.

**Key words:** Uranium mining, mining operator, State, concentration of radionuclides.

## Is ecological food radioecological as well – $^{210}\text{Po}$ and $^{210}\text{Pb}$ studies

D.I. Strumińska-Parulska

University of Gdańsk, Faculty of Chemistry, Environmental Chemistry and Radiochemistry Department, Wita Stwosza 63, 80-308 Gdańsk, Poland

Keywords: ecological and commercial agriculture, polonium  $^{210}\text{Po}$ , radiolead  $^{210}\text{Pb}$ .

Presenting author email: dagmara.struminska@ug.edu.pl

Air and food are the main sources of chemical elements, also natural and artificial radionuclides, transfer to human organisms. The intensity level of radioisotopes intake depends on the place of residence, local contamination quantity, diet habits and food origin. Among natural radionuclides in air, the most important is  $^{222}\text{Rn}$  – emitted mainly from the ground and the construction materials, and in case of Polish inhabitants radon is the most significant part of the total annual radiation dose from natural sources (about 40%, 1.2 mSv).

So far, during annual radiation doses evaluations in Poland, only basic, the most often consumed food products were taken into account. Previous researches showed some products, seemingly negligible as supplements or mushrooms, can have significant contribution in total radiation dose. Also type of agriculture could affect the natural radionuclides content in food. Among naturally occurring radionuclides, their potential ingestion and internal expose, the most important seems to be  $^{210}\text{Po}$  and its parent nuclide  $^{210}\text{Pb}$ .

Considering food origin, some products could be enriched with natural radionuclides when cultivated on soil with higher natural radioactivity background, e.g. Ramsar (Iran), Kerala and Madras (India), Brazil, Sudan, Yangjiang (China) or Pakistan. These agriculture products would have higher amount of natural radionuclides due to accumulation and deposition processes. But some research showed higher topical radionuclides concentrations in soil of an arable fields when compared to surrounding ground. These situation was probably connected to fertilizers used in agriculture (Olszewski et al., 20015). Artificial fertilizers were first created during the mid-19th century, and further chemical pesticides in the 1940s were developed. These new, intensive agricultural techniques, while beneficial in the short term, had serious longer term side effects such as soil compaction, erosion, and declines in overall soil fertility, along with health concerns about toxic chemicals entering the food supply. Khater (2012) noticed that manufactured phosphate fertilizers and their agricultural applications are considerable sources of environmental pollution. Opposite, organic farming methods combine scientific knowledge of ecology and modern technology with traditional farming practices based on naturally occurring biological processes. While conventional agriculture uses synthetic pesticides and water-soluble synthetically purified fertilizers, organic farmers are restricted by regulations to using natural pesticides and fertilizers.

The aim of the study was polonium  $^{210}\text{Po}$  and radiolead  $^{210}\text{Pb}$  activity determination in popular food products in Poland: fruits, vegetables and cereal products that came from different, mainly Polish, traditional and certificate Polish ecological agriculture. Researches showed the mineral fertilizers can impact on uranium and its daughter nuclides, as  $^{210}\text{Po}$  and  $^{210}\text{Pb}$ , content in soil, so plants and animals can accumulated heightened radioisotopes values. The idea was to compare products of two types of agriculture: traditional, where different types of fertilizers are allowed and applied; and ecological where natural fertilizers are allowed; and search for dependency between  $^{210}\text{Po}$  and  $^{210}\text{Pb}$  concentrations in food products and agriculture type. Further the aim was to estimate the radiation doses from  $^{210}\text{Po}$  and  $^{210}\text{Pb}$  decays ingested with analyzed food products and answer the question: is more expensive ecological food is worth buying in case of  $^{210}\text{Po}$  and  $^{210}\text{Pb}$ ?

The results of  $^{210}\text{Po}$  and  $^{210}\text{Pb}$  determination showed their highest concentration were found in red currant, both traditional and ecological:  $1.73 \pm 0.07$  and  $0.67 \pm 0.03$  Bq kg<sup>-1</sup> dry mass for  $^{210}\text{Po}$  and  $1.15 \pm 0.03$  and  $0.10 \pm 0.01$  Bq kg<sup>-1</sup> dry mass for  $^{210}\text{Pb}$  respectively. However, the statistical tests showed there were no statistically significant differences among majority of results. Only “traditional apples and pears” contained more  $^{210}\text{Po}$  when compared to those “ecological”, Mann-Whitney (U test)  $p=0,12$ .  $^{210}\text{Po}$  concentration in traditional apples was calculated at  $0.72 \pm 0.02$ , while in ecological at  $0.30 \pm 0,02$  Bq kg<sup>-1</sup> dry mass.

The authors would like to thank the MNiSW for financial support under grant: DS-530-8635-D646-16.

Khater, A.E., 2012. Uranium and trace elements in phosphate fertilizers Saudi Arabia. *Health Phys.*, 102(1), 63-70.

Olszewski, G., Boryło, A., Skwarzec, B., 2015. Uranium ( $^{234}\text{U}$ ,  $^{235}\text{U}$  and  $^{238}\text{U}$ ) contamination of the environment surrounding phosphogypsum waste heap in Wiślinka (northern Poland). *J. Environ. Radioact.*, 146, 56-66.

## Determination of $^{14}\text{C}$ forms in liquid releases from nuclear power plants: the first results

I.Svetlik<sup>1,2</sup>, M. Fejgl<sup>2</sup>, P.P. Povinec<sup>3</sup>, T. Kořínková<sup>1</sup>, L. Tomášková<sup>1</sup>

<sup>1</sup>Department of Radiation Dosimetry, Nuclear Physics Institute CAS, Na Truhláře 39/64, CZ-180 86 Prague, Czech Republic

<sup>2</sup>National Radiation Protection Institute, Bartoskova 1450/28, CZ-140 00 Prague, Czech Republic

<sup>3</sup>Department of Nuclear Physics and Biophysics, Faculty of Mathematics, Physics and Informatics, Comenius University, Bratislava, SK-842 48, Slovakia

Keywords: chemical forms of  $^{14}\text{C}$ , liquid releases, nuclear power plants, liquid scintillation spectrometry

Presenting author email: svetlik@ujf.cas.cz

There is a lack of data in the scientific literature on  $^{14}\text{C}$  in liquid releases from nuclear power plants (NPPs) with light water pressurised reactors (Kunz 1985; Magnusson et al., 2008; CEC 1984; CEPN 2005). Following the requests of the state regulatory (The State Office for Nuclear Safety in Czech Republic), we developed a method for determination of the chemical forms of  $^{14}\text{C}$  in water samples of liquid releases from NPPs. This analytical method may distinguish the inorganic forms (dissolved  $^{14}\text{CO}_2$  and carbonates) from non-volatile organic forms, using a relatively simple and low-cost apparatus, which can process up to 1.8 L of water. The first step is the liberation of inorganic forms of carbon by diluted sulfuric acid. Once the  $^{14}\text{CO}_2$  is transferred quantitatively into the sorbent (3M NaOH), a condenser is added to the flask, and organic compounds are oxidized in acidic environment at the boiling point of the mixture. The procedure for oxidation of organic compounds in an aqueous environment is derived from the Chemical Oxygen Demand analysis with manganese, where the oxidation is carried out using potassium permanganate at temperatures close to the boiling point of water. The method was analytically tested and experimentally implemented during the end of the year 2015. In our presentation, we will report and discuss both the first results and practical experience

obtained during the first year of experimental monitoring of liquid releases from two Czech NPPs Temelin and Dukovany. We will also compare the first results of the use of  $\text{KMnO}_4$  or  $\text{K}_2\text{Cr}_2\text{O}_7$  for oxidation of organic carbon forms in these samples.

This work was supported by the institutional funding of Nuclear Physics Institute CAS (RVO61389005) and by the Czech Ministry of Interior (project MV-25972-39/OBVV-2010).

Kunz, C., 1985. Carbon-14 discharge at three light-water reactors. *Health Phys.* 49, 25-35.

Magnusson, A., Aronsson, P.O., Lundgren, K., Stenström, K., 2008. Characterization of  $^{14}\text{C}$  in Swedish Light Water Reactors. *Health Phys.* 95(2), S110-S121.

CEC, 1984. Bush, R.P., Smith, G.M., White, I.F., 1984. Carbon-14 waste management. Report EUR8749en, Commission of the European Communities, nuclear science and technology, Luxembourg.

CEPN, 2005. Liquid and Gaseous Activity Released from Pressurised Water Reactors: International Data (1980-2004). Report NTE/05/54 - C413-5, Convention EDF, Etude 3.1.8 livrable 2005.18. Centre d'étude sur l'évaluation de la protection dans le domaine nucléaire (CEPN).

**We prefer a poster form of presentation**



## Lichens and mosses as primary reference organisms of Antarctic terrestrial environment – dosimetric considerations.

K.M. Szufa<sup>1</sup>, J.W. Mietelski<sup>2</sup> and A.M. Olech<sup>3,4</sup>, Kamil Brudecki<sup>1</sup>

<sup>1</sup> The Henryk Niewodniczański Institute of Nuclear Physics, Polish Academy of Sciences, Poland,

<sup>2</sup> Institute of Botany, Jagiellonian University, Zdzisław Czeppe Department of Polar Research and Documentation, Poland.

<sup>3</sup> Institute of Biochemistry and Biophysics, Polish Academy of Sciences, Department of Antarctic Biology, Poland

Keywords: Antarctica, radionuclides, doses

Presenting author email: katarzyna.szufa@ifj.edu.pl

Referenced organisms may be defined as ‘a series of entities that provides a basis for the estimation of the radiation dose rate to a range of organisms that are typical, or representative, of a contaminated environment’ (Larsson, 2004). In Antarctic terrestrial environment such conditions fulfill lichens and mosses, especially due to low generic variation of Antarctic terrestrial flora which consists of mosses, lichens and view grass species only. Therefore those organisms seem to be the only which allow to provide basis to radiological risk assessment (Pentreath and Woodheadb, 2001).

There have been conducted some research in Antarctica to recognize contamination levels in different elements of South Polar ecosystems and indicate sources of those pollution, which are pointed to be global fallout and accident of American satellite over Madagascar (additional input of <sup>238</sup>Pu). Present investigation in Environmental Radioactivity Laboratory of Institute of Nuclear Physic in Cracow is intended to estimate concentration rates of natural (<sup>40</sup>K, <sup>230,232</sup>Th, <sup>234,238</sup>U) and artificial (<sup>137</sup>Cs, <sup>90</sup>Sr, <sup>238,239+240</sup>Pu, <sup>241</sup>Am) in differential biological samples i.a. mosses and lichens collected during the Polish Antarctic Expeditions during four decades (1980–2015) and prepare dosimetric interpretation of data obtained. Such information seem to be crucial to protect and preserve these unique ecosystems, especially that dosimetric considerations about Antarctic terrestrial ecosystem have not been made so far. Radionuclide levels were determined using low background gamma spectrometry, radiochemical sequential procedure (Mietelski et al., 2016) liquid scintillation counter and alpha spectrometry. Dose rates were calculated using Dose Conversion Coefficients for internal and external exposure to considered radionuclides (Gomez-Ros et al., 2004, Ulanovsky and Pröhl, 2008). Estimations were computed using ERICA tool (Brown at al., 2008).

that could be applied to them. *Sci. Total Environ.* 277, 33-43

Larsson, C.M., 2004 The FASSET Framework for assessment of environmental impact of ionising radiation in European ecosystems—an overview. *J. Radiol. Prot.* 24, A1–A12

Gomez-Ros, J.M., Pröhl, G., Taranenko, V. 2004. Estimation of internal and external exposures of terrestrial reference organisms to natural radionuclides in the environment. *J. Radiol. Prot.* 24, A79–A88

Ulanovsky, A., Pröhl, G. 2008. Tables of dose conversion coefficients for estimating internal and external radiation exposures to terrestrial and aquatic biota. *Radiat Environ Biophys.* 47, 195–203

Brown, J.E., Alfonso, B., Avila, R., Beresford, N.A., Copplestone, D., Pröhl, G., Ulanovsky, A. 2008.

*J Environ Radioact. The ERICA Tool.* 99, 1371-1383

Mietelski, J.W., Kierepko, R., Łokas, E., Cwanek, A., Kleszcz, K., Tomankiewicz, E., Mróz, T., Anczkiewicz, R., Szalkowski, M., Wąs, B., Bartyzel, M., Misiak, R. 2016. Combined, sequential procedure for determination of <sup>137</sup>Cs, <sup>40</sup>K, <sup>63</sup>Ni, <sup>90</sup>Sr, <sup>230,232</sup>Th, <sup>234,238</sup>U, <sup>237</sup>Np, <sup>238,239+240</sup>Pu and <sup>241</sup>Am applied for study on contamination of soils near Żarnowiec Lake (northern Poland). *J. Radioanal. Nucl. Chem.* 310, 661–670

The research is supported by National Science Center, Poland; research project no 2015/17/N/ST10/03116

R.J. Pentreath, R.J., Woodheadb, D.J., 2001. A system for protecting the environment from ionizing radiation: selecting reference fauna and flora, and the possible dose models and environmental geometries

## Beryllium-7 correlations in total deposition (dry and wet) measured in Serbia and Slovenia

Rajačić M<sup>1</sup>, Sarvan D<sup>2</sup>, Todorović D<sup>1</sup>, Ajtić J<sup>2</sup>, Krneta Nikolić J<sup>1</sup>, Zorko B<sup>3</sup>, Vodenik B<sup>3</sup>, Glavič Cindro D<sup>3</sup>, Kožar Logar J<sup>3</sup>

<sup>1</sup>*Vinča Institute of Nuclear Sciences, University of Belgrade, P.O.Box 522, 11001 Belgrade, Serbia, milica100@vin.bg.ac.rs*

<sup>2</sup>*Faculty of Veterinary Medicine, University of Belgrade, Bulevar oslobođenja 18, 11000 Belgrade, Serbia*

<sup>3</sup>*Jožef Stefan Institute, Jamova cesta 39, 1000 Ljubljana, Slovenia*

Beryllium-7 is a natural radionuclide whose specific activity at the surface strongly depends on transport history from the upper atmosphere where this isotope is produced. Since the major removal mechanism of beryllium-7 from the atmosphere is wet deposition, local meteorological factors also play an important role in its abundance at the surface.

In this analysis we present the beryllium-7 correlations in total deposition (dry and wet) measured in three locations: Belgrade, the capital of Serbia; Ljubljana, the capital of Slovenia; and Krško, a town in eastern Slovenia where a nuclear power plants located. Air distance between Belgrade and Ljubljana is about 490 km, while Krško lies roughly between them, and is less than 80 km away from Ljubljana. The data in our analysis cover the 1995-2015 period. The beryllium-7 specific activities were measured by standard gamma spectrometry at the Vinča Institute and Jožef Stefan Institute.

A comparison of the three beryllium-7 records in total deposition shows some differences between the measurement sites. For example, the maximum beryllium-7 concentrations in Belgrade are noted in June, while in Ljubljana and Krško, the maximum is observed in August. However, in both cases, the minimum beryllium-7 concentrations occur five months after the maximum, i.e. in November in Vinča, and in February in Ljubljana and Krško. Further, the highest Pearson's linear correlation coefficient ( $r$ ) is obtained for the Ljubljana-Krško records ( $r=0.68$ ). This strong linear correlation decreases down to a weak correlation of  $r=0.35$  and  $r=0.30$  for the Belgrade-Ljubljana and Belgrade-Krško records, respectively.

**Keywords:** *beryllium-7, total deposition, linear correlation*

## Determination of $^{135}\text{Cs}$ and $^{137}\text{Cs}$ in environmental samples by mass spectrometry: Current states and future perspectives

W.T. Bu<sup>1</sup>, J. Zheng<sup>2</sup> and S. Hu<sup>1</sup>

<sup>1</sup>Institute of Nuclear Physics and Chemistry, China Academy of Engineering Physics, Mianyang, 621900, China

<sup>2</sup>National Institute of Radiological Sciences, National Institutes for Quantum and Radiological Science and Technology, Chiba, 263-8555, Japan

Keywords:  $^{135}\text{Cs}/^{137}\text{Cs}$  isotopic ratio, mass spectrometry, environmental monitoring

Presenting author email: wtbu@caep.cn

The radioactive fission products  $^{135}\text{Cs}$ ,  $^{137}\text{Cs}$  have been released into the environment by human activities such as nuclear weapon tests, nuclear fuel reprocessing and nuclear power plant accidents. Monitoring of the two radiocesium is important for dose assessment and attracts increasing scientific and public concerns.

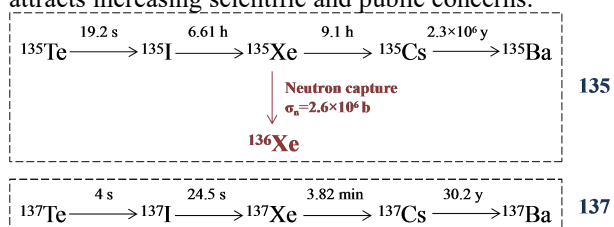


Figure 1. The decay chains at amu 135 and 137

The accumulated fission yields of  $^{135}\text{Cs}$  (6.58%) and  $^{137}\text{Cs}$  (6.22%) from thermal neutron fission of  $^{235}\text{U}$  are similar, indicating an isotopic ratio of  $\sim 1$  at the time of production (Taylor et al., 2008). However, the  $^{135}\text{Cs}$  enhancement in a reactor will be offset by the extremely high neutron-capture cross section of its precursor  $^{135}\text{Xe}$ , resulting in the formation of stable  $^{136}\text{Xe}$  instead of  $^{135}\text{Cs}$  (Figure 1). Thus the truly derived  $^{135}\text{Cs}/^{137}\text{Cs}$  isotopic ratio is highly dependent on the neutron flux (Figure 2). This ratio varies with weapon, reactor and fuel types; therefore, it serves as a new fingerprint for radioactive source identification besides the  $^{134}\text{Cs}/^{137}\text{Cs}$  activity ratio.

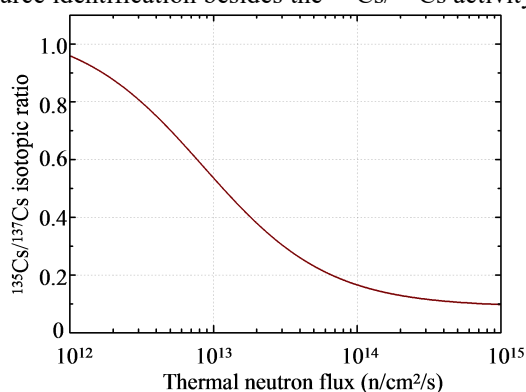


Figure 2. The dependence of  $^{135}\text{Cs}/^{137}\text{Cs}$  isotopic ratio on thermal neutron flux in a nuclear reactor (the irradiation time was set to be one year)

$^{137}\text{Cs}$  has been typically determined by gamma spectrometry and the detection limit with a high-purity germanium (HPGe) can be as low as  $\sim 1$  mBq/g (Hult et al., 2006). Thus gamma spectrometry is suitable for the analysis of  $^{137}\text{Cs}$  at environmental levels. The determination of  $^{135}\text{Cs}$  by radiometric methods, however,

is very difficult due to its long half-life ( $2.3 \times 10^6$  y) and low energy  $\beta$ -decay (76 keV). Therefore, the analytical methods based on mass spectrometry techniques are preferred options when the measurement of  $^{135}\text{Cs}$  is considered.

Mass spectrometry is characterized by the high sensitivity and low detection limit and the relatively shorter sample preparation and analysis times compared with radiometric methods. Recently, analytical methods based on mass spectrometry have been developed for the determination of  $^{135}\text{Cs}$  and  $^{137}\text{Cs}$  in environmental samples and these methods have been applied for the real environmental sample measurements (Russell et al., 2014; Zheng et al., 2016). However, the mass spectrometric determination of radiocesium is affected by the peak tailings of the stable nuclide  $^{133}\text{Cs}$  and the related isobaric and polyatomic interferences. Chemical separation and optimization of the mass spectrometry instrumental setup are strongly needed prior to the mass spectrometry detection.

In this work, we have reviewed the current states about the determination of  $^{135}\text{Cs}$  and  $^{137}\text{Cs}$  in environmental samples by mass spectrometry techniques (TIMS, ICP-MS, AMS etc.). Future perspectives for further related studies are included as well.

This work was supported by the National Natural Science Foundation of China (Grant No. 11605172).

Taylor, V.F, Evans R.D., Cornett, R.J., 2008. Preliminary evaluation of  $^{135}\text{Cs}/^{137}\text{Cs}$  as a forensic tool for identifying source of radioactive contamination. *J. Environ. Radioact.* 99, 109-118.

Hult, M., Preuße, W., Gasparro, J., Kohler, M., 2006. Underground gamma-ray spectrometry. *Acta. Chim. Slov.*, 53, 1-7.

Russell, B.C., Croudace, I.W., Warwick, P.E., Milton, J.A., 2014. Determination of precise  $^{135}\text{Cs}/^{137}\text{Cs}$  ratio in environmental samples using sector field inductively coupled plasma mass spectrometry. *Anal. Chem.* 86, 8719-8726.

Zheng, J., Cao, L.G., Tagami, K., Uchida, S., 2016. Triple-quadrupole inductively coupled plasma-mass spectrometry with high-efficiency sample introduction system for ultratrace determination of  $^{135}\text{Cs}$  and  $^{137}\text{Cs}$  in environmental samples at femtogram levels, *Anal. Chem.*, 88, 8772-8779.

## Particle scavenging of $^{239+240}\text{Pu}$ and $^{230}\text{Th}$ in the western equatorial Pacific Ocean

M. Yamada<sup>1</sup> and J. Zheng<sup>2</sup>

<sup>1</sup>Institute of Radiation Emergency Medicine, Hirosaki University, Hirosaki, Aomori, 036-8564, Japan

<sup>2</sup>National Institute of Radiological Sciences, National Institute for Quantum and Radiological Science and Technology, Inage, Chiba, 263-8555, Japan

Keywords:  $^{239+240}\text{Pu}$  flux, sediment trap experiment, particle scavenging,  $^{230}\text{Th}$ .

Presenting author email: myamada@hirosaki-u.ac.jp

The plutonium isotopes,  $^{239}\text{Pu}$  (half-life:  $2.44 \times 10^4$  y) and  $^{240}\text{Pu}$  (half-life:  $6.58 \times 10^3$  y), have been added to the Pacific Ocean mainly as a consequence of global fallout from atmospheric nuclear weapons testing, while a second source has been close-in fallout from nuclear weapons testing at the Pacific Proving Grounds (Nevissi and Schell, 1975). A number of studies have been made on the water column distributions of  $^{239+240}\text{Pu}$  (e.g., Bowen et al., 1980). Direct measurements of the vertical fluxes of  $^{239+240}\text{Pu}$  remain rare (e.g., Livingston and Anderson, 1983), even though such information is essential for quantifying its scavenging rate in the water column.

$^{230}\text{Th}$  is produced uniformly in seawater from radioactive decay of dissolved  $^{234}\text{U}$ .  $^{230}\text{Th}$  is rapidly adsorbed on settling particles and scavenged from the water column into the underlying sediments. Its flux to the seafloor should approximate its production rate in the water column. These characteristics have led to a wide range of applications as tracers of particle scavenging. Trapping efficiency can be estimated for moored sediment trap by comparing the predicted and measured flux of  $^{230}\text{Th}$ .

The aims of this study were to measure the concentrations of  $^{239+240}\text{Pu}$  and  $^{230}\text{Th}$  in sediment trap time-series samples, to quantify the fluxes of  $^{239+240}\text{Pu}$  and  $^{230}\text{Th}$ , and to understand  $^{239+240}\text{Pu}$  scavenging processes in the water column.

Sediment trap experiments were carried out in the western equatorial Pacific Ocean. Settling particles were collected from the West Caroline Basin by using time-series sediment traps and analyzed for  $^{239+240}\text{Pu}$  and  $^{230}\text{Th}$ . Two sediment traps were deployed at depths of 970 m and 2940 m (1800 m above the bottom). These time-series traps were conical with  $0.5 \text{ m}^2$  collecting area and 26 receiving cups.

Dried and weighed samples were dissolved with nitric, perchloric, and hydrofluoric acids after spiking with chemical yield tracers of  $^{242}\text{Pu}$  and  $^{229}\text{Th}$ . After anion exchange treatment, the Th and Pu isotopes were electrodeposited onto a stainless-steel disc. Their activities were determined with alpha spectrometers equipped with passivated ion implanted silicon detectors and a multichannel analyzer (Yamada and Aono, 2006).

The  $^{239+240}\text{Pu}$  concentrations in settling particles ranged from 2.6 to 8.8 mBq/g. The  $^{239+240}\text{Pu}$  concentrations decreased with increasing total mass fluxes (Figure 1). The  $^{239+240}\text{Pu}$  fluxes showed large seasonal variations. The flux-weighted annual mean fluxes of  $^{239+240}\text{Pu}$  were 0.237 and 0.263 mBq/m<sup>2</sup>/day at

depths of 970 m and 2940 m, respectively. The  $^{230}\text{Th}$  concentrations in settling particles ranged from 12.3 to 44.1 mBq/g at 970 m depth and 39.6 to 112 mBq/g at 2940 m depth. The flux-weighted annual mean concentrations of  $^{230}\text{Th}$  were 17.6 and 71.5 mBq/g at depths of 970 m and 2940 m, respectively. The  $^{230}\text{Th}$  fluxes showed large seasonal variations, similar to the trend of the total mass fluxes. The flux-weighted annual mean flux of  $^{230}\text{Th}$  at 970 m depth was approximately equal to the predicted flux of  $^{230}\text{Th}$  from production in the overlying water column in the western equatorial Pacific Ocean.

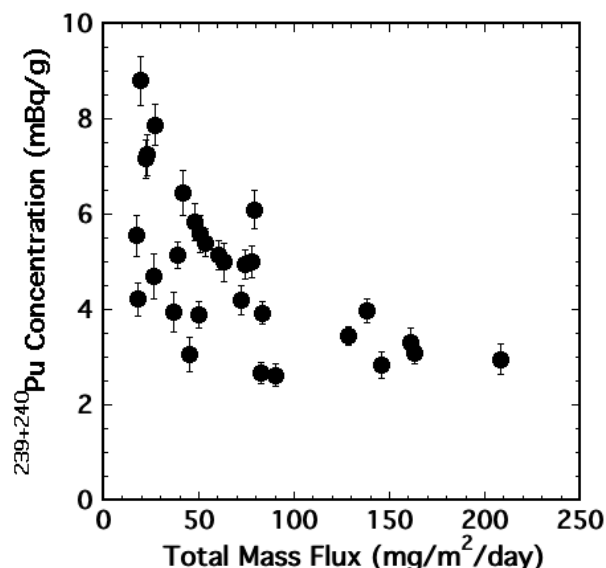


Figure 1. Total mass fluxes plotted against  $^{239+240}\text{Pu}$  concentrations in settling particles.

- Nevissi, A., Schell, W.R. 1975.  $^{210}\text{Po}$  and  $^{239}\text{Pu}$ ,  $^{240}\text{Pu}$  in biological and water samples from the Bikini and Eniwetok atolls. *Nature*, 255, 321-323.
- Bowen, V.T., Noshkin, V.E., Livingston, H.D., Volchok, H.L. 1980. Fallout radionuclides in the Pacific Ocean; vertical and horizontal distributions, largely from GEOSECS Stations. *Earth Planet. Sci. Lett.* 49, 411-434.
- Livingston, H. D., Anderson, R. F. 1983. Large particle transport of plutonium and other fallout radionuclides to the deep ocean. *Nature*, 303, 228-231.
- Yamada, M., Aono, T. 2006.  $^{238}\text{U}$ , Th isotopes,  $^{210}\text{Pb}$  and  $^{239+240}\text{Pu}$  in settling particles on the continental margin of the East China Sea: fluxes and particle transport processes. *Mar. Geol.* 227, 1-12.

## Natural Isotopes as Tracers for the Monitoring of Artificial Groundwater Recharge System

Yoon Yeol Yoon, Yong Cheol Kim, Kil Yong Lee, Soo Young Cho

Geologic Environment Division, Korea Institute of Geoscience and Mineral Resources  
Gwahang-no 124, Yuseong-gu, Daejeon, 34132 Korea

Keywords: groundwater, Rn-222, Sr isotope ratio, artificial groundwater recharge

Presenting author email: kylee@kigam.re.kr

Natural isotopes  $^{222}\text{Rn}$  and  $^{87}\text{Sr}/^{86}\text{Sr}$  ratio variation were used to understand the groundwater - surface water interactions. And also these tracers used to identify groundwater mixing phenomena for the artificial groundwater recharge of the water curtain greenhouse system. Three monitoring well were drilled for monitoring artificial recharge phenomena and groundwater was sampled every month from December 2013 to March 2016. And elements,  $^{222}\text{Rn}$  and  $^{87}\text{Sr}/^{86}\text{Sr}$  ratio variation were analyzed. The concentrations of Fe, Mn, Si, F were varied during the water curtain cultivation period due to the surface water intrusion. This phenomena was occurred by decreasing the groundwater level. And the concentration of  $^{222}\text{Rn}$  was decreased when water curtain cultivation and artificial groundwater recharge were started and slowly increased after water curtain cultivation ended. The concentration of  $^{222}\text{Rn}$  was changed from 400 pCi/L to 2500 pCi/L according to the well. Among three well, OB-14 showed different  $^{222}\text{Rn}$  concentration variation. This well was seriously affected by external environment and  $^{222}\text{Rn}$  concentration showed constant concentration about 500 pCi/L after artificial groundwater recharge. The  $^{87}\text{Sr}/^{86}\text{Sr}$  ratio variation of the three monitoring well showed different appearance. Among them OB-12 and OB-14 showed similar variation during artificial groundwater recharge period but OB-13 showed different ratio variation. This means groundwater-surface water mixing was occurred by different groundwater route.

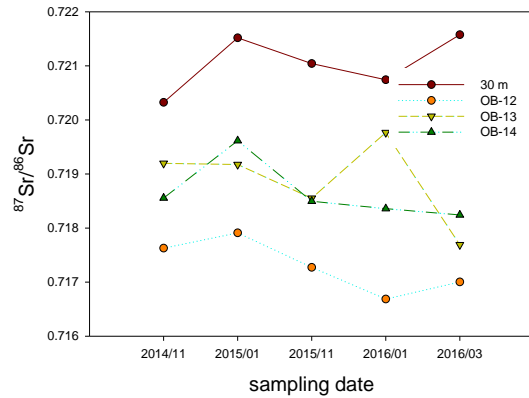


Fig. 2.  $^{87}\text{Sr}/^{86}\text{Sr}$  ratio variation with dam and sampling time

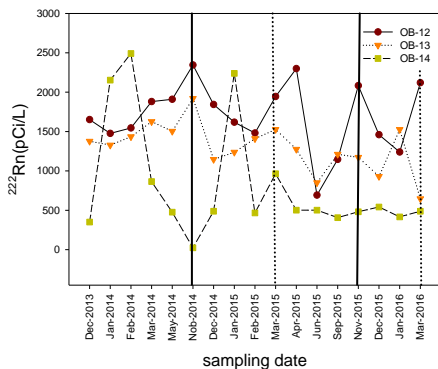


Figure 1.  $^{222}\text{Rn}$  concentration variation with sampling time and point. ( - : artificial recharge started, -- : artificial recharge ended)



## Development of nuclear microscopy techniques for mapping concentrations of radioactive and stable elements in environmental samples

J. Zeman<sup>1</sup>, M. Jeřkovský<sup>1</sup>, J. Kaizer<sup>1</sup>, P.P. Povinec<sup>1</sup>, D. Ozdín<sup>2</sup>

<sup>1</sup>Center for Nuclear and Accelerator Technologies (CENTA), Faculty of Mathematics, Physics and Informatics, Comenius University, Bratislava, 84248, Slovakia

<sup>2</sup>Department of Mineralogy and Petrology, Faculty of Natural Sciences, Comenius University, 84215 Bratislava, Slovakia

Keywords: nuclear microscope, PIXE method, GUPIXWIN software, mineral samples, biological samples

Presenting author email: [jakub.zeman@fmph.uniba.sk](mailto:jakub.zeman@fmph.uniba.sk)

Ion Beam Analysis (IBA) methods such as PIXE (Particle Induced X-ray Emission), PIGE (Particle Induced Gamma-ray Emission), RBS (Rutherford Back Scattering) and others, have been widely used for elemental analysis of samples. Using various combinations of these methods and measuring concentration levels at several points instead of a single point measurement (e.g. by scanning the analyzed sample), it is possible to create distribution maps, which are products similar to other microscope technologies, therefore this new technique has been named a nuclear microscope (Nastasi et al., 2015). The advantage of this method is that it is nondestructive, and that it can provide quantitative concentration maps of elements under study (e.g. uranium in minerals, etc.).

Centre for Nuclear and Accelerator Technologies (CENTA) has recently been established at the Comenius University in Bratislava as a laboratory for Accelerator Mass Spectrometry (AMS) and IBA applications. The laboratory consists of two ion sources (for gas and solid targets), injection system with electromagnet, tandem accelerator with 3 MV nominal voltage (Pelletron), and high energy ion analyzers (Povinec et al. 2015, 2016). The PIXE technology has recently been tested at the CENTA facility with promising results (Zeman et al., 2016).

The aim of the present paper has been to investigate a surface distribution of elements in various environmental (rocks, minerals), space (meteorites), biomedical and technical samples. Narrow beams of 3 MeV protons and 4.5 MeV helium ions have been used for PIXE analysis of such specimen. The possible samples comprise of cuts from minerals, thin cuts and layers of biological samples and some more precious samples which cannot be damaged, so the PIXE method is suitable for this investigation. Ion beams of desired energy are obtained from a 3 MV Pelletron tandem accelerator.



Figure 1. A mineral sample mounted on the sample holder in the reaction chamber.

Emitted X-rays from a specimen are detected by Broad Energy Germanium detector (BEGe, model BE2825). The PIXE spectra have been analyzed using GUPIXWIN software package. Finally, maps of elemental compositions have been obtained from measurements carried out at different points on the specimen surface.

The obtained results have been used for studying processes which caused displacement of elements.

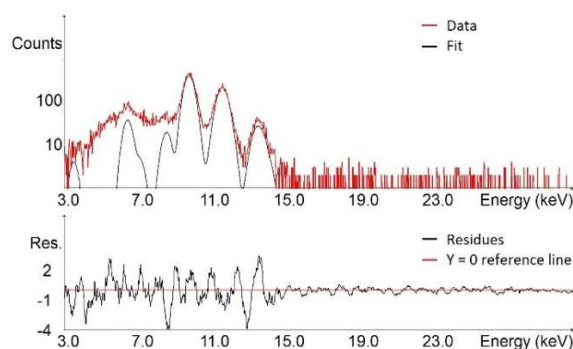


Figure 2. Example of PIXE spectrum analyzed by GUPIXWIN.

The authors are acknowledging support provided by the EU Research and Development Operational Program funded by the ERDF (projects # 26240120012, 26240120026 and 26240220004), and from the International Atomic Energy Agency (project # SLR/0/008), and from the . This study has also been supported by the Slovak Research and Development Agency under the contract # APVV-15-0576.

Nastasi, M., Meyer, J.W., Wang, Y. 2015. Ion beam analysis: fundamentals and applications. CRC Press, Boca Raton.

Povinec, P.P. et al., 2015. A new IBA-AMS laboratory at the Comenius University in Bratislava (Slovakia). Nucl. Instr. Meth. Phys. Res. B 342, 321–326.

Povinec, P.P., et al., 2016. Recent results from the AMS/IBA laboratory at the Comenius University in Bratislava: preparation of targets and optimization of ion sources. J. Radioanal. Nucl. Chem. 307, 20101–2108.

Zeman, J., Jeřkovský, M., Kaiser, R., Kaizer, J., Povinec, P.P., Staníček, J. 2016. PIXE beam line at the CENTA facility of the Comenius University in Bratislava: first results. 2016. J. Radioanal. Nucl. Chem. 311, 1409–1415.

## Possible influence of climate warming on lake water radioactive pollution

Z. Žukauskaitė<sup>1</sup>, B. Lukšienė<sup>1</sup>, N. Tarasiuk<sup>1</sup>, D. Jasinevičienė<sup>1</sup>, A. Puzas<sup>1</sup>

<sup>1</sup>SRI Center for Physical Sciences and Technology, Vilnius, Savanorių ave. 231, LT-02300, Lithuania

Keywords: <sup>137</sup>Cs, evaporation, bottom sediments, second-rate source.

Presenting author email: zita.zukauskaite@ftmc.lt

The climate change is a very relevant problem of these days. In the last century climate started to change rapidly and the temperature of the Earth raised by up to ~0.7 °C and it is considered to continue to rise (IPCC, 2007). Global warming caused by humans is affecting snowpack, glaciers and freshwater ice – they are melting, the weather is getting more extreme, oceans are getting warmer, expanding and becoming more acidic.

Current global circulation models predict an increase in air temperatures by several degrees by the end of the twenty-first century, combined with large changes in the regional distribution and intensity of rainfall (Vincent, 2009). Shifts in precipitation relative to evaporation (the P/E ratio) will cause changes in the water budget and hydraulic residence time of lakes, as well as in their depth and areal extent. For example, some rock basin ponds in the Canadian High Arctic have been drying up as a result of climate warming in the region, perhaps for the first time in millennium. Because of sensitiveness to the climate change, rapid response to it, and rapid changes in the catchment, lakes are effective sentinels for the climate change.

To evaluate the climate warming effect on the lake water radioactive pollution, we carried out two types of experiments: i) a half year experiment under conditions of the decreasing water level with carrier-free lake water and sediments; ii) a year's duration experiment using <sup>137</sup>Cs carrier under the same conditions as mentioned above. Conductivity of the water layer and in the surface sediments was monitored in both types of experiments. Before the experiment the content of chemical elements (Ca, Mg, Na, K, Mn, Fe), anions (SO<sub>4</sub><sup>2-</sup>, NO<sub>3</sub><sup>-</sup>, Cl<sup>-</sup>, F<sup>-</sup>, PO<sub>4</sub><sup>3-</sup>) and cation NH<sub>4</sub><sup>+</sup> in the sediments was measured. Information on the chemical composition of lake water was also obtained. Gamma spectrometric measurements of lake water and sediment samples were carried out using a CANBERRA gamma spectrometric system with an HPGe detector.

Obtained data showed that within half a year, a decrease in the thickness of the water layer above the sediments from ~20 cm down to ~2 cm was followed by a significant increase in conductivities in the above lying water layer and in the surface sediments from ~255 to ~466 and from ~205 to ~452 μS·cm<sup>-1</sup>, respectively. Probably, it was related to the increase in the oxygen flux to the sediment surface inducing more intensive decomposition of the sediment organic substances. In the year's experiment with <sup>137</sup>Cs carrier, the time-dependent <sup>137</sup>Cs activity concentration decrease was observed, with the exception of the last value (Fig. 1).

An increase in the <sup>137</sup>Cs activity concentration was stimulated by the <sup>137</sup>Cs release from the specific

sites induced by an increase in the concentrations of

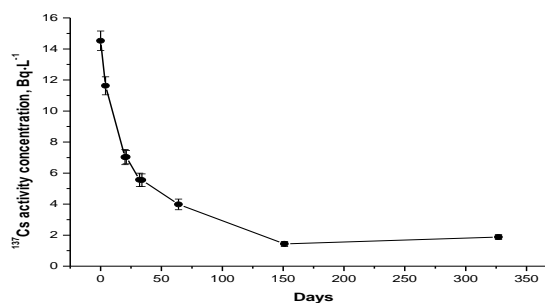


Figure 1. Time-course of the <sup>137</sup>Cs activity concentration in the lake water during the year's duration experiment.

competing ions, such as NH<sub>4</sub><sup>+</sup>. Probably, this process induced the <sup>137</sup>Cs backward flux directed to the above lying water and promoted the radionuclide migration into deeper sediment layers. Such an increase in the NH<sub>4</sub><sup>+</sup> ion concentrations in the sediment pore water was measured in the long-term <sup>134</sup>Cs incubation tests with the 2 cm thickness of the water layer above sediments in (Smith et al., 2000). Data in Fig. 1 show that at the end of the incubation experiment <sup>137</sup>Cs activity concentrations increased from ~1.4 up to ~1.9 Bq·L<sup>-1</sup>. A possible explanation of the concentration increase may be related to the respective <sup>137</sup>Cs pre-concentration effect due to the decrease in the thickness of the water layer above the sediments because of evaporation. An increase in the <sup>137</sup>Cs activity concentrations in the water layer with its declining thickness above the sediments implies the possible second-rate radioactive contamination of the water bodies under conditions of the climate warming. A second-rate source of the water body radioactive contamination may also be the runoff from the lake shore.

This research was funded by a Grant (No. MIP-041/2012) from the Research Council of Lithuania.

IPCC (Intergovernmental Panel on Climate Change), 2007. Contribution of Working Groups I, II and III to the Fourth Assessment Report of the Intergovernmental Panel on Climate Change, Geneva, Switzerland, 30.

Vincent, W.F., 2009. Effects of Climate Change on Lakes In: Pollution and Remediation. Elsevier Inc., 55-60.

Smith, J. T., et al., 1998. The mobility of radiocaesium in lake sediment and implications for dating studies. Dating of sediments and determination of sedimentation rate, STUK A-145, Finland, 76-93.

## Radon in Water: Italian Standard Generator and comparison of different measurement methods.

M. Capogni<sup>1</sup>, F. Cardellini<sup>1</sup>, P. De Felice<sup>1</sup>, E. Chiaberto<sup>2</sup>, F. Berlier<sup>3</sup>, M. Faure Ragani<sup>3</sup>

<sup>1</sup>Italian National Institute of Ionizing Radiation Metrology (INMRI),

<sup>2</sup>Regional Agency for Environmental Protection (ARPA) Piemonte, <sup>3</sup>ARPA Valle di Aosta

Presenting author email: francesco.cardellini@enea.it

Measurement of radon concentration in tap water and natural springs is an important issue both for human health protection and for geological studies. For this reason INMRI ENEA developed a radon in water standard generator to provide reference solution for the calibration of “aqua kit” of commercial radon monitors, HPGe gamma spectrometry system and liquid scintillation counter (LSC).

The circuit (see fig.1) is a closed loop connecting the radon source, the Marinelli beaker, the glass bubbler, the circulation pump and a special dispenser to fill vials for LSC, other vessel may be added according to the needs of the customers.

The aim of the circuit is to provide a set of water samples, all with the same radon concentration, to be measured by different measuring systems, without leakage of radon.

The water samples, with certified radon concentration, are dispatched to the costumers for the calibration of their instruments.

The radon concentration achieved is measured in the primary radon standard operating at INMRI ENEA with 1,5% combined uncertainty (Cardellini 2016).

This work is focused on the description of the circuit and on several calibration tests performed in cooperation with ARPA Piemonte and ARPA Valle d’Aosta.

The measurement techniques investigated are:

1. Liquid scintillation counter;
2. HPGe gamma spectrometry;
3. Commercial “aqua kit” of Saphymo AlphaGuard and Tesys MR1.

Liquid scintillation measurement was performed with Hidex 300sl using the TDCR method and with Tricarb Packard using Ciemat NIST method.

Main results obtained with LSC are listed in Table 1

Water sample	Reference activity (Bq/l)	Tricarb measure (Bq/l)	HIDEX measure (Bq/l)
Sample 1	16971	16693	16640
Sample 2	15117	15160	14780
Sample 3	15363	15280	15150

HPGe gamma spectrometry was performed at ARPA VdA laboratories; water sample was contained in the Marinelli beaker provided by INMRI ENEA and the instruments is an Ortec p-type Coaxial HPGe with 50% relative efficiency.

The Commercial “aqua kit” of Saphymo AlphaGuard and Tesys MR1 where tested with two different sample of water at different radon concentration.

Results in Table 2

Table 2: results of test with “aqua kit” of AlpaGuard, MR1 and HPGe gamma spectrometry (Sample 4).

Water sample	Reference activity (Bq/l)	MR1 (Bq/l)	AlphaGuard (Bq/l)	HPGe (Bq/l)
Sample 4	15215	14974	15391	16056
Sample 5	2900	2920	2951	--

### Conclusion

The result obtained in all the test show the validity of the radon in water generator operating at INMRI ENEA and the good reproducibility of the measurements over different methods.

Measurement with LSC, although satisfactory for standard use, may be improved with better determination of counting dead time.

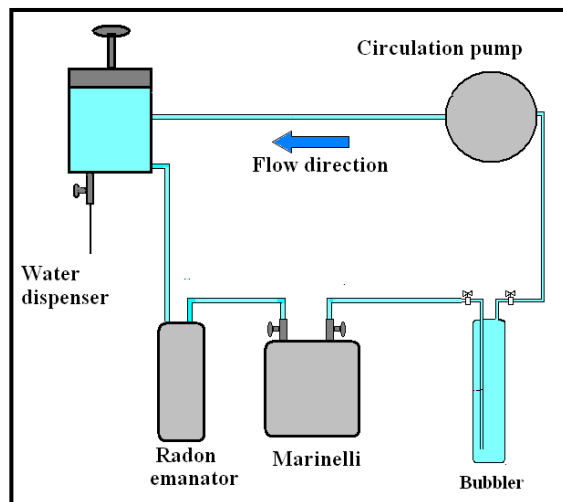


Figure 1. The generator of radon in water operating at INMRI ENEA (Italy)

### Reference

Cardellini, F. Metrological aspects of international intercomparison of passive radon detectors under field conditions in Marie Curie’s tunnel in Lurisia NUKLEONIKA 2016;61(3):257-261  
 Saphymo (2009). AlphaGUARD portable radon monitors user manual, Germany.

## Honey as bioindicators of pollution of the environment in Poland

A. Boryło, G. Romańczyk, B. Skwarzec

Faculty of Chemistry, University of Gdańsk, Department of Chemistry and Environmental Radichemistry

Keywords: honey, biomonitors,  $^{210}\text{Po}$ .

Presenting author email: alicja.borylo@ug.edu.pl

Environmental samples are complex most often in terms of composition and structure, very often heterogeneous and sometimes variable over time, resulting in lack of repeatability at sampling due to rapid changes in material being analyzed. The purpose of the study was to determine the radionuclide.  $^{210}\text{Po}$  in honey samples of nectar and honeydew collected for analysis from four Polish voivodships: Pomeranian, Warmian-Masurian, Kuyavian-Pomeranian and Lesser Poland Voivodeships. Bioindicators are organisms used as an indicator of the state of the environment. These are species with a low tolerance index, or in a specific way responsive to the substance. Popular bioindicator is honey. Bees collecting nectar, pollen and honeydew are often exposed to harmful substances used in agriculture planted on plants and carry these contaminants on the body surface to the hive, and as a consequence impurities get into the honey. Bee honey can be contaminated by various treatments related to apiculture and apiculture as well as xenobiotics in the environment. Its healing properties may be weakened by foreign substances that have come into contact with honey from the following sources: environment (ecotoxins), agricultural and apiculture practices, honey processing and storage. Increasing the intensity of agrochemicals associated with the desire to meet greater crop yields and the use of pesticides to control plant diseases or antibiotics in animals can lead to contamination of crops and food products, including honey produced by bees. Taking into account the fact that bees use the benefits of a radius of up to 3 km from the hive, the origin of the nectar can be determined with great accuracy. With that in mind, bee products can be used as indicators of environmental pollution in a given area.

The average concentration of  $^{210}\text{Po}$  in the analyzed honey samples was in the range of  $0.009 \pm 0.001$  Bq/kg to  $1.182 \pm 0.065$  Bq/g. The highest concentrations of analyzed radionuclides in the samples of honey, both nectar and honeydew, were characterized for Lesser Poland Voivodeship, while similar values were noted for the Pomeranian, Warmian-Masurian and Kuyavian-Pomeranian Voivodeships.

Each honeybee plant is different characteristic biological properties and each apiary has different characteristics, so that even within a single variety there may be differences. As a result of the study, an annual effective dose was calculated on the basis of  $^{210}\text{Po}$  concentration and the consumption in honey (assuming the annual consumption of honey in Poland is estimated to be about 0.61 kg per person), which was  $0,95 \pm 0.08$   $\mu\text{Sv}\cdot\text{year}^{-1}$  respectively. The highest concentration of  $^{210}\text{Po}$  was measured in all analyzed voivodships for honeydew honey, but the highest levels of  $^{210}\text{Po}$  were observed for Lesser Poland Voivodeship. This may be due not only to

high industrial dust emissions but also to the high supply of these elements to the environment with fertilizers and plant protection products. Changes in the natural environment also entail changes in the composition of plants, which indicates the need for constant analysis of particular elements. The content of these radionuclides in the test samples may also be a good reference in later studies of environmental conditions in these areas.

Project funded by the Ministry of Science and Higher Education DS / 530-8630-D505-17.

## Lichens as bioindicators of environmental pollution in Poland

A. Boryło, G. Romańczyk, B. Skwarzec

Faculty of Chemistry, University of Gdańsk, Department of Chemistry and Environmental Radichemistry

Keywords: lichens, biomonitors,  $^{210}\text{Po}$ .

Presenting author email: alicja.borylo@ug.edu.pl

Environmental samples are complex most often in terms of composition and structure, very often heterogeneous and sometimes variable over time, resulting in lack of repeatability at sampling due to rapid changes in material being analyzed. The purpose of the study was to determine the radionuclides  $^{210}\text{Po}$  and  $^{210}\text{Pb}$  in lichen samples (*Xanthoria parietina*, *Parmelia sulcata*, *Physcia adscendens*, *Physcia tenella*, *Caloplaca saxicola*, *Verrucaria Nigrescens*, *Lecanora conizaeoides* and *Amandinea punctata*) collected for analysis from three Polish voivodships: Pomeranian, Kuyavian-Pomeranian and Lesser Poland Voivodeships.

Bioindicators are organisms used as an indicator of the state of the environment. These are species with a low tolerance index, or in a specific way responsive to the substance. Popular bioindicators are lichens.

The mean concentrations of  $^{210}\text{Po}$  and  $^{210}\text{Pb}$  in the analyzed lichen samples were in the range of  $181\pm 9$  Bq/kg to  $1024\pm 9$  Bq/kg for  $^{210}\text{Po}$  and  $184\pm 6$  Bq/kg to  $1024\pm 8$  Bq/kg for  $^{210}\text{Pb}$ . The highest concentrations of  $^{210}\text{Po}$  and  $^{210}\text{Pb}$  were measured for each province in lichen samples with crustose thallus (*Caloplaca saxicola*, *Verrucaria nigrescens*, *Lecanora conizaeoides* and *Amandinea punctata*), while smaller were observed for lichen samples with foliose thallus (*Xanthoria parietina*, *Parmelia sulcata*, *Physcia adscendens* and *Physcia tenella*). In the Lesser Poland Voivodeship the lichens are classified into 3 groups of organisms growing in highly polluted air, which is probably related to the recent high concentrations of particulate matter: PM<sub>10</sub>, PM<sub>2.5</sub> and benzopurene in southern Poland. The norms of particulate matter in the air were practically all the time exceeded. This can be attributed not only to the high emission of industrial dust, but also to the high supply of these elements to the environment with fertilizers and plant protection agents. Changes in the natural environment also entail changes in the composition of plants, which indicates the need for constant analysis of particular elements. The content of these radionuclides in the test samples may also be a good reference in later studies of environmental conditions in these areas.

Project funded by the Ministry of Science and Higher Education DS / 530-8630-D505-17.



## Tritium effect on the anatomical structure of the common reed (*Phragmites australis*)

A.B. Yankauskas<sup>1</sup>, N.V. Larionova<sup>1</sup>, A.N. Shatrov<sup>1</sup>

<sup>1</sup>Institute of Radiation Safety and Ecology NNC RK, Kurchatov, VKO, 071100, Kazakhstan

Keywords: Semipalatinsk Test Site (STS), tritium, plants, anatomical parameter.

Presenting author email: [Yankauskas@nnc.kz](mailto:Yankauskas@nnc.kz)

The Shagan river is the longest superficial watercourse on the territory of the Semipalatinsk Test Site (STS). As a result of nuclear testing river valley has undergone significant radioactive contamination. The concentration of <sup>3</sup>H in surface water amounted to 4\*10<sup>5</sup> Bq/kg, which is more than in 50 times exceeds the permissible level for drinking water (Aidarkhanov, 2010). The first study to assess the influence of <sup>3</sup>H on morpho-anatomical structure of plants was carried out for *Achnatherum splendens* and *Elymus angustus* (Yankauskas, 2012).

In the present work investigates the effect of <sup>3</sup>H on the anatomical structure of the common reed (*Phragmites australis*), which has the highest concentrations (65\*10<sup>3</sup> Bq/kg) (Aidarkhanov, 2010). Research plots were planted at a distance of 1 km from each other along the river Shagan. For anatomical research from each plant were selected fragments of stems and leaves in a 12-20-fold repetition. As the investigated index selected parameters of stem: diameter of stem, thickness of epidermis, thickness of sclerenchyma, the area of vascular bundles located within the parenchyma. The studied parameters of the leaf: the thickness of upper epidermis, thickness of lower epidermis, diameter of stomata, the thickness of the mesophyll, the area of the vascular bundles of the 1-St and 2-nd order. Total produced about 6000 measurements of anatomical parameters.

For the determination of the radionuclide <sup>3</sup>H were sampled in the aboveground part of the plant. Determination of specific activity of <sup>3</sup>H was conducted in the organic component of the method liquid scintillation analysis low background beta-spectrometer Quantulus 1220. Sample preparation was performed on an automated installation of the Oxidizer.

The result of radiometric studies have found that the values of the specific activity of the radionuclide <sup>3</sup>H in the organic components of plants are in the range of 230±30 Bq/kg to 2,4\*10<sup>4</sup>±0,2\*10<sup>4</sup> Bq/kg, which corresponds to the rate of dose of 0,06 µGy/day to 7,0 µGy/day.

According to the obtained data revealed that there is an inverse anatomical parameters of plants in relation to the increase in the content of <sup>3</sup>H. It was found when the specific activity of radionuclide <sup>3</sup>H increased in plant from 230±30 Bq/kg to 2,4\*10<sup>4</sup>±0,2\*10<sup>4</sup> Bq/kg, anatomical parameters reduced: the stem diameter (from 3400±170 µm to 1700±230 µm), the thickness of sclerenchyma (from 170±25 µm to 74±21 µm), the area of vascular bundles (from 40 000±5700 µm<sup>2</sup> to 17 000±2900 µm<sup>2</sup>). The

parameters of the leaf is reduced: diameter of stomata (from 110±13 µm to 78±14 µm), the area of the vascular bundles of the 1-St order (from 26 000±5300 µm<sup>2</sup> to 13 000±3000 µm<sup>2</sup>).

Statistical data processing was conducted to quantify the impact of tritium on the anatomical structure (Table 1.).

Table 1. The results of the statistical analysis

Anatomical parameters	The regression equation	r
Stem		
Diameter of stem	y= -800x+5200	-0.9
Epidermis	y= 0.7x+7,5	0.6
Sclerenchyma	y= -20x+170	-0.7
Vascular bundles	y= -10 000x +53 500	-0.8
Leaf		
The upper epidermis	y= -0.4x+13	-0.6
The lower epidermis	y= -0.5x+16	-0.6
Diameter of stomata	y= -11x+130	-0.7
Mesophyll	y=-10x+200	-0.5
Vascular bundles of the 1-St order	y= -4 200x +33 700	-0.8
Vascular bundles of the 2-nd order	y= -2 000x+15 600	-0.6

*Note: r - correlation coefficient*

Thus, the results of the research showed the existence of influence of the radionuclide <sup>3</sup>H on the anatomical structure of plant common reed *Phragmites australis* – anatomical parameters of stem and leaf decreased by increasing the specific activity of <sup>3</sup>H from n\*10<sup>2</sup> до n\*10<sup>4</sup> Bq/kg. The dose rate not exceed 7,0 µGy/day.

Aidarkhanov, A. O. and others 2010. State of the ecosystem of the river Shagan and basic mechanisms of its formation. In: Actual issues of Kazakhstan radioecology. Vol. 2. 2010. 9-56.

Yankauskas, A. B. and others 2013. Study of the effect of tritium on morpho-anatomical and cytogenetic indices of plant. In: Actual issues of Kazakhstan radioecology. S. N. Lukashenko etc. Vol.4. Vol. 2, 311-332.

## Anthropogenic radionuclide variations in the European atmosphere

P.P. Povinec<sup>1</sup>, J. Bartok<sup>2</sup>, I. Bartoková<sup>2</sup>, M. Ješkovský<sup>1</sup>, A. Kováčik<sup>1,2</sup>, G. Lujanienė<sup>3</sup>, J.W. Mietelski<sup>4</sup>, M.K. Pham<sup>5</sup>, W. Plastino<sup>6</sup>, I. Sýkora<sup>1</sup>

<sup>1</sup>Comenius University, Department of Nuclear Physics and Biophysics, 84248 Bratislava, Slovakia

<sup>2</sup>MicroStep-MIS, Ltd., 84104 Bratislava, Slovakia

<sup>3</sup>SRI Center for Physical Sciences and Technology, Vilnius, Lithuania

<sup>4</sup>Henryk Niewodniczanski Institute of Nuclear Physics, PAN, Krakow, Poland

<sup>5</sup>International Atomic Energy Agency, Environment Laboratories, Monaco

<sup>6</sup>University of Roma Tre, Department of Mathematics and Physics, 00146 Rome, Italy

Keywords: anthropogenic radionuclides, atmosphere, re-suspension, Sahara dust, biomass burning, dispersion modelling

Presenting author email: [povinec@fmph.uniba.sk](mailto:povinec@fmph.uniba.sk)

Samples collected in the South Europe (Monaco – Pham et al., 2013), in the central Europe (Bratislava – Povinec et al. 2012; Sýkora et al., 2012, and Krakow – Blazej and Mietelski, 2014), and in the north-east Europe (Vilnius – Lujanienė et al., 2009) have been used for identification of the recent sources of radionuclide variations in Europe. Radionuclides of cosmogenic (<sup>7</sup>Be), terrigenous (<sup>40</sup>K and <sup>210</sup>Pb) and anthropogenic (<sup>14</sup>C, <sup>137</sup>Cs and <sup>239,240</sup>Pu) origin have been used as proxy for identification of their variations in atmospheric aerosols.

The main sources of radionuclide variations in the atmosphere have included: modulation of galactic cosmic rays with solar activity (for cosmogenic <sup>7</sup>Be only), stratosphere-troposphere processes, re-suspension of radionuclides from soil, desert dust events, biomass burning, and volcanic eruptions (mainly for terrigenous and anthropogenic radionuclides; Livingston and Povinec, 2002).

Variations of <sup>137</sup>Cs concentrations in the ground-level atmosphere, measured by European monitoring stations, have been correlated with Saharan dust events when large amounts of dust were transported over the Mediterranean Sea on the European continent. A weather model has been used to simulate a probability of dust uplift from the Saharan desert.

A dispersion model has been used for propagation of radionuclides through the atmosphere, including their horizontal and vertical transport, and dry and wet deposition of radionuclides on the earth surface.

The Bratislava group acknowledges support provided by the EU Research and Development Operational Program funded by the ERDF (project # 26240220004), and by the International Atomic Energy Agency (TC project SLR9013).

Blazej S. and Mietelski, J.W. (2014) *J. Radioanal. Nucl. Chem.* **300**, 747–756

Livingston, H. D. and Povinec, P. P. (2002) *Health Phys.* **82**, 656-668.

Lujanienė, G., Aninkevicius, V. and Lujanas, V. (2009) *J. Environ. Radioact.* **100**, 108-119.

Pham, M. K., Povinec, P. P., Nies, H. and Betti, M. (2013) *J. Environ. Radioact.* **120**, 45-57.

Povinec, P. P., Holý, K., Chudý, M., Šivo, A., Sýkora, I., Ješkovský, M., Richtáriková, M. (2012) *J. Environ. Radioact.* **108**, 33-40.

Sýkora, I., Povinec, P.P., Brestáková, L., Florek, M., Holy, K. and Masarik, J. (2012) *J. Radioanal. Nucl. Chem.* **293**, 595–606

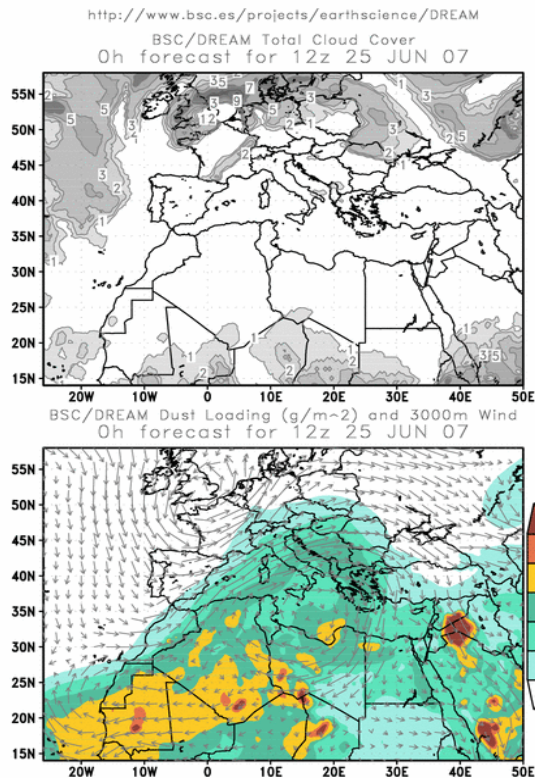


Figure 1 Dry and west deposition over the Europe for the June 2007 case.

## Challenges in assessments of radiological impacts

P. M. Krajewski<sup>1</sup> and G. T. Krajewska<sup>1</sup>

<sup>1</sup>Central Laboratory for Radiological Protection, Warsaw, Mazowia, Poland

Keywords: radioecology, modelling, stochastic, validation

krajewski@clor.waw.pl

At present, assessments of exposures to the public and radiological impacts to the environment, still appears to tackle major issues of prognoses uncertainties. Despite of recent progress in environmental data evaluation in terms of better formulation and description of mechanisms, interactions and radionuclide speciation as well as more accurate quantification of main factors related to transfer and kinetics processes (TRS 472, 2010; TRS 472, 2010; ICRP 114, 2009), the most impact assessments are based on aggregated concepts, applying default values variables therefore usually suffer from large, often orders of magnitude, uncertainties. Indeed, latest publications of the International Commission on Radiological Protection (ICRP) (ICRP 101a, 2006; ICRP 101b, 2006) include requirements and recommendations for the consideration of uncertainties. These have been directly transferred to the IAEA revised Basic Safety Standards (GRS Part 3, 2014) and European Legislation (CD, 2013). Both standards specify that safety assessments which are to be conducted at different stages in the lifetime of an activity or facilities should include, as appropriate, a systematic critical review of any uncertainties or assumptions and their implications for protection and safety. Presumably, the use of probabilistic methods could become the certified technique as it enables to consider any uncertainties intrinsic in dose assessment. Whether the regulators, operators, and stakeholders became familiar with advanced risk prognosis methodology is other question. However, in spite of numerous statistical book there is a lack of practical guidance and harmonized sound scientific supported methodology for the carrying out of such assessments. Moreover, environmental data express not seldom poor statistics and they are aggregated from many various environmental conditions, therefore it is extremely difficult to draw out a shape of PDF function. Also, the structure and complexity of the conceptual model applied and user personal judgement, have significant influence on the overall uncertainties in environmental impact assessments, ( Elert, 1999, Kirchner, 1999, Kirchner, 2008), Thus, the present paper will present and discuss uncertainty of dose prediction from Routine Discharges of Radionuclides to the atmosphere and river base on "Chinon Scenario" in a frame of WORKING GROUP 5 "UNCERTAINTY AND VARIABILITY ANALYSIS FOR ASSESSMENTS OF RADIOLOGICAL IMPACTS ARISING FROM ROUTINE DISCHARGES OF RADIONUCLIDES" for MODELLING AND DATA FOR RADIOLOGICAL IMPACT ASSESSMENTS (MODARIA) IAEA PROGRAMME. The paper discuss the different statistical approaches in selection and of

PDF function base on common used guidance (TRS 472, 2010, TRS 479, 2014) and theirs influence on doses prognosis distribution. The model structure and key elements that may have effect on prognosis uncertainty and distribution shape are reviewed. Several statistics approaches to improve model performance are considered (Guyon, I, 2003; JCGM 106, 2012).

CD, 2013. COUNCIL DIRECTIVE

2013/59/EURATOM of 5 December 2013 laying down basic safety standards for protection against the dangers arising from exposure to ionising radiation, and repealing Directives 89/618/Euratom, 90/641/Euratom, 96/29/Euratom, 97/43/Euratom and 2003/122/Euratom.

Elert, 1999, M. Elert, A. Butler, J. Chen, et al, Effects of model complexity on uncertainty estimates, Journal of Environmental Radioactivity 42 (1999) 255-270

GRS Part 3, 2014, Radiation Protection and Safety of Radiation Sources: International Basic Safety Standards, General Safety Requirements Part 3. No. GSR Part 3, International Atomic Energy Agency Vienna, 2014

Guyon, I, 2003, Guyon Isabelle, An Introduction to Variable and Feature Selection, Journal of Machine Learning Research 3 (2003) 1157-1182

ICRP 101b, 2006. The Optimisation of Radiological Protection - Broadening the Process. ICRP Publication 101b. Ann. ICRP 36 (3).

ICRP 101a, 2006. Assessing Dose of the Representative Person for the Purpose of the Radiation Protection of the Public. ICRP Publication 101a. Ann. ICRP 36 (3).

ICRP 114, 2009, Environmental Protection: Transfer Parameters for Reference Animals and Plants. ICRP Publication 114, Ann. ICRP 39(6)

JCGM 106, 2012, Evaluation of measurement data, The role of measurement uncertainty in conformity assessment. Joint Committee for Guides in Metrology, JCGM 106, 2012

Kirchner, 1999, Gerald Kirchner, S. Ring Peterson", Ulla Bergstrom et al, Effect of user interpretation on uncertainty estimates: examples from the air-to-milk transfer of radiocesium, Journal of Environmental Radioactivity 42 (1999) 255-270.

## Heavy metals and <sup>210</sup>Pb in Finland for the years 2000 – 2005

E. Ioannidou<sup>1</sup>, M. Manousakas<sup>2</sup>, K. Eleftheriadis<sup>2</sup>, J. Paatero<sup>3</sup>, A. Ioannidou<sup>1</sup>

<sup>1</sup>Physics Department, Nuclear Physics Lab., Aristotle University of Thessaloniki, Thessaloniki 54124, Greece

<sup>2</sup>E.R.L., Institute of Nuclear & Radiological Sciences & Technology, Energy & Safety, N.C.S.R. Demokritos, 15310 Ag. Paraskevi, Attiki, Greece

<sup>3</sup>Finnish Meteorological Institute (FMI), Observation Services, P.O. Box 503, Helsinki FI-00101, Finland

Keywords: <sup>210</sup>Pb, heavy metals, trace elements, atmospheric pollution

Presenting author email: [eleioann@physics.auth.gr](mailto:eleioann@physics.auth.gr) (Eleftheria Ioannidou)

In the present work 72 weekly filters collected in Helsinki, Finland during 2000 – 2005 underwent energy dispersive X-ray Fluorescence (ED-XRF) analysis for the determination of their content in Pb, Br, Zn, Cu, Ni, Fe, Mn, Cr, V, Ti, Ca, K, Cl, S, Si, Al, and Na. More specifically, one weekly filter per month and per year was analyzed.

The analysis results indicated that there is a decline trend with the time for Fe and a slight decrease for Ti, Si. The observed concentrations of Pb remain relative stable throughout the time period 2000-2005.

High average concentration of Pb 500 ngr m<sup>-3</sup> was typical of the air in central Helsinki throughout the '60s, but after '70s was decreased to around 150 ngr m<sup>-3</sup> (Mattsson and Jaakkola, 1979). The observed average concentration of lead in the present study equal with 17.7 ngr m<sup>-3</sup>, reveals a decrease of its concentration of the order of one magnitude since '70s.

Other observed mean concentrations in ng m<sup>-3</sup>: Cu: 34.5, Zn: 44.9, Br:15.8, are also lower almost half of those observed during '70s (Cu: 70, Zn: 172, Br:49 ng m<sup>-3</sup>).

The high correlation coefficient observed between the Cu-Zn (R=0.89) is an index of traffic source (Fig. 1). The relative high correlation coefficient between the Ni-V observed values (R=0.66) is an index of heavy oil source. Finally the relative high correlation coefficient between the three elements (Fe-Si-Ti) is a clear index of soil source (Fig. 2).

The Finnish Meteorological Institute has collected daily aerosol samples for the years 2000–2005 for radioactivity monitoring purposes. Airborne <sup>210</sup>Pb is a decay product of <sup>222</sup>Rn emanating from the soil. Due to its long half-life (22.3 years) <sup>210</sup>Pb accumulates relatively into the atmosphere. Thus it can be used as an atmospheric tracer for long-range transported air masses. Anthropogenic lead emissions has low content of <sup>210</sup>Pb, so the anthropogenic lead emissions tend to decrease the specific activity of <sup>210</sup>Pb in the atmosphere. The <sup>210</sup>Pb specific activity is the ratio of the <sup>210</sup>Pb activity concentration to the total concentration of stable lead. The observed values of this ratio vary between 3.5-58 kBq g<sup>-1</sup> (Fig. 3, present study). Previous reported values in Southern Finland ranged between 0.67-39 kBq g<sup>-1</sup> and between 3.9-91 kBq g<sup>-1</sup> in Northern Finland (Kauranen and Miettinen, 2015) with minimum values during the cold winter, due to the increased lead emissions from energy production (Paatero et al., 2015).

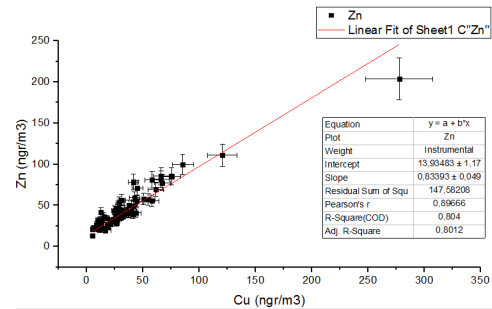


Figure 1. Strong correlation between Cu-Zn is an index of traffic source (years of study 2000-2005)

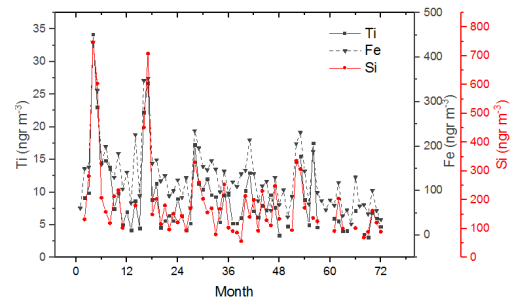


Figure 2. Strong correlation between Fe-Si-Ti is an index of soil source (years of study 2000-2005)

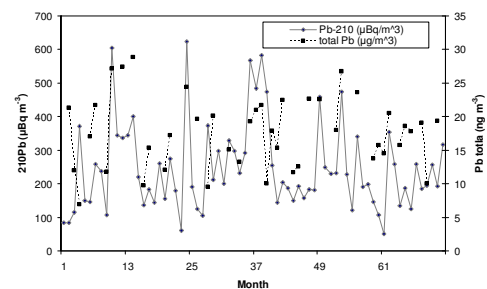


Figure 3. Concentrations for <sup>210</sup>Pb and the Pb<sub>total</sub> for years 2000–2005 in Helsinki, Finland.

### References

- Mattsson R., Jaakkola T., 1979. An analysis of Helsinki air 1962 to 1977 based on trace metals and radionuclides. *Geophysica* 16:1-42.
- Kauranen P. Miettinen JK., 1974. Specific activity of <sup>210</sup>Pb in the environment. *Intern J. Environ Anal Chem.* 3:307-316
- Paatero J., Vaaramaa K., Buyukay M., Kataka J., Lehto J. 2015. Deposition of atmospheric <sup>210</sup>Pb and total beta activity in Finland. *J. Radioanal. Nucl. Chem.* 303: 2413-2420.



## Development of a $^{222}\text{Rn}$ in air secondary standard

M. Krivošík<sup>1,2</sup>, P. Blahušíak<sup>1</sup>, J. Ometáková<sup>1</sup>, M. Chytil<sup>1</sup>, A. Javorník<sup>1,2</sup>, M. Zálešáková<sup>1</sup>

<sup>1</sup>Slovak Institute of Metrology, Department of Ionizing Radiation, Karloveská 63,  
842 55 Bratislava 4, Slovak Republic

<sup>2</sup>Slovak University of Technology in Bratislava, Faculty of mechanical Engineering, Námestie slobody 17,  
812 31 Bratislava 1, Slovak Republic

Keywords: radon chamber, secondary standard, traceability, metrology

Presenting author e-mail: blahusiak@smu.gov.sk

Slovak Institute of Metrology (SMU) received in 2016 a funding for realisation of a secondary standard of  $^{222}\text{Rn}$  in air from the Slovak Research and Development Agency. This standard will serve to provide traceability for laboratories that deal with  $^{222}\text{Rn}$  measurements in environmental samples.

SMU is providing the calibration and verification of various types of the measuring instruments for radon in air and water to determine radiation exposure caused by radon. This demand results from the valid national legislation. Gauges of radon volume activity in the air and in water, and equivalent volume activity of radon in the air, according to Slovak Decree no. 210/2000 Coll. on measuring instruments and metrological control of instruments, are subjected to subsequent verification annually. The project is a response on the European Union legislation and provides metrological support for the development and implementation of the national radon action plan, which the member states of EU are committed to fulfil according Council Directive 2013/59/Euratom.

The secondary standard will consist of two main parts, a radon chamber (a source of radon atmosphere), and an electronic measurement device as a standard of  $^{222}\text{Rn}$ . The chamber (Figure 1) is a horizontal cylinder made from stainless steel with a diameter 0.8 m, length of 2.0 m and a sheet thickness of 5.0 mm. The inner volume of the chamber is about 1.0 m<sup>3</sup>. Considering the construction of the chamber, it will be possible to test the devices directly placing them into the chamber in the radon atmosphere. Due to a visual inspection of measurements, transparent glass door made of soda-lime material was chosen. The entire chamber stands on a mobile chassis. The chamber is connected to a  $^{222}\text{Rn}$  source, air extraction system and other instruments by a vacuum KF system, or special hoses on the top and on the back cap of the chamber for monitoring the radon atmosphere parameters. Radon source is a flow source containing radium salts with  $^{226}\text{Ra}$  activity of 118 kBq. In the present days the tightness of the chamber is tested, and the substantiality of radon source is verified. In the second phase of testing, the chamber will be working in a dynamic regime (López-Coto et al., 2007). The chamber will be continuously filled by radon in order to maintain constant volume activity of radon, and to monitor the thermodynamic parameters of radon gas

mixed with the air. The radon atmosphere inside the chamber will be controlled and the reference value of the  $^{222}\text{Rn}$  volume activity will be determined by a calibrated device Alpha GUARD (Lin et al., 2013).



Figure 1. Cylinder chamber for  $^{222}\text{Rn}$  measurements.

This work was supported by the Slovak Research and Development Agency under the contract No. APVV-15-0017.

- López-Coto, I., Bolivar, J. P., Mas, J. L., Garcia-Tenorio, R., Vargas, A. (2007) Development and operational performance of a single calibration chamber for radon detectors. *Nuclear Instruments and Methods in Physics Research A* 579, 1135-1140.
- Lin, C. F., Wang, J. J., Lin, S. J., Lin, C. K. (2013) Performance comparison of electronic radon monitors. *Applied Radiation and Isotopes* 81, 238-241.



## Behavior of natural radionuclides during a hydrological year in an estuary affected by acid mine drainage and industrial effluents in Southwest of Spain

J.L. Guerrero<sup>1</sup>, A. Hierro<sup>2</sup>, M. Olías<sup>3</sup>, and J.P. Bolívar<sup>1</sup>

<sup>1</sup>Department of Integrated Sciences, Marine International Campus of Excellence (CEIMAR), University of Huelva, Huelva, Andalucía, 21071, Spain

<sup>2</sup>Department of Physics, Autonomous University of Barcelona, Barcelona, Cataluña, 08193, Spain

<sup>3</sup>Department of Geodynamics and Paleontology, University of Huelva, Huelva, Andalucía, 21071, Spain

Keywords: Ría de Huelva estuary, Seasonal behavior, Non-conservative uranium, Acid Mine drainage.

Presenting author email: joseluis.guerrero@dfa.uhu.es

The Ría of Huelva estuary, located at the Southwest of Spain, is formed by the Tinto and Odiel rivers (Figure 1). Tinto and Odiel rivers drain the world's largest sulphide mineral formation: the Iberian Pyrite Belt, which has been worked since 2500 BC. This ecosystem is affected by two facts: 1) the acid mining drainage (AMD) generated in the first section of the river basins, and 2) the chemical industrial complex, located at the estuary

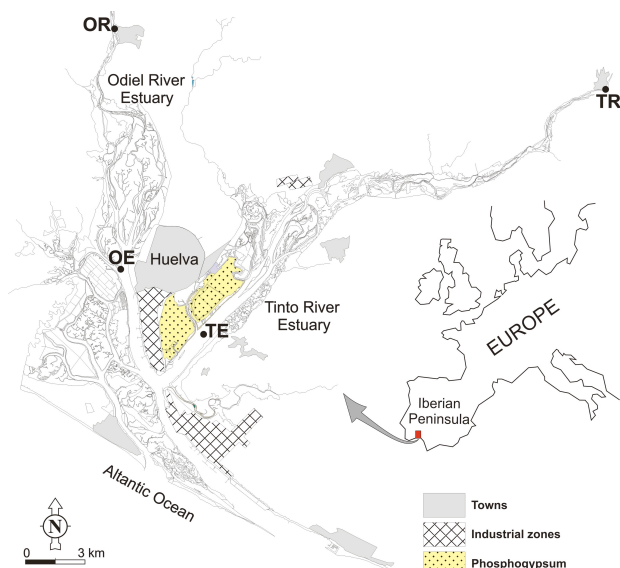


Figure 1. Map of the study area of the Ría de Huelva showing the sampling points.

The AMD (pH = 2-3) gives a singular character to these rivers, keeping high amounts of toxic elements (Hierro et al., 2014), and radionuclides in dissolution. U- and Th-isotopes show concentrations 2-3 orders of magnitude higher than undisturbed continental aquatic system. In addition, very high  $^{234}\text{U}/^{238}\text{U}$  activity ratios (2-3) are observed in these waters.

The objective of this work is to study the behavior of some significant natural radionuclides (U and Th-isotopes) during a hydrological year in the Ría de Huelva Estuary and the end of the rivers (inputs), in order to improve the knowledge of this complex system.

For this study, four sampling points were selected: 1) OR and TR situated at the end of both Odiel and Tinto river, and 2) OE and TE located in the Odiel and Tinto

channels, respectively. OR and TR represent locations having exclusively fluvial composition without any marine influence. In these 4 points, monthly samples for the analysis of natural radionuclides by alpha-particle spectrometry were collected, from September 2009 to September 2010. In total, 52 water samples of 10 L were collected.

The geochemical processes that control the dissolved U in rivers are very complex depending on several factors such as pH, dissolved ions, redox potential, etc. Most of the data for dissolved U in estuaries indicate conservative mixing, but there are examples of non-conservative behavior attributed to oxidation/reduction processes or solubility variations (Church et al., 1996).

The main conclusion from this work was that in the Huelva estuary the U shows a non-conservative behavior due to solubility changes produced by variations in the pH and redox potential. A complete removal of riverine dissolved U is observed in a pH range of 4-6. At pH > 6 a significant fraction of U is released (des-absorbed), from both the suspended matter and bottom sediments, into the dissolved phase. In addition, it highlights the especially high activity concentrations found for Th-isotopes in the mouth river waters, with values up to 100 mBq L<sup>-1</sup> of  $^{230}\text{Th}$ .

### Acknowledgments

This research has been partially supported by the project CTM2015-68628-R (MINECO). José Luis Guerrero thanks the Spanish Ministry of Education, Culture and Sport for a *scholarship* (FPU15/00646).

Church, T.M., Sarin, M.M., Fleisher, M., Ferdelman, T.G., 1996. Salt marshes: an important coastal sink for dissolved uranium. *Geochim. Cosmochim. Acta.* 60, 3879-3887.

Hierro, A., Olías, M., Ketterer, M. E., Vaca, F., Borrego, J., Cánovas C. R., Bolívar J.P., 2014. Geochemical behavior of metals and metalloids in an estuary affected by acid mine drainage (AMD). *Environ. Sci. Pollut. Res.* 21, 2611-2627.

## Outdoor $^{222}\text{Rn}$ concentrations in a city located nearby a large phosphogypsum repository

I. Gutiérrez-Álvarez<sup>1</sup>, J.E. Martín<sup>1</sup>, C. Grossi<sup>2</sup>, A. Vargas<sup>3</sup> and J.P. Bolívar<sup>1</sup>

<sup>1</sup>Departamento de Ciencias Integradas – Física Aplicada, Universidad de Huelva (UHU), 21071 Huelva, Spain

<sup>2</sup>Institut Català de Ciències del Clima (IC3), 08005 Barcelona, Spain

<sup>3</sup>Institut de Tècniques Energètiques (INTE), Universitat Politècnica de Catalunya (UPC), 08028 Barcelona, Spain

Keywords: outdoor radon, continuous monitoring, Huelva, NORM.

Presenting author email: bolivar@uhu.es

The production of phosphoric acid in the Huelva estuary (SW Spain) from 1960 until 2010 employed phosphatic rocks as raw material. These rocks were rich in U series (50 times more than an unperturbed soil). Their  $^{226}\text{Ra}$  content was finally associated with phosphogypsum (over a 90 %). This by-product was stacked in piles into the Tinto river salt-marshes (over 12 km<sup>2</sup> and 1 km away from Huelva city; Bolívar, 2009).  $^{222}\text{Rn}$  exhalation rates from 50 to 750 Bq m<sup>-2</sup> h<sup>-1</sup> have been measured in these piles (Dueñas, 2007), whereas the monthly means for soils of the area range from 13 to 36 (López-Coto, 2013).

For the present study, the outdoor  $^{222}\text{Rn}$  concentration and a set of meteorological variables were measured in Huelva city, in the Campus de El Carmen (UHU, 37.27° N 6.925° W), at 10 and 30 m a.g.l., respectively, during a year, from Spring 2015 through Winter 2016.  $^{222}\text{Rn}$  concentrations corresponded to hourly average values obtained from an air continuous monitoring (ARMON; Vargas et al., 2004). They were deduced from the  $\alpha$ -activity of  $^{218}\text{Po}$  cations produced by the  $^{222}\text{Rn}$   $\alpha$ -decay in the detection volume (a 20 L sphere with a 1  $\mu\text{m}$  filter at the air inlet) and collected over a PIPS detector applying 8 kV between the detector and the sphere surface. The moisture level of the circulating air (1.5 L/min) was kept under humidity lower than 2000 ppmV in order to assure a good system efficiency (reduce the cation neutralization), which depends on it. The valid recorded measurements were about 80 % of the total possible ones (over a 50 % in Spring).

The  $^{222}\text{Rn}$  concentration maximum, average, median and geometric standard deviation were 53.4 (reached in Summer), 7.40, 4.50 and 2.71, in Bq/m<sup>3</sup> (51.5, 10.9, 7.95 and 2.21 in Fall), respectively. The maximum was 39.8 in Spring and 36.4 in Winter. The hourly average  $^{222}\text{Rn}$  concentration showed the expected behaviour associated with the atmospheric stability: a nocturnal increase and a diurnal decrease. The highest values in all the hours took place in Fall. In Winter, in the second part of night, they were clearly lower than those of Summer and Spring, and higher the rest of the day. Three daily patterns were observed for the hourly average  $^{222}\text{Rn}$  concentration doing a weekly average. The first one, a daily smooth oscillation observed in the weeks from the beginning of Winter through the middle of Spring, which was normally under 10 Bq/m<sup>3</sup> (reached two times 15 Bq/m<sup>3</sup>). The second one, a smooth oscillation observed during the last two months of Fall, almost always with a minimum exceeding 5 Bq/m<sup>3</sup> and a maximum beyond 10

(reached 20 Bq/m<sup>3</sup> the 60 % of weeks). And the third one, a less smooth oscillation observed from the middle of Spring through the first month of Fall, with a peak around the sunrise and a flat behaviour in the second part of the diurnal period. This minimum was under 5 Bq/m<sup>3</sup> and the maximum in the range 5-15 Bq/m<sup>3</sup> over the 70 % of times, and between 20 to 30 Bq/m<sup>3</sup> the rest of weeks.

The 3 patterns could be explained considering 3 factors: the more effective  $^{222}\text{Rn}$  dilution associated with a more intense and lasting solar radiation, the annual evolution of  $^{222}\text{Rn}$  exhalation rates from soils of the area, and the occurrence of situations with a higher atmospheric stability in the Huelva estuary. In that sense, every maximum higher than 20 Bq/m<sup>3</sup> occurred in hours around the sunrise with winds with a speed lower than 3 m/s and blowing from NE quadrant (land). It happened 80 % of days in Fall and over 50 % of them in the rest of seasons. Moreover, every maximum higher than 40 Bq/m<sup>3</sup> occurred only with an evolution of wind direction following a breeze regime land-Atlantic ocean (SW quadrant). This fact reflects a high degree of atmospheric stability (Hernández-Ceballos, 2015). Our study has not detected any influence from piles in  $^{222}\text{Rn}$  concentration. Despite of the scarce of days (8) with slow winds in the second part of night from SE quadrant (piles, land), the maximum of  $^{222}\text{Rn}$  was under 20 Bq/m<sup>3</sup> in those days, as occurred from the opposite quadrant (NW, land).

- Bolívar, J.P., Martín, J.E., García-Tenorio, R., Pérez Moreno, J.P., Mas, J.L., 2009. Behaviour and fluxes of natural radionuclides in the production process of a H<sub>3</sub>PO<sub>4</sub> plant. *Appl. Radiat. Isot.* 67-2, 345-356.
- Dueñas, C., Liger, E., Cañete, S., Pérez, M., Bolívar, J.P., 2007. Exhalation of  $^{222}\text{Rn}$  from phosphogypsum piles located at the Southwest of Spain. *J. Environ. Radioact.* 95(2-3), 63-74.
- López-Coto, I., Mas, J.L., Bolívar, J.P., 2013. A 40-year retrospective European  $^{222}\text{Rn}$  flux inventory including climatological variability. *Atmos. Environ.* 73, 22-33.
- Vargas, A., Ortega, X., Martín Matarranz, J.L., 2004. Traceability of radon-222 activity concentration in the radon chamber at the technical university of Catalonia (Spain). *Nucl. Instrum. Methods Phys. Res., Sect. A*, 526(3), 501-509.
- Hernández-Ceballos, M.A., Vargas, A., Arnold, D., Bolívar, J.P., 2015. The role of mesoscale meteorology in modulating the  $^{222}\text{Rn}$  concentration in Huelva (Spain) – impact of phosphogypsum piles. *Meteorol. Atmos. Phys.* 119(3), 163-175.

## Monte Carlo simulation gamma spectrometry of radon in air

R. Breier<sup>1</sup>, P.P. Povinec<sup>1</sup>, M. Krivošík<sup>2,3</sup>, P. Blahušíak<sup>2</sup>, J. Ometáková<sup>2</sup>, A. Javorník<sup>2,3</sup>

<sup>1</sup>Department of Nuclear Physics and Biophysics, Faculty of Mathematics, Physics and Informatics, Comenius University, 84248 Bratislava, Slovakia

<sup>2</sup>Slovak Institute of Metrology, Department of Ionizing Radiation, Karloveská 63, 842 55 Bratislava 4, Slovak Republic

<sup>3</sup>Slovak University of Technology in Bratislava, Faculty of mechanical Engineering, Námetieslobody 17, 812 31 Bratislava 1, Slovak Republic

Keywords: Monte-Carlo, HPGe, Background, muon, cosmic rays, contamination, radon

Corresponding author email: breier@fmph.uniba.sk

### Background

The background of HPGe gamma-spectrometers, which is placed at sea-level, is become from three basic source (Oeschger et al., 1981; Povinec et al., 2008):

(a) cosmic-ray induced component,  
(b) radioactive contamination of construction parts of the spectrometer,

Every material is contaminated with radioactive isotopes. For gamma spectrometry is interesting decay chain of <sup>238</sup>U, <sup>232</sup>Th and isotope <sup>40</sup>K

(c) radioactive contamination of a shield.

For radio-purity research material compound of detector system is necessary use low level background gamma laboratory. Important problem in low level detection system is cosmic ray. Secondary cosmic ray is created by interaction of galactic and solar cosmic ray with atmospheres nuclei. At sea-level it is possible observed free compound of cosmic ray.

(a) hard component (muons),  
(b) nucleonic component (neutrons, protons),  
(c) soft component (electrons, positrons, photons).

In presented work we predicted due to background from cosmic ray and contamination.

### Efficiency

For measurement radon by gamma spectrometry in gas sample was used Marinelli Style Gas Analysis Containers. Monte-Carlo simulation was used for finding of efficiency various isotope in radon chain.

### Monte Carlo

For monte Carlo simulation For the simulation of interactions of particle with the HPGe detector we use the GEANT4 code developed at CERN for high-energy physics interaction studies (Allison et al., 2006). Interactions of muons with matter are included in the GEANT4 package in four mechanisms (Agostinelli et al., 2003): muon ionization, muon bremsstrahlung, production of electron-positron pairs, and muon photonuclear reactions. Depending on the definition of the physics list, we can optimize the simulation for specific applications (Breier and Povinec, 2009). We have been using a predefined physics list, QGSP\_BIC\_HP. This package allows simulation of

high-energy interactions of muons, and includes low energy interaction of gamma and neutrons.

Detail information of the physics of the simulations, a distribution of cosmic-ray muons, their intensities and energies, and their transport through the rock has been covered in our previous papers (Povinec et al., 2008, Breier and Povinec, 2009, Breier et al., 2016).

Oeschger, H., Beer, J., Loosli, H.H., Schotterer, U. 1981. Low-level counting systems in deep underground laboratories In: *Methods of Low-Level Counting and Spectrometry*. IAEA, Vienna, pp. 459–474.

P.P. Povinec, M. Betti, A.J.T. Jull, P. Vojtyla New isotope technologies in environmental physics *Acta Phys. Slovaca*, 58 (2008), pp. 1–154

J. Allison, et al. Geant4 developments and applications *IEEE Trans. Nucl. Sci.*, 53 (2006), pp. 270–278

S. Agostinelli, et al. Geant4 - a simulation toolkit *Nucl. Instrum. Methods Phys. Res. A*, 506 (2003), pp. 250–303

R. Breier, P.P. Povinec Monte Carlo simulation of background characteristics of low-level gamma-spectrometers *J. Radioanal. Nucl. Chem.*, 282 (2009) (79920)

P.P. Povinec, et al. New isotope technologies in environmental physics *Acta Phys. Slov.*, 58 (2008), pp. 1–154

R. Breier, Y. Hamajima, P.P. Povinec

Simulations of background characteristics of HPGe detectors operating underground using the Monte Carlo method *J. Radio. Nucl. Chem.*, 307 (2016), pp. 1957–1960

## Temporal changes of $^7\text{Be}$ , $^{137}\text{Cs}$ , $^{241}\text{Am}$ and Pu isotopes activity concentrations in surface air at Lithuania

S. Byčenkienė<sup>1</sup>, G. Lujanienė<sup>1</sup>, B. Šilobritienė<sup>2</sup>, P.P. Povinec<sup>3</sup>

<sup>1</sup> Department of Environmental Research, SRI Center for Physical Sciences and Technology, Vilnius, Lithuania,

<sup>2</sup> The Environmental Protection Agency, Radiology Division, Lithuania

<sup>3</sup> Faculty of Mathematics, Physics and Informatics, Comenius University, Bratislava, Slovakia

Keywords:  $^7\text{Be}$ ; long-lived radionuclides; aerosol transport

Presenting author email: bycenkiene@ar.fi.lt

In spite of their low activities, the anthropogenic radionuclides introduced into the atmosphere from various sources have been applied as tools for investigation of contaminant behaviour and transport phenomena in the atmosphere.

Measurements of activity concentrations of  $^{137}\text{Cs}$ ,  $^{241}\text{Am}$ ,  $^7\text{Be}$  and Pu isotopes in aerosol were carried out in daily samples in Vilnius (1993-2011), Preila (1994-1999) and Utena (1997-2015) with special emphasis on better understanding of their behaviour as well as their application in tracer studies.

The ground level air samples were collected on FPP-15 filters made of chlorinated polyvinyl chloride (~1 m<sup>2</sup> surface). High volume samplers with flow rates (2400 m<sup>3</sup> h<sup>-1</sup> - 6000 m<sup>3</sup> h<sup>-1</sup>) were operated. The activity concentrations of gamma-emitters were measured in 12 or 24 h samples by gamma-ray spectrometry using HPGe detector (relative efficiency of 42 %, resolution of 1.9 keV at 1.33 MeV). The combined uncertainty of measurements by gamma-spectrometry was better than ± 7 % ( $k = 2$ ).

The radiochemical analyses of Am and Pu were performed on monthly samples (total volume ~2.0x10<sup>6</sup> m<sup>3</sup>) of aerosol ashes (~30 g). The applied radioanalytical procedures are described in detail by Lujanienė (2011). The measurements of Pu and Am isotopes deposited on stainless-steel discs were carried out with the Alphaquattro (Silena) spectrometer. The precision of Pu and Am measurements was better than ±8 % and ±10%, respectively ( $k = 2$ ).

$^{239,240}\text{Pu}$  monthly activity concentrations in Vilnius ranged from 0.9 to 300 nBq/m<sup>3</sup> (mean value of 13.4 nBq m<sup>-3</sup>). The highest  $^{239,240}\text{Pu}$  activity concentration within the 1995–2011 record with the  $^{240}\text{Pu}/^{239}\text{Pu}$  atom ratio close to the Chernobyl value was found in 1995, and it was attributed to the transport of “hot” particles from the areas contaminated after the Chernobyl accident.

The radionuclide activity concentrations measured in Vilnius in March-April of 2011 were approximately by 4 orders of magnitude lower as compared to those after the Chernobyl accident. The activity concentrations of  $^{131}\text{I}$  and  $^{137}\text{Cs}$  ranged from 2 to 3800 mBq m<sup>-3</sup> and from 0.2 to 1070 mBq m<sup>-3</sup>, respectively (Lujanienė et al., 2012). Among other radionuclides, also activities of  $^{239,240}\text{Pu}$  and  $^{241}\text{Am}$  were measured in aerosol samples in April 2011. Concentrations of  $^{239,240}\text{Pu}$  and  $^{241}\text{Am}$  in aerosol samples were found to be 44.5 - 2.5 nBq m<sup>-3</sup> and 15.6 - 3.2 nBq m<sup>-3</sup>, respectively, with  $^{241}\text{Am}/^{239,240}\text{Pu}$  activity

ratio of 0.35 - 0.04 (comparable with 0.37 - 0.04 of global fallout), and high  $^{239,240}\text{Pu}/^{239}\text{Pu}$  atom ratio of  $0.244 \pm 0.018$ .

In samples collected at the Preila background station  $^{137}\text{Cs}$  monthly activity concentrations varied from 0.2 to 5.2 mBq m<sup>-3</sup> with the mean value of 1.9 mBq m<sup>-3</sup>. It is evident that higher activities in aerosol samples and wider variations were found in Vilnius as compared to those found in Preila. Although the  $^{137}\text{Cs}$  activity concentrations in daily samples in Vilnius varied within the factor of 2500, the monthly  $^{137}\text{Cs}$  activities tended to decline for the data obtained between 1993 and 2006.

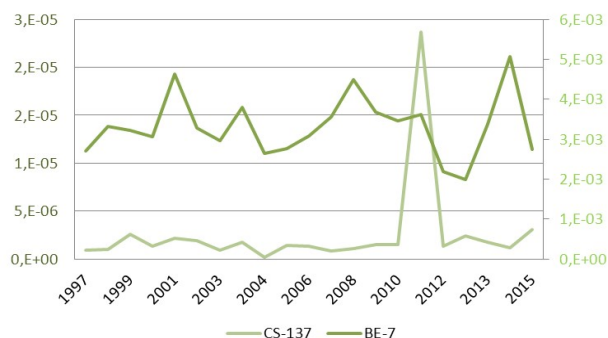


Figure 1.  $^{137}\text{Cs}$  and  $^7\text{Be}$  activity concentrations (Bq m<sup>-3</sup>) in Utena during 1997-2015.

The minimum and maximum  $^7\text{Be}$  activity concentrations were observed during 2001 and 2014 (Figure 1). Temporal course of  $^7\text{Be}$  activity concentrations measured in Vilnius in 1993-1999 showed a clear seasonal variations and relation to 11 year solar cycle.

- Lujanienė, G., 2013. Determination of Pu, Am and Cm in environmental samples. In: *Isotopes in hydrology, marine ecosystems and climate change studies: proceedings of the international symposium held in Monaco, March 27 - April 1, 2011*. Vol. 2. Vienna: International Atomic Energy Agency, 411-418
- Lujanienė, G., Byčenkienė, S., Povinec, P.P., Gera, M. (2012) *J. Environ. Radioact.* **114**, 71-80.
- Lujanienė G., Byčenkienė S., Povinec P.P. (2013) *Appl. Radiat. Isot.* **84**, 330-334.



## Radioactive elements and stable metals in uranium mine drainage

F. P. Carvalho, J.M. Oliveira, M. Malta, M. Santos

Laboratório de Protecção e Segurança Radiológica, Instituto Superior Técnico/Universidade de Lisboa,  
Estrada Nacional 10, km 139, 2695-066 Bobadela LRS, Portugal

Keywords: uranium mines, mine drainage, radionuclides, stable metals, ecotoxicity.

Presenting author email: carvalho@itn.pt

Liquid effluents from uranium mines often are acidic and charged with dissolved radionuclides and stable metals. The most common procedure to treat these radioactive effluents is co-precipitation of radionuclides and metals with barium chloride, decantation of the precipitate in ponds, and release of the overlaying water into rivers while the sludge is disposed as contaminated mud (Carvalho et al., 2011; Pereira et al., 2014). Often, rivers receiving treated and untreated mine drainage display enhanced concentrations of radionuclides (Carvalho et al., 2016).

An investigation was carried out on the acid drainage (pH 3.96) of an old uranium mine containing  $61000 \pm 7300$  mBq/L  $^{238}\text{U}$ ,  $886 \pm 60$  mBq/L  $^{226}\text{Ra}$  and  $504 \pm 27$  mBq/L  $^{210}\text{Po}$ , and relatively high concentrations of Ni, Al, Fe, Mn, and Zn. After the mine water treatment with addition of  $\text{BaCl}_2$  and pH rise with addition of calcium hydroxide, the overlying water released into streams was found to contain still  $8740 \pm 747$  mBq/L of  $^{238}\text{U}$ ,  $250 \pm 22$  mBq/L of  $^{226}\text{Ra}$  and  $30 \pm 1$  mBq/L of  $^{210}\text{Po}$  in the dissolved phase. The radionuclide activities remaining in treated mine water still ranged from 6% to 26% of initial activities. Also, the stable elements still remaining in treated water were at 3-76% of their initial concentrations (Figure 1).

The sludge from water treatment contained most of radionuclides and metals removed from mine water by co-precipitation. After sun drying for several months at the disposal pit, this sludge was leached with water and large fractions of contaminants could be re dissolved. Barium, used in the water treatment, was the only element in concentrations higher in treated water and sludge elutriates than in the original mine water.

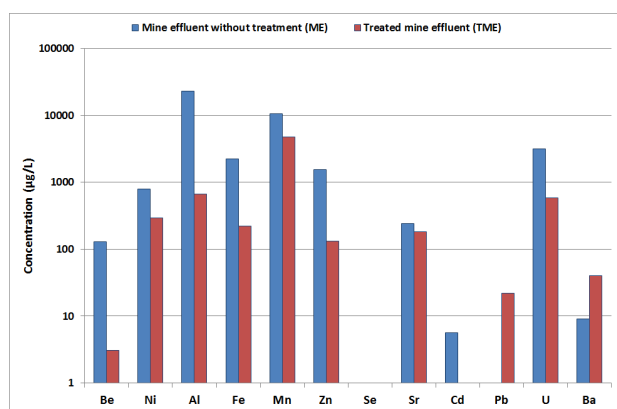


Figure 1. Concentration of metals in mine water and treated mine water.

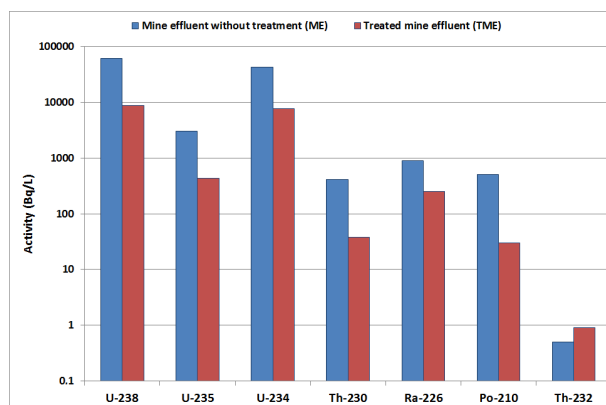


Figure 2. Concentration of radionuclides in mine water and treated mine water.

Results indicate that current uranium mine water treatment with barium are reasonably effective in reducing concentrations of radioelements and stable metals, but treated water still contained contaminants in concentrations that might be toxic to aquatic biota. Disposal of sludge in uncovered landfills may also originate leachates toxic to aquatic fauna. Improved treatment of mine drainage seems therefore needed.

### References

- Carvalho, F. P., Oliveira, J. M., Malta M., 2016. Radioactivity and Water Quality in Areas of Old Uranium Mines (Viseu, Portugal). *Water Air Soil Pollut*, 227:252.
- Carvalho, F. P., Oliveira, J. M., Malta M., 2011. Radionuclides in plants growing on sludge and water from uranium mine water treatment. *Ecol. Eng.* 37, 1058-1063.
- Pereira, R., Barbosa, S., Carvalho, F. P., 2014. Uranium mining in Portugal: a review of the environmental legacies of the largest mines and environmental and human health impact. *Environ Geochem Health* 36, 285–301. (DOI 10.1007/s10653-013-9563-6).
- Lourenço J. , Marques S. , Carvalho F. P., Oliveira J., Malta M., Santos M., Gonçalves F., Pereira R., Mendo S.(Submitted). Evaluation of the teratogenicity and genotoxicity of uranium mine effluents and soil elutriates using the Fish Embryo Toxicity (FET) test.



## Radon Concentration estimation for the working area within the Radioactive Waste Treatment Station from Bucharest, Romania

L.C. Tugulan<sup>1</sup>, A. Chiroasca<sup>2</sup>, D. Vlaicu<sup>1</sup>, C. Ciobanu<sup>1</sup>, F. Dragolici<sup>1</sup> and G. Chiroasca<sup>3</sup>

<sup>1</sup>Horia Hulubei National Institute for Physics and Nuclear Engineering, IFIN-HH, POB MG-6, Magurele, Bucharest 077125, Romania

<sup>2</sup>University of Bucharest, Department of Structure of Matter, Earth and Atmospheric Physics and Astrophysics, 405, Atomistilor str., P.O. MG-11, RO - 077125 Magurele (Ilfov), Romania

<sup>3</sup>University of Bucharest, Doctoral School for Physics, 405, Atomistilor str., P.O. Box MG-11, RO - 077125 Magurele (Ilfov), Romania

Keywords: natural radionuclide, radon concentration, dose estimation.

Presenting author email: liviu.tugulan@nipne.ro

The main component for human exposure to radiation is the Rn-222 present within all enclosed areas. Due this, the EU Directive 2013/59/EURATOM recommends to all member countries to establish an accurate assessment for the Radon (Rn-222) concentration within working places. All Radon concentrations were performed within air with an AlphaGUARD PQ2000 produce by Saphymo GmbH.

Table 1. Effective annual dose for each analysed workspace

Chamber	Dose [mSv/an]			
	media	max	min	with ventilation
0-16	0,75	1,30	0,14	0,15
0-21	0,53	1,10	0,05	0,37
0-22	0,55	1,06	0,11	0,20
0-23	1,63	2,66	0,74	0,21
0-23C	3,14	4,26	1,11	0,20
0-24	0,56	1,14	0,04	0,16
1-06	0,62	1,23	0,18	0,14
1-08	0,55	0,93	0,27	0,19
1-10	2,58	5,63	0,50	0,29
1-13	1,17	1,69	0,17	0,34
1-14	1,62	2,40	0,41	0,29

All results from Table 1 show that we can define two distinct groups, the working areas and the waste treatment and characterization areas.

In order to apply the constraints from 2013/59/EURATOM, the annual effective dose was estimated using the concentration to dose rate conversion coefficients proposed by UNSCEAR, 2008; ICRP, 1993 and L.C. Tugulan et al., 2015. The results from this computations are presented in Table 1 were also average values are presented.

The concentration to dose rate conversion coefficients present specific issues related to the average value used for the conversion, as you can see in Figure 1, the concentration determined with the active detector have specific large amplitude oscillations and an average is hard to assess. The biggest amplitude oscillation is due the ventilation system when the concentration drops rapidly from 200 Bq/m<sup>3</sup> to less than 30 Bq/m<sup>3</sup> within less than two hours after the system is started (in the case of Liquid Treatment Centre – Figure 1).

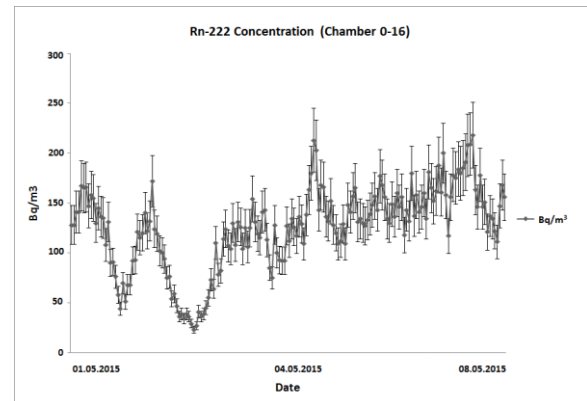


Figure 1. Radon concentration within the Liquid Treatment Centre

The raw results from Table 1 show that for certain workplaces the annual effective dose is above the 1 mSv/year constraint and especially for this type of workplace the use of the ventilation system and the reduction of the exposure time are highly recommended as they are effective in lowering the exposure of human workers employed within the Treatment Station. For workplaces like 0-23, 0-23C, 1-10, 1-13 and 1-14 the authors recommends that the activity to start within them only after completing a 2 hours ventilation cycle.

Directive 2013/59/EURATOM. Laying down basic safety standards for protection against the dangers arising from exposure to ionizing radiation.

National Commission for Nuclear Activities Control, 2000. Fundamental Norms for Radiological Safety NSR 01, Official Bulletin, part I, no.404/29.08.2000.

L.C. Tugulan et al., 2015. Radiation exposure in underground low activity radioactive waste repository. Rom. Journ. Phys., Vol. 60, Nos. 9-10, P. 1598–1605.

United Nations Scientific Committee on the Effects of Atomic Radiation, 2010. UNSCEAR 2008. Report to General Assembly with Scientific Annexes. United Nations, New York.

## The contribution of the natural radionuclides to the radiological hazard at the National Radioactive Waste Repository Baita Bihor, Romania

L. C. Tugulan<sup>1</sup>, C. Ricman<sup>2</sup>, F. N. Dragolici<sup>1</sup>, O. G. Dului<sup>3</sup>

<sup>1</sup>Horia Hulubei National Institute for Physics and Nuclear Engineering, IFIN-HH, POB MG-6, Magurele, Bucharest 077125, Romania

<sup>2</sup>Geological Institute of Romania, National Geological Museum, 2, Pavel Dimitrievici Kiseleff avn., 011345, Bucharest, Romania

<sup>3</sup> University of Bucharest, Faculty of Physics, Department of Structure of Matter, Earth and Atmospheric Physics and Astrophysics, 405, Atomistilor str., P.O. Box MG-11, RO-077125 Magurele, (Ilfov), Romania

Keywords: natural radioactivity, radioactive waste, gamma-rays spectrometry, annual effective dose.

Presenting author email: liviu.tugulan@nipne.ro

The high-resolution gamma spectrometry was used to estimate the contribution of the natural  $^{238}\text{U}$  series,  $^{232}\text{Th}$  and  $^{40}\text{K}$  radionuclides to the annual effective dose within the National Radioactive Waste Repository (DNDR) Baita, Bihor County, Romania. By using the activity to dose conversion coefficients as recommended by United Nations Scientific Committee on the Effects of Atomic Radiation Report (2000), the final results obtained for the annual dose due to natural radionuclides showed values between  $0.29 \pm 0.09$  and  $1.98 \pm 0.14$  mSv/y with an average value of  $0.46 \pm 0.45$  mSv/y, values which are significantly lower than the TLD results previously reported of  $1.55 \pm 0.11$  mSv/y. The relatively steadiness of the total annual effective dose distribution within repository as well as its higher average value than those due to natural radionuclide points towards a certain contribution of the disposed radioactive waste to the annual effective dose. In the same time, it is worth mentioning that the annual effective dose of  $1.55 \pm 0.11$  mSv/y is about 13 times lower the maximum permitted value of 20 mSv/h, established by National Regulations.

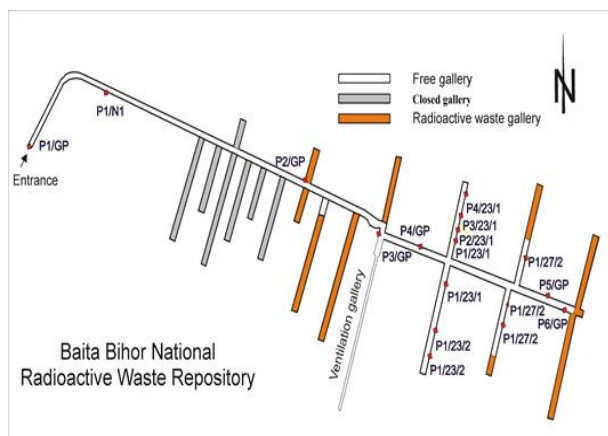


Figure 1. The schematic representation of the Baita Bihor galleries with the location of sampling points

The location of sampling points being presented in Figure 1. Each sample used for radiometric and XRF measurements was about 1 kg of rocks. The contents of  $^{232}\text{Th}$ ,  $^{238}\text{U}$  and  $^{40}\text{K}$  were determined by means of high resolution gamma-ray spectrometry (Tugulan and Dului, 2014).

From the Table 1 data it can be remarked that the average activity concentrations of  $^{238}\text{U}$  series of 83.2 Bq/kg is about two times greater the similar reports for

volcanic and metamorphic rocks of Romania (Cristache et al., 2009).

Table 1. The experimental values of  $^{238}\text{U}$ ,  $^{232}\text{Th}$  and  $^{40}\text{K}$  as determined by high resolution gamma ray spectrometry, the calculated dose rate (D) and annual effective doses (AED).

Sample	Th-232 Bq/kg	U-238 Bq/kg	K-40 Bq/kg	D nGy/h	AED mSv/year
P1/GP	45.7 ± 5.3	424 ± 51	1275 ± 147	277	1.36
P2/GP	67.6 ± 7.8	57.1 ± 6.8	964 ± 111	107	0.53
P3/GP	33.6 ± 3.9	42.6 ± 5.1	767 ± 88	72	0.35
P4/GP	13.1 ± 1.5	58.1 ± 7.1	351 ± 40	50	0.24
P5/GP	28.2 ± 3.2	57.6 ± 6.9	494 ± 57	64	0.32
P6/GP	41.5 ± 4.8	20.6 ± 2.5	918 ± 106	73	0.36
P1/N1	23.2 ± 2.7	52.4 ± 6.3	344 ± 40	53	0.26
P1/23/1	42.6 ± 4.9	61.9 ± 7.4	989 ± 125	96	0.47
P2/23/1	64.1 ± 7.4	699 ± 84	1018 ± 117	404	1.98
P3/23/1	14.7 ± 1.7	173 ± 21	311 ± 36	102	0.50
P4/23/1	34.9 ± 4.0	25.9 ± 3.1	750 ± 86	64	0.32
P1/23/2	38.2 ± 4.4	22.3 ± 2.7	680 ± 78	62	0.30
P2/23/2	54.1 ± 6.2	97.3 ± 11	890 ± 94	115	0.56
P3/23/2	56.1 ± 6.4	48.5 ± 5.8	1212 ± 139	107	0.52
P1/27/1	46.7 ± 5.4	44.5 ± 5.3	844 ± 100	84	0.41
P1/27/2	21.6 ± 2.5	24.4 ± 2.9	834 ± 96	59	0.29
P2/27/2	38.2 ± 4.4	12.1 ± 1.4	1166 ± 134	72	0.38
Average ± SD	39.1 ± 16.0	113 ± 180	739 ± 85	93 ± 92	0.46 ± 0.45

According to the presented results and the effectiveness of the radioprotection system implemented on site, is one more demonstrated the compliance of the activities with the National Regulations and best practices in the field.

National Commission for Nuclear Activities Control, 2000. Fundamental Norms for Radiological Safety NSR 01, Official Bulletin, part I, no.404/29.08.2000.

United Nations Scientific Committee on the Effects of Atomic Radiation, 2000. UNSCEAR 2000. Report to General Assembly with Scientific Annexes. United Nations, New York.

Cristache, C.I. et al., 2009. Epithermal neutron activation, radiometric, correlation and principal component analysis applied to the distribution of major and trace elements in some igneous and metamorphic rocks from Romania. Applied Radiation and Isotopes, 67, 901-906.

Tugulan, L.C., Dului, O.G., 2014. Annual dose rate determination by high resolution gamma spectrometry for TL dating of loess deposits in South-Eastern Dobrudjea, Romania. Romanian Reports in Physics, 66, 862-876

## Environmental dose assessment for the radionuclides embedded in building materials used in residential buildings

L.C. Tugulan<sup>1</sup>, A. Chiroasca<sup>2</sup>, A. F. Miclaus<sup>1</sup>, F. Dragolici<sup>1</sup>, D. Vlaicu<sup>1</sup> and G. Chiroasca<sup>3</sup>

<sup>1</sup>Horia Hulubei National Institute for Physics and Nuclear Engineering, IFIN-HH, POB MG-6, Magurele, Bucharest 077125, Romania

<sup>2</sup>University of Bucharest, Department of Structure of Matter, Earth and Atmospheric Physics and Astrophysics, 405, Atomistilor str., P.O. MG-11, RO - 077125 Magurele (Ilfov), Romania

<sup>3</sup>University of Bucharest, Doctoral School in Physics, 405, Atomistilor str., P.O. MG-11, RO - 077125 Magurele (Ilfov), Romania

Keywords: natural radionuclide, gamma spectrometry, hazard indexes, dose estimation.

Presenting author email: liviu.tugulan@nipne.ro

Our environment is constantly emitting radiation from natural radionuclides embedded in earth, soils, living materials and cosmic sources. As we basically live with radiation and this radiation is mainly due to natural occurring radioisotopes, a correct assessment for the radionuclides we enclose in our walls and buildings may raise specific concerns. This paper we performed a dose and radiation risk assessment of specific major radionuclides present in common building materials.

In order to achieve this, two type of residential buildings were analysed – one flat on second floor for a building so that the soil radon emissions can be ignored and a house build on the ground currently under construction. Both places are within close range to Bucharest, the flat is from Popesti-Leordeni and the house is located in Magurele, Ilfov.

The radionuclide concentrations from the building materials were evaluated using High Performance GeHP spectrometry and the initial results (for the major radionuclides) are present in table 1.

Table 1. Radioisotope concentration results for the building materials

sample	U-238 [Bq/kg]	Th-232 [Bq/kg]	K-40 [Bq/kg]
Ceramic Brick Flat	68.1 ± 12	47.7 ± 8.2	571 ± 98
Cement (after maturing) Flat	32.3 ± 5.6	17.5 ± 3.9	225 ± 39
Ceramic tile Flat	33.8 ± 5.7	42.9 ± 8.5	268 ± 46
Hone Flat	487 ± 81	60.5 ± 10.2	196 ± 34
Sand Flat	48.8 ± 8.3	12.5 ± 4.8	482 ± 83
Concrete (B250) House	14.2 ± 2.5	11.2 ± 3.8	315 ± 54
autoclaved aerated concrete House	14.4 ± 2.4	12.8 ± 3.2	296 ± 36
Ceramic Brick House	70.0 ± 10.1	50.0 ± 7.3	733 ± 85

From this results we can perform an accurate assessment for the dose given by the exposure to the building itself without being affected from the other radionuclides from soil, ground and other materials within the house. For this assessment, conversion coefficients were taken from UNSCEAR 2000 leading to a dose rate and annual equivalent dose (AED) for each of the materials under evaluation (see table 2).

The last column contains the activity concentration index for each of the materials and it is obtained from the procedure presented in EU directive 2013/59/EURATOM.

The global values were obtained by taking into account the proportion of materials used (based on architectural and structural projects) we can estimate the annual equivalent dose for the two residential places. The lower value was obtained for the Flat where annual equivalent dose is  $(0.34 \pm 0.04) \text{ mSv/year}$  –dose rate is  $(69.4 \pm 6.9) \text{ nGy/h}$ . For the second case, the house has a dose rate of  $(74.2 \pm 7.9) \text{ nGy/h}$  leading to an annual equivalent dose of  $(0.36 \pm 0.04) \text{ mSv/year}$ .

Table 2. Dose rate evaluation for the analysed radionuclides from the building materials

sample	D [nGy/h]	AED [mSv/an]	I [Bq/kg]
Ceramic Brick Flat	84.1 ± 3.79	0.41 ± 0.01	0.66 ± 0.03
Cement (after maturing) Flat	34.9 ± 1.91	0.17 ± 0.01	0.27 ± 0.02
Ceramic tile Flat	52.7 ± 2.6	0.26 ± 0.01	0.42 ± 0.02
Hone Flat	270 ± 12	1.32 ± 0.02	1.99 ± 0.09
Sand Flat	50.2 ± 5.2	0.25 ± 0.01	0.39 ± 0.04
Concrete (B250) House	26.5 ± 2.3	0.13 ± 0.01	0.21 ± 0.02
autoclaved aerated concrete House	26.7 ± 1.4	0.13 ± 0.01	0.21 ± 0.01
Ceramic Brick House	93.1 ± 2.6	0.46 ± 0.01	0.73 ± 0.02

The dose equivalent effective annually for these two houses is low than limit of 1 mSv/y (CNCAN, 2000), required in Romania, for population.

Directive 2013/59/EURATOM. Laying down basic safety standards for protection against the dangers arising from exposure to ionizing radiation.

National Commission for Nuclear Activities Control, 2000. Fundamental Norms for Radiological Safety NSR 01, Official Bulletin, part I, no.404/29.08.2000.

United Nations Scientific Committee on the Effects of Atomic Radiation, 2000. UNSCEAR 2000. Report to General Assembly with Scientific Annexes. United Nations, New York.

## Use of gamma spectrometry for detection of $^{222}\text{Rn}$ pre-earthquake anomalies

G. Eleftheriou<sup>1</sup>, V.K. Karastathis<sup>1</sup>, K. Tsinganos<sup>1,3</sup>, M. Kafatos<sup>2</sup>, T. Aspiotis<sup>1</sup>, D. Ouzounov<sup>2</sup> and G. Tselentis<sup>1,3</sup>

<sup>1</sup>Institute of Geodynamics, National Observatory of Athens, Athens, Thessio, 11810, Greece

<sup>2</sup>EESMO, Chapman University, CA, Orange, 92866, USA

<sup>3</sup>National and Kapodistrian University of Athens, Athens, Zografou, 15772, Greece

Keywords: Radon, Earthquakes,  $\gamma$ -spectrometry, SW Peloponnese.

Presenting author email: geoelefthe@noa.gr

In order to investigate pre-earthquake phenomena and forecast strong seismic events, many types of earthquake precursors have been proposed and applied worldwide (Cicerone et al., 2009). Among them,  $^{222}\text{Rn}$  anomaly in soil gas has been evidenced as a particularly effective middle-term pre-earthquake precursor (Gosh et al., 2011). Traditionally  $^{222}\text{Rn}$  measurements are performed by means of alpha spectrometry, however recently the use of gamma sensors for subsurface  $^{222}\text{Rn}$  monitoring has been proved clearly advantageous (Zafirir et al., 2011).

In this work, we are presenting long-term measurements of  $^{222}\text{Rn}$  in the soil applying gamma ray spectrometry. The measurements were performed as part of an innovative integrated study of pre-earthquakes phenomena (Tsinganos et al. 2016), where three gamma radiation sensors (NaI(Tl) scintillators) for continuous real-time monitoring of  $^{222}\text{Rn}$  accumulation in the ground have been installed at the region of SW Peloponnese. All gamma ray sensors have been energy calibrated and installed in the ground at a depth of 1 m. Local meteorological parameters (precipitation, atm. pressure, temperature, humidity) for atmospheric corrections were also continuously monitored. The  $^{222}\text{Rn}$  measurements were performed indirectly by means of gamma ray spectrometry of its radioactive progenies  $^{214}\text{Pb}$  and  $^{214}\text{Bi}$ . Automatic in-situ Full Spectrum Analysis (FSA) technique was applied, with sampling rate of 30 min, for direct quantitative determination of  $^{222}\text{Rn}$ ,  $^{232}\text{Th}$  and  $^{40}\text{K}$  ( $\gamma$ ). An additional alpha radiation spectrometer (Barasol unit) has been used for the inter-calibration of all gamma radiation monitoring stations after their installation.

Time series from the stations have been recorded and statistically analyzed in order to determine the background level and identify anomalous variations. The results are very promising since radon anomalies are in good correlation with earthquakes in many cases. The radon anomalies occur between 1 to 10 days, approximately, before the earthquakes. The duration and the variation depend on distance from the epicentre and the earthquake magnitude. The radon concentration increment reached up to 35% while the duration of the anomalies varies from hours up to several days.

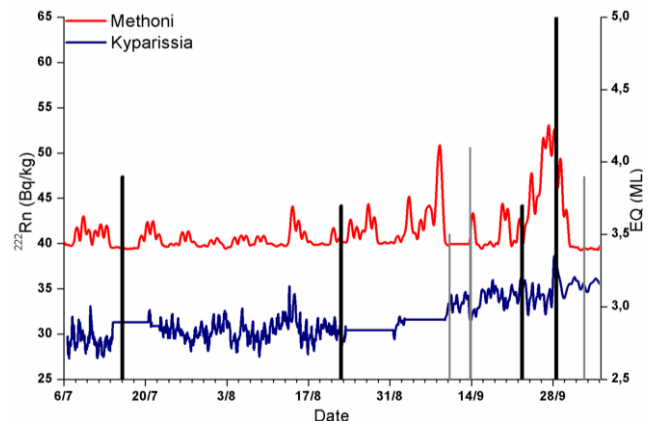


Figure 1. Radon anomalies recorded at two  $^{222}\text{Rn}$  stations before significant earthquakes occurred at the region of SW Peloponnese.

This work was supported by the Hellenic General Secretariat for Investments and Development under project ARISTOTELIS: “GSRT Excellence Program in Environment, Space and Geodynamics / Seismology 2015-2017”.

- Cicerone, R.D., Ebel, J.E., Britton, J., 2009. A systematic compilation of earthquake precursors. *Tectonophysics* 476, 371-396.
- Ghosh, D., Deb, A., Sengupta, R., 2011. Anomalous radon emission as precursor of earthquake. *J. Appl. Geophys.* 69, 67-81.
- Tsinganos, K., Karastathis, V.K., Tselentis, A., Papadopoulos, D., Kafatos, M., D. Ouzounov, G.A., Velez, A.P., Eleftheriou, G., Mouzakiotis, E., Liakopoulos, S., Aspiotis, T., Gika, F., Voulgaris, N., 2016. A pilot study of the Earthquake Precursors in the Southwest Peloponnese, Greece. *AGU Fall Meeting 2016, NH51C-1976*.
- Zafirir, H., Haquin, G., Malik, U., Barbosa, S.M., Piatibratova, O., Steinitz, G., 2011. Gamma versus alpha sensors for Rn-222 long-term monitoring in geological environments. *Radiat. Meas.* 46, 611-620.



## <sup>210</sup>Po determination in sandy soils by alpha-particle spectrometry

C. Bañobre<sup>1</sup>, I. Diaz-Francés<sup>2</sup>, A. Noguera<sup>1</sup>, H. Bentos Pereira<sup>1</sup>,  
L. Fornaro<sup>1</sup>, G. Manjón<sup>2</sup> and R. García-Tenorio<sup>2</sup>

<sup>1</sup> Grupo de Desarrollo de Materiales y Estudios Ambientales, Centro Universitario Regional del Este, Universidad de la República, Rocha, Uruguay

<sup>2</sup> Grupo Física Nuclear Aplicada, Universidad de Sevilla, Sevilla, Spain

Corresponding author: gtenorio@us.es

### Introduction

<sup>210</sup>Po is a naturally occurring radionuclide, which can be considered one of the most radiotoxic natural radioactive isotopes known by man due to its high specific activity and its emission of high linear energy transfer (LET) alpha radiation.

<sup>210</sup>Pb ( $T_{1/2} = 22.3$  y) is the parent nuclide of <sup>210</sup>Po and is formed by the decay of radon (<sup>222</sup>Rn) in the uranium series. Radon gas exists in atmospheric air, originated from exhalation from the ground, being its formed daughters (e.g. <sup>210</sup>Pb and <sup>210</sup>Po) wet and dry deposited onto terrestrial surface and surface of the seas where they can be incorporated into the food chain. Hence, man is exposed to radioactive polonium by natural processes, mainly from the oral intake of foodstuff.

Because <sup>210</sup>Pb is a soft beta emitter with an additional low-energy gamma emission (its direct radiometric measurement is no trivial), the <sup>210</sup>Pb determination, particularly in soils, is performed in many cases by the measurement of its daughter <sup>210</sup>Po, pure alpha emitter, by alpha-particle spectrometry, assuming secular equilibrium. These determinations are useful for example to study potential transfer factors soil to plants in radioecological studies or in the evaluation of erosion rates in environmental studies and requires assuring the complete dissolution of the sample, especially in soils with a high proportion of sand where a fraction of this radionuclide can form part of the crystalline structure.

In this work a couple of radiochemical methods for <sup>210</sup>Po determinations by alpha-particle spectrometry in sandy soils has been tested and validated based in the complete digestion of the treated aliquots and the self-deposition of the liberated <sup>210</sup>Po onto copper or silver discs.

### Materials and Methods

The activity concentrations of <sup>210</sup>Po in all the samples analyzed have been determined by applying the high-resolution alpha-particle spectrometric technique. In particular, an alpha-particle spectrometric system, Alpha-Analyst from Canberra Co., formed by a total of eight independent chambers working in parallel, each one equipped with a PIPS type silicon detector (450 mm<sup>2</sup> active area), has been employed, being reached typical minimum detectable activities in the order of 10<sup>-1</sup>mBq.

The application of this technique implies the previous isolation and deposition in thin layers of the radioelement of interest in order to avoid interferences in the measurements. The two radiochemical methods

tested for <sup>210</sup>Po determination are based in the complete microwave digestion of sandy soils aliquots with mixture of acids (nitric, hydrochloric and hydrofluoric acids), differing in the posterior treatment of the obtained solution: in one case the solution is directly conditioned for the posterior self-deposition of the <sup>210</sup>Po onto silver discs without any previous radiochemical isolation, while in the other case the solution obtained from the microwave digestion is submitted to a liquid-liquid extraction procedure in order to isolate the Po from other elements or radionuclides, being afterwards the isolated Po fraction self-deposited onto copper discs.

The second radiochemical method, more laborious due to the application of a liquid-liquid separation procedure, allows the sequential obtention of another fraction containing the U-isotopes isolated.

### Results and Discussion

The <sup>210</sup>Po determinations performed in aliquots of sandy soil samples for the two described procedures indicate that both give results in good agreement between them and reproducible, allowing to conclude that when the only alpha emitter of interest to be determined is the <sup>210</sup>Po, the most simple method based in its direct self-deposition from the solution obtained from the digestion (after conditioning) can be applied with confidence. The use of the more laborious method could be considered as an alternative when in addition to the <sup>210</sup>Po, the determination of the U-isotopes alpha emitters (<sup>234</sup>U, <sup>235</sup>U and <sup>238</sup>U) is needed. Both methods conduit to obtain high radiochemical yields and clean deposits, allowing a complete separation of the <sup>210</sup>Po and the <sup>209</sup>Po (used as chemical tracer) peaks in the alpha-spectra.

In the sandy soils analyzed, the <sup>210</sup>Po levels found are in agreement with the levels of <sup>238</sup>U and <sup>234</sup>U determined sequentially also by alpha-particle spectrometry, and with the levels of <sup>226</sup>Ra determined by gamma-ray spectrometry, with a High Pure Germanium Detector 35 % efficiency and 1.75 % photopeak resolution for <sup>60</sup>Co, indicating the existence of secular equilibrium along all the uranium series in the analyzed samples, and giving additional confidence about the methods proposed. These sandy soils present, as expected, a negligible fraction of atmospheric <sup>210</sup>Pb, because the deposited atmospheric fraction of this radionuclide is fixed in a minimum proportion in soils with very little content of organic matter.



## Dynamics of radionuclide concentration in components of the Chernobyl NPP cooling pond ecosystem during drawdown of water level

D.I. Gudkov<sup>1</sup>, S.I. Kireev<sup>2</sup>, A. Ye. Kaglyan<sup>1</sup>, S.M. Obrizan<sup>2</sup>, A.B. Nazarov<sup>2</sup> and V.V. Belyaev<sup>1</sup>

<sup>1</sup>Department of Aquatic Radioecology, Institute of Hydrobiology, Kiev, UA-04210, Ukraine

<sup>2</sup>State Specialized Enterprise “Ecocentre”, Chernobyl, UA-07270, Ukraine

Keywords: Chernobyl NPP cooling pond, radioactive contamination, water, aquatic biota.

Presenting author email: digudkov@gmail.com

The Chernobyl NPP cooling pond (CP) is one of the most contaminated water bodies within the Chernobyl Exclusion Zone (CEZ). In May 1986 water radioactivity was determined mainly by <sup>131</sup>I and other short-lived radionuclides and according to some sources was 1.5 kBq l<sup>-1</sup> (Kryshev, 1995), others - reached the order of 10<sup>5</sup> Bq l<sup>-1</sup> (Kazakov et al., 1994). The density of contamination of the CP's sediments by <sup>90</sup>Sr in early 1990s was 14.8 GBq km<sup>-2</sup> - 24.3 TBq km<sup>-2</sup> and <sup>137</sup>Cs - 0.4-28.4 TBq km<sup>-2</sup> (Kazakov et al., 1994).

In 2008, under the “Program of the Chernobyl nuclear power plant decommissioning”, it was decided on the CP drawdown. In late 2014, after the cessation of pumping water into the CP, the natural decline in the water level, mainly due to the filtering of water through the body of the dike, has began. Examples and analogues of decommissioning of the cooling pond of such volume and levels of radioactive contamination, as well as the transformation of the semi-natural ecosystem in the water level drawdown conditions do not exist.

The CP is an artificial water body, located on the right bank floodplain area of the Pripyat River. The waterfront of the CP was formed partially by above the floodplain terrace, and preferably by protective dam with length of 25 km, width of 70-100 m and 5.7 m in height. Before the start of the drawdown of water level in the CP its length was 11 km, average width - 2 km, surface area - 22.7 km<sup>2</sup>, prevailing depth - 4-7 m but on separate areas – up to 18-20 m and the amount of 149 million m<sup>3</sup>.

Our studies were carried out during 1998-2017. The <sup>137</sup>Cs concentration in water and hydrobionts was measured by  $\gamma$ -spectrometry complex: PGT IGC-25 detector (France), “Nokia LP 4900 B” analyser (“Nokia”, Finland), low-volt feeding source – crate NIM BIN, amplifier NU-8210 (“Elektronikus Merokeszulekek Gyara”, Hungary) and 100 mm thickness leaden protection. The <sup>90</sup>Sr content was measured on low-background NRR-610  $\beta$ -radiometer (“Tesla”, Czech). Minimal detectable activity was 0.04 Bq under 1000 s sample exposition.

The declines of water level in the CP at the present stage first of all have caused a drastic change in the hydrological, hydrobiological and hydrochemical regime. In February 2017, the water level and volume of water masses decreased respectively by 4.5 m and 70%. In place of the CP three water bodies with different size and volume were formed. There was a mass death of periphyton (aquatic organisms, that live attached to rocks or other surfaces) communities of plants and animals (especially bivalves) and littoral aquatic plants, leading

to organic pollution of the pond ecosystem and deterioration in its sanitary and biological indicators. During the period 2015-2016 the concentration of <sup>90</sup>Sr and <sup>137</sup>Cs in water increased by 35-40% (Figure).

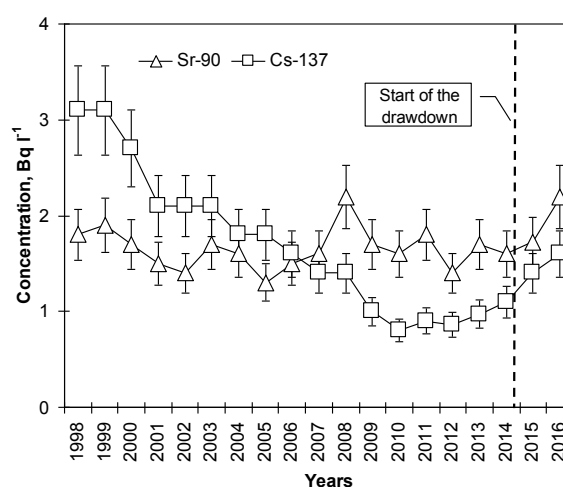


Figure. Dynamics of <sup>90</sup>Sr and <sup>137</sup>Cs concentrations in water of the CP during 1998-2016.

During 2016, due to annual update of higher aquatic plants' biomass, an increase in the concentration of radionuclides in plant tissues by 20-30% has marked in comparison to 2014. A significant increase in the activity of radionuclides in shellfish and fish for a period of water levels drawdown has not determined.

Due to changes in the hydrological and hydrochemical regime of the CP in the coming years is expected to change the physicochemical forms of the radionuclides in the bottom sediments, their transition into a dissolved state and a more intense accumulation by living organisms.

This study was supported by the NAS of Ukraine and by the State Agency of Ukraine on the Exclusion Zone Management. The authors wish to thank personnel of State Specialized Enterprises “Chernobyl NPP” and “Ecocentre” for the promoting research within the CEZ.

Kazakov S.V., Vovk P.S., Fil'chagov L.P. 1994. Radioecological state of the Chernobyl NPP cooling pond. Problems of the Chernobyl exclusion zone. 1, 129-138 (in Russian).

Kryshev I.I. 1995. Radioactive contamination of aquatic ecosystems following the Chernobyl accident. J. Environmental Radioactivity. 27, 207-219.

# Study on the correlation of the variation of $\gamma$ dose rate and radon progeny in the atmosphere

Lei Zhang<sup>1</sup>, Qiuju Guo<sup>2</sup> and Yunxiang Wang<sup>2</sup>

<sup>1</sup>State Key Laboratory of NBC Protection for Civilian, Beijing, 102205, China

<sup>2</sup>State Key Laboratory of Nuclear Physics and Technology, School of Physics, Peking University, Beijing, 100871, China

Keywords:  $\gamma$  dose rate, radon progeny, precipitation, <sup>214</sup>Bi.

Presenting author email: [qjguo@pku.edu.cn](mailto:qjguo@pku.edu.cn)

There are several reasons can cause the variation of  $\gamma$  dose rate in environmental monitoring stations surrounding nuclear facilities. It is very important to clarify the variation of natural background radiation from man-made reasons, such as an accident.

Experiment study on the correlation of the variation of  $\gamma$  dose rate and radon progeny in the atmosphere was carried out by on-site continuous measurements on  $\gamma$  dose rate, concentrations of radon and its progeny in Beijing, China. Figure 1 is the outlook of the monitors. Data of precipitation is from China Meteorological Database.

Figure 2 is the measurement results of  $\gamma$  dose rate and concentration of radon and its progeny(July 15 to 1<sup>st</sup> August, 2016).

It is found that during the period of no precipitation, the variation range of  $\gamma$  dose rate is 77.70 – 93.39 nSv<sup>-1</sup> with an average of 84.25 nSv<sup>-1</sup>; while during or after strong precipitation, the highest value of  $\gamma$  dose rate can reach 137 nSv<sup>-1</sup>, 63% higher than that of the average.

It is also found that during the period of on precipitation, the correlation between  $\gamma$  dose rate and radon progeny in low level atmosphere is quite week, R=0.2826. the variation of radon progeny in low level atmosphere causes the variation of  $\gamma$  dose rate less than 5%.

During or after big precipitation, however, a strong correlation between  $\gamma$  dose rate and the concentration of <sup>214</sup>Bi, which is washed down from higher level atmosphere, is indicated by Figure 3.



Figure 1. Outlook of related monitors.

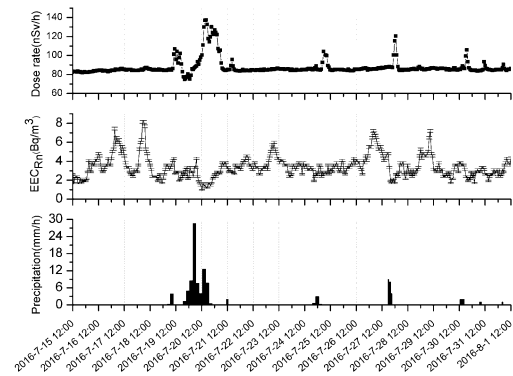


Figure 2. Measurement results on  $\gamma$  dose rate and concentrations of radon and its progeny

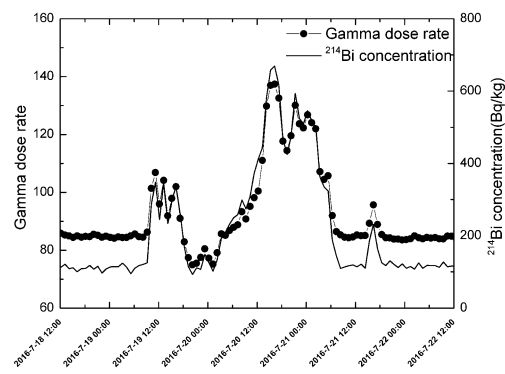


Figure 3. Correlation between  $\gamma$  dose rate and <sup>214</sup>Bi

This work was supported by the National Found of Natural Sciences of China (No. 11355001).

Lei Zhang, Jinmin Yang and Qiuju Guo. STUDY ON A STEP-ADVANCED FILTER MONITOR FOR CONTINUOUS RADON PROGENY MEASUREMENT. Radiation Protection Dosimetry (2016), pp. 1–4.

SARAD GmbH. A2M4000 Area activity monitor. AM4000\_InfoSheet\_DataSheet\_EN\_08-04-2014.docx.

M. Lebedyte, D. Butkus, G. Morkunas. Variations of the ambient dose equivalent rate in the ground level air. Journal of environmental radioactivity. 2003. Vol.64: 45-57.

N. Fujinami. Study of radon progeny distribution and radiation dose rate in the atmosphere. Japanese journal of health physics. 2009. Vol. 44:89-94.

## The fate of contaminated radiocesium in forest litter during fungal lignin degradation as the late stage of decomposition process

S.N. Hashida and T. Yoshihara<sup>1</sup>

<sup>1</sup>Environmental Science Research Centre, Central Research Institute of Electric Power Industry, Abiko, Chiba, 270-1194, JAPAN

Keywords: Bioleaching, litter degradation, lignin, white rot fungus.

Presenting author email: shashida@criepi.denken.or.jp

Besides physicochemical processes, biological process acts important role in the migration and immobilization of radionuclide. Soil microorganisms decompose forest litter fall under bioactive natural environment and this process acts as the first step of radionuclide remobilization. Thus, their activity profoundly influences the fate of radionuclide by leaching from organic matter, enabling environmental biocycling. Consequently, the period of radionuclide retention is attributed to microbial and forest litter property (Steiner et al., 2002). Previously, we demonstrated that the retention of Fukushima-derived radiocesium correlated with recalcitrant lignin macromolecules of decomposing Japanese cedar litter, but not in decomposing Japanese flowering cherry litter (Hashida et al., 2016). Lignin chemical structures are known to be complex, including an assembly of three types of lignin subunits, i.e., *p*-hydroxyphenyl (H), guaiacyl (G), and syringyl (S), and the proportions of these subunits vary among distinct woody species. Therefore, the behaviour of Fukushima-derived radiocesium contaminated in litter fall may vary depending on tree species and the lignin degradation activity.

In this study, we investigated that 1) the cesium absorbing capacity of lignin derivative prepared from various tree species, 2) the impact of nutrient condition on lignin degradation in our *in vitro* decomposing assay and 3) isolation of local white-rot fungi with high lignin degradation activity. Well-dried lignin derivative (TGAL) extracted from various tree species was capable of absorbing stable cesium in the column experiment (Table. 1). The variation of absorbing capacity was greater in deciduous broad leaf (DB) species than evergreen needle leaf species (EN). Generally, DB lignin consists of both G- and S-subunit while EN lignins are composed of exclusively G-subunit. The structural complexity could cause the larger variation in DB lignins.

**Table 1.** Cesium absorbing capacity of various TGAL

Tree	Species	Absorbing capacity, ng/mg
<i>Cryptomeria japonica</i>	EN	375
<i>Taxus cuspidata</i>		375
<i>Ostrya japonica</i>	DB	475
<i>Acer pictum</i>		375
<i>Maackia amurensis</i> var. <i>buergei</i>		350
<i>Juglans nigra</i> L.		325
<i>Tilia japonica</i>		325
<i>Kalopanax pictus</i>		300
<i>Prunus jamasakura</i>		345

In previous report, lignin degradation by whit-rot fungal inoculation was poor under our experimental condition (Figure 1A, PDA). Here, nitrogen starvation efficiently decreased lignin content during two weeks cocultivation with milled cedar litter (Figure 1A, KIRK). Moreover, we collected local white-rot fungi with various lignin degradation activities (Figure 1B). Combined with optimum cultivation condition and fungi with high lignin degradation activity, we are now evaluating the fate of contaminated radiocesium in forest litter during later decomposition process, namely fungal lignin degradation.

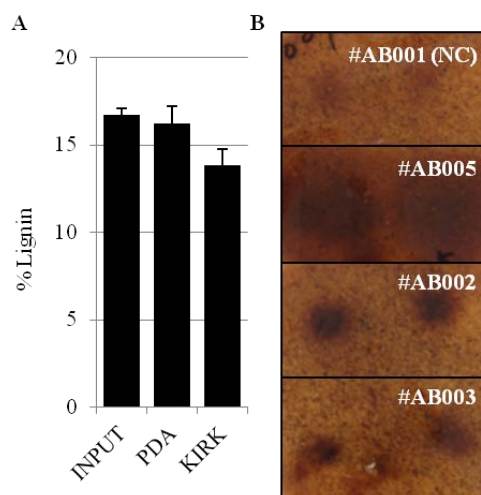


**Figure 1.** Lignin degradation assay

**A.** Quantification of lignin two weeks after white-rot fungi cocultivation with milled cedar litter. PDA means normal nitrogen condition and KIRK means nitrogen starvation condition. **B.** Activity of lignin degradation of isolated local white-rot fungi on cedar litter-guaiacol medium.

This work was supported by the Japan Society of the Promotion of Science (JSPS) Grant-in-Aid for Scientific Research (B) [Grant Number 15H04621 to T.Y. and S-n.H.].

Steiner, M., Linkov, I. and Yoshida, S. 2002. The role of fungi in the transfer and cycling of radionuclides in forest ecosystems. *J. Environ. Radioact.* 58, 217-241.  
 Hashida, S.N. and Yoshihara, T. 2016. Disparate radiocesium leaching from two woody species by acceleration of litter decomposition using microbial inoculation. *J. Environ. Radioact.* 162-163, 319-327.

## Elaboration and use of heat maps to assess of nuclear risk

M.A. Hernández-Ceballos<sup>1</sup>, L. De Felice<sup>1</sup>

<sup>1</sup>Joint Research Centre, Nuclear Safety and Security Directorate, Knowledge for Nuclear Security and Safety Unit, Radioactivity Environmental Monitoring Group, Ispra, Varese, 21021, Italy

Keywords: Radioactivity, Forward trajectories, heat maps, EURDEP

Presenting author email: miguel.hernandez@jrc.ec.europa.eu

### Introduction

Following the Fukushima accident, interest in off-site Emergency Preparedness and Response (EP&R) increased substantially at national, regional and global levels. Most countries have reviewed their EP&R arrangements and capabilities and many are implementing improvements as a consequence.

In this sense, the possibility to report a first and quick estimation in the early phase of an emergency event about the areas that could be potentially affected is quite useful for the civil protection authorities to address this kind of events and mitigate its impact in the area of interest.

However, the complexity and the risk of addressing the radiation-releasing nuclear accidents at any specific place is a function of several factors, such as, the large-scale release of radionuclides, the amount and composition of the radionuclides released (source term), the atmospheric transport and deposition of the released radioactivity, the vulnerability of the people and economic assets (involving dose-effects relationship),...

### Objective

Due to the key role of the meteorological fields, specifically wind dynamics, in the temporal and spatial variability of radioactivity releases in the atmosphere, in the present work, we suggest a methodology to estimate the spatial impact, in terms of probability, of a hypothetical release from a given European Nuclear Power Plant (NPP).

This method is based on obtaining the corresponding heat map, based on the Kernel Density Estimation techniques (Wand and Jones, 1995), of each NPP from the base of the information provided by a large set of forward trajectories calculated from each NPP.

### Methodology

1) To calculate the set of four daily forward trajectories in each one of the 56 European NPPs during a period of five years (2011-2015). The total number of trajectories for each NPP was 7,304, and they have been calculated using the HYSPLIT model at an initial height of 100 m and with a temporal horizon of 96 hours.

2) A PostgreSQL DB with PostGIS extension for supporting geographical features has been designed for storing all trajectories as points (40,516,900 points for each NPP)

3) A plugin for QGIS software has been used for visualizing and processing all stored trajectories and the

corresponding points reading the data directly from the DB e performing the heat maps.

4) A search radius (kernel bandwidth) of 55 km and the uniform kernel shape (this parameter controls the rate at which the influence of a point decreases as the distance from the point increases (radius)), were used to calculate the heat maps. The radius specifies the distance around a point at which the influence of the point will be felt, while this kernel option gives the same weight to all points within this radius. For more information, we refer to <http://docs.qgis.org/2.0/ca/docs/>

### Results

A general and four seasonal heat maps comprising the 2011-2015 period were obtained for each EU NPP. Figure 1, as an example, displays the general heat maps of three NPPs in Europe, such as Almaraz (Spain), Paks (Hungary) and Heysham (United Kingdom).

More than the logical maximum number of heats reached in the surroundings of each NPP, as it was expected, the spatial coverage and the distribution of the affected areas are quite different comparing the results in each NPP. In this sense, it is clear that the key factor to understand and justify these results is the combination of wind dynamics and orography features of the region in which the NPP is located. In addition, the seasonal analysis has revealed temporal differences in the affected areas during the year.

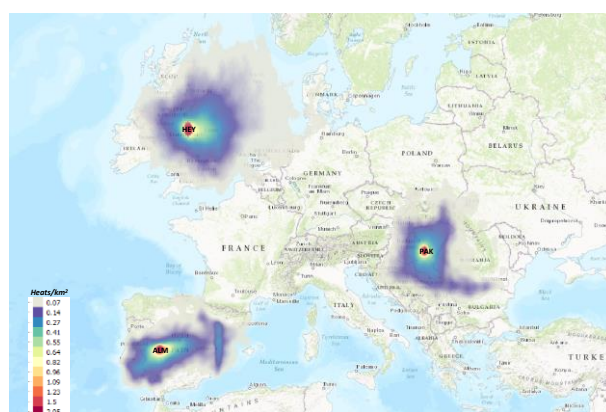


Figure 1. Example of heat map in three EU NPP. (The legend of the figure represents the number of heats (points) that fall within a km<sup>2</sup>)

### Reference

M. P. Wand & M. C. Jones. Kernel Smoothing Monographs on Statistics and Applied Probability Chapman & Hall, 1995.



## Experimental Measurement and Indirect Assessment Methods to Determine the Natural Background Gamma Radiation Dose Rate in Urban Region

S.M.T Hoang<sup>1</sup>, D.K. Tran<sup>2</sup>, Y. Truong<sup>2</sup>, and N.S. Le<sup>2</sup>

<sup>1</sup>Korea Atomic Energy Research Institute, Daejeon, 34057, Republic of Korea

<sup>2</sup>Nuclear Research Institute, Dalat, 670100, Vietnam

Keywords: natural radiation, dose rates, environmental measurements, fourth.

Presenting author email: tuanhsm@kaeri.re.kr

The determination and assessment of the ambient dose rate from the natural background are always the main objects of environmental monitoring programs. Mankind has in fact evolved in a natural background radiation environment which have an original source from basic components as primordial formed before the earth formation (mainly include 238-U, 235-U, and 232-Th series and 40-K), cosmogenic, and human produced. Most radionuclides in the U and Th series and 40-K emit gamma radiation, giving rise to exposures from gamma-ray outdoor. The natural background gamma radiation levels differ from place to place because of differing concentrations of radionuclides from fallout in the soil, and from cosmic radiation that changes with altitude and latitude.

This study has determined the dose rate of natural background gamma radiation at the altitude of 1 m above the ground, the accumulated dose of environmental gamma radiation, and radioactivity of the mainly natural and human-made radioisotopes in soils in the urban environment (Ho Chi Minh City, Vietnam). Based on the acquired data, the maps of dose rates have been composed to the Ho Chi Minh City, which can be used to estimate public exposure as well as having a database for impact assessment from environmental.

determination of dose-rate component methods, and cumulative dose monitoring. With the first one, the mobile monitoring system installed on a box type vehicle contains the radiation measuring instruments of gamma-ray dose rate monitor (Model FH-40-Eberline), data processing unit, GPS, etc. The second one was an indirect method through to the collection and analysis of gamma radioactive isotope in soil: Collect and determine the specific activity of natural radioactive isotopes and artificial soil, thereby applying the system dose conversions and specialized software to calculate the radiation dose outside projection, and a Thermoluminescent Dosimeter (TLD) was used in the last method.

The distribution of dose rate fluctuation at 2245 measured locations is presented in Figure 1. Besides it, Figures 2 presents the average activity of radioactive isotopes (238-U, 232-Th series and 40-K) in soil samples under the districts. The map showing gamma dose rate environment at 120 soil-sampling locations shown in detail (Figure 3).

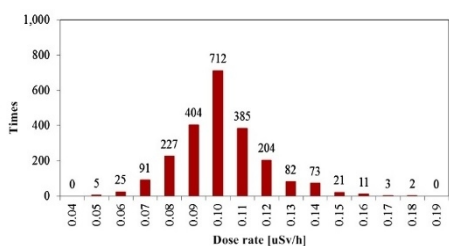


Figure 1. The distribution of dose rate fluctuation at 2245 measured locations.

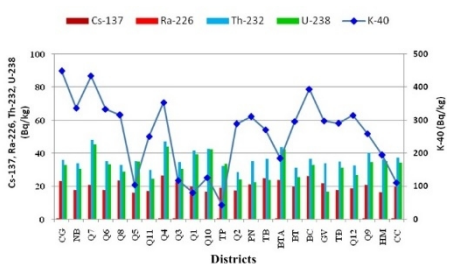


Figure 2. The average activity of radioactive isotopes in soil samples.

Three methods were applied in this study as environmental radiation monitoring system with GPS,

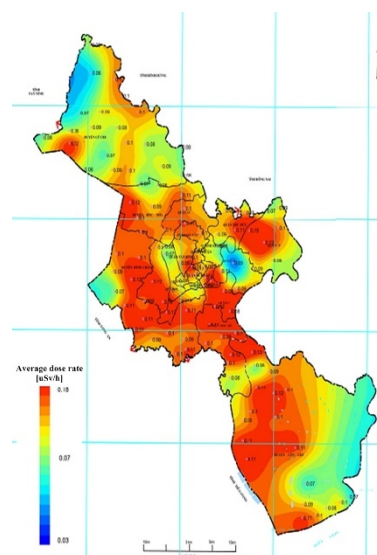


Figure 3. The map of environmental gamma dose rate.

The resulted values were widely fluctuated in the range from 0.05 to 0.18µSv/h, with the average value of 0.10 µSv/h. Approximately, there are 86.2% of the obtained dose rates within the range from 0.08 to 0.12 µSv/h equivalent to 0.70 to 1.05µSv/year, and this range is in agreement with the natural radiation background in the whole world. The average values were as 33.1, 21.1, 36.6, 279.0, and 0.42 Bq/kg.



## On the relation between outdoor $^{222}\text{Rn}$ and atmospheric stability determined using a modified Turner method

M. Bulko, K. Holý, M. Müllerová

Faculty of Mathematics, Physics and Informatics, Comenius University, Mlynská dolina F-1,  
842 48 Bratislava, Slovakia

Keywords: atmosphere,  $^{222}\text{Rn}$ , stability, Turner method.

Presenting author email: [Karol.Holy@fmph.uniba.sk](mailto:Karol.Holy@fmph.uniba.sk)

Atmospheric stability plays the most important role in the dispersion and transport of air pollutants. In practise, information about atmospheric stability is often obtained from discrete stability classes determined from routine meteorological observations. Radioactive gas,  $^{222}\text{Rn}$ , present in the atmosphere has also been considered a good indicator of vertical dispersion and atmospheric stability. The works dealing with the relation between two different approaches of atmospheric stability determination (Pasquill or Turner stability classes vs. radon concentration in the air) are relatively sparse in the literature (e.g. Chambers et al., 2015; Duenas et al., 1996). This study focuses on a detailed analysis of the mutual relationship between the atmospheric radon and Turner stability classification modified for the Central European region.

Outdoor  $^{222}\text{Rn}$  measurements were carried out in Bratislava, the capital of Slovakia (48°9'4" N; 17°4'14" E; 170 m a.s.l.) since 1991 (Holý et al., 2010). Radon activity concentration (RAC) has been continuously recorded at a height of 1.5 m above the ground. A scintillation chamber with an active volume of 4.5 L was used for radon measurements (Beláň et al., 1992). Atmospheric stability classes were determined by the Turner method modified by Polster (Polster, 1967). Input variables were solar altitude, cloud cover, cloud ceiling height and wind speed.

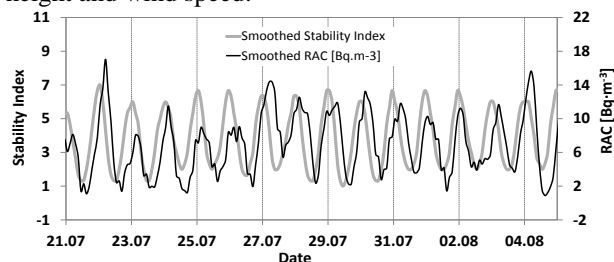


Figure 1. Smoothed time series of radon activity concentration and stability indexes.

The analysis of the time series of radon activity concentration and stability indexes (SI) determined by the modified Turner classification, adjusted for temperate climate regions, implies the existence of a notable time lag between these time series - the time series of RAC lag approximately 4 hours behind the time series of SI (Fig. 1). This lag is likely caused by an immediate “reaction” of stability indexes to the changes in meteorological parameters, which is in contrast with

the fact that naturally it must take some time until the change occurs in the real atmosphere (or in the radon concentration, since radon gas is an inseparable part of the atmosphere). Time lags of various lengths were also found between the time series of RAC and meteorological variables like solar altitude, wind speed and temperature. If the time lag of 4 hours was taken into account, statistical analysis of one year’s worth of data revealed a roughly linear dependence between RAC and SI, suggesting a close relationship between these variables.

The findings outlined in this study imply that outdoor radon and the stability classification based on meteorological parameters are equivalent indicators of atmospheric stability.

This work has been supported by the Scientific Grant Agency of the Ministry of Education of the Slovak republic under the VEGA projects No. 1/3046/06, 1/0678/09 and 1/0143/14.

Beláň, T., Chudý, M., Ďurana, L., Holý, K., Levaiová, D., Povinec, P., Richtáriková, M., Šivo, A., 1992. Investigation of radionuclide variations in the Bratislava air. Rare Nuclear Processes. Proc. 14th Europhys. Conf. Nucl. Phys., editor P. Povinec, Singapore: World Scientific, 441 p.

Chambers, S. D., Williams, A. G., Crawford J., Griffiths, A. D., 2015. On the use of radon for quantifying the effects of atmospheric stability on urban emissions. Atmos. Chem. Phys. 15, 1175–1190.

Duenas, C., Perez, M., Fernandez, M. C., Carretero J., 1996. Radon concentrations in surface air and vertical atmospheric stability of the lower atmosphere. J. Environ. Radioact. 31, 87-102.

Holý, K., Bulko, M., Polášková, A., Holá, O., Müllerová, M., Böhm, R., 2010. Fifteen years of continual monitoring of  $^{222}\text{Rn}$  activity concentration in the Bratislava atmosphere. Proc. Int. Conf. Environ. Radioact., Vienna, IAEA-CN-145, 5 p.

Polster, G., 1967. Zur Anwendung der Turnerschen Klassifizierung der Diffusionskategorien in der mitteleuropäischen Klimaregion. Zentralabteilung Strahlenschutz der Kernforschungsanlage Jülich. Interner Bericht No. 94.

## Hot particles in air filters collected in Finland immediately after the Chernobyl accident

J. Paatero<sup>1</sup>, F. Groppi<sup>2</sup>, A. Ioannidou<sup>3</sup>

<sup>1</sup>Finnish Meteorological Institute, (FMI), Observation Services, P.O. Box 503, Helsinki FI-00101, Finland

<sup>2</sup>Università degli Studi di Milano, Physics Department, LASA Lab, Segrate (MI), 20090 Italy

<sup>3</sup>Aristotle University of Thessaloniki, Physics Department, Thessaloniki 54124 Greece

Keywords: hot particles, nuclear accident, air monitoring, NPP

Presenting author email: [anta@physics.auth.gr](mailto:anta@physics.auth.gr) (Alexandra Ioannidou)

Following the accident at the Chernobyl nuclear power plant on 26 April 1986, about  $2 \times 10^{18}$  Bq of condensable radioactive materials were released, the majority of which was deposited in Europe (IAEA, 1986).

Most of the released radioactive material was in particulate form, whereas noble gases and most of iodine were in gaseous form. Sometimes the activity of even a single “particle” may be so high that may cause a severe health hazard. Radioactive particles released from Chernobyl have been described by many as “hot particles” where “hot” is synonymous with “highly radioactive”.

In the Chernobyl accident most of the particulate material was deposited within 20 km of the plant, but about one-third was transported even thousands of kilometres. Radioactive materials from Chernobyl were transported throughout Europe during the 10-day release period. About one-quarter of the total radioactive material was released during the early stages of the accident (IAEA, 1986). The emissions later decreased, reaching a minimum on 2 May 1986 but then increased again until 6 May 1986, when the release practically ceased. Trajectory analyses showed that Finland was affected by air masses originating from Chernobyl accident very early after the accident as well as during 5-6 of April 1986 (Pollanen et al., 1997).

All filters collected in Helsinki, Finland immediately after the Chernobyl accident up to the end of June were analyzed for “hot particles” by autoradiography technique (Cyclone Plus of PerkinElmer) in the University of Milano, Italy.

The evidence of “hot particles” in three filters collecting in Helsinki Finland between 27-28 April 1986 (Fig. 1), 28-29 April 1986 (Fig. 2) and 5-12 of May 1986 (Fig. 3) after the Chernobyl accident are consistent with the results of trajectory analysis. Also the concentrations of <sup>137</sup>Cs in the filters are consistent with the above discussion.

Table 1. <sup>137</sup>Cs activity concentration in air filters collected in Helsinki, Finland

Date of Sampling	<sup>137</sup> Cs (mBq m <sup>-3</sup> )
27-28 April	367.6
28-29 April	251.8
29-30 April	4.3
30 April – 2 May	2.5
2-5 May	17.1
5-12 May	2.7

The aim of this study is to characterise such particles with regard to their elemental, mineralogical and radionuclide composition. Morphology and elemental information for particle characterization will be given by SEM analysis. Elemental distribution and structure information will be given by  $\mu$ -XRF analysis. Analyses are still in progress.

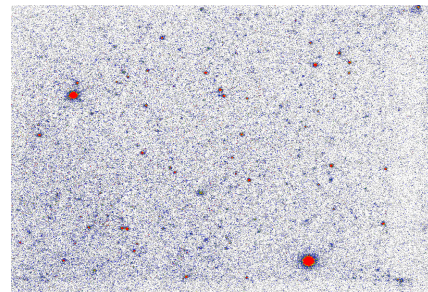


Figure 1. Autoradiography image of filter collected between 27-28 April 1986

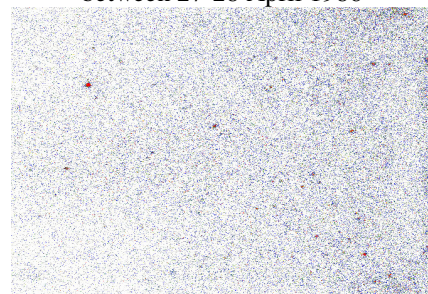


Figure 2. Autoradiography image of filter collected between 28-29 April 1986

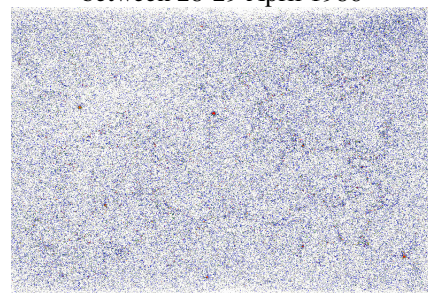


Figure 3. Autoradiography image of filter collected between 5-12 May 1986

### References

- IAEA (1986). Safety Series No. 75-INSAG-1. Summary report on the post Hot particles from Chernobyl accident review meeting on the Chernobyl accident. International Atomic Energy Agency, Vienna.
- Pöllänen, R., Valkama, I., Toivonen, H. 1997. Transport of radioactive particles from the Chernobyl accident. Atmosph. Environ. 31(21), 3575-3590.

## Development of a rapid radioanalytical method for quantification of low levels of Ra-226 in aqueous samples by radiochemistry separation followed by $\alpha$ -spectrometry

E. M. van Es<sup>1,2</sup>, B. Russell<sup>1</sup>, D. Read<sup>1,2</sup>, P. Ivanov<sup>1\*</sup>

<sup>1</sup>National Physical Laboratory, Hampton Road, Teddington, Middlesex, TW11, United Kingdom

<sup>2</sup>Chemistry Department, University of Surrey, Guildford, Surrey, GU2 7XH, United Kingdom

Keywords: Ra-226 analysis, radiochemistry separation,  $\alpha$ -spectrometry, ICP-MS

\*Presenting author email: peter.ivanov@npl.co.uk

Radium-226 is a long-lived ( $T_{1/2} = 1600$  years) naturally occurring radionuclide, member of the uranium decay series. Due to its high solubility, Ra is naturally present in aqueous environmental systems at concentrations determined by the local geology and the chemical composition of the ground water.

As a result of activities related to mining, oil or gas extraction and other NORM (naturally occurring radioactive materials) industries, radium can be occasionally concentrated in scales and by-products to elevated and potentially hazardous levels. Therefore, NORM industries are required to comply with stringent discharge limits imposed by the environmental and health protecting authorities. For instance, in the United Kingdom the limit for  $^{226}\text{Ra}$  in discharged waters is  $10 \text{ mBq L}^{-1}$  (EPR, 2011). However, quantification of sub-Becquerel amounts of radium not only requires radioanalytical methods with low enough limits of detections but could also represent a challenge to differentiate natural background from industrial contamination (Read et al., 2013).

The current study aims at the development and validation of a rapid radioanalytical method for determination of low levels of  $^{226}\text{Ra}$  in aqueous solutions by radiochemistry separation and pre-concentration of radium ions on  $\text{MnO}_2$ -PAN resin followed by  $\text{BaSO}_4$  micro-precipitation on Resolve™ filters prior to  $\alpha$ -spectrometry counting.

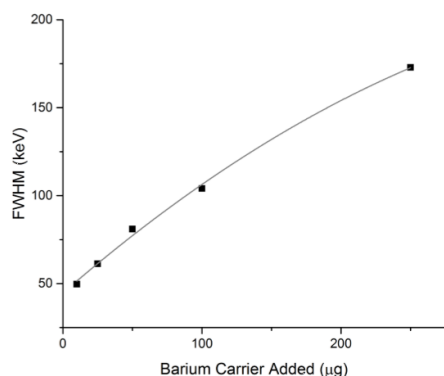


Figure 1. Full width at half maximum (FWHM) of the  $^{226}\text{Ra}$  4.78 MeV  $\alpha$ -peak vs. the amount of Ba carrier

As part of the method development work the effect of Ba carrier used for micro-precipitation on the quality of the resulting  $\alpha$ -spectrometry source was evaluated against the full width at half maximum (FWHM) of the  $^{226}\text{Ra}$  4.78 MeV  $\alpha$ -peak (Fig. 1). The homogeneity and the

thickness of the micro-precipitated sources was examined by scanning electron microscope (SEM), as shown on Fig. 2. Furthermore, the combined  $^{226}\text{Ra}$  counting efficiency was measured as a function of the amount of Ba carrier added and optimum barium content was determined to be  $50 \mu\text{g}$ .

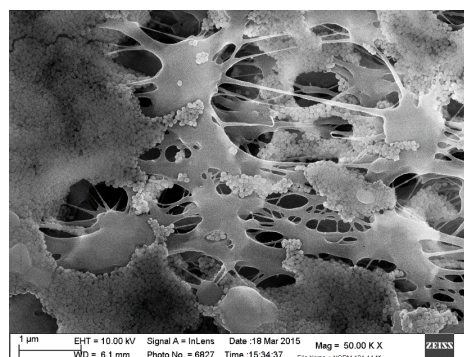


Figure 2. SEM image of  $^{226}\text{Ra}$  source for  $\alpha$ -spectrometry, prepared by micro-precipitation of  $\text{BaSO}_4$  on Resolve™ filter. Image magnification is 50 000 and the amount of Ba carrier added is  $50 \mu\text{g}$ .

The chemistry yield of radium was measured using  $^{223}\text{Ra}$  ( $T_{1/2} = 11.4 \text{ d}$ ,  $E_\alpha = 5.72 \text{ MeV}$  (52.6 %)) as a tracer. The procedure was validated by measuring of spiked water samples with known  $^{226}\text{Ra}$  activity and then applied to determine the radium content in ground water samples from Lancashire, UK. It was found that background concentrations of  $^{226}\text{Ra}$  ranged from 2 to  $200 \text{ mBq L}^{-1}$ .

The radioanalytical method is discussed in comparison with the recently developed ICP-QQQ-MS techniques for  $^{226}\text{Ra}$  analysis in ground water (van Es, 2017) in terms of sample throughput, removal of interferences and limits of detection.

EPR (The Environmental Permitting (England and Wales) (Amendment) Regulations) 2011. Statutory Instruments 2043.

Read, D., Read, G. D., Thorne, M. C., 2013. Background in the context of land contaminated with naturally occurring radioactive material. *J. Radiol. Prot.* 33, 367–380.

van Es, E.M., Russell, B.C., Ivanov, P.I., Read, D., 2017. Development of a method for rapid analysis of Ra-226 in groundwater and discharge water samples by ICP-QQQ-MS. *Appl. Radiat. Isot.* Feb 20, doi: 10.1016/j.apradiso.2017.02.019



## Assessment of natural radiation exposure caused by the <sup>222</sup>Rn progeny gamma radiation in underground parking places in Vilnius

D. Jasaitis<sup>1</sup>, M. Pečiulienė<sup>1</sup>, A. Girgždys<sup>1</sup> and R. Girgždienė<sup>1,2</sup>

<sup>1</sup>Department of Physics, Vilnius Gediminas Technical University, Vilnius, Saulėtekio Ave. 11, LT-10223, Lithuania

<sup>2</sup>Department of Environmental Research, Center for Physical Sciences and Technology, Vilnius, Saulėtekio Ave. 3, LT- 10257, Lithuania

Keywords: natural radiation, equivalent dose rate, radon progeny, car parking places.

Presenting author email: Dainius.Jasaitis@vgtu.lt

In controlling the natural radiation exposure for the human in buildings, it is necessary to determine the levels of natural radioactivity (external exposure) and radon exhalation rate (internal exposure) from building materials. The most important natural sources of exposure in buildings are products of uranium (<sup>238</sup>U) and thorium (<sup>232</sup>Th) radioactive decay process as well as kalium (<sup>40</sup>K). Gamma radiation of these elements causes external human exposure. Internal human exposure is caused by radon (<sup>222</sup>Rn) and its progeny. It has been found out that the equivalent dose rate (EDR) caused by ionizing radiation of radon decay products <sup>214</sup>Pb and <sup>214</sup>Bi can vary from 2 to 20% of the total value of the EDR (Chibowski and Komosa, 2001).

The aim of this work is to evaluate exposure caused by natural background radionuclides in underground car parking places and to estimate which part of the total equivalent dose rate is due to the <sup>222</sup>Rn progeny in the air. The research was carried out in underground parking places in Vilnius city (Lithuania) during the period 2014 April - 2015 March.

The specific activities of <sup>226</sup>Ra, <sup>232</sup>Th and <sup>40</sup>K in structural materials used for building underground parking places are shown in Table 1 (Jasaitis et al., 2016).

Table 1. Specific activities of natural radionuclides in building materials and activity index

Building material	Specific activity, Bq/kg (mean value ± standard deviation)			I
	<sup>226</sup> Ra	<sup>232</sup> Th	<sup>40</sup> K	
Structural materials				
Concrete	49.3±1.7	35.1±1.4	539.4±22.6	0.52
Ferroconcrete	88.1±3.4	33.3±1.7	591.1±23.4	0.66
Binding agents				
Cement	35.9±1.2	4.1±0.2	127.2±4.6	0.18
Clay	27.2±0.7	9.9±0.4	541.6±3.7	0.32
Mineral fillers				
Gravel	11.6±0.4	3.5±0.1	287.0±10.6	0.15
Sand	12.7±0.4	5.4±0.2	245.3±8.3	0.15
Parking place floor coverings				
Asphalt	38.1±1.3	22.0±0.8	680.0±28.6	0.46

The lowest specific activities of natural radionuclides have been found in binding agents and mineral fillers, while their highest specific activities have been measured in ferroconcrete, concrete and asphalt. The activity indexes of natural radionuclides in mostly

used building materials vary from 0.15 to 0.66. They do not exceed the values established in HN 85-2011 and regulated by the European Commission.

Having assessed the EDR distribution in various car parking places, it has been found out that radiation is mostly influenced by radionuclides <sup>40</sup>K, <sup>226</sup>Ra and <sup>232</sup>Th and <sup>226</sup>Ra decay product, i.e. <sup>222</sup>Rn, contained in structural materials of parking places.

In order to estimate which part of the total equivalent dose rate is due to the <sup>222</sup>Rn progeny the equivalent dose rate in the air was measured, and the <sup>222</sup>Rn activity concentration in the air was determined at the same time and at the same site.

It was determined that the external equivalent dose rate caused by the <sup>222</sup>Rn progeny radiation in the underground car parking varies from 6 to 27% of the total equivalent dose rate (Fig. 1).

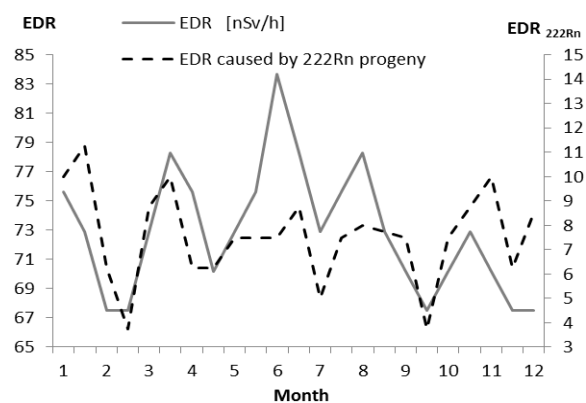


Figure 1. Variations of the total EDR and EDR caused by <sup>222</sup>Rn progeny in the underground car parking places

It has been estimated that radon progeny concentration in underground parking places provides annual human exposure of 1.7 mSv. This would represent about 70 % of annual human exposure caused by natural sources.

Chibowski, St., Komosa, A., 2001. Radon concentration in basements of old town buildings in the Lublin region, Poland. J. Radioanal. Nucl. Chem. 247, 53-56.  
 Jasaitis, D., Chadyšienė, R., Pečiulienė, M., Vasiliauskienė, V. 2016. Research on change of natural ionizing radiation in car parking places. Romanian journal of physics. 61, 1657-1676.

## Assessment of External Exposure to the Public from Natural Radionuclides in Soil in Iran

M. R. Kardan<sup>1</sup>, N. Fathabdi<sup>2</sup>, A. Attarilar<sup>2</sup>, N. Rastkhah<sup>2</sup>

<sup>1</sup> Reactor and Nuclear Safety Research School, Nuclear Science and Technology Research Institute, Tehran, Iran,

<sup>2</sup> Iran Nuclear Regulatory Authority, Tehran, Iran

Keywords: Natural Radioactivity, Terrestrial Sources, Absorbed gamma dose rate, Annual Effective Dose, Public Exposure.

Presenting author email: mkardan@aeoi.org.ir

In this study external exposure to the public due to the natural radionuclides in soil was calculated based on their activity concentrations. A total of 979 Soil samples from 31 Provinces were collected. The <sup>226</sup>Ra, <sup>232</sup>Th and <sup>40</sup>K concentrations in soil samples were determined directly using a shielded coaxial High Purity Germanium (HPGe) detector (Hafezi, 2005). The external gamma dose rate in the air at 1 m above ground level was calculated from average measured specific activities in each province according to the following equation (UNSCEAR, 2000):

$$D = 0.462ARa + 0.604ATh + 0.042AK \quad (1)$$

where D is the dose rate in nGy h<sup>-1</sup> and ARa, ATh and AK are the specific activities (Bq.kg<sup>-1</sup>) of <sup>226</sup>Ra, <sup>232</sup>Th and <sup>40</sup>K, respectively.

The outdoor and indoor annual effective dose equivalent was calculated as follows (UNSCEAR, 2000):

$$OAEDE = Dave \times DCF \times OF \times T \quad (2)$$

$$IAEDE = Dave \times DCF \times IF \times T \times Rio \quad (3)$$

Where OAEDE and IAEDE are outdoor and indoor annual effective dose equivalent,

Dave, average absorbed dose rate

DCF, dose conversion factor (Sv/Gy)

OF and IF, outdoor and indoor occupancy factor

Rio, the ratio of indoor to outdoor and

T, time (8760h.y<sup>-1</sup>)

A dose conversion factor (DCF) of 0.7 Sv/Gy, outdoor occupancy factor (OF) of 0.2, indoor occupancy factor (IF) of 0.8, the ratio of indoor to outdoor gamma dose rate (Rio) of 1.4 were used as recommended by the UNSCEAR(UNSCEAR, 2000).

The activity concentrations of naturally occurring radionuclides, from the samples were found to vary from 13.00 to 1040.00 with an average of 464.00 Bq/kg for <sup>40</sup>K, from 1.30 to 70.30 with an average of 26.84 Bq/kg for <sup>232</sup>Th and from 2.00 to 68.40with an average of 24.20 Bq/kg for <sup>226</sup>Ra. The calculated absorbed dose rate varied from 12.71 to 91.39 nGy.h<sup>-1</sup>. Population-weighted average of calculated absorbed dose rate was 46.74 nGy.h<sup>-1</sup>. Which is lower than the world average outdoor exposure due to terrestrial gamma radiation 58 nGy.h<sup>-1</sup> (UNSCEAR, 2000).

Gamma absorbed dose rate and total annual effective dose were calculated for each sample location then the effective dose assign to the population proportional to the population of the province divided to the number of samples in the province. Fig. 1 shows the distribution of population with respect to total annual effective dose for Iran. The distribution follows normal distribution. It can be seen that the largest population fraction is in the 0.4-0.49 mSv/y which is about 33% of population also about 61% of Iran population falls within the range 0.3-0.49 mSv/y.

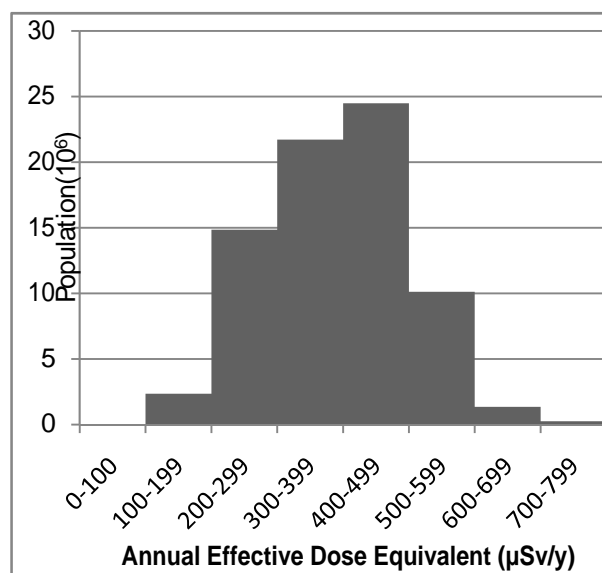


Figure 1. Distribution of population with respect to ranges of annual effective dose equivalent due to natural radionuclides in soil in Iran

Hafezi S., Amidi J., Attarilar A., 2005, Concentration of natural radionuclides in soil and assessment of external exposure to the public in Tehran, Iran. J. Radiat. Res., 3, 85-88.

UNSCEAR (United Nations Scientific Committee on the Effects of Atomic Radiation), 2000 Sources and effects of ionizing radiation, United Nations, New York.



## Transitions of radon from groundwater to indoor air; Shower stall model

K.Y. Lee, K.S. Ko, S.Y. Cho, D.H. Kim, Y.Y. Yoon, D.H. Koh, K. Ha

Geologic Environment Division, Korea Institute of Geoscience and Mineral Resources,  
124 Gwahag-ro, Yuseong-gu, Daejeon, Korea

Keywords: Radon, transition rate, groundwater, indoor air

Presenting author email: kylee@kigam.re.kr

Radon ( $^{222}\text{Rn}$ ) is a radioactive gas formed by the decay of radium ( $^{226}\text{Ra}$ ) within the uranium ( $^{238}\text{U}$ ) series. Radon has been recognized as a lung carcinogen by the World Health Organization (WHO, 2009) and considered to be the major contributor to public exposure from natural sources (UNSCEAR, 2000). Most common radon concerns have focused primarily on indoor air radon that comes from soil and rocks surrounding the building foundation. In some cases, water radon might become a dominant source of indoor air radon. Radon in water usually originates in water wells that are drilled into bedrock containing radon gas. These wells could be private water wells or wells that are utilized by a public water supply system. Dissolved radon in groundwater will be transferred into indoor air during household utilizations such as showering, laundering, and dishwashing. Estimates are that indoor air radon concentrations increase by approximately 1 pCi/L for every 10,000 pCi/L in water (Bryan Swistock, 2016).

In this work, transition of radon from groundwater to indoor air was measured experimentally using a shower stall with shower head and kitchen faucet. The shower stall was constructed with dimensions of 50 cm ( $\Phi$ ) and 150 cm height with a volume of 295 L and consisted of a shower head at 150 cm height and a kitchen faucet at 50 cm height from the bottom. During the experiment, the shower stall was supplied groundwater containing around 155 Bq/L of radon. Three different water utilization methods were examined to measure the transition effects by water utilization methods. At first, groundwater was supplied through the shower head with flow rate of 10 L/min for 2 hours. Secondly, groundwater was supplied through the kitchen faucet with the same methods as in the shower head experiment. Finally, shower head and kitchen faucet were utilized simultaneously to supply the groundwater into the shower stall with flow rate of 15 L/min for 2 hours. The groundwater supplied into the shower stall was drained continuously through the bottom drainage of the stall.

Radon in air of the shower stall was measured continuously during groundwater utilizations with Rn-in-air monitors (RAD7, Durrige Co., US) in closed loop. Transition rate ( $T_r$ ) of radon from groundwater to air of the shower stall was estimated using the Eq. (1).

$$T_r(\%) = 100 \cdot \frac{C_a V_a}{C_w V_w} \quad (1)$$

Where,  $C_w$  and  $C_a$  are radon activity concentration (Bq/L) of radon in water and air, respectively.  $V_w$  and  $V_a$

are volume (L) of water supplied and air of the water stall, respectively. Transition rates of radon by water utilization methods can be shown in the Figure 1.

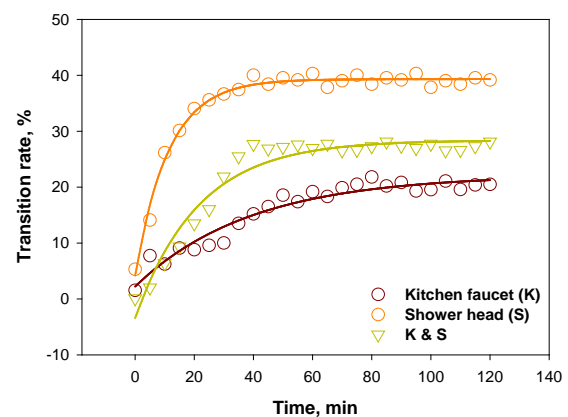


Figure 1. Transition rate of radon from groundwater to air of the shower stall by water utilization methods.

(K): water supplied by kitchen faucet, (S): water supplied by shower head, T & S: water supplied by (K) and (S) simultaneously.

The results revealed that transition of radon from groundwater to the air should be affected by water utilization methods as well as some parameters for air-water equilibrium partitioning of radon such as water and air temperature and atmospheric pressure.

WHO, 2009. In: Zeeb, H., Shannoun, F. (Eds.), Handbook on Indoor Radon.

UNSCEAR, 2000. Sources and Effects of Ionizing Radiation. UNSCEAR 2000 Report to the General Assembly with Scientific Annexes. United Nations, New York.

Bryan Swistock, 2016. Reducing Radon in Drinking Water, WATER FACTS 30, Pennsylvania State University. <http://extension.psu.edu>

## Radioactive contamination of soils of Japan and problems of their rehabilitation

L.N. Maskalchuk

International Sakharov Environmental Institute of Belarusian State University, Minsk, 23/1 Dolgobrodskaya str., 220070, Belarus

Keywords: radiocaesium, soil contamination and rehabilitation, spropels, clay-salt slimes. soil amendments  
maskal@bsu.by; leonmosk@tut.by

The nuclear accident at the Fukushima Daiichi NPP in 2011 was the second large-scale accident (INES Level 7) in the history of the world atomic power engineering and led to the radioactive contamination of environment. The total area of the radioactive contamination resulting from that accident is about 13 782 000 km<sup>2</sup>, that is approximately 3,6% of the total territory of Japan. Herewith, the average concentration of radiocaesium in radioactively contaminated soils varies from 800 to 50 000 Bq/kg, and the maximal concentration of <sup>137</sup>Cs is 1 300–230 000 Bq/kg.

The comprehensive research conducted by the Ministry of Education, Culture, Sports, Science and Technology of Japan revealed that after the Fukushima Daiichi nuclear accident the level of radioactive contamination of agricultural soils in a range of Japanese prefectures exceeds the maximum permissible limits.

The following soil types are the most extended in Japan: brown forest soils (cambisols) (53.4%), andosols (17.3%), fluvisols (15.0%), regosols (5.5%), etc. At the Fukushima Daiichi NPP site and the adjacent territories, which are radioactively contaminated now, the most common are the following soil types: brown forest soils (cambisols), andosols (with small inclusions of peat soils), podzols and fluvisols (fluvial gley soils developing on alluvial sediments), etc. Cambisols, andosols and gleysols, including brown forest and gray lowland soils prevail among the Japanese agricultural grounds and account for approximately 82% from their total area.

The generally accepted methods of radioactively contaminated agricultural soils rehabilitation are: 1) physical (ploughing of the contaminated topsoil); 2) chemical (fertilizing with various soil amendments); 3) biological (cultivation of certain crops on the contaminated soils).

Currently, physical methods of radioactively contaminated soils rehabilitation are primarily used in Japan. Because of these rehabilitation actions, it has been accumulated more than 35 mln tons of radioactively contaminated soils, foliage and other radioactive waste which require further reprocessing and disposal.

Per Japan's legislation concerning radioactively contaminated soils, to prevent the direct impact of radioactive pollutants the following methods may be employed as one of possible countermeasures: mechanical removal of the contaminated topsoil and chemical processing.

Considering the above and given the specificity of Japanese soils, divers soil amendments such as spropels or clay materials (including potassium production

wastes – clay-salt slimes) may be effectively used to reduce <sup>137</sup>Cs migration into plants.

Spropels are the substances of biogenic origin, which are formed by animal and vegetable remains at the bottom of freshwater lakes where there is a lack of oxygen. As for determination of spropel types, the main feature is the content of organic matter. Besides, colloidal structure of spropels, the big specific surface and considerable cation exchange capacity allow to use spropels as an effective sorbent of radionuclides. Clay-salt slimes (CSS) are characterized by high selective sorption properties towards <sup>137</sup>Cs, and their use as a mineral amendment to spropels allows to improve their sorption properties and significantly increase of <sup>137</sup>Cs fixation on soils.

The long-term comprehensive research carried out within the framework of the national programs for rehabilitation of the radioactively contaminated soils in Belarus, as well as the results of the ISTC projects #859 and #3189, allowed to get the following results:

1) The physicochemical, agrochemical and sorption properties of soils, spropels (organic; silicon; carbonate), hydrolyzed lignin (acid, neutralized), clay-salt slimes and based on them organomineral sorbents were studied.

2) The kinetics of <sup>137</sup>Cs and <sup>90</sup>Sr sorption-desorption processes was studied for the laboratory specimens of soils, spropels, clay-salt slimes and hydrolyzed lignin.

3) The effect of the organomineral sorbents application for radioactively contaminated soils rehabilitation was investigated: physicochemical properties of soils and amendments were determined; the dependence of radionuclides behavior in soils and amendments from quantitative parameters describing their physicochemical properties was revealed.

4) The methodology of targeted search of selective to <sup>137</sup>Cs and <sup>90</sup>Sr sorption materials was developed and the technical specifications for the proposed soil amendments production were prepared.

Based on the available experimental data, it can be concluded that CSS-based organomineral sorbents are the most effective soil amendments preventing radionuclides migration (<sup>137</sup>Cs and <sup>90</sup>Sr) in the soil – plant system.

The given approach could be used in Japan for minimization of the Fukushima Daiichi nuclear accident consequences, namely for rehabilitation of radioactively contaminated soil and territories, purification of aquatic medium and ecosystems from <sup>137</sup>Cs and for safety radioactive waste management.

## Multi-Nuclide Adsorption Properties of Granulated Composite Zeolites for Fukushima Advanced Decontamination

Hitoshi Mimura, Minoru Matsukura, Fumio Kurosaki, Tomoya Kitagawa

UNION SHOWA K.K., 1-8-40, Konan, Minato-ku, Tokyo 108-0075, JAPAN

Keywords: multi-nuclide decontamination, zeolite, adsorption property, breakthrough property.

Presenting author email: hmimura@st.cat-v.ne.jp

In Fukushima NPP-1, large amounts of highly contaminated water over 900,000 m<sup>3</sup> accumulated in the reactor, turbine building and the trench in the facility have been treated by circulating injection cooling system: Cs and Sr decontamination processes of SARRY and KURION using zeolites and crystalline silicotitanates, and multi-nuclide (62 nuclides including Co) decontamination systems of ALPS using various adsorbents (**Fig. 1**). Zeolites, a kind of inorganic ion-exchanger, are well known to have high selectivity for different nuclides depending on their crystal structures. In this study, three kinds of zeolite mixtures, Zeolite A, Mordenite and Zeolite X, having high selectivity towards Sr, Cs and Co, respectively, were converted to granulated composite zeolites for multi-nuclide decontamination.

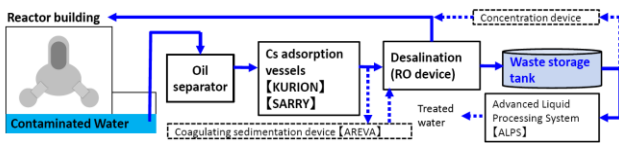


Figure 1. Decontamination system of SARRY, KURION and ALPS in Fukushima NPP-1.

The mixtures of three kinds of Zeolites, Zeolite A (A50 powder, UNION SHOWA K.K.), Natural mordenite (M, Ayashi, Miyagi Pref., Japan) and Zeolite X (LSX, UNION SHOWA, K.K.), were granulated, and two kinds of granulated composite zeolites, AMX<sub>α</sub> (Mixing ratio: A:M:X=1:1:1, 0.5~1 mm φ) and AMX<sub>β</sub> (Mixing ratio: A:M:X=0.5:1:0.5, 0.5~1 mm φ) were used for the batch adsorption of <sup>85</sup>Sr, <sup>137</sup>Cs and <sup>60</sup>Co and breakthrough experiments. The uptake (%) and distribution coefficient ( $K_d$ ) of these nuclides in seawater were estimated by batch method. The adsorption properties are as follows.

### (1) Cs adsorption property:

The uptake (%) of Cs<sup>+</sup> in pure water for AMX<sub>α</sub> and AMX<sub>β</sub> was over 90% ( $K_d$ : >10<sup>3</sup> cm<sup>3</sup>/g), and the uptake (%) in seawater was 56 and 70%, respectively (**Fig. 2**). Relatively large uptake (%) for AMX<sub>β</sub> is due to the larger content of mordenite with high Cs selectivity. The Cs uptake (%) decreased with increasing the coexisting Na<sup>+</sup> and K<sup>+</sup> concentrations above 1,000 and 500 ppm, respectively. The Cs breakthrough property was examined by using the packed columns with AMX<sub>α</sub> and AMX<sub>β</sub> (2.5g) and feed solution (seawater containing 100 ppm Cs<sup>+</sup>). No breakthrough was observed up to 100 cm<sup>3</sup> of the effluent passed through the column, and the adsorption capacity was estimated at least over 6 × 10<sup>-2</sup> mmol/g.

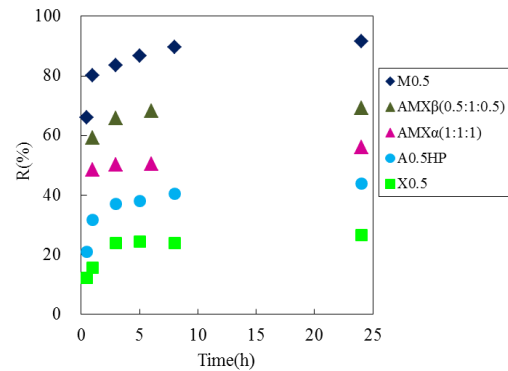


Figure 2. Cs uptake (%) vs shaking time for composite zeolites and single zeolite.

### (2) Sr adsorption property:

The uptake (%) of Sr<sup>2+</sup> ions for AMX<sub>α</sub> and AMX<sub>β</sub> was 65 and 58% in seawater, respectively, indicating the excellent adsorbability of AMX<sub>α</sub> with larger content of A and X zeolites. The equilibration time was about 10 h, which was longer than that for Cs uptake. The uptake (%) of Sr<sup>2+</sup> markedly decreased with coexisting Ca<sup>2+</sup> concentration above 100 ppm, while unaffected by coexisting Mg<sup>2+</sup> concentration up to 1,000ppm. The uptake (%) was enhanced by dilution of seawater; 80% and 95% for 1/2 diluted seawater and 1/10 diluted one, respectively, which was similar to that of zeolite mixture. The breakthrough was affected considerably by flow rate; the breakthrough capacity was 1.7 × 10<sup>-3</sup> and 5 × 10<sup>-4</sup> mmol/g at 0.2 and 0.8 cm<sup>3</sup>/min, respectively.

### (3) Co adsorption property:

The uptake (%) of Co<sup>2+</sup> in seawater for AMX<sub>α</sub> and AMX<sub>β</sub> was estimated to be 47% and 92%, respectively. The equilibration time was over 24 h, which was longer than those for Cs and Sr uptake. The uptake (%) of Co<sup>2+</sup> slightly decreased with coexisting concentration of Mg<sup>2+</sup>, Ca<sup>2+</sup> and Sr<sup>2+</sup> above 50 ppm. The uptake (%) of Co<sup>2+</sup> for AMX<sub>α</sub> was enhanced with diluting seawater: 96 and 99% for 1/2 diluted seawater and 1/10 diluted one, respectively. The breakthrough profile was very gentle due to the low adsorption rate. No breakthrough was observed up to 100 cm<sup>3</sup> of the effluent passed through the column at 0.2 cm<sup>3</sup>/min of flow rate and the breakthrough capacities at 0.4 and 0.8 cm<sup>3</sup>/min were estimated to be 4.2 × 10<sup>-3</sup> and 3.1 × 10<sup>-3</sup> mmol/g, respectively. In the case of Co adsorption, the equilibrium pH increased markedly over pH 7, and hence the surface adsorption and sedimentation of hydrolysis species such as Co hydroxides are probably occurred.

## Activity Concentration of $^{210}\text{Pb}$ , $^{40}\text{K}$ , $^{237}\text{Cs}$ in surface soil samples from Southern Algeria

M. Nadri<sup>1</sup>, C. Khiari<sup>1</sup>, A. Iouannidou<sup>2</sup>

Physics Department, L'Ecole Normale Supérieure (ENS) V-Kouba, 16050 Algiers, Algeria

Physics Department, Aristotle University of Thessaloniki, 54124 Greece

**Keywords:** Algeria, Nuclear tests, Radioactivity, Surface distribution

Presenting author email: [nadri@ens-kouba.dz](mailto:nadri@ens-kouba.dz)

The activity concentrations of  $^{210}\text{Pb}$ ,  $^{137}\text{Cs}$  and  $^{40}\text{K}$  in surface soil samples from different areas of Algeria are examined and presented in this study.

Sixteen soil samples were collected from Sahara area, near the location where in the early 1960s France conducted a series of above-ground and underground nuclear tests in the south of Algeria (IAEA, 2005).

Measurements of  $^{137}\text{Cs}$  fallout are of major importance on environmental studies. Most of these studies are based on processes related to  $^{137}\text{Cs}$  migrations in soils, which is affected of number of factors

The concentration of  $^{210}\text{Pb}$ ,  $^{137}\text{Cs}$ , and  $^{40}\text{K}$  in surface soil samples ranged between 9.7 - 62.2 Bq kg<sup>-1</sup>; between 0.21 - 4.51 Bq kg<sup>-1</sup> and between 76.9 - 303.0 Bq kg<sup>-1</sup> respectively (Table 1).

**Table.** Activity concentration of  $^{210}\text{Pb}$ ,  $^{40}\text{K}$ ,  $^{237}\text{Cs}$  in surface soil samples in Southern Alheria

A/A	Activity concentration (Bq/kg)		
	Pb-210	Cs-137	K-40
1	21.7±2.2	3.20±1.40	120.0±11.1
2	12.8±1.9	1.05±0.21	303.0±20.3
3	62.2±7.2	0.91±0.20	173.0±13.4
4	21.4±4.3	2.34±0.41	224.0±21.1
5	14.4±1.7	2.00±0.37	132.1±12.8
6	15.4±2.3	4.51±0.87	181.4±15.4
7	16.6±2.7	3.37±0.75	118.3±12.3
8	24.2±2.6	1.85±0.82	97.8±8.9
9	24.3±4.7	1.60±0.32	237.2±19.6
10	35.6±3.6	1.70±0.46	154.8±13.3
11	45.7±6.1	2.05±0.44	76.9±7.2
12	47.0±7.2	2.44±0.55	91.4±8.2
13	55.4±8.1	4.03±0.54	138.6±18.7
14	49.3±5.0	3.84±0.53	137.8±18.7
15	9.7±1.3	0.21±0.06	232.9±2.3
16	10.3±2.2	0.30±0.09	246.3±2.7

The observed activity concentrations of  $^{210}\text{Pb}$ ,  $^{137}\text{Cs}$  and  $^{40}\text{K}$  are in good agreement with results reported in other investigations contacted in Algeria (Baggoura et al., 1998; Kadum et al., 2013).

The  $^{137}\text{Cs}$  concentrations are lower than most  $^{137}\text{Cs}$  values observed in many regions in Europe (Ioannidou et al., 2013, 2014).

The concentrations of  $^{40}\text{K}$  are lower than the world average.

Not any correlation observed between the concentrations of the three radionuclides.

### Acknowledgments

This work was supported by Physics Department, (ENS) V-Kouba, 16050 Algiers, Algeria.

### References:

- IAEA., 2005. Radiological Conditions at the Former French Nuclear Test Sites in Algeria: Preliminary Assessment and Recommendations Radiological assessment reports series, Vienna: IAEA.1-60.
- Baggoura, B., Noureddine, A., Benkrid, M. 1998. Levels of natural and artificial radioactivity in Algeria, Appl. Radiat. Isot. 49 (7), 867-873.
- Kadum, A., Bensaoula, B., Dahmani, B. 2013 Radioactivity Investigation of sand from the Northern region Tlemcen-Algeria, using well shape NaI(Tl) detector, Civil & Environm. Research 3(12), 171-179.
- Ioannidou, A., Giannakaki, E., Manolopoulou, M., Stoulos, S., Vagena, E., Papastefanou, L. Ginid, d., Manenti, S., Groppi, F. (2013) An air-mass trajectory study of the transport of radioactivity from Fukushima to Thessaloniki, Greece and Milan, Italy. Atmospheric Environment 75,163-170.
- Ioannidou, A., Manolopoulou, M., Stoulos, S., Vagena, E., Papastefanou, C., Bonardi, M., Gini, L., Manenti, S., Groppi, F. (2014) Radionuclides from Fukushima accident in Thessaloniki, Greece (40°N) and Milano, Italy (45°N) J Radioanal Nucl Chem, 299(1), 155- 159



## Secondary contamination of agricultural products by resuspension of radiocesium

N.Nihe<sup>1</sup>, Y. Ohmae<sup>1</sup>, K.Tanoi<sup>1</sup>, H. Mukai<sup>2</sup>, T. Kogure<sup>2</sup>, and T.M.Nakanishi<sup>1</sup>

<sup>1</sup> Graduate School of Agricultural and Life Sciences, The University of Tokyo, Tokyo, 113-8657, Japan

<sup>2</sup> School of Science, The University of Tokyo, Tokyo, 113-0033, Japan

Keywords: radiocesium, secondary contamination, resuspension

Presenting author email: anaoto@mail.ecc.u-tokyo.ac.jp

Since the occurrence of the TEPCO Fukushima Daiichi Nuclear Power Plant accident 6 years ago, decontamination has progressed in Fukushima Prefecture and cancelation of evacuation is under progress. To restart farming, secondary contamination of agricultural products by resuspended matter is a matter of concern; therefore, we examined the amount of agricultural products that may have been contaminated by resuspended matter.

Komatsuna (*Brassica rapa* L. var. *perviridis*) was cultivated using non-contaminated soil and water in a pot (30 cm × 30 cm × 30 cm). Pots were arranged 30 cm, 60 cm, and 120 cm from the ground surface. The installation site was set at six locations in Fukushima Prefecture: A (approximately 50 km from the Fukushima Daiichi Nuclear Power Plant, ambient dose rate of approximately 0.1 μSv/h, not decontamination area, the same below), B (35 km, 0.9 μSv/h, decontamination until August 2016), C (12 km, 0.1 μSv/h, decontamination until August 2016), D (4.5 km, 0.7 μSv/h, decontamination area), E (4.5 km, 1.4 μSv/h, not decontamination area), and F (3.5 km, 1.0 μSv/h, not decontamination area). Komatsuna was cultivated four times: from June 18th to July 30th, 2016 (Iidate village, Minamisoma city Odaka, Iwaki city only), from July 30th to August 29th, from August 29th to October 10th, and from October 10th to December 12th. After harvesting the ground part, half of them were washed with water and the amount of radiocesium was measured (after washing); the amount of radiocesium in the other half was measured after harvesting (without washing).

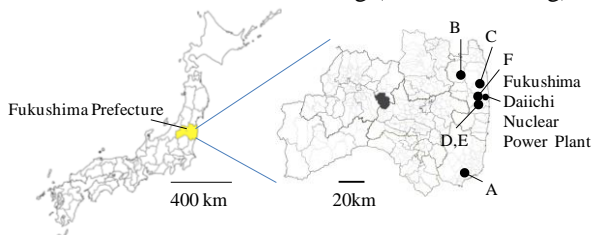


Fig. 1. Installation site

The radiocesium concentration in the aboveground parts without washing at sites A, B, C, D, E, and F was 3–205 Bq/kg (dry weight), 9–112 Bq/kg (dry weight), 9–55 Bq/kg, 30–113 Bq/kg (dry weight), 29–849 Bq/kg (dry weight), and 41–2536 Bq/kg (dry weight), respectively. The radiocesium concentration in plants after washing was mostly lower than that in those without washing. Furthermore, when comparing Komatsuna by height, Komatsuna closer to the ground surface tended to have a higher radiocesium concentration than those further from the ground. Therefore, it can be presumed that

radiocesium detected in Komatsuna leaves was present because of adhesion of floating matter from the ground surface. Particles containing radiocesium adhered to the filter of the atmospheric dust sampler installed at points B and C until August when decontamination was performed at both points. Because X-ray analysis of one of the particles revealed radiocesium, particles containing high cesium concentration covered with silica (known as a cesium ball, Adachi et al., 2013) were confirmed. Just for an added precaution, agricultural products produced in Fukushima has been verified the safety (under 100 Bq/kg) before shipment.

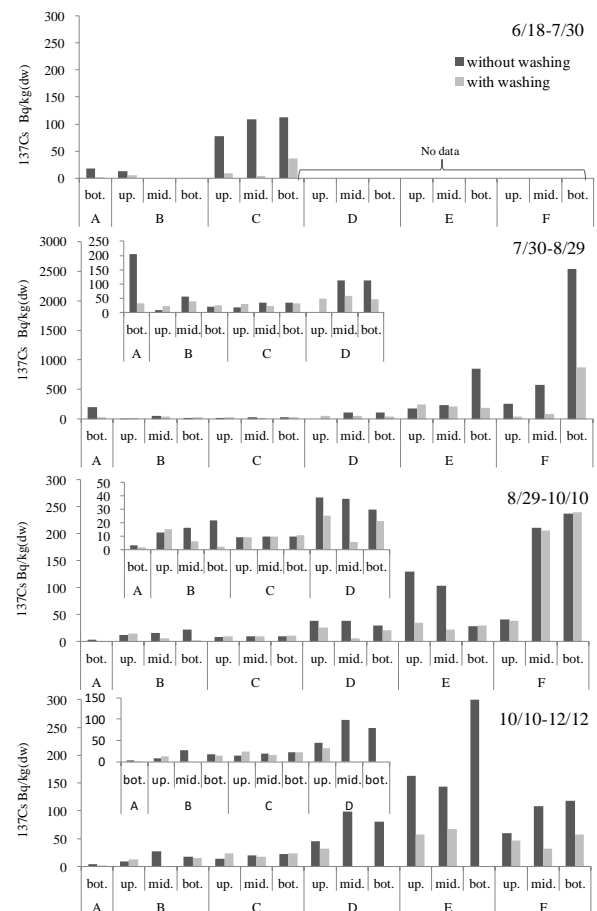


Fig. 2. Radiocesium concentrations in the aboveground parts of Komatsuna at each site

This work was supported by the Ministry of Agriculture, Forestry, and Fisheries.

Adachi, K., Kajino, M., Zaizen Y., Igarashi, Y., 2013. Emission of spherical cesium-bearing particles from an early stage of the Fukushima nuclear accident. Scientific Reports. Doi:10.1038/srep01554.



## Monitoring the concentration of actinides and lanthanides in the Chernobyl exclusion zone

D. Plausinaitis<sup>1</sup>, A. Budreika<sup>2</sup>, A. Karaliunas<sup>2</sup>, Y. Balashevskaja<sup>3</sup> and L. Bogdan<sup>3</sup>

<sup>1</sup>Department of Physical Chemistry, Vilnius University, Naugarduko str. 24, LT-03225, Lithuania

<sup>2</sup>Company LOKMIS, Visoriu str. 2, LT-08300, Vilnius, Lithuania

<sup>3</sup>Central Analytical Laboratory for RAW Characterization, Center for Individual and Environmental Radiation Monitoring "EcoCenter", Shkilna str. 6, 07270, Chornobyl, Ukraine

Keywords: lanthanide, uranium, REE, Chernobyl.

Presenting author email: deivis.plausinaitis@chf.vu.lt

The environmental monitoring for the detection of actinides (Act) and lanthanides (Lan) is becoming an ever more important role in today's research. It is known that lanthanides and long-lived actinides (Th and U) are evenly distributed in the earth's crust. However, due to human activities, this distribution may be affected (Yoshida et al., 1998). In the Chernobyl Exclusion Zone this change may be associated primarily with the nuclear accident. At that time, large amounts of actinide and lanthanide isotopes got into the environment. Uranium and other transuranic isotopes (TRU) were spread out as nuclear fuel particles, meanwhile the dispersion of lanthanides could be various in nature. In particular, most of the lanthanides are nuclear fuel fission products. However, these elements could be used as nuclear reactor design materials or as nuclear fuel additives (Schlieck et al., 2001).

For this reason, the main goal of our study was to carry out the analysis of samples from the Chernobyl zone to determine the concentrations of Act, Lan and other radionuclides. The measurements were carried out using ICP-MS and classical radiochemical techniques. It was to investigate the samples of surface and ground waters, soil and vegetation. The Concentrations of lanthanides, <sup>232</sup>Th and <sup>235,238</sup>U were registered by applying the ICP-MS technique. The activities of <sup>137</sup>Cs, <sup>90</sup>Sr, <sup>238</sup>Pu, <sup>239+240</sup>Pu and <sup>241</sup>Am were determined by using classical radiological and radiochemical methods (alpha, beta and gamma spectroscopies).

During the investigation of soil samples, a linear correlation ( $r^2 = 0.97$ ) between the total lanthanides and actinides concentration was found (fig.1). In surface water samples, similar linear dependence was also observed, but its correlation was lower ( $r^2 = 0.56$ ).

It was found that in all soil samples the concentration of <sup>235</sup>U was higher than natural, e.g. in a range of 0.78 - 0.95%. This showed that all samples have been contaminated with nuclear fuel particles. This result was also confirmed by measurements of TRU nuclides with radiochemical methods. The total concentration of TRU isotopes in soil samples amounted to an average 0.17% of total actinide concentration. Therefore, it must be concluded that natural actinides, e.g. Th and U make the greatest impact on the data shown in figure 1.

After concentration measurements, the distribution profiles of lanthanides were determined. Figure 2 shows the data obtained of soil samples in which the positive concentration anomaly of Gd can be seen. In a similar manner, the anomalous high concentration of Er has been determined in surface water samples. In our view, these anomalies have an

anthropogenic nature and are associated with the nuclear power plant accident.

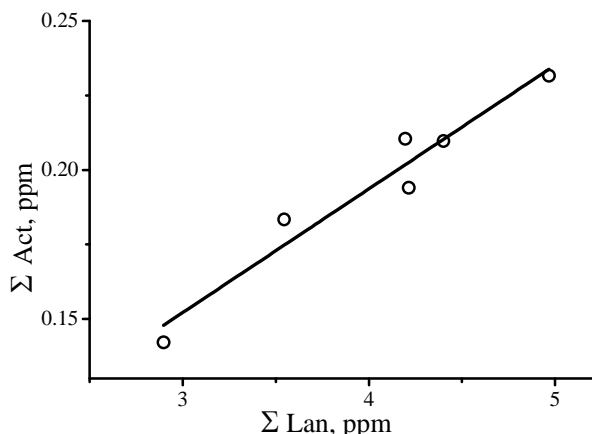


Figure 1: Correlation between the total concentrations of lanthanides and actinides in Chernobyl zone soil.

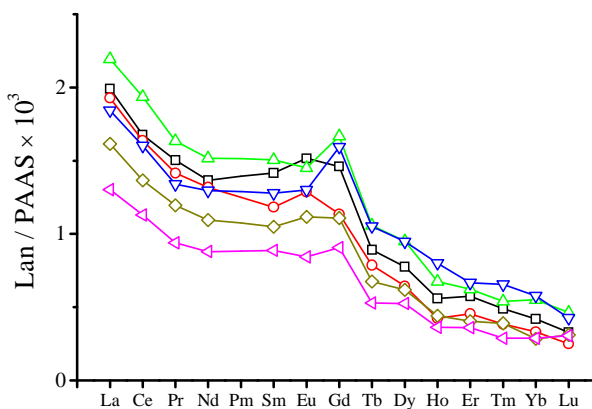


Figure 2: Lanthanide patterns of Chernobyl zone soil samples normalized to Post-Archean Australian Shale (PAAS).

This work was supported by the company LOKMIS, which works under its project for Nuclear Waste Characterization Research.

Yoshida, S., Muramatsu, Y., Tagami, K., Uchida, Sh. 1998. Concentrations of lanthanide elements, Th, and U in 77 Japanese surface soils. *Environ. Intern.* 25, 275-286.

Schlieck, M., Berger, H. D., Neufert, A. 2001. Optimized gadolinia concepts for advanced in-core fuel management in PWRs. *Nucl. Eng. Des.* 205, 191-198.

## Radionuclides in tree rings from the Fukushima region

P.P. Povinec<sup>1</sup>, M. Jeřkovský<sup>1</sup>, J. Kaizer<sup>1</sup>, I. Kontul<sup>1</sup>, I. Sýkora<sup>1</sup>, A. Šivo<sup>1</sup>, X. Hou<sup>2</sup>, M. Laubenstein<sup>3</sup>, L. Steinnes<sup>4</sup>, I. Svetlik<sup>5</sup>, S. Xu<sup>6</sup>

<sup>1</sup>Faculty of Mathematics, Physics and Informatics, Comenius University, 84248 Bratislava, Slovakia

<sup>2</sup>Technical University of Denmark, Riso, Denmark

<sup>3</sup>Laboratori Nazionali del Gran Sasso – INFN, 67100 Assergi (AQ), Italy

<sup>4</sup>Department of Chemistry, Norwegian University of Science and Technology, Trondheim, Norway

<sup>5</sup>Department of Radiation Dosimetry, Nuclear Physics Institute CAS, 180 86 Prague, Czech Republic

<sup>6</sup>Scottish Universities Environmental Research Centre, East Kilbride, G75 0QF, UK

Keywords: tritium, radiocarbon, cesium, plutonium, AMS,  $\gamma$ -spectrometry, tree rings, Fukushima

Presenting author email: povinec@fmph.uniba.sk

Several medium- and long-lived radionuclides were released during the Fukushima accident to the atmosphere, and later were transferred to the biosphere. Among the most interesting medium- and long-lived radionuclides are tritium ( $^3\text{H}$ ,  $T_{1/2} = 12.32$  yr),  $^{134}\text{Cs}$  ( $T_{1/2} = 2.06$  yr),  $^{137}\text{Cs}$  ( $T_{1/2} = 30.17$  yr), radiocarbon ( $^{14}\text{C}$ ,  $T_{1/2} = 5730$  yr), and radioisotopes of plutonium, mainly  $^{239}\text{Pu}$  ( $T_{1/2} = 24.1$  kyr), and  $^{240}\text{Pu}$  ( $T_{1/2} = 6.56$  kyr). The largest release rates to the atmosphere have been estimated for radiocesium (about 16 PBq for  $^{134}\text{Cs}$  and  $^{137}\text{Cs}$  each) (Povinec et al., 2013).

To study the transfer of these radionuclides to the biosphere, tree ring samples were collected from the vicinity of the Fukushima Dai-ichi nuclear power plant, in the northwest direction, where the largest radionuclide atmospheric concentrations, and radionuclide levels deposited on land were observed (Povinec et al., 2013). Those tree ring samples could be suitable biomarkers for studying the annual transport of radionuclides in the environment.

The tree sections were collected (from north to the south) at Yamakiya, Shimotsushima, Ogaki and Iwaki (Fig. 1). Annual tree rings (Fig. 2) were first manually dated and then separated from the sections, and prepared for physical and chemical treatments. The tree-ring samples were then dried in an oven for about one week, crushed into small particles, homogenized, and then separated into three portions for further treatments and analyses:

- (i) Non-destructive radiocesium analysis – the tree ring samples were dried again and compressed into pellets of different geometries for gamma-ray spectrometry. Low-level gamma-ray spectrometers operating in the Gran Sasso underground laboratory (at 3800 m water equivalent depth) and in Bratislava were used for analyses of  $^{134}\text{Cs}$  and  $^{137}\text{Cs}$ .
- (ii) Tritium analysis – the tree ring samples were combusted in a stream of oxygen. The water vapor was collected, distilled and then mixed with a scintillator cocktail. The sample vials were analyzed in a liquid scintillation spectrometer.
- (iii) Radiocarbon analysis – the tree ring samples were combusted to form  $\text{CO}_2$ , and graphite targets

were later prepared for accelerator mass spectrometry (AMS) analyses.

- (iv) Plutonium analysis – it is planned that the tree-ring samples after the gamma-spectrometric measurements will be used for preparation of targets for AMS analysis of plutonium isotopes.

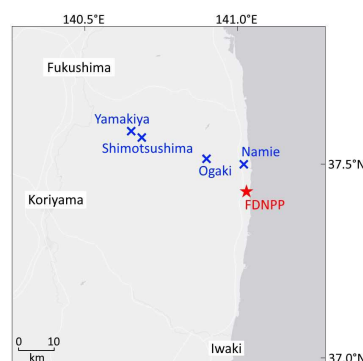


Figure 1. Sampling sites of tree rings in the vicinity of the Fukushima Dai-ichi nuclear power plant.



Figure 2. Picture of the tree section from the Yamakiya site. Annual tree-rings are well visible.

Results of radiocesium, tritium and radiocarbon measurements in the Fukushima tree ring samples will be presented and compared with available atmospheric and soil radionuclide data obtained after the Fukushima accident.

This work was supported by the EU Research and Development Operational Program funded by the ERDF (projects No. 26240120012, 26240120026, and 26240220004), and by the International Atomic Energy Agency (TC project SLR9013).

Povinec, P.P., Hirose K., Aoyama M., 2013. Fukushima Accident: Radioactivity Impact on the Environment. Elsevier, New York, 382p.

## Radioactive Contamination Source Determination by $^{137}\text{Cs}$ , $^{129}\text{I}$ and Pu Isotopic Ratios and its Emission Fallout Inhomogeneity Assessment

A. Puzas<sup>a</sup>, M. Konstantinova<sup>a</sup>, A. Gudelis<sup>a</sup>, Ž. Ežerinskis<sup>a</sup>, X. Hou<sup>b</sup>, R. Gvozdaitė<sup>a</sup>, J. Šapolaitė<sup>a</sup>, R. Druteikienė<sup>a</sup>, E. Lagzdina<sup>a</sup>, D. Lingis<sup>a</sup>, V. Juzikienė<sup>a</sup>, V. Remeikis<sup>a</sup>

<sup>a</sup>Center for Physical Sciences and Technology, Savanoriu ave. 231, Vilnius, Lithuania

<sup>b</sup>Center for Nuclear Technologies, Technical University of Denmark, Risø Campus, DK-4000 Roskilde, Denmark

Keywords:  $^{137}\text{Cs}$ , Pu isotopes, soil, radioecology.

Presenting author email: Andrius.Puzas@ftmc.lt

During the last century the Northern hemisphere was significantly influenced by the fallout of nuclear weapon tests, Chernobyl accident releases. In 2011 the accident in Fukushima spread a significant amount of volatile and semi-volatile radionuclides into the atmosphere (Lujanienė et al. 2012, Povinec et al. 2013). Occasional emissions from nuclear fuel recycling facilities, isotope production for medical use still prevail nowadays, as well. The assessment of radionuclide isotopic composition is important for determination of the artificial radionuclide emission source as an every source could be identified by a certain radionuclide isotopic composition as its “fingerprint” pattern (Varga et al. 2007, Hou et al. 2009). Secondly, due to peculiarities of radionuclides dispersion in the atmosphere the fallout of radionuclide emission creates a significantly inhomogeneous pattern detected whereas air mass travel-path models show definite backward trajectories pointed out to the possible emission source. In order to determine radioactive contamination sources and to understand nuclear fallout inhomogeneity reasons up to one hundred undisturbed meadow and forest soil samples were collected in the territory of Lithuania, especially, in certain places where the Chernobyl accident plume travelled over. For a comprehensive sample analysis different techniques were used: HPGe gamma spectrometry for  $^{137}\text{Cs}$  assessment, alpha spectrometry - for  $^{238}\text{Pu}$  and  $^{239,240}\text{Pu}$  atomic ratios and activities determination, accelerator mass spectrometry – for  $^{129}\text{I}$  determination, inductively coupled plasma mass spectrometry combined with a state-of-the-art high sensitivity APEX sample introduction system combined with the PCM sample desolvation module - for revealing the  $^{239}\text{Pu}$  and  $^{240}\text{Pu}$  isotopic ratio. Although the mixture of global nuclear tests fallout and the negligible Chernobyl plume emissions prevailed, the results showed a substantial concentration increase (up to one hundred times) of  $^{137}\text{Cs}$  and Pu and considerable atomic and isotopic ratios differences of  $^{137}\text{Cs}/^{239,240}\text{Pu}$ ,  $^{238}\text{Pu}/^{239,240}\text{Pu}$ ,  $^{240}\text{Pu}/^{239}\text{Pu}$  in sampling locations nearby and in medium-scale, sometimes revealing Chernobyl contribution up to 43% in certain places. It was found a significant inhomogeneity of global fallout and the Chernobyl accident releases prevailing in nearby sampling locations in undisturbed meadows and between undisturbed meadows and forest soils. The  $^{129}\text{I}/^{127}\text{I}$  isotopic ratios and no correlation between  $^{129}\text{I}$  and  $^{137}\text{Cs}$  showed a different  $^{129}\text{I}$  source of contamination prevailing, possibly, pointing out to nuclear fuel

reprocessing facilities operated in the Europe. Places to perform sampling under air mass trajectories of the possible radionuclide emission for the best its detection sensitivity are discussed. A possible numerical model to explain inhomogeneous radionuclide contamination fallout depending on various surface and near-ground troposphere parameters is discussed as well.

Lujanienė G., Valiulis D., Byčėnėnė S., Šakalys J., Povinec P.P. 2012. Plutonium isotopes and  $^{241}\text{Am}$  in the atmosphere of Lithuania: A comparison of different source terms. *Atmospheric Environment* 61:419-42.

Povinec P.P., Hirose K., Aoyama M. 2013. Fukushima Accident: Radioactivity Impact on the Environment. Elsevier.

Varga Z. Origin and release date assessment of environmental plutonium by isotopic composition. 2007. *Anal Bioanal Chem.*, 389:725–732.

Hou X., Hansen V., Aldahan A., Possnert G., Lind O.C., Lujanienė G. A review on speciation of iodine-129 in the environmental and biological samples. 2009. *Anal Chim Acta.* 26;632(2):181-96.

## Assessment of radioactive contamination of surface water and sediments in Poland in 2016

M.Kardaś, A.Fulara, B.Rubel, M. Suplińska, E.Starościak, K.Pachocki

Central Laboratory for Radiological Protection, 03-194 Warsaw, Konwaliowa 7, Poland

Keywords: monitoring,  $^{137}\text{Cs}$ ,  $^{90}\text{Sr}$ ,  $^{239,240}\text{Pu}$

Presenting author email: rubel@clor.waw.pl

In the frame of monitoring of radioactive contamination of surface waters and bottom sediments in year 2016, samples of water and bottom sediment were collected twice a year (in spring and autumn) in 18 sampling points. These sampling points were located along the Vistula river (7 sampling points), and along the Odra river (5 sampling points). Six sampling points were located in the selected Polish lakes.

$^{137}\text{Cs}$  and  $^{90}\text{Sr}$  in water and plutonium in bottom sediments were determined by radiochemical methods.  $^{137}\text{Cs}$  in bottom sediments was determined using gamma spectrometry.

The average activity concentrations of  $^{137}\text{Cs}$  in water from basins of the Vistula River and Odra River and from Polish lakes were on an even level and ranged from 2,13 mBq l<sup>-1</sup> (for lakes) to 2,96 mBq l<sup>-1</sup> (Odra river basin). The average activity concentrations of  $^{90}\text{Sr}$  ranged from 3,61 mBq l<sup>-1</sup> for Vistula river basin – 4,27 mBq l<sup>-1</sup> for lakes (Table 1).

Table 1. Annual average concentrations of  $^{137}\text{Cs}$  and  $^{90}\text{Sr}$  in the water of the basin of the Vistula river, Odra river and lakes.

Location of sampling	$^{137}\text{Cs}$ [mBq l <sup>-1</sup> ]	$^{90}\text{Sr}$ [mBq l <sup>-1</sup> ]
Basin of the Vistula (7) <sup>a)</sup>	2,20 ± 1,07 <sup>b)</sup> (14)	3,61 ± 0,78 (14)
Basin of the Odra (5)	2,96 ± 0,71 (10)	4,27 ± 2,62 (10)
Lakes (6)	2,13 ± 1,00 (12)	3,72 ± 2,80 (12)
Average overall (18)	2,39 ± 1,00 (36)	3,83 ± 2,13 (36)

<sup>a)</sup> Number of samales, <sup>b)</sup> Average value ± Standard deviation

In bottom sediments of rivers and lakes, large variations in the activity concentrations of  $^{137}\text{Cs}$  and  $^{239,240}\text{Pu}$  were observed. The largest difference was observed for lakes. The smallest differences in concentrations of these isotopes were observed in the bottom sediments for basin of the Vistula River (Table 2).

The average activity concentrations of  $^{137}\text{Cs}$  in bottom sediments were varied also: the lowest was observed in the basin of the Odra river (3,90 Bq kg<sup>-1</sup>), and the highest for lakes (16,03 Bq kg<sup>-1</sup>).

Table 2. Annual average concentrations of  $^{137}\text{Cs}$  and  $^{239,240}\text{Pu}$  in bottom sediment of the basin of the Vistula river, Odra river and lakes.

Location of sampling	$^{137}\text{Cs}$ [Bq kg <sup>-1</sup> ]	$^{239,240}\text{Pu}$ [mBq kg <sup>-1</sup> ]
Basin of the Vistula (7) <sup>a)</sup>	4,86 ± 4,09 (14) <sup>b)</sup>	35,00 ± 36,43 (14)
Basin of the Odra (5)	3,90 ± 4,18 (10)	29,54 ± 49,29 (10)
Lakes (6)	16,03 ± 31,54(12)	50,98 ± 118,59(12)
Average overall (18)	8,32 ± 17,34 (36)	38,81 ± 62,00 (36)

<sup>a)</sup> Number of samales, <sup>b)</sup> Average value ± Standard deviation

In case of plutonium, its annual average activity concentrations in bottom sediments were similar for both rivers and amounted to 35,00 mBq kg<sup>-1</sup> for the basin of Vistula River, 29,54 mBq kg<sup>-1</sup> for Odra River Basin and significantly higher for lakes – 50,98 mBq kg<sup>-1</sup> (Table 2).

Both, the annual average concentrations of analysed radionuclides and the data obtained for single determinations for water and sediment samples do not differ from data obtained in previous years (Suplińska et al., 2014) but well reflected in large time periods (Wardaszko et al., 2001)

Monitoring of radioactive contamination of surface waters and sediments leads to the conclusion that  $^{137}\text{Cs}$  and  $^{90}\text{Sr}$  contamination of surface waters is low. Also, the concentration of radioactive  $^{137}\text{Cs}$  and  $^{239,240}\text{Pu}$  in bottom sediments of rivers and lakes remains on low level.

Our determinations confirm that there were no new releases of radioactive isotopes into the environment.

The work done on request of the National Fund for Environmental Protection

Suplińska M, Kardaś M, Rubel B, Fulara A, Adamczyk A, 2015, Monitoring of radioactive contamination in Polish surface waters in 2012-2013. J. Radioanal. Nucl. Chem. 304, 81-87.

Wardaszko T, Radwan I, Pietrzak-Flis Z, 2001, Radioactive contamination of rivers and lakes in Poland in 1994–2000 (in Polish). Inspection of Environmental Protection, Warsaw, pp 2–82.

## Cs-137 levels in Peruíbe Black Mud: a Medicinal Clay

Paulo Sergio Cardoso da Silva<sup>1</sup>, Renato Semmler<sup>1</sup>, Guilherme Soares Zahn<sup>1</sup>, Paulo Flávio de Macedo Gouvea<sup>1</sup>

<sup>1</sup>Instituto de Pesquisas Energéticas e Nucleares - CNEN/IPEN, CP 11049, 05508-000 São Paulo-SP, Brazil

Keywords: Cs-137, gamma spectrometry, Peruíbe, peloid.

Presenting author email: pscsilva@ipen.br

Cesium-137 is not found naturally in soil and sediment but can appear as a product of radioactive fallout, being one of the radioactive pollutants of environmental concern.

In Peruíbe City, Southeast Brazil, the sediment known as Black Mud is traditionally used as topical infusion for healing articular and skin diseases such as osteoarthritis and psoriasis. During the applications, the black mud, heated to approximately 40 °C, is used to cover the patient skin, for periods of 20 minutes daily, up to three months.

Clay sediments from estuary system are well known to accumulate trace elements from natural and anthropogenic origin. The natural radionuclides of uranium and thorium series and <sup>40</sup>K activity concentrations as well as the dose resulting from used of topical applications of black mud has already been evaluated indicating an average dose of less 5 μSv y<sup>-1</sup>. Nevertheless the contribution of anthropogenic <sup>137</sup>Cs has not been measured yet.

A low level <sup>137</sup>Cs measurement methodology was applied to evaluate the activity concentration of this nuclide in the Peruíbe black mud clays. The method consists in calibrating the detector, determining the detector counting efficiency, accumulative counts at regular time intervals of both sample and background and smoothing the 661.6 keV <sup>137</sup>Cs photopeak.

The methodology was validated by using the reference materials IAEA-Soli-6 (radionuclides in soil), IAEA-414 (radionuclides in mixed fish from the Irish sea and North sea) and IAEA/SD-N-2 (radionuclides in marine sediment samples).

Ten samples of Peruíbe black mud were measured, five samples collected and analyzed direct from the black mud deposit and five matured samples, i.e., black mud washed with sea water to eliminate impurities and then let to stand in sea water for at least five months in order to be used as a medicinal peloid.



## Determination of activity concentration of $^{234}\text{U}$ , $^{238}\text{U}$ , $^{210}\text{Po}$ , $^{210}\text{Pb}$ , $^{90}\text{Sr}$ , $^{134}\text{Cs}$ and $^{137}\text{Cs}$ in the water from wells Oligocene in Warsaw

E. Starościk, M. Kardaś

Central Laboratory for Radiological Protection, 03-194 Warsaw, Konwaliowa 7, Poland

Keywords: water, uranium,  $^{210}\text{Po}$ ,  $^{137}\text{Cs}$

Presenting author email: starosciak@clor.waw.pl

The consumption of water is one of the ways passage of radioactive substances to the human body. Council directive 2013/51/EURATOM of 22 October 2013 “Laying down requirements for the protection of the health of the general public with regard to radioactive substances in water intended for human consumption” and Polish Minister of Health regulation of November 27, 2015 “On the quality of water intended for human consumption” (Dz. U. 2015. pos. 1989) determine the levels of natural and artificial radionuclides permitted in these waters.

The aim of the study was to determine the activity concentrations of natural isotopes: uranium-234, uranium-238, polonium-210, lead-210 and artificial isotopes: strontium-90, cesium-134 and cesium-137 in water samples from wells Oligocene located in Warsaw. The waters were taken from ten Oligocene water intakes located in different streets (districts) of Warsaw: Hallera (Praga Północ), Inflancka (Śródmieście), Porajów (Białoleka), Szaserów (Praga Południe), Łuczek (Włochy), Zagłoby (Ursus), Kazubów (Bemowo), Gajowiczyńskiej (Żoliborz), Płocka (Wola), Wolumen (Bielany).

The activity concentration of  $^{210}\text{Po}$  ranged from  $<0,3 \text{ mBq}\cdot\text{l}^{-1}$  for water intake at Kazubów to  $2,02 \pm 0,12 \text{ mBq}\cdot\text{l}^{-1}$  for water from Szaserów. In the case of  $^{210}\text{Pb}$  concentration range is from  $0,98 \pm 0,09 \text{ mBq}\cdot\text{l}^{-1}$  for water from Porajów to  $4,04 \pm 0,22 \text{ mBq}\cdot\text{l}^{-1}$  for water from Inflancka. In the four water samples (Szaserów, Porajów, Inflancka and Hallera) activity concentration of  $^{234}\text{U}$  were above the limit of detection ( $0,5 \text{ mBq}\cdot\text{l}^{-1}$ ) and ranged from  $1,18 \pm 0,24 \text{ mBq}\cdot\text{l}^{-1}$  to  $1,56 \pm 0,28 \text{ mBq}\cdot\text{l}^{-1}$ . Activity concentration of  $^{238}\text{U}$  in three samples were above  $0,5 \text{ mBq}\cdot\text{l}^{-1}$ : Hallera  $0,75 \pm 0,23 \text{ mBq}\cdot\text{l}^{-1}$ , Szaserów  $0,81 \pm 0,22 \text{ mBq}\cdot\text{l}^{-1}$  and Porajów  $0,82 \pm 0,51 \text{ mBq}\cdot\text{l}^{-1}$ . For all tested samples of Oligocene water activity concentration of  $^{90}\text{Sr}$  were below  $0,45 \text{ mBq}\cdot\text{l}^{-1}$ . For  $^{134}\text{Cs}$  determined by gamma

spectrometry results obtained below  $0,13 \text{ Bq}\cdot\text{l}^{-1}$  for all tested samples of water.  $^{137}\text{Cs}$  were determined by radiochemical method. Activity concentration of  $^{137}\text{Cs}$  ranged from  $<0,32 \text{ mBq}\cdot\text{l}^{-1}$  for water intake at Łuczek to  $3,91 \pm 0,45 \text{ mBq}\cdot\text{l}^{-1}$  for water from Porajów. The resulting activity concentrations of studied isotopes are shown in Figure 1.

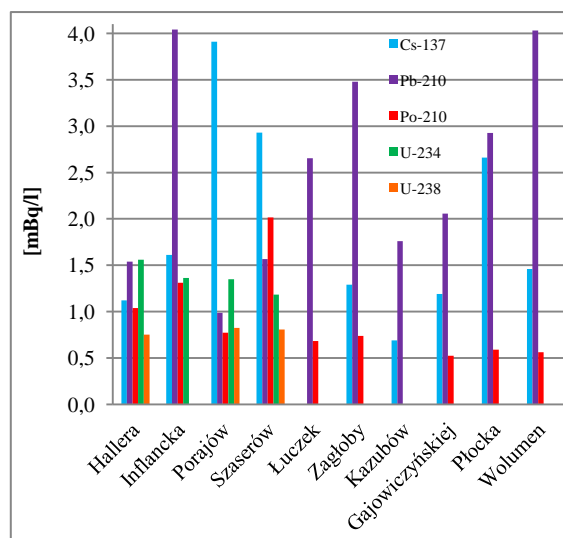


Figure 1. Activity concentrations of studied isotopes in the Oligocene waters of the area of Warsaw.

All tested water from wells Oligocene meet the requirements stored in the Polish Minister of Health regulation of November 27, 2015 “On the quality of water intended for human consumption”.

This work was supported by the Ministry of Science and Higher Education Republic of Poland.

## Polonium $^{210}\text{Po}$ , radiolead $^{210}\text{Pb}$ and uranium $^{234}\text{U}$ , $^{238}\text{U}$ in mushrooms from Northern Poland

D.I. Strumińska-Parulska, K. Szymańska, B. Skwarzec and J. Falandysz

University of Gdańsk, Faculty of Chemistry, Environmental Chemistry and Radiochemistry Department, Wita Stwosza 63, 80-308 Gdańsk, Poland

Keywords: polonium  $^{210}\text{Po}$ , radiolead  $^{210}\text{Pb}$ , uranium  $^{234}\text{U}$ ,  $^{238}\text{U}$ , mushrooms.

Presenting author email: dagmara.struminska@ug.edu.pl

The aim of the research was polonium  $^{210}\text{Po}$ , radiolead  $^{210}\text{Pb}$  as well as uranium  $^{234}\text{U}$  and  $^{238}\text{U}$  determination in caps, stipes and soil substrate of edible mushrooms collected in northern Poland. The analyzed radionuclides were determined in five mushroom species from *Leccinum*: orange birch bolete (*L. aurantiacum*), Hazel Bolete (*L. pseudoscabrum*), Red-capped scaber stalk (*L. quercinum*), Foxy bolete (*L. vulpinum*) and Slate bolete (*L. duriusculum*). Mushrooms typically grow in forests and fields, but almost all ecosystems will favor their growth in the correct substrate medium. The fruiting bodies of mushrooms are generally considered as absorbing mineral constituents, including heavy metals and radionuclides. They could be used as environmental biomonitoring indicators to evaluate the level of the environment contamination as well as the quality of the ecosystem. Mushrooms and microbes biological activities effect on long-term radionuclides retention in organic layers of forest soil and the soil represents the major reservoir of radionuclides - thus they can be easily available for mushrooms and mycelium located in organic layers.

Among analyzed *Leccinum* mushrooms, the highest concentrations of  $^{210}\text{Po}$  and  $^{210}\text{Pb}$  as well as  $^{234}\text{U}$  and  $^{238}\text{U}$  were observed in Hazel bolete (*L. pseudoscabrum*): 0.71-10.9  $\text{mBq}\cdot\text{g}^{-1}$  dry mas and 0.50-4.92  $\text{mBq}\cdot\text{g}^{-1}$  d.m. for  $^{210}\text{Po}$  and  $^{210}\text{Pb}$  as well as 0.06-0.43  $\text{mBq}\cdot\text{g}^{-1}$  d.m. and 0.05-0.58  $\text{mBq}\cdot\text{g}^{-1}$  d.m. for  $^{234}\text{U}$  and  $^{238}\text{U}$  respectively.

In order to identify the potential radiotoxicity, on the basis of previously calculated  $^{210}\text{Po}$ ,  $^{210}\text{Pb}$ ,  $^{234}\text{U}$  and  $^{238}\text{U}$  content in dried and unprocessed culinary fruiting bodies of analyzed mushrooms, the annual effective radiation doses were calculated, on the basis of the effective dose conversion coefficients from analyzed radioisotopes ingestion for adult members of the public recommended by ICRP (ICRP, 2012). The results showed the consumption of 0.5 kg of whole dried mushrooms, the highest annual effective radiation doses could be 5.33  $\mu\text{Sv}$  from  $^{210}\text{Po}$ , 1.42  $\mu\text{Sv}$  from  $^{210}\text{Pb}$ , 21.2 nSv from  $^{234}\text{U}$  and 25.9 nSv from  $^{238}\text{U}$  decay. The total annual effective dose from natural radiation in Poland was estimated at 2.1-2.6 mSv (including  $^{222}\text{Rn}$ ) while the annual effective dose from  $^{210}\text{Po}$  and  $^{210}\text{Pb}$  intake with different foodstuffs and water was estimated at 54  $\mu\text{Sv}$  per year for both (Jagiela et al., 1997; Pietrzak-Flis et al., 1997; Dobrzyński et al., 2005). It means if consumers would eat the analyzed mushrooms, they should not increase significantly the total effective radiation dose from  $^{210}\text{Po}$ ,  $^{210}\text{Pb}$ ,  $^{234}\text{U}$  and  $^{238}\text{U}$  from typical dietary intake. For comparison eating *B. edulis* collected in Białogard could

result an annual effective dose from  $^{210}\text{Po}$  decay at 37  $\mu\text{Sv}$  (Skwarzec and Jakusik, 2007).

The authors would like to thank the MNiSW for financial support under grant: DS-530-8635-D646-16.

Dobrzyński, L., Droste, E., Trojanowski, W., Wołkiewicz, R., 2005. Spotkanie z promieniotwórczością. IPJ, Świerk.

Jagiela, J., Biernacka, M., Henschke, A., Sosińska, A., 1997. Radiologiczny Atlas Polski. PIOŚ, CLOR, PAA, Biblioteka Monitoringu Środowiska, Warszawa.

Pietrzak-Flis, Z., Chrzanowski, E., Dembińska, S., 1997. Intake of  $^{226}\text{Ra}$ ,  $^{210}\text{Pb}$  and  $^{210}\text{Po}$  with food in Poland. Sci Total Environ. 203(2), 157-165.

Skwarzec, B., Jakusik, A., 2003.  $^{210}\text{Po}$  bioaccumulation by mushrooms from Poland. J Environ Monit., 5, 791-794.

## Calcium and magnesium supplements as a source of polonium $^{210}\text{Po}$ and radiolead $^{210}\text{Pb}$

D.I. Strumińska-Parulska and B. Skwarzec

University of Gdańsk, Faculty of Chemistry, Environmental Chemistry and Radiochemistry Department, Wita Stwosza 63, 80-308 Gdańsk, Poland

Keywords: calcium and magnesium supplement, polonium  $^{210}\text{Po}$ , radiolead  $^{210}\text{Pb}$ , radiation doses.

Presenting author email: dagmara.struminska@ug.edu.pl

Polonium  $^{210}\text{Po}$  ( $T_{1/2}=138.376$  days) and radiolead  $^{210}\text{Pb}$  ( $T_{1/2}=22.2$  years) appear at the end of the decay-chain of uranium  $^{238}\text{U}$  and are radio-ecologically interesting natural elements to investigate due to their high radiotoxic characteristics. These radionuclides are introduced into the biosphere through various routes of terrestrial and marine radioecological pathways and are continuously deposited from the atmosphere in association with aerosols. Both  $^{210}\text{Po}$  and  $^{210}\text{Pb}$  radionuclides are, together with radon, the natural radioactive material delivering the highest natural dose to living organisms. Next calcium and magnesium are one of the most essential elements in living organisms and their deficiencies are common so their supplements have become extremely popular.

The aim of this pioneer study was to investigate the most popular calcium and magnesium supplements as a potential additional source of polonium  $^{210}\text{Po}$  and radiolead  $^{210}\text{Pb}$  in human diet. The analyzed Ca and Mg pharmaceuticals contained their organic or inorganic compounds; some from natural sources as shells, fish extracts, or sedimentary rocks. The objectives of this research were to investigate the naturally occurring  $^{210}\text{Po}$  and  $^{210}\text{Pb}$  activity concentrations in calcium and magnesium supplements, find the correlations between  $^{210}\text{Po}$  and  $^{210}\text{Pb}$  concentration in medicament and the element chemical form, and calculate the effective radiation dose connected to analyzed supplement consumption.

The highest  $^{210}\text{Po}$  and  $^{210}\text{Pb}$  activity concentrations in Ca pharmaceuticals were measured in mineral tablets made from sedimentary rocks,  $3.88\pm 0.22$  and  $2.97\pm 0.18$   $\text{mBq}\cdot\text{g}^{-1}$  respectively. The results obtained for natural origin calcium supplements (shells, sedimentary rocks) were much higher than the other analyzed samples. Also the results of  $^{210}\text{Po}$  analysis obtained for inorganic forms of calcium supplements in comparison to organic were significantly higher. The highest  $^{210}\text{Po}$  and  $^{210}\text{Pb}$  activity concentrations in magnesium supplements were also measured in dolomite pills –  $3.84\pm 0.15$   $\text{mBq}\cdot\text{g}^{-1}$  and  $2.97\pm 0.18$   $\text{mBq}\cdot\text{g}^{-1}$  respectively. The differences, mainly in  $^{210}\text{Po}$  activities, are representatives of the individual supplement and its raw material properties as well as technological processes. If high temperature during supplement production is used, significant part of polonium can volatilize due to low sublimation point of polonium. Also time influences polonium activity decrease in the supplements.

On the basis of  $^{210}\text{Po}$  and  $^{210}\text{Pb}$  content calculated in analyzed calcium and magnesium supplements, the annual effective radiation doses were estimated – for daily intake of 1 pill of pharmaceutical or

RDI value of pure element. In both cases, for each supplement, the highest annual effective radiation doses calculated for RDI value were calculated for natural origin supplements – sample of dolomite (sedimentary rocks): in case of 1 g of pure Ca:  $12.7\pm 0.70$   $\mu\text{Sv}\cdot\text{year}^{-1}$  from  $^{210}\text{Po}$  and  $5.57\pm 0.34$   $\mu\text{Sv}\cdot\text{year}^{-1}$  from  $^{210}\text{Pb}$ ; in case of 0.4 g of pure Mg:  $3.38\pm 0.13$   $\mu\text{Sv}\cdot\text{year}^{-1}$  from  $^{210}\text{Po}$  and  $3.72 \pm 0.02$   $\mu\text{Sv}\cdot\text{year}^{-1}$  from  $^{210}\text{Pb}$ . Obtained results of the annual effective radiation dose in case of the highest  $^{210}\text{Po}$  activity in dolomite supplement ( $12.7$   $\mu\text{Sv}\cdot\text{year}^{-1}$ ) would be similar to Polish fish consumption.

According to Polish conditions, the annual effective dose from  $^{210}\text{Po}$  and  $^{210}\text{Pb}$  total intake with different foodstuffs and water was estimated at  $54$   $\mu\text{Sv}$  per year for each isotope and the total annual effective dose from all sources was estimated at  $2.1$ - $2.6$   $\text{mSv}$ . It means if consumers would choose dolomite supplement as additional Ca and Mg source, they would receive additional value of radiation dose at level close to 25% of the total effective radiation dose from  $^{210}\text{Po}$  and close to 10% of the total effective radiation dose from  $^{210}\text{Pb}$  from typical dietary intake.

The authors would like to thank the Ministry of Sciences and Higher Education for the financial support of this work under grant: DS/530-8635-D646-16.

### Indoor Radon in Ardenne: A multivariate analysis

V.De Heyn<sup>1</sup>, C.Licour<sup>1</sup>, F.Tondeur<sup>1</sup>, I.Gerardy<sup>1</sup>, B. Dehandschutter<sup>2</sup>, G. Ciotoli<sup>3</sup>, G. Cinelli<sup>4</sup>

<sup>1</sup>Laboratoire de Physique Nucléaire, ISIB, Haute Ecole Bruxelles-Brabant, Brussels, BE1000, Belgium

<sup>2</sup>Federal Agency for Nuclear Control, Brussels, BE1000, Belgium

<sup>3</sup>Istituto di Geologia Ambientale e Geoingegneria, Consiglio Nazionale delle Ricerche, Rome, I00016, Italy

<sup>4</sup>Independent Researcher, Italy

Keywords: natural radioactivity, soil uranium, soil radon, indoor radon

Presenting author email: [vdeheyn@he2b.be](mailto:vdeheyn@he2b.be)

Indoor radon being a product of the decay of <sup>238</sup>U present in the soil or sub-soil, it is often assumed that a correlation must exist between indoor <sup>222</sup>Rn the concentration of U in the soil or sub-soil, as well as with <sup>222</sup>Rn in the soil. These correlations should also be influenced by other physical and geochemical properties, like soil permeability, which in turn can be related to pedological, geological and lithological classes. Analyzing the relations between all these factors could allow developing a model that would predict areas affected by <sup>222</sup>Rn, even without any measurement in homes. This model would use the available data, which may differ according to the country or even the region.

Several data are available in Ardenne, a region of ~4000 km<sup>2</sup> in the south of Belgium: indoor Rn and soil gas Rn concentrations, soil permeability, soil U from an airborne campaign, which all show an important variability, although the area as a whole can be considered as radon-affected. Geological, pedological and lithological information is also available. As the datasets were not collected at the same sampling points, a first step of interpolation / smoothing was necessary for some of them before the multivariate analysis. The data were mapped on a kilometric grid. Soil Rn and soil permeability were combined into a “radon potential” applying the Czech definition. The numerical variables were transformed in a way to obtain roughly normal distributions (e.g. log-transform of indoor Rn data).

Figure 1 summarizes the absence of clear relationships between indoor Rn, soil Rn and permeability, and airborne soil U. As the radon potential is a function of soil Rn, the better correlation between them is obvious.

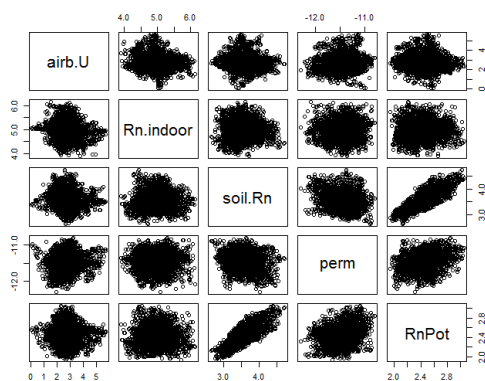


Figure 1. Scatterplot matrix of data collected in Ardenne

In Table 1, Pearson’s correlation coefficients of the global data lead to the same conclusion.

	Airb. U	indoor Rn	Soil Rn	perm	RnPot
Airb U	1.000				
indoor Rn	-0.110	1.000			
Soil Rn	-0.033	0.048	1.000		
Perm.	-0.085	0.030	0.817	1.000	
RnPot	0.086	0.033	0.368	-0.179	1.000

Table 1. Pearson Correlation coefficients of the smoothed and normalized data (N=3729)

We note a strong absence of correlation between indoor Rn and soil Rn or airborne soil U in this Rn-affected area. This result prevents further study by principal component analysis and leads to consider cartography by geological or lithological zone rather than on the kilometric grid. Table 2 gives the correlation coefficients between weighted mean values calculated for the 20 possible classes defined as lithology-geology pairs.

Data grouped by pairs lithology-geology					
Ave-rages	Airb. U	indoor Rn	Soil Rn	perm	RnPot
Airb U	1.000				
indoor Rn	-0.405	1.000			
Soil Rn	-0.044	0.375	1.000		
Perm.	-0.101	0.264	0.811	1.000	
RnPot	0.028	0.341	0.555	0.062	1.000

Table 2. Pearson Correlation coefficients of the smoothed and normalized grouped data by pairs lithology-geology (N=20)

## Solvent effects in the colorimetric detection of $\text{UO}_2^{2+}$ by substituted tetraphenylethene

Jun Wen, \* Sheng Hu, Xiaolin Wang

Institute of Nuclear Physics and Chemistry, China Academy of Engineering Physics, Mianyang, 621900, Sichuan Province, China

Keywords: Solvent effects, uranyl, colorimetric detection.

Presenting author email: junwen@caep.cn

Uranium is a representative element of an actinide metal that has naturally radioactivity and widely distributed in the environment [1]. Uranium is one of the main fuel in nuclear energy generation, and it also has been used in nuclear weapons [2]. With the growing human demand for nuclear energy, the worldwide uranium consumption is continuous increasing. For uranium, the most stable and common ionic form is appears as a complex of the uranyl ion ( $\text{UO}_2^{2+}$ ), because uranyl is water soluble, it is readily migrated to environment. Unfortunately, uranium is radioactive and chemically toxic, it was reported that human exposure to uranium could give rise to lung cancer, urinary system disease and genetic diseases.

Considering the widespread use of uranium and its toxic properties, the development and improvement of analysis methods for the determination of uranium are vital. Therefore, many techniques have been used for the determination of uranium. Among these analysis methods, colorimetric detection is a simple, rapid, highly selective, and low-cost method for metal ion determination. However, only few reports on the application of this technique to uranium ion analysis have been published. Moreover, solvents are only considered as reaction media in the system of determination, even though solvents have been known to effect metal ion coordination for some time.[3]

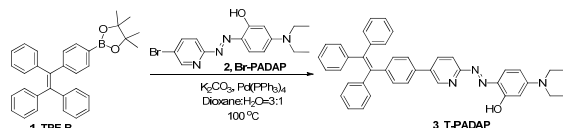


Figure 1. Synthesis of T-PADAP

In order to obtain insight into the impact of solvent on selectivity, we synthesized a novel molecule, T-PADAP, and found that the coordination of metal ions could be adjusted by varying the amounts of H<sub>2</sub>O and DMSO. Under the optimized conditions, T-PADAP exhibited a high selectivity, low detection limit, wide effective pH range, and good anti-interference qualities as a colorimetric sensor for  $\text{UO}_2^{2+}$ . This work provides a simple method for the detection of uranyl ions, and illustrates the use of solvent effects to regulate the coordination ability of sensors.

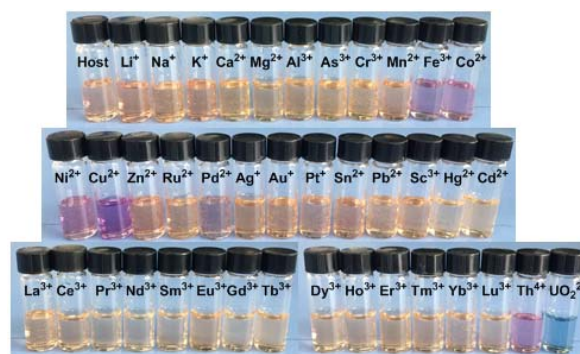


Figure 1. Image of the solutions of T-PADAP ( $10^{-5}$  M)/cation ( $10^{-5}$  M) mixtures at a  $f_w$  of 40% taken under natural light.

This work was supported by the National Science Foundation of China (Nos. 21401175), the Radiochemistry 909 Project in the China Academy of Engineering Physics

[1] K.B. Gongalsky, Environ. Monit. Assess., 2003, 89, 197.

[2] J. Li, Y. Zhang, Proc. Environ. Sci., 2012, 13, 1609.

[3] C. Gaillard, A. Chaumont, I. Billard, C. Hennig, A. Ouadi, G. Wipff, Inorg. Chem. 2007, 46, 4815-4826.





## Calculation of net doses and their characteristic limits from readings of environmental stray-radiation monitors at CERN

P. Vojtyla and F. Malacrida

Occupational Health and Safety and Environmental Protection Unit, CERN, Geneva 23, CH-1211, Switzerland

Keywords: environmental dosimetry, accelerator, stray radiation, ISO 11929, characteristic limits

Presenting author email: pavol.vojtyla@cern.ch

The exposure to stray radiation from CERN's sites usually dominates the external exposure of members of the public living or working close to the sites. There are a number of stray radiation monitors that measure the exposure to neutrons, rem-counters, and to photons and penetrating charged particles, pressurized ionization chambers (Scibile et al., 2008). The quantity of interest is the *net* ambient dose equivalent.

In the past, there have been periods of long accelerator shutdowns when background dose rates of each individual station could be measured during a long time. This is not the case anymore and it appears to be more convenient to use periods without particle beams in the crucial accelerators for measuring the background dose rates also during operation seasons. Furthermore, a simple deduction of the background dose rate could not reveal whether a positive result was an effect or just a random fluctuation. A method based on the international standard ISO 11929 (ISO, 2010) was developed to calculate the characteristic limits using the Bayesian approach.

Unlike in radioactivity measurements in which the uncertainty of the measured value can be estimated from physics principles, in environmental dose rate measurements, there are many unpredictable influences, like temperature drifts of signals from ionization chambers or photon exposure burst caused by washout of the radon progeny by rain. Hence, empirical variances are used instead of standard uncertainties usually derived from the model of the signal generation process.

There are three types of characteristic limits:

1. Decision threshold, which is unique to each measurement result and the value of which decides whether a signal is or is not attributable to an effect at the given confidence level;
2. Detection limit, which characterizes the measurement process. It defines the smallest effect that will be detected with the probability defined by the given confidence level;
3. Limits of the confidence interval.

In practice, one is interested in the ambient dose equivalent integrated over longer intervals, such as a month or a quarter, however, readings are stored as a time series of doses integrated over much shorter intervals, typically from 10 minutes to 1 hour. In this way, the monitoring function of the system is preserved and the effect of inevitable faults of the instrumentation is limited in time.

The dose rate data series is compared with the data series of the accelerator operation (Ozelton and Baird, 2008). The latter defines the data points corresponding to the background conditions. To account for exposure to gamma radiation from rests of radioactive plumes after stopping a facility, tagging of a dose rate reading as a background reading starts only 1 hour after the beam stop.

Planned accelerator operation periods extend over months but there are always stops for preventive and corrective maintenance and machine development. Samples of the background dose rate can be taken during each longer period. This makes the method very robust not only against long-term background dose rate changes (e.g. periods with snow, cosmic-ray intensity variations) but also against bursts of the external exposure due to washout of radon progeny from air following an onset of rain because onsets of precipitation and accelerator stops are not correlated.

Detection limits around 1  $\mu$ Sv per year can be obtained. Such a small *net* dose represents about 0.1% of the annual external exposure from natural sources and makes only 10% of CERN's dose objective for members of the public. Some real data will be shown and interpreted.

Systematic uncertainties of the operational dosimetry quantity ambient dose equivalent so as measured by the used instruments is out of the scope of this work.

### Acknowledgment

The authors acknowledge the IT support of N.P. Jacinto in preparing scripts for data extraction from various databases.

### References

- ISO, 2010. Determination of the characteristic limits (decision threshold, detection limit and limits of the confidence interval) for measurements of ionizing radiation – Fundamentals and application, ISO 11929, International Organization for Standardization, Geneva.
- Ozelton, E.C., Baird, J.A., 2008. Timber designers' manual. Hoboken, NJ, Wiley.
- Scibile, L., Perrin, D., Segura Millan, G., Witorski, M., Menzel, H.G., Vojtyla, P., Forkel-Wirth, D., 2008. The LHC radiation monitoring system for the environment and safety: From design to operation, in Proc. EPAC08, Genoa.

## FEATURES TRITIUM DISTRIBUTION IN THE WATERS AT THE SEMIPALATINSK TEST SITE

*Aktaev M.R., Lukashenko S.N., Aidarkhanov A.O.*

*Institute of Radiation Safety and Ecology of the NNC RK, Kurchatov, Kazakhstan*

The work provides results of research on distribution of artificial radionuclides in water of "Atomic" lake and Shagan river, located at the territory of the former Semipalatinsk Test Site.

To determine content of artificial radionuclides in water of "Atomic" lake, point sampling of surface water was made as well as in-depth sampling with the vertical interval of 5-10 m. Water samples from Shagan river were collected with sampler from different depths with the vertical interval of 5 cm.

According to obtained data, in "Atomic" lake non uniform spatial distribution of concentrations of artificial radionuclides was observed. Maximal values of tritium and strontium-90 were found in the central part of the body of water at the depth of 60-80 m, and they were 20 000 and 15 Bq/kg, respectively, and the minimal values were found at the depth of up to 10 m. According to monitoring data, artificial radionuclides distribution in the central part of the lake has a stable character.

Presence of tritium was noticed in water of Shagan river, from the "Atomic" lake to inflow into Irtysh river. Maximal concentration of tritium was found at the distance of 5 km downstream from "Atomic" lake, with activity of 350 000 Bq/kg. Also at the area with maximal concentrations non uniform areal distribution of tritium is observed, both in width and depth of the stream.

In the place of flowing of Shagan river into Irtysh river specific activity of tritium does not exceed 100 Bq/kg.

## PECULIARITIES OF BURNING THE GRAPHITE SAMPLES

Vladimir Abdulajev<sup>1</sup>, Andrius Garbaras<sup>1,2</sup>, Elena Lagzdina<sup>1</sup>, Danielius Lingis<sup>1,2</sup>, Jevgenij Garankin<sup>1</sup>, Artūras Plukis<sup>1</sup>, Rita Plukienė<sup>1</sup>, Vidmantas Remeikis<sup>1</sup>, Arūnas Gudelis<sup>1</sup>

<sup>1</sup> Institute of Physics, Center for Physical Sciences and Technology, Lithuania

<sup>2</sup> Faculty of Physics, Vilnius University, Lithuania

vladimir.abdulajev@ftmc.lt

Nuclear reactor graphite is a source of dangerous radioactive waste, it is particularly important to determine radiological characteristics of graphite as it is a part of nuclear power plant decommission process. Decommissioning of old reactors and planned use of graphite in the new ones force to look for solutions of irradiated graphite management and disposal [1]. There are several principal solutions possible: disposal of graphite in appropriate repositories, incineration of graphite as a combustible radioactive waste, or recycling and reuse [2]. In order to evaluate radioactive impurities in the graphite is need to burn the graphite. In this work the peculiarities for the burning of graphite were investigated.

Graphite was burned in the oven at 1000 °C in the He flow adding oxygen as oxidiser. It was determined that graphite didn't burn completely during one burning cycle. Burning bigger samples of graphite proved to a challenge for this method as it didn't completely burn down, even after running the cycle for few times. However smaller samples burned down completely. The burning results are presented in the Table 1.

Table 1. The mass of the burned graphite.

Sample nr 1.	Cycle Nr.	Mass of the released carbon, $\mu\text{g}$
	1	29.85
	2	34.38
	3	38.16
	4	30.77
	5	17.3
Total mass of carbon in the burned sample		150.46

The amount of released carbon in the CO<sub>2</sub> form was detected using thermal conductivity detector. The chromatogram of the burned graphite sample is presented in the Figure 1. Further investigations are needed to optimize the instant burning of the graphite sample.

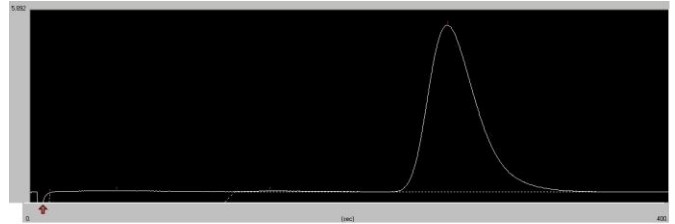


Figure 1. The chromatogram of the burned graphite sample.

- [1] V. Remeikis, A. Plukis, R. Plukiene, A. Garbaras, R. Bariseviciute, A. Gudelis, R. Gvozdaite, G. Duskesas, L. Juodis, Method based on isotope ratio mass spectrometry for evaluation of carbon activation in the reactor graphite, *Nuclear Engineering and Design*, **240** 2697–2703, (2010).
- [2] A. Garbaras, E. Bruzas, V. Remeikis, Stable Carbon Isotope Ratio ( $\delta^{13}\text{C}$ ) Measurement of Graphite Using EA-IRMS System, *Material Science* **21** (2), (2015)

## Prediction of the spectrum for a Cerium Bromide ( $\text{CeBr}_3$ ) detector combining RASCAL code and Monte Carlo simulations

F. Legarda<sup>1</sup> and N. Alegría<sup>1</sup>

<sup>1</sup>Department of Nuclear Engineering and Fluid Mechanics, University of the Basque Country, Bilbao, 48013, Spain

Keywords:  $\text{CeBr}_3$  detectors, gamma spectrometry, MCNP simulations

Presenting author email: natalia.alegria@ehu.eus

Some computational codes can assess the release of radionuclides and the dose rate from a Nuclear Accident and one of them is the RASCAL code (Radiological Assessment System for Consequence AnaLysis) which was developed for the U.S. Nuclear Regulatory Commission (NRC).

The present study tries to obtain spectra for  $\text{CeBr}_3$  detector combining the RASCAL 4.3 code results with MCNP-6

Several parameters have to be chosen for the RASCAL code:

- Event Type: Nuclear Power Plant
- Event Location: A generic site
- Type of Reactor and Reactor Source Term
  - Reactor type PWR, 2940 MWt, 30000 MWd / MTU, with containment volume of  $5,1\text{E}+04 \text{ m}^3$  and a design leak rate of 0,10 %/d
  - Accident type: LOCA (NUREG-1465) with a damage estimate of 30 percent cladding failure (gap)

- Reactor Release Paths: Containment leakage, being the release height of 10 m with the sprays off

- Meteorological conditions: Summer Afternoon Windy, that means stability class B, wind speed of 25 km/h and no rain

- Dose Calculation: the point where dose is assessed is 1 km away from containment building axis and in the direction of prevailing wind. Doses are calculated at 8 hours after start of release

After that, the case is prepared for calculation by RASCAL, and the activity results are shown in the following table.

Table 1. Activity release

	At shutdown	At end (8,25h)
Core activity	$2,2\text{E}+22 \text{ Bq}$	$1,7\text{E}+22 \text{ Bq}$
Containment	0 Bq	$1,2\text{E}+19 \text{ Bq}$
Environment	0 Bq	$6,3\text{E}+15 \text{ Bq}$

The released radionuclides are: Rb-88, I-131, I-132, I-133, I-135, Xe-133, Xe-135, Kr-88, Cs-134, Cs-136, Cs-137, between others.

The External Gamma Exposure Rate obtained is  $2,66\text{E}-04 \text{ (mSv/h)}$ , being the ground shine dose rate of  $1,67\text{E}-04 \text{ (mSv/h)}$  and the cloud shine dose rate of  $0,99\text{E}-04 \text{ (mSv/h)}$

The next step in our study is to obtain the photon spectrum at the measuring point.

For the MCNP- 6 simulation, in the input file, the following information was included:

- The geometry
- The materials
- Photon flux at the measuring point
- Photon energy spectrum
- The FWHM equation
- Energy bins for the spectra

- Number of particles  
After that, the results of the simulation, the total spectrum, is shown in figure 1:

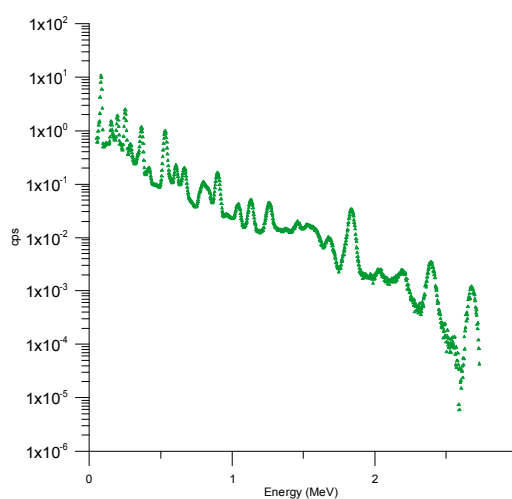


Figure 1: Total spectrum

Experimentally, the dead time of the  $\text{CeBr}_3$  detector has been obtained in our laboratory using the two sources method, being that dead time of  $1.33\text{E}-06 \text{ s}$ . Considering the total counts (Cloud Shine + Ground Shine) of 165 cps, the dead time at this counting rate is 0.022%

So, it can be concluded that at this activity release rate the dead time is very low and there is a light peak overlapping. However, for more severe accidents with core melt and containment building failure, the dead time would be several orders of magnitude higher and the detector would saturate and overlapping will be much more severe.

### References

RASCAL: Description of Models and Methods (NUREG-1887). Office of Nuclear Security and Incident Response. U.S. Nuclear Regulatory Commission. Washington, DC 20555-0001  
Los Alamos National Laboratory. MCNP-6. Monte-Carlo N-Particle Transport Code System, versión 6. New México. USA, 2005.



## Assessment of the possibility of farm animal breeding on the Semipalatinsk nuclear test site conditions

Zh.A. Baigazinov, S.N. Lukashenko

Institute of Radiation Safety and Ecology, Kurchatov, 070011, Kazakhstan

Keywords: radioactive contamination; farm animal breeding; Semipalatinsk nuclear test site

Presenting author email: baigazinov@nnc.kz

Semipalatinsk Nuclear Test Site (SNTS) operated in Eastern Kazakhstan during 1949 – 1989 and its territory has local areas with high concentrations of radionuclides in the environment (Lukashenko et al., 2015). After the test site was shut down, people in the neighboring locations started quite active unauthorized commercial activities at the site: more than a hundred farms are currently running year-round uncontrolled breeding there. Grazing pasture sheep and horse breeding at vast steppe territories is typical there.

Total area of SNTS is about 18 thousand square kilometers with a major part of the lands considered as “background” ones in terms of radiology (Lukashenko et al., 2010). Formal transfer of these “clean” lands for commercial utilization is currently in progress. For that, a reliable radiological contamination forecast for livestock products from animals bred at STS is needed for assessment of the dose loads on consumers of these products.

Knowledge about the  $^{137}\text{Cs}$  and  $^{90}\text{Sr}$  radionuclides transition to livestock products is quite extensive. Still, prevailing portion of this knowledge has been obtained in laboratory experiments or at the territories contaminated due to radiological accidents (Green et al., 2003; Fesenko et al., 2009), which are different from STS conditions in terms of radiological contamination, natural and climatic conditions. Few works are devoted to transition of transuranium radionuclides, such as Pu and Am, to livestock products and the gaps in data are common (IAEA, 2010, Sutton et al., 1979).

One should also note that the main studies of such transitions and, particularly, of the transfer coefficients are performed for the chain “forage – livestock product” based on the common assumption that the radionuclides are mainly delivered to animal bodies with forage. It is important that such assumption does not work for STS conditions: for instance, the major contribution to livestock products contamination at the sites of surface nuclear explosions comes from contaminated soil – more than 90% of  $^{137}\text{Cs}$  and  $^{90}\text{Sr}$  content in mutton is due to the radionuclides intake with soil (Lukashenko et al., 2015).

Since 2007 at the Institute of Radiation Safety and Ecology (Kazakhstan) conducted research of parameters of radionuclide transfer in livestock and poultry products on SNST condition. The focus is on radionuclides  $^3\text{H}$ ,  $^{137}\text{Cs}$  and  $^{90}\text{Sr}$ , transuranic radionuclides  $^{241}\text{Am}$  and  $^{239+240}\text{Pu}$  (Baigazinov, 2016).

To assessment of the possibility to use for breeding animals the SNTS territory were used transfer

parameters of radionuclide into farm animals’ product, which obtained on the STTS condition.

The results of assessment show that animal products (milk, meat) will meet the hygienic standards for radiation safety.

Firstly, this is due to the fact that the area of contamination of test areas are small and local, than the pasture territory of animals. The second reason is the relatively low migration bioavailability of radionuclides in the system “soil-forage-farm animals’ product” on the SNTS.

The exception is the district Shagan river and water sources of “Delegen” site (underground test site). When animals grazing at these sites high concentration of 3H can be pass into products.

In general, it can be argued that more than 95% of the SNTS territory can be used for farm animal breeding.

This work was supported by the Government of the Republic of Kazakhstan RBP-036.

The authors are thankful to the staff of the Department for Comprehensive Ecosystems Studies of the IRSN (Kurchatov, Kazakhstan) for their help in radiological environmental studies.

- Lukashenko, S.N., et al. 2015. Topical Issues of Radiation Ecology in Kazakhstan. Issue 5. Dom Pechati, Pavlodar, (in Russian).
- Lukashenko, S.N., et al. 2010. Topical Issues of Radiation Ecology in Kazakhstan. Issue 1. “Dom Pechati”, Pavlodar, (in Russian).
- Green, N., Woodman, R.F.M., 2003. Recommended transfer factors from feed to animal products. NRPB-W40. Nation. Radiol. Protec. Board, Chilton.
- Fesenko, S., Isamov, N., Howard, B.J., Beresford, N.A., Barnett, C.L., Sanzharova, N., Voigt, G., 2009. Review of Russian language studies on radionuclide behaviour in agricultural animals: part 3. Transfer to muscle. J. Environ. Radioact. 100, 215–231.
- International Atomic Energy Agency, 2010. Handbook of Parameter Values for the Prediction of Radionuclide Transfer in Terrestrial and Freshwater Environments. TRS 472. IAEA, Vienna.
- Baigazinov, Zh.A., Parameters for the transfer of  $^{239+240}\text{Pu}$ ,  $^{241}\text{Am}$ ,  $^{137}\text{Cs}$ ,  $^{90}\text{Sr}$ , and  $^3\text{H}$  to farm animals under the conditions of the Semipalatinsk Test Site: dissertation abstract of candidate of biological sciences (radiobiology), Obninsk, 2016 (in Russian).

## Dissolved uranium and radon in groundwater of the Goesan area, Korea

B.W. Cho<sup>1</sup>, M.S. Kim<sup>2</sup>, H.K. Kim<sup>2</sup>, B.K. Ju<sup>2</sup>, J.H. Hwang<sup>1</sup>, U. Yun<sup>1</sup>, C.O. Choo<sup>3\*</sup>,

<sup>1</sup>Korea Institute of Geosciences and Mineral Resources (KIGAM), 124, Gwahakro, Yuseonggu, Daejeon, Korea

<sup>2</sup>National Institute of Environmental Research (NIER), Hwangyongro 42, Seogu. Incheon, Korea

<sup>3</sup>Department of Geology, Kyungpook National University, 80 Daehakro, Bukgu, Daegu Korea

Keywords: Uranium, Radon, Concentration, groundwater

Presenting author email: cbw@kigam.re.kr

Uranium and radon concentration was measured in 200 groundwater samples taken from Goesan area known as contains Ogcheon metamorphic rock zone (OG2) which partly include coal bed bearing high uranium content of 361 ppm (Shin and Kim, 2011). Well depth ranged from 10 to 220 m having an average depth of 82 m. The geology of the area was classified as three metamorphic rock zones (OG1, OG2, and OG3) and two granite zones (Cretaceous granite and Jurassic granite).

Uranium and radon in groundwater is originated from uranium in bedrock. To see uranium content of rocks of the 5 zones, equivalent of uranium (eU) in rocks was measured using portable gamma ray spectrometer (GR-320A) at the groundwater sampling point if possible (Table 1). Higher median value of eU (8.2 ppm) was found on CGR outcrops. The median eU value of OG2, known as having high uranium content at the some point, was not as high as that of CGR and similar to those of JGR, OG1, and OG3.

Table 1. Eequivalent of uranium (eU) of the 5 zones in the area (ppm)

Zone	Samples	Min.	Max.	Med.
JGR	56	1.1	6.8	3.8
CGR	25	3.8	11.6	8.2
OG1	43	1.1	8.0	3.5
OG2	38	1.4	14.9	3.9
OG3	38	1.7	6.8	3.1

The uranium level in groundwater of the area ranged from 0.02 to 293.0 µg/L with a median value of 0.87 µg/L. The uranium level in groundwater was highest in CGR zone (Figure 1) and it is well consistent with the results of uranium content of rocks (Table 1). Most of the samples were found to have uranium concentrations below 30 µg/L, the WHO guideline value based on its chemical toxicity (WHO, 2011), and only four samples from granite zones (JCR and CGR) exceeded 30 µg/L.

The radon level in groundwater of the area was found to vary from 1.8 to 1,540.9 Bq/L with a median value of 58.8 Bq/L which is similar to the national median radon level of 52.1 Bq/L (NIER, 2015). The percentage of samples having radon concentration equal to or greater than 100 Bq/L of WHO guideline value (WHO, 2011) was found to 25.5 %. The radon concentration was high in the samples from the CGR (range of 18.9-1,540.9 Bq/L) and JGR zones (range of 3.3-523.9 Bq/L) (Figure 2). The percentage of samples having radon level above 100 Bq/L in CGR zone was 64.0 % while those in JGR,

OG2, OG1, OG3 zones were 39.3, 18.4, 9.3, and 5.3 %, respectively. Although there is still no guideline value for radon in drinking water in Korea, it is highly recommended to reduce radon concentration of groundwater having greater than 100 Bq/L before drinking, especially in granite zone.

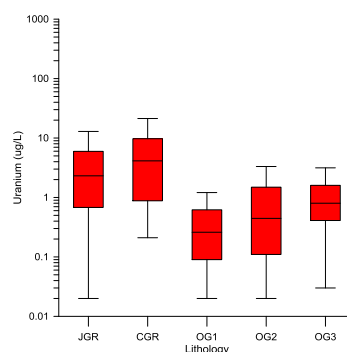


Figure 1. Uranium levels in groundwater from 5 geology.

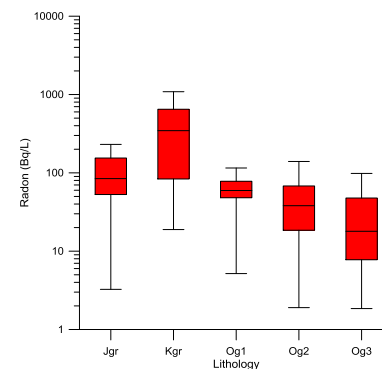


Figure 2. Radon levels in groundwater from 5 geology.

This work was supported by the National Institute of Environmental Research (NIER-SP2015-386) and Korea Institute of Geosciences and Mineral Resources (Gp2015-014-2016(2))

Shin, D. B., and Kim, S. J., 2011. Geochemical characteristics of black slate and coaly slate from the uranium deposit in Deokpyeong area, *Econo. and Environ. Geol.*, 44, 373-386.

NIER, 2015. Studies on the naturally occurring radionuclides in groundwater in the multi-geologic areas. NIER Report No. SP2015-386, 235.

WHO, 2011. Guidelines for drinking water quality. Chapter 9. Radiological aspects, 4th edition. World Health Organization, Geneva.

## CONCENTRATION FACTORS OF FISH, CRUSTACEAN, CEPHALOPOD, MOLLUSCS, MACROALGAE, AND ECHINODERM

S.W. Choi<sup>a</sup>, D.J. Kim, J.S. Chae<sup>b</sup>

<sup>a</sup> Korea Institute of Nuclear Safety Korea

<sup>b</sup> Korea Institute of Nuclear Safety Korea

\* Email: k166csw@kins.re.kr

The concentrations factor of 14 heavy metals in marine organisms at the neighbouring sea of Korea were measured and investigated, respectively. The 261 seawater samples, 261 fish samples, 16 Cephalopods and 17 Crustaceans, 7 Molluscs, 9 Macroalgae were measured the concentrations of heavy metals. The concentration factors in 314 sampling locations were analyzed in concentration of seawater and marine organisms.

The concentrations in seawater were Sr( $7,430 \mu\text{g}\cdot\text{kg}^{-1}$ ), Rb( $110 \mu\text{g}\cdot\text{kg}^{-1}$ ), Fe( $18.4 \mu\text{g}\cdot\text{kg}^{-1}$ ), and Cs( $0.167 \mu\text{g}\cdot\text{kg}^{-1}$ ), respectively. The concentrations of muscle of marine organism were Sr( $56.4 \text{mg}\cdot\text{kg}^{-1}$ ), Fe( $20.0 \text{mg}\cdot\text{kg}^{-1}$ ), Zn( $7.84 \text{mg}\cdot\text{kg}^{-1}$ ), and Mn( $1.61 \text{mg}\cdot\text{kg}^{-1}$ ), respectively.

Concentration factors in all of organism were highest in P, Mn, Ba and lowest in Na, Sr, Rb, Mo. Highest concentration factors of P(276,000), Cu(246,000), Mn(155,000), and Sr(14.6) were measured in Molluscs, respectively. The concentration factors of muscle in fishes showed strikingly high P(277,000), Mn(45,500), Fe(5,890) and Sr (3.22), respectively. The concentration factors of macroalgae showed P(237,000), Mn (88,900), Fe(38,900), and Sr(5.88). The results indicated that the concentration factors of 14 heavy metals in the Echinoderms, Molluscs were higher than that in the fish and cephalopods.

The mean concentration factors of the heavy metal were similar to the recommended value from IAEA (2004) and IAEA (2010).

## Radiological assessment of natural radioactivity level in some sediment samples along the coastal see of Limbe-Cameroon

E.J.M. Nguelem<sup>1,2\*</sup>, M.M. Ndontchueng<sup>1,3</sup>, A. Simo<sup>1</sup>, C.J.S. Guembou<sup>1,4</sup>

1. The National Radiation Protection Agency P.O.Box 33732 Yaounde-Cameroon
2. Fundamental Physics Laboratory, Mathematics, Applied Computer Sciences and Fundamental Physics, University of Douala P.O.Box: 24157 Douala, Cameroon
3. Department of Physics, University of Douala, P.O.Box 24157 Douala-Cameroon
4. Atomic and Nuclear Spectroscopy, Archeometry, University of Liege-Belgium, POBOX 4000, Liege 1 Belgium

**Abstract:** The measurement of natural radioactivity level in sediment samples from four different beaches along the coastal see of Limbe-Cameroon was performed using high-resolution gamma spectrometry based high purity germanium detector. To measure activity concentration of radionuclides with low gamma-ray energy, the self-absorption correction was conducted. The measured specific activity of primordial radionuclides of  $^{226}\text{Ra}$ ,  $^{232}\text{Th}$ ,  $^{40}\text{K}$ ,  $^{238}\text{U}$ ,  $^{210}\text{Pb}$  and  $^{235}\text{U}$  were ranged from 22.09 to 64.40, 24.22 to 81.80, 108.56 to 246.48, 17.44 to 38.81, 23.68 to 130.48 and 0.28 to 1.79Bqkg<sup>-1</sup>, respectively. To validate the results and to check the performance of the equipment, two references materials from the International Atomic Energy Agency (IAEA) were used. The observed values of the radioactivity levels were compared with some published data available worldwide. From the fact that the studied beaches are frequently visited by the population, radiological risk was assessed by calculating the radiological hazards parameters such as radium equivalent activity, gamma absorbed dose rate, annual effective dose and hazard index. The overall radiological health hazards parameters ranged from 76.45 to 198.35Bqkg<sup>-1</sup> for radium equivalent activity, from 0.21 to 0.54 for external hazard index, from 35.83 to 91.17nGyh<sup>-1</sup> for gamma absorbed dose rate, and from 43.49 to 110.67μSvyear<sup>-1</sup> for outdoor annual effective dose equivalent. Following the comparison of the observed radiological risk parameters values in sediment under investigation with the recommended safe limits of UNSCEAR, it can be concluded that no radiological risk to human can be observed in all these beaches.

**Keywords:** Gamma radiation . Sediment samples . Radiological assessment . self-absorption

## Annual cycle of <sup>7</sup>Be in soil in a micro-watershed of Mato Frio River, (Brazil)

A.D. Esquivel L.<sup>1</sup>, R.M. Moreira<sup>2</sup>, J. Juri Ayub<sup>3</sup> and D.L. Valladares<sup>3</sup>

<sup>1</sup>Universidad Tecnológica de Panamá, Ciudad de Panamá, Centro de Investigaciones Hidráulicas e Hidrotécnicas - (CIHH), Ciudad de Panamá, 0819-07289, El Dorado-Panamá, República de Panamá

<sup>2</sup>Setor de Meio Ambiente - (SEMAM), Centro de Desenvolvimento da Tecnologia Nuclear - (CDTN-CNEN), Belo Horizonte, Minas Gerais, 31270-901 Belo Horizonte, Brasil

<sup>3</sup>Grupo de Estudios Ambientales - (GEA), Instituto de Matemática Aplicada San Luis - (IMASL). Universidad Nacional de San Luis - CONICET, Ciudad de San Luis, Ejercito de los Andes 950, D5700HHW San Luis, Argentina

Keywords: Berillyum-7, atmospheric deposition, soil content, wet deposition.

alexander.esquivel@utp.ac.pa

Beryllium-7 (<sup>7</sup>Be) is a natural radionuclide formed in the atmosphere by spallation nitrogen and oxygen atoms impacted by cosmic rays atoms (Lal et al., 1958). It can be used to estimate soil erosion and/or sedimentation caused by rainfall events. Kaste et al. (2011) pointed out that, in order to evaluate the potential of <sup>7</sup>Be as a tracer in this application, it is necessary to know its seasonal and spatial depositional variability as well as quantify the relationship between precipitation and surface inventories. The aim of the present work research is to investigate the content of <sup>7</sup>Be in soil, its seasonal variation along the year and its relationship with the rainfall regime in the Mato Frio creek micro-watershed (Brazil).

### Results

A highly linear relationship between <sup>7</sup>Be deposition and the amount of rainfall, has been observed in the studied region (Fig. 1). Similar results have been found in others environments (Kaste et al., 2011; Juri Ayub et al., 2012). Thus the expected value of the <sup>7</sup>Be

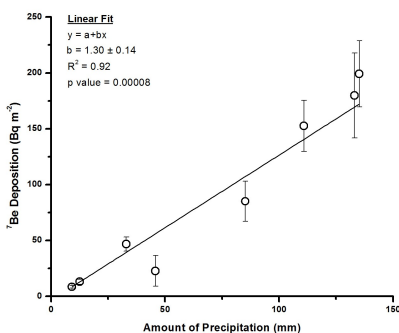


Figure 1. <sup>7</sup>Be deposition versus rainfall amount.

content in the soil due to wet deposition could be calculated from the slope ( $1.30 \pm 0.14 \text{ Bq L}^{-1}$ ) and the daily precipitation record of the 2015/2016 biennium. In the upper part of Figure 2 is shown the expected <sup>7</sup>Be soil content, whereas the bars in the lower part show the <sup>7</sup>Be atmospheric input. From October 2015 to October 2016, soil samples were sampled monthly down to a depth of 5 cm, and the <sup>7</sup>Be total content measured (Fig. 2, circles). This figure reveals that: 1) the <sup>7</sup>Be deposition exhibits oscillation cycles due to the asymmetric precipitation pattern, 2) the measured <sup>7</sup>Be content is close to the value expected from wet deposition; 3) seasonal changes in

soil <sup>7</sup>Be content could be predicted from the atmospheric deposition in rainfall episodes.

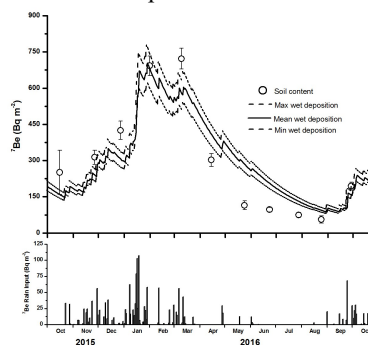


Figure 2. <sup>7</sup>Be wet deposition and <sup>7</sup>Be soil content (upper) and <sup>7</sup>Be input by rains (lower).

The <sup>7</sup>Be content in soil indicates a marked seasonal variation along the year. This could be explained by the local precipitation pattern; the region shows well marked rainy and dry seasons, with at least 80% of the precipitation occurring during the wet season. The good agreement between the measured <sup>7</sup>Be content in the soil and the expected value due to wet deposition confirms: 1) that the general assumption that wet deposition is the main mechanism by which <sup>7</sup>Be reaches the soil, 2) that the <sup>7</sup>Be content in the soil can be accurately estimated by the <sup>7</sup>Be content in the rain.

This work has been supported by the Brazilian Nuclear Energy Commission (CNEN).

Lal, D., Malhotra, P.K., Peters, B., 1958. On the production of radioisotopes in the atmosphere by cosmic radiation and their application to meteorology. *Journal of Atmospheric and Terrestrial Physic.* 12. 306 to 328.

Kaste, J.M., Elmore, A.J., Vest, K.R., Okin, G.S., 2011. Beryllium-7 in soils and vegetation along an arid precipitation gradient in Owens Valley, California. *Geophysical Research Letters.* 38.

Juri Ayub, J., Lohaiza, F., Velasco, H., Rizzotto, M., Di Gregorio, D., Huck, H., 2012. Assessment of <sup>7</sup>Be content in precipitation in precipitation in a South American semi-arid environment. *Science of the Total Environment.* 441. 111 to 116.



## Tracing the migration of radionuclides using *Betula pendula* and *Pinus sylvestris* (Lithuania)

A. Gudelis, L. Gaigalaitė, V. Abdulajev, D. Valiulis

Center for Physical Sciences and Technology (FTMC), Vilnius, LT-02300, Lithuania

Keywords: tree rings, birch sap,  $^{137}\text{Cs}$ , tritium.

Presenting author email: lina.gaigalaite@ftmc.lt

Biota samples can effectively represent an impact on the environment by both global and local radiological events. To detect low activities of radionuclides or low concentrations of stable isotopes modern analysis methods are used.

In this work, the gamma-ray spectrometry, the liquid scintillation counting (LSC) and the inductively coupled plasma mass-spectrometry (ICP-MS) were applied.

In order to determine the distribution of a fission product  $^{137}\text{Cs}$  in old tree stem the pine tree (*Pinus sylvestris*) rings samples were measured with a gamma-ray spectrometer equipped with a well-type HPGe detector of a 170 cm<sup>3</sup> crystal volume. Figure 1 shows a course of  $^{137}\text{Cs}$  massic activity (dry weight) in the rings overwhelming the time span of 94 years (one sample corresponds to a period of approx. 5 years).

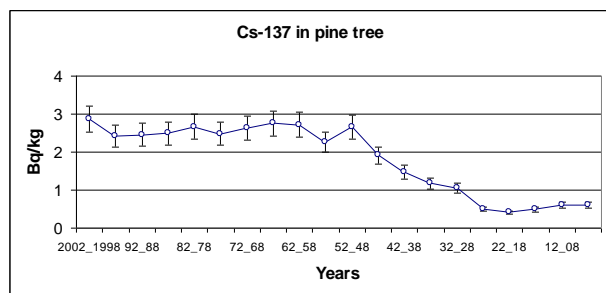


Figure 1.  $^{137}\text{Cs}$  massic activity in pine tree rings covering the period 1908-2002.

In Japan, distribution of  $^{137}\text{Cs}$  was measured in cryptomeria (*Cryptomeria japonica*) and cypress (*Chamaecyparis obtusa*) trees heartwood and sapwood. The maximum massic activity of 1.8 Bq kg<sup>-1</sup> was found in cypress tree heartwood while the mean massic activity was 3 to 4 times lower in the sapwood in both trees (Kohno et al., 1988). In Croatia, the maximum massic activity of 1.7 Bq kg<sup>-1</sup> was found in silver fir-tree (*Abies alba* L.) rings those covered the period 1925-1992 (Lovrencic et al., 2008).

Stable elements  $^{95}\text{Mo}$ ,  $^{133}\text{Cs}$  and  $^{134}\text{Ba}$  were determined with ICP-MS in other pine tree rings samples covering the period 1931-2009.  $^{95}\text{Mo}$  is a decay product of  $^{95}\text{Zr}$ - $^{95}\text{Nb}$  released to the environment after both Chinese nuclear tests in atmosphere in seventies of the last century and Chernobyl accident in 1986. The latter event was also responsible for releases of  $^{134}\text{Cs}$  that decayed to  $^{134}\text{Ba}$ .

The courses of both relative  $^{137}\text{Cs}/^{133}\text{Cs}$  concentration ratio and relative  $^{137}\text{Cs}$  deposition are shown in Figure 2.

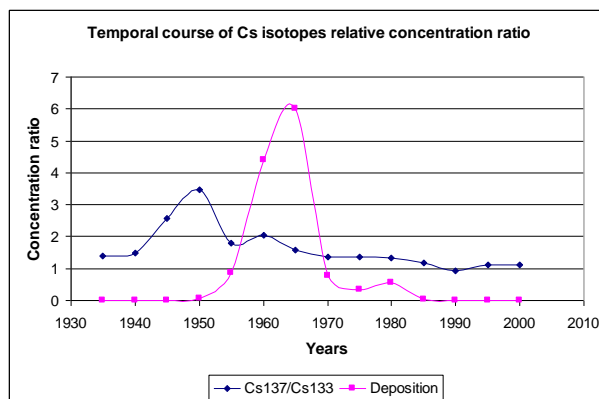


Figure 2. Relative  $^{137}\text{Cs}/^{133}\text{Cs}$  concentration ratio and relative deposition of  $^{137}\text{Cs}$ .

The LSC method was used for the determination of tritium in birch (*Betula pendula*) sap samples. The birch trees growing nearby a radioactive waste repository are suitable bioindicators for assessment of radionuclides transfer to the biota. LSC spectrum revealed presence of  $^{137}\text{Cs}$  in birch sap (Figure 3).

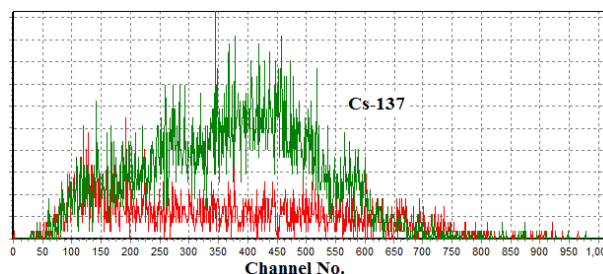


Figure 3. LSC spectrum (green) of birch sap sample demonstrating presence of  $^{137}\text{Cs}$ .

The original birch sap sample was re-measured with a well-type HPGe detector, the determined massic activity of  $^{137}\text{Cs}$  was  $(5.0 \pm 0.4)$  Bq kg<sup>-1</sup> ( $k = 1$ ). This result could be a consequence of the long-term radionuclides accumulation in Lithuanian forest ecosystem.

Kohno, M., Koizumi, Y., Okumura, K., Mito, I., 1988.

Distribution of environmental  $^{137}\text{Cs}$  in tree rings. J. Environ. Radioact. 8, 15-19.

Lovrencic, I., Volner, M., Barisic, D., Popijac, M., Kezic, N., Seletkovic, I., Lulic, S., 2008. Distribution of  $^{137}\text{Cs}$ ,  $^{40}\text{K}$  and  $^7\text{Be}$  in silver fir-tree (*Abies alba* L.) from Gorski Kotar, Croatia. J. Radioanal. Nucl. Chem. 275, 71-79.

## Temporal variations of <sup>210</sup>Pb in groundwater near radioactive waste repository

I. Gorina, A. Gudelis

Ionizing Radiation Metrology Laboratory, Department of Metrology,  
Center for Physical Sciences and Technology (FTMC), Vilnius, LT-02300, Lithuania  
Keywords: radioactive waste repository, groundwater, <sup>210</sup>Pb, gamma-ray spectrometry.  
Presenting author email: inga.gorina@ftmc.lt

A near-surface “Radon” type radioactive waste repository had been operating in 1963-1989, then it was closed and later, after 17 years of the closure, reconstructed in 2006 (Nedveckaitė et al. 2013). The initial inventory of radionuclides was assessed in (LEI, 2004).

The inventory reaching 1 GBq was as follows (decay-corrected to February 2016, in Bq): <sup>3</sup>H 5.49E+13, <sup>137</sup>Cs 2.99E+13, <sup>239</sup>Pu 9.14E+11, <sup>90</sup>Sr 3.37E+11, <sup>60</sup>Co 2.07E+11, <sup>14</sup>C 1.76E+11, <sup>226</sup>Ra 1.10E+11, <sup>63</sup>Ni 3.42E+10, <sup>204</sup>Tl 4.84E+10, <sup>152</sup>Eu 1.34E+10, <sup>36</sup>Cl 1.20E+09.

There were ten monitoring wells installed in the territory of the repository at different distances and directions from the vault. At the beginning of a research a significant leakage of tritium was confirmed. Since January 2005, groundwater samples for the determination of tritium were taken on the monthly basis.

Later on, monitoring results in groundwater near the storage facility revealed that <sup>210</sup>Pb activity concentration values were considerably higher than they could be expected in groundwater and exceeded the permissible norms (EURATOM, 2001). A new monitoring programme started with special emphasis to higher volume monthly samples from groundwater wells no.41 and no.42 in order to determine time-dependent activity concentrations of <sup>210</sup>Pb. These two wells are located in 0.5 m distance from the vault.

<sup>210</sup>Pb is the decay product of <sup>238</sup>U series with a half-life of 22.23 years (DDEP, 2013). This radionuclide may disperse as a decay product of <sup>222</sup>Rn, which comes from the vault, in turn, as a decay product of <sup>226</sup>Ra.

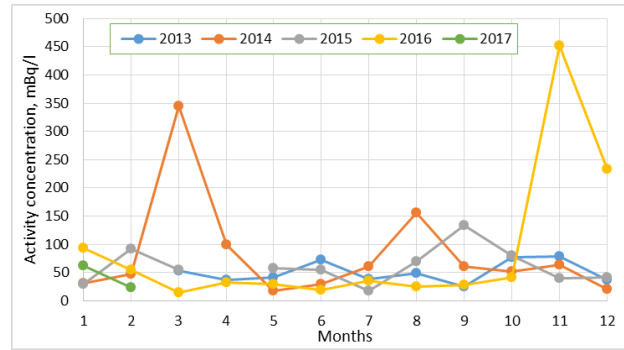


Figure 2. Variation of <sup>210</sup>Pb activity concentration in groundwater well no.42 in 2013-2017.

Groundwater samples were evaporated and residues measured with a gamma-ray spectrometer with a well-type HPGe crystal detector. The maximum values of 447 mBq/l and 452 mBq/l in the wells no.41 and no.42, respectively, were determined in November 2016 (Figure 1, Figure 2). They are about 3.5 times higher than the average value.

Variations of <sup>210</sup>Pb activity concentration in groundwater demonstrate rather episodic character of sharp increases.

Nedveckaitė, T., Gudelis, A., Vives i Batlle, J., 2013.

Impact assessment of ionizing radiation on human and non-human biota from the vicinity of a near-surface radioactive waste repository. Radiat. Environ. Biophys 52, 2, 221-234.

LEI, 2004. Radionuclide inventory at Maisiagala repository. Lithuanian Energy Institute Report No. S/14-625.4.6-G-V:01.

European Commission Recommendation 2001/928/EURATOM. Official Journal of European Communities L., 344, 28.12.2001.

DDEP, 2013. Decay Data Evaluation Project.

<[http://www.nucleide.org/DDEP\\_WG/DDEPdata.htm](http://www.nucleide.org/DDEP_WG/DDEPdata.htm)>.

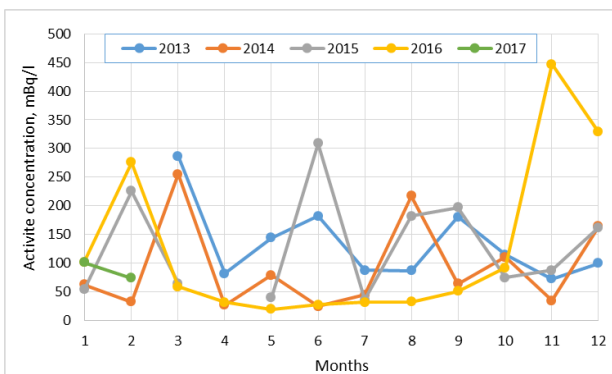


Figure 1. Variation of <sup>210</sup>Pb activity concentration in groundwater well no.41 in 2013-2017.

## <sup>210</sup>Pb geochronology for the assessment of historical pollutants in the touristic area of Snagov Lake, Romania

A.R. Iurian<sup>1</sup>, R.C. Begy<sup>1</sup>, K. Szabolcs<sup>1</sup>, H. Simon<sup>1</sup>, I.M. Martonos<sup>1</sup>, D. Ciobotaru<sup>1,2</sup>, I. Dumitrascu<sup>2</sup>, R.M. Margineanu<sup>3</sup>

<sup>1</sup>Faculty of Environmental Science and Engineering, Babeş-Bolyai University, Cluj-Napoca, Cluj, 400294, Romania

<sup>2</sup>Environmental Health Centre, Cluj-Napoca, Cluj, 400240, Romania

<sup>3</sup>Horia Hulubei National Institute for R&D in Physics and Nuclear Engineering, Bucharest-Magurele, MG-6, Romania

Keywords: <sup>210</sup>Pb dating, sediment, metals, hydrocarbons.

Presenting author email: iurian.andra@ubbcluj.ro

Since 1963 (Goldberg, 1963), the fallout component of <sup>210</sup>Pb (namely <sup>210</sup>Pb in excess) has been widely used as environmental tracer for sediments or ice core dating, for understanding recent contamination processes in a range of sedimentary environments, including lakes, reservoirs, floodplains, estuaries and coastal marine environments. Lacustrine sedimentary archives are known to preserve a record of pollution impacts potentially over centuries, reflecting temporal changes of the contamination sources and of variations in the transport path regimes.

Heavy metals and hydrocarbons historical content were investigated in undisturbed sediment columns from Snagov Lake, an area of special ecological national interest from Ialomitei River Basin, SE Romania. The temporal context for the study was provided by <sup>210</sup>Pb geochronology with Chernobyl-derived <sup>137</sup>Cs as independent chronological marker. Two core sections at 1 cm intervals were analysed by gamma-ray spectrometry for <sup>226</sup>Ra and <sup>137</sup>Cs, while the <sup>210</sup>Pb was derived by alpha-ray spectrometry, through the measurement of its daughter <sup>210</sup>Po assuming secular equilibrium conditions. In terms of sediment quality with respect to anthropogenic contamination, core sections were analysed using (i) the atomic absorption spectrometry (AAS) for heavy metal determination (e.g. Pb, Cd, Zn, etc), and additionally, (ii) gas-chromatography (GC) combined with mass spectrometry (MS) techniques for the evaluation of polycyclic aromatic hydrocarbons (PAHs) and total hydrocarbons concentrations. Sediment grain size distribution and organic content (by LOI method) were employed for the identification of historical storminess events or to detect discontinuities in the sediment record. The major contribution to the total PAHs ( $\Sigma 16\text{PAH}$ ) content was attributed to the high molecular weight PAH. The highest value (4.604 ng/g, dry weight) for the  $\Sigma 16\text{PAH}$  was detected in surface sediment layers. Source apportionment was evaluated through the ratios of specific PAH compounds suggesting petroleum combustion to be the primary source of PAH in the sediments (see Figure 1). Depth distribution of metal content is also given for selected species (see Figure 2). Pb, Zn and Cd present similar depth characteristics, having increasing values towards surface layers and relative constant below 15 cm depth. A possible explanation is the increase of touristic activities in the area in the last decades, accompanied by an increase in the population number with about 20% in the last 15 yr.

Historical pollutant information is crucial in decision-making for an efficient management of the region since Snagov area presents an increased touristic interest due to its close proximity to the Bucharest capital city.

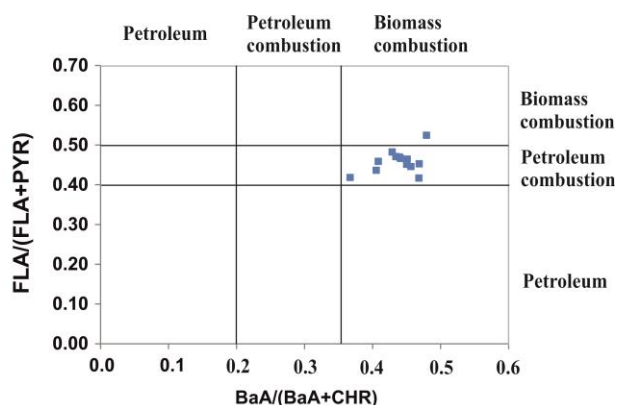


Figure 1. Evaluation of possible PAHs sources in sediments (fluoranthene=FLA, pyrene=PYR, benz[a]anthracene=BaA, chrysene=CHR)

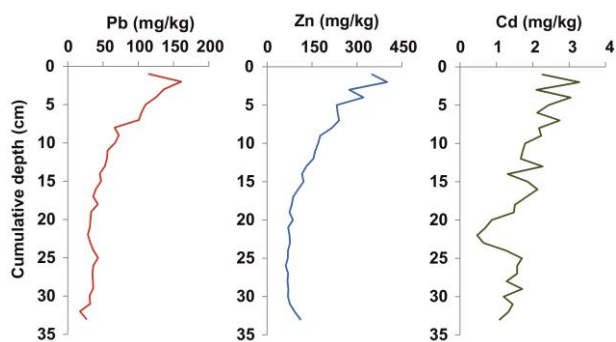


Figure 2. Depth distribution of Pb, Zn and Cd in a sediment column from Snagov Lake

This work was supported by a grant of the Romanian National Authority for Scientific Research and Innovation, CNCS – UEFISCDI, project number PN-II-RU-TE-2014-4-1772.001.

Goldberg ED, 1963. Geochronology with <sup>210</sup>Pb. In Radioactive Dating. Proceedings of a Symposium. IAEA, Vienna, pp. 21-131.

## The distribution of tritium in the aquatic environments, Lithuania

O. Jefanova<sup>1</sup>, J. Mažeika<sup>1</sup>, R. Petrošius<sup>1</sup> and Ž. Skuratovič<sup>1</sup>

State Research Institute Nature Research Centre, Vilnius, Akademijos St. 2, LT-08412, Lithuania

Keywords: Ignalina NPP, tritium, surface water, groundwater.

Presenting author email: skuratovic@geo.lt

Tritium (<sup>3</sup>H) is mobile radionuclide of hydrogen, which is important in investigating water flow processes (Cartwright and Morgenstern, 2016), (Gusyev et al., 2016). The properties of tritium gives opportunity to use it for various applications. Tritium continues to be a valuable tracer in a post nuclear bomb pulse world (Patrick A. Harms et al., 2016), also is useful tracer for dating young waters.

Tritium is the radioactive component of liquid releases and gaseous discharges of nuclear power plants. The radioactivity monitoring around the NPPs involves measuring tritium activity to see the dynamics in aquatic environment of NPP (Momoshima et al., 1987), (Jean-Baptiste et al., 2007).

In Lithuania tritium concentration studies were carried out in groundwater, surface water bodies – in rivers and lakes, the Baltic Sea, Curonian Lagoon, continuous measurements of precipitation have been carried out, as well (Fig. 1).

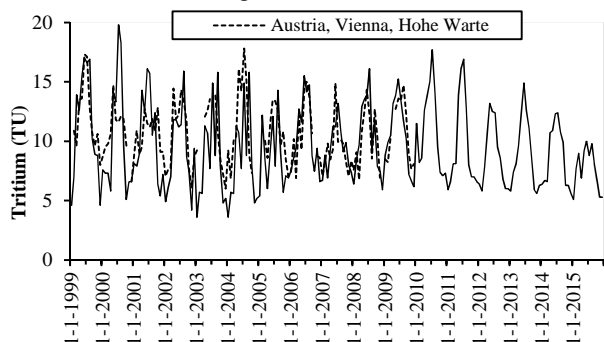


Figure 1. <sup>3</sup>H concentration in monthly precipitation of eastern Lithuania compared with GNIP station (<http://www.iaea.org/water>) in 1999–2015

<sup>3</sup>H monitoring of the water bodies in the Ignalina NPP (INPP) environment, with the occurring breaks, begun before the construction of INPP.

The aim of the study is to evaluate the significance of tritium release in the environment during INPP operation in comparison with a background of natural formation of <sup>3</sup>H in the atmosphere, and its global distribution in consequence of the nuclear weapon testing in the atmosphere.

The resulting time series of <sup>3</sup>H data were used for the assessment of scales of <sup>3</sup>H release into the environment during the INPP operation in context of natural <sup>3</sup>H production in the atmosphere, as well as of its global distribution after nuclear weapons tests in the atmosphere. <sup>3</sup>H traces of INPP origin were found only in close proximity to INPP (Fig 2.).

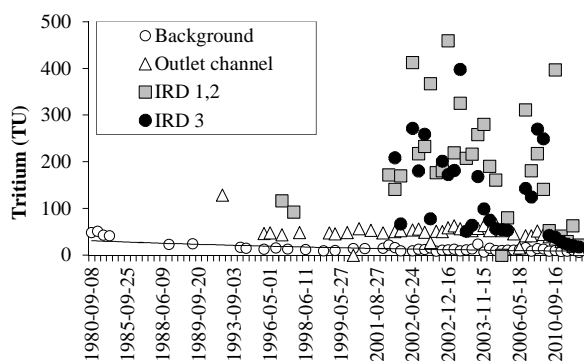


Figure 2. <sup>3</sup>H activity concentration in the channels related to the industrial site of INPP in 1980–2012

- Cartwright I., Morgenstern U., 2016. Using tritium to document the mean transit time and sources of water contributing to a chain-of-ponds river system: Implications for resource protection, *Applied Geochemistry*. Volume 75. 9-19.
- Gusyev, M. A., Morgenstern, U., Stewart, M. K., Yamazaki, Y., Kashiwaya, K., Nishihara, T., Kuribayashi, D., Sawano, H., and Iwami, Y., 2016. Application of tritium in precipitation and baseflow in Japan: a case study of groundwater transit times and storage in Hokkaido watersheds. *Hydrol. Earth Syst. Sci.*, 20, 3043-3058.
- Jean-Baptiste P., Baumier D., Fourré E., Dapoigny A., Clavel B., 2007. The distribution of tritium in the terrestrial and aquatic environments of the Creys-Malville nuclear power plant (2002–2005), *Journal of Environmental Radioactivity*. Volume 94. Issue 2. 107-118.
- Momoshima N., Okai T., Inoue M., Y. Takashima Y., Tritium monitoring around a nuclear power station in normal operation, *International Journal of Radiation Applications and Instrumentation. Part A. Applied Radiation and Isotopes*, Volume 38, Issue 4, 1987, Pages 263-267.
- Patrick A. Harms, Ate Visser, Jean E. Moran, Brad K. Esser, 2016. Distribution of tritium in precipitation and surface water in California. *Journal of Hydrology*. Volume 534.63-72.



### Distribution of <sup>241</sup>Am and <sup>137</sup>Cs in forest soil at «plumes» of radioactive fallout

I.N. Kamenova, N.V. Larionova, A.O. Aidarkhanov, S.N. Lukashenko

Branch «Institute of Radiation Safety and Ecology» of the RSE «NNC RK », Kurchatov, Kazakhstan».

Keywords: forest ecosystems, soil, radionuclides, forest litter.

email: sobina@nnc.kz

The tests carried out at the territory of Semipalatinsk Test Site (STS) have caused contamination of not only the test site territory but also the lands beyond. So after the first ground nuclear test carried out by 29 August 1949 under adverse conditions, strong winds led to the rapid movement of the radioactive cloud in an easterly direction. This fact has led to the formation of «plumes» of radioactive fallout (Logatchev, V.A., 1997). One of the territories suffered from radioactive fallouts is the pine forest of Priirtyshie. The zone of the pine forest growth extends to the northeast from the STS.

To study the surface of distribution of radionuclides in 10 points was produced conjugate selection of mixed soil samples (0-5 cm) and litter (3-10 cm). The forest litter was divided into organic and mineral components, by drying and sieving via 2 mm sieve. The forest litter was sampled based the techniques used for studying it in the zone suffered from contamination resulted from the Chernobyl accident (Goldfinches, A.I., 2000). To assess the vertical migration of radionuclides three soil profiles were laid. Soil samples were collected at depth intervals of 5 cm, to a depth of 50 cm. Determination <sup>241</sup>Am and <sup>137</sup>Cs performed by gamma spectrometry. The detection limit for <sup>241</sup>Am and <sup>137</sup>Cs was 0.5 Bq/kg. The error in <sup>137</sup>Cs and <sup>241</sup>Am measurement did not exceed 10-20%.

As the result of researches conducted, it was found that <sup>241</sup>Am specific activity in organic and mineral components of the litter vary from <0.7 to 3.5±0.7 Bq/kg and from 0.6±0,3 to 330±70 Bq/kg respectively, while for soil this value ranges within <1 to 5.1±1.1 Bq/kg. Specific activity of <sup>137</sup>Cs in organic and mineral components of the litter vary from 7±1.4 to 350±70 Bq/kg and 18±4 to 350±70 Bq/kg respectively, while for soil this value ranges within 21±4 to 130±10 Bq/kg. Figure 1 shows distribution of radionuclides in surface soil layer (5cm) and the litter (3-10 cm).

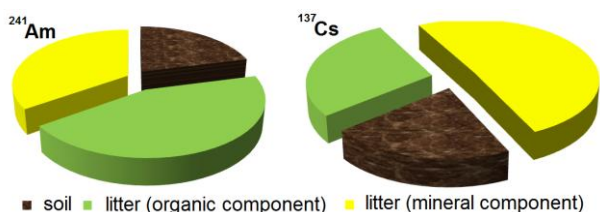


Figure 1. Distribution of <sup>241</sup>Am and <sup>137</sup>Cs radionuclides in surface soil layer and the litter

The maximum concentration of radionuclides <sup>241</sup>Am (≈ 45%) belongs to the organic components of the litter, <sup>137</sup>Cs (≈ 50%) – to the mineral component of the

litter. This fact can speak of difference in migration abilities and bioavailability of these radionuclides.

The distribution of radionuclides in the vertical profile of forest soil is uneven. The specific activity of the radionuclide <sup>137</sup>Cs installed only in the upper soil layer, below the profile is below the detection limits of the equipment used. Specific activity of <sup>241</sup>Am varies from <0.5 to 64±13 Bq/kg. Distribution of <sup>241</sup>Am radionuclide is graphically described at the figure 2.

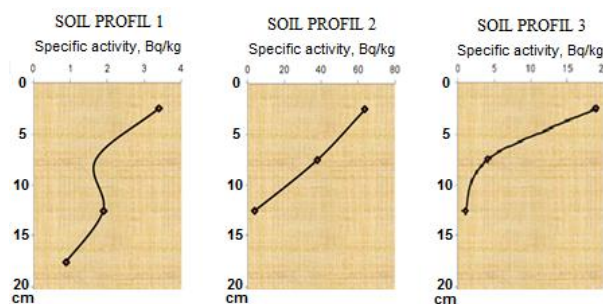


Figure 2. Distribution of <sup>241</sup>Am in the vertical soil profile

The maximum values specific activity of <sup>241</sup>Am are in the top 5-cm layer of soil. Below along vertical profile of forest soil the concentration of this radionuclide is reduced. In the 20-cm layer and below values specific activity of <sup>241</sup>Am are below the detection limits of the equipment used. Thus, The main storage element of the soil profile of forest ecosystems is a litter.

This work was supported by the Government of the Republic of Kazakhstan RBP-036.

The authors are thankful to the staff of the Department for Comprehensive Ecosystems Studies of the IRSN (Kurchatov, Kazakhstan) for their help in radiological environmental studies.

Logatchev, V.A., 1997. USSR Nuclear Tests. Semipalatinsk test site: to provide general and radiation safety of nuclear tests. / M.: Second typography FU "Medbioextrem" at Russian Ministry of Health, 1997.

Goldfinches, A.I., 2000. Biochemistry artificial radionuclides in forest ecosystems: - M: Science, - 269.



## Transfer parameters of $^{137}\text{Cs}$ and $^{241}\text{Am}$ into the tissues of sheep with soils in dependence to radioactive contamination form

B.A. Kenessarın, Zh.A. Baıgazinov, S.N. Lukashenko

Institute of Radiation Safety and Ecology NNC RK, Kurchatov (071100), Kazakhstan

Keywords: radioactive contamination, transfer parameters, sheep

E-mail: Kenessarın@nnc.kz

As a result of different nuclear tests (underground, aboveground, airdrop) on the Semipalatinsk nuclear test site (STNS) the local and spotted places with different levels of radioactive contamination were formed (Lukashenko, 2010). Earlier studies on the STNS have shown that the parameters of radionuclides in the organism of farm animals higher in the soil, than with forage (Baıgazinov, 2016).

Experimental studies with animals were conducted during the summer period in the conditions of stall contents in the territory the STNS. The most widespread species of farm animals for this region is Kazakh coarse wool breed sheep, at the age of about 1 year, with a live weight of 27-30 kg was chosen as an object of the research.

Animals were divided into 4 groups with 3 sheep on each group. The daily diet of sheep included 100 g per day dried, screened to 500 microns radioactive polluted soil sampled from the STNS. First group of animals feeds the soil from the location of aboveground nuclear tests (site No. 1), the 2nd group – from places of experimental-industrial underground nuclear test (site No. 2), the 3rd group – the soil from zones of radioactive water currents (underground nuclear tests), the 4th group – from the site of combat radioactive elements operation site. Duration of the experiment was 50 days and after the animals slaughtered. Daily intake of radionuclides shown in Table 1.

Table 1. Total daily intake with soil

Location #	total daily intake,	
	Bq/day	
	$^{137}\text{Cs}$	$^{241}\text{Am}$
1	12000±600	5000±250
2	2700±140	250±13
3	2000±100	100±5
4	87±5	130±7

As a result of the conducted research the transfer factors of radionuclides to the tissues of sheep are defined. Dependence of transfer rate to the character of radioactive contamination is also determined (Table 2).

In most cases, the concentration activity of  $^{241}\text{Am}$  in tissues, was below of the detection limit of used apparatus- methodological support, in connection with which, for most organs and tissues calculated estimated transfer coefficients.

It was determined that in locations 1, 2 and 3, the transition coefficients are almost identical.

However, very unexpected results was obtained for Loc. №4.  $^{137}\text{Cs}$  level transition in the location №4 in to

Table 2. Transfer parameters  $^{137}\text{Cs}$ ,  $^{241}\text{Am}$  to the body and tissue

Location #	Transfer factor to the different tissue of sheep, kg/day			
	$^{137}\text{Cs}$ , $n \times 10^{-2}$		$^{241}\text{Am}$ , $n \times 10^{-3}$	
	Muscle tissue	liver	Muscle tissue	liver
1	<u>1.1</u> 1.3-1.0	<u>0.65</u> 0.83-0.53	<u>&lt;0.02</u>	<u>0.11</u> 0.11 - 0.1
2	<u>1.6</u> 2.4-1.1	<u>1.1</u> 1.2-1.0	<u>&lt;0.4</u>	<u>&lt;1</u>
3	<u>1.3</u> 1.6-0.75	<u>0.75</u> 0.84-0.41	<u>&lt;1</u>	<u>&lt;2</u>
4	<u>42.2</u> 140.0-11.0	<u>16.1</u> 28.7-5.3	<u>&lt;0.7</u>	<u>&lt;2</u>

Note: The numerator - geometric mean, in the denominator - Max-min.

mutton was in  $32 \pm 7$  times more than in other areas. At the same time of the earlier work it is known that the coefficient of  $^{137}\text{Cs}$  transition in mutton, in the "food-mutton" system amounts to  $(12,3 \pm 3,0) \times 10^{-2}$  (Baıgazinov, 2016), which is 3.5 times lower than the coefficient transition in the system "soil (loc.4) - mutton".

In the present case, the formed assertion that forage is the main source of incomes and a major contributor to contamination of animal products, and in our situation does not find its confirmation.

This fact shows that it is necessary to revise approaches to the assessment of ways of forming contamination of animal products.

This work was supported by the Government of the Republic of Kazakhstan RBP – 036.

The authors are thankful to the staff of the IRSE (Kurchatov, Kazakhstan) for their help in radioecological environmental studies.

Lukashenko, S.N. et al. 2010. Topical Issues in Radioecology of Kazakhstan. Issue 2. Dom Pechati, Pavlodar (in Russian).

Baıgazinov, Zh.A., Parameters for the transfer of  $^{239+240}\text{Pu}$ ,  $^{241}\text{Am}$ ,  $^{137}\text{Cs}$ ,  $^{90}\text{Sr}$ , and  $^3\text{H}$  to farm animals under the conditions of the STNS: dissertation abstract of candidate of biological sciences (radiobiology), Obninsk, 2016 (in Russian).

## Technique to identify ground zeros of nuclear events of the Semipalatinsk test site

P.Ye. Krivitsky, S.N. Lukashenko, M.A Umarov.

Branch “Institute of Radiation Safety and Ecology”  
RSE NNC RK, Kurchatov, Kazakhstan

Keywords: Semipalatinsk test site, Experimental Field, neutron activation products, ground zeros of nuclear events.  
Presenting author email: Krivitskiy@nnc.kz

In the territory of the “Experimental Field” ground (EF) of the Semipalatinsk test site (STS) there are a great number of ground zeros of nuclear events that took place during the period of 1949 to 1962. (Lukashenko et al., 2010; Lukashenko et al., 2011; Lukashenko et al., 2013). Ground zeros can be divided into three kinds: ground zero with a crater, remediated ground zero and the one with no technogenic disturbances.

In case there is a crater, a ground zero is quite easy to identify, however, in case of no technogenic disturbances, it is impossible to spot it visually. A detailed analysis of <sup>137</sup>Cs and <sup>241</sup>Am has also shown that due to these meteorologically transported products, this forms a displacement of real ground zero, and in some cases, a ground zero cannot be detected at all which does not enable to identify it for these radionuclides. In this context, neutron activation products are assumed to be the most effective to reveal ground zeros of nuclear events, in particular, <sup>152</sup>Eu.

Based on this a goal was set to develop a technique of how to determine ground zeros of nuclear explosions for neutron activation products (<sup>152</sup>Eu, <sup>60</sup>Co, <sup>3</sup>H) Activation products unlike <sup>137</sup>Cs and <sup>241</sup>Am form a distinct contamination contour, and only fine particles are exposed to transfer (<0.1 mm). <sup>152</sup>Eu, <sup>60</sup>Co, <sup>3</sup>H were selected as the most-long-lived radionuclides.

For the technique to be processed, surface soil samples were collected at different distances from the supposed ground zero of a nuclear event. Fractional and mineralogical sample analysis was carried out; extra deep-earth soil sampling was made.

Based on the fractional analysis it is found that <sup>152</sup>Eu concentration in all fractions is approximately the same (Figure 1, 2) which enables usability of a coarse fraction. A coarse fraction is least exposed to transfer which allows minimization of uncertainty for ground zero determination.

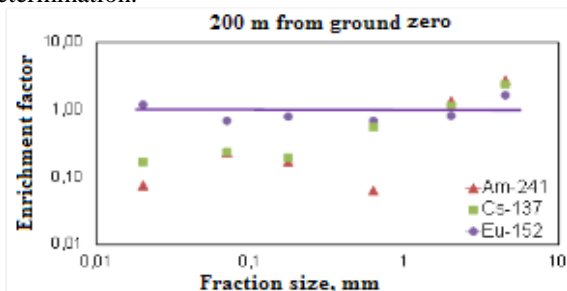


Figure 1 Dependency of <sup>152</sup>Eu enrichment factor on fraction size at a distance of 200 m

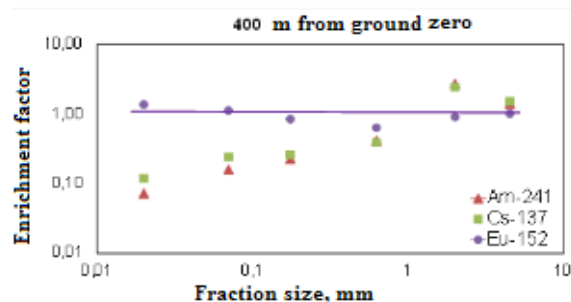


Figure 2 Dependency of <sup>152</sup>Eu enrichment factor on fraction size at a distance of 400 m

Based on the mineralogical analysis, a mineral of maximum concentration was found –sand stone (<sup>152</sup>Eu concentration is 1 500 Bq/kg, <sup>3</sup>H – 12 000 Bq/kg). Based on deep-earth sampling results it was determined that <sup>152</sup>Eu and <sup>3</sup>H are across the depth which allows sampling at depth rather than on the surface.

Thus, identification of nuclear venues is expedient based on the data on radionuclides formed owing to neutron activation (<sup>152</sup>Eu, <sup>60</sup>Co, <sup>3</sup>H). Sampling should be made at a depth of 5-10 cm rather than on the surface, as the surface layer is subjected to contamination due to radionuclides fallout after the explosion. For research one should use a coarse fraction because it is less subjected to transfer. One should also consider a particular mineral because concentrations of activation products in various minerals vary greatly. A P-3 spot was explored and identified using these principles.

This work was supported by the Government of the Republic of Kazakhstan RBP-036.

- Lukashenko, S.N., et al. 2010. Topical Issues of Radiation Ecology in Kazakhstan. Issue 1. “Dom Pechati”, Pavlodar, (in Russian).
- Lukashenko, S.N., et al. 2011. Topical Issues of Radiation Ecology in Kazakhstan. Issue 3. “Dom Pechati”, Pavlodar, (in Russian).
- Lukashenko, S.N., et al. 2013. Topical Issues of Radiation Ecology in Kazakhstan. Issue 4. “Dom Pechati”, Pavlodar, (in Russian).

## Radionuclides as tracers for assessing the radiocapacity and reliability of ecosystems

Yu.A. Kutlakhmedov

Institute of Cell Biology and Genetic Engineering of NASU. Kiev

Keywords: tracers, reliability, ecosystems, radiocapacity.

Presenting author email: ecoetic@yandex.ru

Our experimental studies were carried out in aquatic plant culture, using  $^{137}\text{Cs}$  as a tracer, through the behavior of which it is possible to evaluate the effect on ecosystems of various factors of biotic and abiotic origin (gamma radiation and heavy metals- Cd, Pb, Zn). Studies of the behavior and redistribution of the tracer  $^{137}\text{Cs}$  of Chernobyl origin were also carried out in field expedition studies on a slope near the river, already in the 30-km zone of the Chernobyl NPP, and in Volyn district and Belarus. We used boxes models for selected ecosystems. The theory and models of the radiocapacity and reliability of complex systems are widely used in the work (Kutlakhmedov, 2013). At the ecosystem level, this parameter is the magnitude of the radiocapacity factor, determined using chamber models (Kutlakhmedov, 2015). As a result, using such parameters, we obtained the possibility of using mathematical models of reliability and radio capacity at different levels of integration of biosystems (Kutlakhmedov, 2015). The radiocapacity and reliability of the ecosystem is considered by us as the reliability of the tracer radionuclide transport system ( $^{137}\text{Cs}$ ) for ecosystem components from environment to people, in accordance with the theory of reliability of complex systems (Kutlakhmedov, 2015). In terms of chamber models, the reliability of radionuclide transport can be estimated through the radionuclide migration rates for ecosystem components and is calculated by the formula for  $F_j$  (the reliability of the element for retaining radionuclides in this component of the ecosystem:  $F_j = \Sigma a_{ij} / (\Sigma a_{ij} + \Sigma a_{ji})$ ). Where  $\Sigma a_{ij}$  is the sum of the radionuclide-pollutant transfer rates from the different components of the ecosystem to the specific J-element of the ecosystem and/or landscape, according to boxes models, and  $\Sigma a_{ji}$  is the sum of the rates of outflow of pollutants from the investigated box-J to other components of the ecosystem, conjugate with them. In terms of this approach at the ecosystem level, reliability can be determined through the parameters of the radiocapacity, that is, the accumulation of the radionuclide  $^{137}\text{Cs}$ , as an analog of the vital macro -K. High radioactivity - the reliability of the biotic component of the ecosystem to retain and accumulate tracer in it,

indicates the well-being and viability of the biotic component of the ecosystem under consideration. The peculiarity of this approach is that the more reliable the biota of an ecosystem holds radionuclides of a tracer, the less radionuclides it gets to a person, which means that it is safer to have it in the regime of nature management in this ecosystem (that is, with minimal dose loads). For ecosystems of real landscapes, we developed a variant of analytical GIS technology (Kutlakhmedov, 2013). The source materials for the mathematical model and GIS analysis we applied are cartographic materials, field research and remote sensing data, statistical materials on the natural and anthropogenic characteristics of the study area, As well as any other materials that are spatially referenced and can be translated into a computer format for use within this model. This method allows you to receive maps of distribution and redistribution tracer in a real landscape in Koncha Zaspas (near Kiev). The conducted cycle of studies on the model ecosystem (aquatic plant culture) showed that the radiocapacity factor of the biota relative to the tracer ( $^{137}\text{Cs}$ ) introduced specifically into the aquatic plant culture is a very sensitive indicator. The higher the radiocapacity factor of the biota of the model ecosystem, the better the tracer in biota is retained and the greater the degree of biota welfare. We extended this approach to real ecosystems - the lakes, the cascade of the Dnieper reservoirs. It is shown that, in fact, changes in the radioactivity parameters can serve as an adequate indicator of the distribution and redistribution of radionuclides in the ecosystem and a measure of the welfare of the biota in it.

Kutlakhmedov Yu.A. Reliability of ecological systems / Rodina VV, Matveeva IV / Monograph, 2013, Palamarium Academic Publishing. Saarbruckem. Russian.

Kutlakhmedov Yu.A. The road to theoretical radioecology. Monograph. 360 s. Kiev-2015, Phytosociocentre. Russian

## Artificial radionuclides in the vegetation cover at areas adjacent to Semipalatinsk test site

N.V. Larionova<sup>1</sup>, V.V. Polevik<sup>2</sup>, Yu.S. Shevchenko<sup>1</sup>, I.N. Kamenova<sup>1</sup>, A.O. Aidarhanov<sup>1</sup>, S.N. Lukashenko<sup>1</sup>

<sup>1</sup> Institute of Radiation Safety and Ecology NNC RK, Kurchatov city, Kazakhstan

<sup>2</sup> Shakarim State University in Semey city, Semey city, Kazakhstan

Keywords: Semipalatinsk Test Site (STS), artificial radionuclides, plants, transfer factors (Tf)

email: Larionova@nnc.kz

Extensive territories, adjacent to Semipalatinsk Test Site (STS) and those subjected to radioactive contamination as the result of passing radioactive fallout "plumes". Vegetation cover here is mostly presented by steppe ecosystems as well as a pine forest in the Near-Yrtysh area.

The areal vegetation study was performed using specific methods of geo-botanical description, including determination of the main vegetation types, as well as the estimation of projective cover and species composition of plants. To assess accumulation of artificial radionuclides in herbaceous plants the sites located in assumed hayfields and pasturelands, as well as forest massifs of territory of interest were chosen. In total 20 research sites, uniformly distributed over the entire territory were arranged (Figure 1).

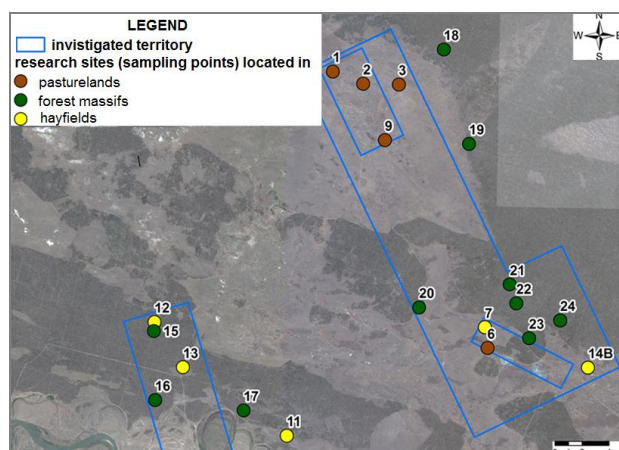


Figure 1. Schematic arrangement of research sites

At each the research site were collected samples plants (from the area of ~2 sq. m) represented by mixed samples of steppe (or meadow herbs). Together with plants was sampled soil using "envelope" method (2×1 m) at the depth of 5 cm. Specific activity of radionuclides <sup>137</sup>Cs and <sup>241</sup>Am was measured by gamma spectrometry, for <sup>90</sup>Sr and <sup>239+240</sup>Pu method of radiochemical extraction with further beta and alpha spectrometry was used. Specific activity of <sup>241</sup>Am and <sup>137</sup>Cs in plants was determined in carbonized, preliminarily milled samples, <sup>90</sup>Sr and <sup>239+240</sup>Pu – were determined in ash followed by converting into dry matter.

It was found that vegetation cover is characterized by several vegetation associations: wormwood-herbal pinery, fescue-herbal pinery, woodreed-herbal pinery, wormwood-feather grass

pinery. Dominating plants here is Culundian pine (*Pinus culundensis*), a subspecies of Common pine (*Pinus sylvestris*). Grass cover of each association is formed depending on ecological growth conditions of, and is mainly represented by cereals (*Stipa capillata*, *Festuca valesiaca*) with herbs (*Artemisia austriaca*, *Gypsophylla paniculata*, *Linaria vulgaris*, *Helichrysum arenarium*, *Chenopodium urbicum*). The territories between massifs of the pine forest are also occupied by cereals (*Festuca valesiaca*, *Stipa capillata*) and herbal-cereal (*Artemisia austriaca*, *Stipa sareptana*, *Festuca valesiaca*). In these communities, bushes *Caragana pumila* and *Spiraea hypericifolia* can also be found.

Specific activity of <sup>241</sup>Am and <sup>137</sup>Cs in soils vary from <1 to 5.1±1.1 Bq/kg and 5.4±1.1 to 120±20 Bq/kg respectively, in plant samples – proved to be below the detection limit for instrumentation used. Specific activity of <sup>90</sup>Sr in soils is 1.7±0.5 to 30±4 Bq/kg, <sup>239+240</sup>Pu – is characterized by a wide scatter in values (from <0.2 to 270±20 Bq/kg).

For quantitative assessment of <sup>90</sup>Sr and <sup>239+240</sup>Pu accumulation in herbaceous plants, transfer factors (Tf) have been calculated. So, <sup>90</sup>Sr Tf for plants of proved to be sufficiently high (1.7-1.8) and comparable with Tf of this radionuclide for zones of radioactive streamflows at "Degelen" site (1.7). Tf for <sup>239+240</sup>Pu, vice versa, proved to be lower on the whole (0.00036-0.0085) than minimum values for herbaceous plants at epicenters of the aboveground nuclear testing (0.0014) in the STS territory (Larionova, 2013).

In general specific activity of radionuclides <sup>90</sup>Sr and <sup>137</sup>Cs in vegetation collected at assumed hayfields and pasturelands, as well as forest massifs of the researched territory, are below the maximum permissible levels of radioactive contamination of forage plants (111 Bq/kg and 74 Bq/kg respectively), established by the Ministry of Agriculture of the Republic of Kazakhstan (1994). Specific activity of <sup>241</sup>Am and <sup>239+240</sup>Pu in plants is not rated, however, based on the general level of radiotoxicity of each, one can assume, That permissible level for them will be approximately an order of magnitude lower than for <sup>90</sup>Sr (≈10 Bq/kg), that significantly overcomes the values set.

Larionova, N.V., Accumulation artificial radionuclides in plants at the territory of the former Semipalatinsk test site: dissertation abstract of candidate of biological sciences (radiobiology), Obninsk, 2013 (in Russian).



## Optimized Strontium-90 Analytical Methods for Groundwater Based on Properties

Jung-Hyup Lee<sup>1</sup>, Yo-Han Kim, Yong-Jae Kim, Ju-Yong Yoon, Sung-A Yim, Kyu-Jung Chae<sup>2\*</sup>

<sup>1</sup>Center for Environmental Radiation & Radioactivity Assessment (CERA), Korea Institute of Nuclear Safety (KINS),  
Yu-Sung Ghahak-ro 62 Daejeon, 34142 South Korea

<sup>2</sup>Department of Environmental Engineering, College of Engineering, Korea Maritime and Ocean University, 727  
Taejong-ro, Yeongdo-gu, Busan 606-791, South Korea

Keywords: Sr-90, Groundwater, Ion exchange, radiostrontium .  
email: ckjdream@kmou.ac.kr

Environmental radiation monitoring is necessary at vicinity of nuclear waste disposal site. Among many radioactive materials, strontium-90 is a one of the important radioactive materials in environmental surveillance monitoring at nuclear power plant and waste disposal site. However, it is demands for time-consuming, complicated pre-treatment process, lots of analysis costs and low analysis reliability at proficiency compare to other radionuclides. Groundwater Strontium-90 is focused on the analysis especially based on groundwater properties. To increase analysis reliability, various pre-treatment methods and techniques are applied such as precipitation, ion-exchange, fuming nitric acid mainly at same geometry of three groundwater samples taken from different points of nuclear waste disposal site. Groundwater characterization using electro-conductivity, drying, and ICP-AES are conducted before determination of analytical procedures to figure out optimized methods for each groundwater sample. A groundwater sample is identified for seawater intrusion. The rest two samples are observed different iron amount visibly. As an above each different properties of three groundwater sample, different analytical procedures were determined based on each properties. It is refer to as below Table-1 for each sample elements properties.

Table 1. Groundwater samples elements contents (mg/L)

Sample	Ca	Fe	Mg	Sr
EM-01	458±22.8	12.4±3.30	173±3.50	1.73±0.10
EM-02	22.3±1.35	3.30±0.63	14.1±1.38	0.08±0.01
EM-03	9.4±2.91	1.73±0.10	5.78±2.56	0.08±0.01

Groundwater sample amount is used 60L for analysis and categorized three methods below table 2.

Table 2. Pre-treatment methods for each sample

Method	Procedures
Type 1	S.C.E → Car. Pre. → F. N
Type 2	M.C.E → Car. Pre. → F. N
Type 2	Oxal. Pre. → F. N → S.I.E → Car. Pre. → F. N

S.I.E : Single Cation Exchange

M.C.E: Multi Cation Exchange

F.N : Fuming Nitric acid precipitation

Car. Pre. : Carbonate Precipitation

Oxal. Pre : Oxlate Precipitation

All samples are tested type 1~3 methods for figuring out optimized methods at different groundwater properties. Type 1 for EM-01, Type 2, 3 for EM-02, 03 is determined as optimized pre-treatment methods based on chemical recovery and obtained data reliability. EM-02, 03 can be also applicable type 3 proved by data reliability and chemical recovery. Analytical methods determination of strontium-90 must be considered at various aspects. It should be located at first analysis result reliability and following safety, time consuming, costs etc.

### References

- Jumpei T., 2015 Determination of low-level radiostrontium with emphasis on in-situ pre-concentration of Sr from large volume of freshwater sample using powdex resin. J. Environmental Radioactivity 146, 88-93.
- Nora V.,2010 Determination of radiostrontium isotopes: A review of analytical methodology. A. Radiation and Isotopes 68 2306-2326 .



## Sorption of $^{137}\text{Cs}$ on aluminosilicate sorbents based on clay-salt slimes of JSC “Belaruskali”

T.G. Leontieva, L.N. Maskalchuk

International Sakharov Environmental Institute of Belarusian State University, Minsk, 23/1, Dolgobrodskaya str. 220070, Belarus

Keywords: clay-salt slimes, radiocesium, illite, selective sorption, sorbents.  
leontieva@bsu.by

Thus, the radioecological problems caused by the proliferation and accumulation of radionuclides in the environment must be solved, in many countries various sorption materials for radionuclides binding are investigated. For  $^{137}\text{Cs}$  removal from water environments (reservoirs, ponds, technical waters) natural sorbents are used (clinoptilolite, vermiculite, bentonite, glauconite, illite, etc) (Hilton et al., 2006). They are characterized by high selective sorption properties towards several radionuclides ( $^{137}\text{Cs}$ ,  $^{90}\text{Sr}$ ), low cost price and commercial availability. As follows from the extensive practical experience in minimization of the Chernobyl accident consequences, the most effective sorbents for reduction of radionuclides migration in soils are clay materials with layered structure (montmorillonite, vermiculite, illite, etc.) (Sangarova et al., 2005).

To obtain aluminosilicate sorbents of radionuclides it is proposed to use the waste of potassium industry of “Belaruskali” – clay-salt slimes (CSS), representing a weighted clay sediment in a saturated salt solution. CSS were sampled from the special slime storages (N 1-3) of “Belaruskali” and 3 batches of specimens were prepared for laboratory testing.

The main mineral fractions of CSS are montmorillonite, illite, potassium feldspar, dolomite, calcite, quartz; the solid phase is represented by a finely dispersed fraction. The selective sorption properties towards  $^{137}\text{Cs}$  were studied on the specimens obtained after the initial CSS samples water (w) and aqueous acid (m) treatment (Popov et al., 2011). The results are presented in Table 1 and show that after 24 h contact with the radioactive solution ( $^{137}\text{CsCl}$ ,  $[\text{K}^+] = 0.5 \text{ mmol/l}$ ) the degree of  $^{137}\text{Cs}$  sorption ( $F_s$ ) for the studied sorbents is around 99% and the distribution coefficient ( $K_d$ ) of  $^{137}\text{Cs}$  is  $10^4 \text{ l/kg}$ .

Table 1. Selective sorption properties of aluminosilicate sorbents towards  $^{137}\text{Cs}$

Sample	$F_s$ , %	$K_d \cdot 10^4$ , l/kg	RIP(K), mmol/kg
CSS-1w	99.2	1.3	6 364
CSS-2w	98.5	0.7	3 313
CSS-3w	99.1	1.1	5 491
CSS-1m	99.2	1.2	6 099
CSS-2m	99.0	1.0	4 988
CSS-3m	99.3	1.3	6 724

The Radiocaesium Interception Potential (RIP(K)) is of a great practical importance and indicates the ability of materials to selectively absorb  $^{137}\text{Cs}$  in the presence of the competing cation  $\text{K}^+$ . The maximum value of RIP(K), obtained for the CSS-3m sample, is

higher than the value of RIP(K) for illite, bentonite and clinoptilolite. (Popov et al., 2011).

The kinetics of  $^{137}\text{Cs}$  sorption on the aluminosilicate sorbents was studied. The results obtained for the sample CSS-3m (Figure 1) show that sorption is a very fast process: for 1 min  $F_s$  reaches 98.2% and by 30 days  $F_s$  is 99.6%. Establishing equilibrium sorption time of 20 min and the value at the same  $K_d(^{137}\text{Cs}) - 10^4 \text{ l/kg}$ , after 30 days of contact with the radioactive solution the  $K_d$  value increases in 2.3 times.

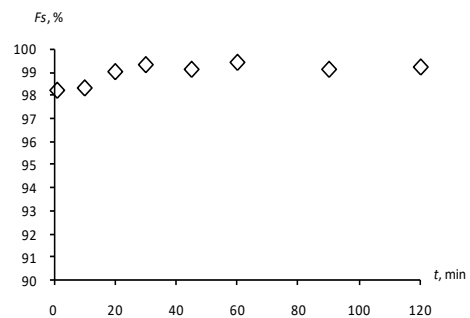


Figure 1. Dependence of  $F_s(^{137}\text{Cs})$  from time contact

To sum up the availability in Belarus the industrial waste of “Belaruskali” (CSS) in large amount (more than 110.5 mln t on 01.01.2016), high sorption properties of CSS and selectivity to radionuclides, as well as possibility of use simple and well-known reprocessing technologies, the proposed material can be used as a secondary mineral resource for getting of radionuclides sorbents aimed at purification of aquatic medium and ecosystems from  $^{137}\text{Cs}$  and solving of radioecological problems.

Hilton T.G., Kaplan D.I., Knox A., Coughlin D., Rice R., Watson S. I., Fletcher D. E. and Koo B. 2006. Use of illite clay for in situ remediation of  $^{137}\text{Cs}$ -contaminated water bodies: field demonstration of reduced biological uptake. Environ. Sci. Technol. 40, 4500-4505.

Sangarova N.I., Sysoeva A.A., Isamov N.N., Alexakhin R.M., Kuznetsov V.K., Zhigareva T.L. 2005. The role of chemistry in the rehabilitation of agricultural land affected by radioactive contamination. Russian Chem. J. 49, N 3, 26-34 (in Russian).

Popov V.E., Il'icheva N.S., Maslova K.M., Stepina I.A. 2011. The study of kinetics of selective sorption of  $^{137}\text{Cs}$  by dynamic method with measurement of radioactivity in the solid phase of soil. Pedology. 5, 556-563 (in Russian).

## Tritium research in air at the territories affected by nuclear explosions

O.N. Lyakhova, S.N. Lukashenko, L.V. Timonova and D.V. Turchenko

Institute of Radiation Safety and Ecology, National Nuclear Centre RK, Kurchatov, 071100, Kazakhstan

Keywords: tritium, air contaminate, radioactivity, nuclear explosion

Presenting author email: lyahova@nnc.kz

During 1949 – 1989 years at the Semipalatinsk Test Site (STS) more than 450 nuclear explosions were made. These events have resulted in large amount of tritium (T) in the environment. Concentrations of tritium in surface and ground waters, vegetation and soil varies from several Bq/kg to several hundreds of thousands Bq/kg. Of course, such a high concentrations of tritium in natural objects have contributed to contamination of air with tritium.

Results of the researches carried out at the sites of underground nuclear explosions show that there was an active process of T emanation from rocks and soils into air. It was assumed that T can enter the atmosphere not only as a component of tritiated water (HTO) but as a gaseous compounds ( $T_{\text{gas}}$ ), such as  $T_2$ , HT,  $CH_3T$  and etc. as well.

Therefore together with researching the concentration of HTO the possible content of  $T_{\text{gas}}$  in the atmosphere was considered in this research. The work is aimed at researching the concentrations of HTO and  $T_{\text{gas}}$  in the atmospheric environment in venues of nuclear tests of various types carried out at the STS territory.

Results of analysis of all the researches show that in most cases the area with high tritium concentration in air environment are associated with epicentral sites of nuclear tests.

### I. MATERIALS AND METHODS

The researches have been carried out in venues of various types of nuclear tests of STS: «Experimental Field», «Degelen», «Balapan» sites and the crater of the «Atomic» lake.

Concentration of T in the air environment of radiation-hazardous objects was studied by assessing its concentrations in both atmospheric and soil air. Samples were taken using tritium collector, which allows to trap tritiated hydrogen from air using 2-step sequential extraction of T in form of tritiated water (HTO) and gaseous compounds ( $T_{\text{gas}}$ ). To sample atmospheric air the tritium collector was installed at selected site at the height of 70 cm above the ground. For sampling soil air the sampling spot was covered by cylindrical insulating reservoir with the volume of 100 l. Edges of the reservoir were buried into the ground. Before sampling, air was pumped out from the reservoir via vacuum pump to make a discharge of 25-30 Pa.

### II. RESULTS

«**Experimental Field**». According to the data obtained emanation of T into the near-surface layer of the atmosphere is insignificant at this site. It was not registered presence of  $T_{\text{gas}}$ . However presence of HTO was detected in two researched point. Volumetric activity of HTO was 0.8 and 0.3 Bq/m<sup>3</sup> respectively.

Thus, emanation of T into the near-surface layer of the atmosphere is insignificant at this site.

«**Balapan**» site. At the «Balapan» site nuclear tests have been carried out in vertical boreholes. Maximal values of HTO and  $T_{\text{gas}}$  were registered in the well-mouth area, however, it was found that the places of T emission into the atmosphere are not territorially associated with the well-mouth. Numerical values of HTO and  $T_{\text{gas}}$  were registered at the distance of 10 to 50 m to the borehole in various directions. Volumetric activity of HTO ranged from 7 to 15 Bq/m<sup>3</sup>,  $T_{\text{gas}}$  – from 70 to 150 Bq/m<sup>3</sup>.

«**Degelen**» site. The «Degelen» site was used for underground nuclear tests in horizontal tunnels. The researches were carried out at the portals of 4 tunnels: №503, 511, 176 and 177. Volumetric activity of HTO in air at the tunnel portals ranged from 1.0 to 30 Bq/m<sup>3</sup>, one of the main sources of that is radioactively contaminated streamflows. Insignificant concentration of  $T_{\text{gas}}$  in the air (0.5 Bq/m<sup>3</sup>) was registered only in the tunnel 511. It was assumed that tunnel cavities could be the source of  $T_{\text{gas}}$ . However, no researches in this area have been carried out till the moment.

**The «Atomic» lake.** The lake was created as the result of the excavation explosion. The researches show presence of HTO and  $T_{\text{gas}}$  in the air. One of the sources of HTO entry into air can be water, specific activity of T in water is 100 to 1000 Bq/l. The processes of evaporation from the soil surface and transpiration of plants can also make their contribution.

Presence of gaseous tritium at these territories have probably result of transformation crystalline-bound T from soil to air. T content in the surface soil layer could reach up to 150 kBq/kg at this site.

### CONCLUSION

Results of analysis of all the data obtained showed the presence of tritium emanation processes from the soil surface into the atmosphere in venues of different nuclear tests. In general, the researches show that the level of HTO and  $T_{\text{gas}}$  in air vary depends on mechanisms of T transformation or formation in various environmental objects and also it depends on type of the nuclear test.

However it should be noticed, that the values of volumetric activity of HTO and  $T_{\text{gas}}$  in air of the researches area do not exceed permissible volumetric activity values of T in inhaled air for population, that equals to 1900 Bq/m<sup>3</sup>.

## Method for accurate determination of ultratrace level $^{241}\text{Am}$ in soil and sediment samples by SF-ICP-MS

Z.T. Wang,<sup>1,2</sup> J. Zheng,<sup>2</sup> K. Tagami,<sup>2</sup> and S. Uchida<sup>2</sup>

<sup>1</sup>Institute of Nuclear Physics and Chemistry, China Academy of Engineering Physics, Mianyang, Sichuan, 621900, China

<sup>2</sup>Biospheric Assessment for Waste Disposal Team, National Institute of Radiological Sciences, National Institutes for Quantum and Radiological Science and Technology 4-9-1, Anagawa, Inage, Chiba, 263-8555, Japan

Keywords: Americium, SF-ICP-MS, soil and sediment, ultratrace level

Presenting author email: zhongtang\_wang@caep.cn

Americium is one of the toxic radionuclides that released from nuclear weapon tests and nuclear industry. It is radiologically important to identify the source term of released Am, its environmental behavior and associated environmental impact. Soil and sediment are two mostly investigated matrix in Am study. In this work, a new method was proposed to accurately determine  $^{241}\text{Am}$  in soil and sediment samples, with emphasis on the removal of spectral interferences and mitigation of matrix effect. The developed method consists of five steps (Figure 1), including  $\text{HNO}_3$  leaching to release Am from sample,  $\text{CaC}_2\text{O}_4$  co-precipitation to remove major metals, extraction chromatographic separation using UTEVA and DGA-N resins to remove interfering elements (Bi, Hg, Hf, Pb, Pt, Pu and Tl), extraction chromatographic separation using TEVA resin to remove rare earth elements (REEs) and Am isotopic determination by Aridus-SF-ICP-MS analytical system. This method exhibited high decontamination ability of interfering elements (IEs), resulting in thorough removal of IEs from large soil samples up to 20 g. In particular, the decontamination factor of Pu was  $7 \times 10^5$ , allowing this method to analyze  $^{241}\text{Am}$  in samples contaminated with  $^{241}\text{Pu}$ . The REEs-derived matrix effect in SF-ICP-MS measurement of  $^{241}\text{Am}$  was quantified for the first time by this study, and the proposed REEs removal approach sufficiently removed REEs and thus eliminated matrix effect. On the basis of thorough removal of IEs and REEs, this method can determine  $^{241}\text{Am}$  accurately in soil and sediment samples and this was validated by analyzing six standard reference materials. In addition,

the low of detection (0.012 mBq/g) and high chemical recovery of Am (79-82%) enables this method to analyze ultratrace level  $^{241}\text{Am}$  in environmental soil and sediment. This method provides technical support in radiological assessment and applications of using Am as a tracer.

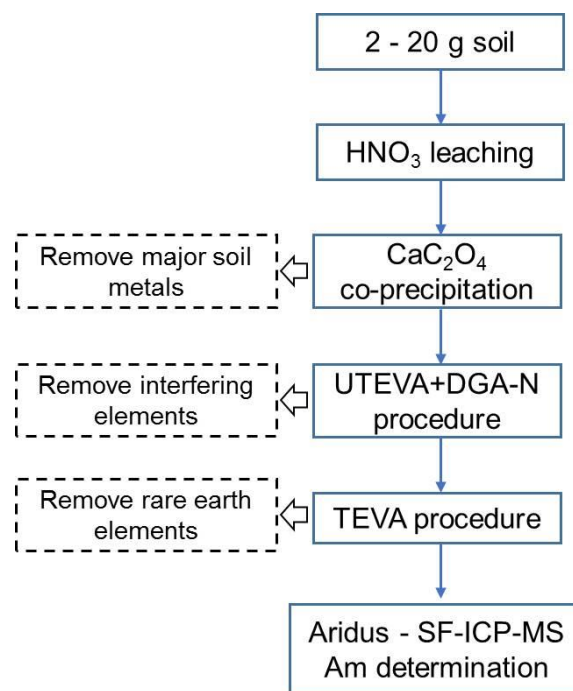


Figure 1. Analytical procedure for Am determination

This work was supported by the Agency for Natural Resources and Energy, the Ministry of Economy, Trade and Industry (METI), Japan.

## Environmental effects of low doses of ionising radiation: How do we deal with non-targeted effects?

Carmel Mothersill and Colin Seymour

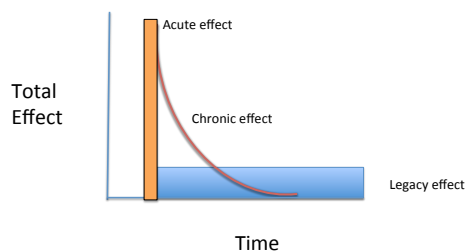
Department of Medical Physics and Applied Radiation Sciences, McMaster University, Main Street West, Hamilton, ON L8S 4K1, CANADA

Keywords: Non-targeted effects, historical dose effects, delayed mutations, environmental dose effects  
Presenting author email: [mothers@mcmaster.ca](mailto:mothers@mcmaster.ca)

Ionising radiation is a known mutagen and carcinogen and is conventionally thought to cause biological effects in humans and in non-human biota by causing mutations in DNA at critical sites. Radiation protection models assume a linear-no-threshold (LNT) relationship between dose (i.e. energy deposition) and effect (in this case probability of an adverse DNA interaction leading to a mutation) although in practice a dose limit or benchmark approach is employed to enable regulators to decide on intervention doses. This model does not consider non-targeted effects (NTE) such as bystander effects or delayed effects which occur in cells or organisms not directly receiving energy deposition from the dose. These effects can manifest in organisms in the population which were not exposed to an actual energy deposition (dose) or in distant progeny of organisms which were exposed or were bystanders at the time of the initial exposure (Seymour and Mothersill 2000). Figure 1 is a conceptual depiction of the potential contribution initial, historical and ambient dose effects.

There is huge controversy concerning the role of NTE with some saying they reflect “biology” and that repair and homeostatic mechanisms sort out the apparent damage while others consider them to be a class of damage which increases the size of the target (reviewed in Mothersill and Seymour 2012). One thing which has recently occurred these authors and others but has yet to be tested in environmental scenarios is that NTE may be very critical for measuring or modelling long-term environmental effects at the level of the population rather than the individual. The issue is that NTE resulting from an acute high historical dose such as occurred after the A-bomb or Chernobyl occur in parallel with chronic effects induced by the continuing residual impacts due to radiation dose decay. This means that if ambient radiation doses are measured for example 25 years after the Chernobyl accident, they only represent a portion of the dose effect because the contribution of NTE is not included. Current attempts in our laboratory to calculate separate contributions of actual residual dose and contribution of NTE to effects will be presented for discussion.

CONCEPTUAL DIAGRAM OF THE COMPONENTS INVOLVED IN TOTAL EFFECT



### References

Seymour CB, Mothersill C. [Relative contribution of bystander and targeted cell killing to the low-dose region of the radiation dose-response curve.](#) Radiat Res. 153:508-511 (2000)  
Mothersill C, Seymour C. [Changing paradigms in radiobiology.](#) Mutat Res. 750(2):85-95. 2012

## Soil as a barrier determining the radionuclide transport and availability

L. Nedzveckienė<sup>1</sup>, B Lukšienė<sup>1</sup>, N. Tarasiuk<sup>1</sup>, R. Gvozdaite<sup>1</sup>

<sup>1</sup>SRI Center for Physical Sciences and Technology, Vilnius, Savanorių ave. 231, LT-02300, Lithuania

Keywords: <sup>137</sup>Cs, plutonium isotopes, sorption, K<sub>d</sub>

Presenting author email: [laima.nedzveckiene@ftmc.lt](mailto:laima.nedzveckiene@ftmc.lt)

The term „barrier“ in the environmental sciences is mainly associated with the high, intermediate and low level radioactive waste disposal or storage. Each of radioactive waste repositories is equipped with a system of barriers, which reduces the possibility of release of radionuclides from the storage site. Repositories consist of the natural geological barrier provided by host rocks of the repository and its surroundings as well as an engineered barrier system (EBS). The EBS may itself comprise a variety of sub-systems or components, such as waste forms, canisters, buffers, backfills, seals and plugs (Olszewska et al., 2015). For example, huge deposits of naturally occurring swelling clays (e.g. montmorillonite, vermiculite) are abundant all over India. This material is regarded as the backfill material in the engineered barriers of high-level radioactive waste forms. The characteristic properties of these swelling clays ensure that the long-lived radioactive fission products are retained in the clay for more than 10<sup>3</sup> years, so that the radioactivity of the fission products decays to very low levels (Sivaiah et al., 2004).

The dissemination of materials from the storage site is stimulated by associated gradual process with disintegration of containers and engineered barriers due to external effects (groundwater, microorganisms, cement degradation, corrosion, etc.) which could worsen the isolation of waste. Radionuclide solubility is one of the factors that can determine the potential migration from the repository to the near and far fields in geosphere and biosphere.

On the other hand, the deposition of man-made radionuclides on the soil surface in Lithuania has taken place since the outset of nuclear weapon testing and which as a result of accidental releases by the nuclear industry cannot be excluded in the future. The fixation of radionuclides by the soils is of great importance, because the adsorption processes to a considerable extent determine the transport and availability of the radionuclides. The dynamics of Cs and plutonium isotope sorption by soils as influenced by soil components are not fully understood. Especially data about the migration ability of Pu isotopes in different types of soils are very limited.

In this study peculiarities of the plutonium isotope and <sup>137</sup>Cs sorption by selected soils in Lithuania were investigated to facilitate the understanding of the dynamics of redox sensitive and monovalent radionuclides in the barrier system of soils.

A series of pH-variation experiments in which selected soil samples were divided according to the grain size (0.25 and 0.50 mm) using a dynamic flow column method were carried out. In all the cases the solid-liquid

distribution coefficient (K<sub>d</sub>) for direct radionuclide adsorption, denoting the amount of adsorbed radionuclide (Bq·kg<sup>-1</sup>) and the equilibrium concentration of radionuclide in solution (Bq·L<sup>-1</sup>), was evaluated. The experimental results have shown that Pu adsorption is strongly dependent on solution pH values, the concentration of macroelement pairs (Fe+Mg, Mg+K, Fe+Ca) and the soil texture. Moreover, K<sub>d</sub> values were significantly higher in the experiments with soil fractions of the 0.25 mm size (Fig.1).

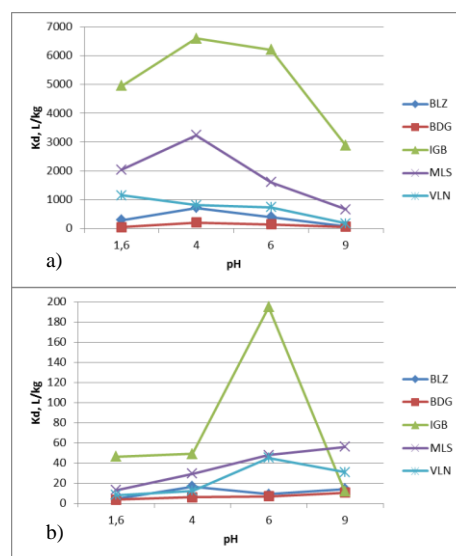


Figure 1. K<sub>d</sub> dependence on pH value: a) particle size 0.25 mm, b) particle size 0.5 mm.

The <sup>137</sup>Cs and plutonium isotope activity concentrations in profiles of upland and wetland soils of lake banks indicated that the upland soil is distinguished as a better system for the radionuclide barrier. All experimental results provide a framework for development of a comprehensive plan in which soils of different geochemical/geophysical properties and radioactive tracers are being applied to study soil as a barrier system.

Olszewska, W., Miśkiewicz, A., Zakrzewska-Kołtuniewicz, G., Lankof, L., Pająk, L., 2015. Multibarrier system preventing migration of radionuclides from radioactive waste repository. NUKLEONIKA 60(3), 557 - 563.

Sivaiah, M.V., Kumar, S.S., Venkatesan, K.A., Sasidhar, P., Krishna, R.M., and Murthy, G.S., 2004. Sorption of Strontium on Zirconia Modified Vermiculite. J. Nucl. Radiochem. Sci. 5(2), 33-36.



# Radioactivity levels in maize from high Background radiation areas and dose estimates for the public in Tanzania

Leonid Leopold Nkuba<sup>1</sup> and Yesaya Yohana Sungita<sup>2</sup>

<sup>1</sup>Tanzania Atomic Energy Commission, Radiation Control Directorate  
P.O Box 80479, Dar es Salaam - Tanzania. Tel: +255 22 2927555  
Email: leonid\_nkuba@yahoo.co.uk

<sup>2</sup>Tanzania Atomic Energy Commission, Nuclear Technology Directorate  
P.O Box 80479, Dar es Salaam - Tanzania. Tel: +255 22 2927555  
Email:ysungita@hotmail.com

## Abstract

Natural radioactivity levels in maize which is one of the staple foods in various regions in Tanzania have been studied. The radioactivity concentration of  $^{238}\text{U}$ ,  $^{232}\text{Th}$  and  $^{40}\text{K}$  were determined using  $\gamma$  ray spectrometry employing HPGe detector of relative efficiency of 51 %. The average radioactivity concentrations in maize from five regions were ranged from  $1.8 \pm 0.2$  to  $23.6 \pm 0.7$  Bq/kg  $^{238}\text{U}$ ,  $2.2 \pm 0.1$  to  $38.9 \pm 1.0$  Bq/kg for  $^{232}\text{Th}$  and  $42.0 \pm 0.4$  to  $434.6 \pm 18.7$  Bq/kg for  $^{40}\text{K}$  respectively. Total annual committed effective dose due to total  $^{238}\text{U}$  and  $^{232}\text{Th}$  intakes as a result of consumption of maize in five Regions were as follows; Manyara (1.46 mSv/y), Mbeya (0.31 mSv/y), Dodoma (0.21 mSv/y), Ruvuma (0.19 mSv/y) and Dar es Salaam (0.08 mSv/y). The dose value from Manyara was almost the same to the annual dose guideline for the general public which is 1 mSv/y, where else for other regions the doses are low. Hence a conclusion could be made that food crops cultivated at Minjingu village might expose the population to high radiation dose which might be detrimental to their health.

**Keywords:** Radioactivity, Minjingu phosphate deposit, committed effective dose, Uranium Deposit

## Radionuclides in Bodies of Wild Animals of Semipalatinsk Test Site

A.V. Panitskiy, S.N. Lukashenko and N.Zh. Kadyrova

branch "Institute of Radiation Safety and Ecology" of the RSE "National Nuclear Center of the Republic of Kazakhstan"

Kurcharov city, 071100, Kazakhstan

Keywords: radioecology, concentration ratios, Semipalatinsk Test Site.

Presenting author email: Panitskiy@mail.ru

As the result of testing nuclear weapons and adverse factors of radioactive agents at the territory of Semipalatinsk Test Site (the STS) the sites, with high concentration of radionuclides in natural environmental media – soil, vegetation and water were formed. As a rule, these sites are associated with the epicenters of surface nuclear explosions, channels of radioactively-contaminated streamflows out of testing tunnels, where the underground nuclear tests were conducted, venues of testing warfare radioactive agents and the venues of underground excavation explosions (Panitskiy, 2015). Also the contamination at the test site was registered in form of "plumes" of radioactive fallouts resulted from passage of radioactive fallouts, those in their turn have resulted from the nuclear tests (Larionova, 2013).

At these sites quite high concentrations of artificial radionuclides were registered in soil, vegetation and water. These components of natural environment also serve as the components of the food and habitation area for many representatives of wild animals.

Therefore, as the object of these researches the animals, constantly living at these radioactively-contaminated sites, consuming vegetable food of various degree of radioactive contamination, and living in holes digged in radioactively- contaminated soil were chosen.

As the result of research, the data, characterizing present radioecological state of the STS fauna was obtained. According to results of research, the parameters of radionuclides transfer into wild animals' bodies depend on many factors as follows: the character of radioactive contamination, daily activity radius, behavior peculiarities of animals and etc. (Panitskiy, 2017)

The parameters of radionuclides transfer into wild animals' bodies obtained as the result of research can be use for various predictive models of risk assessments for biota. The tables (Table 1, Table 2.) provide CR values of radionuclides in bodies of wild animals, inhabiting the venues of testing nuclear weapons and adverse factors of radioactive agents.

Table 1. CR values  $^{137}\text{Cs}$  and  $^{90}\text{Sr}$  for animals STS

Animals	CR values (Mean±SD)			
	$^{137}\text{Cs}$		$^{90}\text{Sr}$	
Sand lizard ( <i>Lacerta agilis</i> )	n-30	$(6,2\pm 9,9)\times 10^{-3}$	n-11	$(1,1\pm 1,4)\times 10^{-2}$
Partridge ( <i>Perdix perdix</i> )	n-5	$(3,3\pm 2,5)\times 10^{-3}$	n-5	$\frac{*(4,2\pm 6,3)\times 10^{-4}}{(2,7\pm 2,2)\times 10^{-2}}$
Ground squirrel ( <i>Spermophilus erythrogegnys</i> )	n-6	$(1,2\pm 0,9)\times 10^{-2}$	-	-
Siberian jerboa ( <i>Allactaga saltator Ewersm</i> )	n-27	$(2,2\pm 1,2)\times 10^{-3}$	n-8	$(2,4\pm 1,1)\times 10^{-2}$
Hare ( <i>Lepus europaeus</i> )	n-2	$(9,9\pm 6,8)\times 10^{-4}$	-	-
*Muscular tissue				
Bone tissue				

Table 2. CR values  $^{241}\text{Am}$  and  $^{239+240}\text{Pu}$  for animals STS

Animals	CR values (Mean±SD)			
	$^{241}\text{Am}$		$^{239+240}\text{Pu}$	
Partridge ( <i>Perdix perdix</i> )	n-5	$< 5,9\times 10^{-4}$	n-5	$< 1,9\times 10^{-5}$
Ground squirrel ( <i>Spermophilus erythrogegnys</i> )	n-1	$2,5\times 10^{-4}$	-	$9,9\times 10^{-4}$

The researches in this direction have been continued and this table is been constantly refreshed

Larionova, N.V., Lukashenko, S.N., 2013 Transport of radionuclides from soil to plants in the area of radioactive fallout at the former Semipalatinsk test site. J. Radiation and Risk 3, 65-71. (in Russian)

Panitskiy, A.V., Lukashenko, S.N., 2015. Nature of radioactive contamination of components of ecosystems of streamflows from tunnels of Degelen massif. J. Environ. Radioact. 32-40

Panitskiy, A.V., Lukashenko, S.N., Kadyrova, N.Zh., 2017.  $^{137}\text{Cs}$  and  $^{90}\text{Sr}$  in lizards of Semipalatinsk test site J. Environ. Radioact., 166P1, 91-96

## Spatial distribution of natural radionuclides in soils surrounding a lignite-fired power plant in Greece

H. Papaefthymiou, M. Manousakas and M. Soupioni

Department of Chemistry, University of Patras, Patras, Achaia, 265 04, Greece

Presenting author email: [epap@chemistry.upatras.gr](mailto:epap@chemistry.upatras.gr)

Coal contains nearly all the elements of the periodic table and also naturally occurring radioactive elements in concentrations, in some cases, higher than those in most sedimentary rocks. During coal combustion for the production of heat and electrical energy, trace elements and natural radionuclides may be released into the atmosphere, associated with fine fly ash particles or as vapors. Many studies have shown that these fine fly ash particles are considerably enriched in several toxic elements and radionuclides (Seams and Wendt, 2000). Greek lignites appear to have higher concentrations of the  $^{238}\text{U}$  series radionuclides, compared to those reported by UNSCEAR for coal (Papaefthymiou et al., 2008; UNSCEAR, 2000).

In this study, the spatial distribution of the natural radionuclides  $^{238}\text{U}$ ,  $^{226}\text{Ra}$ ,  $^{232}\text{Th}$  and  $^{40}\text{K}$  in the vicinity of coal power plants in Megalopolis, Greece was examined. Moreover, their correlation with each other and the total organic carbon (TOC %) were also examined.

### Experimental

In the Megalopolis lignite centre, two lignite power plants are in operation: the Megalopolis-A (550 MW) and the Megalopolis-B (300 MW). At full load, the units consume  $\sim 22\text{--}25 \times 10^6$  kg of pulverised lignite per day. The produced fly ash is collected by electrostatic precipitators, with practical collection efficiency of 95%.

Fourteen surface soil samples (S1-S14), up to 5 cm, were collected from areas within a radius of 10 km of the coal-fired power plants in 2006. Almost all soil samples were collected from undisturbed flat areas having short-cropped vegetation. A differential global positioning system was used for the positioning of each sampling site. The collected samples were analysed for their natural radionuclide concentration by using  $\gamma$ -ray spectrometry set-up, combined with a Canberra HPGe coaxial detector. The counting time was 24 h in order to have statistically relevant results.

The total organic carbon content (TOC %) of the collected samples was determined using the Walkley-Black method.

### Results

The activity concentration values of  $^{238}\text{U}$ ,  $^{226}\text{Ra}$ ,  $^{232}\text{Th}$  and  $^{40}\text{K}$  are presented in Table 1. It should be noticed that the average values for  $^{238}\text{U}$  and  $^{226}\text{Ra}$  (both members of the  $^{238}\text{U}$  decay series) were found to be higher compared with the Greek (25 and 25  $\text{Bq kg}^{-1}$ , respectively) and world (35 and 35  $\text{Bq kg}^{-1}$ , respectively) average values for soil, but fall within the range reported by UNSCEAR (UNSCEAR, 2000). As concerns the average concentrations of  $^{232}\text{Th}$  and  $^{40}\text{K}$  (33 and 337  $\text{Bq}$

$\text{kg}^{-1}$ , respectively), they were found to be comparable with the values for the world and Greek soil (UNSCEAR, 2000) and were also low in lignite and fly ash samples from the Megalopolis-A plant (Papaefthymiou et al., 2007).

Table 1. Activity concentration values ( $\text{Bq kg}^{-1}$ ) of  $^{238}\text{U}$ ,  $^{226}\text{Ra}$ ,  $^{232}\text{Th}$  and  $^{40}\text{K}$  in the surface soil samples (0-5 cm) from the Megalopolis basin area.

Sample code	$^{238}\text{U}$	$^{226}\text{Ra}$	$^{232}\text{Th}$	$^{40}\text{K}$
S1	53±7	35±1	35±1	412±28
S2	40±3	22±1	26±1	317±21
S3	69±6	44±1	35±2	320±25
S4	26±5	31±1	33±1	320±24
S5	56±6	41±1	34±1	359±27
S6	64±3	47±1	39±1	387±29
S7	77±6	31±1	29±2	352±28
S8	36±4	25±3	27±1	320±24
S9	87±8	46±2	36±2	392±33
S10	29±3	46±3	25±1	228±29
S11	129±10	125±3	40±3	404±33
S12	59±8	51±1	26±2	382±30
S13	30±5	47±1	29±2	293±23
S14	57±7	33±1	30±2	234±18
Average	58±27	45±25	33±5	337±58
Megalopolis lignite	510	530	20	170

The values of the TOC% content in the samples ranged from 2.5 to 13.4 with an average value of  $7.4 \pm 4.6$ .

The calculated binary Pearson correlation coefficients showed, as expected, strong significant correlation between  $^{238}\text{U}$  and  $^{226}\text{Ra}$ . Medium, but significant correlation between  $^{238}\text{U}$  -  $^{40}\text{K}$ ,  $^{238}\text{U}$  -  $^{232}\text{Th}$  and  $^{232}\text{Th}$  -  $^{40}\text{K}$  also were found. TOC did not present any significant correlation with the examined radionuclides.

### References

- Papaefthymiou, H., Symeopoulos, B., Soupioni, M., 2008. Neutron activation analysis and natural radioactivity measurements of lignite and ashes from Megalopolis basin, Greece. *J. Environ. Radioact.* 10, 1653-1655.
- Seams, .S., Wendt, J.O.L., 2000. The partitioning of radionuclides during combustion. *Adv. Environ. Res.*, 4, 45-58.
- UNSCEAR, 2000 (United Nations Scientific Committee on the Effects of Atomic Radiation). United Nations (2000).

## Honey as an environmental indicator in Achaia (Greece)

M. Soupioni, A. Kaponi and H. Papaefthymiou

Department of Chemistry, University of Patras, Patras, Achaia, 26504, Greece

Keywords: honey, heavy metals, natural and artificial radionuclides, Achaia (Greece)

Presenting author email: [epap@chemistry.upatras.gr](mailto:epap@chemistry.upatras.gr)

Bee honey is a very important natural energy food, which contains mainly a mixture of carbohydrates, such as fructose, glucose and maltose (P. Vinas et al. 1997). The mean content of mineral substances in honey is about 0.17 % m/m, although it varies within a wide range. Generally, the chemical composition of honey varies with the surrounding environment (major floral, soil and water contamination), because bees from an individual hive may forage in an area over 7 km<sup>2</sup> contacting flowering plants and trees, from which they gather pollen, nectar etc. Consequently, honey may be useful as an environmental indicator of heavy metals and radionuclides pollution (P. Przybyłowski and A. Wilczynska, 2001).



Figure 1. The regional unit Achaia in Greece

Achaia is a regional unit of Greece at the northwestern part of the Peloponnese peninsula. In the present study certain major, minor and trace metals concentrations, as well as the activity concentration values of the <sup>40</sup>K and <sup>137</sup>Cs were measured in honey from Achaia (Greece) in order to consider for the pollution of this area, but also for its own quality control and nutritional aspect.

### Experimental

Thirteen commercial honey samples were collected from hives located at representative rural and urban-industrial wide areas of Achaia. In water diluted honey samples Ca concentration was measured by Flame Atomic Absorption Spectrometry. For the trace elements analysis the inductively coupled plasma mass spectrometry (ICP-MS) was used after the microwave digestion of the samples. The precision and the accuracy of the results were evaluated by analyzing the reference material "Wheat flour" SRM 1567a, provided by NIST. The activity concentration measurements were performed by  $\gamma$ -ray spectrometry, using a Canberra HPGe coaxial detector. The counting time was 24 h in order to have statistically relevant results.

### Results

The results revealed that the determined Ca concentration (~3 ppm) in honey was very close to the bibliographic values for greek honeys, while the Pb and Cd concentrations were under the European Union guideline limits. The activity concentration of <sup>40</sup>K (~77.35 Bq kg<sup>-1</sup>) in honey samples was fairly lower than the Greek average for soil (UNSCEAR, 2000) and <sup>137</sup>Cs was not detected at all.

### References

- P. Przybyłowski, A. Wilczynska, 2001. Honey as an environmental marker. *Food Chem.* 74, 289
- P. Vinas, I. Lopez-Garcia, M. Lanzon, M. Hernandez Cordoba, 1997. Direct Determination of Lead, Cadmium, Zinc, and Copper in Honey by Electrothermal Atomic Absorption Spectrometry using Hydrogen Peroxide as a Matrix Modifier. *J. Agric. Food. Chem.* 45, 3952
- UNSCEAR (2000) Sources and Effects of Ionizing radiation. United Nations Scientific Committee on the effects of atomic radiation. Report to General Assembly with Scientific Annexes. United Nations, New York.

## Burullus lake, Egypt: Using natural and artificial radioisotopes for a chronology

M. Perez-Mayo<sup>1</sup>, N. Imam<sup>2</sup>, D. Pittauer<sup>3</sup>, H.W. Fischer<sup>1</sup>

<sup>1</sup>Institute of Environmental Physics, University of Bremen, Bremen, 28359, Germany

<sup>2</sup>National Institute of Oceanography and Fisheries, Cairo, 11516, Egypt

<sup>3</sup>MARUM – Center for Marine Environmental Sciences, University of Bremen, Bremen, 28359, Germany

Keywords: Gamma-spectrometry, lake sediment, Chronology, <sup>137</sup>Cs.

Presenting author email: manuel@iup.physik.uni-bremen.de

Burullus lake is an ecologically important wetland site with high anthropogenic influence. Radioisotope content and distribution has been studied earlier (El-Reefy et al. 2014). Pollen and macrofossils allowed for a sediment chronology, whilst a radiochronology could not yet be established (Appleby et al. 2001)

We present a new intent of chronology based on radioisotopes measured with gamma spectroscopy.

### Methodology

Sediment chronology based on <sup>210</sup>Pb is a method with a long history (Appleby 1978), well tested and with well known problems (Sanchez-Cabeza and Ruiz-Fernández 2012).

We determine the natural radioisotopes as: <sup>214</sup>Bi, <sup>214</sup>Pb, <sup>40</sup>K and <sup>210</sup>Pb from the uranium chain, <sup>228</sup>Ac, <sup>212</sup>Bi, <sup>212</sup>Pb, <sup>208</sup>Tl from the thorium chain and anthropogenic <sup>137</sup>Cs measured by high-resolution, low-background gamma spectroscopy.

Modelling of the sedimentation rate will be realized based on classical models (Robbins, Edgington and Kemp 1978, Appleby 1978).

### Material

A core of 50cm length and 8cm diameter from the western part of the lake was taken in May 2016. (31°25'N 30°37'E). The core was divided into layers of 2cm, dried and milled.

Samples were pressed into pellets of 70mm diameter, and sealed into metalized foil to obtain the secular equilibrium between <sup>226</sup>Ra, <sup>222</sup>Rn and its progeny, after three weeks of ingrowth time.

### Preliminary results

First results (Fig.1) shows both <sup>210</sup>Pb<sub>exs</sub> and <sup>137</sup>Cs concentration values decrease monotonically with depth and are consistent with values reported earlier (El-Reefy et al. 2014, Appleby et al. 2001). Whilst <sup>210</sup>Pb<sub>exs</sub> data would allow for a preliminary chronology resulting in a mean sedimentation rate of about 1mm/yr for the upper 10cm. The high concentration of <sup>137</sup>Cs at the top of the core might indicate erosion or deposition effects.

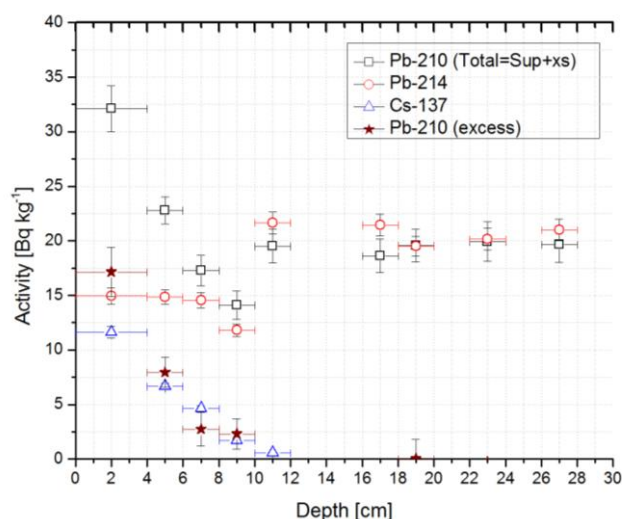


Figure 1. Preliminary results for: <sup>210</sup>Pb, <sup>214</sup>Pb radioisotopes and <sup>137</sup>Cs.

### References

- Appleby, P. G., H. H. Birks, R. J. Flower, N. Rose, S. M. Peglar, M. Ramdani, M. M. Kraiem & A. A. Fathi (2001) Radiometrically determined dates and sedimentation rates for recent sediments in nine North African wetland lakes (the CASSARINA project). *Aquatic Ecology*, 35, 347-367.
- Appleby, P. G. O., F. (1978) The calculation of lead-210 dates assuming a constant rate of supply of unsupported 210Pb to the sediment. *Catena*, 5, 1-8.
- El-Reefy, H. I., H. M. Badran, T. Sharshar, M. A. Hilal & T. Elnimr (2014) Factors affecting the distribution of natural and anthropogenic radionuclides in the coastal Burullus Lake. *Journal of Environmental Radioactivity*, 134, 35-42.
- Robbins, J. A., D. N. Edgington & A. L. W. Kemp (1978) Comparative 210Pb, 137Cs, and pollen geochronologies of sediments from Lakes Ontario and Erie. *Quaternary Research*, 10, 256-278.
- Sanchez-Cabeza, J. A. & A. C. Ruiz-Fernández (2012) 210Pb sediment radiochronology: An integrated formulation and classification of dating models. *Geochimica et Cosmochimica Acta*, 82, 183-200.



## Experimental studies of specifics of <sup>3</sup>H transport in plant by root uptake

Y.N. Polivkina, N.V. Larionova, O.N. Lyakhova, S.N. Lukashenko

Institute of radiological safety and ecology NNC RK, Kurchatov, VKO, 071100, Kazakhstan

Key words: <sup>3</sup>H, migration, tissue free water tritium, organically bond tritium.

email: [polivkina@nnc.kz](mailto:polivkina@nnc.kz)

Isotope <sup>3</sup>H is one of the first places in radioecological studies, because it is a high risk as a source of internal irradiation and can be incorporated of important biomolecular cell structure.

There are areas with high levels of <sup>3</sup>H on the Semipalatinsk test site (STS) (Lukashenko et al., 2015), these plots can be of serious dangerous to surrounding areas due to the transport activity of the radionuclide. As known plants play an important role in the migration of <sup>3</sup>H so purpose of the experimental studies was to investigate the specifics of the entering and redistribution of <sup>3</sup>H in plants by root uptake.

A sunflower (*Helianthus Annus*) was grown in background soil in plastic pots which were placed greenhouse. During vegetation the plants were watered with tunnel water with high specific activity of <sup>3</sup>H which was brought from the territory of the STS. The specific activity of <sup>3</sup>H in the tunnel water and plant samples was controlled every 10 days.

Measurement of specific activity of <sup>3</sup>H was determined with a scintillation cocktail Ultima Gold LLT with QUANTULUS 1200 instrument (ISO 9698-1989 /E/). Tissue free water was extracted from the plant samples by means of a special installation (Lukashenko, Larionova, Zarembo, 2015), the preparation of samples for determination of organically bond tritium (OBT) has been performed with a Sample Oxidizer.

Figure 1 shows direct correlation between plant tissue free water tritium (TFWT) concentration and HTO concentration in tunnel water.

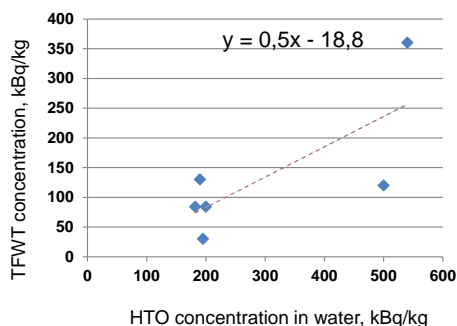


Figure 1. Changes of TFWT concentration.

Figure 2 shows that OBT concentration increased in 4 times at the end of vegetation. This fact perhaps indicates that TFWT participates in metabolic processes due to <sup>3</sup>H can be incorporated of organic structure of cells.

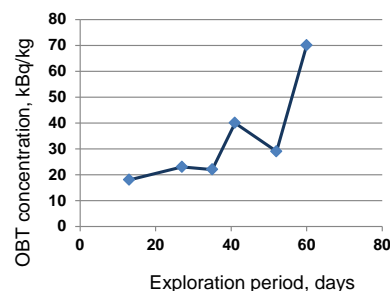


Figure 2. Changes of OBT concentration.

The plant organ distribution of TFWT and OBT was studied at the end vegetation. According figure 3 the highest concentration of TFWT was indicated in roots resulting from this organ perform the function of uptake water from soil. As figure 3 shows the concentration of OBT in root was lower than in above-ground organs. OBT accumulation in above-ground organs may be related to high metabolic activity in this part of plant resulting from <sup>3</sup>H incorporated of organic cell structures.

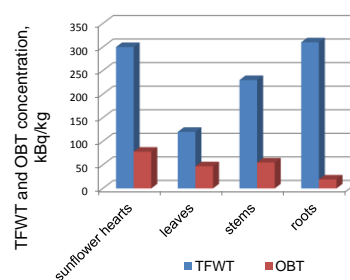


Figure 3. The distribution of TFWT and OBT.

Thus, plants can participate actively in transport of <sup>3</sup>H radionuclide environment.

Actual issues of Kazakhstan radioecology. Lukashenko S. N. etc. Vol. 5. 2015. 230. 243-245.

Installation for the extraction of water from samples / S. N. Lukashenko, N. In. Larionov, V. P., Zarembo; innovative patent of RK No. 29721, 15.04.2015, bull. No. 4.

Water quality – determination of tritium activity corresponding to the concentration – liquid scintillation counting method ISO 9698-1989 /E/

## RESEARCH TRITIUM MIGRATION WITH GROUNDWATER AT THE SITE BALAPAN IN THE TERRITORY OF THE SEMIPALATINSK TEST SITE

*Pronin.S.S., Lukashenko S.N., Lyakhova O.N., Aktayev M.R.*

Institute of Radiation Safety and Ecology NNC RK, Kurchatov, Kazakhstan  
e-mail: Proninss@nnc.kz

At the present time the territory of «Balapan» site represents a reserve of ground waters radioactively contaminated as the result of secondary washing out of artificial radionuclides from cavities of "warfare" boreholes. According to results of previous researches, the main contaminant of ground (fracture) waters is tritium ( $^3\text{H}$ ) with activity ranging from 0.07 to 4,700 kBq/kg. The content of other artificial radionuclides  $^{137}\text{Cs}$ ,  $^{90}\text{Sr}$  and  $^{239+240}\text{Pu}$  was had extremely low activity levels (Subbotin S.B.et. al., 2003-2007). It was found that fracture waters of Palaeozoic basement are focused in the zone of exogenic fracturing, and depending on geo-structural conditions, lie at the depth of 4 to 100 m. Research of state of ground water, wide-spread in near-surface layers of sedimentary deposits (ground waters) have not been carried out.

Work objective: research of modern state of ground waters, distributed in formations of Palaeozoic basement (fracture waters) and modern sediments (ground waters).

Research of fracture water was carried out in existing boreholes of "Balapan", site by restoring water inlet (cleaning). For research of the state of near-surface ground waters drill works were carried out.

Upon the result of fracture waters, specific activity of  $^3\text{H}$  varies within a wide range from 0.01 to 450 kBq/kg. No other artificial radionuclides such as  $^{137}\text{Cs}$ ,  $^{90}\text{Sr}$ ,  $^{239-240}\text{Pu}$  was found. It was found, that maximum concentrations of  $^3\text{H}$  with activity from 240 to 450 kBq/kg belong to local spots. It was noted that a distance from hydrogeological to «warfare» boreholes does not affect  $^3\text{H}$  activity in ground waters. Conditions and degree of ground waters contamination, are associated with geological characteristics of individual sites.

Comparative analysis of results for 2003 – 2015 (a half-life period of  $^3\text{H}$ ) have shown, that contamination of ground waters with  $^3\text{H}$  is clear and completely developed. In some cases decrease and increase in  $^3\text{H}$  specific activity from 2 to 70 times is noticed.

Primary data was obtained on levels and character of near surface waters contamination with  $^3\text{H}$  radionuclide. Presence of  $^3\text{H}$  in ground waters was found almost at all surveyed sites. Maximum concentrations of  $^3\text{H}$  were found in the western part of «Balapan» site – boreholes KAR - 1 (25 kBq/kg), KAR - 2 (15 kBq/kg) and the southwestern part of the site in the borehole Sh.B.-3 (33 kBq/kg). It was found that, artificial radionuclides enter near surface ground waters by means of unstopped rise of fracture waters, in places without seat clays and with presence of permeable rocks.

## Determination of important radionuclides in soil samples from the Island of Mljet, Croatia

S. Dulanská<sup>1</sup>, M. Nodilo<sup>2</sup>, P. Rajec<sup>1</sup>, L. Mátel<sup>1</sup>, Ž. Grahek<sup>1</sup>, I. Tucaković<sup>1</sup>

<sup>1</sup>Department of Nuclear Chemistry, Comenius University, Bratislava, Mlynská Dolina, Ilkovičova 6, 842 15, Slovakia

<sup>2</sup>Laboratory for Radioecology, Ruđer Bošković Institute, Zagreb, Bijenička c. 54, 10 000, Croatia

Keywords: radionuclides, *terra rossa*, soil, Mljet

Presenting author email: rajec@fns.uniba.sk

Radiochemical analysis of soils samples collected from the locations National Park Mljet (the north-west part of the Island of Mljet, Croatia) have been performed in this study using beta, alpha and gamma spectrometric measurements. The research included determination of the <sup>90</sup>Sr, alpha emitters (<sup>241</sup>Am, <sup>238</sup>Pu, <sup>239,240</sup>Pu, <sup>241</sup>Pu) and anthropogenic gamma emitters.

The sampling collected from undisturbed land, covered with minimum grass and/or foliage of nearby trees, neighbouring with land used for farming, sightseeing and human living situated in north and central part of the National Park. Soils (*Terra rossa*) are collected during August 2015 from 11 locations with additional sampling on March 2016 from 2 locations. Grass and foliage leftovers are removed together from the surface soil. The soil sampling was done with a paddle within area of approximately 300 cm<sup>2</sup> in the interval from surface to 10 cm in the deep. *Terra rossa* soil is mixture of insoluble red clays, left after water dissolved out the carbonate from limestone and dolomite, and wind deposited particles.

Table 1. Massic activities (Bq kg<sup>-1</sup>) in soil samples

Soi	A <sup>137</sup> Cs (Bq kg <sup>-1</sup> )	A <sup>90</sup> Sr (Bq kg <sup>-1</sup> )	A <sup>239,240</sup> Pu (Bq kg <sup>-1</sup> )	A <sup>241</sup> Am (Bq kg <sup>-1</sup> )
1	46.3 ± 3.7	66.0 ± 5.9	0.382 ± 0.033	0.004 ± 0.001
2	18.9 ± 1.5	92.8 ± 8.3	0.505 ± 0.040	0.529 ± 0.051
3	24.7 ± 2.0	133.6 ± 11.9	0.598 ± 0.051	0.061 ± 0.007
3*	123 ± 9.8	209.9 ± 18.7	1.545 ± 0.121	0.376 ± 0.041
4	185 ± 15	330.1 ± 29.4	2.876 ± 0.268	0.286 ± 0.025
4*	140 ± 11	174.6 ± 15.5	3.912 ± 0.320	0.429 ± 0.069
5	25.5 ± 2.0	198.7 ± 17.7	0.200 ± 0.014	0.957 ± 0.091
6	118 ± 9	204.0 ± 18.2	2.946 ± 0.279	0.243 ± 0.022
7	27.1 ± 2.2	125.5 ± 11.2	0.602 ± 0.005	0.208 ± 0.019
8	80.2 ± 6.4	186.2 ± 16.6	2.129 ± 0.190	0.566 ± 0.06
9	82.6 ± 6.6	136.6 ± 12.2	1.750 ± 0.181	0.005 ± 0.001
10	0.5 ± 0.1	131.3 ± 11.7	0.107 ± 0.008	0.007 ± 0.001
11	70.1 ± 5.6	166.4 ± 14.8	1.066 ± 0.102	0.128 ± 0.011

Table 2. Ratios of activity concentrations in soil samples

<sup>137</sup> Cs/ <sup>90</sup> Sr	0.417 ± 0.080
<sup>239,240</sup> Pu/ <sup>137</sup> Cs	0.019 ± 0.006
<sup>239,240</sup> Pu/ <sup>90</sup> Sr	0.008 ± 0.002

Correlations between concentrations of the analysed radionuclides were tested by the statistical analysis method. Regression diagnostics procedures for

examination of the regression triplet were used. The results shows strong correlation between <sup>239,239,240</sup>Pu/<sup>90</sup>Sr R=0.71, <sup>239,240</sup>Pu/<sup>137</sup>Cs R=0.89 and <sup>90</sup>Sr/<sup>137</sup>Cs R=0.84. The radioactivity ratio of studied anthropogenic radionuclides in soil can be explained by global fallout. The most important radionuclides in global fallout are <sup>90</sup>Sr and <sup>137</sup>Cs, because of their long half-lives, association with particles of submicron sizes and radiation hazard. The observed distribution of <sup>90</sup>Sr and <sup>137</sup>Cs in global contamination is determined by number of factors as the character of the nuclear weapons tests, the general systematic of the atmospheric circulation.

Measured radioactivity of <sup>90</sup>Sr in all analyzed soil samples were higher than <sup>137</sup>Cs. The highest <sup>90</sup>Sr radioactivity was found for the soil sample No. 4. (330.1 ± 29.4) Bq kg<sup>-1</sup> and the lowest for the soil sample No. 1 (66.0 ± 5.9) Bq kg<sup>-1</sup>. The value of radioactivities in Croatian measured soil samples were higher than that soil samples, that were collected from the exclusion zone (< 30 km) of the earthquake-damaged Fukushima Daiichi nuclear power plant (Sahoo, 2016). Sahoo determined <sup>90</sup>Sr radioactivity in soil within the span (3.0 ± 0.3 to 23.3 ± 1.5) Bq kg<sup>-1</sup>. Results show presence of the important anthropogenic radioisotopes in the collected soil samples, most probably as a result of nuclear bombs testing in the atmosphere in the 60s (Sahara desert) and the Chernobyl accident.

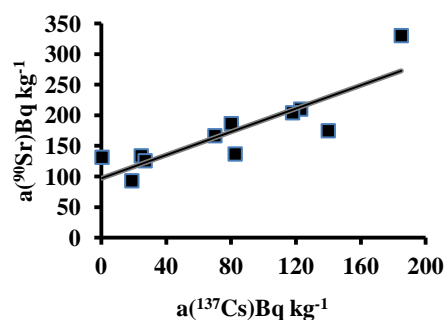


Figure 1. Correlation between activity of <sup>90</sup>Sr vs. <sup>137</sup>Cs in soil samples.

This work was supported by the KEGA 002UK-4/2016.

### References:

Barišić, D., Vertačnik, A., Lulić, S., 1999. [Caesium contamination and vertical distribution in undisturbed soils in Croatia](#). J. Environ. Radioact. 46, 361-374.

## Radionuclides distribution in the artificial reservoir biota

A.K. Rozhkova<sup>1</sup>, N.V. Kuzmenkova<sup>1</sup>, I.E. Vlasova<sup>1</sup>, E.A. Pryakhin<sup>2</sup>, S.N. Kalmykov<sup>1</sup>

<sup>1</sup>Department of Chemistry, Lomonosov MSU, Moscow, 119991, Russia

<sup>2</sup>Urals Research Center for Radiation Medicine, Chelyabinsk, 454076, Russia

Keywords: hydrobionts, fish, artificial reservoir.

Presenting author email: rozhkovaak@gmail.com

Hydrobionts are part of the food chain and actively involved in radionuclides migration processes. The investigations of real samples from radioactively contaminated water reservoirs were studied. The reservoir R-4 of the "Mayak" Production Association using as a low-level waste (LLW) storage and it is unique in the number and radionuclides composition. The study purpose was to establish the radionuclide distribution parameters within the artificial reservoir R-4 hydrobionts.

The reservoir R-4 characteristics: the water area is 1.3 km<sup>2</sup>, the water volume is 3.8 mln.m<sup>3</sup>, the maximum depth is 3.5 meters, the average depth is 3.1 m. The total activity is 555·10<sup>6</sup> Bq. As a result of field work in 2013, the following samples were selected: fish (pike, roach), chironomids (predatory and peaceful), zooplankton and phytoplankton. Zooplankton and phytoplankton were divided using a sequential filtration system - 100 µm filters were used to collect zooplankton, and 0.45 µm for phytoplankton. Samples of fish were divided into organs: scales, muscles, liver, gills and frozen.

Samples preparation for alpha, beta and gamma measurements included the following steps: ashing in a muffle furnace (8 hours, 450°C), acidic autopsy (HNO<sub>3</sub> conc., 4 hours) and co-precipitation ((NH<sub>4</sub>)<sub>2</sub>HPO<sub>4</sub> + NH<sub>4</sub>OH). All samples were analyzed using gamma-spectrometry (Canberra GR 3818), strontium-90 was determined by Cherenkov counting. Alpha spectrometry was used for alpha-emitted nuclides determination (CANBERRA Model 7401) after separation using extraction chromatography (DGA, UTEVA, TRU (TrisKem International)).

Phyto- and zooplankton intensively absorb radionuclides from the aquatic environment. The phytoplankton activity is higher than in zooplankton. This radionuclides distribution can be associated with a larger phytoplankton specific surface area.

Chironomids larvae are living in soft mud in natural conditions. Particles of bottom sediments sticks to chironomids, hence the activity of chironomid samples is much higher than phyto- and zooplankton.

Caesium-137 maximum accumulation observed in chironomids samples (total activity – 1,7·10<sup>4</sup> Bq/g). Strontium-90 accumulates more in roach scales (1,8·10<sup>3</sup> Bq/g), because it's properties are similar with calcium cation.

The radionuclides total activity in external organs is to 2-3 orders higher than in internal organs. High uranium and plutonium activities in the internal organs correlates with the actinides in phytoplankton

(9,2 и 2,4 Bq/g) and zooplankton (1,8 и 1,4 Bq/g) activities. The high americium activity in all studied organs indicates its bioavailability. The greatest content of plutonium (141,3 Bq/g) and americium (5,8 Bq/g) observed in roach gills; uranium – in scales (3,4 Bq/g).

This work was supported by the Russian Scientific Foundation (project 16-13-00049).

## Analysis of the $^{137}\text{Cs}$ and $^{90}\text{Sr}$ content in freshwater fish from northern Poland

B. Rubel, M. Suplińska, K. Pachocki, M. Kardaś

Central Laboratory for Radiological Protection, Konwaliowa 7, 03-194 Warsaw, Poland

Keywords: fish,  $^{137}\text{Cs}$ ,  $^{90}\text{Sr}$ .

Presenting author email: rubel@clor.waw.pl

This contribution is focused on the determination of the radioactive contamination of freshwater fish. Species of *Perca fluviatilis*, *Esox Lucius*, *Carassius carassius* and *Abramis brama* originating from Piaśnica river and lakes Łebsko and Gardno (all in northern Poland) were analyzed for the presence of  $^{137}\text{Cs}$  and  $^{90}\text{Sr}$ . The study was carried in year 2016 for whole fish (eviscerated) and subsamples: fillets with the skin, fish bones and whole fish heads and a few ichthyosis samples. The determination of the  $^{137}\text{Cs}$  and  $^{90}\text{Sr}$  content in samples of water lake Łebsko and river Piaśnica was also performed.

Measurement of activity concentration of  $^{137}\text{Cs}$  and  $^{90}\text{Sr}$  in *Perca fluviatilis* revealed significant differences related to the place of fish origin. Fish samples from lakes Łebsko and Gardno were characterized by a much higher concentration of  $^{137}\text{Cs}$  ( $9.44 \text{ Bq kg}^{-1}_{\text{f.w.}}$  and  $8.17 \text{ Bq kg}^{-1}_{\text{f.w.}}$ ) than from Piaśnica river ( $0.90 \text{ Bq kg}^{-1}_{\text{f.w.}}$ ). Significant differences were also observed in the activity concentration of  $^{90}\text{Sr}$  between *Perca fluviatilis* originated from lakes ( $0.221\text{-}0.239 \text{ Bq kg}^{-1}_{\text{f.w.}}$ ) compared to those from the river ( $0.086 \text{ Bq kg}^{-1}_{\text{f.w.}}$ ). Differences in  $^{90}\text{Sr}$  concentration in *Perca fluviatilis* were also noticed in other waters on the territory of Poland (Zalewska et al., 2016). Such differences were not detected for other species in which the  $^{137}\text{Cs}$  concentration was in the range  $1.22\text{-}1.99 \text{ Bq kg}^{-1}_{\text{f.w.}}$  in samples taken from river Piaśnica and the aforementioned lakes. The highest activity of  $^{90}\text{Sr}$  was measured in *Abramis brama* ( $0.393\text{-}0.474 \text{ Bq kg}^{-1}_{\text{f.w.}}$ ).

Analyses of different species of fish confirm that 67,2-82,2% of  $^{137}\text{Cs}$  is accumulated in fish fillets, while 1.1 - 7.5% in fish bones. The content of  $^{90}\text{Sr}$  in fish fillets showed significant differences related to method of their preparation. Fillets together with ichthyosis (*Perca fluviatilis* and *Esox Lucius*) were characterized by one order of magnitude higher  $^{90}\text{Sr}$  content, 34.1-38.8%, than the fillets of *Carassius*

*carassius* and *Abramis brama* analyzed without ichthyosis: 4.2-5.4%. Whereas the measurements carried out in the separated ichthyosis showed that the content of the  $^{90}\text{Sr}$  was in the range from 29.2% to 31.1%. This confirms that  $^{90}\text{Sr}$  is accumulated mainly by ichthyosis, while the accumulation in muscle tissue plays minor role. The content of  $^{90}\text{Sr}$  in fish bones amounts on average to 19.7 %.

Activity concentration of  $^{137}\text{Cs}$  in lake Łebsko and river Piaśnica was at the level  $3.33 \text{ mBq l}^{-1}$  and  $1.50 \text{ mBq l}^{-1}$ , whereas  $^{90}\text{Sr}$  was  $1.0$  and  $0.9 \text{ mBq l}^{-1}$ , respectively. Those values do not differ from values measured in other inland waters of Poland (Suplińska et al., 2015).

Analyzed species of fish characterized a high coefficient concentration both  $^{137}\text{Cs}$  ( $\text{CF}_{\text{Cs-137}}$ ) and  $^{90}\text{Sr}$  ( $\text{CF}_{\text{Sr-90}}$ ), despite the low concentrations of these radionuclides in water, confirming that they may be good indicators of aquatic organisms.

The average concentrations of  $^{137}\text{Cs}$  and  $^{90}\text{Sr}$  in freshwater fish fillets allowed us to estimate the annual dose due to fish consumption:  $0,009 \mu\text{Sv}$  and  $0,004 \mu\text{Sv}$ , respectively, giving only fraction of a percent contribution to the annual effective dose received by the inhabitants of Poland, as a result of consuming foods containing isotopes  $^{137}\text{Cs}$  and  $^{90}\text{Sr}$ .

This work was supported by the Ministry of Science and Higher Educations

- Zalewska T., Saniewski M., Suplińska M., Rubel B., 2016,  $^{90}\text{Sr}$  in fish from the southern Baltic Sea, coastal lagoons and freshwater lake. J. Environ. Radioact. 158-159, 38-46.
- Suplińska M., Kardaś M., Rubel B., Fulara A., Adamczyk A., 2015, Monitoring of radioactive contamination of polish surface waters in 2012-2013. J. Radioanal. Nucl. Chem. 304, 81-87.



## Constraints in the application of $^{210}\text{Pb}$ dating method in a sediment core from a reservoir affected by Acid Drainage Mine

E.G. San Miguel<sup>1</sup>, C.R. Cánovas<sup>2</sup>, J.P. Bolívar<sup>1,a</sup>

<sup>1</sup>Dept Física Aplicada, Universidad de Huelva, Campus de Excelencia Internacional del Mar (CEIMAR), 21071 Huelva, Spain

<sup>2</sup>Dept of Geology, Universidad de Huelva, Campus de Excelencia Internacional del Mar, Huelva

Keywords:  $^{210}\text{Pb}$ ,  $^{226}\text{Ra}$ ,  $^{137}\text{Cs}$ , sediment dating

*a*, Presenting author email: bolivar@uhu.es

In this work, a discussion of the feasibility of application of  $^{210}\text{Pb}$  dating method is accomplished. The main hypothesis in which the traditional models used rely on are examined. The dates provided by each of the models are compared with those obtained based on  $^{137}\text{Cs}$  dates which seem to be well-established in this sediment core.

Vertical profiles of  $^{210}\text{Pb}$ ,  $^{226}\text{Ra}$  and  $^{137}\text{Cs}$  have determined in a sediment core from Sancho Reservoir, which is a reservoir strongly affected by acid mine drainage (AMD). Vertical profile of these radionuclides seem to be influenced by the increase of acidity of the reservoir waters as a consequence of AMD pressure.

The Sancho reservoir is located in the Iberian Pyrite Belt in the River Meca Valley. Due to the intense mining activities, the Meca River is currently deeply contaminated by AMD, transporting huge amounts of contaminants to the Sancho Reservoir. These pollutants are mainly transferred to the bottom sediments where high metal concentrations are observed in pore waters (Sarmiento et al., 2009).

$^{210}\text{Pb}$ ,  $^{226}\text{Ra}$  and  $^{137}\text{Cs}$  were determined by gamma-ray spectrometry using a Well Ge detector (Canberra). Spectra were collected for at least 80,000 s and analysed by Genie 2000 software (Canberra Industries). The photopeaks used in the radionuclides determination were:  $^{210}\text{Pb}$  (46.5 keV),  $^{226}\text{Ra}$  (352 keV from  $^{214}\text{Pb}$ ) and  $^{137}\text{Cs}$  (661 keV). Efficiency calibration with self-absorption corrections were determined according to procedures detailed elsewhere (Appleby and Piliposian, 2004).

The vertical profile of  $^{137}\text{Cs}$  shows a clearly distinct peak that allows the determination of an average sedimentation rate.

On the other hand, the vertical profile of  $^{210}\text{Pb}_{\text{XS}}$  ( $^{210}\text{Pb}$  in excess with respect to  $^{226}\text{Ra}$ ) versus depth (Fig. 1) shows an exponential decreasing suggesting the possibility of applying of the model CF:CS (Robbins, 1978). In this case, despite of the exponential decreasing profile of  $^{210}\text{Pb}_{\text{XS}}$ , it is evidenced that this particular model does not provide a reliable chronology in this sediment core. It is interesting to note that there are a number of applications of model CF:CS in literature that obtain  $^{210}\text{Pb}$  chronologies based only in the vertical profile of  $^{210}\text{Pb}_{\text{XS}}$  without other considerations.

The ages obtained from each of the simple models used in the  $^{210}\text{Pb}$  dating method do not match with that obtained from Fallout radionuclides. As a consequence, it is evidenced that  $^{210}\text{Pb}$  dating method always needs to be validated with at least one another independent method.

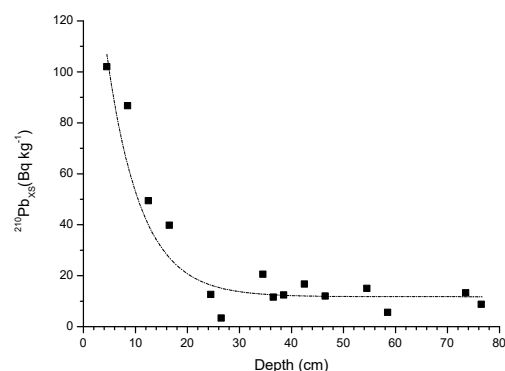


Figure 1.-  $^{210}\text{Pb}_{\text{XS}}$  vs depth. Dotted line shows the CF:CS results.

This is a publication No. from CEIMAR Publication Series. This research has been partially supported by the Project of Spanish Ministry of Economy and Competitiveness "Flujos de Radionucleidos emitidos por las balsas de fosfoyeso de Huelva; evaluacion de su dispersion, riesgos radiologicos y propuestas de restauracion (Ref: CTM2015-68628-R)

### References

- Appleby, P.G., Piliposian, G.T., 2004. Efficiency corrections for variable sample height in well-type germanium gamma detectors. *Nucl. Instr. Meth. Phys. Res. B* 225, 423–433. doi:10.1016/j.nimb.2004.05.020
- Sarmiento, A.M., Olías, M., Nieto, J.M., Cánovas, C.R., Delgado, J., 2009b. Natural attenuation processes in two water reservoirs receiving acid mine drainage. *Sci. Total Environ.* 407, 2051–2062. <http://dx.doi.org/10.1016/j.scitotenv.2008.11.011>
- Robbins, J.A., 1978. Geochemical and geophysical applications of radioactive lead. In: Nriagu (Ed.), *The Biogeochemistry of Lead in the Environment*, pp. 285–393.

## Radionuclides and heavy metal removal using chitosan-graphene oxide composite

S. Šemčuk<sup>1</sup>, G. Lujanienė<sup>1</sup>, D. Valiulis<sup>1</sup>, A. Leščinskytė<sup>1</sup>, S. Tautkus<sup>2</sup>, D. Laurinavičius<sup>1</sup>

<sup>1</sup>SRI Center for Physical Sciences and Technology, Savanorių ave. 231, LT-02300, Vilnius, Lithuania

<sup>2</sup>VU Faculty of Chemistry and Geosciences, Naugarduko g. 24, LT-03225, Vilnius, Lithuania

Keywords: chitosan-graphene oxide composite, radionuclides, heavy metals.  
Presenting author email: sergej.semчук@gmail.com

The development of new technologies based on the efficient and environmental friendly materials such as graphene oxide (GO) and GO based nano-composites resulted from the rapid industrial development, energy needs and, on the other hand, the high requirements of the environmental protection. These nano-composites belong to the group of the most promising sorbents capable of efficiently removing heavy metals and radionuclides from various kind solutions. GO has a large surface area and a number of oxygen containing groups such as epoxy (C-O-C), hydroxyl (-OH), carboxyl (-COOH), and carbonyl (-C=O) capable of binding metals and radionuclides via coordination and electrostatic interaction. Recent studies of GO chemistry have shown its significance as a precursor of graphene and a substrate for a variety of chemical modifications. Numerous studies, various methods and materials involving GO testify its importance. GO and its composites were applied to wastewater treatment and to adsorptive remediation of environmental pollutants. The aim of this work was to apply GO and chitosan-graphene oxide (CS-GO) composite for removing heavy metals and radionuclides from liquid media.

GO was synthesized using a modified Hummer's method, by oxidation of graphite powder (Marcano et al., 2010). CS-GO composite was prepared as described in literature with some modifications (Yan et al, 2016). Prepared materials were characterized using TEM and FTIR. Both sorbents were used in sorption experiments which were carried with metals (Cu, Co, Ni, Pb) and radionuclides (Pu, Cs, Am). The sorption efficiency has been studied using modelling solutions and natural seawater.

A fast adsorption of heavy metals and radionuclides to sorbents has been observed, and the equilibrium was reached after 10-60 minutes. pH dependences were studied in a wide range of the initial pH values from 2 to 11 for radionuclides and from 3 to 7 for heavy metals. The maximum of Pu and Am sorption to CS-GO was observed at pH between 4 and 5. It has been found that CS-GO composite has a better adsorption ability for Pu isotopes as compared to GO (Figure 1).

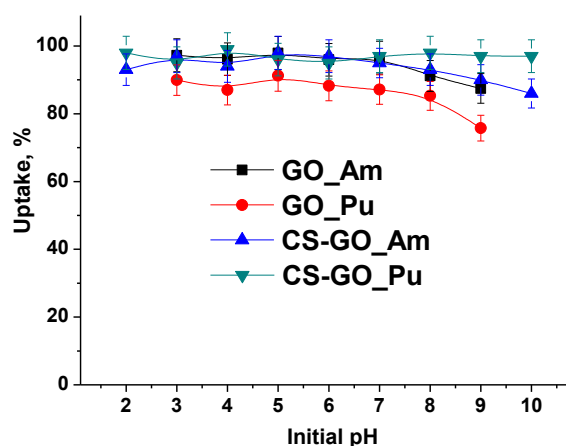


Figure 1. pH dependences of Am and Pu(IV) sorption to GO and CS-GO.

Marcano D.C., Kosynkin D.V., Berlin J.M., Sinitzkii A., Sun Z., Slesarev A., Alemany L.B., Lu W., Tour J.M. Improved Synthesis of Graphene Oxide. ACSNANO 4 (2010) 4806–4814.

Yan H., Hu H., Li A., Cheng R. pH-tunable surface charge of chitosan/graphene oxide composite adsorbent for efficient removal of multiple pollutants from water. Chemical Engineering Journal 284 (2016) 1397–1405.

## Tritium speciations in soil as a factor, characterizing migration processes

Z.B. Serzhanova, A.K. Aydarkhanova and S.N. Lukashenko

Branch "Institute of Radiation Safety and Ecology" of the NNC RK, Kurchatov city, East-Kazakhstan, 071100, Kazakhstan

Keywords: tritium, soil, speciation, Semipalatinsk test site.

E-mail: serzhanova@nnc.kz

Tritium ( $^3\text{H}$ ) is one of the most widely spread artificial radionuclides at the territory of Semipalatinsk Test Site (the STS). Being a hydrogen isotope,  $^3\text{H}$  comprises many compounds, including those of biological importance. Therefore a necessity of more detailed studying  $^3\text{H}$  and its speciations in soils arises, since soil is the primary component in biological chain, while  $^3\text{H}$  speciations is the main parameter, characterizing the processes of its secondary redistribution in environmental objects.

Tritium in soils is contained in the same forms as the hydrogen does. These forms are:  $^3\text{H}$  in surface-adsorbed and interlayer water, those are the forms met in free water (Lopez-Galindo, A., et al., 2008; Pushkaryov, A.V., et al., 2007). Hydroxylic, organically and crystalline bound  $^3\text{H}$  are bound tritium speciations. An outstanding feature of each  $^3\text{H}$  speciation is the bond strength between hydrogen-containing compounds and the soil.

To determine  $^3\text{H}$  occurrence forms in soil radioactively hazardous objects of the STS were chosen as follows: «Degelen» and «Balapan» sites. At these sites increased  $^3\text{H}$  concentration was registered in water and soil as well (Aidarkhanov, A.O., et al., 2010).

The technique used for determining  $^3\text{H}$  occurrence forms included stepwise extraction of each of the speciations. Tritium speciations contained in free water were determined using the method of distillation at different temperatures. Bound  $^3\text{H}$  speciations were determined using two-stage autoclave decomposition with intermediate ignition for the purpose of removal of organically bound  $^3\text{H}$ .

As the result of works it was found that,  $^3\text{H}$  distribution has non-uniform character. Such a distribution arises from the mechanism of  $^3\text{H}$  formation and entrance to this object. Obtained results are shown in the table 1.

Table 1. Distribution of  $^3\text{H}$  speciations in soils of the testing sites

Sampling place	Sampling point	Tritium specific activity, Bq/kg			
		$^3\text{H}$ surface-adsorbed water	$^3\text{H}$ in interlayer water	Hydroxylic $^3\text{H}$ + organically bound $^3\text{H}$	Crystalline bound $^3\text{H}$
"Degelen"	Karabulak stream	4400±440	2100±210	230±120	<120
	Baitles stream	10300±1000	4100±420	<120	<120
	Uzynbulak stream	2200±210	1700±160	<120	<120
	Aktybay stream	2000±200	1300±130	<120	<120
	Bezmyanny stream	2300±250	1050±100	420±120	190±20
	Toktakashuk stream	6800±600	4000±370	<120	<120
	Bezmyanny stream 2	1970±180	350±40	<120	<120
"Balapan"	Shagan river, p.1	10000±900	-	560±120	<120
	Shagan river, p.2	28000±2500	15500±1200	2400±200	<120
	Shagan river, p.3	650±120	60±10	430±120	250±120
	"Atomic" lake, p.1	850±80	5500±560	11000±1100	730±120
	"Atomic" lake, p.2	750±70	1100±420	11000±1200	700±120
	"Atomic" lake, p.3	1700±170	3200±320	4400±500	710±120

- speciation not registered

Tritium speciations, contained in free water, dominate in places of inflow of contaminated soil water, those are the channel of Shagan river and "Degelen". In soil of these sites high concentrations of  $^3\text{H}$  were registered in surface-adsorbed water, being the most available form. At these sites  $^3\text{H}$  can be transferred into plants, water and air.

Bound  $^3\text{H}$  speciations dominate in epicentral parts of the nuclear testing venues. One of such venues is the "Atomic" lake, where the organically bound  $^3\text{H}$  dominates. Organically bound  $^3\text{H}$  is the form available for plants, that causes presence of  $^3\text{H}$  in vegetation of the "Atomic" lake.

Obtained results allow to assume that presence of some or other  $^3\text{H}$  speciations, is probably caused by the mechanism of their formation or entry.

Aidarkhanov, A.O., et al., 2010. Ecosystem condition of Shagan river and the main mechanisms of how it is formed. Topical issues in radioecology of Kazakhstan, Proceedings of the Institute of Radiation Safety and Ecology over 2007-2009, 9-55.

Lopez-Galindo, A., et al., 2008. Tritium redistribution between water and clay minerals. Applied Clay Science, 151-159.

Pushkaryov, A.V., et al., 2007. Kinetics of isotope-hydrogen exchange in a bentonite-sand mixture Institute of Environmental Geochemistry: collected papers. Kiev, issue 15, 27-36.

## Tritium in soils of the «Experimental Field » of Semipalatinsk Test Site

L.V. Timonova, O.N. Lyakhova, S.N. Lukashenko

Branch “Institute of Radiation Safety and Ecology” of the NNC RK, 2 Krasnoarmeiskaya str., 071100, Kurchatov city, Kazakhstan

Keywords: «Experimental Field», tritium, europium.  
E-mail: Timonova@nnc.kz

Research of tritium (<sup>3</sup>H) content in soil of the STS territory have been initiated recently (since 2011).

### Research technique

At the territory of the «Experimental Field» <sup>3</sup>H content in soil was studied at the epicenters of nuclear explosions.

Soil samples were collected in venues with the maximal radionuclide contamination upon the results of pedestrian gamma-survey. Soil samples were analyzed not only for <sup>3</sup>H, but also for <sup>152</sup>Eu content. This was occasioned by the fact that <sup>3</sup>H, and <sup>152</sup>Eu, can be formed as the result of neutron activation during nuclear explosions. Specific activity of <sup>152</sup>Eu was determined using gamma-spectrometric method (Measurement procedure 2143-91). To determine <sup>3</sup>H concentrations, soil samples were prepared by means of autoclave decomposition (Operating Instruction 03-02-03). Specific activity of <sup>3</sup>H was determined via beta-spectrometry (ISO 9698 (E)).

### Results and discussions

As the result of researches, carried out at the sites of the «Experimental Field », concentrations of <sup>3</sup>H in soil vary from < 150 to 70 000 Bq/kg (Table 1).

To reveal the mechanism of <sup>3</sup>H formation in soil based on obtained results about <sup>3</sup>H and <sup>152</sup>Eu concentration a dependence of their activity ratios was built for each site. Obtained ratio values are characterized by linear dependence (Figure 1).

As the result of comparative analysis for each site <sup>3</sup>H/<sup>152</sup>Eu ratio factors were found to be 2 in average.

Table 1. Specific activity values of <sup>3</sup>H and <sup>3</sup>H/<sup>152</sup>Eu ratio.

Site	Range of specific activity of <sup>3</sup> H, Bq/kg	Ratio <sup>3</sup> H/ <sup>152</sup> Eu
P-1	< 150 – 70000	1.8
P-5	< 150 – 18000	2.6
P-3	< 150 – 14000	2.3
P-2, P-7	< 150 - 11000	2.1

Obtained linear dependence proofs the fact that one of the routes for <sup>3</sup>H formation in soil of the «Experimental Filed» testing sites is neutron activation process that took place during the tests.

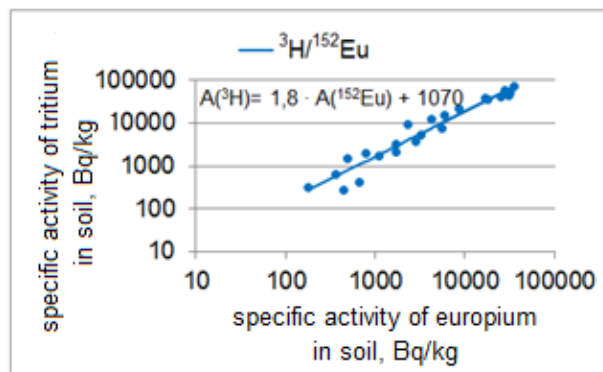


Figure 1. <sup>3</sup>H/<sup>152</sup>Eu ratio for P-1 site.

In the equation <sup>3</sup>H/<sup>152</sup>Eu ratio factor is one of the indexes, that depend on typical physical peculiarities of one test or another. Free term value shows the amount of residual <sup>3</sup>H, resulted from other mechanisms during the tests.

ISO 9698 (E), 1989. Water quality – Determination of Tritium Activity Corresponding to a Given Concentration – Liquid Scintillation Counting Method.

Measurement procedure 2143-91 № 5.06.001.98 Activity of radionuclides in volumetric samples. Procedure of measurement using gamma-spectrometer. Recommendation. State system ensuring the unity of measurements. – Introduction.1998-06-02. -1991. – p.17.

Operating Instruction 03-02-03 (A). Sample preparation for elemental analysis by autoclave decomposition. – Kurchatov: IRSE NNC RK, 2011. – P.12.

## Speciation of artificial radionuclides in water objects of Semipalatinsk Test Site

A.S. Toropov<sup>1</sup>, A.K. Aidarkhanova<sup>1</sup>, S.N. Lukashenko<sup>1</sup>

<sup>1</sup>Branch of Institute of Radiation Safety and Ecology of National Nuclear Centre of the Republic of Kazakhstan, Kurchatov, 071100, Kazakhstan

Keywords: migration, colloids, speciation, radionuclides.  
Presenting author email: torop990@gmail.com

Anthropogenic radionuclides may be contained in significant and detectable amounts in the surface water bodies of the Semipalatinsk Test Site (STS) and pose a potential risk to ecosystems and human, moving beyond the territory of the test grounds. Thus, the radionuclides migration process could considerably affect by the speciation of radioactive elements along with landscape-geochemical conditions of the environment.

In this work speciation of radionuclides in the surface water objects were studied.

In this work speciation of radionuclides in 3 surface water objects were studied. There were 2 water streams outflowing from tunnels 177 and 503 of Degelen test ground, and an artificial lake «Telkem-2». These water objects were investigated before and considered as a most contaminant at STS (Aidarkhanova, 2015).

In order to study distribution of radionuclides speciation in water objects samples were subjected to a cascade filtration with separation the following forms: coarse suspended matter (1-10 µm), fine suspended matter (1-0.45 µm), pseudocolloids (0.1-0.45 µm), macromolecular colloids (0.1-100 kDa), low-molecular mass organic colloids (10-) and dissolved (<10 kDa).

Results of radionuclides speciation in water bodies of STS has shown in Tables 1-3.

Table 1. Speciation of radionuclides in water stream of 177 tunnel, Bq l<sup>-1</sup>

Speciation	<sup>137</sup> Cs	<sup>90</sup> Sr	<sup>239+240</sup> Pu
<10 µm	5.0±0.5	680±70	0.58±0.06
<1 µm	5.0±0.5	690±70	0.53±0.05
<0.45 µm	4.3±0.4	660±70	0.44±0.04
<0.1 µm	3.7±0.4	680±70	0.4±0.04
<100 kDa	3.8±0.4	670±70	0.68±0.07
<10 kDa	3.6±0.4	720±70	0.32±0.03

Table 2. Speciation of radionuclides in water stream of 503 tunnel, Bq l<sup>-1</sup>

Speciation	<sup>137</sup> Cs	<sup>90</sup> Sr	<sup>239+240</sup> Pu
<10 µm	<0.3	150±15	0.70±0.07
<1 µm	<0.3	160±20	0.6±0.06
<0.45 µm	<0.3	150±15	0.52±0.05
<0.1 µm	<0.3	150±15	0.37±0.04
<100 kDa	<0.3	130±15	(7.2±0.7)·10 <sup>-2</sup>
<10 kDa	<0.3	110±10	(6.2±0.6)·10 <sup>-2</sup>

Table 3. Speciation of radionuclides in water of Telkem-2, Bq l<sup>-1</sup>

Speciation	<sup>137</sup> Cs	<sup>90</sup> Sr	<sup>239+240</sup> Pu
<10 µm	<0.4	190±20	0.35±0.03
<1 µm	<0.4	170±20	0.24±0.02
<0.45 µm	<0.4	170±20	0.26±0.03
<0.1 µm	<0.4	160±20	0.30±0.03
<100 kDa	<0.4	160±20	0.11±0.01
<10 kDa	<0.4	160±20	(4±0.4)·10 <sup>-2</sup>

<sup>137</sup>Cs activity in water stream outflowing from tunnel 177 was 5.0±0.5 Bq l<sup>-1</sup>, declining to 3.6±0.4 5 Bq l<sup>-1</sup> in less than 10 kDa speciation form. Thus about 30 % of <sup>137</sup>Cs was bounded with particles existing in surface water. Activity of <sup>137</sup>Cs in 503 tunnel water stream and Telkem-2 was below the detection limit.

It was found the main speciation of <sup>90</sup>Sr is dissolved matter for all water objects explored.

It was found that <sup>239+240</sup>Pu were capable to stay in the forms of suspensions, different size colloids and remain in dissolved form as well. For example, for water stream of tunnel 503 <sup>239+240</sup>Pu activity changed gradually from 0.7 Bq l<sup>-1</sup> to (6.2 ± 0.6)·10<sup>-2</sup> after filtration through the 10 kDa membrane. The distribution of speciation f as follows: the membrane 1 micron was retent 17% of the <sup>239+240</sup>Pu, 0.45 - 6%, 0.1 microns - 21%, 100 kDa - 43%, and 10 kDa - 1%.

For 177 tunnel water stream more than 50 % <sup>239+240</sup>Pu were dissolved.

For Telkem-2 activity of <sup>239+240</sup>Pu decreased in one order of magnitude from 0.35 to 0.04 Bq·l<sup>-1</sup> with maximum retention in colloid associated speciation.

The ratio between speciation distributions highly depend on water source peculiarities and can easily change under environmental conditions.

This work was supported by the Ministry of Education and Science of the Republic of Kazakhstan under grant 0122/14.

Aidarkhanova A.K. Lukashenko S.N. Investigation of character of distribution of radioactive contamination in the "water – sediments" system of Semipalatinsk Test Site and adjacent territories. // ENVIRA-2015 International Conference proceedings. Greece, 2015. P. PS3-43.



## $^{239,240}\text{Pu}$ activity concentrations in biota of the Baltic Sea

D. Tracevičienė<sup>1</sup>, G. Lujanienė<sup>1</sup> and B. Šilobritienė<sup>2</sup>

<sup>1</sup>SRI Center for Physical Sciences and Technology, Vilnius, Savanorių pr. 231, LT-02300, Lithuania

<sup>2</sup> Environmental Protection Agency, A. Juozapavičiaus g. 9, LT-09311 Vilnius, Lithuania

Keywords: seaweed, fish, plutonium, Baltic Sea.

Presenting author email: diana.traceviciene1989@gmail.com

Plutonium isotopes were mainly introduced into the Baltic Sea ecosystem after the global fallout, while the Chernobyl accident insignificantly contributed to the Pu activity concentrations (Holm, 1995; Livingston and Povinec, 2000). The aim of this study was to estimate  $^{239,240}\text{Pu}$  activity concentrations in seaweed (*Cladophora glomerata*, *Flucelloria lumricalis* and *Fucus vesiculosus*) and fish (*Platichthys flesus*, *Clupea harengus membras*, *Abramis brama*). Samples were collected in the Curonian Lagoon and in the Baltic Sea in 2012-2015. All dried samples were ashed and Pu isotopes were separated from the matrix as well as from interfering radionuclides using the extraction chromatography method.  $^{242}\text{Pu}$  was used as a tracer for the chemical yield determination. First plutonium and americium were extracted with TOPO/cyclohexane solution. TEVA and TRU resins were applied for the final cleaning (Lujanienė, 2013). Then plutonium isotopes were electrodeposited on the stainless steel discs.  $^{239,240}\text{Pu}$  activity activities were measured by means of alpha spectrometry.

$^{239,240}\text{Pu}$  activity concentrations in seaweed ranged from 0.48 mBq/kg to 17.6 mBq/kg, dry weight (d. wt.). The lowest activities were found in the *Cladophora glomerata* collected in the Curonian Lagoon, while the highest ones in the *Fucus vesiculosus* from the Baltic Sea. The *Fucus vesiculosus* was collected at the seashore (Palanga, Šventoji) of the Baltic Sea and used for comparison.

Activity concentrations of  $^{239,240}\text{Pu}$  in fish species varied from 0.5 mBq/kg to 5.9 mBq/kg, wet weight (w. wt.). Low plutonium activity concentrations were measured in the *Abramis brama* from the Curonian Lagoon, whereas higher activities were characteristic of the *Platichthys flesus* species collected in the Baltic Sea.

Our results have shown that plutonium activity concentrations depend on the fish species because some species (e.g., *Platichthys flesus*) are more populated at the bottom of sea, where the concentration of radionuclides is higher than in surface waters, while other species could migrate from one area to another. Activity concentrations of  $^{239,240}\text{Pu}$  in seaweed depend on the sampling location, on species and their origin. In general, the observed  $^{239,240}\text{Pu}$  variations in biota of the Baltic Sea were close to those reported by other researchers (e.g., Strumińska-Parulska and Skwarzec, 2010).

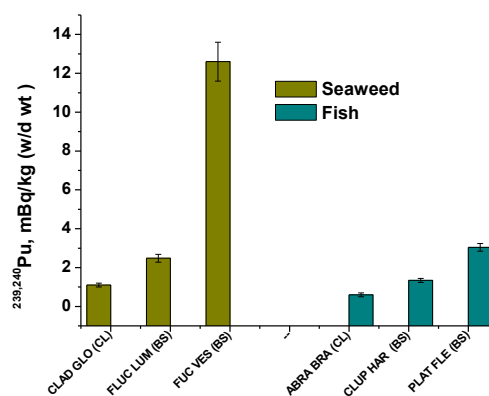


Figure 1. Average  $^{239,240}\text{Pu}$  activity concentrations in seaweed (mBq/kg, d. wt.) – *Cladophora glomerata* (CLAD GLO), *Flucelloria lumricalis* (FLUC LUM) and *Fucus vesiculosus* (FUC VES) as well as in fish (mBq/kg, w. wt.) – *Platichthys flesus* (PLAT FLE), *Clupea harengus membras* (CLUP HAR) and *Abramis brama* (ABRA BRA) from the Curonian Lagoon (CL) and the Baltic Sea (BS).

Holm, E., 1995. Plutonium in the Baltic Sea. Appl Radiat Isot 46, 1225–1229.

Livingston H. D., Povinec P.P., 2000. Anthropogenic marine radioactivity. Ocean & Coastal Management 43, 689-712.

Lujanienė, G., 2013. Determination of Pu, Am and Cm in environmental samples. In: Isotopes in hydrology, marine ecosystems and climate change studies: proceedings of the international symposium held in Monaco, March 27 - April 1, 2011. Vol. 2. Vienna: International Atomic Energy Agency, 411-418.

Strumińska-Parulska, D.I., Skwarzec, B., 2010. Plutonium isotopes  $^{238}\text{Pu}$ ,  $^{239+240}\text{Pu}$ ,  $^{241}\text{Pu}$  and  $^{240}\text{Pu}/^{239}\text{Pu}$  atomic ratios in the southern Baltic Sea ecosystem. Oceanologija, 52(3), 499-512.

## Background of HPGe gamma spectrometers: What can particle physics tell us?

P. Vojtyla

Occupational Health and Safety and Environmental Protection Unit, CERN, Geneva 23, CH-1211, Switzerland

Keywords: low-level counting, HPGe spectrometer, cosmic muons, detector background.

Presenting author email: pavol.vojtyla@cern.ch

High-purity germanium gamma spectrometers are very popular in the field of environmental radioactivity.

Background of such spectrometric systems was studied since about half a decade, with the appearance of the first Ge(Li) gamma spectrometers. At the very beginning, the studies were mostly based on experience and on the common sense. Dedicated systems placed very deep underground are rare and mostly available only for the cutting-edge physics research. A major part of laboratories is placed in cellars of common buildings and use low-level systems available commercially.

The background of such common low-level HPGe gamma spectrometers is dominated by penetrating radiation – high-energy muons of the cosmic origin, electromagnetic showers created by them and neutrons. Neutrons from the nucleonic component of the cosmic radiation at the surface level are (partially) absorbed even by moderate concrete shielding but replenished in muon interactions, including the negative muon capture (Vojtyla et al., 1994).

It is a long time since first Monte-Carlo models were applied to the studies of muon-induced background in common low-level HPGe systems for the first time, for example (Vojtyla, 1995) and (Vojtyla, 1996). Such Monte-Carlo tools had been originally developed for particle physics due to the complexity of interactions that high-energy particles may initiate. Mastering the process and validating the codes and its assumptions by experiments enabled us to analyse the governing dynamics of the whole process and to understand it quantitatively – the condition to control it.

Figure 1 illustrates a collision of a 50 GeV/c muon with a 35% HPGe system in a descending-Z lining (15 cm Pb, 1 mm Cd, 2 mm Cu) leading to an energy deposition of 1.77 MeV. Besides visualisation as shown in Figure 1, statistical treatment of all tracks enables us to reconstruct the full pedigree of a particle cascade and confirm hypotheses from the past or discover unexpected behaviour.

For example, the primary muon interactions that leads to counts in the energy region of interest are effective as follows: ~80%  $\delta$ -rays produced by muons, ~10%  $e^+e^-$  production, ~4% muon decay, ~6% the remainder: direct ionisation, muon bremsstrahlung, etc. The multiplicity of the primary muon vertices is very low: Only 2% of all muon events generate more than one particle cascade causing an event of interest. The prevailing part of primary interaction points leading to an effect is situated within a few cm of the inner lead shield. Hence, the laboratory arrangement outside the shield does not play a significant role.

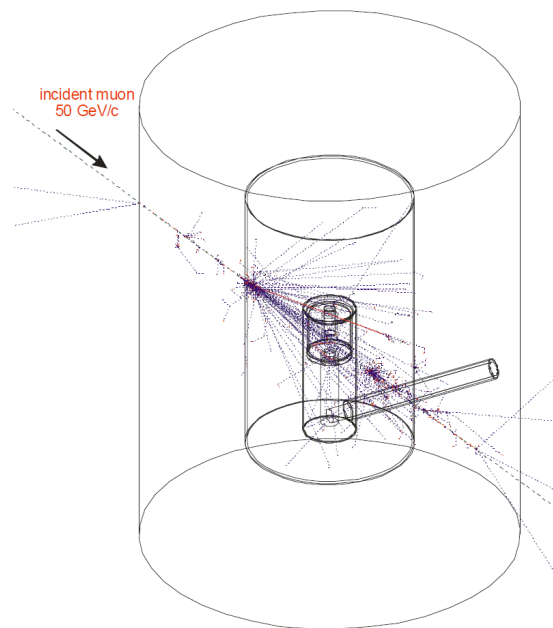


Figure 1. Interaction of a 50 GeV/c muon in an HPGe spectrometer.

On the other hand, investigation of radiation fields inside a shield shows that particle fluxes are anisotropic, as expected, but almost homogenous in space. The photon multiplicities (numbers of photons emitted during a single event) have average values around 4 and events with more than 10 photons are not rare. Hence, simulation of this background component cannot be simplified as it is the case of  $^{210}\text{Pb}/^{210}\text{Bi}$  contamination of lead.

The paper will provide further interesting findings that cannot be mentioned in the abstract due to the lack of space.

- Vojtyla, P., Beer, J., Šťavina, P., 1994. Experimental and simulated cosmic muon induced background of a Ge spectrometer equipped with a top side anticoincidence proportional chamber. *Nucl. Instr. Meth in Phys. Res. B.* 86, 380–386.
- Vojtyla, P., 1995. A computer simulation of the cosmic-muon background induction in a Ge  $\gamma$ -spectrometer using GEANT. *Nucl. Instr. Meth in Phys. Res. B.* 100, 87–96.
- Vojtyla, P. 1996. Influence of shield parameters on cosmic-muon induced backgrounds of Ge  $\gamma$ -spectrometers. *Nucl. Instr. Meth. In Phys. Res. B.* 111, 163–170.

## Peculiarities of artificial radionuclides speciation in soils of Semipalatinsk test site

A.Ye. Kunduzbayeva<sup>1</sup>, S.N. Lukashenko<sup>1</sup>

<sup>1</sup>Department of Physics, University of Somewhere, City, Region, Postcode, Country  
 Institute of Radiation safety and Ecology of the National Nuclear Center, Kurchatov city, East-Kazakhstan, 071100,  
 Republic of Kazakhstan  
 kunduzbaeva@nnc.kz

Speciation of radionuclides in soils is one of the parameters, widely used in complex radioecological studies. Speciation of radionuclides are used in assessing and predicting bioavailability and migration ability of radionuclides (migration in food chain, washing out with surface and ground waters) in soils, as a scientific basis to validate the choice of remediation method used for contaminated lands and etc. (B.Salbu et al., 2009; Bacon et al., 2008).

The STS territory has a unique feature: there are several objects with different levels and character of radioactive contamination of soil (depending on the type of test, mechanism of radioactive particles formation). Longstanding studies (2008-2015) allowed to accumulate a significant amount of materials regarding speciation of artificial radionuclides in soils of various STS objects. This work is aimed at summarizing results of longstanding studies of <sup>137</sup>Cs, <sup>90</sup>Sr, <sup>241</sup>Am, <sup>239+240</sup>Pu artificial radionuclides' speciation in soil of various STS objects and at revealing distribution peculiarities of radionuclides' speciation at the STS territory depending on character of radioactive contamination of soil cover.

The paper provides quantitates of <sup>137</sup>Cs, <sup>239+240</sup>Pu and <sup>241</sup>Am and <sup>90</sup>Sr artificial radionuclides' speciation in soils of the STS testing sites as follows "Experimental Field" (surface explosions), "Degelen" (underground explosions with takeout of radionuclides to the day surface with tunnel water), "4a" (testing warfare radioactive agents), object "Atomic lake" (excavation explosion) and conditionally "background" STS territories (territories beyond the testing sites, suffered from global fallouts and fallouts from surface nuclear tests). For the purpose of study, the subsequent extraction method modified by F.I. Pavlotskaya was used (Pavlotskaya, 1974).

It was found, that distribution of radionuclides' speciation in the STS soils depends on physical and chemical properties of radionuclides and the character of soil cover radioactive contamination. The lowest mobility and bioavailability of all the radionuclides studied was registered at the "Experimental Field" site and the "Atomic" lake, where the radionuclides were mainly found in tightly bound form (over 91,7%). This is mainly due to peculiarities of formation mechanisms of the radioactive particles resulted from surface and excavation explosions. The highest mobility of radionuclides was registered in soils of WRA testing sites ("4a" site), influence zones of radioactive streamflows from the "Degelen" site and conditionally "background" lands of the STS, for that sorption, mechanism of radioactive contamination of

contaminated particles is typical. In particular, there was found insignificant increase in exchangeable and mobile <sup>137</sup>Cs form, <sup>239+240</sup>Pu organic form and <sup>241</sup>Am mobile form, maximum concentration of exchangeable and mobile <sup>90</sup>Sr forms at the STS (Kunduzbayeva et al., 2013).

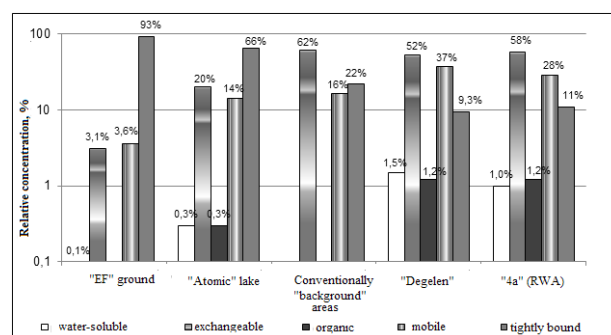


Figure 1. Speciation of <sup>90</sup>Sr radionuclide.

The results of study conducted at the STS can be used in assessing and forecasting radionuclides behavior in soils of contaminated lands with similar mechanisms of radioactive contamination (the territory within the influence zone of nuclear industry objects, nuclear test sites, influence zones of radioactive fallout traces and etc.).

Speciation of radionuclides in the environment / B.Salbu, L.Skipperud // Journal of Environmental Radioactivity. – 2009. – No.100. – P. 281-282.

Jeffrey R. Bacon. Is there a future for sequential chemical extraction / Jeffrey R. Bacon, Christine M. Daidson // Analyst. – 2008. - No.133. - P. 25 - 46.

Pavlotskaya, F.I. Migration of radioactive products of global fallout in soils. / F.I. Pavlotskaya. – M.: Atomizdat, 1974. – 215 p.

Kunduzbayeva, A.Ye. Speciation of artificial radionuclides in soils of "Experimental Field" ground. / A.Ye. Kunduzbayeva., S.N.Lukashenko, R.Yu. Magasheva // Proceedings of the National Nuclear Center of the Republic of Kazakhstan over 2011-2012. /edited by S.N. Lukashenko. – Vol.2. - Issue 4. - Pavlodar: Dom Pechati, 2013. – P. 181-208.